Allan Pentecost

Travertine

Springer

Allan Pentecost

Travertine

Allan Pentecost

Travertine

With 102 Figures and 22 Photoplates, some in color

Springer

Author

Dr. Allan Pentecost

Reader in Geomicrobiology
School of Health and Life Sciences
King's College London
Stamford Street 150
London SE1 9NN
United Kingdom

Library of Congress Control Number: 2005926090

ISBN-10 1-4020-3523-3
ISBN-13 978-1-4020-3523-4

Springer is a part of Springer Science+Business Media
springeronline.com

Printed in The Netherlands

Cover design: Erich Kirchner, Heidelberg
Typesetting: Camera ready by the author
Production: Almas Schimmel
Printing: Krips, bv, Meppel

Printed on acid-free paper 30/3141/as – 5 4 3 2 1 0

Preface

During the spring of 1960, an uncle showed me a 'petrifying spring' near Plaxtol in Kent where twigs had been encased in a calcareous jacket. A twig was collected and having recently been given I. Evan's Observer's Book of Geology by my parents, I found a photograph of another petrifying spring and an explanation of its origin. In those days, Derbyshire was too far for a holiday destination, and I took little further interest until a research studentship with Professor G. E. Fogg became available in 1971. Tony Fogg had recently moved to the University College of North Wales, Bangor and the research was to be into cyanobacterium mats, with fieldwork along the Red Sea coast. The fieldwork never materialised but my interest in algal mats had been aroused. A chance stroll along the Bangor shore revealed beautifully calcified cyanobacterium mats, and Tony generously allowed me to investigate these instead. The old Plaxtol collection was retrieved and yielded abundant cyanobacteria. It became apparent that here was a wealth of information about a rock whose formation was so rapid, that the process could be studied in days rather than years – an exceptional state of affairs. A search of the literature also revealed that the rock, a form of travertine, had other unusual features. The decision to bring this information together in a book was soon made, but it was to be many years before time allowed its initiation. Progress was sometimes slow, when heavy German tomes had to be translated, and obscure publications had to be found. This was punctuated by amusing encounters such as Weed's description of the cowboy who bathed in the waters of Mammoth Hot Springs, only to find that he was becoming 'petrified', no doubt making a rapid retreat! The literature on travertine is widely scattered and references are encountered in a surprising number of disciplines. Indeed, travertine has played an important but neglected role in our understanding of nature. Not only does it continue to inspire millions of visitors to caves and travertine dammed-lakes – it was also the careful observation on the growth of travertine in the 19th Century that led to an appreciation of the true age of the Earth, and the foundation of the science of geology.

Many travertines develop at the Earth's surface where they were often covered in plants, while others form in caves where they form flowstone, stalactite and stalagmite. In a work of this kind it is impossible to ignore cave deposits and they are widely referred to, although the original intent was to concentrate on the surface forms. It was soon apparent that the definitions of these forms were often vague and confusing and were badly in need of clarification. In the cool British climate, travertine formation has not occurred on a large scale, but in warmer latitudes, travertines can be extensive and of considerable economic value. Most of the largest deposits are formed around hot springs, in which Britain is impoverished. Despite this, British deposits are of great variety and have taught us much about biogeochemical processes and of the organisms that once inhabited them, and it is within this region that the author began his interest before venturing to warmer climes.

Allan Pentecost · London, May 2005

To my family

Acknowledgements

I am grateful to the following for permission to reproduce copyright material: Carol Hill, Paolo Forti and the National Speleological Society, Alabama for the upper part of Fig. 24; Martyn Pedley and the Yorkshire Geological Society, Fig. 19; the British Bryological Society for reproduction of Fig. 68; the Geologist's Association for reproduction of Fig. 27; the Henry Moore Foundation for use of Photoplate 20E, Hodder Arnold and Andrew Goudie for permission to reproduce Fig. 82; the British Cave Research Association for Fig. 69; Dr. M. P. Kerney, Dr. R. C. Preece and the Royal Society for Fig. 75; Dr. Zhang Dian and the American Geophysical Union for Fig. 102.

I am also indebted to Dr. C. Clelia, Dr. Paolo Tortora, Dr. A. Waltham, and K. Gardner for the provision of photographs and Dr. C. Clelia, Prof. R. L. Folk, Prof. W. F. Giggenback, Prof. A. Goudie, Dr. A. G. Irwin, T. C. Lord, Debora Rougeaux, Dr. B. Spiro, Dr. Heather Viles, Dr. B. Winsborough, and Dr. P. Withers, for helpful suggestions and advice.

Financial assistance is gratefully acknowledged from the British Bryological Society, English Nature, the Geologist's Association and the Royal Society.

I am also grateful to Blackwell Publications for permission to use Fig.4, the *Naturalist* for Fig. 14, *Cave and Karst Science* for Figs. 22 and 69, the CIBA Foundation for Fig. 26, the Quaternary Research Association for Figs. 47, 58 and 79, E. Schweizerbart'sche Buchhandlung, Stuttgart for Fig. 51, *Radiocarbon* for Fig. 71, USGS for Fig. 88 and *New Scientist Magazine* for Fig. 92.

Contents

Chapter 1

Introduction

The work is divided into 17 chapters covering, it is hoped, most of the accumulated knowledge of this unusual stone. The first chapter provides definitions and looks at the history of our understanding of travertine formation. The second deals mainly with the properties of active travertines and begins with their classification using a broad range of criteria, from their geochemical origins to their gross morphology. In Chapter 3, hydrogeological processes leading to the formation of travertine-depositing waters are considered, including the role of the soil-atmosphere and factors controlling spring emergence. The chemical properties of travertine-depositing water are considered next according to the groundwater source. The range of springwater compositions is explored in Chapter 6 and compared with non-depositing waters. In Chapter 7, the mineralogy and gross composition of travertines is examined. The two common polymorphs of calcium carbonate, aragonite and calcite both form travertines and during their growth, trap other atoms, ions and molecules. These trace constituents together with other precipitating and trapped minerals can provide useful environmental and historical evidence in older travertines. Of equal significance are the stable isotope compositions of carbon and oxygen in the travertine carbonate. The ratios of the two stable isotopes of oxygen, ^{16}O and ^{18}O for example, are capable of providing valuable information on the conditions under which travertines were deposited in the past. Cave travertines in particular have been useful in unravelling climate change in the Quaternary. This topic is addressed in Chapter 8.

The flora and fauna of actively-depositing travertines has fascinated biologists for more than two hundred years. It was soon established that the specialised physico-chemical environment was home to a great diversity of plants and animals with some peculiar adaptations to a rapidly depositing environment. In Chapter 9, this diversity is explored with reference to the ecology and biology of the organisms involved. The process of travertine formation is arguably the most revealing and important aspect of any book devoted to a freshwater carbonate. The chemical changes leading to calcium carbonate deposition are considered in Chapter 10 and include the important of carbon dioxide evasion, the nucleation and growth of calcite crystals and the significance of the associated organisms. The chemical dynamics of travertine-depositing systems are described and processes ranging from carbonate nucleation to crystal cohesion investigated. The next four chapters deal with organic remains of travertines and their use as biostratigraphic markers and indicators of past climates. Chapters 11 and 12 concentrate on the Quaternary and its numerous and important interglacial travertines. Their floras and faunas are described, methods of dating are elaborated and the impacts on travertine formation by man are described. With the recent interest in climate change, interest in the recent past, as revealed by the Quaternary sediments has increased, leading to advances in our understanding of climate variation over the past two million years. Epigean (surface) travertine formation is both sensitive to climate and replete with terres-

trial fossils, providing valuable evidence of local and regional climates. The effects of climate and man on travertine formation is taken up in Chapter 13. Travertines cannot form in organically polluted waters and are sensitive to catchment interference by man. As a result, the recent history of travertine formation can often be linked directly to human activity. The remaining chapters cover topics mainly relevant to inactive travertines and related deposits. Travertine is but one of a wide variety of Earth's continental limestones and in Chapter 14, the older deposits, dating from Archaean to Pliocene are considered. Marls, calcretes and beachrocks – other forms of continental carbonate, are often associated with travertine and are sometimes confused with them. They are described briefly in Chapter 15 along with industrial deposits of calcium carbonate. The latter are responsible for much of the scaling of industrial and domestic pipework, and the use of inhibitors and other forms of remediation are also described here. Some consideration is given to the likely occurrence of extraterrestrial travertines in Chapter 16. Such deposits almost certainly exist on other planets of the Solar System. Since microbes are frequently found entombed within travertine, they could provide a focus for the search of microbial activity on other planets.

While travertine-like deposits can be a nuisance in industry, the 'natural' travertines can be financially rewarding. Some are renowned for their visual impact and used extensively in art and architecture. The topic has a long and interesting history. In addition, many of the world's most scenic spots are travertine locations, bringing huge sums of money to those countries fortunate enough to possess them. They too are the subject of Chapter 17.

1.1 Definition of Travertine

Several recent definitions of travertine can be found in the literature. They vary from a single phrase to a short paragraph in length. Some emphasise temperature while others point to hydrologic setting or process. The latter is emphasised throughout this book. Process of formation should be of fundamental significance in the definition of all limestones. Among the more brief though not particularly concise definitions of travertine is that of Mitchell (1985): 'formed by evaporation of spring and river waters' while Whitten and Brooks (1972) define it as a 'kind of calc-tufa deposited by certain hot-springs'. Temperature also enters into the definitions of Riding (1991) who defined travertine as

> … a product of warm carbonate springs where the elevated temperatures, together with the dissolved materials present in these warm waters, excluding most eukaryotic organisms.

He also lists them as one of five forms of microbial carbonate: 'a layered benthic microbial deposit with a dendritic microfabric', while Glover and Robertson (2003) define travertine simply as 'hot spring deposits (>20 °C)'.

Emig (1917) wrote one the best early 20th Century accounts of travertine formation and defined it as 'deposition from the water of springs or streams holding calcium bicarbonate in solution'. Fouke et al. (2000) apply a broader definition:

> All non-marine carbonate precipitates in or near terrestrial springs, rivers, lakes and caves.

Although some the above definitions pay attention to process, they are insufficiently precise. For example, evaporation is not normally considered to be an important process in travertine formation, and all natural waters contain at least traces of calcium and bicarbonate. Restricting a definition on temperature alone would lead to difficulties with old, inactive deposits, while lake and playa deposits are varied and include the lake marls, not normally equated with travertine.

Of interest is the proposal of Koban and Schweigert (1993) who provide definitions based on the mode of precipitation (organic/inorganic), the hydrological setting (vadose/phreatic), and the porosity, on a triangular diagram distinguishing lacustrine limestones, sinters, travertines and tufas. The diagram is conceptually appealing and in placing emphasis on the hydrology, makes an important contribution. However, it would be difficult to apply in most situations. Bates and Jackson (1987) provide three definitions:

a a dense finely crystalline, massive or concretionary limestone, of white, tan or cream, often having a fibrous or concentric structure and splintery fracture formed by rapid chemical precipitation of calcium carbonate from solution in surface and groundwater, as by agitation of stream water or by evaporation around the mouth or in the conduit of a spring, especially a hot spring. It also occurs in limestone caves where it forms stalactites, stalagmites and other deposits; and as a vein filing, along faults, and in soil crusts. The spongy or less compact variety is *tufa*. Synonym *calcareous sinter*.
b a term sometimes applied to any cave deposit of calcium carbonate.
c a term used inappropriately as a synonym of *kankar* (a type of calcrete).

Definition a) is more informative than most, but fails to clearly identify the main process leading to travertine formation, namely the degassing of aqueous carbon dioxide, although this is implied, along with evaporation. Deposits associated with soils are normally referred to as calcretes.

Travertine is defined here as:

A chemically-precipitated continental limestone formed around seepages, springs and along streams and rivers, occasionally in lakes and consisting of calcite or aragonite, of low to moderate intercrystalline porosity and often high mouldic or framework porosity within a vadose or occasionally shallow phreatic environment. Precipitation results primarily through the transfer (evasion or invasion) of carbon dioxide from or to a groundwater source leading to calcium carbonate supersaturation, with nucleation/crystal growth occurring upon a submerged surface.

This definition attempts to emphasize inorganic processes, namely reactions involving gaseous carbon dioxide and a calcium bicarbonate solution leading to the precipitation of calcium carbonate in a non-marine setting. It does not preclude biological processes nor evaporation, but regards them as subsidiary. The principal reaction involves the loss of carbon dioxide gas from a calcium bicarbonate solution leading to calcium carbonate deposition. Most definitions fail to cover all cases of a particular process and the above is no exception. For example, on rare occasions, travertine is formed under the influence of seawater, while algal and bryophyte photosynthesis is locally important. These processes are detailed below, but it should be emphasized that they remain exceptional and apply to few deposits considered here as travertines.

Travertine deposition frequently occurs on steep slopes, and bedding within the deposit, where present, is usually inclined and undulatory. Travertines formed *in situ* are rarely horizontally bedded. Laminations on a millimetre to centimetre scale are common and often the result of daily/seasonal growth rhythms. Bacteria, algae, bryophytes and reeds are frequently encrusted with travertine and photosynthetic activity will enhance calcium carbonate precipitation. In caves, these fabrics are normally absent. Most frequent morphologies are mounds, pendants and terraces associated with dams. Key travertine

features are lack of horizontal bedding and formation by chemical precipitation. Clastic travertines resulting from autochthonous travertine erosion are common and often occur as terraces and fans. These deposits often show horizontal bedding but their clastic nature is usually obvious. Deposits formed by the common ion effect would not be classed as travertines, although in practice, some of the resulting forms would be difficult to distinguish from them and they are considered here along with the travertines as defined above.

1.2 Travertine Compared with Other Non-marine Carbonates

Travertine is distinguished from:

- *lake marl* which is deposited on the beds of lakes and results largely from the precipitation of calcium carbonate through phytoplankton /macrophyte photosynthesis augmented by CO_2 evasion and evaporation. Precipitation occurs either within the lake water and subsequently deposited as a calcareous mud, or upon submerged benthic macrophytes such as *Chara* that become incorporated into a fine, weakly laminated sediment in a fully phreatic environment. Lake travertines are normally more localised, being deposited at the emergence points of submerged springs by *in situ* precipitation to form mounds, and also as travertine dams at the lower end of a lake in a vadose/phreatic setting. Littoral deposits associated with microalgae may also occur. Deposition is focussed and horizontal bedding is lacking. Where travertine forms into dams across rivers and streams, impounded lakes or ponds usually form into which marls accumulate. In these cases, the marl contains a significant amount of clastic travertine and is best regarded as part of a 'travertine-depositing system'.
- *lake reef:* Occasionally, reefs form at calcareous lake margins which appear to result from the coagulation of fine planktonic carbonates (e.g. Green Lake, N.Y.). The deposits may result from precipitation in the lake water as a combined result of degassing of CO_2 and photosynthesis. They may not be deposited *in situ* but consolidated in the lake littoral as carbonate reefs. Their fabrics can be travertine-like but they cannot be strictly classified as travertine and they are referred to here as lake-reef carbonates. The mechanism of reef formation is uncertain and they will be referred to briefly in Chapter 15.
- *calcrete* (caliche), a subaerial deposit formed by evaporation and CO_2 evasion of water at the moist soil surface. These deposits are typically laterally extensive and usually no more than a few metres in thickness and of low porosity. They reach their maximum development in warm, arid climates. Travertines may become 'calcretised' during periods of aridity but this is a secondary process, and evaporation is rarely an important factor in travertine formation.

In modern settings, travertines are usually readily separated from marine limestones, lake marls and calcretes as the process of formation is easy to recognise. Travertine deposition tends to be localised around points of spring emergence, or associated with calcium-rich river systems. Bedding, if present, is often irregular. Cave travertines contain little or no mouldic porosity but form characteristic pendants, pillars and curtains, often with bizarre shapes. Old inactive travertines may be more difficult to recognise. Their hydrological settings may be obscure and their morphologies much modified by erosion and diagenesis. Examination of thin sections is normally required where characteristic microfabrics are often revealed.

1.3 Etymology

The word travertine is thought to originate from the *lapis Travertinus* used for the volcanic spring deposits of Bagni di Tivoli in Lazio, Italy. Other spellings are sometimes encountered in the early literature, notably *trevertine* and *travertin*. In Italian it is *travertino*. Travertinus was originally *tiburtinus* or *Tivertino*, from the Roman name of Tivoli, a town 26 km east of Rome. There are several references to travertine in the classical literature. Vitruvius noted its strength; '*Tiburtina vero et quae eodum genere sunt omnia, sufferunt et ab oneribus et a tempestibu iniuria*', and it is mentioned in Plinius' *Natural History*; '*lapides Tiburtini ad reliqua fortes, vapore dissiliunt*'. Travertine was quarried near Bagni di Tivoli to provide building materials during the Roman period, but these sites have been largely if not entirely destroyed by more recent excavations. During the Roman Empire, the rock was probably won from many quarries in the vicinity of important towns, but those near Tivoli were likely to be among the most important as it could be sent directly to Rome by barge. Bagni di Tivoli should therefore be regarded as the type locality for travertine.

Several other names have been applied to travertine and are in common use. In English-speaking lands, *calcareous tufa* is used, often reduced simply to *tufa*. Barker (1785) used the term *tuft*. These terms apply to soft, poorly consolidated deposits that abound in the British Isles. The French use *le tuf calcaire*, and occasionally *touviere* or *tout* (Blot 1986). In Germany, *Kalktuff* is often used, with *alm* to distinguish the soft, unconsolidated forms (Jerz 1983). More rarely it was called *Duckstein* (Damm 1968), and occasionally *Sprudelstein* or *Quellekalk*. The travertine of Cannstatt was referred to specifically as *Sauerwasserkalk*. Many of these words are derived from the Latin *tofus*, and in early English writings, *towfe* or *tophus* can be found (Leland c. 1538 in Hearne 1711; Rudder 1779). Townson (1797) distinguished 'the common calcareous Tophus, (tophus communis)' from both volcanic tufa and the travertino, along with other writers such as Baier (1708) and Naumann (1850).

Tofus is an ambiguous term which seems to have been applied to a range of soft rocks. Ovid compared it with pumice, as a material unsuitable for building and Plinius wrote; *'e reliqua multitudine lapidum tofus aedificis inutilis est mortatilate, mollitia*.'

Statius observed its use in road building but the identity of the material is uncertain. However, *tofus rubrum* has been equated with 'lithoidal tufa', a term applied to pyroclastic deposits erupted from the Colli Albani volcanoes, southeast of Rome (Platner 1830). Vitruvius states; '*sunt etiam alia genera plura, uti in Campania rubrum e nigrum tofum*', though Virgil considered *tophus scaber* a general term. In modern Italian, *tufo* is used for pyroclastic deposits consisting of volcanic ash, lapilli and pumice fragments found in great quantity in the vicinity of Naples, Rome and elsewhere. This description extends to ash sufficiently consolidated to be cut for building stone and has been used widely since the Roman period. Poorly consolidated deposits of travertine, which many would call calcareous tufa, are uncommon in this region, and it is unlikely that such deposits represent the original tufo. Blake (1947) clearly distinguishes between this tufa, with its variable colour and strength, and travertine.

The term *algal tufa* has been used in the early 20th Century literature for a range of algae-associated intertidal and evaporite carbonates (Warren 1982). Intertidal carbonates are outside the scope of this work and will be only briefly referred to. There is in fact a much earlier reference to this form of sediment. According to Agricola (1546), Theophrastus (c. 370–287 B.C.) used *poros* for such deposits, but this was not taken up by later writers.

Another term occasionally used to describe travertine is *sinter*, which originated in Germany for the dross formed during the smelting of iron (Damm 1968). *Sprudelsinter* is still used for hot spring deposits formed at spas, such as Carlsbad (Karlovy Vary) in the Czech

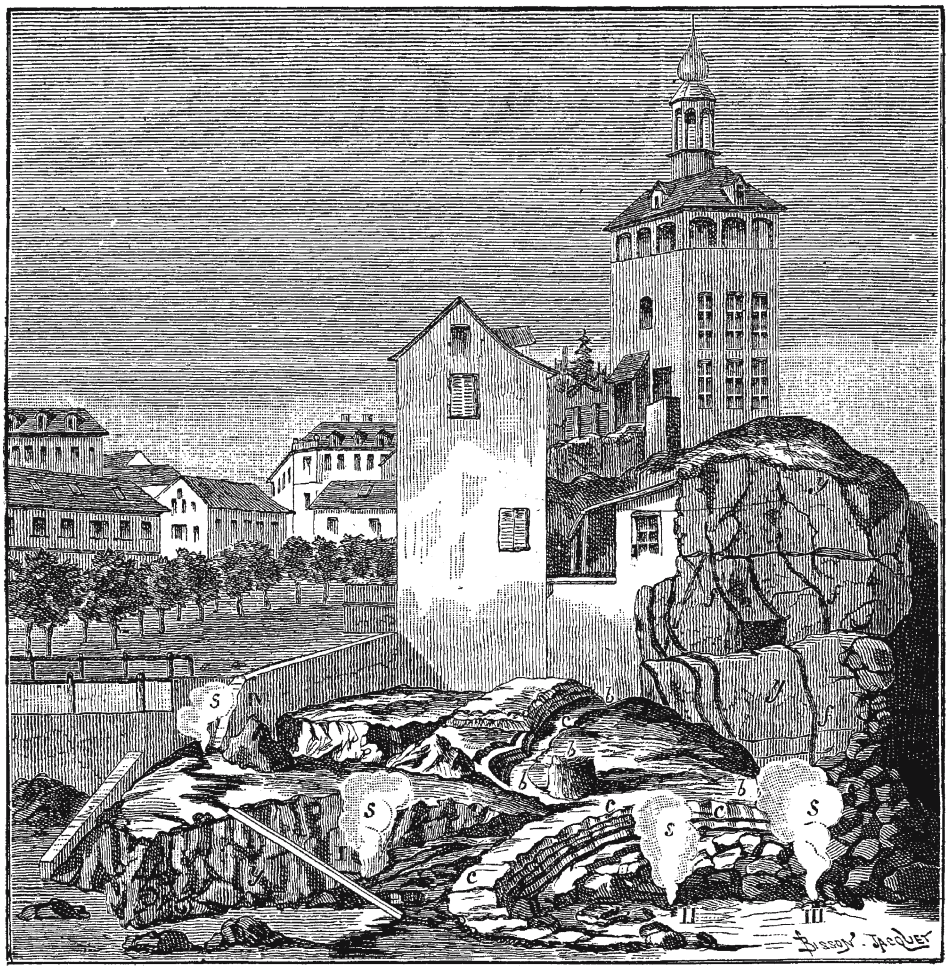

Fig. 1. The hot spring of Carlsbad, Czech Republic where many early observations of travertine formation (c) were undertaken. From Daubrée (1887)

Republic (Fig. 1). Walch (1773) considered sinter 'feiner und compakter als die Tophstein'. Sinter could apply to the travertine of Bagni di Tivoli, though it would then be confused with siliceous sinter, used for the opaline silica deposits of hot springs. Sinter, according to Pia (1933) should be applied to inorganically formed deposits, whereas the Bagni travertine contains layers of 'shrubs' thought to have formed through bacterial activity (Chafetz and Folk 1984). A more accurate term *calc sinter* has found occasional use. Hubbard and Herman (1990) revived the term *travertine-marl* as an alternative, including the softer clastic sediments.

Ought these terms be distinguished in the light of current knowledge? Recent research has revealed a rich microbial flora in many modern hot spring travertines, but their role in its formation remains equivocal and it is clear that at Bagni di Tivoli, shrubs occur only in discrete layers. Not only would it be impracticable to distinguish layers and give them separate names, but it is difficult, if not impossible to determine the precise origins of many ancient travertines.

Should the term *calcareous* (*calc*) *tufa* be encouraged as an alternative to travertine ? It is well enough understood in much of Europe, and Blot (1986) coined the term *tufologie* for the study of such deposits, but it might be misunderstood in Italy. It could be argued that the softer, poorly consolidated varieties should be so described, as indeed they are in numerous publications (e.g. Pedley 1990). The problem here is one of definition. There is no practical way of unambiguously setting a degree of strength or consolidation to these deposits. Julia (1983) recognised this and used travertine for all carbonate encrustations on plants without reference to pore volume or density. While admitting the impracticability of porosity measurements during field surveys, a classification into tufa and travertine is difficult to apply in cases where deposition is not obviously associated with plants. There are therefore good reasons in the author's view for reassessing these terms, and in this work, the term *tufa* will be not be used, though its use will no doubt continue, and be reasonably well understood in most parts of the world.

1.4 History of the Science of Travertine Formation

Travertine has been exploited as a building material for at least two thousand years but is mentioned little in classical texts, and an understanding of travertine formation has come to us only recently. That certain springs could deposit a stony material on submerged objects has been known since the first century B.C. Strabo (c. 20 B.C.) mentions the petrifying waters of the hot springs at Hierapolis, Turkey and recounts a legend concerning a bird overflying them. In China, cave travertines were described as early as the 4th Century B.C. in the Chi Ni Tzu (Needham 1959) and epigean travertine has been recognised since the Thang dynasty (A.D. 618–907). According to Yao Yuan-Chih (c. 1650), 'not only wood, but also herbs can change into stone when this happens to plants and the water-absorbing stone (*shang shui shih*) is produced'. The term *han shui shih* is applied to plant encrustations, and *chiang shih*, a more general term, aptly translated as the 'ginger stone'. An illustrated Chinese account is provided by Chang (1927).

After the collapse of the Roman Empire, nothing seems to have been written on the subject in the 'Dark Ages' that followed. However, the terms were known in the German area as early as A.D. 750. In the Middle Ages references are also sparse. Cohn (1876) recalled the hymn of Boleslau von Lobkowitz, c. 1500, where the algal colours of Carlsbad are described and Agricola (1546) notes a *tofus*, providing a brief description. 'Petrifying springs' were objects of curiosity in Europe and received passing reference in alchemical works such as Libavius (1597). Hot springs have always attracted interest and use made of their supposed medicinal qualities, but their calcareous and siliceous deposits passed by almost without comment. The travertine springs of Zerka Ma'in, Jordan once famous for their cures, were visited by Herod the Great (*Genesis* 36; 24). The encrustation of Rome's aqueducts, and doubtless the city's plumbing could hardly have gone unnoticed, but no written records have come to light.

Our current understanding of travertine formation can be traced back as far as the 11th Century but sound principles could not be formulated until the overturn of the 'Phlogiston Theory' late in the 18th Century when the true nature of matter began to unfold. The properties of calcium bicarbonate solutions were studied throughout the 19th Century when empirical formulae were superseded by equilibrium constants at the start of the 20th Century. This allowed chemists to determine the ionic constitution of natural waters and obtain predictions of the chemical changes occurring when temperature, pressure and composition was altered. Today we have a reasonably good understanding of travertine formation, but it would be a mistake to believe that our understanding is complete. Much remains to be done.

The precipitation of calcium carbonate at the Earth's surface is a major geochemical process that has played a significant part in the history of inorganic chemistry. The discovery and chemical properties of carbon dioxide are central to an understanding of the mechanism. Before the 17th Century, little was known of the nature of matter and its chemical transformation. Plinius (c. A.D. 70) mentions types of vapours that probably included carbon dioxide and also the speleothems of Mount Corycus, Greece. During the 11th–17th centuries, travertine is mentioned as speleothem in several influential works and three classes of mechanisms proposed to account for them (Shaw 1997). The first regarded speleothem as a plant-like growth and this is easy to understand in structures such as stalagmites with their root-like bases and concentric layers when seen in cross section. The second held that the deposits resulted from vapours rising from the depths of the Earth. The third maintained that some process of solidification from water occurred and this eventually led to our current understanding of the process. An important early development was the observation of dissolution and precipitation of salts. Experiments with the poorly soluble potassium nitrate led Palissy (1564) to conclude that speleothems formed by deposition of a salt taken up by water. The role of carbon dioxide in the process was not revealed until much later although the gas was known in other contexts. Helmont (1648) described *spiritus sylvestris* through the action of vinegar on limestone and the same gas was recognised in mineral springs. Later, Cavendish (1767) undertook experiments on the lime scale ('fur') forming on cooking utensils in London and found that the fur was held in solution by 'fixed air' but did not explain the process further. In 1770, Scheele recognised that carbonates and bicarbonates were different salts and noted the solvent action of carbon dioxide on limestone, and Black (1757) undertook experiments on the burning of lime and magnesia which were found to release carbon dioxide. Once Lavoisier (1780–90) overthrew the confusing 'Phlogiston theory' and deduced the proportion of carbon and oxygen in carbon dioxide, the correct formula was soon discovered. Not long after, Cuvier (1812) pronounced that water dissolves carbonates by means of abundant carbonic acid, allowing them to later crystallise after the acid has evaporated. This provided the correct solution, but did not explain where the carbonic acid came from. Bourguet (1742) proposed much the same mechanism but failed to mention the part played by 'fixed air' (CO_2). More detailed accounts of the early history of speleothem research may be found in Shaw (1997).

Geologists and botanists have long recognised epigean travertine as spring-deposited limestone and speculated upon its origin. Leopold von Buch (1774–1853) a German geologist and pupil of Werner travelled to Italy in 1799 and described the deposits at Tivoli, distinguishing several forms (Buch 1809), noting their association with plants. Joseph Priestley discovered photosynthesis in 1776 and its formulation ($CO_2 + H_2O + \text{light} = O_2 + \text{organic matter}$) was given by Ingen-Housz (1796). Charles Lyell (1829) described some British travertines remarking that:

> the water of the springs … must also contain lime, since oxalate of ammonia renders the water turbid … and carbonic acid is very evident.

Raspail (1833) is attributed by Julius Pia as the first to recognise that CO_2 uptake by plants could result in calcium carbonate precipitation. Agardh (1827) visited the travertine-depositing hot springs of Carslbad and prepared the first list of algae from such deposits. Ferdinand Cohn, Professor of Botany at Breslau (now Wróclaw, Poland) made detailed studies of travertine and their associated algae. At Carlsbad he collected and described the cyanobacterium *Fischerella thermalis* (*laminosus*), observing that 'presst man die Polster dieser Alge aus, so fühlt man zwischen den Fingern einen äusserst feinen Sand zurückbleiben'. The 'sand' was found to be calcium carbonate and Cohn describes the close association

between algae and the travertine deposits. Cohn supported Raspail's view that plant metabolism could result in the precipitation of calcium carbonate, but did not cite his work. He also observed that not all plant species deposit carbonates in otherwise favourable circumstances and that CO_2 loss to the atmosphere was responsible for some travertine formation (Cohn 1862). He later turned his attention to the travertines of Italy, making a study of samples collected at the 'Cascatelle' of Tivoli, a series of travertine-encrusted waterfalls on the Anio River (Cohn 1864). He found further support for his plant hypothesis and also visited the springs at Bagni di Tivoli containing the 'volcanic' travertines used by the Romans. He distinguished, as had Buch, between the Cascatelle and Bagni travertines and described their algal flora in detail. One of his significant observations, for long overlooked, is the distinction between intracellular and extracellular biomineralization based in part on his observations of travertine.

Advances in carbonate chemistry were few in the first half of the 19th Century and awaited an understanding of the nature of ions and chemical equilibrium. Measurements by Schloesing (1872) showed that the amount of calcium carbonate dissolved by carbon dioxide could be expressed as a simple empirical equation and in the same decade it was found that for dilute solutions, the quotient [base][acid]/[salt] was constant at a given temperature and pressure. A few years later the ionic product of water was obtained. Hassack (1888) confirmed Cohn's views that aquatic plants could precipitate calcium carbonate by performing laboratory experiments, and the great deposits of travertine and siliceous sinter at Yellowstone were described in detail by Weed (1889a). Walter Harvey Weed provided a review of the algae of hot springs, noting the preponderance of cyanobacteria and showed that the amount of calcium carbonate held in solution greatly exceeded that held by water in contact with the epigean atmosphere.

By the end of the 19th Century, chemists were able to obtain equilibrium constants for some of the carbonate system reactions and these were essential if the dissolution and precipitation of carbonates were to be understood. Equations relating the activity of the Ca^{2+}-HCO_3^- system to dissociation constants were standardised by Johnston (1915) and the combined equations used to predict solution composition as a function of the CO_2 partial pressure, although it would be some years before biologists recognised their importance. One of the first influential works on travertine written in English was that of the American W. H. Emig who worked for a while as a biologist for the Oklahoma Geological Survey. He provided a well-informed account of the travertines of the Arbuckle Mountains (Emig 1917) that included speculation regarding their recent history, an account of their flora and some early chemical analyses of the waters. Emig was born at Coulterville, Ill. and graduated from the University of St. Louis in 1911.

Julius Pia reviewed the earlier work relating plant metabolism to calcium carbonate deposition (Pia 1933, 1934) and described eight theories to explain the precipitation process. These included the 'Water loss theory' whereby plants take up water, concentrating the calcium bicarbonate remaining in the water, and the 'Carbon dioxide loss theory' which is essentially calcium carbonate precipitation brought about by photosynthesis. During the past 50 years knowledge of travertine has increased rapidly and papers on travertine now appear regularly in many fields of science, as well as in the arts. Influential post-war developments include the application of stable and radioactive isotope measurements, the latter permitting dating, advancing studies of palaeoclimatology and palaeobiology. Further progress arose through the advent of the electron microscope, computers and more refined methods of chemical analysis plus a realisation of the environmental significance of many deposits and their relationships with plants. More recently, the possibility of travertine deposits on other planets has been given serious attention in relation to the discipline of exobiology. These and other uses of this remarkable rock are described in the following chapters.

Origins of the Components

Travertines exist in a variety of forms and are classifiable on a range of criteria. A review of the literature by Pentecost and Viles (1994) identified four salient features; the precipitation process, carbon dioxide geochemistry, the travertine fabric and its morphology. The first two are considered below along with schemes applied to limestone in general. Chapters 3 and 4 consider the travertine fabric and morphology and their use in classification. Travertines may also be classified according to their hydrological setting and this is also referred to in Chapter 4.

2.1 Travertine Precipitation

Four chemical processes are responsible for almost all travertine formation on Earth. Most travertines form from the degassing of surfacing carbon dioxide-rich groundwaters containing >2 mmol L^{-1} (c. 80 ppm) calcium. A groundwater capable of depositing travertine is produced when dissolved carbon dioxide ('carbonic acid') attacks carbonate rocks to form a solution containing calcium and bicarbonate ions ('calcium bicarbonate') (Eq. 2.1):

$$CaCO_3 + CO_2 + H_2O = Ca^{2+} + 2(HCO_3)^- \quad (2.1)$$

Travertine deposition is the reverse of reaction (1). Carbon dioxide is lost from solution on contact with an atmosphere whose CO_2 concentration is lower that that in equilibrium with the 'attacking' below-ground solution. The sources of underground carbon dioxide capable of contacting and dissolving carbonate rocks (hence termed the carrier CO_2 or 'carrier') are manifold but two are of particular importance, the respired soil-zone CO_2 and thermally-generated CO_2. Where the evasion of carbon dioxide occurs to the epigean (i.e. above-ground and illuminated) atmosphere, additional CO_2 loss frequently occurs through the photosynthesis of aquatic plants and evaporation.

A few travertines are formed by the reaction between atmospheric carbon dioxide and hyperalkaline groundwater (Eq. 2.2):

$$Ca(OH)_2 + CO_2 = CaCO_3 + H_2O \quad (2.2)$$

These groundwaters most frequently occur in regions undergoing serpentinization (O'Neil and Barnes 1971) or those in contact with natural or industrially produced calcium hydroxide. This process may be considered *invasive* rather than *evasive* with respect to the carrier.

Travertines arising from (Eq. 2.2) are widely distributed but uncommon. Another process may be described as groundwater alkalisation and is observed when groundwaters rich in

calcium mix with alkaline surface water. Hydroxyl ions in the lake water react with bicarbonate (HCO_3^-) to form carbonate (CO_3^{2-}) followed by precipitation of calcium carbonate (Eq. 2.3).

$$Ca(HCO_3)_2 + OH^- = CaCO_3 + HCO_3^- + H_2O \quad (2.3)$$

This reaction is mainly confined to a class of saline lakes where the OH^- concentration is elevated as a result of geochemical processes. These carbonates do not form through a direct transfer of carbon dioxide to or from the atmosphere and are not strictly travertines. However, they may be described as 'travertine-related' and are included in this book.

Another travertine-related process is the 'common ion effect'. The best known example is provided by the reaction of groundwaters infiltrating evaporites that become saturated with gypsum or anhydrite ($CaSO_4$). Gypsum-saturated waters contain high concentrations of $CaSO_4$, approaching 2 g L^{-1}. When mixed with a Ca-bicarbonate water, Ca is sufficiently elevated to exceed the solubility product of calcite and precipitation follows. In this case, precipitation may be subsurface and within stratified sediments when mixing occurs underground. Again, the resulting deposits are not strictly travertines as described in Section 1.1.

To summarise, precipitation of calcium carbonate results from: evasion/invasion of CO_2; reactions involving OH^-; and increase in Ca. Deposits resulting from these five processes often appear similar both in their microfabric and gross morphology.

2.2 Classification on Carrier CO_2

In this section, consideration will be given to the reactions which give rise to the carrier CO_2. It will be seen again that a small number of independent processes are involved in the majority of cases, but as some of them are believed to originate deep in the Earth's crust, a number rely on indirect evidence or are merely speculative. However, useful classifications can result which have implications for the prospecting of travertines, and impinge upon some aspects of their morphology, fabric and biota. In the majority of cases the carrier originates either from the soil (meteogene) or from more deeply seated thermal processes (thermogene) providing a primary subdivision into two categories. This classification has the value of being independent of scale but is more difficult to apply to ancient travertines since it is ultimately dependent upon source water composition. As Riding (1999) and others have pointed out, purely descriptive definitions, irrespective of their origin, may be so broad as to have little value.

2.2.1 Meteogene Travertines

Soil-zone and atmospheric carbon dioxide may be regarded as meteoric in origin, since the terrestrial vegetation and associated soil contains carbon fixed from the atmosphere. Travertines formed from groundwaters charged with a meteoric carrier are termed meteogene (Pentecost and Viles 1994). They form typically in cold-water springs in regions underlain by carbonates, or occasionally evaporites (gypsum). Their dissolved inorganic carbon content (DIC) and dissolved calcium rarely exceeds 8 mmol L^{-1} (480 ppm as HCO_3) and 4 mmol L^{-1} (160 ppm as Ca) respectively and the stable carbon isotope composition averages around –10‰ (see 8.2). Occasionally, such waters circulate deep beneath the ground where they become heated and rise as hot springs, but contain only the meteoric carrier. These travertines, often the result of artesian flow, have been described as thermometeogene

(Pentecost 1995a). This is probably not the most suitable term because the name suggests that thermal water issues from the source. While the water is indeed warm or even hot in most of these springs this not always so. For example at high latitudes, where the mean air temperature is close to 0 °C, the groundwater temperature may be 10 °C higher due to deep circulation, but water at 10 °C is hardly 'thermal' (a term usually associated with 'hot'). The problem is discussed in more detail by Pentecost et al. (2003) and a better term for these waters is *superambient*. This implies that the groundwater issues significantly above the ambient temperature (the mean annual air temperature). *Invasive meteogenes* include those formed through the reaction of atmospheric CO_2 with hyperalkaline groundwater as described in (Eq. 2.2) above.

The soil atmosphere is by far the most important contributor of carbonic acid leading to limestone dissolution and the CO_2 enrichment of groundwaters. Concentrations of carbon dioxide gas in the soil air vary from about 0.2–10% (Jakucs 1977; Brook et al. 1983; Ford and Williams 1989) and a large proportion is dissolved by percolating rainwater. The epigean atmospheric CO_2 concentration of 0.03% is too low to contribute significantly to direct carbonate dissolution where soils are present.

Thus the meteogene travertines are divided into two categories; the *evasive meteogenes* where carbon dioxide evasion leads to travertine deposition and the *invasive meteogenes* where the reverse process leads to deposition. Both may be further subdivided into the *ambient meteogenes*, the most frequently encountered where waters rise at ambient temperature, and the *superambient meteogenes* where, through deep circulation, the waters rise at a temperature above ambient and often as hot springs (>37 °C). Since all invasive meteogenes so far investigated are ambient, the terms *ambient* and *superambient* may be used without qualification as 'evasive' or 'invasive'.

2.2.2 Thermogene Travertines

The second group usually contains some meteoric carrier, but the bulk of the carbon dioxide originates from thermal processes within or even below the Earth's crust. Thermally generated carbon dioxide dissolves in groundwater, often under considerable pressure and the resulting high concentrations of CO_2 are capable of dissolving large volumes of rock, the solutions rising as hot, bubbling springs, forming a hydrothermal circuit (see 5.1.2). Typical dissolved inorganic carbon (DIC) and Ca levels are 10–100 mmol L^{-1} (400–4000 ppm as HCO_3) and 2–20 mmol L^{-1} (80–800 ppm as Ca) respectively, two to ten times higher than most meteogene sources. Rates of degassing and precipitation are correspondingly higher, providing distinctive fabrics and the travertine stable carbon isotope composition is generally heavier than meteogene waters (typically –3 to +8‰). Thermogene deposits have a more localised distribution than meteogenes and are often associated with regions of recent volcanic or tectonic activity. For example, the waters giving rise to Mammoth Hot Springs in the USA are heated by magma chambers close to the surface and the extensive deposits of Central Italy are associated with a number of Quaternary volcanic centres. High geothermal gradients may also exist locally in areas containing large blocks of radioactive igneous intrusions resulting in hydrothermal activity.

It is important to note that thermogene source waters are not necessarily hot, although this is frequently the case, the term applying to the source rather than the exit temperature of the water. Hot springs, with exit temperatures of 37 °C or above, are likewise not necessarily of thermogene character as noted above.

2.2.2.1 Magmatic Generation of Carrier

Deep sources of carbon dioxide have long been suspected to occur in thermal discharges of spring-water as they are often accompanied by ^3He, thought to be present in the upper mantle (Piperov et al. 1988). Carbon dioxide is a common magma constituent and significantly affects its melting point (Deines 1992). In fact the amount of CO_2 within the Earth is now thought to far exceed that at the surface. As magma rises toward the Earth's surface, pressure reduction leads to outgassing, with the vertical migration and eventual release of carbon dioxide to the epigean atmosphere. This may be encouraged by the presence of deep faults in regions of crustal tension. Circulating groundwaters are capable of dissolving large quantities of gas under high hydrostatic pressures. The resulting solutions dissolve calcium carbonate at depth, providing highly concentrated bicarbonate solutions that begin degassing as the waters rise. Hydrothermal solutions often ascend along fractures and Khoury et al. (1984) noted that within a region of Jordan with an elevated geothermal gradient, basalt was releasing CO_2 into deep faults and precipitating travertine at the surface. In the Carpathian Mountains, Dowgiallo (1976) provides evidence for the magmatic origin of some high-CO_2 springs on isotopic evidence while conceding that the bitumen oxidation hypothesis of Nowack (1938) may account for some of the CO_2. In a Japanese site, helium isotope studies suggest that decarbonation was responsible for up to 90% of the deep carbon source (Sano 1996) while at Huanglong, China, Yoshimura et al. (2004) suggest that most of the CO_2 originates in the upper mantle. Some mantle-derived carbon dioxide could be juvenile as carbon compounds occur frequently in meteorites, though a proportion may also come from sediments having entered the upper mantle via subduction. This probably explains at least in part the wide range of $\delta^{13}C$ values reported from travertines and their associated waters (Barnes et al. 1984; Allard 1988; Deines 1992). The topic will be considered further in Chapter 8.

2.2.2.2 Decarbonation

Baking of carbonate sediments in the presence of clay and other minerals leads to the formation of carbon dioxide gas. The importance of these processes has been advocated by Germann and Ayres (1941), White (1957), Hurley et al. (1966), Muffler and White (1968), Panichi and Tongiorgi (1976), Barnes et al. (1984), Amundson and Kelly (1987), D'Amore (1989) and Cathelineau et al. (1989). Both contact- and regional metamorphism provide sufficiently high temperatures to release carbon dioxide from carbonate-silicate rock. Reactions proceed at temperatures ranging from 100–800 °C (Cathelineau et al. 1989; D'Amore 1989) and at depths of up to 5 km. The mineral products include chlorite, epidote, forsterite, wollastonite and more rarely portlandite, $Ca(OH)_2$ dependent upon the composition of the associated country rocks, limestone impurities and fluid compositions. Portlandite may itself produce hyperalkaline groundwaters as noted above (Saines et al. 1980; Barnes et al. 1982). Some relevant reactions are shown in Table 1. Many of these reactions are easily reversible and some (e.g. iv) occur at moderate temperatures (100–150 °C) producing thermogene carrier within regions of average geothermal gradients and shallow depths. Such reactions are thought to occur in oil fields (Hutcheon and Abercrombie 1989) but their overall significance in travertine formation and CO_2 evasion in general is unknown.

While the reactions in Table 1 may proceed to the right, liberating gaseous CO_2, the associated pressure-temperature field and activities/fugacities of the species involved are conjectural. Where geothermal gradients are high, such as regions of active vulcanism, or in mountain-building areas where hot radioactive rock underthrusts limestone, decarbonation could proceed at a low lithostatic pressure close to the surface. The overall significance of decar-

Table 1. Carbon dioxide generation by subsurface thermal processes. From Germann and Ayres (1941); Barnes et al. (1982, 1984) and Hutcheon and Abercrombie (1989)

A) Reactions between silicate minerals and carbonates	
i)	$2CaMg(CO_3)_2 + SiO_2 = Mg_2SiO_4$ (forsterite) $+ 2CaCO_3 + 2CO_2$
ii)	$CaCO_3 + SiO_2 = CaSiO_3$ (wollastonite) $+ CO_2$
iii)	$7CaMg(CO_3)_2 + 2.5Al_2Si_2O_5(OH)_4$ (kaolinite) $+ 3H_2O + 3Fe^{2+} + 3.5O_2 =$ $Mg_7Al_2Fe_3Si_5Al_3O_{20}(OH)_{16}$ (chlorite) $+ 7CaCO_3 + 7CO_2$
iv)	$5FeCO_3 + SiO_2 + Al_2Si_2O_5(OH)_4$ (kaolinite) $+2H_2O = Fe_5Al_2Si_{13}O_{10}(OH)_8$ (chlorite) $+5CO_2$
v)	$4CaCO_3 + K_2Al_4Si_6Al_2O_{20}(OH)_4$ (mica) $+6SiO_2 + 2Fe^{2+} + O_2 =$ $2Ca_2Al_2FeSi_3O_{12}(OH)$ (epidote) $+ 2KAlSi_3O_8$ (feldspar) $+ H_2O + 4CO_2$
vi)	$CaCO_3 + H_2O = Ca(OH)_2$ (portlandite) $+ CO_2$
B) Reactions of carbon and some of its non-carbonate compounds	
vii)	$C + 2H_2O = CO_2 + 2H_2O$
viii)	$CO + H_2O = H_2 + CO_2$
ix)	$CH_4 + 2H_2O = 4H_2 + CO_2$
x)	$(COOH)_2$ (oxalic acid) $=HCOOH$ (formic acid) $+CO_2$ (decarboxylation)

bonation is disputed by some geochemists because of the relative ease of reaction reversal and restricted access to carbonates of hydrothermal fluids.

2.2.2.3 CO_2 from Heated Organic Matter

Most oil fields possess a cap of gas containing 1–5 vol-% carbon dioxide. Its origin is unclear but may include thermally-generated sources (Tiratsoo 1972; Hutcheon and Abercrombie 1989). Oil is also accompanied by large volumes of interstitial and 'bottom' connate water, often with a high alkalinity, though this may be due to the presence of organic acids rather than CO_2. Carbon dioxide also occurs with methane in coal and other carbonaceous deposits resulting from a low temperature reaction (Eq. 2.4; Tiratsoo 1972):

$$C_{57}H_{56}O_{10} = C_{54}H_{42}O_5 + 3H_2O + CO_2 + CH_4 \quad (2.4)$$

A significant source of CO_2 may be the reaction between methane and ferric oxide (haematite) and could account for some gas field CO_2 (Eq. 2.5: W. F. Giggenback, *pers comm.*)

$$CH_4 + 8Fe_2O_3 = CO_2 + 2H_2O + 8FeO \quad (2.5)$$

Few travertines seem to be associated with such processes. One example may be the Colusa Oil Spring, in California (Feth and Barnes 1979). Bituminous limestones in Greece also give rise to travertines containing hydrocarbons (de Boer et al. 2001) and others probably occur in the Pannonian Basin of central Europe.

Decarboxlyation of organic acids occurs between 200–300 °C, but can begin as low as 100 °C due to cleavage of the weak C-COOH bond. The extent of decarboxylation is also dependent upon pressure and its geochemical significance is unclear at present.

2.2.3 'Orgamox' Waters and Other CO_2 Sources

Significant oxidation of buried (non-soil) organic matter can occur at low temperatures (0–30 °C) and it is conceivable that large quantities of carbon dioxide could be released by this process and dissolve in groundwater. This is clearly not a case of thermally-generated carbon dioxide but is likely to occur where there are shallow organic-rich sediments.

Deposits of peat have been suggested as a possible CO_2 source for the Plitvice travertines (Srdoc et al. 1983). Carbon dioxide is also formed in anaerobic waters and sediments by bacteria, particularly sulphate-reducers (Eq. 2.6):

$$2C_3H_6O_3 \text{ (lactate)} + SO_4^{2-} + 4H^+ = 2CH_3COOH \text{ (acetate)} + S^{2-} + 2H_2O + 2CO_2 \qquad (2.6)$$

Sulphate reduction may occur deep underground providing a suitable organic substrate is available, and may become a significant CO_2 source (Chapelle and McMahon 1991). Acetate fermentation by methanogenic bacteria may also produce carbon dioxide.

These processes could not be readily distinguished form the organic oxidation processes above using standard analyses of groundwaters but are included for the sake of completion. At least one minor travertine deposit probably results from this kind of process, namely the Harrogate Sulphur Springs of the UK. It has been classified as a 'cool orgamox' (cool non-soil organic matter oxidation) travertine (Pentecost 1996a).

Another uncommon but well-known process of CO_2 formation is by near-surface spontaneous combustion. This occurs within bituminous carbonates in Jordan, and also forms portlandite leading to extensive travertine deposition (Clark et al. 1991).

Carbon dioxide generation is also possible by the oxidation of pyrite. The resulting sulphuric acid could then react with carbonate to produce CO_2. Some Chinese caves have high CO_2 atmospheres as a result of this process which could lead to increased limestone solution (Waltham et al. 1993). Its relevance to carbonate deposition is unknown.

Thus three geochemical types of travertine, meteogene, thermogene and 'cool orgamox' may be distinguished. While the distinction can often be made on the basis of source water chemistry, intermingling of thermogene and meteogene waters can occur (Boni et al. 1980; Scheuer and Schweitzer 1981; Yoshimura et al. 2004), and a mixed water will result. A summary of the distinguishing features of meteogene and thermogene source waters is shown in Table 2. Cool orgamox waters have been excluded since too few have been recognised and investigated.

2.3 Other Classifications

Mention must be made of other limestone classifications since they may be applied to the travertines. Folk (1962) recognised three main limestone constituents: allochem (=grain); matrix (micrite) and sparite (cement). He also described four families of allochems; peloid. ooid, bioclast and intraclast. Using these, four families of limestone, capable of further subdivision were obtained, namely: 1) allochem cemented by sparry calcite; 2) allochem with micrite matrix; 3) microcrytalline limestone lacking allochems and 4) limestone with *in situ* organic remains – biolithites. Most travertines would fall under groups 3 and 4.

Another scheme was devised by Dunham (1962). Three subdivisions are made between limestones which are: 1) matrix-supported (lime mudstones and wackestones and micrite taken as <20 μm by Dunham); 2) grain-supported limestones (packstones and grainstones) and 3) biologically bound (boundstones) with a further category for crystalline limestones.

Table 2. Geochemical characters of the autochthonous travertines and associated waters

Origin		Carrier	DIC mmol L^{-1}	pCO_2 vol-%	$\delta^{13}C$ (PDB‰) of travertine	pH	Typical morphology	Typical fabrics
Meteogene								
Evasive	Ambient	soil	2–8	1–10	−12 to −3	7–8.1	Stream crust, cascade, river dam, oncoids, stalagmites	Algal bushes and laminae, bryophytes and phytoclasts. Mouldic porosity
	Super-ambient	soil	2–8	1–10	−12 to +2	7–8.1	Stream crust, cascade, river dam	Algal bushes and laminae, bryophytes and phytoclasts. Mouldic porosity
Invasive		atmosphere	<1	<0.03	−20 to −9	9–11	Stream crust, river dam	Limited biofabric, usually sinter-like
Thermogene								
		mantle, magma, decarbonation	12–50	20–70	−1 to +10	6–7	Mounds and fissure ridges	Bacterial and cyanobacterial shrubs and laminae, abiogenic shrubs. Fenestral porosity.

Some travertines belong to this fourth category, whilst others may be described as lime mudstones and boundstones. Neither scheme is closely related to a particular depositional environment or origin and all schemes are complicated by post depositional change. However, they have found use in the description of travertine deposits, particularly where a range of different limestones need to be distinguished.

2.4 Sources of Bedrock Carbonate and Calcium

It is impracticable to classify travertines according to the source of bedrock carbonate mineral or calcium but these sources require consideration as they influence the distribution of travertine deposits. Most travertines originate from calcium bicarbonate waters, and these have been shown to arise, in most cases, from the reaction between dissolved carbon dioxide and a carbonate rock. The marine carbonates (calcite, dolomite) are the most abundant carbonate source in the Earth's crust. Of these, calcite is more rapidly dissolved by CO_2 solutions and travertines are often uncommon in regions underlain entirely by dolostones. Continental carbonates such as older travertines, calcretes and lake marls may themselves provide a carbonate source for further travertine deposition but this has been little documented. Another source is carbonatite, an uncommon igneous rock containing a high proportion of calcite and/or dolomite (Deines 1989). Carbonatites are widespread along the African Rift where they have been identified with at least two travertines (Holmes 1965; Casanova and Hillaire-Marcel 1992). Another calcium-containing carbonate, ankerite $(Ca,Fe,Mg)CO_3$ occurs in metamorphic rocks and occasionally provides the calcium source for travertine (Spötl et al. 2002). Other carbonates include magnesite ($MgCO_3$), siderite ($FeCO_3$), natron ($Na_2CO_3 \cdot 10H_2O$) and trona ($Na_2CO_3 \cdot NaHCO_3 \cdot 2H_2O$). It is not known to what extent, if any, they serve as a CO_2 source.

Calcium enters solution mainly from limestones of varying purity. Gypsum can be a significant source in some regions leading to common-ion precipitation. Thermogene waters may undergo bedrock reactions allowing calcium to enter from other sources. For example it can be removed from the biotite of gneisses and from anorthite during kaolinisation (Yoshimura et al. 2004). There are several stable isotopes of calcium but no attempts have yet been made to use them as tracers.

The Travertine Fabric

This chapter describes the fabric of travertine under two main headings, the microfabric and the mesofabric. The former relates to mainly microscopic characters identifiable in thin section and the scanning electron microscope (SEM), and the latter to characters visible mainly in hand specimens visible to the naked eye. Microscopic characters are by far the most important and lead to an understanding of travertine formation, its subsequent mineralogical history (diagenesis) and provide explanations for many of its physical characteristics. Meso-fabrics merge with microfabrics but permit discussion of travertine porosity and banding, both of which provide characteristic features of the rock, and are normally evident in polished hand specimens. They also include descriptions of small mobile forms of travertine known as ooids and oncoids.

Many factors are responsible for the fabric of travertines. In speleothems, Frisia et al. (2000) list seven: kinetics of growth processes, discharge, carbonate mineral supersaturation, CO_2 evasion rate, presence of growth inhibitors, ion transport mechanism and temperature. For the epigean travertines there are additional factors such as plant growth characteristics and animal burrows. In addition, most of these factors have multiple effects and are interdependent. For example, discharge affects the hydrodynamics at the travertine surface (laminar or turbulent flow) influencing the CO_2 evasion rate, as well as providing energy which can be used to build oncoids and form clastic travertines. These factors will be discussed more fully in Section 10.5. Here, the emphasis will be upon structural features of the fabric, rather than its genesis.

3.1 The Microfabric

Fabric refers to the textural and structural features of a rock on a range of scales, including spatial relationships between the constituent mineral grains to the degree of lamination and the jointing system, where present. Important textural features are grain size, grain shape and the relationships between adjacent mineral grains. As a limestone, the great majority of travertine grains are of calcium carbonate, either as calcite or aragonite. Individual calcite grains, often consisting of single crystals, vary greatly in size, from submicroscopic (<0.2 μm) to macroscopic (>10 mm), while aragonite usually occurs as microscopic acicular crystals. The term *micrite* is commonly used for the fine-grained calcite <5 μm in diameter, and is the major constituent of many limestone matrices, with *microspar* used for crystals in the range 5–15 μm (Folk 1959). Unfortunately, these definitions have not been adhered to universally. Special terms are also used for grain shape. Equant crystals are approximately equidimensional and are common in travertine. Grains without distinguishable crystal faces are termed *anhedral*, those showing at least one plane crystal face are *subhedral*, while grains showing well developed rational faces throughout are termed *euhedral* (Bates and Jackson 1987). Micrite is normally equant and

anhedral, while microspar is frequently equant and euhedral. Equally common are narrow, elongate grains loosely termed 'blades' often aggregated into a multiplicity of forms. They have been described as columnar when more than 10 μm wide and with a length to width ratio of > 6:1 and acicular when less than 10 μm wide with a greater length to width ratio. Both may form aggregates consisting of hundreds of crystals and are rarely present as isolated individuals. Plate-like grains, common in some limestones, are infrequent in travertine.

The above constituents form a range of characteristic microfabrics dependent upon their spatial interrelationships. These in turn are responsible for the mesofabrics evident in hand-specimens. The microfabrics depend upon the depositing environment and are influenced by the physicochemical and biological conditions prevailing during $CaCO_3$ nucleation and crystal growth. Further modifications (diagenesis) frequently occur soon after the travertine has been deposited.

The most significant textural components of travertines are micrite, three simple forms of sparite and more complex dendrites. While all of these may constitute the original, or primary fabric of a travertine, it is important to realise that secondary fabrics resulting from diagenesis are usually present and cannot always be reliably distinguished. For example, while a primary micrite is being precipitated around the surface of an algal colony, it may be recrystallizing into a sparite a few mm below the surface, or a layer of sparite might be in the process of micritization by bacteria and fungi. The resulting fabric will be a combination of primary and secondary (diagenetic) processes. For the initial discussion, it is impracticable to separate the two processes and textures are considered here without direct reference to diagenesis.

Bacteria, algae and bryophytes often occur in abundance and several authors have distinguished *biofabrics* which may be characteristic of certain groups or species of plants. The influence of plants on fabric will be explored with reference to the bulk constituents and the spatial relationships.

Bulk constituents are explored by examining a range of travertine fabrics classified exclusively on crystal size into micrite (0–5 μm), 'microspar' (5–35 μm) and 'macrospar' (>35 μm) in thin sections (Fig. 2). While the spar size definitions do not conform to other classifications and include more complex dendritic types, they are useful when describing freshwater limestones such as travertine. Some travertines, developing in the absence of plants and without obvious clumps of bacteria, are listed under 'calcareous sinter' in Fig. 2a which shows a set of four stick charts and a summary pie chart. The four examples demonstrate a preponderance of spar with an average 16% micrite. A calcareous sinter from a thermogene site in Wyoming, (Chart 4) shows a spar content exceeding 95%. Travertines containing recognisable bacterial clumps but otherwise negligible plant material are shown in Fig. 2b. The first four charts are of modern travertines and demonstrate a wide range in composition. Micrite is a minor component in the calcites of Charts 1 and 2, but is dominant in 3 and 4 representing aragonite travertines from Wyoming (for convenience small aragonite crystals are included here under 'micrite'). Two Pleistocene bacterial travertines composed of calcite (Charts 5, 6) contain more than 50% micrite.

Travertines dominated by algae are shown in Fig. 2c. Charts 1–8 are modern deposits colonised by a range of common species. Charts 1 and 2 represent travertines colonised by the cyanobacterium *Phormidium incrustatum* and consist almost entirely of micrite. A similar cyanobacterium, *Schizothrix* (3 and 4) is also associated with abundant micrite, while *Rivularia haematites*, a well-known freshwater stromatolite-forming cyanobacterium forms a sparry travertine (5). Charts 6–8 show travertines associated with the common eukaryotic algae *Gongrosira, Oocardium* and *Vaucheria.* They all contain significant micrite but it does not exceed the amount of sparite. One of the older travertines (10) is associated with *Vaucheria* and contains considerably less micrite than the modern *Vaucheria* (8). Travertines associated with bryophytes also vary widely in composition (Fig. 2d). The first three, representing

different moss taxa, are micrite-dominated, but the fourth is dominated by spar. This is interesting since both 3 and 4 represent the same species from the same geographical region, yet their microfabrics are clearly different. Charts 5–8 represent older travertines and micrite remains significant in all of the samples.

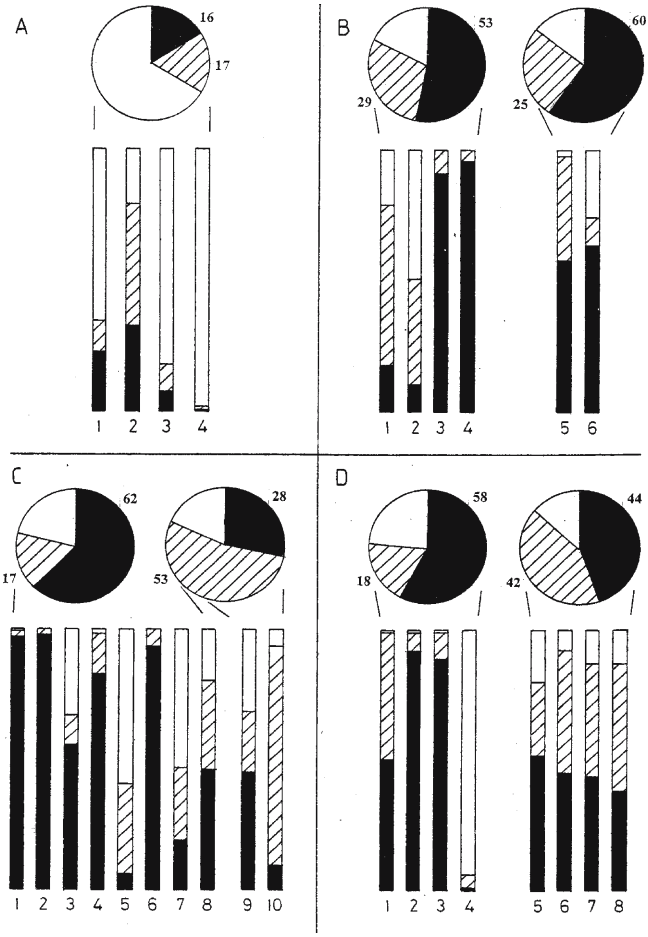

Fig. 2. Stick and pie charts of travertine fabrics giving percent compositions obtained from 10 random fields of thin sections. Micrite 0–5 μm, black; 'microspar' 5–35 μm, hatched; larger spar >35 μm, white. Pie charts show mean compositions for a range of fabric types. a) *modern sinter:* 1 Fleinsbrunnen, Germany; 2 Ingleton, UK; 3 Matlock, UK; 4 Firehole Lake, Wyoming b) *bacteria:* 1 Bagno Vignoni, Italy; 2 Lago delle Collonelle, Italy; 3 Mammoth Hot Springs basin facies, Wyoming; 4 Mammoth Hot Springs terracette; 5 Bagni di Tivoli, Italy; 6 Cave Bruno Poggi, Italy. 1–4 modern, 5,6 Pleistocene. c) *algae:* 1 *Phormidium incrustatum*, Fleinsbrunnen, Germany; 2 *P. incrustatum*, Menai, UK; 3 *Schizothrix sp.*, West Malling, UK; 4 *S. pulvinata*, Maolan, China; 5 *Rivularia haematites*, Malham, UK; 6 *Gongrosira incrustans*, Cuatro Cienegas, Mexico; 7 *Oocardium stratum*, Lahage, Belgium; 8 *Vaucheria sp.* , Wateringbury, UK; 9 *Phormidium incrustatum*, Gordale, UK; 10 *Vaucheria* sp., Matlock, UK 1–8 modern, 9,10 mid-late Holocene. d) *bryophyte:* 1 *Gymnostomum subrigidulum*, Jiuzhaigou, China; 2 *Fissidens grandifrons*, Jiuzhaigou, China; 3 *Palustriella commutata*, Gordale, UK; 4 *P. commutata*, Matlock, UK; 5 *P. commutata*, Gordale, UK; 6 Menai, UK; 7 Penmon, UK; 8 *Palustriella commutata*, Wateringbury, UK 1–4 modern, 5–8 mid-late Holocene. All calcite except the Mammoth aragonites. Note that the spars include a range of composite forms consisting of crystallites invisible under the polarising microscope

Crystal-size compositions reveal interesting features of the travertine fabric. In general, it appears that 'calcareous sinters' contain less micrite than travertines associated with microbes or plants. Among algal travertines, there is great variation, but a suggestion that some species, such as *Oocardium stratum* and *Rivularia haematites* exercise control over crystal size. While bryophytes also tend to be associated with micrite, there is variation, and no evidence that particular species of bryophyte influence crystal size. The results suggest that environmental rather than biological factors play a role in determining the microfabric. There is also evidence to show that overall, older travertines contain less micrite than modern travertines. These observations imply that the interpretation of older travertines on their crystal size alone will reveal little of their origin, but it appears that travertines containing an abundance of micrite are more likely to have been associated with biological activity. Any conclusions are of course tentative considering the small sample size and the fact that none of the travertines consisted of 'pure' biofabrics. For example, bryophytes are nearly always colonized by algae, and bacteria are ubiquitous. However, similar observations to these have been reported by other authors. The topic of crystal size will be considered further under diagenesis and some specific algal fabrics will be found in Sections 9.1–2 (Photoplates 14 and 15).

In speleothems, many fabrics have been described, reflecting the diversity of their origins (Hill and Forti 1997). Frisia et al. (2000), working on Alpine and Irish caves, describe five basic types for travertine speleothems: columnar, fibrous, microcrystalline, dendritic and calcareous tufa. The two former were the most frequently encountered and the differences were attributed to the degree of wetting and mineral supersaturation.

3.1.1 Calcite Fabrics: Micrite and Sparite

Thin sections often reveal micrite as dark, almost opaque regions with indeterminate boundaries (Photoplate 4A). However, micrite usually occurs in well-defined areas, as 'clumps', 'strings' or in layers alternating with other textures. Irregular clumps of micrite are common. More regular, subspherical structures ranging from 5 μm to 1 mm in diameter termed *peloids* are a frequent constituent, and usually thought to be associated with microorganisms (Pedley 1994; Riding 2000) although in marine settings they would often be identified with faecal pellets. The clumps occur in a wide range of travertines and are probably largely microbial in origin, although faecal material may contribute in the marl-like and paludal deposits occurring in low-flow regimes. Aggregates of peloids often form a characteristic 'clotted' structure (Photoplate 4B,C) and have been reported from a wide range of travertine types especially those associated with colonies of bacteria and cyanobacteria (Das and Mohanti 1997). Peloidal layers occur in the Pleistocene Cannstatt travertines of Germany with a presumed biological origin (Koban and Schweigert 1993). Clotted mesofabrics are termed *thrombolites* and they have occasionally been reported from lake travertines (Riding 2000; Pache et al. 2001). Micrite laminations are often evident in algal travertines, where the millimetre-scale layers are due to a variation in density or colour, and often related to the seasonal growth of algae.

Micrite is deposited around, and probably within bacterial colonies, around algae such as *Vaucheria* (Irion and Müller 1968) and especially cyanobacteria (Monty 1976; Freytet and Plet 1996; Janssen et al. 1999). Transverse thin sections across deposits containing cyanobacteria often reveal localised clumps of micrite closely resembling peloids. Some clastic travertines, such as 'spring chalks' and dam fills are sometimes composed almost entirely of micrite where an admixture of fine authigenic precipitate combined with mechanically disintegrated clastics is to be expected.

Sparite is distinguishable in thin sections by its transparent, frequently interlocking crystals. Spanning a range of 5 μm to many cm, the crystals form numerous textures ranging from simple and equant merging into more complex dendritic structures. 'Equant' spar may be euhedral or anhedral, with a length-to-breadth ratio (LTB) ranging from 1 to about 2. Mosaics of equant spar are a common feature of travertine thin sections, and frequently occur in a range of sizes in a single sample. The mosaics range from equidimensional to polydimensional but the latter is the norm. Spar is often found in irregular or rounded patches representing secondary infills of pore spaces, and in coarse to fine laminations. The c-axes of spar mosaics often appear to be randomly oriented under the crossed polars of a petrological microscope, but may be radially disposed when present in colonies of algae such as *Rivularia* or approximately normal to the deposit surface in the case of spar palisades. In *Rivularia*, the sparite is primary, but in many other cases it is secondary and the result of diagenetic processes (Freytet and Verrecchia 1999). Some spars consist of tight mosaics with few intercrystalline spaces and plane crystal boundaries indicative of competitive growth (Bathurst 1976) while others, often associated with algae in modern travertines, have a more open texture with large intercrystalline spaces. Equant spar is often the most common textural component of epigean travertine, but there is always the possibility that crystals have been sectioned perpendicular to a long axis. This will not be apparent unless two mutually perpendicular sections are examined from the same sample or scanning electron microscopy is used. Most spar, when examined carefully, has been shown to be composed of smaller crystals or crystallites (Kendall and Broughton 1978; Frisia et al. 2000). These smaller structures are often referred to as 'subcrystals' in the literature but the former term is to be preferred. Good examples of crystallites have been found in the cemented rudites of the Dluga Valley, Poland (Gradzinski et al. 2001).

Crystals with an LTB of 2–6 and their c-axes parallel to the longest side have been referred to as *columnar* and are well known in speleothems, where they probably represent the most frequently encountered fabric (Kendall and Broughton 1978). Columnar spar exhibits uniform extinction under the polarizing microscope with their c-axes approximately perpendicular to the surface upon which they develop. In speleothems, this spar is often composed of crystallites 50–100 μm in width terminating in flat apices (Frisia et al. 2000). They are also common in epigean travertines where they may be primary or the result of diagenesis (Chafetz et al. 1994). A related form referred to as 'bladed spar' is more pointed, tooth-like with the crystals weakly radiating in vertical section (Chafetz et al. 1994, Fig. 3e) but the forms intergrade with columnar calcite. Bladed spar has been used for at least two different fabrics, as radial aggregates or as approximately parallel bundles. When present as parallel arrays, they can be described as palisades (Photoplate 4D) but as the radius of curvature decreases, palisades merge imperceptibly into radial spar. Radial spar occurs in at least two well-defined forms in travertine. It is a common constituent of algal colonies such as those of *Rivularia*, and it is also found as cement on the surface of microbial filaments, tubes or bubbles or of plant surfaces, especially bryophyte stems (Photoplate 4E). The edges of the crystals are frequently ragged and they may contain a fine colloform banding of colloidal organic matter. Intergranular spaces are common in modern algal bladed spar but less evident in other forms, including cement. Crystal boundaries are frequently irregular and the blades range from equidimensional to polydimensional. Layers of radial spar may form spheres, hemispheres or cylinders depending upon the nature of the supporting surface. Palisades usually form layers of cement on approximately planar surfaces so that the crystal c-axes are parallel. Where layers retain a constant thickness they are termed *isopachous cements*. When they are laterally continuous, as around cavities or other fabrics, they are often referred to as *fringe ce-*

ments (e.g. Pedley 1987; Garcia del Cura et al. 2000). Drusy crystals are often found in these cements where they line cavities (Photoplate 5A). Equidimensional spar is often revealed when spar palisades are cross-cut as noted above. Cements are space-filling crystals which have grown attached to a free surface. As defined, the great bulk of travertine calcite could be considered cement.

Fibrous crystals have an LTB >6 and include spars and some forms of micrite, dependent upon their overall dimensions. Most fibrous calcite is 'length fast', with c-axes parallel to the long axis of the crystal. Less common forms, known mainly from speleothem are 'length slow' (Folk and Assereto 1976). Length-fast fibrous calcite has been classified into 'columnar calcite' where crystal width exceeds 10 μm, and 'acicular calcite' with width <10 μm (Tucker and Wright 1990). As with bladed calcite, radial forms and palisades are often dependent upon the radius of curvature of the supporting surface. Radial calcites (both columnar and acicular) occur in unattached spherical forms of travertine known as oncoids and ooids. They are also widely distributed in other travertines, where they form well-defined layers resembling isopachous cements. They also occur in algal colonies (columnar calcite). In the large crystals of radial fibrous sparite, under crossed polars, extinction progresses smoothly across the crystal face and the crystals are clearly composites of smaller crystallites invisible under the light microscope, and often show colloform banding (Photoplate 5B). Janssen et al. (1999) comment upon the likely primary nature of fan laminae of this type associated with cyanobacteria, but it is also found in invasive meteogene travertines where algal activity is minimal. An unusual variant, *radaxial calcite*, with wavy extinction known from some marine limestones, does not appear to have been recorded in modern travertines. Fibrous calcite, also known as 'elongate columnar calcite' has been described from cave flowstones by Frisia et al. (2000). Here, crystals developing from thin layers of microspar, showed evidence of competitive growth, and crystal-splitting (see Kendall 1993). Frisia et al. also describe a 'microcrystalline' fabric from strongly laminated speleothems consisting of crystallites < 4μm wide and 5–50 μm in length. The resulting polycrystalline spar possesses extinction domains with serrated edges.

Due to the difficulties in distinguishing between equant and columnar spar in thin section (see Kendall 1993 for an example), little is to be gained by classifying quantitatively, the various forms. However, to provide some idea of the overall range of size, and length-to breadth ratios of spar, some data are presented in histogram form from thin sections of two representative types of epigean travertine (Fig. 3). A modern and old sample each of a thermogene Italian travertine and a meteogene moss travertine are shown, and in all the spar ranged mostly from 5–50 μm, with the mode usually between 5–25 μm. In Fig. 3 there is no convincing evidence of an increase in crystal size from young to old travertine, and large spar averaging >100 μm diameter is uncommon. In all four samples, the bulk of the spar would be described as equant since the length-to-breadth ratios have their modes in the range 1–2. Ratios exceeding 5 are scarce. Again there are no obvious differences between the modern and old samples. Little can be concluded from such a small data set, but it is at least apparent that young and old travertines need not necessarily differ greatly in their fabric, and there appears to be a preponderance of 'equant spar', at least when samples are viewed as vertical thin sections.

Cave calcite or 'speleothem', being free from photosynthetic plants, excepting cave thresholds, and usually containing few heterotrophic microbes is, to a good approximation, an abiotic 'calcareous sinter'. These travertines, while sharing a common origin with their epigean relatives, are virtually free of mouldic porosity and contain little, if any micrite. There have been several detailed studies of speleothem fabrics, mainly devoted to stalagmites and stalactites. Columnar calcite is the most common constituent of speleothem, consisting of large

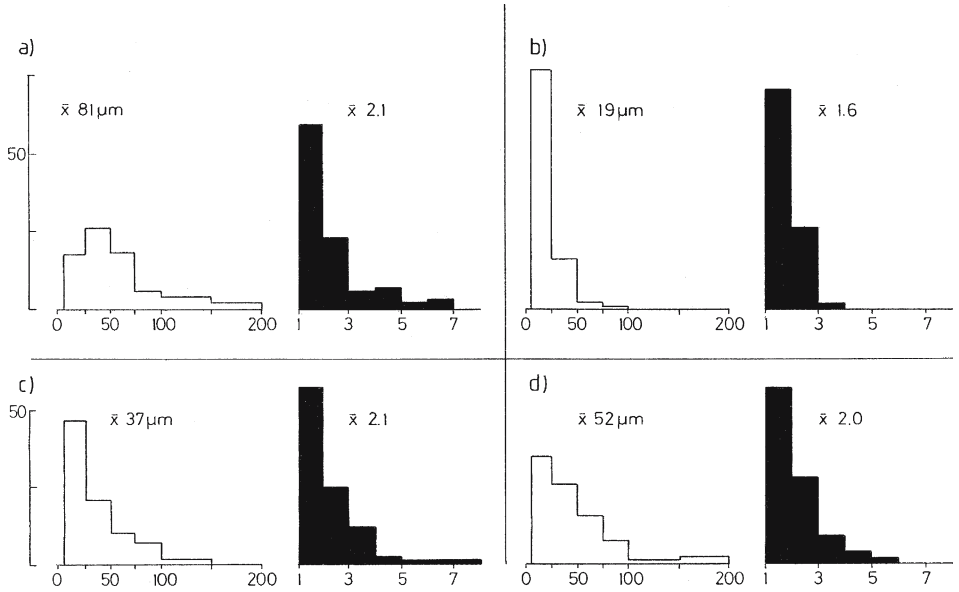

Fig. 3. Frequency histograms of calcite crystal size (mean diameter in µm, unfilled) and length-to-breadth ratio (LTB, filled) taken from four vertical thin sections. Crystals below 5 µm diameter (micrite) excluded from all measurements. Based on 100 observations from each sample. a) Bagni di Tivoli modern travertine (thermogene); b) Bagni di Tivoli Pleistocene travertine; c) Matlock Bath *Palustriella* travertine, modern (superambient); d) Matlock Bath *Palustriella* travertine, postglacial

length-fast crystals with LTB <6 and orientated perpendicular to the deposit surface. The crystals are typically 0.5–5 cm in length but may be much larger, occasionally forming a large part of a single speleothem (White 1976). Columnar calcite usually has irregular crystal boundaries and uniform extinction although the crystals can be shown to be made up of smaller crystallites 4–100 µm wide and >100 µm long (Kendall and Broughton 1978; Frisia et al. 2000). These crystals sometimes show lateral overgrowths and evidence of crystal splitting. Narrower crystals, referable to fibrous calcites with LTB>>6 are less common but may be found as layers between columnar calcite. They sometimes show evidence of competitive growth where they are indicative of a primary origin. With an absence of vegetation and large gas bubbles, most speleothem has a more regular, evenly laminated structure, although a number of 'erratic forms' occur such as shields, helictites and concretions (Hill and Forti 1997). Most interest has centered upon stalagmite bosses as they have been found useful for palaeoisotope studies (Section 13.1). The different types of fabric appear to develop largely as a response to the rate of water flow (Gonzalez et al. 1992; Kendall 1993). White (1976) observed that in caves, speleothem near thresholds was more fine-grained than that within deeper, previously sealed sections. This is thought to be due to the more rapid growth and greater contamination of threshold speleothem with foreign particles.

3.1.2 Calcite Fabrics: Dendritic and Similar Forms

At high precipitation rates and usually at higher temperatures, more complex forms of calcite appear as dendritic (single, tree-like) crystals. These crystals are commonly encountered in frozen metals, but the flattened 'two-dimensional' ice snowflakes provide the most

familiar examples. Dendrites are uncommon in the ionic crystals of calcium carbonate, and best known from the thermogene travertines. Crystal morphologies resembling true dendrites were first described as 'cedar-tree crystals' from Japanese travertines (Kitano 1963) but they were not investigated in detail until the 1980s. Intensive field and petrographic studies of the Central Italian travertines by Chafetz and Folk (1984), and Folk et al. (1985), revealed them as widespread in Italy, where they were referred to under a number of terms including 'ray crystals'. Two forms were described, 'thicker radial crusts' where the individual layers, and crystals, measured mostly 2–8 cm, but occasionally much larger, and 'fine ray crystal fans' where the layers were only a millimetre or so in thickness. The fine crystal fans consisted largely of radial calcite showing sweeping extinction under crossed polarizers. Under the SEM, however, the fans were seen to be composed of strings of diamond-shaped plates about 3 μm long and 1 μm wide showing a high intercrystalline porosity (Folk et al. 1985). These complex, composite structures often resemble feathers in vertical section (Photoplate 5C). The 'thicker radial crusts' were also composed of radial fibrous calcite in the form of fans, with axial divergences of 10–30°. Fans are common in the Italian thermogene travertines. The calcite strings were not seen and the rays consisted of larger plate-like crystals 20–40 μm in length. In Fig. 2g of Folk et al. (1985) the crystals appear to be composed of crystallites 5–10 μm in length.

A study of the thermogene travertines at Terme San Giovanni, Rapolano Terme, Italy by Guo and Riding (1992) revealed 'feather crystals' 1–10 cm high which they equated with the 'ray crystals' of Folk et al. (1985). The crystals formed well-defined layers separated by laminae of aragonite. The crystals were built either of rhombohedral units about 20 μm in length, or by 'chevron-shaped' crystals of similar size. Similar fabrics, termed 'cone-in-cone' structures have been described from some inactive German travertines (Koban and Schweigert 1993).

The hot springs of the East African Rift Valley often produce travertines and dendritic structures were reported from the shores of Lake Bogoria by Casanova (1994). A later investigation by Jones and Renaut (1995) revealed two types of dendritic calcite forming at water issuing >90 °C. Feather dendrites grew irregularly in quiescent pools and scandulitic dendrites occurred as more compact and regular layers on the sloping minidams. Both dendritic forms were distinguished as 'non crystallographic' as their branches did not follow the predicted crystallographic patterns for calcite. They are presumably composed of crystallites with large variations in orientation. The 'feather dendrites' grow up to 4 cm in length and exhibit curved branching through splitting of the crystals. Splitting may result in two or many separate branches at one location, giving rise to a complex morphology. The branches develop around a stem 0.2–0.3 mm in diameter exhibiting uniform extinction under crossed polarizers. 'Crossbars' occasionally join the branches together. The scandulitic dendrites consist of 'en echelon' calcite plates building into a complex, branched structure, usually with a distinguishable stem about 0.1 mm wide as seen in vertical section. The plates are approximately rectangular and about 0.35 x 0.4 mm in size. The dendrites are well characterized in transverse section where the crystals appear rectangular and faintly zoned. The crystals are unusual in growing from the outside inwards, a process known as skeletal growth (Jones and Renaut 1996). The units are stacked in a fairly regular pattern, but sometimes show feathering at the edges. There is a resemblance between this structure and a form of needle-fibre calcite termed 'lublinite', also composed of 'en echelon' plates and often associated with evaporating environments (Verrecchia and Verrecchia 1994). Feather crystals closely resembling scandulitic dendrites also occur associated with needle-fibre calcite at Pamukkale, Turkey (Pentecost et al. 1997) and at Bagno Vignoni, Italy (Photoplate 5D).

Questions remain concerning the relationships between these forms. The ray crystals of Folk et al. (1985, Fig. 2g) bear a close resemblance to some of the Bogorian scandulitic dendrites such as those illustrated by Jones and Renaut (1995, Fig. 11b). The main difference appears to be crystal size, an order of magnitude longer in the Kenyan examples. Other figures in Folk et al. (1985), e.g. Fig. 5a, show a resemblance to the feather crystals of Jones and Renaut, but differ in detail. It may be that diagenesis has obscured some of the details and they have the same origin. The crystals of Guo and Riding (1992) have crystallographic branches according to Jones and Renaut (1994) and are described by them as crystallographic dendrites. Crystallographic dendrites are known associated with a range of microorganisms from diverse calcifying environments, including thin travertine crusts and cave deposits (Friedmann 1979; Jones and Kahle 1986; Frisia et al. 2000) and the crystals tend to be more delicate. An example is shown in Photoplate 5E. The three-dimensional structures of the various forms would help solve the issue, but would be difficult to accomplish, even with serial sections. One of the noteworthy features of the Bogoria travertines is the low level of Ca in the water, amounting to just a few ppm. Jones and Renaut (1995) discuss hypotheses leading to dendritic growth and note that in experimentally-produced dendrites, a large excess of CO_3 over Ca produces a range of dendritic structures.

Dendritic calcite also occurs in speleothems. Frisia et al. (2000) describe dendritic fabrics composed of branching polycrystals >100 μm in length and about 10 μm wide consisting of small crystallites <0.1 μm to >1 μm in diameter. Several of the above forms have also been classified as 'shrubs' (see below).

3.1.3 Calcite Fabrics: Shrubs and Bushes

The term 'shrub' was used by Kitano (1963) to describe structures in some Japanese travertines and subsequently by Chafetz and Folk (1984) in their extensive and important studies of the central Italian deposits. The latter were the first to recognise the significance of these structures in the Italian travertines and to demonstrate their close association with colonies of bacteria. Chafetz and Guidry (1999) went on to distinguigh three kinds of shrub: bacterial, crystal and ray crystal. The former were considered to be bacterially mediated while the latter were thought to be formed by a combination of bacterial and abiotic processes, being types of crystallographic and non-crystallographic dendrites as noted above. Shrubs are easily recognised in polished hand specimens (Photoplate 6A). Most typically they occur as well-defined layers of opaque, white calcite showing a characteristic pattern of branching with rounded, knobbly terminations. The layers are usually 1–6 cm in thickness and may extend laterally for many metres. Superficially they resemble dendritic calcite, but examination in thin section reveals complex structures built of two components. In modern bacterial shrubs, the building unit consists of micrite clumps about 10 μm across associated with abundant bacteria (Photoplate 6B). These clumps are interspersed with rhombic spar 10–20 μm in length (Guo and Riding 1994) to form aggregates about 100 μm in diameter. The aggregates are stacked or linked together to form complex, upwards-branching shrubs (Fig. 4). Shrubs vary in the proportion of 'bacterial micrite' and spar and those with the latter predominating begin to resemble the scandulitic dendrites previously described (Guo and Riding 1994, Fig. 7c). Indeed, Chafetz and Guidry (1999) recognised a continuum of form between 'bacterial' and 'ray crystal' shrubs and provide micrographs of these intergradations. The spar component may be abiotic, but at Terme San Giovanni, Rapolano, it has been found associated with the diatom *Achnanthes*. Chafetz and Folk (1984) based their original observations of shrubs on the Italian Pleistocene travertines, and here,

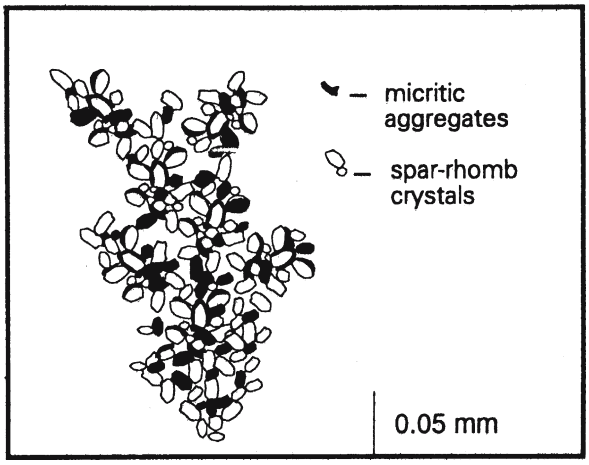

Fig. 4.
Schematic diagram of a modern shrub showing co-occurrence of micrite aggregates and spar rhombs. The aggregates are associated with bacteria. From Guo and Riding (1994) with permission

the shrubs were found to consist of aggregates of a different structure. These consisted of an equant spar core 10–60 μm in diameter containing abundant bacterial inclusions, surrounded by a clear spar coating. Again, the units constructed complex branched structures with the intervening spaces filled with spar cement. There is no doubt that bacteria have a role to play in the formation of these shrubs, and their preponderance in the sulphide-rich springs of Central Italy is probably significant, since bacteria often predominate in this environment today. Bacterial calcite shrubs are a widespread and sometimes a major component of thermogene travertine fabric, but they are far from ubiquitous. For example they are almost absent from the large deposits of thermogene travertine of the Gerecse Mountains, Hungary. They may be associated with particular water chemistries, perhaps those containing high dissolved sulphide, but this needs further investigation. Shrubs appear to form preferentially in quiescent shallow pools on travertine slopes and they are also known from coated grains. Again however, clear distinctions between shrubs and feather crystals are not always evident. The travertines of San Marco Mesa at Cuatro Cienegas consist of fibrous calcite feather crystals, yet they are infested with numerous bacteria-like inclusions similar those reported in the Italian thermogene shrubs (Photoplate 6C). Iron and manganese-rich shrubs have also been described from some travertines (Chafetz et al. 1998). The diagenesis of shrubs is considered later.

There are many reports in the literature of 'algal bushes' where there is also clear evidence of organisms strongly influencing the fabric (e.g. Monty 1976; Schäfer and Stapf 1978;Ordoñez and Garcia del Cura 1983; Love and Chafetz 1988; Freytet and Plet 1996). Bushes normally consist of radiating structures, anything from <1 mm to several cm in height. They are not as evident as shrubs in hand specimens but clearly revealed in thin sections. They usually radiate from a single point and consist of sparite, micrite or both, but at least when first formed, they rarely consist of single crystals, but rather a radiating mass, with the radiating algal filaments directing the control of crystal growth. Algal bushes are most frequently associated with cool meteogene travertines. Well-known examples of algae forming bushes are the prokaryotes *Dichothrix, Rivularia, Schizothrix* and *Phormidium* and the eukaryotes *Gongrosira* and *Oocardium* (Section 9.2.1). Several species also form vertical arrays of filaments on the travertine surface leading to the development of less bush-like swards. The *Dichothrix*-like structures of the Pleistocene Cannstatt travertines of Germany (Koban and Schweigert 1993) may be of this type.

3.1.4 Aragonite Fabrics

Aragonite fabrics have been described from several epigean thermogene travertines. Unlike calcite, orthorhombic aragonite is not known to grow into large crystals in travertine and is almost invariably found as fine, needle-shaped crystals often a few tens of microns long. Aragonite was first identified in the deposits at Carlsbad but most of our knowledge comes from elsewhere. Aragonite needles may occur in massive random aggregates, but more regular arrays as spherulites and sheaves may be more common, especially in recently deposited travertine. For example, at Mammoth Hot Springs, the modern travertines are composed of a mixture of 'sprays', sheaves ('fuzzy dumbells' of Folk et al. 1985) and spherulites with the former building into more complex shrub-like structures (Pentecost 1990b; Fouke et al. 2000). Individual crystals at Mammoth are acicular and range from 0.1–1 μm wide and 10–200 μm in length. They are aggregated into radiating sprays consisting of 100 or more needles. Aragonite sheaves probably form in the water of travertine-dammed pools, with some growing at the water surface (Fouke et al. 2000). Frequently the sprays develop into larger more complex and branched structures up to 2 cm length, which were originally described as shrubs by Pentecost as they superficially resemble the Italian shrubs of Chafetz and Folk (Photoplate 6D). They also develop in the same environmental setting, namely quiescent pools containing sulphide-rich water. Riding (1991) preferred to call these structures 'needle dendrites' to distinguish them from the biotic Italian shrubs. A better term might be 'needle crystal shrubs' as used by Guo and Riding (1994). Chafetz and Guidry (1999) refer to the aragonite shrubs at Mammoth Hot Springs as 'bacterial shrubs', although the bacterial component is not always obvious (Section 10.7.2). Casanova (1986) describes similar shrubs from some African travertines. Dendritic aragonite has also been noted from caves (White 1976; Hill and Forti 1997). Guo and Riding (1992) describe aragonite layers in the modern Italian Rapolano Terme travertines. Here, the needle aggregates also formed sheaves, rosettes, spherulites and 'crosses'. In many cases, the spherulites appeared to nucleate on foreign structures such as bacteria or pollen. Occasionally, the Mammoth spherulites were also observed to nucleate in this way (Pentecost 1990b) and in the Dead Sea lacustrine stromatolites, aragonite needles are associated with algae (Buchbinder 1981). Spherulites and sheaves of aragonite are known mostly from studies of artificial precipitates (Lippmann 1973). Jones and Renaut (1995) consider them to form under conditions of high disequilibrium. Aragonite needles have also been described from some thermogene travertines bordering the Dead Sea (Khoury et al. 1984) and the meteogene travertines of Orissa State, India (Das and Mohanti 1997). Other microfabrics identified at Mammoth include centimetre-sized botryoids close to the vents and composed of masses of aragonite needles. Aragonites also forms radiating anthodites, helictites and satin-like laminations in speleothem. Aragonite-encrusted bubbles have been found in a Sardinian cave (Hill and Forti 1997) with the c-axes perpendicular to the bubble surface, and the outer bubble walls found at Mammoth Hot Springs are also coated with small (<15 μm) aragonite crystals (Fouke et al. 2000). At Durango, Colorado, thermogene travertines include encrusted bubbles formed by photosynthesising algae consisting of an inner layer of aragonite and outer layer of calcite (Chafetz et al. 1991a). Several thermophilic bacteria, including *Chloro-flexus* and members of the Aquificiales produce striking thread-like forms where the flowing water aligns the growths into parallel bundles encrusted with aragonite. Some are superficially reminiscent of the feather crystals of Jones and Renaut (1995). Vaterite, another polymorph of calcium carbonate also occurs in travertine but the fabrics have not so far been described. It is unstable and rapidly reverts to calcite.

3.2 Mesofabrics

Features visible in polished hand specimens of travertine are considered here with a number of smaller mobile forms known as coated grains. Microfabric blends into the mesofabric so no hard and fast rules apply, but the porosity and lamination of travertine are best considered here.

3.2.1 Porosity

Voids are a characteristic feature of almost all travertines, and part of the fabric (Heimann and Sass 1989). Choquette and Pray (1970) classified limestone porosity into fabric selective and non-fabric selected. The porosity of most travertines is fabric selective and can be divided into four sub-types: intercrystalline; mouldic; fenestral, and shelter porosity (Fig. 5). While some of these may be classified as microfabric, the mesofabrics are more characteristic for most travertines. Non-fabric selective porosity occurs through fracturing and includes cavernous porosity formed through dissolution. Porosity also results from the activities of burrowing invertebrates such as *Lithotanytarsus* and *Tinodes*. Intercrystalline porosity is common to all travertines but varies according to the density and form of the crystals. Some of the most porous travertines are the freshly precipitated aragonites of Mammoth Hot Springs which may have a pore space volume of 80%. Porosities become as low as 2% in travertines where the majority of voids have been filled by secondary calcite (Török 2003). These travertines no doubt contain a reduced intercrystalline porosity, but mouldic porosity tends to be largely maintained, at least in Quaternary deposits. Intergranular porosity is important in clastic travertines where the clasts range from a few micrometres to many centimetres in diameter. Mouldic porosity is commonly observed and often associated with plant fragments. Leaves, for example, often fall into travertine-depositing streams where they become encrusted with a thin layer of carbonate. Beneath the leaf, a sizeable cavity can form, due to irregularity in the leaf surface, ('shelter porosity') whilst travertine accumulates above. Eventually, the leaf decays forming both a cavity and a void once occupied by the leaf tissue. Thus it is possible to distinguish a primary shelter porosity followed by secondary mouldic porosity developing as the tissues decay. Likewise, buried twigs, branches and roots of trees produce mouldic porosity. Bryophytes, particularly *Palustriella* (*Cratoneuron*) *commutata* produce travertines with high framework porosity (Photoplate 7A). The open framework of the moss cushions provides a scaffold off hollow calcite tubes formed by the internal decay of moss stems. These travertines are often remarkably porous and light, yet strong as a consequence of the intricate scaffolding forming around the moss stems and were previously sought as building material. The macroscopic cavities developing in thermogene travertines are usually caused by the inclusion of gas and are often associated with algal mats, providing

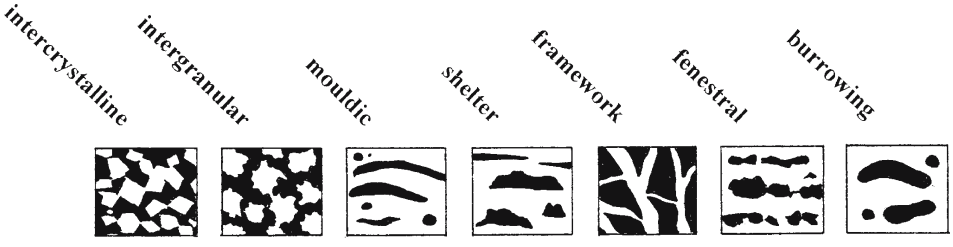

Fig. 5. The main types of fabric-controlled porosity in travertine (void space shown in black; modified and redrawn from Choquette and Pray 1970)

fenestral porosity. The sideways growth of aragonite sinter ridges to form a fenestral framework is described by Farmer and Des Marais (1994a). 'Foam rock' provides an extreme example through the accumulation of encrusted gas bubbles resulting from gas evasion and photosynthesis (Photoplate 7B). At a microscopic level, voids left by decayed bacteria, algae and leaky fluid inclusions also occasionally contribute significantly to the porosity.

There are few data relating to porosity measurements in travertine, and most of these are estimates based on the 'water absorption capacity' (WAC). This is obtained by drying a small sample, removing air with a pump, flooding the sample with water, releasing the vacuum then blotting and reweighing. The weight difference obtained provides a measure of the air volume displaced providing penetration is complete, and the void spaces are not too large to drain the water. In tight rocks, where there is a lack of hydraulic connectivity, the WAC invariably underestimates the true porosity. Data on porosity as WAC, reported as % void volume, are available for meteogene and thermogene travertines (Dublanski et al. 1983; Ferreri and Stanzione 1978; Irion and Müller 1968; Pentecost 1989, 1990b; Pentecost et al. 2000a and unpublished). It is impractical to measure the contributions of the various types of porosity independently, so they represent combined figures. A wide range in the porosity is apparent for both meteogene and thermogene travertines. The meteogene mode of 52.5% make them among the most porous limestones known, rivalling coquinas. Few epigean Quaternary travertines have porosities above 70% or below 10%. The available data so far indicate no significant difference between the porosities of algal and bryophyte travertines, but in the latter, framework porosity is often more significant and pore space volumes can exceed 80%. Cyanobacterial travertines inhabited by burrowing chironomids have porosities up to 60% and the bulk appears to be intercrystalline which presumably makes burrowing easier. The denser travertines probably contain a reduced intercrystalline porosity. Porosities of allochthonous (clastic) travertines include a variable intergranular component and are often in the range 40–50% in meteogene deposits. Thermogene travertines possess widely varying porosities (mean 25.6%, range 4–78%) reflecting in part the degree of secondary precipitation and diagenesis, and the available data, albeit limited, indicate that thermogenes, at least those composed of calcite, tend to possess lower porosities than meteogenes. The lowest porosities are frequently associated with well-cemented deposits and include abiotic forms such as speleothem. For the latter it has been generally assumed that the porosity is negligible, but measurements obtained by Baker et al. (1998) show that it may be as high as 14.9%. It is clear from the data that porosity measured as relative void volume cannot be used to reliably distinguish travertine types.

Size distributions of the macroscopic cavities >2.5 mm diameter (fenestral/mouldic porosity) in a meteogene and thermogene sample have been found to be surprisingly similar despite their different origins (Fig. 6, unpublished data). Voids were formed in one case by bryophytes and in the other, gas accumulation, and in both, cavities exceeding 30 mm diameter were uncommon and most numerous in the range 2.5–5 mm. However, the form of the cavities is distinctive. Those formed in the thermogene travertine by gas entrapment possess a large length to breadth ratio (often >5) with the long axis parallel to the bedding. In meteogene deposits, the form of the cavities is approximately isodiametric, and in cascade forms show little relationship to bedding. These differences might allow ancient travertines to be more clearly distinguished although a few meteogene lake travertines in Africa also show some evidence of gas entrapment (Casanova 1994). Since meteogene travertines tend to possess higher porosities than thermogenes, despite their similar fenestral frameworks, it seems likely that meteogenes contain a higher intercrystalline porosity. It is the occurrence of voids in the low cm size range which give most travertines their distinctive appearance when viewed in the field.

3.2.2 Bedding and Jointing

Well-defined bedding planes have been described from the smooth travertine quarry faces of Lazio, Italy by Chafetz and Folk (1984 p. 298). Bedding frequently pinches out and represents mound slope accumulations with an irregular change in the deposition rate downflow. Erosional surfaces also occur in these travertines and may contribute towards the bedding. In many accumulations, the travertine may consist of numerous fine partings corresponding to weak layers in the lamination, particularly on weathered surfaces. Where deposition has resulted in approximately sheet-like layers of travertine, vertical jointing is also common, and often associated with settlement over an incompetent sediment or tectonic activity.

3.2.3 Floe, Nodules and Thinolite

When carbonate precipitates at the air-water interface in still water, floe carbonate, also known as 'raft' or 'hot water ice' is formed, supported by surface tension. As deposition continues the floe thickens and increases in mass, until it sinks to the bottom of the pool (Photoplate 7C).

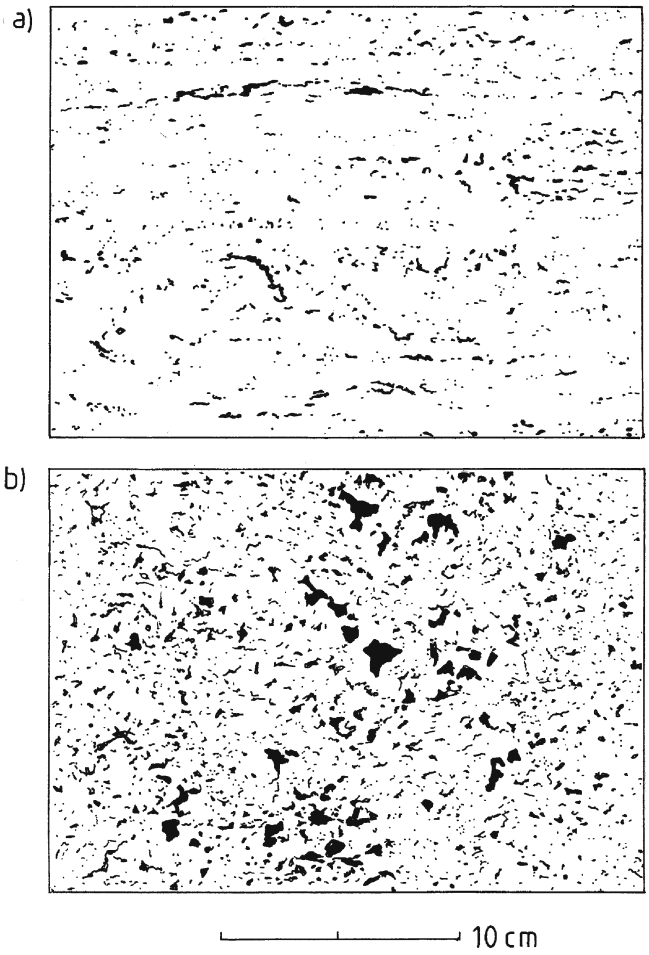

Fig. 6.
Cavity patterns in cut slabs of travertine. a) thermogene travertine from central Italy showing traces of bedding; b) meteogene cascade travertine with bryophyte remnants, West Malling, UK

Floe is frequently found in thermogene deposits (Allen and Day 1935), but also forms in dam pools of meteogene deposits including cave travertines (Fouke et al. 2000; Drysdale et al. 2003a). Floe calcite rafts are typically 1 mm or less in thickness and are composed of small spar crystals growing approximately vertically downwards from the water surface sometimes showing a shrub-like microfabric. Fluids, presumably creeping over the exposed surface as a result of capillarity, then proceed to precipitate more spar in an upwards direction leading to a bipartite structure in some cases which often continues once the floe has sunk. In caves these structures are usually known as rafts and are often of free-floating aragonite or calcite (Hill and Forti 1997). Nodular splash-deposits are a common and widely distributed type of deposit sometimes developing on damp surfaces just above the water line of travertine-depositing springs and in calcareous rock seepages. They consist of small nodules or protuberances just a few mm high, often showing evidence of corrosion and form from evaporation of water splashes. Similar splash deposits are well known from caves (e.g. White 1976; Hill and Forti 1997). Their mechanism of formation is not known in detail. Related deposits consisting of siliceous sinter occur in New Zealand where they are known as spicules or 'coccolithosilici' (Henley 1996).

Dunn (1953) and Bischoff et al. (1993) describe several mesofabrics from the travertine towers of Mono Lake, California based upon crystal arrangement and porosity termed 'dendritic', 'lithoidal' and 'thinolitic'. Lithoidal tufa forms an inner core to the towers and is usually dense; dendritic tufa consists of a series of compact upwardly branching columns, though its relationship with the dendritic calcite described in 3.2.1.2 is unclear, and thinolitic tufa consists of tetragonal pyramids forming a kind of latticed structure. The term 'lithoidal' has also been used widely and imprecisely for a variety of massive, low porosity deposits in Europe. Thinolitic tufa results from the transformation of ikaite and is discussed further in Section 7.3.

3.2.4 Biofabrics

Plants profoundly influence travertine structure and several biofabrics are recognisable, particularly in meteogene deposits. These fabrics also provide the basis of several classification schemes for travertine, most of which emphasize the influence of plants. Prát (1929) classified Czechoslovakian deposits into 'moss' and 'algal' types and Pevalek (1935) distinguished four types: '*Cratoneuron*', '*Bryum*', '*Agrostis-Schizothrix*' and '*Schizothrix*'. A similar scheme was adopted by Irion and Müller (1968) for deposits of the Schwäbische Alb, Germany. Biofabrics can be distinctive, permitting identification of the original plant material, as in the case of *Vaucheria*-tufa (Wallner 1934a; Pentecost 1990a) (Photoplate 7D). In *Vaucheria*, the size and arrangement of the perforations caused by decay of the algal filaments in transverse thin section, combined with the mesofabric are sufficient for identification. With somewhat less certainty, *Schizothrix*-tufa (Schäfer and Stapf 1978) and deposits associated with the bryophytes *Conocephalum, Cratoneuron*, *Eucladium* and *Hymenostylium* are sometimes recognisable. Colonial cyanobacteria produce a range of small radiating structures that are often concentrically laminated and sometimes classified as freshwater stromatolite. They are considered further in 9.1.3. Larger plants also influence fabric, the incorporation of leaves, branches and twigs providing a distinctive mouldic porosity as noted in Section 3.3.1. The fabric of some high-porosity deposits is influenced by tube-dwelling Diptera such as *Lithotanytarsus*, producing a fine honeycomb structure (Thienemann 1950; Symoens et al. 1951). In Australia, Drysdale et al. (2003b) show how the remnants of caddis tubes may be used to predict the direction of water flow in travertine-depositing streams.

3.2.5 Coated Grains: Ooids and Oncoids

Included here are a range of small (<1 mm–30 cm) unattached biotic and abiotic forms of travertine. Coated grains consist of a nucleus upon which a cortex of carbonate is accreted in an approximately even, radial manner. The adjective 'approximate' needs stressing and the terminology and classification of coated grains is currently confusing (Tucker and Wright 1991). Two types of coated grain are found in travertine fabrics, the ooid and oncoid. The cortex of an ooid is smoothly and evenly laminated, particularly in its outer layers. Ooids are spherical or occasionally spheroidal and there are no obvious biotic structures in the cortex. The cortex of an oncoid consists of irregular, frequently overlapping laminae. Oncoids are normally spheroidal and may possess a recognizable biofabric, particularly cyanobacteria (Flugel 1982; Peryt 1983; Hartkopf-Fröder et al. 1989; Tucker and Wright 1990). Further terms have been used to account for biotic structures within oncoids. For example, cyanoid has been proposed for modern oncoids containing calcified cyanobacteria (Riding 1991). Ooids and oncoids are often described from travertines but the above terminology has rarely been adhered to and it is questionable whether the two forms are always distinguished or are indeed distinguishable. With reference to travertine, the depositional environment is the most important factor. Coated grains occur in waters with a wide range of salinity. Oncoids are also known from terrestrial limestones such as calcretes (Wright and Tucker 1991).

3.2.5.1 Ooids

Ooids were first described from travertine by Agricola (1546) in the hot springs of Carlsbad, where they were

> 'as porous as honeycomb… and the size of a pea (where) they are formed from dripping water'.

These ooids are composed of aragonite and are described briefly by Hatch et al. (1938). They also occur near Tekke Ilica, Turkey (Richter and Besenecker 1983) and are widespread in the Denizli area. Here they range from <1 mm to 5 cm in diameter and occur in well-sorted layers, in the bottom of shallow hot spring pools. They consist of strontium-enriched tangentially layered aragonite needles up to 2 μm in length. The narrow concentric laminae were however, frequently disrupted by erosion events (cf. definition above) but closely resembled the well known marine Bahamian ooids in other respects, containing few biotic structures. Flugel (1982) applied the term pisoid for a non-marine ooid, but there is confusion regarding the definition of 'pisoid' and 'pisolith' and the terms are not stressed here. Indeed, the term ooid could be replaced without detriment, by the term micro-oncoid (see below) although spelean concretions termed 'cave pearls' should perhaps remain distinct. Meteogene ooids are described and figured by Love and Chaftez (1990) and travertine oolites of Pleistocene age have been described from a fluvial deposit by McGannon (1975). They consist of irregular or spheroidal calcite grains 1–2 mm in diameter with up to 20 concentric laminae. Some nuclei consist of charophyte fruits suggesting nearby lacustrine conditions. The ooid cortices had a radial fibrous structure. Ooids are also known from several lakes containing more massive accumulations of travertine, such as the Great Salt Lake, Utah (Rothpletz 1892). Travertines deposited from warm springs in Idaho, possess 'bacterial pisoliths' ranging from 0.5–16 mm in diameter (Chafetz and Meredith 1983) and they are abundant in some of the central Italian deposits (Photoplate 7E). The cortices of these ooids contain single and branching bacterial clumps radiating approximately perpendicular to the surface showing a shrub-like form.

Deposits formed around gas bubbles should not perhaps be classified as ooids, as they often lack concentric laminations, although their mode of formation, in some respects, is not very different. They are common in some thermogene travertines, often accumulating in large numbers as 'foam rock' (Photoplate 7B) where precipitation rates are rapid. They have also been reported from cold springs (Schreiber et al. 1981) and caves (Hill and Forti 1997).

3.2.5.2 Oncoids

Concentrically-laminated unattached forms of travertine with an irregularly laminated cortex are usually referred to as oncoids (Riding 1991). Oncoids tend to be larger than ooids, but according to Tucker and Wright (1990) there is no compelling argument for a different term, and they use 'micro-oncoid' for structures <2 mm diameter. Most oncoidal travertines consist of spheroidal accretions of diameter 5–500 mm (Photoplate 8A,B). Oncoids are a common travertine component and are found in streams, rivers and lakes. Many oncoids approximate prolate spheroids (spindle-shaped) but some lake forms are oblate spheroids (disk- or biscuit shaped) and yet others, whilst describable as spheroidal, have widely differing values for all three axes. The sphericity of oncoids is dependent upon several factors. The nuclei of many, particularly those developing in wooded streams, are twig or branch fragments which first give rise to a cylindrical crust, and later a prolate spheroid. Oblate forms can likewise be generated from shale fragments with a high length to thickness ratio, such as those of Canandaigua Lake, New York State. Shape is also influenced by the rate of movement. Most, if not all actively accreting oncoids are mobile to some extent. This is necessary to ensure that deposition occurs over the entire surface and prevent them from becoming cemented into the stream bed. If the rate of movement is low, extreme forms such as 'biscuits' develop.

3.2.5.2.1 *Fluvial Oncoids*

The many descriptions of fluviatile oncoids are made primarily with reference to the colonising algae (Penzig 1915; Roddy 1915; Pia 1933; Fritsch and Pantin 1946; Minckley 1963; Adolphe and Rofes 1973; Schäfer and Stapf 1978; Szulc 1983). Little is known of their development in relation to hydrology. Oncoids occur in streams with a moderate gradient subject to the occasional flooding necessary to overturn them. They are frequently found in the pools separating travertine dams, often being washed down to the next pool, gaining size as they go (Braithwaite 1979). Pentecost (1989) found that individual oncoids with mean diameter 1.2 cm moved between 0 and 30 cm a^{-1} over a gradient of 5% and from 0–23 m a^{-1} over a gradient of 30%. Eventually oncoids cease moving and become incorporated into the substratum. Once wedged into the stream bed they may continue growing laterally and finally become cemented. Graded beds of oncoids sometimes occur but they are often found ungraded and dispersed in a finer travertine matrix to form an oncolitic facies. The nuclei of fluviatile oncoids may be rock fragments, including older oncoids, gastropod shells or wood fragments. Jaag (1938) and Golubic (1973) observed that fragments of stream crust at Stein am Rhine, Switzerland became detached and formed oncoids.

The oncoid cortex is usually seasonally laminated, often consisting of radial fibrous calcite (Ordoñez and Garcia del Cura 1983) with most growth occurring during the warmer months (Adolphe and Rofes 1973; Pentecost 1989). They tend to be intimately associated with filamentous cyanobacteria, but occasionally, photosynthetic microbes are almost entirely lacking, such as those described from an invasive meteogene deposit in Wales by Braithwaite (1979). The laminae characteristically display 'basal rings' since oncoids remain in one place

sufficiently long to develop a crust only on the exposed upper surface. Thus growth occurs as a series of overlapping layers which overall provide a rounded morphology (Golubic 1973; Schäfer and Stapf 1978). Some oncoids and their sections are illustrated in Photoplate 8A and B.

Adolphe and Rofes (1973) plotted the size distribution of oncoids down a 2 km stretch of the Levrière River, France but no obvious patterns occurred. The oncoids ranged from 1–3 cm in diameter and the current speed averaged 0.3 m s^{-1}. The shape of fluviatile oncoids can be highly variable, even within a single sample. This was evident in a small wooded stream at Priory Mill, Oxfordshire, where most specimens had a maximum: minimum diameter ratio ranging from 1.5 to 2, but values exceeding 5 were not uncommon. Over half of the nuclei were twig fragments, accounting for the extreme forms. In this sample of 120, 14% could be described as prolate, 15% oblate and the remaining 71% 'spheroidal' with the three axes differing from each other by less than 10%. Their mean sphericity was about 2. Oncoids taken from an unwooded site near Malham Tarn were significantly smaller and less extreme in their shape (mean sphericity c. 1.4) and the nuclei consisted of grains of limestone or travertine. The mean radial growth rate of the larger oncoids from the woodland site was estimated from annual laminae as 1.6 mm a^{-1} and they had an average age of about eight years. These oncoids could not have moved great distances since they were collected 25 m below the spring. The smaller oncoids from the unwooded site had a mean radial growth rate of 0.14 mm a^{-1} and averaged about 30 years old. They were collected 100 m below the spring. Both samples were colonised by cyanobacteria and the chemical composition and calcite saturation index of the water was similar at both. Clearly there is much to be learned about the genesis of these unusual sediments.

Most oncoids occur in meteogene deposits, probably because the rate of accretion is sufficiently low to allow the regular movement necessary to maintain their shape. Where deposition rates are high, any coated grain would soon coalesce with others to form a crust, as occurs in foam rock. Thermogene oncoids have however been described from the Bolivian Altiplano where they are found in shallow hollows of carbonate sand on a playa lake surface (Risacher and Eugster 1979; Jones and Renaut 1994). The last authors termed the structures 'pisoids', noting that diatoms were associated with their formation. These oncoids ranged in diameter from 1–300 mm, and consisted of layers of radial calcite, micrite and sparite. Some contained shrub-like fabrics.

3.2.5.2.2 *Lacustrine Oncoids*

One of the earliest references to littoral oncoids is that of Buckland (1846) who mentioned 'petrified potatoes' on the shores of Lough Neagh, Northern Ireland. As with fluvial oncoids, interest was initially in the associated algae which grow abundantly on the surface and assist in the entrapment and consolidation of the cortex (Thiselton-Dyer 1891; Clarke 1900; Davis 1900, 1901; Kindle 1927; Raymond 1937; Smith and Mason 1991; Winsborough et al. 1994). These oncoids are found principally at the edges of shallow lakes (Kindle 1923) and usually possess a stone or shell nucleus. Both Shäfer and Stapf (1978) and Jones and Wilkinson (1978) noted that oncoid size increased with water depth. This correlation may reflect lake level fluctuation, with the deeper oncoids receiving more continuous deposition. In water exceeding a few metres in depth, movement is presumably too restricted to allow oncoid development. Wave action on or near the shore must be important and probably explains why oncoids are frequently found only in certain areas. Data on oncoid movement are sparse, but in parts of Lake Constance, a well-studied site, the largest oncoids were found in the vicinity of the

Rhine current, where flow rates up to 1 m s^{-1} were recorded (Schäfer and Stapf 1978). The oblate spheroid (disc) is a common morphology (Schöttle and Müller 1967) and may reflect the form of the nucleus or site hydrology. The remarkable 'water biscuits' described by Mawson (1929) from South Australia appear to have grown in shallow seasonal pools. Presumably, water depth was just sufficient to cover the oncoids, allowing strong horizontal growth. Flooding may have been responsible for flipping them over, exposing the other side. The original site is lost to land development, but 'biscuits' have been reported near Augusta, Western Australia (L. A. Moore, *pers. comm.*). An unusual biscuit morphology has been described by Casanova and Tiercelin (1982) from Lake Magadi, Kenya, where the oncoids possess a raised and thickened margin, thought to be caused by evaporation. All lacustrine oncoids described above possess seasonal laminae and consist largely of radial fibrous calcite. Casanova (1994) believes that turbulence *per se* does not influence oncoid morphology but merely the rate of displacement.

3.2.6 Lamination

Few travertines are devoid of lamination, and often, lamination is the most obvious structural feature of the rock. It is present in a wide range of forms, from irregular layers, evident in the field, but not in thin section, to microscopic lamination only visible under high magnification. Lamination is evidence of periodic change in sedimentation. This can be induced by purely physical factors such as flood events or other weather patterns. Often it is linked, directly, or indirectly to biological activity. Lamination may be present at a range of scales so that a travertine may preserve a detailed record of its past history. Lamination may be plane, undulate or regularly wavy (corrugate). Corrugate lamination is often due to periodic phenomena associated with minidams (Section 4.1.4.1).

Several types of lamination can be distinguished (Fig. 7) namely repetitive, alternate and cyclothemic. In the former, only one type of lamination is present, but with sharp discontinuities between adjacent layers. Alternate lamination occurs where two different fabrics alternate regularly, and this is best observed in speleothems. Cyclothemic lamination occurs where a more complex sequence shows regular repeats. It is also possible to distinguish between banding *within* the same fabric, and banding caused by an alternation of two or more fabrics.

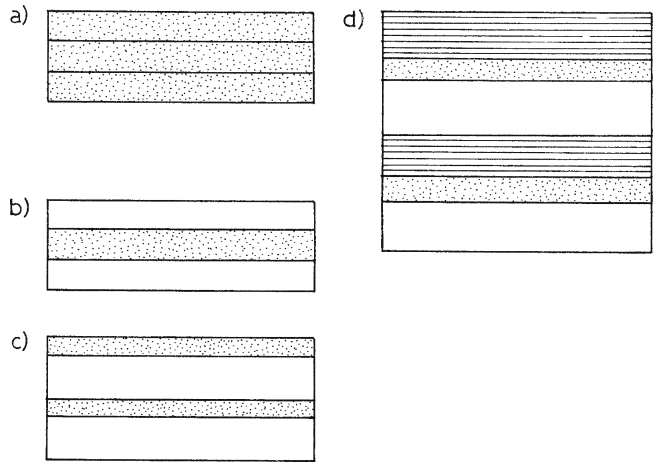

Fig. 7.
Types of lamination. a) repetitive; b) alternate homopachous; c) alternate heteropachous; d) cyclothemic

3.2.6.1 Banding within a Fabric

Examples are known from several travertines but they have been little studied. In the *Phormidium* travertines of North Wales, millimetre-scale banding is evident in polished hand sections, but thin sections reveal structureless micrite. This banding is probably the result of differing amounts of algal biomass. Since the growth rate of this travertine is known to be 1–2 mm a^{-1} the lamination was probably seasonal, with the darker, organic-rich layers corresponding to the summer period. More obvious, and potentially more useful banding is often seen in columnar calcite. The bands have been intensively studied in speleothems (e.g. Tan et al. 1999) and consist of layers of brown pigmentation presumed to represent organic matter trapped within crystals. The lamination is usually on a fine scale and in speleothems, a combination of flourescence microscopy and mass spectroscopy has demonstrated that the banding may be annual and due to inputs of soil-derived organic matter. Similar fine-scale banding occurs in the columnar calcites of some epigean travertines but is probably the result of shorter term processes resulting from their more rapid growth (e.g. Folk et al. 1985). In epigean travertines, the organic matter banding is not necessarily allochthonous. For example, fine scytonemin banding is produced *in situ* by the cyanobacterium *Rivularia* and may persist in the fabric. It is thought to result from short-term (order of days) variation in the level of insolation (Pentecost and Edwards 2003). Chafetz and Folk (1984) figured diel intracrystalline banding in an altered aragonite from the thermogene deposits at Mammoth. It appears to represent an uncommon example of repetitive lamination. Lamination may also be caused within crystals by layers of inclusions, and through the zoning of other elements trapped in the calcite or aragonite lattice.

3.2.6.2 Alternation of Fabrics

This is responsible for the more obvious lamination of travertine hand specimens. In its simplest form it consists of a regular alternation of two fabrics showing as a variation in colour and/or texture. The fabrics often vary in their erodability resulting in differences of relief, accentuating the layering in old travertine sections. Lamination ranges in scale from sub-millimetre to metres reflecting deposition rates and the mode of formation. Coarse, irregular lamination occurs in clastic travertines deposited behind dams during flood episodes where the content of clay and organic matter varies according to the local conditions. Fining-up sequences may occur, or in more arid areas, the lamination may be due to hiatuses, or erosion events during drought. Lamination on a centimetre scale is often seen in cascade travertines colonised by bryophytes. It is probably the result of seasonal growth of these plants, sometimes combined with a change in species-composition as a response to variation in flow.

More interest has been taken in the smaller-scale laminations of 1 cm or less. Most of the lamination is of the alternate type, where bands of dark and light laminae may persist over many centimetres and number in the hundreds (Fabré and Fiche 1986). Thin sections usually reveal differences in the fabric, with the lighter bands often containing a greater density of carbonate than the darker bands. The individual light and dark layers (referred to here as singlets) may be of approximately equal thickness (termed here *homopachous*) or of unequal thickness (*heteropachous*). A light and dark layer combined produces a couplet, which in some cases represents an annual or daily accumulation of travertine. A form of cyclothemic lamination (Fig. 7) occurs in deposits colonised by tube-dwelling Chironomid larvae. The tubes are formed in late spring, followed by a spongy summer algal layer and a more dense

winter layer. The sequence is repeated the following year eventually forming thick buildups of cascade travertine. Another example is reported by Arp et al. (2001) for a stream deposit where an alternation of two *Phormidium* (cyanobacterium) fabrics and a winter layer of diatoms mixed with detritus is described. A range of algal lamination types is illustrated by Freytet and Plet (1991) where some group-specific characters were apparent. Lamination of this type is common in speleothems, and is often revealed by differences in colour and porosity (Genty 1993).

Examples of the small-scale alternate lamination in several types of modern travertine are provided in Table 3 and Photoplate 8 C,D. Detailed studies of travertine lamination are limited and several questions remain. It is usually possible to identify alternate lamination as daily or seasonal, with most thermogene travertines displaying the former. Thermogene deposition rates are usually rapid, permitting greater resolution, and occasionally, a superimposed seasonal lamination is found on a daily lamination. This has been reported from some of the Pleistocene thermogene travertines of central Italy, where annual layers of shrubs alternate with thin layers of lime mud. The shrubs sometimes contain fine laminae 0.1–0.5 mm wide, interpreted as daily accumulations (Chafetz and Folk 1984). In small-scale alternate lamination, the 'dark' bands in transmitted light usually represent the more porous layers of micrite precipitated during summer or daytime (Irion and Müller 1968; Jones and Wilkinson 1978). However this is not always found to be the case. At Bagno Vignoni, Italy, the dark micrite layer represented a night-time accumulation resulting from dust fall which disrupted the precipitation of feather crystals (Pentecost 1994). In some Japanese meteogene stream crusts, the dark and more porous layers were found to be deposited in the winter (Kano and Fuji 2000). In reflected light, the more porous 'summer' laminations of annual couplets usually appear darker than the winter bands with the difference being due to increased pigmentation, probably caused by the higher organic matter content and lower porosity (Photoplate 8D). When describing the banding of travertine, it is important to make reference their appearance in reflected and transmitted light otherwise confusion may result.

In most cases the lamination appears to be heteropachous, with the light laminae often wider than the dark laminae (Ordoñez and Garcia del Cura 1983; Guo and Riding 1992, see also Table 3). This is counterintuitive, since the dark laminae forming under the influence of greater solar radiation should favour travertine deposition through increased CO_2 evasion and photosynthesis. In several cases however, measurements on laminae are insufficient to afford firm conclusions. Care is also required in their interpretation, since there is at least one case where the lamination has been attributed to flood events (Golubic and Fischer 1975). In the soft *Phormidium* travertines common in wooded European karst streams, lamination often appears to be caused by differences in porosity rather than crystal size. Here there is clear evidence that the dark summer layers are significantly wider than the pale winter layers (Pentecost and Viles, unpublished, see also Table 3). Lamination may also be caused by regular changes in algal filament orientation, or alternations of algal species (Freytet and Plet 1991, 1996). Some comparative data from tropical streams would be useful in this respect, where insolation remains roughly constant, but discharge often varies seasonally. In the travertines of the Deinschwanger Bach, Germany, Arp et al. (2001) attributed a seasonal lamination pattern to two growth forms of *P. incrustatum*: α and β. In the former the trichomes are loosely scattered while in the latter they form regular, often dense bundles perpendicular to the deposit surface. The laminations consist of alternations of these forms with *P. incrustatum* α forming a light porous layer in the summer and *P. incrustatum* β a dense layer in spring associated with micrite.

Table 3. Examples of small-scale (0.5–5 mm) travertine lamination viewed in transmitted light

Type	Dark singlet: fabric an interpretation	Light singlet: fabric and interpretation	Associated microbes	Reference
Meteogene				
stream crust	sparse micrite, summer growth	dense micrite, winter growth	*Phormidium*, *Schizothrix*	Monty (1976)
stream crust	-	spar, daytime growth		Folk et al. (1985)
stream crust, cascade	spongy micrite, summer growth	dense micrite, winter growth	*Phormidium incrustatum*	Pentecost and Viles (unpublished)
stream crust, cascade	micrite, winter growth	sparite, summer growth		Chafetz et al. (1991b)
oncoid	microspar, flood events	spar	*Gongrosira*	Golubic and Fischer (1975)
oncoid	micrite, summer growth	sparite, winter growth	*Calothrix*	Pentecost (1989)
oncoid	micrite, 'seasonal'	sparite	*Phormidium*	Freytet and Plet (1991)
Thermogene				
cascade	aragonite needles, photo-synthesis	dendritic calcite, abiotic	fungal spores, bacteria, pollen	Guo and Riding (1992)
cascade	micrite, night-time with dust accumulation	feather calcite, photosynthesis	*Achnanthes*, *Phormidium*, *Spirulina*	Pentecost (1994)

There are numerous references to lamination in older travertines, but in most cases the original fabric has been altered by diagenesis, and interpretation is difficult. Among the Quaternary travertines, lamination is figured, and briefly discussed in meteogenes by Heimann and Sass (1989) and Smith and Mason (1991). Older travertine laminations are described by Weiss (1969), Anadón and Zamarreño (1981), Monty and Mas (1981) and Chaftetz et al. (1991b). Quaternary thermogene lamination is considered briefly by Schreiber et al. (1981), Folk and Chafetz (1983), Richter and Besenecker (1983) and Jones and Renaut (1994). Most of these papers are concerned with coated grains.

3.2.6.3 Stromatolites

Riding (1999) redefined stromatolite as 'a laminated benthic microbial deposit'. Many travertines can be so described and it was Walcott (1914) who first made comparisons between modern cyanobacterium-containing travertine and ancient stromatolite, concluding that the latter contained cyanobacteria. Needless to say, most ancient stromatolites are of marine origin, and the number that can be referred to as travertine is small.

A problem arises when one examines ancient laminated travertines – are they epigean or spelean? If epigean, is the lamination directly related to temporal variations in microbial activity or entirely inorganic? Providing diagenesis has not been too severe, examination of facies may be sufficient to elucidate the sedimentation process and distinguish between epigean and spelean deposits but the interpretation of lamination requires care. Formerly, Semikhatov et al. (1979)

included inorganic forms such as speleothem and sinter crusts as stromatolite, but a microbial association is normally recognised at present. In the case of the laminated travertines, facies where the daily laminae can be attributed to microbial activity could be regarded as stromatolite along with many of the annually laminated *Phormidium* travertines. Freytet et al. (1996), Freytet and Verrecchia (1998) and Das and Mohanti (1997) all consider algal tufas as stromatolitic. The well-defined *Phormidium* and *Rivularia* colonies of some travertines are clearly referable as modern freshwater stromatolites particularly when they occur on lake shores (Casanova 1994). Where oncoids contain calcified cyanobacteria they have been referred to as a cyanoids, a type of skeletal stromatolite (Riding 1991). Riding (2000) also uses the term 'tufa stromatolite' and oncoids as 'unattached spherical stromatolites', classing tufa stromatolite as one of six stromatolite categories. Some calcretes are also recognised as terrestrial stromatolites where there is evidence of microbial activity.

Some interesting but rare forms of stromatolite have been found on thermogene travertines. In shallow quiescent pools of Mammoth Hot Springs, Walter et al. (1976) and Brock (1978) described *Phormidium* conophytons. The structures are formed by the coalescing trichomes of *P. tenue* var. *granuliferum* and consist of ribbed pinnacles a few centimetres high with a regular spacing. *Conophyton* stromatolites are well known in the fossil record and have also been found in modern siliceous sinters.

3.3 Diagenesis

This is the name given to the alteration of a rock fabric after it has been deposited. It may be divided into processes operating during three sequential stages: pre-burial, early burial and late burial. The processes are not mutually exclusive, and for the purpose of this discussion it is more useful to consider just two stages: meteoric diagenesis operating pre- and early burial, and late burial diagenesis. The changes include the effects of dissolution, recrystallisation, microbial micritisation, bioturbation, cementation, compaction, oxidation of organic matter and formation of authigenic minerals (Tucker and Wright 1991). Diagenesis has important consequences for ^{14}C and uranium-series dating of travertine and the interpretation of original fabrics. Microfossil taphonomy is likewise affected by the diagenetic history of a sediment. In his seminal work on carbonate diagenesis, Bathurst (1976) states that 'carbonate rocks are as much the products of diagenesis as they are of primary deposition', and the carbonates, by virtue of their mineralogy, are altered to a far greater extent than other sediments. These observations are pertinent to travertines, but most of our understanding of carbonate diagenesis comes from studies of marine sediments. In the Recent marine carbonates, where diagenesis is reasonably well understood, two major changes occur at the pre-burial and early-burial stages: cementation of an unconsolidated sediment, and the transformation of aragonite and high-magnesian calcite into low magnesian calcite. Other less predictable changes occur as the result of microbial activity at the pre-burial stage, but bioturbation, often significant in marls and other weakly consolidated sediments, is rarely significant in travertine. In Recent travertines, cementation is the most important process, and mineralogical transformations are of less importance, since the primary carbonate of a travertine is normally low-magnesian calcite. In the small number of travertines containing significant aragonite or vaterite as their primary fabrics, mineralogical changes are more important. While low-Mg calcite is thermodynamically stable under the conditions of deposition with respect to high-Mg calcite and aragonite, crystal size effects are important and recrystallization of low-Mg calcite (aggradational neomorphism) is often observed. Both cementation and recrystallization require the presence of liquid water. Before discussing this, the relationship between the primary travertine fabric and cement must be considered.

3.3.1 Primary Fabric and Cement

One of the greatest difficulties facing the travertine petrologist is distinguishing the primary fabric from cement. Although a travertine may be laminated and built up of a primary fabric layer by layer, the relationships between the contributing precipitates are rarely obvious. For example, in a cascade travertine colonised by bryophytes, the bryophytes play a reef-like role, forming a framework into whose interstices other organisms and sediments may become trapped and lithified. The bryophytes represent the 'primary fabric' yet initially they are unmineralised and consist only of organic matter. Their subsequent encrustation by calcium carbonate is a secondary process and as such this carbonate can be considered as cement binding the fabric together. The early encrustation is not part of the original structure, but acts as an early binder adding rigidity to the deposit. In the case of a coral reef, the primary fabric consists largely of biomineralised coral skeleton and the associated calcified biota. After death, the reef intertices often become filled with a readily identifiable, and secondary cement. If one accepts that some of the bryophyte carbonate is precipitated directly as a result of photosynthesis, the 'primary' framework will include a proportion of biologically-precipitated carbonate, thus becoming part of the primary fabric. Chafetz et al. (1994), observed that the initial spar coatings of the Plitvice travertines 'form a framework for later deposition' and distinguished them from later cements while Pedley (1992) described organic frameworks onto which polycyclic sheets of cement were bound. The same argument applies to precipitation of carbonate around an algal or bacterial colony. The carbonates associated with these plants would in most cases consist largely of 'cement' in addition to a normally indeterminate fraction of 'primary' biologically-induced (photosynthetic) carbonate. This can be contrasted with the precipitation of cave travertine where plants play no role in the framework and the carbonate is precipitated in layers by an inorganic process. The primary fabric consists almost entirely of calcium carbonate, but it might equally be regarded as a primary 'cement', as it provides a rigid structure upon which more carbonate can precipitate. Such a 'cement' may be regarded as a primary fabric. One way of tackling this dilemma is to define the primary fabric as that present at the active travertine surface. Secondary fabrics, including cement, then develop below the travertine surface. Since a 'surface' has no thickness, a more realistic and practical 'surface' would include the top 1 mm of travertine. Even this is not entirely satisfactory however, as will be seen below. The term 'cement' has been borrowed from the marine carbonate literature, where initially soft, or blocky sediments undergo cementation to form hard grounds for example. Since travertine is often hard to begin with, the term loses much of its meaning, but it is deeply embedded in the literature and its abandonment might cause further confusion. Care is clearly needed to distinguish primary from secondary fabrics in travertines, and in many cases, the distinction will not be possible to make. Similar problems have been encountered with siliceous sinter (Jones and Renaut 2003).

3.3.2 Meteoric Diagenesis

This occurs in surface or near-surface environments at ambient pressures and temperatures, in contrast with burial diagenesis occurring at high pressures and temperatures (typical lithostatic pressures >=300 m rock; >40 °C). As most of the investigated travertines are geologically young rocks, the study of burial diagenesis has been neglected and most investigations relate to meteoric diagenesis. The process does not result in significant compaction or dolomitization, but cementation, sparmicritisation, neomorphism and dissolution have been widely documented.

Meteoric diagenesis occurs as the result of the changes brought about by percolating groundwater or rainwater below the 'primary' fabric at the travertine surface. Percolation can result in the dissolution or precipitation of carbonate depending upon its saturation state with respect to the mineral with which it is in contact. Included under this heading are the biological effects of dissolution and sparmicritisation that also operate at or near the travertine surface.

3.3.2.1 Percolation of Stream and Groundwater

Water from which travertine is deposited penetrates below the surface and may continue to deposit minerals within the porous framework. The flow of water through the travertine mass varies according to its fabric. Two forces allow water to penetrate: the small head of water present in the stream channel and capillarity. For most travertines, the head of water would rarely exceed a few decimetres, and a large resistance is usually offered by the small channels between the mineral grains and voids. Where the layer of depositing water is less than a few millimetres, the head is negligible, and water will penetrate by capillarity alone. There appear to be no published infiltration rates for travertines, but with a head of 4 cm water, the author measured a mean rate of 9.3 μm s^{-1} (ca 0.001 cm^3 cm^{-2} s^{-1}) for a meteogene *Phormidium incrustatum* deposit in the UK. The low rate of infiltration should ensure that deposition occurs most rapidly at or very close to the surface. With a large framework porosity, infiltration rates will be much higher, but have not been measured.

In cases where a dense primary fabric is formed, the porosity may be as low as 10%, but as shown in Section 3.3.1, the average porosity of Recent epigean travertine is 50–60%, providing ample space for further mineralisation. As a stream water, supersaturated with respect to the carbonate of which the deposit is composed, penetrates the surface, precipitation will continue both upon pre-existing mineral grains and other surfaces. As penetration continues, the supersaturation will fall, until finally, saturation is reached and no further precipitation will be observed. In an 'ideal' travertine where deposition is continuous, at a fixed rate, and the mineral deposited as equal-sized grains of a single polymorph, the effects of infiltration will occur throughout the deposit. The porosity of the deposit may be assumed to be initially constant, but as cement is precipitated within the intertices, porosity will decline toward the surface. Natural deposits rarely if ever approach this ideal but the author is unaware of any data supporting this hypothesis.

During the formation of travertine cascades, a rapid building phase is often followed by a quasi-equilibrium where erosion prevents further accretion (Section 4.1.3). In this situation, the travertine close to the surface can be old, and infiltration in the upper layers may persist for decades forming a hard rind protecting the softer layers below. The phenomenon has been observed on the 'Hole in the Wall' travertine in the UK (Pentecost et al. 1990) and may be widespread on dams and cascades. On the Plitvice lake dams in Croatia, a 'hardground' develops in winter where the water remains supersaturated with calcite and lithifies the surface crust (Emeis et al. 1987). Infiltration is particularly rapid in the open bryophyte fabrics of meteogene travertines and a dense sparry deposit usually results. Infiltration diagenesis of is often patchy and unpredictable within travertine. A study of stream oncoids from the UK showed an increase in the proportion of sparite and decrease in porosity with age (c. 0–4 ka) but the associated clastic travertines were unaltered (Pentecost 1989). This may be caused by early oncoid diagenesis perhaps assisted by high water permeability within oncoid layers.

The above processes relate to the percolation of stream water in a region of permanent saturation, and the water may be referred to as phreatic, rather than vadose, where water

percolates above the water table. Much of the cement deposited by phreatic waters form layers of equal thickness (isopachous) and they have been widely reported (e.g. Pedley 1987). In some circumstances, phreatic water may not originate from direct percolation but by lateral or even vertical movement of groundwater. While the active travertine surface is unlikely to be influenced by this, buried, inactive travertines may be in contact with phreatic waters for long periods. These waters are often low in dissolved oxygen and charged with reduced Fe and Mn. If further precipitation occurs, then ferroan calcites could form, and if oxygen is encountered, local oxidation may result in the precipitation of authigenic Fe and Mn oxides and hydrates. The saturation-state of these waters with respect to the travertine carbonate will likewise affect their carbonate content and ultimate composition. An isotopic study by Manfra et al. (1974) on the Italian travertines provides some evidence for groundwater diagenesis, and iron-pans reflecting former piezometric surfaces have been recorded at some UK sites (Pentecost et al. 1990).

Where inactive travertines are exposed above the water table, or liable to periodic inundation, they lie in the vadose zone and may be prone to desiccation. There are two characteristic forms of vadose cementation, 'meniscus' and 'gravitational' and both have been observed in travertine fabrics (Ordoñez and Garcia del Cura 1983; Love and Chafetz 1990; Gradzinski et al. 2001a). As the surface dries, water may rise, and evaporation at the surface provides another source of secondary mineralisation. In hot and arid climates, the result may be an extremely dense travertine crust recalling the 'clinker' of the exposed Bahamian shelf carbonates. Such forms, which closely resemble calcrete are well documented in Turkey (Burger 1990).

3.3.2.2 Dissolution of Carbonate

Where travertines become exposed to solutions undersaturated with respect to a carbonate mineral, such as direct rainfall and soil-percolation water, surface dissolution may be expected leading to typical limestone karstification (Vitek 1973; Viles and Goudie 1990a). The percolation of rainwater, in the absence of strong evaporation does not appear to have any other significant diagenetic effect, at least according to the ^{14}C assays of rainwater percolating travertine (Srdoc et al. 1983). 'Mixing-corrosion' is possible where vadose and phreatic waters contact and is well documented in other limestones, sometimes producing diagnostic fabrics (James and Choquette 1984). This is especially likely to occur where percolating rainwater mixes with a bicarbonate-rich groundwater, or deep thermal waters intermingle with shallow groundwaters.

Once a travertine has become soil-covered, karstification proceeds apace and the dissolved products may be capable of re-precipitating carbonates lower in the sequence. This must be the mechanism by which small stalactites and flowstones are formed within old travertine caves. Good examples can be seen in the Olgahöhle, Germany and Lillafüred, Hungary. At Plitvice, Chafetz et al. (1994) recognised three generations of calcite deposition terminating in a centimetre-thick late stage flowstone forming on the inactive cascades. Love and Chafetz (1990) also report 50 cm stalactites and associated botryoidal deposits from travertine caves in Oklahoma.

'Spiked crystals' have sometimes been observed on travertine surfaces with the electron microscope (Love and Chafetz 1990) and are probably the result of localised dissolution. 'Spiky' calcite (Folk et al. 1985) was found upon calcite rhomb faces, with the spike axes in the direction of the c-axis. Although Folk et al. argue that these acicular crystals are primary and arise via screw dislocations, they are suggestive of crystal dissolution.

3.3.2.3 Recrystallisation of Calcite

Chave and Schmalz (1966) concluded on experimental grounds that particles of calcite <0.1 μm in diameter would be unstable in water and this is supported by theory. Smaller crystals are more soluble than larger ones of the same mineral and a tendency towards increasing crystal size over time has often been observed in carbonate sediments. The process of re-solution and precipitation until a stable crystal is formed is known as Ostwald ripening. The recrystallisation of micrite into sparite *in situ* is termed aggradational neomorphism and has been investigated in detail by Love and Chafetz (1988, 1990). The travertines of the Arbuckle Mountains in Oklahoma are among the finest examples of travertine cascades in the United States and contain extensive laminated fabrics (alternate homopachous) with bushes of cyanobacterial filaments, and singlet widths of about 1–2 mm. In the younger travertines the laminations consist of layers of 'bushes' enclosed by fan-shaped crystals in vertical section, alternating with darker layers of finer crystals. In the older travertines, laminations consisted largely of coarse columnar calcite, but staining with methylene blue revealed traces of former algal bushes. It was clear that almost complete recrystallisation of the darker layers had occurred and the upward growth of the spar crystal layers eventually collided with the spar layer above as indicated in Fig. 8. Rarely reported poikilotopic cements, usually taken to indicate neomorphism were also found in this travertine. This form of diagenesis is probably widespread in algal travertines, and may well occur in other biofabrics. For example, aggradational neomorphism has been widely recognised as occurring in bushes and colonies of the cyanobacteria *Phormidium* and *Schizothrix*, resulting in an early post-mortem alteration of micrite (Janssen et al. 1999; Freytet and Verrecchia 1999; Arp et al. 2001). Recrystallisation has also been described, but in less detail by Shafer and Stapf (1978) in the Lake Constance oncoids. Geurts (1976), Braithwaite (1979); McGannon (1975); Cipriani et al. (1977); Thorpe (1981); Julia (1983) and Heimann and Sass (1989) also report on the phenomenon. In an alpine speleothem, the stable isotopic composition of primary and secondary calcites was found to be identical suggesting neomorphism in the cave environment (Spötl et al. 2002).

Despite neomorphism, micrite may persist in travertines for long periods, presumably in situations where percolation is retarded or the crystal surfaces are poisoned or occluded by organic matter or other minerals. The Pleistocene travertines of the Hula Valley, Israel con-

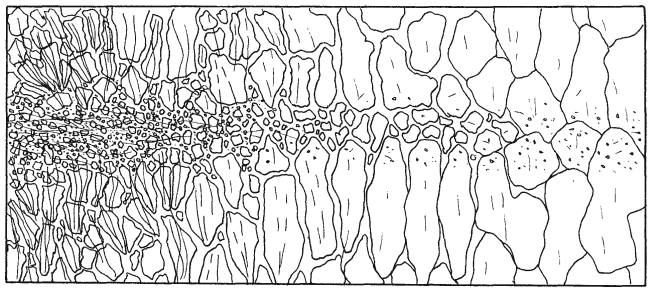

Fig. 8. Neomorphism of a cyanobacterium (*Phormidium*) meteogene travertine shown as a pictorial time-series. The original fabric is shown left consisting of a laminated travertine with two winter layers of calcite spar and a summer layer of micrite with *Phormidium* filaments. As neomorphism progresses to the right, the lower layer of spar grows up and engulfs the micrite layer. At far right the calcite spar contains traces of *Phormidium* filaments together with diverse microscopic inclusions coincident with the micrite layer. While re-rystallisation is indicated, an additional source of $CaCO_3$ will be required to reduce the porosity. Bar 1 mm

tain abundant primary micrite and microspar vug linings, and there was no evidence for recrystallisation in these deposits (Heimann and Sass 1989). In some Mesozoic travertines, Steinen et al. (1987) report a primary fabric, including micrite. In the case of speleothems, and some epigean travertines, Kendall and Broughton (1978) have shown that recrystallization, if it occurs at all, is confined to a narrow surface layer, where calcite crystallites are transformed into large radiating crystals of sparite. The same may well occur in epigean travertines and explain the frequent occurrence of bladed spar with sweeping extinction.

3.3.2.4 Recystallisation of Aragonite

Some travertine is deposited initially as aragonite and here neomorphism has been frequently recorded. Aragonite transforms to calcite, due to its higher solubility and microcrystalline form. The rate of transformation is variable and depends upon both water composition and the rate of percolation (Cipriani et al. 1977). Transformation can be surprisingly rapid. Malesani and Vannucchi (1975) reported that the aragonite of Bagni san Fillipo is completely transformed into calcite in 10–15 days. At Mammoth Hot Springs, old cascade deposits near Elephant Back terrace can be found where transformation is actively taking place, and extensive neomorphism is apparent only a few years after deposition (Sturchio 1990). In some cases, virtually all of the original aragonite fabric is obliterated. Sparite replaces aragonite sprays forming structures reminiscent of the ray-crusts described by Folk et al. (1985). In a study of the active travertine fabrics at Mammoth, Fouke et al. (2000) found that aragonite was often closely associated with calcite, especially on the lower slopes. It was suggested that at these lower temperatures, aragonite crystals, washed down from the hotter waters above, could have been rapidly transformed to a dendritic form of calcite. Gibert et al. (1983) and Richter and Beseneker (1983) also report aragonite transformation in thermogene travertine ooids. Using the differing ability of the two polymorphs to accommodate strontium, Malesani and Vannucchi (1975) found evidence for aragonite diagenesis in several active Italian travertines and noted the repartition of strontium during the process. Repartition of both Mg and Sr has also been reported in travertine ooids (Richter and Besenecker 1983). In some alpine speleothems, Spötl et al. (2002) observed aragonite replacement by calcite. The transformation of aragonite to calcite is not however, always a rapid process. Gregor (1982) for example, records aragonite from the Miocene Bottingen travertines but in the Pleistocene Rapolano Terme travertines, all of the original aragonite laminae had been converted to calcite, or the aragonite dissolved (Guo and Riding 1992). While calcite-aragonite transformations are the norm, aragonite-aragonite transformations, involving the formation of larger, lower energy crystals is suspected in some high-altitude travertines from South America (Valero-Garcés et al. 2002).

Much of the above relates to thermogene and spelean travertines, but most epigean meteogene travertines will also contain traces of aragonite. Mollusc shells are frequently incorporated into deposits and are composed of both calcite and aragonite. Partial dissolution of shell is frequently observed, even in recently deposited travertines and this is probably due to their aragonite content.

3.3.2.5 Sparmicritisation

A term devised by Kahle (1977) to describe the destructive activities of microrganisms etching sparry carbonate rocks. The process is recognised as important in the diagenesis of shallow marine carbonates (Bathurst 1976). Microbes, particularly algae, bore (more correctly, etch) the carbonate, breaking up the crystals and, at least in marine limestone, leave tubes filled

with micrite, forming 'micrite envelopes'. In marine limestones, the envelopes have a high preservation potential, possibly due to the inclusion of recalcitrant organic matter inhibiting recrystallisation. In travertine, Chafetz et al. (1994) describe some convincing examples of sparmicritisation from the Plitvice Lakes travertine dams and cascades. Most of the travertine appears to have been originally spar, but extensive areas of micrite occur, and thin sections revealed ghosts of former bladed and equant spar within layers of micrite, and spar in the process of becoming micritised. In some areas, thin sections revealed filamentous microorganisms penetrating spar crystals. In Waterfall Beck, a travertine-depositing stream in the UK, sparmicritisation occurs beneath the travertine crust to a depth of 1.3 mm, and the main agent appears to be the cyanobacterium *Leptolyngbya (Schizothrix) perforans* (Pentecost 1978, 1992a). The process is most likely due to the secretion of an acid or Ca-chelator.

Sparmicritisation could account for a significant fraction of the micrite in some travertines and is most clearly demonstrated in deposits with abundant sparry calcite (Fig. 9). Where the deposit is composed of micrite from the start, sparmicritisation is not of course possible, though the microbes might serve to prolong the life of a micrite, retarding aggradational neomorphism. The thermogene deposits at Bagno Vignoni, Italy possess a dense surface calcite rind consisting of radiating sparite bushes. A few mm below the surface, a green-brown layer colonised by cyanobacteria and diatoms occurs in a much more porous layer with a more open bushy structure. This suggests that the endoliths are opening up small parts of the crystal, possibly by local dissolution. Ironically, it is within the endolith layer that microbial

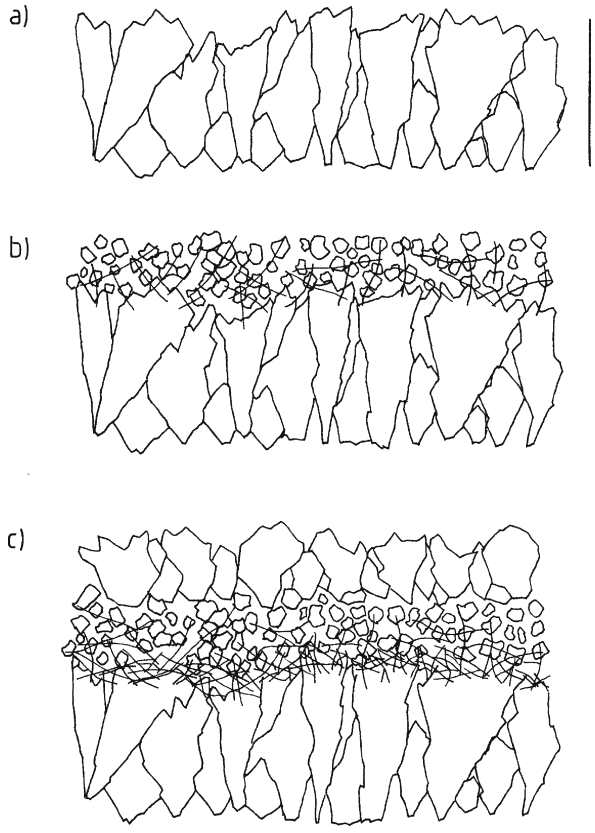

Fig. 9.
Sparmicritisation of a laminate travertine. a) 'Winter' layer of abiogenic columnar and bladed spar. b) 'spring/summer' layer of microspar and micrite associated with filamentous cyanobacteria. The 'winter' spar is beginning to be etched by the overlying cyanobacterium community developing in the warmer part of the year. c) 'second early winter' spar forming on top of the summer micrite. The first winter layer is now buried by 1 mm of travertine but endolithic cyanobacteria continue to etch the top of the first spar layer, breaking it up into micrite. Further etching is limited owing to the limitation of light but endolithic fungi and heterotrophic cyanobacteria could continue the sparmicritisation at greater depths. Bar 1 mm. Based on observations at Waterfall Beck, UK, where *Hyella fontana, Phormidium favosum* and *Leptolyngbya* (*Schizothrix*) *perforans* comprise the endolithic cyanobacterium community. Travertine surface at top

growth, and presumably microbially-induced precipitation reaches its maximum (Pentecost 2001). In another Italian travertine, Guo and Riding (1994) noted sparmicritisation of shrubs and Galli and Sarti (1989) observed it in some Italian stream deposits.

3.3.3 Burial Diagenesis

Travertines older than Quaternary may be buried under several hundred metres or more of overburden. In common with other limestones, various kinds of burial diagenesis are likely to occur. They result from increased lithostatic and hydrostatic pressure, heating, and the ingress of mineral-enriched solutions, generally in the absence of dissolved oxygen. Diagenetic effects include compaction and porosity reduction resulting from further cementation by a wide range of minerals, dissolution of the original fabric, sometimes with replacement by other minerals, and reactions between the original carbonate component and accessory minerals. The final product may be difficult to interpret. Dolomitisation resulting from ingress of Mg-enriched solutions could lead to complete replacement and loss of organic matter, while pressure-solution could lead to dissolution and recrystallisation. The stable oxygen isotope ratio ($\delta^{18}O$) of buried carbonates may also vary in a predicable manner with depth as a result of further cementation (Tucker and Wright 1990). There have been few studies of the effects of burial diagenesis on these rocks. Donovan (1973) observed dolomitisation of a Devonian travertine-like deposit from Scotland, which contained a ferroan dolosparite, but the period of dolomitisation is uncertain. Steinen et al. (1987) found quartz and dolomite in a Jurassic travertine. The increased occurrence of chert in older travertines suggests ingress of later Si-enriched solutions.

Chapter 4

Morphology and Facies

The study of landscape topography with emphasis on the erosional processes encompasses geomorphology, and in a geographical context, geomorphology may be used to classify land surface features. In contrast with most of the land surface, travertine morphologies are frequently constructive in nature. The counterintuitive observation that waterfalls, good examples of erosive features, are locations where travertine is preferentially deposited has intrigued geomorphologists (Gregory 1911). These 'constructive' events epitomise travertine formation. They are of geologically short duration and the constructive process can be terminated rapidly by erosion. Travertine is perhaps unique in the sense that the events of deposition and erosion can be investigated simultaneously side by side. Depending upon the degree of cohesion between the crystals, deposits range from soft and chalky with low relief to dense and massive with high relief.

Several attempts have been made to classify deposits according to their morphology and setting. One of the first schemes was that of Klähn (1923) who described three forms of travertine from German rivers based primarily on stream gradient. In a modified form this scheme was followed by Stirn (1964), Gruninger (1965) and Frey and Probst (1974) working in the German Swabian Alps. Three forms were recognised: Taltuff, consisting of river dams and backfills developing along low gradients, <10%; Gehängetuff, terraced slope deposits forming at an angle of 25–40° and Falltuff, protuberant masses, normally developing on steeper slopes. In Slovakia, Scheuer and Schweitzer (1981) classified travertines into valley-barrage, valley side (cascade), paludal and sinter cones. Several other authors also describe dams and cascades e.g. Gregory (1911), Matonickin and Pavletic (1962), Heinrich (1967), Jux and Kempf (1971) and Mongini (1973), but no comprehensive classifications appeared. More recently, the morphology of several mainly thermogene travertines were described by Chafetz and Folk (1984) who recognised five basic forms: waterfall/cascade; lake-fill; sloping mound; terraced mound and fissure ridge. In France, Fabré (1986) describes six travertine typologies including an artificial 'travertin anthropique'. Scheuer and Schweitzer (1989) illustrate morphologies of many thermal Hungarian travertines, explaining them in terms of the local geomorphology. Freytet (1990) provides a morphological classification of spring and fluvial travertines in northern France, splitting them into 'moss travertine', 'mobile' forms (oncoids) and 'encrusted' forms and focuses on medium to small-scale features. Magnin et al. (1991) split the travertines of southeast France into two main types; spring and river-valley. The valley-fills include travertine dams and backfill deposits, which together form a 'travertine system'. A number of travertine types were classified by Pedley (1990) according their environmental setting: 'perched springline', 'cascade', 'fluviatile' (braided and barrage types), 'lacustrine' and 'paludal'. This was further elaborated by Ford and Pedley (1992), who proposed a three-way split into 'cool water', 'thermal' and 'saline' travertines. A study of British travertines revealed that most of these deposits could be classified into seven

groups (Pentecost 1993) but the scheme is of limited value worldwide because Britain contains comparatively few forms, and modern thermogene travertines are lacking. In Japan, Kano and Fuji (2000) proposed another morphological classification for travertine-depositing streams. They include five types: encrusted boulder; plane slope; mound; terrace, and cascade.

Scale is an important factor when considering any classification of this kind. Ordoñez et al. (1986) use a three-fold classification: macrostructure – controlled by position relative to the water table and topography; mesostructure controlled by ecology; microstructure controlled by the efficiency of degassing. Although an oversimplification, it demonstrated the range of effects operating over different scales. It will be apparent that the classification of travertines on their morphology is confounded by the juxtaposition of forms of a variety of types and origins within the same area. Pentecost and Viles (1994) attempted a revised classification of the travertines and placed them into eleven categories, divided into two sub-groups. The first sub-group with eight categories contains all of the autochthonous (*in situ*) travertines associated with springs, streams, rivers, lakes and marshes and concluded with the allochthonous (clastic) travertines. The scheme embodied descriptions from many published sources, plus their own observations (Table 4). Virtually all known travertines can be assigned to one of these categories, but we emphasised, along with previous writers, that 'travertine complexes' consisting of a range of intergrading forms are common, and defy a simple classification. For example, it is normal to find allochthonous and autochthonous deposits closely associated giving complex morphologies. Travertine dams range from less than 1 cm to over 100 m in length, the former normally part of a larger cascade system while the latter are often free-standing structures. A good classification scheme is dependent upon well-marked discontinuities in characteristics and these are lacking in most travertines and indeed in limestones generally. The morphological forms described below are based largely on our 1994 review. We make no claims for its universality, but despite its shortcomings, it provides a summary of the travertine morphologies so far discovered.

The facies of a sediment are its total characteristics, allowing it to be related to a particular depositional environment. To a large extent, the facies constitute the main elements of the travertine fabric and its morphology but to this may be added particular sedimentary features such as the bedding type and bedding relationships within the travertine-complex.

Table 4. A morphological classification of travertine (after Pentecost and Viles 1994)

Autochthonous	Hydrological position	Allochthonous	Hydrological position
Mound	Spring	Alluvial cone	Stream/river
Fissure ridge	Spring	Bar	Stream/river
Paludal	Spring	Lake and valley fill	Spring/stream/river
Cascade (inc. dripstone)	Seep/stream/river		
Dam	Seep/stream/river		
Fluvial crust	Seep/stream/river		
Cemented rudite/clast	Seep/stream/river		
Lacustrine crust and reef	lake		

Several investigators have identified and named travertine facies, explaining them in terms of the sedimentation process. Ferreri (1985) made a detailed study of the Central Italian travertines, dividing them into autochthonous and detrital (allochthonous) forms and then subdividing on grain size and type of plant encrustation. She recognised phytohermal and microhermal types and classified the autochthonous forms as boundstones. For meteogene travertines ('tufas' of several authors), Blot (1986) considered five facies, two dominated by bryophytes, one a dam/cascade type, a paludal and a detrital type. Pedley (1990) divided the facies into two main types, autochthonous and clastic, and then subdivided primarily on petrology, paying particular attention to clastic forms (Table 5). Arenas et al. (2000) recognised six facies in a Quaternary paludal-lacustrine deposit: macrophyte encrustations, bryophyte buildups, coated grains and oncoid rudstones, biomicrites, stromatolites and marls. In some areas the oncoidal facies allowed identification of palaeowater flows. Similar facies have also been described by Buccino et al. (1978). Glover and Robertson (2003) used Pedley's model to describe the large travertine of Antalya adding two further types; 'pisolith tufa' and 'tufa breccia'. His model has also been used to describe the Ruidera Lakes system in Spain, along with further terms such as a 'vertical tube facies' for encrustations around emergent macrophytes (Garcia del Cura et al. 2000).

Thermogene travertines have been classified using similar schemes. Guo and Riding (1998) placed the facies of the Rapolano Terme thermogene travertines into eight categories with emphasis on changes in deposition rate downflow. At Mammoth Hot Springs, Fouke et al. (2000) identified five facies bearing relationships with distance from source and fabric. They are: 1) a vent facies, formed of centimetre-sized botryoids of aragonite needles built upon bacterial filaments; 2) apron and channel facies of aragonite precipitated onto bacterial filaments; 3) pond facies with shrubs of aragonite at higher temperatures, ridged networks among cyanobacteria at lower temperatures, calcite bubbles and calcite ice; 4) proximal slope facies composed of aragonite shrubs, often dendritically branched and forming microterracettes; 5) distal slope facies of dendritic feather crystals of calcite and irregular spherules up to 5 mm diameter.

Table 5. Facies types in tufa (after Pedley 1990)

Facies type	Description
Autochthonous	
Phytoherm framestone	In situ cemented plant material with highly porous framework
Phytoherm boundstone	In situ stromatolitic build-ups with fringe-cements and often associated with oncoids
Clastic allochthonous	
Phytoclast tufa	Fragments of encrusted plants cemented before and/or after transport
Cyanolith 'oncoidal' tufa	Oncoids, often with woody fragments for nuclei
Intraclast tufa	Reworked deposits often dominated by silt and sand-sized fragments, carried in spate and deposited as calciclastic grain-supported fabrics in fluvial channels
Microdetrital tufa	Fine, often structureless lacustrine and paludal deposits of micrite
Peloidal tufa	Only detectable petrologically, can be grain-supported
Palaeosols	Soil profiles may develop as a result of water table lowering

4.1 Autochthonous Travertines

4.1.1 Spring Mounds

These comprise domes of travertine, <1 m to >100 m in height surrounding a spring orifice. Most mounds require a hydrostatic head, and the orifice shape (circular and pipe-like, or linear and sheet-like) determine their solid geometry. Mounds may be subdivided on position and hydrology. Terrestrial and submerged forms can be recognised, and mounds formed via capillarity in bryophyte cushions can be distinguished from those resulting from artesian flow. Mounds resulting from capillarity rarely exceed 1 m in height and have been little documented. The largest terrestrial domes are of thermogene travertine and many examples are known. Damm (1968) provides a detailed account of one of the most substantial, Zendan-I Suleiman (Solomon's prison) in Iran, about 100 m in height. The cone appears to have taken about 10 Ka to form and its internal structure is clearly seen in a tunnel driven to the centre, but is no longer active. The orifice contains fine sediments with travertine fragments and artefacts. An even larger example, and perhaps the largest in the world occurs in the Rio Salado Valley of New Mexico (Harrington 1948). Descriptions of ten Slovakian mound types are given by Scheuer and Schweitzer (1985). They include the 'regular cone' with a simple cross section and central orifice and the 'parasitic cone' where the original cone has become inactive and a lower cone has developed. These and several other forms are shown in Fig. 10. Other notable mounds occur at Hammam Meskoutine, (Algeria), Homestead, Utah and in Wyoming (Auburn and Mammoth Hot Springs, Photoplates 1A, 1E). In the Great Artesian Basin of Australia, mounds occur in at least eleven large groupings and number in their hundreds (Ponder 1986). One of the best known is Blanche Cup in the Lake Eyre Group. Some of these mounds consist of admixtures of mud, silt and travertine. Mounds such as Blanche Cup and the Heber group in Utah (Photoplate 9A) have wide orifices with smooth walls containing deep pools of water. Similar mounds are also said to be abundant in parts of Peru (Liddle 1928), and at Colluco, (Argentina), Chongo (India) and Hammam Bou Hadjar, Algeria (Waring 1965). Many mounds are of low relief and consist of sheet-like layers of travertine with a dip of just a few degrees and in these cases, the mound outlines become irregular, presumably in response to minor differences in ground level surrounding the springs. The huge deposits at Bagni di Tivoli provide good examples. The mounds of the Great Artesian Basin of Australia form along the western fault of the Lake Eyre basin, and elsewhere (Wopfner and Twidale 1967; Mabbutt 1977; Kerr and Turner 1996) and consist of superambient meteogene travertine. Similar mounds are found in the Kimberley region of Australia (Viles and Goudie 1990b) and in parts of Egypt (Butzer and Hanesen 1968). The orifices of thermogene mounds frequently self-seal due to the rapid deposition. This results in the migration of springs and a complex build-up of deposit.

In Europe, meteogene mounds are uncommon. Small spring mounds from the UK are known for their rich flora (Pentecost 1981) and form via capillarity in cushions of the moss *Palustriella commutata*. A relict mound has been described from Poland (Gradzinski et al. 2001b) and they are also known from the Paderborn district, Germany (D. Burger, *pers. comm.*). On rare occasions, mounds occur within caves where they are known as geysermites, examples being known from several parts of Europe and America (Hill and Forti 1997). In Cuba, the geysermites, formed from upwelling thermal water, are about 10 cm high and 40 cm in diameter, but elsewhere, their height may exceed 1 m.

The formation of mounds is not understood in detail but it is clear that most of them require water under pressure. The hydrostatic pressure needed to form the largest mounds is considerable, approaching 7 kg cm^{-2} at ground level. These pressures can be realised in artesian systems and most mounds probably develop in this way, but geyser-like activity may be responsible on

rare occasions as noted by Cohn (1862). Mound height must be limited by the hydrostatic head, and the rate of flow presumably falls as the mound builds. Bargar (1978) records a mound at Mammoth Hot Springs that grew in height by 20 cm in a period of nine months. The remarkable symmetry of many mounds may be related to the formation of dam-like rims at the orifice. These rims build so that the overflow of water is approximately equal all round the mound as in the case of travertine dams, ensuring its regular form. In a series of experiments, and on the basis of theoretical work, Kerr and Turner (1996) have shown that the overflow of water at a mound orifice is controlled by surface-tension effects. Blanche Cup, Australia with an orifice diameter of 25.5 m, can only overflow about 1% of its rim at a discharge rate of 0.2 L s^{-1}. With higher discharges, mound orifices can be overtopped all-round so flow rate will influence the build-up of travertine on the mound. The orifice necks of old mounds are often surprisingly smooth and regular and presumably related to either regular dissolution or precipitation. Kerr and Turner made artificial mounds and terraces by allowing saturated solutions of sodium carbonate to flow within a small tank. Convective cooling allowed the salt to nucleate and crystallise in a range of mound- and terrace-like morphologies on a rough surface placed within the tank. They demonstrated that the composition of the salt was unimportant and that the morphologies were dependent only upon the process of crystallisation as a function of the fluid supersaturation. Mound profiles range from steep-sided structures with slopes exceeding 50° to low mounds with barely perceptible slopes of 1° or less. Mound slope and overall geometry are likely to be functions of surface topography, flow rate, head and the degree of carbonate supersaturation at the orifice. A high degree of supersaturation will lead to rapid deposition around the vent giving a steep mound, while waters closer to saturation are likely to deposit at increasing distances, providing a more modest profile under conditions of equal discharge.

The second type of travertine mound is formed entirely under water, usually in saline lakes. Subaqueous mounds usually result from the mixing of Ca-rich springwaters with saline, carbonate-rich lake water leading to the rapid precipitation of calcium carbonate. Their formation does not result from CO_2 evasion and strictly, these deposits are not travertines, but included on account of their close similarity to their epigean counterparts. The results can be dramatic, with the formation of spectacular towers, mounds and 'tombstones' once the lake level has lowered sufficiently to expose them. Good examples are known in the Western Great Basin of the United States and include those of Mono (Fig. 11), Pyramid, Searles and Washoe Lakes and the ancient submerged mounds of Buffalo Springs, Nevada (Dunn 1953; Scholl 1960; Scholl and Taft 1964; Feth and Barnes 1979; Rieger 1992; Bischoff et al. 1993). Similar structures occur in Lake Van, Turkey (Kempe et al. 1991), Inner Mongolia (Arp et al. 1998) and Greece (Hancock et al. 1999). Due to fluctuating lake-levels, many of the Great Basin mounds are now exposed. Dunn (1953) describes forms 1–5 m in height with the circular spring openings still visible whilst Scholl and Taft (1960) describe Pleistocene pinnacles, spires and 'tombstones' up to 40 m in height on the dry bed of Searles Lake. About 500 examples are known from this site. In Mono Lake, the mounds occur with spring-derived 'defluidisation structures' (Cloud and Lajoie 1980). Several African rift lakes contain mounds (Casanova 1994) the largest being the tower of Abbé Lac, Djibouti (Fontes and Pouchan 1975).

Small marine mound-springs occur in the intertidal zone where upwelling groundwater is subject to intense evaporation to form a type of beach rock (Warren 1982). At low temperatures, a hydrated calcium carbonate, ikaite may precipitate into remarkable tube-like structures and spectacular columns. First described from the thermal upwellings in Ika Fjord, Greenland, they are also known to have formed in some of the Great Basin lakes of the USA. (Bischoff et al. 1993). In caves a type of inverted cone formed by the precipitation of calcium carbonate in cave sands and muds from dripping water is known as a 'conulite' (Fig. 24).

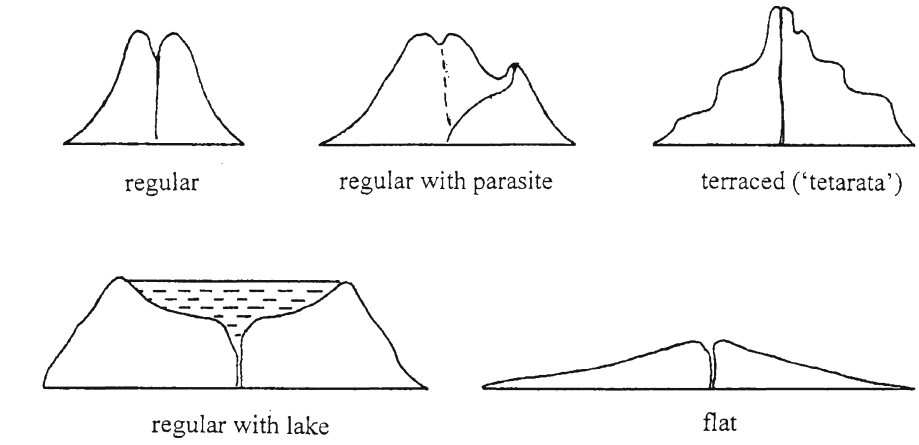

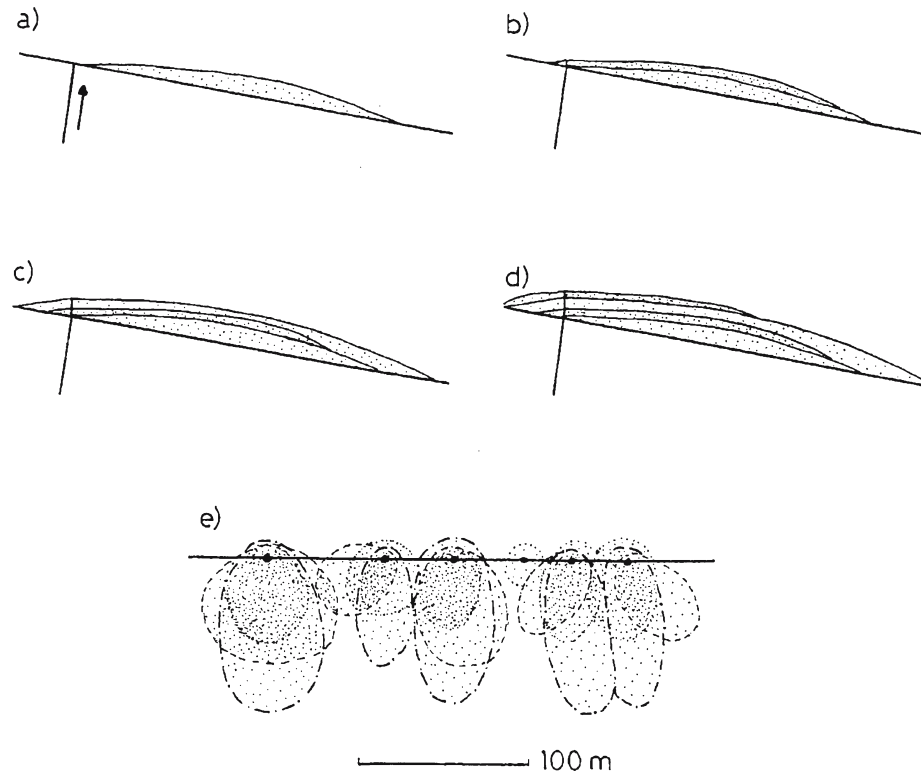

Fig. 10. Sections and plans of travertine mounds. Above: Types of travertine mound, adapted from Scheuer and Schweitzer (1985). Below: The development of a mound/fissure ridge complex, interpreted from sections in the Budakalász Quarry, Hungary. a-d) Growth of a series of mounds from a faultline; e) Plan view showing a linear array of travertine-depositing springs with three series of mounds superimposed. Vertical scale exaggerated x10

4.1.2 Fissure Ridges

Travertine build-ups around spring orifices along fractures such as joints or faults (Bargar 1978) form elongate, wedge-like structures termed fissure ridges. Ridges range from 1->15 m in height, and may exceed 0.5 km in length. Khoury et al. (1984) describe a calcite-vein ridge at Zerka Mai'in, Jordan where fractures have been filled with subsurface calcite and later undergone differential weathering below travertine mounds. Many inactive ridges are known such as those of Hamman Mescoutine, Algeria; the Elephant Back, Mammoth Hot springs, Wyoming; and Soda Dam, New Mexico (Chafetz and Folk 1984). Altunel and Hancock (1993) found fissure ridges over extensional fractures in Turkey but at Pamukkale they contribute little (c. 1%) to the crustal extension in the opening graben. Where fissure ridges have been exposed in section, it is clear that travertine becomes deposited upon the inner as well as the outer walls and progressive widening of the fracture takes place (Photoplate 9B). This may be the result of continuing crustal tension, or high hydrostatic pressure within the ridge. Pressures exceeding 750 kg m^{-2} have been estimated within some of the fissure ridges at Mammoth Hot Springs (Bargar 1978). With reference to the mound springs above, these pressures must often be exceeded. Hancock et al. (1999) suggest that mounds and cones occur where fissures underlay soft sediments while fissure ridges occur where the fractures continue to the surface. They show that the ridges tend to develop over the fractures in fault step-over zones rather than the fault itself.

A spectacular partially active ridge occurs at Terme San Giovanni Battista, Rapolano near Siena, where most of the spring-water responsible for its formation has been piped to nearby baths (Guo and Riding 1999) (Photoplate 9C). L'Apparent (1966) described a fissure ridge-like structure impounding a lake at Band-e-Hajar, Afghanistan. These ridges have also been observed on the floor of the former Searles Lake, California (Scholl and Taft 1964). They are primarily a thermogene feature.

Fissure ridges form a continuum with travertine mounds since the flow of water from the fracture is often discontinuous leading to a linear array of individual springs. Local buildups will result in a series of small interconnected and interdigitating mounds gradually increasing in height. On low to moderate gradients a complex accumulation of travertine may develop. This is given support by the long sections exposed in some of the large travertine quarries of Hungary (Fig. 10b) and this form of deposition is likely to account for the structure of many of the large thermogene deposits of Italy and Turkey.

Fig. 11.
Silhouettes of three exposed travertine mounds c. 5 m high, Mono Lake, California

4.1.3 Cascades

Two types of cascade can be distinguished at active sites: *erosively-shaped* deposits, approximately paraboloid in section and frequently with fluted channels, the morphology largely controlled by spate water trajectory, and *accretionary* deposits, irregular and prograding where deposition outpaces erosion over long periods. The former are typical of high-discharge streams with vertical falls formed along resistant rock layers (Dennen et al. 1990). Examples include Sitting Bull Falls, New Mexico; Turners and Prices Falls, Oklahoma (Photoplate 1C); the upper falls at Urach, Germany (Photoplate 9D); Terni Falls, Italy, and the Huangguosho and Gaotang Falls, China. In the UK good examples occur at Gordale and Waterfall Beck, Yorkshire. Waterfall Beck has been monitored for more than 30 years during which time no net increase in deposition has occurred. Travertine formation during summer on mats of the bryophyte *Palustriella* (*Cratoneuron*) *commutata* is stripped bare by winter spates, maintaining the profile illustrated in Figure 12a. Discharge ranges from <1 to 150 l. s^{-1}, but the trajectories of suspended stones during spate, when current speeds range from 1–2 m s^{-1}, demonstrate that the profile is not dictated by this. Instead, the shearing force of water, and to a lesser extent descending pebbles, maintain the form of the cascade. The same is true in one of the nearby Gordale cascades where carbon dating has shown that the present form was reached soon after deposition began 240 years ago (Pentecost et al. 1990). Travertine accretion is likewise prevented on the much larger Huangguoshu Fall of China (Fig. 12). Here the flow of water is seasonal, reaching minimum values in early winter (16 m^3 s^{-1}) and maximum in summer (1450 m^3 s^{-1}). These huge flows over a 74 m cliff, strip the spring bryophyte growth, maintaining the shape. At Urach, Germany the upper vertical section is controlled by erosion but below where the gradient is much reduced, the travertines are crossed by braided streams permitting accretion. Cascades, in common with mounds, occur over a range in scales and may be a major feature of travertine-depositing systems.

Some cascades appear to be indefinitely accretionary where the flow of water is so slight that shearing stress and erosion is negligible. Examples include the falls of Topolje in former Yugoslavia, the Rio Salitre Falls, Brazil (Branner 1911), the 'carapaces' of the Ghaap Escarp-

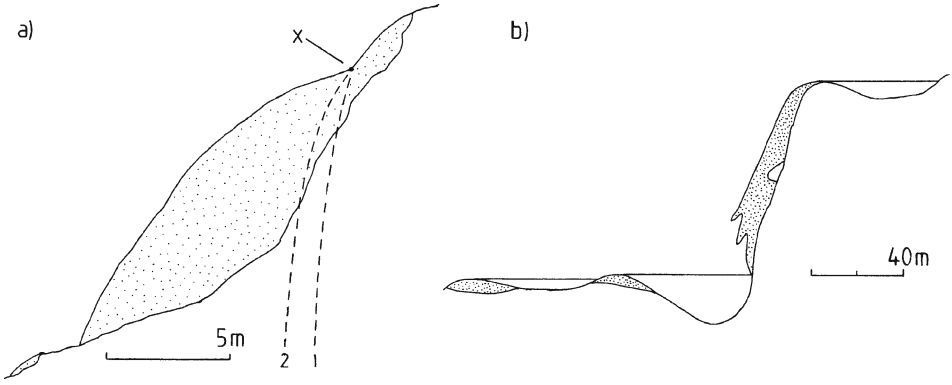

Fig. 12. Two cascade travertine profiles showing features of erosion. Horizontal and vertical scales are equal, travertine is stippled. a) Waterfall Beck, UK. A small cascade deposit 13 m high. Two trajectories for waterborne particles are shown by the broken lines, beginning at point X. Particle trajectories are shown with horizontal velocity components of 1 and 2 m s^{-1}, typical for spate conditions in this stream. b) Huangguoshu Fall, Guizhou Province, China where travertine forms on a 74 m cliff. Note the travertine cave, pound pool and two degraded travertine dams below. Discharge ranges from 16–1450 m^3 s^{-1}. (after Zhang Yingjun and Mo 1982)

ment, South Africa (McKee 1993a) and the Gütersteiner Falls in Germany (Fig. 13, Photoplate 1D). Thermogene travertines forming on hillsides often develop this morphology to an extreme degree as shown by the Reotier travertine (Photoplate 3A). In these cases, lateral extension is restricted only by the mechanical strength of the travertine. Dam walls may progress in a similar fashion, as has been demonstrated by the ^{14}C dating of dam profiles (Srdoc et al. 1980) and is probably responsible for the extensive 'shoals' above the Jiuzhaigou dams in China. Deposits may become so bulky that they topple over or crack leading to the formation of blocky rubble at the base of rejuvenated cascade deposits. The form of these accretionary cascade deposits can be modified by other processes. Spray loses its dissolved chemical load rapidly on waterfalls, and where sprayfall is persistent, 'spray tufa' can result (Zhang et al. 2001). These often produce irregular knobbly deposits at the sides of waterfalls.

A number of prograding cascade sub-types are recognisable. They include the keeled cascade where the water flows along a narrow slot before plunging over a prominent travertine nose. Examples are the Rohrbach, Germany (Von der Dunk and Von der Dunk 1980), parts of the upper Gütersteiner Falls and the Maurienne Falls, France (Gignoux 1937). Travertine 'tubes' (röhren), described from Croatia by Pevalek (1935) consist of a protuberant cylinder of travertine forming a natural spout at the top of small waterfalls (Fig. 14a). A frequent prograding form is the Belgian 'cron', ('gehängetuffe') characterised by a series of small dams with a staggered step-like structure (Fig. 14b).

There is often a rich flora in the boggy hollows of these cascades (Verhulst 1914; Mosseray 1938; Symoens et al. 1951; Pentecost and Lord 1988; Pentecost 1991a). Crons represent a transition between cascades and travertine dams.

A remarkable series of keeled structures occur at Pamukkale, Turkey termed 'self-built canals' (Bean 1971; Altunel and Hancock 1993). They are thought to form through the vertical accretion of travertine along the edges of watercourses. Bean mentions one following the main street of Hierapolis, over 2 m high. Self-built canals are of exceptional height compared with their width, and the h/w ratio may exceed 12. The structures are no longer forming but according to Altunel and Hancock (*op cit*) are mentioned by Plinius as irrigation canals. Within Hierapolis, it is clear that some at least were purposefully constructed on account of their regular geometry. The canals at the margin of the modern Pamukkale deposits are up to about 1 km in length, winding in arcs down a slight gradient. In some, several periods of deposition are apparent in the walls (Photoplate 1B). The canals contain a narrow and shal-

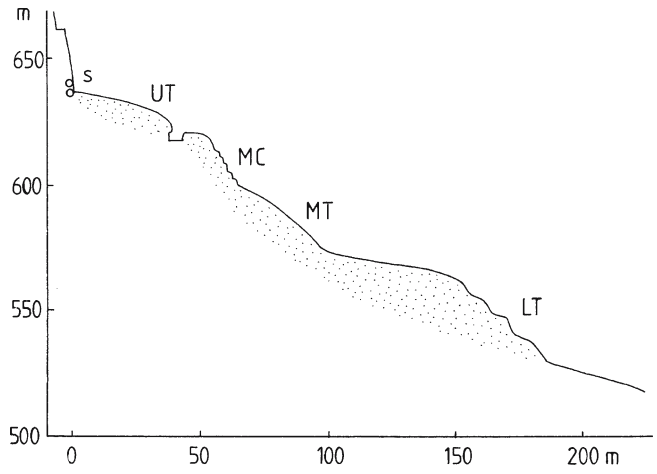

Fig. 13.
Profile of the Güterstein travertine, Germany. LT Lower Gehängetuffe and cascades; MC Middle cascade; MT Middle Gehängetuffe; UT Upper Gehängetuffe and pond; *s* springs. Travertine area stippled (after Gruninger 1965)

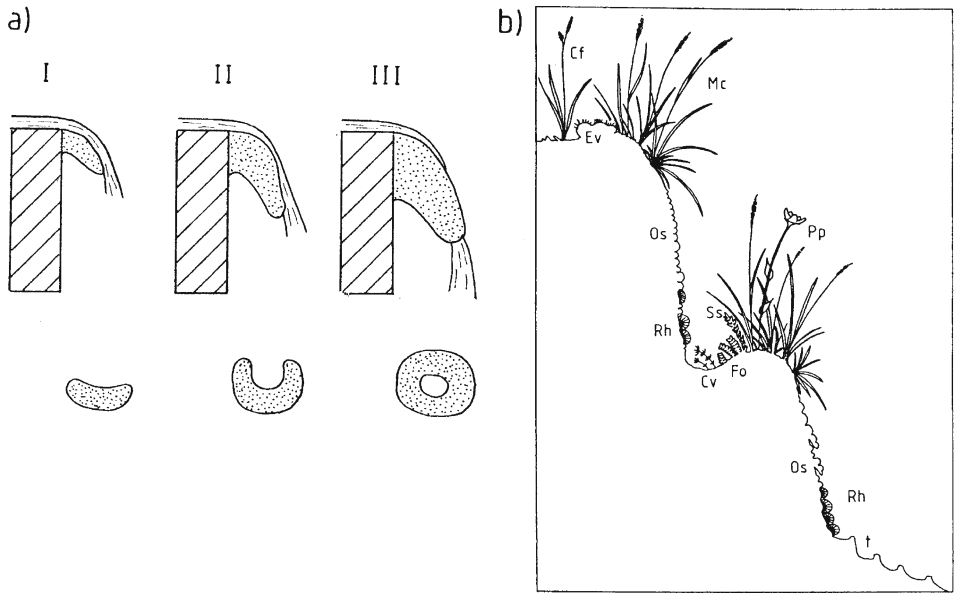

Fig. 14. Travertine tubes and crons. a) Development of travertine tubes (after Pevalek 1935). I. Small protuberant mass develops on waterfall; II mass extends and the sides begin to form a water channel; III sides meet above and tube is formed. b) Diagrammatic section through a cron in Yorkshire, UK showing some of the vegetation and the micromorphology. Cf *Carex flacca*; Cv *Chara vulgaris*; Ev *Eucladium verticillatum*; Fo *Fissidens osmundoides*; Mc *Molinia caerulea*; Os *Oocardium stratum*; Pp *Parnassia palustris*; Rh *Rivularia haematites*; Ss *Selaginella selaginoides*; t travertine minidams. (from Pentecost 1991a)

low slot like channel about 40 cm wide carrying the flowing water. The slots appear to form via dissolution and they are often surprisingly invariant in their dimensions. Water overtops the slot and seeps downslope, depositing travertine in the process, thus building up the sides of the keel, slowly raising the height. Deposition must cease soon after the water flows down the wall, since otherwise, the walls would soon extend outwards and would no longer assume their almost vertical form. Eventually the slot disappears as the flow of water diminishes. Channels are also recorded from Kocobas, Turkey (Özkul et al. 2002) and similar structures termed *tecoatle* (stone snakes) occur at Tehuacan, Mexico (Winsborough et al. 1996). They qualify as some of the most remarkable travertine structures in the world.

Other prograding structures are no less fascinating for their bridge-like forms several of which have been described from Turkey. In every case, powerful karst springs break out of steep valley sides and form protuberant cascades overhanging the main river. Eventually the growing deposit spans the ravine to form a bridge. Rivers passing beneath these deposits are often fast-flowing and aggressive, helping to maintain an arched structure and preventing dam formation. The Zamanti River of the eastern Taurus Mountains flows beneath three bridges named Yerköprü 1, 2 and 3 (Bayari and Kurttas 1997; Bayari 2002). They span a river 16–30 m in width, and are a minimum of 3–4 m in thickness, thickening towards the bank. The upper surfaces of these bridges are almost horizontal and in places support mature soils, Yerköprü meaning 'earth bridge' in Turkish (Fig. 15a,b). The bridges usually develop from unilateral perched springs, but a type forming from bilateral springs is seen in the Yerköprü-1 bridge (Fig. 15a). In this example, perched springs deposit travertine on both sides of the river, eventually coalescing over the rushing water. This bridge contains about 40,000 m^3

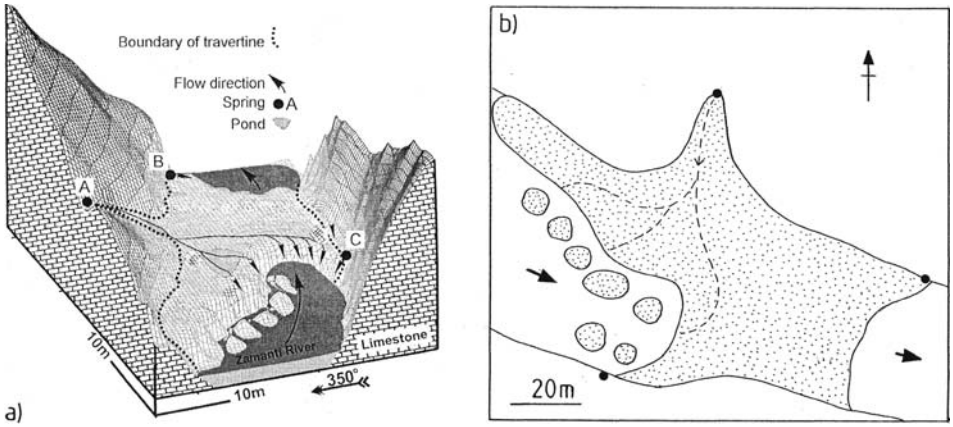

Fig. 15. The Yerköprü-1 ('Bridge 1'), Zamanti River, Turkey. a) Orthographic view of bridge. Note spring positions on both sides of the gorge (From Bayari 2002 with permission). b) Plan view showing springs (filled circles). Several blocks have fallen into the river. Travertine stippled. (after Bayari and Kurttas 1997)

travertine. By assuming the prograding structures take a half-pyramid form, Bayari estimated that the travertine could extend up to at least 20 m over the river without support. The tensile strength of the travertine would appear to limit bridges forming from unilateral springs to about 25 m, while bilateral springs could conceivably span a 50 m river. Nevetheless, even wider bridges are known. The Yerköprü Hadim of Turkey may be the largest of its kind in the world, being 250 m in length and 50 m high and wide. Another large bridge is that of the Gokteik Gorge, Burma (La Touche 1906). This structure stands 160 m above the Chaungzon River with an arch height of 60 m. Here, substantial downcutting of the river must have taken place subsequent to bridge formation. The structure provides a natural line of communication across the gorge as does the Yauli River bridge in Peru (Howard 1948). Bridges are rare in Europe, though they are known from the Auvergne (Scrope 1858; Boule 1902) and Provence (Nicod 1981).

Martel (1894) mentions a further type of bridge from the Cañon de la Scagne in the Maritime Alps formed by the breaching of a travertine dam. Tonto Natural Bridge, Arizona and the bridge at Fremont, Wyoming provide other examples from the United States (Feth and Barnes 1979). Similar bridges up to 2 m in width are fairly common among the large eroding dams of southeast China.

4.1.4 Dams

Distinguished from cascades by their localised vertical accretion leading to water impoundment as pools, ponds and lakes. The term 'barrage' is often used for this form, but implies a specific type of obstruction in English, and 'dam' is used here in common with artificial overflow dams. The essential features of travertine dams are shown in Fig. 16. Dams usually occur in series along watercourses, sometimes in a fairly regular and predictable pattern. The distance between successive dams (inter-dam distance, or IDD) ranges from about a centimetre to over a kilometre and appears to depend largely upon the gradient of the stream bed and the discharge. Each dam is usually separated by a pool or lake whose depth ranges from a few millimetres to several metres. The pools of the larger dams often contain marl, but the shallower dams may possess a range of stream crusts including oncoids. The dam itself is composed largely of travertine formed *in situ,* with the two walls meeting at a crest.

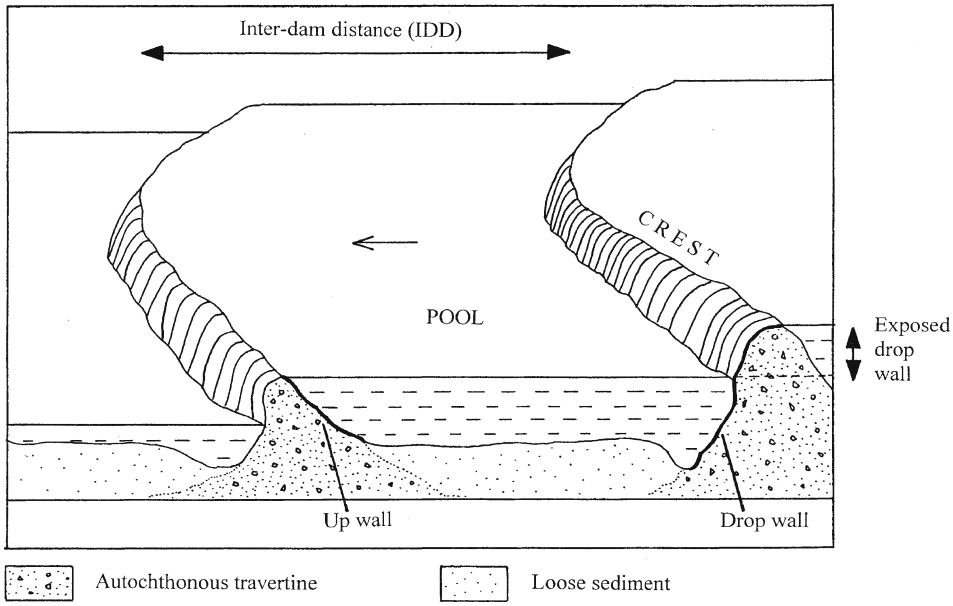

Fig. 16. Morphological features of travertine dams. For minidams some of these features are modified owing to surface tension effects

The wall over which the water cascades is termed the *drop wall* in accordance with engineering practice, and the wall facing upstream, the *up wall.* Height is best measured on the exposed drop wall, from the water level in the tailwater pool to the crest, as shown in Fig. 16 and is termed here the *exposed drop wall height* (EDW) to distinguish it from the total dam height which includes the submerged wall. The EDW varies from a few cm to >40 m, but most dams range from 0.2–5 m. With a range of five orders of magnitude, one might expect to see large differences in the morphology passing from the smallest to the largest dams. While some differences are evident, they are not as great as might be supposed, and it takes a leap of faith to accept that processes leading to dam formation are the same over the entire range of scale.

To facilitate comparisons, travertine dams have been split artificially into two groups based on their IDD. Dams with the IDD ranging from 1 cm to 1 m are termed here *minidams*, and are normally associated with trickling, rather than fast-flowing water. Surface tension forces may be more important than gravity in the formation of these structures (Section 10.2). However there is at present no evidence for a discontinuity between the stuctures of minidams and the larger *dams*, but it facilitates discussion of the various forms at the different scales. It should be noted that the IDD is a function of stream gradient, so that dams of a range of sizes may sometimes be observed in the same stream section.

4.1.4.1 Minidams

These are small-scale features most often seen in thermogene travertines (Geurts et al. 1992) and in caves where the total discharge of water is low, of the order of litres per second. On moderate slopes of about 30° the IDD is typically 1–3 cm, increasing to several decimetres on slopes less than 5°. The relationship between slope and the IDD has often been commented upon but there have been few detailed investigations. A study of a small sample of minidams

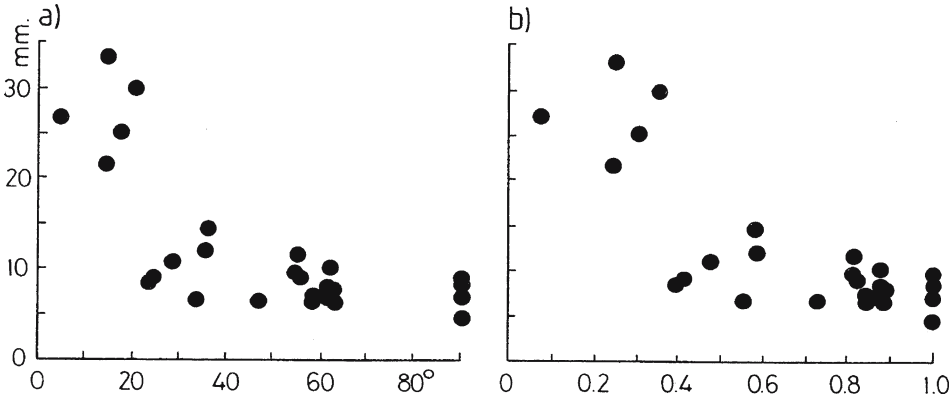

Fig. 17. Relationship between slope and inter-dam distance (IDD) for minidams. a) IDD versus angle of slope; b) IDD vs sin(slope); Unpublished data from Ingleborough Cave and the River Skirfare UK; Reotier, France and Suio, Italy

by the author showed a significant negative correlation between the average IDD and slope (Fig. 17). It appears that the IDD declines almost linearly as the slope increases to about 40°, but then changes little to 90°. The overall trend is therefore nonlinear, with a minimum IDD of about 7 mm on the steepest slopes. The relationship becomes more linear when the sine of the angle is plotted against the IDD (Fig. 17b). These dams produce some of the most intricate and remarkable surface patterns found anywhere in nature (Photoplate 10A,B). If cross sections through minidams are examined, they are found to be of several kinds (Fig. 18). The dams may be steep-sided and approximately symmetrical, rounded and asymmetrical, or cusped, with the apex (crest) pointed upstream. Cusped dams tend to be more common on the steeper slopes, with the up-walls slightly overhanging. In minidams developing on vertical surfaces, the drop walls are often almost plane and at an angle of about 20–30° to the vertical. On such surfaces, the dams often form regular, almost horizontal sets of sharply defined crests persisting over 50 cm or more. Occasionally the sets branch to form loose anastomosing structures or the crests thin out until they become imperceptible. Anastomoses are characteristic of minidams and are encountered less often in larger dams. The lines of crests, while approximately parallel, often possess regular undulations with a 'wavelength' of 5–10 mm. Similar structures are found on more gentle slopes but the crests tend not to be parallel but more anastomosing and often with broader, convex-downflow undulations. The hollows between the crests frequently have a rough, minutely botryoidal, or shrubby surface when compared with the smooth crests. Minidams appear to be especially prevalent on slopes receiving intermittent flow.

More information can be gained from the pools of water separating the dams. Length-to-depth ratios have been calculated for the series of minidams of Ingleborough Cave illustrated in Fig. 18. If one neglects the 'meniscus head' of the water droplets filling the depressions, it is possible to estimate approximate length-to-depth (IDD/total drop wall height) ratios from sections. For the Ingleborough samples, this ratio shows a significant increase with the angle of slope ($r_{Spearman}$ 0.34, P=0.04), so that for gentle slopes, the IDD is much greater than the pool depth and here, 90% of the ratios ranged from 0.15–0.8. Warwick (1952) noted a similar phenomenon in caves and described two kinds of minidam: type 'A' along steep gradients where the ratio of the pool area to depth is small; type 'B' over slight gradients where the pool area to depth ratio is much higher.

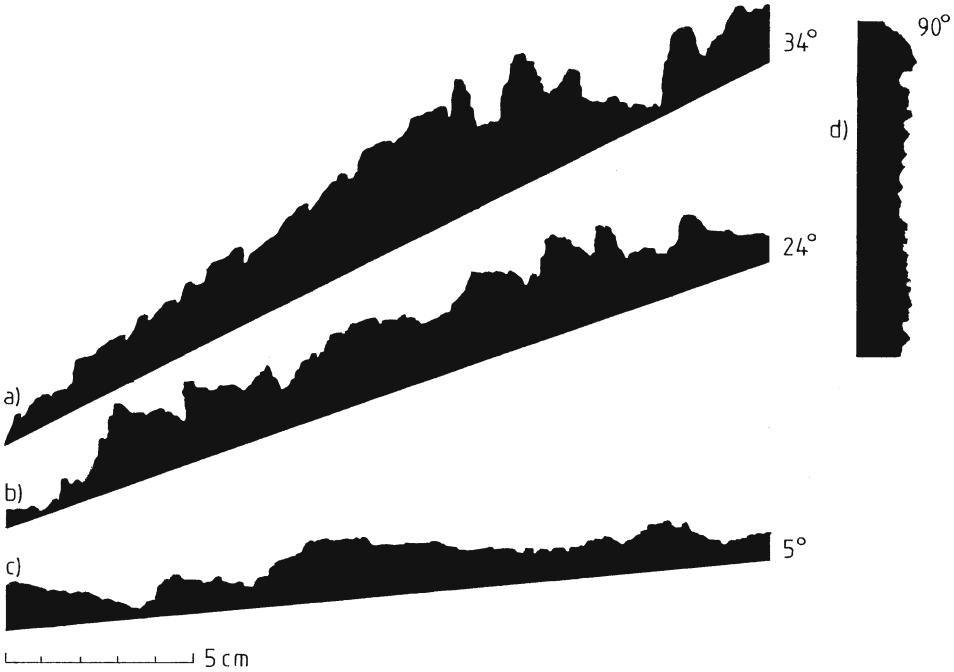

Fig. 18. Vertical profiles through some minidams. a-c) Profiles from a flowstone deposit in Ingleborough Cave, UK obtained with a mechanical tracer. d) Vertical travertine sheet from Suio, Italy obtained by 'printing' a polished rock slice directly onto the paper. Note the cusps in a) and d). Vertical and horizontal scales equal

In reality, a continuum of forms exists. The minidams of caves are usually termed 'rimstones' or 'gours'. Unfortunately, neither term is well defined. Gours include erosional features and rimstones have not been delineated in terms of size, unhelpful in morphological terms. In central Europe, travertine facies consisting of minidams are sometimes referred to as 'tetarata'. A number of formation mechanisms have been proposed (e.g. Warwick 1952) and are taken up in Chapter 10.

Certain 'corrosion rims' found on exposed limestones are similar to minidams, but are formed by quite different processes (Jennings 1985). Battistini (1981) describes peculiar rims in intertidal eolianite and limestone from Madagascar, possibly aided by cyanobacteria. Several other periodic phenomena of similar dimensions resemble minidams in their mophology, namely the ribbing of icicles, tidal ripple marks in mud, and 'sand ripples' resulting from the weathering of soft sandstones (Pentecost 1999b). The periodicity of icicle ribbing matches quite closely the periodicity of vertical minidams and both share a Gaussian distribution. There are also some physico-chemical similarities between the two phenomena. Icicle ribbing appears to be the result of surface instability induced by thermal diffusion coupled with laminar flow (Ogawa and Furukawa 2002).

4.1.4.2 Macrodams

Buildups 0.1–>2 m in height, with inter-dam distances of 1–100 m are a common feature of epigean travertines and are sometimes found in caves. Many of these structures seem to start around local obstructions such as landslide rubble, woody debris or on slope breaks

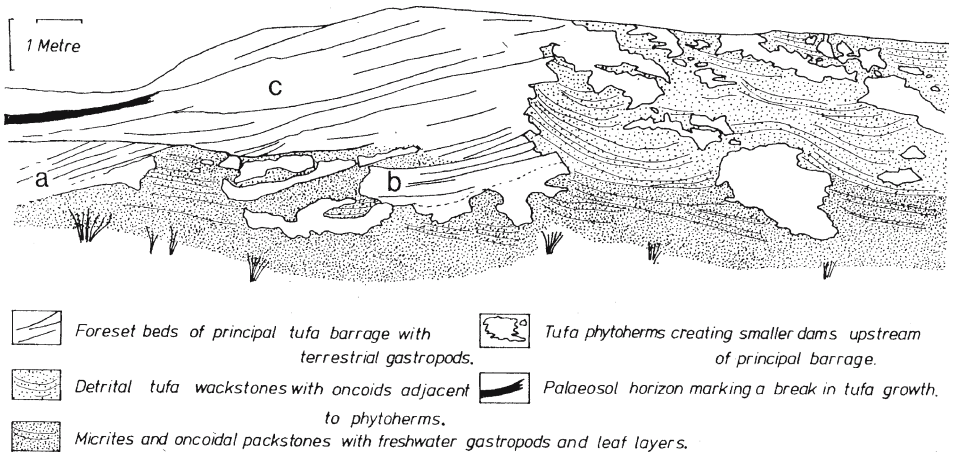

Fig. 19. Section through a Holocene meteogene dam at Caerwys, UK. a,b; early dams, c; final dam (from Pedley 1987 with permission)

(Lambert 1955; Heinrich 1967; Golubic 1969; Wright 2000; UNEP 2004) but little else is known of their genesis. Golubic (1969) suggests that initiation begins with a quiescent pool serving as a trap for detritus, locally reducing erosion and allowing a dam to build. In common with the larger cascades, they often reveal a wedge-shaped section, with extensive, frequently laminated back-fills (Emig 1917; Szulc 1983; Pedley 1987; Chafetz et al. 1994) (Fig. 19).

The larger river dams sometimes impound spectacular lakes, the best known being those of Krka (Skradin) and Plitvice, in Croatia (Emeis et al. 1987; Ford and Pedley 1992). The Skradin Falls, with a maximum height of 45 m is one of the world's single largest active travertine dams although the stepped Panda Lake Fall in China is 15 m higher (Pentecost and Zhang 2001). These dams have been subject to a number of studies and have revealed complex growth dynamics, with the faster-growing structures resulting in the flooding of slower-growing or breached dams uplake (Pevalek 1935; Kempe and Emeis 1985; Brnek-Kostic 1989). Other active dam systems have been described from the Rio Pinilla, Spain (Andrews et al. (2000), the Velin River, Italy (Warwick 1952), the Vallée de Sept Lacs, Madagascar (Salomon 1986), Band e Amir, Afghanistan (Jux and Kempf 1971; Lindner and Petelski 1984) and from Queensland, Australia (Drysdale and Gale 1997). The colourful dammed lakes along the Jiuzhaigo and Huanglong Rivers in Szechuan, China are famous tourist attractions (Photoplate 3B), replete with legendary monsters. Some sections of these valleys have broad, gently sloping expanses of turbulent water with rapid travertine deposition termed 'shoals' (Photoplate 10C). The largest is Jinsa Podi at Huanglong, measuring 1.3 km long and up to 125 m wide. They appear to be unique to this region. Large inactive dams also occur at Antalya, Turkey (Burger 1985), in Morocco (Ahmamou et al. 1989) and in southern China. Lang et al. (1992) recognise two macrodam types, namely 'cascade' and 'retention' the latter characterised by clastic backfills. The history of dam development in the Lathkill Valley, Derbyshire, UK has been investigated using a combination of ground penetrating-radar and augering (Pedley et al. 2000). Here an early Holocene phase of dam formation was followed by ponding and sapropel accumulation, ending in the almost complete cessation of deposition, possibly as a result of human activity.

In common with minidams, the larger inter-dam distances tend to be recorded on the more gentle slopes. For example, at Plitvice, the mean IDD is about 1 km and the slope 1°

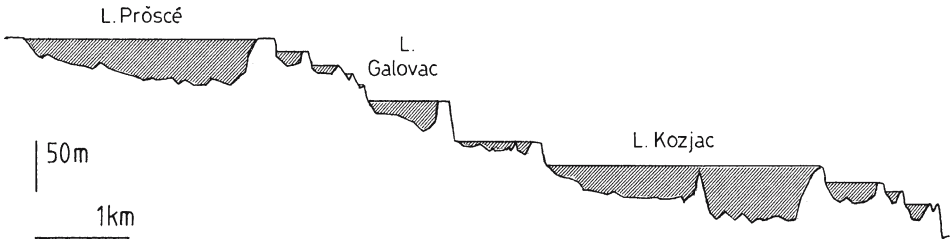

Fig. 20. Longitudinal section through the Plitvice Lakes showing the major dams. Vertical scale exaggerated x10. Redrawn from Emeis et al. (1987)

(Fig. 20). At Jiuzhaigou, China, the slope is similar with a mean IDD of 4 km. A series of dam profiles is provided in Fig. 21. The limited data indicate that the IDD increases with discharge. Large dams are rarely found on slopes exceeding 25°, but smaller ones are characteristic of certain thermogene travertine mounds. Ekmekci et al. (1995) found that the size of the thermogene Pamukkale dams and pools both became smaller as the gradient increased. Spelean dams also have shorter pools on steeper gradients but the dam height tends to increase as a result of more rapid deposition (Veni 1994; Hill and Forti 1997). A general rule therefore applies; steeper slopes support smaller dams with shorter inter-dam distances. One reason for this may be that large dams on steep slopes are too unstable to persist, but other hydrological factors such as discharge and deposition rate are also likely to influence the pattern.

Dams also develop on pre-existing travertine surfaces where deposition rates are high. Many of the Huanglong dams in China fall into this category and their morphology has been investigated in some detail. Taken as a whole, the area of the travertine-dammed pools of Huanglong decreases in an approximately exponential pattern, with pools of area 0–10 m^2 being by far the most common (Lu and Li 1992). The ratio of dam height to IDD may approach unity (Fig. 21, Photoplate 3B) and these more extreme forms are often referred to as 'pulpit basins' (Weed 1889a; Geurts et al. 1992). Pulpit basins are characterised by their steep, usually bowed and ribbed drop-walls (Photoplate 10D). A more general term for these structures, including those with less relief is 'terracette' (Bargar 1978). Terracettes often develop in a staggered arrangement and are best developed in invasive-meteogene and thermogene travertines. The term has also been used for much smaller structures however which could lead to confusion (Warwick 1952).

In a study of the Nash Brook dams in Wales, Viles and Pentecost (1999) investigated a series of 69 dams along a 250 m section of stream. Statistical analysis of their spacing indicated a random pattern and a significant positive correlation was obtained between the exposed drop wall height and the length of the dammed pool below. This would not be unexpected if the IDD was random along a stream section whose overall gradient varied little. Random patterns are not always observed in dam spacings. Three of the profiles illustrated in Fig. 21 have high variance-to-mean ratios indicating overdispersion. Log jams or beaver dams may initiate some of these structures by providing a local zone of turbulence, but others occur in deforested regions. However, in the Nash Brook, the pattern of dams could have been initiated by obstructions caused by large woody debris (LWD). There have been several studies of log dams on rivers (e.g. Marston 1982) and they are often found to be random but persistent structures capable of induration with travertine. The density of dams in the Nash Brook however was considerably higher than previously reported values

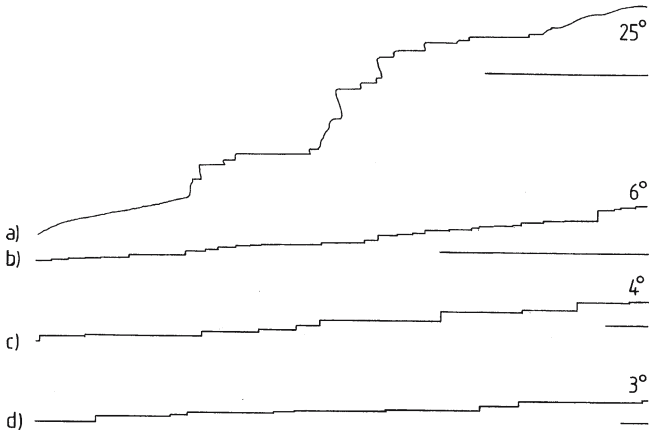

Fig. 21.
Dam profiles. a) Bather's Basins, Pamukkale; b) Nash Brook, UK; c) Hydrostation dams, Maolan Forest Reserve, Guizhou, China; d) Beishuihei River, Guizhou, China. Note increase in the inter-dam distance as the slope declines. Horizontal and vertical scales equal. After Pentecost et al. (1997) and Pentecost, Viles and Zhang (unpublished)

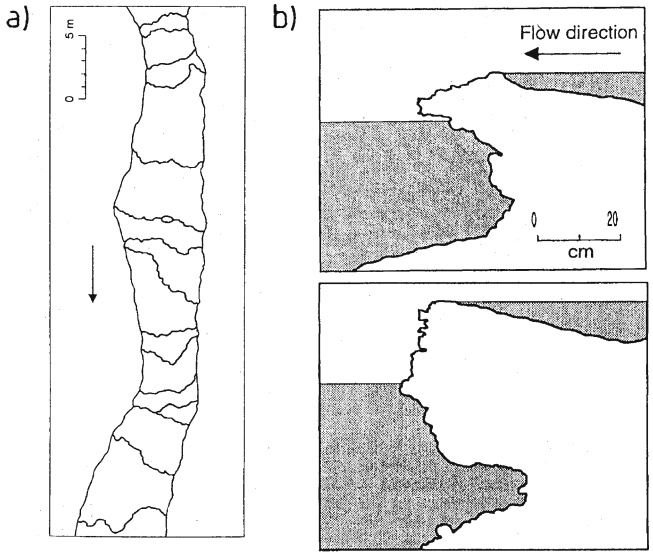

Fig. 22.
Dam morphologies.
a) Plan view of part of the Nash Brook dams, Wales showing a random pattern and tendency for some dams crests to follow a convex-downflow form and two anastomoses. Arrow shows direction of flow. b) Vertical profiles of two of the dams showing steep and undercut drop wall and gently sloping up wall. Crests colonised by *Vaucheria*. From Viles and Pentecost (1999)

for LWD, even though the site occurs in a wooded catchment. The uppermost 15 dams of Nash Brook (Fig. 22) were measured in detail and the crest lengths were found to average 1.2 times the stream width, usually convex downstream. Crests were occasionally anastomosing, but to a much less extent than those of minidams. Emig (1917) provided a detailed plan of some Oklahoma Dams and it would be interesting to revisit his sites to examine any changes in crest position and geometry. An analysis of the form of dam crests over a range of scales would also provide an interesting exercise in fractal geometry.

Profiles of macrodams often demonstrate a complex morphology. For example, most of the Cwm Nash drop walls were overhanging and this was accentuated by calcifying tufts of the alga *Vaucheria* (Fig. 22b). Similar morphologies were observed for some north Australian dams (Wright 2000) and dams densely colonised by net-spinning invertebrates are described by Humphreys et al. (1995). Geurts et al. (1992) noted some unusual dam profiles from the Coal River Springs, Yukon. They describe how the growth of algae and bryophytes

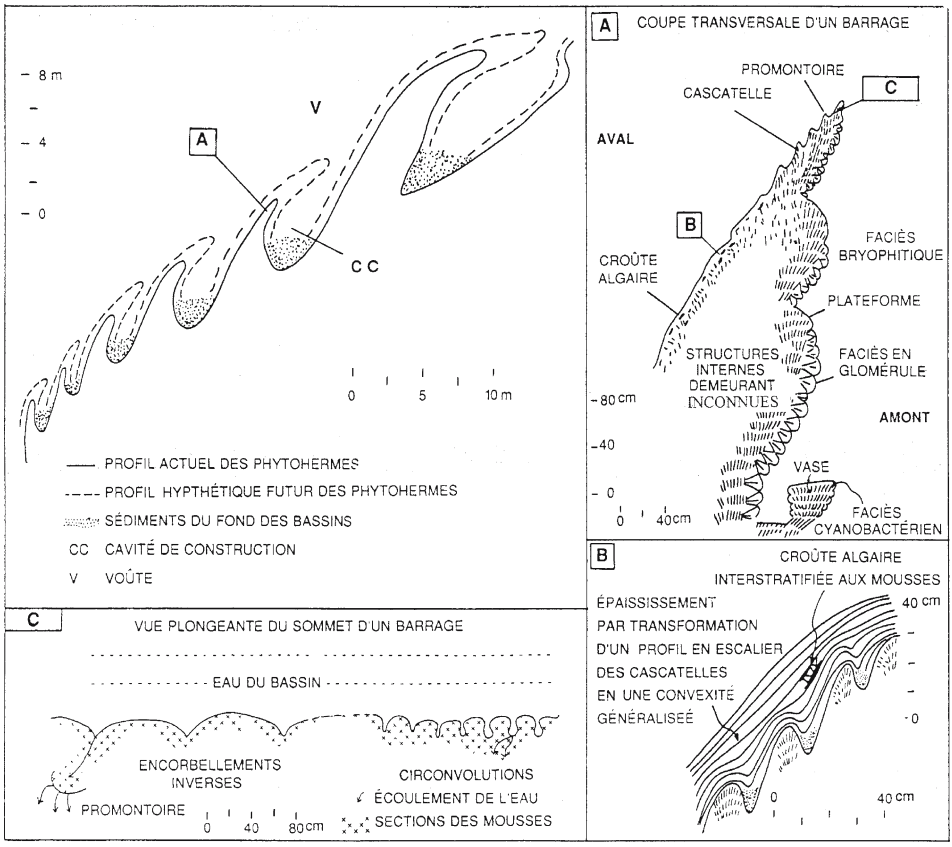

Fig. 23. The Coal River dams of Yukon showing their structure and probable mode of formation. The diagram top left shows the upstream inclination of the upper part of the biggest dams with detail of an individual dam (A) on right. Development of the hypothetical profile accompanied by the formation of vaults and cavities is illustrated. Growth of algae and bryophytes on the up-wall side cause the dam to overhang. Detail of part of a section through the drop-wall of a dam is shown in (B) illustrating the laminated fabric and the covering of minidams with a non-periodic algal crust. Inversed corbelling is shown in an elevated view directly facing a dam, with the dam pool behind in (C). Low points between the corbels allow the pool water to overtop the dam periodically along the dam crest. From Geurts et al. (1992) with permission

modify dam morphology in non-turbulent flow regimes to produce rims with 'inversed corbelling' (Fig. 23). These structures, resembling a series of regular inverted cones, possess on their up-wall side, concretionary growths of cyanobacteria while the dam crests and drop walls are colonised by mosses. The resulting structures overhang significantly on their up-wall side so that the pools are deep in relation to their width (Fig. 23b). Although the morphology is partially explained by the growth of plants in response to capillarity from the flowing water, it is also connected with slope and turbulence. The genesis of this corbelling is further elucidated by Geurts (1997). The regular buildups of convex-downstream crest segments result from radiating water waves generated by water falling with a regular spacing from the dam above. Wave interference from adjacent cascades provides overflow points and perpetuates the regular structure. Periods of quiescence associated with low water levels leads to localised deposition at the apices of the crescents further accentuating the form.

4.1.5 Fluvial Crusts

Included here are superficial deposits formed in running water but not directly associated with cascades. They develop on a variety of substrata and may be smooth and sheet-like or nodular and coralloid and frequently accompanied by oncoids. In Germany, the deposits are recognised as Bachtuffe (Klähn 1923) and in the UK they are currently the most frequently encountered active deposits (Pentecost 1993). Fluvial crusts are to be found along all gradients and merge with cascades/dam deposits. They are common along river courses in arid regions, for example, in many of the Wadi tufas of North Africa and the Middle East (Butzer and Hanesen 1968). In Britain, fluvial crusts form thin, 1–5 cm thick irregular coatings over tree roots, pebbles, gravel or bedrock (Photoplate 11A). These coatings are easily dislodged, forming cores for oncoids, and with the eroded fragments accumulate downstream as clastics. The deposits are usually colonised by algae, especially cyanobacteria, frequently resulting in a nodular form. They are found at water depths ranging from a few mm to several metres and form on steeper slopes a continuum with travertine cascades. Thermogene travertine crusts sometimes grade into low-relief mounds around spring orifices, such as those of Bullicame, Italy. Oncoids are also known but are less common. In Oman, many of the invasive meteogene travertines described by Clarke and Fontes (1990) are fluvial crusts, forming thin but extensive sheets over the bedrock. Stream crusts are analogous to the flowstones developing in caves, but their surface tends to be more irregular due to plant growth and entrapment of detritus.

4.1.6 Lake Deposits

Lakes with inflows and outflows are part of the fluvial system, and the carbonates deposited within them are often formed by similar processes and possess similar fabrics to travertines formed in rivers. Thus, at least some of these carbonates can be classified satisfactorily as travertines, resulting largely from gas evasion. The slow passage of water through lakes means that CO_2 evasion is reduced, while photosynthesis and evaporation become increasingly important as progenitors of carbonate precipitation. Lake travertines are usually confined to the littoral regions, unless submerged springs occur (sect above) and carbonate precipitation is probably enhanced by shallow water evaporation and algal photosynthesis. These travertines sometimes intergrade with lake marls, forming in deeper water as a result of the sedimentation of suspended carbonate grains. Saline lakes, frequently encountered in closed basins, often possess a 'travertine-like' littoral crust where evaporation must play an important role in carbonate precipitation.

4.1.6.1 Lacustrine Crusts

These share some features with fluvial crusts. They consist mainly of oncoids and superficial coatings on littoral sediments (Photoplate 11B) and larger reef-like accumulations. Oncoids up to 30 cm diameter occur in regions subject to significant currents (e.g. Bodensee, Germany) but are usually found in the range 2–15 cm. Well-known sites include the Finger Lakes, New York State (Clark 1900); Plitvice (Stoffers 1975); the lakes near Zahle, Lebanon (Adolphe et al. 1976); the Oligocene deposits of Limoges (Freytet and Plaziat 1982), and numerous lakes in the East African Rift (Casanova 1994) where oncoids consolidate and develop a columnar growth form. Some unusual lake crusts occur in Lago Grande (Mexico), associated with a range of cyanobacteria (Winsborough et al. 1994). Travertines occur in lakes with salinities ranging from <1 to >300‰ TDS, and evaporation aided by degassing is probably responsible for deposition at many sites. At some there are intergradations with calcretes and other evaporites.

4.1.6.2 Reefs

Sizeable accumulations of travertine-like reef are sometimes found attached to sediments or rock walls at lake margins. Their origin is unclear, but in Green Lake, New York State the reefs are associated with 'whitings', where some form of agglutination process, possibly microbially mediated occur (Thompson and Ferris 1990). These deposits although resembling travertine, may not be primarily the result of degassing and need further investigation. Similar reefs occur in Lake Annecy, France and Pozzo Azulas, Mexico (Photoplate 11C). The latter is a small spring-fed lake remarkable for the occurrence of large blade-like calcite morphologies in deeper waters. Whitings do not appear responsible for these deposits but diatom activity is suspected (Winsborough and Golubic 1987). The 'algal biostromes' of Great Salt Lake, Utah consist of ring-like structures, elongate mounds and 'tongue festoons' in shallow (<4 m) water, associated with the cyanobacterium *Aphanothece packardii* (Carozzi 1962) and cover an area of 250 km^2. Other anomalous forms include the 'big heads' of Walker Lake, Nevada, (Newton and Grossman 1988); the columnar reefs of the Idaho Hot Spring Limestone (Straccia et al. 1990); the peculiar bowl-shaped crusts 0.3–3 m in diameter along the shore of the ancestral Dead Sea (Buchbinder et al. 1974) and the nodular, stromatolitic crusts of Wondergat, South Africa (Gomes 1985). Deposits may also form in dam pools and include concretions, shrubs, and ooids. There are numerous examples of fossil reefs from the East African lakes including 'Ox-tongue' forms in Suguta Valley, Kenya and the columnar stromatolites of Lake Manyara (Casanova 1994). Lake depth has a considerable influence and many of these forms are classified as freshwater stromatolites.

4.1.7 Paludal Deposits

Low-relief accumulations forming in areas of impeded drainage are included here. Local centres of consolidation are provided by grass and moss cushions leading to small irregular accumulations of protuberant travertine, often divided by braided stream channels. Deposits occur worldwide but active sites appear to be limited in populated regions such as Europe where wetland drainage and water-table lowering seem to have led to their demise (Goudie et al. l993). Many inactive paludal travertines have come to light in former wetland areas, but there are few descriptions of modern sites. A well known relict example occurs at Ehringsdorf, Germany (Steiner and Wagenbreth 1971).

Situated in low-lying terrain, with an elevated water table, paludal sites are often associated with shallow standing water. In the UK, the calcareous mires at Malham and Sunbiggin Tarns provide good if small examples (Photoplate 11D). These deposits are often found mixed with *Chara* marls and a rich malacofauna, often providing useful material for palaeoenvironmental investigations (Section 12.2). Where thermal springs break out in areas of impeded drainage, rapid deposition often occurs around the stems of reeds and grasses to form a 'reed' or 'macrophytic' travertine' (Guo and Riding 1998; Valero-Garcés et al. 2002; Özkul et al. 2002). The deposits frequently contain a high proportion of terrigenous material, are vulnerable to erosion, and often possess a deltaic structure including a large proportion of clastic carbonate. Apart from the localised impregnation of large bryophyte cushions, the deposits are soft and marly providing little relief. After burial, they are often difficult to locate unless auguring is undertaken or rabbits are present. Paludal travertines usually contain a large amount of clastic material and may grade into entirely clastic accumulations. Numerous examples of this type of deposit are known from the Western Desert in Egypt (Crombie et al. 1997).

4.1.8 Cemented Rudites and Clasts

Surface-cemented rudites and clasts consist of cemented scree, alluvium, breccia, and gravel formed as a result of ground- and surface water degassing to the epigean atmosphere, but it is not always possible to distinguish between near-surface and hypogeal cementation, the latter resulting from precipitation from calcite supersaturated groundwaters. Mixing of groundwaters leading to common-ion precipitation and evaporation may be significant in some areas, particularly at lower latitudes resulting in calcrete formation. Coarse sediments provide easy pathways for flowing water and gas exchange providing they occur close to the surface. Cemented gravels are highly resistant to erosion, forming pronounced benches in many regions of the world. Numerous examples are known in the UK where river gravels and coastal shingles are frequently involved (Davies and Keen 1985; Pentecost 1993). Cementation is usually localised and irregular lumps of cemented gravel weighing several tonnes and often displaced by slippage, are a common feature along some river systems (Photoplate 11E). In these cases, cementation appears to have been achieved via the degassing of shallow seepage waters. Cemented breccias have been described widely from Poland and adjacent countries where they were shown to be deposited under vadose conditions (Gradzinski et al. 2001a). Cemented rudites are also found on coasts, where calcium bicarbonate groundwater seepage occurs onto shingle banks in the upper littoral and supralittoral (Pentecost 1993). On Shetland, UK, travertine-cemented screes appear to originate from the local dissolution and reprecipitation of calcite and other minerals (Flinn and Pentecost 1995). They have also been observed in some travertines from the Italian Alps (Spötl et al. 2002). Most of the travertine cements are of calcite, but aragonite is an important component of cemented gravels at Las Coladas, an Andean salar (Valero-Garcés et al. 2001). In this case, it is unclear to what extent the deposition is due to CO_2 evasion by the thermal springs entering the lake, or the mixing of the saline lake waters and spring waters. If however evaporation plays a major role they would best be termed beachrocks (Section 15.3). Some forms of calcrete are also very similar to these deposits, especially in arid regions where subsurface cementation is common.

4.1.9 Speleothems

Speleothems composed of calcite or aragonite are hypogean travertines. Caves contain a great variety of travertine morphologies from the familiar stalactites and stalagmites to rarely seen conulites buried in the sand of cave floors. Hill and Forti (1997) provide a good overview of these forms and recognise five hydrological mechanisms responsible for most of the variation: dripping, flowing, seeping, pooled and splashing water. Other processes such as evaporation, airflow, and joint geometry account for much of the remaining variation. As with epigean travertines, 'depositing systems' are recognisable where two or more of these processes operate in juxtaposition providing an endless variety of speleothem forms (Fig. 24).

Water drops suspended from the ceilings of limestone caves lose a small quantity of CO_2 and a trace of calcium carbonate is deposited on the ceiling as a ring about the same size as the drop. With a slow and steady drip-rate, the ring of carbonate increases in length and the drop becomes suspended at the end of short carbonate tube. The tubes continue growing until their weight exceeds the cohesive force holding the tube to the ceiling. The diameter of these stalactites has been shown to be a function of the drop surface tension and the acceleration due to gravity (Curl 1972). These stalactites are called 'straws'. They are noteworthy because crystal growth only occurs at the basal drip-point to produce one, or at most a few calcite crystals with their c-axes vertically oriented (Kendall 1993). Conical stalactites prob-

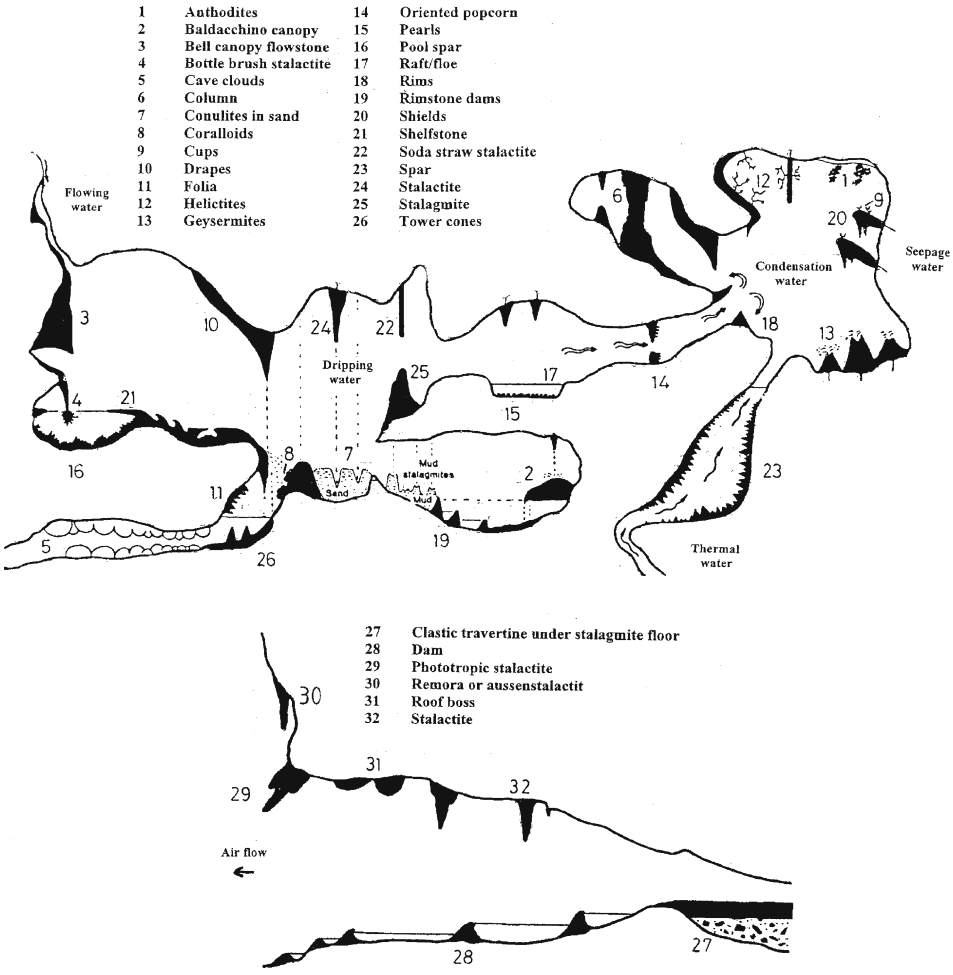

Fig. 24. Diagrams of the main spelean travertine types. Above: deep cave deposits (upper diagram modified from Hill and Forti 1997, with permission). Below: deposits at cave thresholds

ably begin as straws, but receive additional carbonate largely from external seepage from other sources on the cave roof and calcite crystals with a different orientation. They are rarely symmetrical due to the irregular pattern and seasonality of seepage points. Where seepages follow a crack, 'curtains' often result.

Drops falling to the cave floor continue to lose CO_2 and form stalagmites. Stalagmite size is not limited by weight in caves and they can form far more massive structures, often approaching the cave ceiling, or merge with stalactites to form pillars. Stalagmites are often found to be of similar diameter to the stalactites forming above them, and this is presumably related to the extent to which the drip water can be dispersed from its point of impact and the thickness of the water film (Dreybrodt 1988). Despite this, stalagmites tend to be larger than the overhanging stalactites, possibly because the drip residence time is longer. Stalagmites have a growth pattern quite unlike that of stalactites and are termed 'cuspate'. Their diameters can be predicted theoretically (Section 10.4.1).

A distinction is often made between speleothems developing from dripping water (dripstones) and those forming through more general seepage or surface flow. Cave flowstones more closely resemble the cascade and stream crust deposits of epigean travertines but they are generally more dense and with a smoother surface. Where the flow of water is reduced to a film, complex and often fluted draperies are common. The fluting is often periodic with a cm-scale spacing that is probably a manifestation of the Rayleigh-Taylor instability (see deBruyn 1997).

A number of 'erratic' speleothems are described by Moore and Halliday (1953) and detailed by Hill and Forti (1997) under the terms helictites, anthodites, coralloids and concretions. They also include shields, subcircular masses of travertine with a flat surface and an overhanging and often fluted drop wall (Fig. 24). They are 1–5 m in diameter and may form from water seeping from horizontal cracks in the cave wall.

Helictites are related to straw stalactites but they are highly irregular in form and usually no more than a few decimetres in length. Their unusual shape is thought to originate from a reduced supply of drip water and frequent blockage of the feeder canal. They are composed of aragonite or calcite and several subtypes are known. The most common are the vermiform helictites and they sometimes take a helical form. All possess a small central canal through which the cave water flows and numerous hypotheses, summarised by Hill and Forti have been proposed for their formation. Localised hydrostatic pressure in a calcite film, followed by CO_2 evasion and the sequential crystallisation of calcite with rotating crystallographic axes appears to go some way in explaining their unusual form.

Botryoidal forms are common on cave walls and range from small pin-head like protuberances to large grape-like masses up to 1 m in diameter. Some are associated with pool deposits or water splashes. Anthodites are formed of aragonite and consist of finely textured radiating structures with individual crystals ranging from a few mm to several cm. In some cases the characteristic prism angle of 63° 48' can be identified in the orientations of the branches. They are often flower-like, extremely delicate and a wide range of forms has been described. They are frequently associated with helictites and probably form slowly from seeping water, usually with significant evaporation.

Coralloids are delicate but more robust speleothems known under a variety of names such as 'cave popcorn' and 'cave coral'. Formed of calcite or aragonite, they are also known to form in subaqueous and subaerial environments. Most coralloids appear to be subaerial, developing from seepage waters or splashes. Stable isotope measurements have shown that evaporation is important in their formation. Subaqueous coralloids, known as 'tower coral' also appear to result from evaporation, and sometimes occur in the pools of minidams.

Concretions are distinguished from botryoidal speleothem in being unattached to a surface of which cave pearls are the best known. Cave pearls form in shallow pools and range in size from <1 mm to 15 cm in diameter, but mostly 5–20 mm. A layer of travertine builds around a central, foreign nucleus and normally consists of calcite with the c-axes perpendicular to the surface. The rounding of these concretions may be supposed to be similar to those leading to the growth of oncoids, namely frequent random movement leading to an overall equal exposure to supersaturated solutions and equidimensional growth. There are however, two important differences. In cave pearls, the energy for movement is supplied by water drips so that the pearls move within a confined space. Also, the 'ball mill' effect arises from their close proximity, where abrasion between adjacent pearls helps to maintain their shape and imparts a smooth lustre to the surfaces. Water drips can only move the smaller pearls and the largest must continue to grow almost statically, subject to little more than the crystal growth forces (Hill and Forti 1997). A rare type of cave pearl, known from Castleguard

Cave in Canada is divested of its spherical symmetry and takes on a cubical form (Robèrge and Caron 1983). Their origin is not understood.

Calcite bubbles also occur in caves, and are probably formed in similar manner to the foam-rock bubbles of epigean travertines. The bubbles occur in quiet pools. They are less than 1 cm across with walls of about 0.2 mm (Hill and Forti 1997).

Less satisfactorily defined deposits have been described from caves but have received little attention. They include two forms of coatings and crusts, distinguished as subaqueous and subaerial. The subaerial forms include deposits formed as a result of condensation water. They are believed to develop through the deposition of calcite particles present in aerosols onto cave walls, modified by water condensates. These deposits cannot be regarded as travertines. Subaqueous crusts line cave pools and often become concretionary with time and are formed through CO_2 evasion. They are sometimes called 'cave clouds' (Fig. 24). Parallels may be found with epigean stream crusts and littoral lake deposits.

Also associated with quiescent pools are surface deposits of calcite resembling ice. They are variously described as 'floe' or 'raft' calcite and are also commonly found in epigean travertines, especially thermogenes and invasive meteogene deposits. Minor disturbances eventually lead to the disintegration of the floe and it falls into the pool where it may accumulate to from substantial layers of confetti-like sediment. Occasionally, the rafts sink at a single location as a result of ceiling drips where they may accumulate to form subaqueous 'cave cones' (Photoplate 12A). Raft-like deposits often thicken at the edges of pools and become attached to the margins to form 'shelfstone'. Another most unusual form of calcite also occurs in such pools. These are the hollow 'cave cups' whose rim is level with the water surface while the cup itself remains dry. Most cups are polycrystalline, but occasionally monocrystalline cups are found with a pyramidal form (Gèze 1968). They are formed from calcite rhombohedra at the water surface where the pyramidal sides prevent water from covering the crystal. Growth proceeds at the crystal edge and a stepped hopper crystal results with a cup-like form. The more regular, rounded cups form in a similar manner.

Another common variant, occurring mainly in warmer parts of the world at cave thresholds is known by a variety of names: 'Aussen stalaktiten' (Lehmann 1954); 'Stalactitevorhang' and 'remora' (Pentecost 1993). They develop in slow or intermittent water flow over steep slopes (Matonickin and Pavletic 1962) and consist of stalactite-like masses often of grotesque, gravity-defying forms. These deposits merge into the classical prograding cascades where flow is more persistent. Remora also occurs on steep limestone cliffs and is well developed in the tower karsts of Guilin, China where there is high seasonal rainfall and a warm climate. The deposits are exceptionally dense and hard, often forming below bedding plane seepages and they are probably formed in part through evaporation of thin water films. They are poorly laminated but often associated with black or brown growths of cyanobacteria. An example is provided by the 'Christmas tree', a tourist attraction in Mexico (Photoplate 12D). In the UK these deposits are uncommon, but good examples occur at Boggle Hole Gorge, Yorkshire. In rare instances, remora depart from the vertical due to the preferential deposition of carbonate on the more illuminated side. These forms have been described as 'deflected stalactites' and have even been noted developing under the influence of seawater (Taborosi et al. 2003). The phenomenon has been attributed to algal photosynthesis (Dobat 1966; Rong et al. 1996) but might also be the result of increased evaporation and CO_2 evasion on the warmer illuminated surface. For example, DeSaussure (1961) described 'phototropic cave coral' growing out toward cave entrances, subsequently explained by Hill (1978) as resulting from evaporation by the drier inflowing air. At thresholds, cave dripstones often give way to the 'Aussen stalactiten'.

4.2 Allochthonous (Clastic) Travertines

Forming in turbulent environments, travertines often undergo erosion soon after formation and many deposits contain a significant proportion of clastic material (Garcia del Cura et al. 2000). Travertine-marls forming in paludal environments are especially prone to redeposition and a range of predominantly clastic deposits have been distinguished. Typical morphologies include bars, lenticular 'spreads' in flood horizons (Minckley 1963; Evans 1972) (Photoplate 12B), valley-fills ('Taltuffe') and alluvial fans forming at the foot of escarpments (Burger 1990). Levees and 'overbank deposits' occur along some rivers (Lyell 1829). Back-fills in travertine-dammed lakes often consist of a mixture of clastic travertine and lake marl. Pedley (1990) classified clastic travertines into five types: phytoclast tufa – cemented crusts formed around plants; oncoidal tufa; intraclast tufa -silt to sand-sized particles carried downstream and redeposited as calciclastic grain-supported fabrics in fluvial channels; microdetrital tufa consisting of micrite which is either structureless or clotted, sometimes referred to as 'spring chalk'. These deposits have been collectively referred to as 'detrital' by Julian and Martin (1981). Oncoids provide an unusual example of a deposit which oscillate from autochthonous to allochthonous depending upon whether they are in a state of motion or fixed and accreting. Buccino et al. (1978) followed by Pedley (1987, 1990) use the term 'phytoherm' to distinguish travertines formed in association with bacteria and plants developing *in situ* but including a variable amount of clastic material. The term is not strictly a botanical equivalent to 'bioherm', which has also been used to describe travertines (e.g. Lang and Lucas 1970) and generally understood to imply a mass of cemented bioclasts, the latter consisting of actively calcifying marine organisms (e.g. algae, coral). Travertine algae, though encrusted with carbonate, rarely biomineralise in the sense of common marine algae such as *Halimeda* and are not strictly bioclasts (see Pentecost 1990c).

There have been few investigations of clastic travertines *per se*. Kite and Allomong (1990) describe an alluvial deposit from Virginia and Mathews et al. (1965) noted that travertines are moved several km downstream during floods. Many of the large Italian deposits contain a significant proportion of clastic material, often as dam fill (Chafetz and Folk 1984). Pentecost and Spiro (*unpublished*) made a grain-size analysis of back-fill deposits at Caerwys, Wales but found no evidence of fining-upwards sequences where deposition occurs under declining flow.

4.3 Travertine Caves

Several types of travertine cave are known. The most common form is the primary cave system frequently occurring beneath cascades (Photoplate 12E). These develop as the travertine builds a protuberance over a steep cliff or dam which eventually meets the ground leaving a cavity behind it in the same manner as a travertine bridge (Stirn 1972). Three primary caves are well known tourist attractions. The Olgahöhle at Honau, Germany (Ziegler 1972) consists of a dual passageway 50 m long and up to 6 m wide, parallel to an old dam system. A similar cave occurs at Lillafured, Hungary where a series of chambers interconnected by artificial tunnels are developed within a massive travertine cascade. Travertine caves, often with sediment infills, are common in this country (Korpás 2003). The third is the Huangguosho Falls Cave in Guizhou Province, China which provides spectacular glimpses of the falls from a series of natural windows (Fig. 12b). Numerous caves occur in the great deposits at Antalya, Turkey (Burger 1990) and in the United States, a travertine cave at Twin Buttes, Arizona is used by Zuni Indians for ceremonies (Feth and Barnes 1979). Another Holocene cave is described from Switzerland by Eikenberg et al. (2001). The undermining of travertine mounds built upon soft sediments also results in small caves (Gradzinski et al. 2001b).

Caves are noteworthy for their mammalian remains and artefacts, and those in travertine are no exception. In fact, some of the most important primate finds occurred in primary travertine caves of the Ghaap Escarpment, South Africa. A study of many caves along this escarpment led McKee (1993a) to classify them into four types: 'carapace' (= primary) caves, pipes (solution cavities and potholes), river-carved rock shelters and vadose caves. Previous work by Peabody (1954) identified pipes of two types in these travertines. The first appeared to result from the corrosive action of plant roots, usually terminating as a hollow cone. Similar perforations have been attributed to the growth of *Pistacia integerrima* roots in some Indian travertines (Pant and Tewari 1984). The second consist of helicoidal pipes or potholes and result from the well-known rotary action of stones on stream beds. McKee (*op cit.*) found examples with diameters as large as 3.5 m with the bottoms filled with water worn-pebbles. Even larger examples can be seen along the Beishuihei River in Guizhou, China. Another cave type is formed by the erosive action of flowing water on travertine-lined river banks. At bends, the water often carves a cup-shaped cavity, rarely more than a few metres deep either as a result of corrasion, or by undercutting, as in Lost Sole Cave, Mokgareng (McKee 1993b). Finally, there is evidence of vadose caves in these travertines. The origin of relict travertine caves is obviously important when they contain major fossil assemblages. Caves may also form through other processes. Springs emerge from gypsum-lined travertine caves near Banff, Canada, and their formation attributed to carbonate dissolution by sulphuric acid. The acid appears to form via sulphide oxidation, the sulphide being generated by bacteria (Van Everdingen et al. 1985). A similar phenomenon occurs in Virginia (Hubbard et al. 1990). At Mammoth Hot Springs, Wyoming, Bargar (1978) describes collapse features 1–6 m deep sometimes opening into small caves. The 'Grottoes' of Elephant Back terrace and the Stygian Cave are well known features possibly resulting from 'inverse solubility', i.e. dissolution engendered by cooled water which has become undersaturated with respect to aragonite/calcite (Bargar 1978). Alternatively they may be vadose caves formed by CO_2-enriched groundwater percolation. Collapse features opening into small caves also occur at Pamukkale, Turkey. This site boasts the celebrated Plutonium of Hierapolis, an old travertine cave containing high concentrations of carbon dioxide.

4.4 Postdepositional Effects On Morphology

The rapid and localised build-up of a resilient limestone will modify the surrounding environment by altering the drainage and subsequent erosion patterns, as well as undergoing erosion itself. Some of the changes are difficult to predict, while the karstification of the travertine progresses in a manner similar to that of other limestones. Less obvious processes can also lead to change. In Spain, a large lacustrine-paludal travertine complex situated in the central Ebro depression, has been shown to have become downwarped by the the dissolution of underlying evaporite deposits by rising groundwater (Arenas et al. 2000). As the mass subsided, further travertine was deposited in the developing basin.

4.4.1 Karstification

Some deposits have undergone considerable modification by groundwater percolation (karstification), exhibiting all of the features seen in hard limestones. In the Drevenik Mountains, Slovakia, Vitek (1973) described karren, surface pitting and honeycombing typical of bare and covered karstified travertine. Karren are also well developed in parts of the Antalya deposits in Turkey (Burger 1990). Much of the 'high level' travertine possesses rundkarren,

produced by aggressive waters dissolving the rock under a soil cover. Rillen karren also occur along parts of the '50 m level'. Many of the Italian Pleistocene travertines are also karstified with old erosion surfaces and palaeosols seen in quarry sections (Chafetz and Folk 1984) and large solution hollows occur in several areas. The deep depressions now occupied by Lago Regina and Lago delle Collonelle, Tivoli have relict stalactites on their walls indicating that they were once dry (Pentecost and Tortora 1989) and other richly fossiliferous depressions are known (Segre and Ascenzi 1956). Small poljes occur in the eastern part of the Antalya deposit (Burger 1990) one of which is drained by a swallow hole (Photoplate 12C), but the nature of the corrosion is unclear. They may be initiated by collapses over large caves. Glover and Robertson (2003) made a re-appraisal of the Antalya deposit and considered that some of the dam structures described by Burger were also solutional features.

Burger (1990) recognised two types of calcretisation on the Antalya travertines. Exposed surfaces become intensely indurated and transformed into a massive almost unstructured limestone, no longer recognisable as a travertine. Such duricrusts are widely distributed in the warmer regions of the world. A second type termed *bodensinter* formed beneath a soil cover and is also widespread. It is more sparry than the surface crust and 'rings' when struck with a hammer recalling the Caribbean karst 'clinker'. It is covered in rundkarren and develops to a depth of about 2 m below the surface. It appears to form a fairly well defined layer and is plowed out by farmers to improve the land. Such deposits are probably widespread. Similar material occurs on the Piano del Diavolo, near Canino Italy -probably the most extensive area of travertine in that country. Soil-derived CO_2 corrosion may also be responsible for planation of the Antalya travertines (Burger 1990). The Pleistocene Cannstatt travertines of Germany show evidence of karstification, associated with the deposition of iron, manganese and other heavy elements (Koban and Schweigert 1993).

4.4.2 Soils

Soil development on a rock with a traceable history should prove rewarding but little is known of the soils developing on travertines. McFarland and Sherwood (1990) describe a soil developing over a deposit and provide a profile and analysis of the section. They found evidence for secondary calcite induration at the travertine surface attributed to capillary movement of shallow groundwater. Edmonds and Martens (1990) describe the exchange capacity and carbonate content of several Virginian mollisols overlying or associated with travertine. They possessed an organic A-horizon depleted in calcium carbonate suggesting solution with reprecipitation at lower levels. In England, a rendzina 3–8 cm in depth has developed upon a 250 year-old travertine. About half the deposit was covered in a soil supporting 47 plant species (Pentecost 1981). Palaeosols are a common feature of travertines and often provide useful palaeoenvironmental data. Pedley (1987) described palaeosols from a Postglacial travertine dam complex in Wales. They were a few centimetres in thickness and often interdigitated within the deposit and represented temporary cessation of carbonate precipitation. Palaeosols have also been described from Hungary (Scheuer and Schweitzer 1981) and Denizli, Turkey (Özkul et al. 2002).

4.4.3 Mass Movement

Manfra et al. (1976) suggest that epeirogenic movements have probably altered springline positions and affected travertine deposition in several parts of Lazio, Italy. Similar phases of uplift may have been responsible for the sequence of eight terraces in the Gerecse Moun-

tains, Hungary beginning in the late Pliocene (Scheuer and Schweitzer 1973). Such phenomena may also be responsible for the huge terraces of Antalya with the lowest currently below sea level, indicating a period of downwarping and/or sea level rise (Burger 1990). Four step-like sequences occur in the Granada Basin, Spain dating back to the late Pleistocene and have been likened to prograding marine carbonate platforms (Martín-Algarra et al. 2003). Tilting, warping and faulting of the Algerian crust has led to drainage reversal, and the progress of activity has been followed by travertine formation (Julian and Martin 1981). Similar observations have been made in France (Ellenberger and Gottis 1967). More extensive post-depositional faulting is probably responsible for alignments detected by remote sensing the Antalya travertine (Aydar and Dumont 1979). Open fissures parallel to active extensional faults have been identified in the deposits at Pamukkale, Turkey (Altunel and Hancock 1993) and earthquakes are thought responsible for the travertine collapse at La Roche Fontaine, France (Pareyn and Salimeh 1990) and the fracturing of a New Guinea deposit (Humphreys et al. (1995). Heimann and Sass (1989) show how travertine deposition over a wide area prevailed under sluggish water in the Hula Valley, Israel for hundreds of thousands of years but deposition ceased when tectonic activity led to the incision of river channels and water table lowering.

Smaller movements occur when the mass of accumulated travertine causes displacement of underlying incompetent beds, or downslope movements following fracture. Good examples of tensional fractures are known at Mammoth Hot Springs (Bargar 1978) and the travertine landslide at the Silver Gate deposit was probably initiated by this process. Block slippage on a substantial scale has been noted at Vysne Ruzbachy, Slovakia (Lozek 1969), Aveyron, France (Ambert and Tavoso 1981) and Shelsley Walsh, UK. (Pentecost et al. 2000a). Many of the large fractures seen in the Italian travertine quarry faces are probably of tensional/settlement origin.

4.4.4 Effects on Fluvial Systems

The presence of travertine in fluvial systems can profoundly influence their development. For example, dams can change the pattern of erosion and alluviation dramatically within a river system. This in turn has implications for further development of 'travertine systems' providing clastic materials and a range of new environments for travertine deposition. In Derbyshire, England, the Wye Valley dams are today undergoing degradation due to reduced accretion accompanied by increased erosion (Pedley 1993). Where a sequence of travertine deposits exists, the palaeogeomorphology may be interpreted. Pedley (1987) showed how the Caerwys travertines in Wales developed after the initial incision of a tributary of the River Wheeler from a braided stream. Ultimately, the Wheeler tributary breached the main dam leading to incision, water table lowering and the end of travertine deposition. At Matlock Bath, UK, the River Derwent has been diverted 100 m to the east by an impinging travertine forming below a thermal outfall (Pentecost 1999a). Cemented alluvium has also been reported to modify river courses in arid regions (Carthew and Drysdale 2003).

Limestone Solution, Groundwater and Spring Emergence

Groundwater solutes source the ions responsible for most travertines. Rainwater and snowmelt infiltrates soil, then reaches the water table and flows along a potential gradient until it is returned to the Earth's surface as a spring or seep. The flow of underground water is complex, especially in regions underlain with folded and faulted rock or where mixing occurs with deeper thermal sources. Springs occur where a water table intersects the land surface and the level of the water table varies with topography, geology, climate and time. This chapter explores relationships between travertine deposition, groundwater circulation and subsurface geology.

5.1 Limestone Solution and Groundwater

Most groundwater originates from percolating precipitation. Rainwater seeps through the upper layers of rock and soil by gravity to a depth where other forces come into play, and the flow gains a lateral component. Most soils contain a significant fraction of organic matter. Microbial decomposition and root respiration add carbon dioxide to the percolating water, reducing the pH. These waters are capable of dissolving calcium carbonate in the soil and underlying bedrock forming a dilute solution containing calcium and bicarbonate ions.

5.1.1 Meteogene Source Waters

The solubility of limestone in carbon dioxide solutions was well established in the latter part of the nineteenth century. Geologists soon recognised the importance of this in sedimentary cycling and landscape evolution and there have been many studies on the nature and rate of limestone solution (White 1988). Carbon dioxide is the major 'solvent' of limestone but other acids are present in precipitation, e.g. H_2O, HNO_3 and H_2SO_4 all of which dissolve limestone. The strong acids are normally present in trace amounts but sulphuric acid may be released in considerable quantities from limestone via pyrite oxidation or indirectly from the soil through bacterial activity. Weaker humic and fulvic acids are released from soil but their corrosion potential is not thought to be significant. The carbon dioxide responsible for limestone solution comes from several sources, as explained in Chapter 2. These sources differ in their location and reaction rates may be expected to vary as a result of this. The kinetics of carbonate dissolution are also complex. If it is assumed initially that the concentration and supply rate of CO_2-rich water remains constant, then the rate of solution depends upon five major factors: the surface area of rock in contact with this water; the type of flow, i.e. laminar or turbulent; the type of rock, particularly the proportion of calcite to dolomite; pressure; and temperature. Temperature is probably the most significant because of the strong dependence of chemical reaction rates, plus its effect on water viscosity and the diffusivity of

ions. As temperature rises, these factors combine to increase the dissolution rate. Rock surface area can vary over orders of magnitude; low in tight, jointed rocks characterised by conduit flow; high in porous rocks like the Chalk where diffuse flow is important. The presence of other ions in the water may also be of interest. If a common ion is present, such as Ca from gypsum, then dissolution declines but other ions in high concentration (e.g. sodium and chloride) may increase solution more than twofold. Kinetic factors assume little importance in hydrological systems where groundwater contacts limestone for extended periods, but in systems with large conduits and short path lengths with flow-through times of a few days, reaction rates can be important in determining the chemical composition of emergent waters. Conduits are often complex and follow bedding planes, joints and other fractures. Diffuse flow in poorly jointed but porous carbonates such as the pelagic chalks is probably Darcian (Shuster and White 1971).

Karst hydrologists recognise waters as *autogenic*, which develop within the karst itself, and *allogenic* which run into karst from non-karst regions. In large conduits, allogenic waters sometimes remain aggressive throughout their length. In situations where the flow varies, solutional rates will be found to be dependent upon the rate of flow, since kinetic factors will come into play. Several techniques can be used to show whether equilibrium has been achieved between the dissolved carbon dioxide and limestone (calcite), some of which will be described in Chapter 10.

In systems where soil-derived carbon dioxide predominates, hydrologists recognise two end-member solution pathways, termed 'open' and 'closed'. The open system may be visualised as a jar containing limestone immersed in water with an air space above. The carbon dioxide content of the air is allowed to remain constant by keeping the lid of the jar open until the reaction proceeds to equilibrium. Under constant temperature and pressure, the amount of limestone dissolved is a function solely of the partial pressure of CO_2 in the atmosphere. Under closed conditions, the atmosphere above the water-rock mixture is isolated by capping the jar before solution begins. The equilibrium composition will be found to be

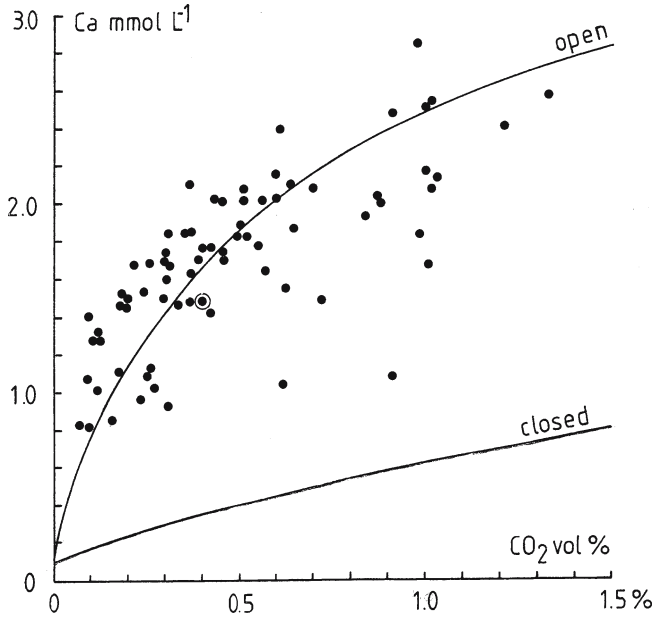

Fig. 25.
Relationship between dissolved Ca and the calculated equilibrium partial pressure of CO_2 in 75 limestone springwaters from the Yorkshire Dales, UK. The two curves represent pure open- and closed solution compositions at 10 °C (curves from Atkinson and Smith 1976). Waterfall Beck spring is encircled

different from the open system composition, with the calcium concentration significantly lower than that of open system at the same CO_2 partial pressure. The quantity dissolved is now a function of the absolute amount of carbon dioxide present in the atmosphere at the time of closure. In a study of limestone springs in northern England, many of which deposited travertine, the great majority were found to have compositions approximating to open system dissolution (Fig. 25). This is not always the case however since Usdowski et al. (1979) and Dandurand et al. (1982) found evidence for both open and closed system pathways in travertine-depositing waters from continental Europe. Drake (1980, 1983) suggests that closed system dissolution pathways should be widespread beneath deep tropical soils. These pathways should also occur in thermogene systems but are less accessible to analysis. It is likely that most solutional pathways include a combination of both processes. The influence of the solutional pathway on travertine formation is considered later (6.1).

5.1.2 Thermogene and Superambient Meteogene Source Waters

Thermal water trajectories are less well understood than those of cool karstic waters, and are likely to be more complex, with wide-ranging compositions. Meteoric water gains heat by a variety of processes as outlined in Chapter 2 and this often involves flow at depths of 300 m or more with closed-system dissolution prevailing. Deep within the crust, lithostatic pressures squeeze the rock tight and prevent water flow, restricting it to shallower depths, where it may be heated by conduction from hot rock or by rising gases. In general, water is scarce below 1000 m excepting deep sedimentary basins where it may persist to about 3000 m. Hydrostatic pressure prevents the water from boiling at great depths, but as it ascends, the boiling point may be reached below the surface. The resulting water vapour will rise and may condense again into water, or discharge as steam. In these situations, a variety of hydrothermal minerals may be deposited below ground level, and primary minerals thermally altered *in situ*, while the water itself may have undergone several changes of phase until it is finally discharged. The temperature fields of the uppermost crust are reasonably well known around hot spring discharges in parts of New Zealand and Wyoming and allow some understanding of the underlying hydrology (Fig. 26).

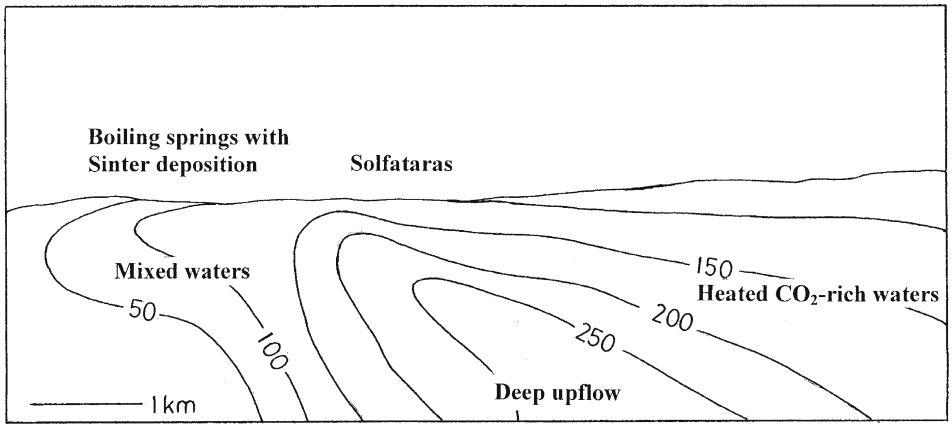

Fig. 26. Temperature field (°C) of a hydrothermal system illustrating groundwater relationships and surface hydrothermal activity. Based on drill logs at Yellowstone National Park, Wyoming and North Island, New Zealand. Vertical and horizontal scales equal. Redrawn after Henley (1996)

In parts of Latium, Italy, many of the thermogene travertines occur on structural highs in a sedimentary basement which acts as a confined aquifer. On these highs, faulting and fracturing allow the deeper waters to mix with an upper, unconfined aquifer in recent volcanics (Turi 1986). In the Pannonian Basin of Hungary, a shallow aquifer is recharged by precipitation over topographic highs and discharges at topographic lows (e.g. the Tisza River) whilst a confined aquifer containing saline connate water occurs at depth (Ballentine, et al. 1991). Again, faulting provides connections between the systems forming a complex 'thermomineral circuit'. In these circuits, it appears that the descent of water is much slower than its ascent, since the latter is facilitated by open fractures less resistant to flow, plus reduced density and viscosity resulting from higher temperatures. Thus solute acquisition most likely occurs on descent rather than ascent as it is a time-dependent process.

Drill logs at Mammoth Hot Springs, Wyoming have shown that water temperature attained a maximum of 70–80 °C and was invariant in some boreholes. Geothermometry predicted equilibration temperatures in the range of 88–100 °C (Fournier 1989; Fouke et al. 2000). Well-head pressures of 5 kg cm^{-2}, thought to result from the presence of gas were reported here (White et al. 1975). The Mammoth groundwater circuits however are known to be complex with at least two identifiable sources. It is evident that the pressure was sufficient to force water along conduits and influence the discharge. Similar pressures must be common in thermal systems to build travertine mounds tens of metres high as noted in 4.1.1. Water feeding the Mammoth springs is known from radiogenic work to be meteoric in nature and has either migrated laterally or more likely risen through sediments buried deeply below the surface, starting as dilute brines at temperatures of 340–370 °C (Leeman et al. 1977). According to their δD signatures, these waters do not appear to have undergone a change in phase (liquid-vapour-liquid) before reaching the surface (Fouke et al. 2000).

At Matlock Bath, UK, a superambient travertine is deposited from a water, shown by geothermometry not to have exceeded 35 °C at any time (Pentecost 1999a). Examination of the local geothermal gradient has shown it could have descended no deeper than 500 m below ground, assuming that little heat was lost in the ascent. The water probably percolates grits, then limestone, before becoming trapped beneath a tilted basalt sill where it ascends as a line of warm springs near a river (Fig. 27).

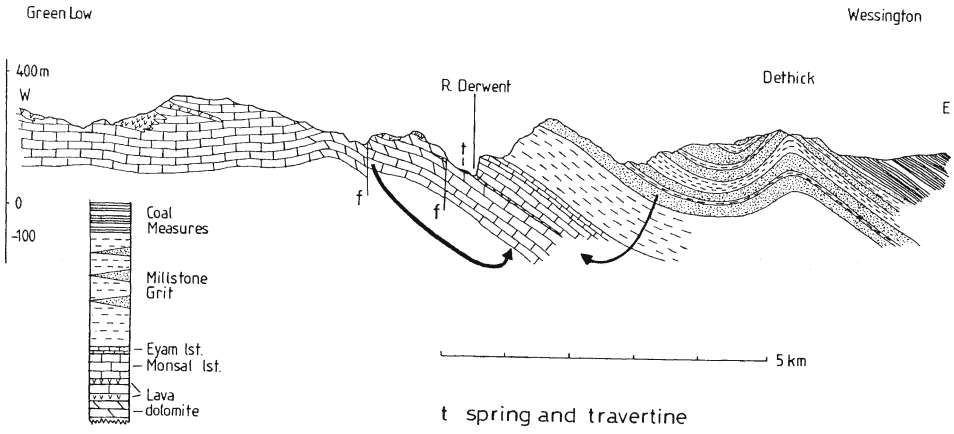

Fig. 27. Geological section through the superambient-meteogene spring at Matlock Bath, UK showing the position of the lava aquiclude and probable pathway of groundwater. From Pentecost (1999a) reproduced with permission from the Geologist's Association from *Proceedings of the Geologist's Association*

5.2 Spring Emergence – Structural Controls

Most travertine is deposited below springs and spring position influences the form and amount deposited. Springs breaking out on steep slopes often give rise to cascade deposits whilst those breaking out on level ground may form mounds or paludal deposits. Spring position is controlled by the water table in unconfined aquifers, but may be controlled by the piezometric surface in confined aquifers. In Estonia, Lookene (1968) found that many travertines occurred at the 75–80 m level corresponding to a groundwater horizon. Most meteogene deposits, at least in Europe, form below springs issuing from perched water tables (Fig. 28a) and are frequently confined to first-order streams. Such water tables are common in gently folded rock containing an alternation of aquicludes and aquifers, such as limestone and clay sequences. Perched water tables frequently result in springs breaking out on slopes leading to rapid deposition. These streams often occur at the head of obsequent (i.e. anti-dip) valleys where the comparatively steep slope may be instrumental in travertine deposition. As a result, lines of springs can deposit a series of travertines for many kilometres along a valley side. Occurrences are common along the Chalk rim in the UK (Fig. 29)

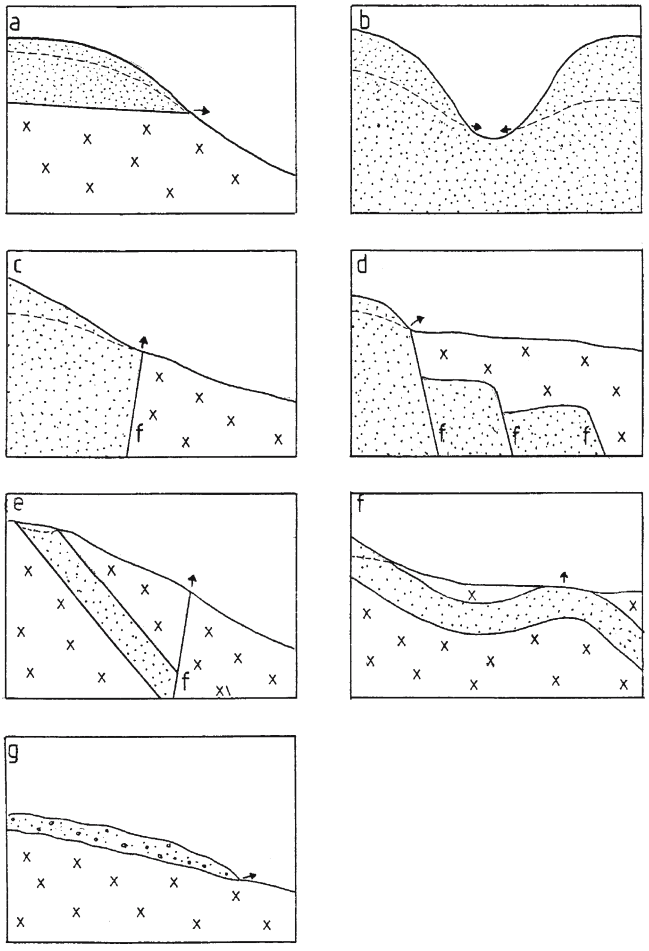

Fig. 28.
Relationships between travertine-depositing springs and geological structure. a) A gravity spring issuing from a perched water table; b) Water table intersecting ground surface in a valley; c) Fault-controlled 'overflow' spring; d) An impounded spring; e) A fault-controlled artesian spring. Many thermogene and superambient deposits are formed in this manner. Some springs rise below lakes; f) Artesian spring in folded rock; g) An interflow spring through calcareous soil. Calcareous aquifer stippled, aquicludes with crosses. F faults; broken line shows water table. Arrows show springs. Partly based on Scheuer and Schweitzer (1981)

and the Schwäbische Alb, Germany (Gwinner 1959). Alternatively, the water table may intersect the ground surface in valleys resulting in seepages or springs in valley bottoms, often directly into a river. In these cases, marine transgression can lead to groundwater rise and reactivation of travertine deposition at a higher level (Segré 1957). Sometimes, impervious strata may be faulted against an aquifer leading to an 'overflow spring' (Fig. 28c). Few of these are known to give rise to travertine, but the springs at Bewcastle and Ironbridge UK are of this type. An example also occurs at Burgtonna, Germany (Kahlke 1978) and they are known at Mszana Polna, Poland (Gruszczynski and Mastella 1986). Alternatively, faulted terrain may become buried by impervious sediments forming an 'impounded spring'. Travertines deposited from such springs are known from Slovakia (Scheuer and Schweitzer 1981). In the Velino Valley of Italy, irregular fault movements since the Mid-Pleistocene are believed to be responsible for spring migration leading to the deposition of a range of travertines at different levels along the valley side (Soligo et al. 2002).

Artesian systems also occur as a result of faulting, folding or both. For example, a steeply dipping aquifer faulted against an aquiclude, will allow water rise along the fracture (Fig. 28e). A head of pressure is needed to drive the flow and may be provided by precipitation percolating into higher ground. Examples include Canino, Italy (Fig. 30), Langensalza, Germany (Wagenbreth 1968) and the numerous mound springs of Australia, where overflow springs also occur (Ponder 1986).

Fault intersections appear to be particularly favourable sites for springs (Pecsi et al. 1982). Tensional faults developed along grabens are commonly associated with thermogene travertines. The large west- and northwest-trending faults of the Pamukkale graben, Turkey provide pathways for the thermal travertine-depositing waters (Altunel and Hancock 1993; Hancock et al. 1999) and many other examples are known such as those of Greece (de Boer et al. 2001) and Morocco (Akdim et al. 2004). An example of a complex faulted terrain giving rise to a series of travertine terraces is shown in Fig. 31. Though conjectural, the structure

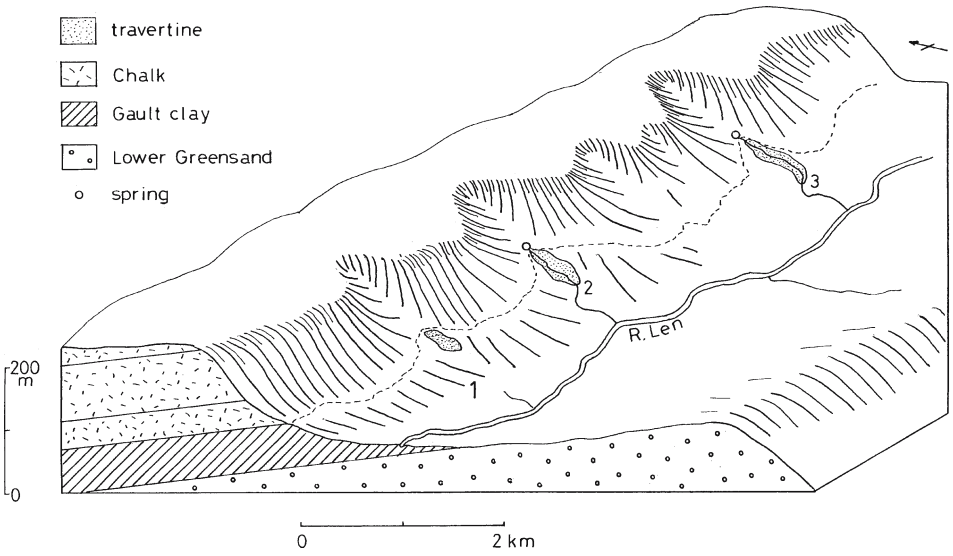

Fig. 29. Block diagram showing the positions of travertine deposits originating from springs breaking out of small obsequent valleys, from a perched water table. North Downs, Southern England. Springline indicated by dashed line. 1. Thurnham Village; 2 Hollinbourne; 3 Harrietsham

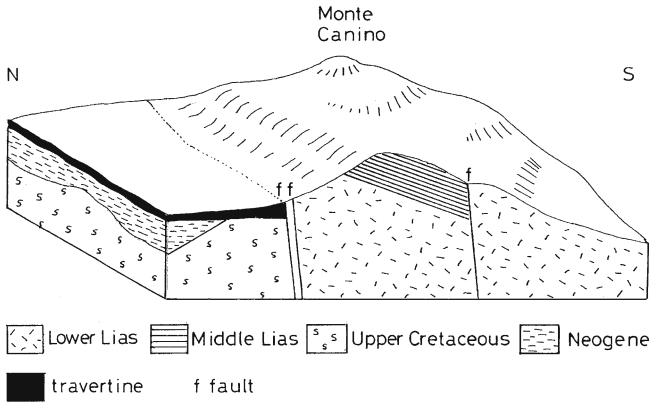

Fig. 30.
Block diagram of the Canino travertine deposit, Italy shown in relation to normal faulting of Mesozoic sediments on Monte Canino. Redrawn after Cocozza (1963)

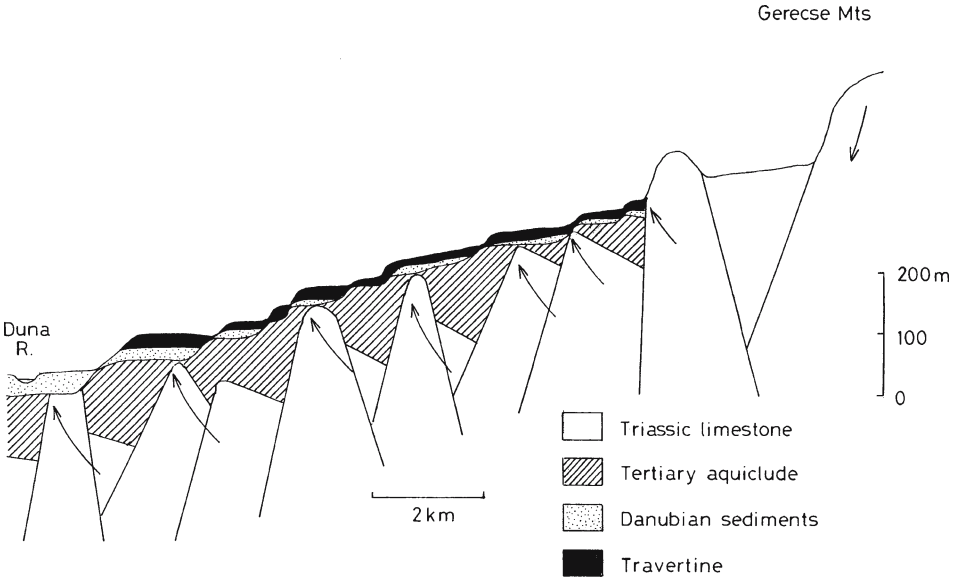

Fig. 31. Geological section of the travertine sequences on the northern margin of the Gerecse Mountains, showing the influence of water emergence on travertine deposition. Complex faulting is shown in Triassic limestones. Arrows show direction of water flow (conjectured). Redrawn after Scheuer and Schweitzer (1981)

illustrates how water from the same source could rise at a number of springs several kilometres apart. Travertines may also be deposited from interflow waters passing through a calcareous soil capping an aquiclude, (Fig. 28g) though none have so far appear to have been reported. However, calcareous aeolianites are often associated with small travertines in the western UK and may be of this type.

The karst springs of the Yorkshire Dales, UK have short residence, times, usually less than a year. In the Plitvice region of Croatia, a hydrologic retention ranging from 1–10 years was estimated on the basis of ^{3}H measurements (Horvatincic et al. 1989). In Turkey, residence time is considered a significant factor in travertine deposition where only those springs with waters 10–15 years old are depositing (Bayari 2002). The superambient waters at Matlock Bath have been tritium-dated at about 20 yr (Edmunds 1971).

Chemical Composition of Source Waters

As emerging springwaters contact the epigean atmosphere, a sequence of chemical changes unfold downstream sometimes leading to the precipitation of calcium carbonate, iron oxides and other compounds. It is therefore important to have a chemical inventory at the start of this journey, to understand how the solutes are acquired, and determine if possible, the subsequent chemical pathways. While the Ca-H-CO_2 system is paramount in any investigation of calcium carbonate deposition, many minor elements have influence over the subsequent reactions. The Group II elements Mg and Sr enter the crystal lattice of calcite or aragonite, influencing their structure and solubility. The alkali metals and some transition elements such as Fe and Mn likewise substitute in the lattice, altering the mineral properties. Several trace elements such as P, Mn, Co, Cu and Zn influence plant and microbial growth, often reducing it if concentrations are either too high or too low, thus potentially influencing the travertine fabric and its biodiversity. Other elements may be concentrated far above their background levels, providing potential economic deposits of Ag, Au and Sb in some thermogene travertines.

Groundwaters from which travertine is precipitated vary greatly in their chemical composition. Calcium hydroxide waters may have undetectable levels of CO_2 and a low ionic strength while thermogene springs may have in excess of 30 mmol L^{-1} CO_2 and a high salinity. The pH can range from less than 6 to more than 12. Travertines have previously been shown to fall into a number of fairly well defined groups based upon the source of the carrier carbon dioxide and the reactions leading to carbonate precipitation. This section is divided accordingly into meteogene and thermogene water types with further consideration given to hyperalkaline (invasive meteogene) and saline waters. The chemical composition and properties of each type will be described, beginning with the Ca-H-CO_2 system. It will be necessary to distinguish between the source water, emerging at the Earth's surface, and the active water, in contact with and forming the deposits. This section will consider the composition of the source waters, and the active water will be considered later, when the mechanisms and dynamics of travertine formation are discussed (Section 10.3). Thermogene springs often deposit at source, in which case the source water is the active water, but in many cases, travertine is deposited a significant distance below the spring. This distinction applies particularly to the CO_2-Ca-H system where large changes in composition often occur downstream.

6.1 Meteogene Source Waters

The majority of these waters have compositions typical of cold karstic springs, where rainwater has percolated through a soil horizon into a layer of carbonate bedrock. The total dissolved solids rarely exceed 1 g L^{-1} and are most often in the range 0.1–0.5 g L^{-1}. Most of the dissolved load consists of calcium and bicarbonate ions with smaller amounts of Mg, Na, SO_4 and Cl. Magnesium, and some sulphate may originate from the bedrock, while Na and Cl usually come from marine aerosols.

6.1.1 The CO_2-Ca-H System

Some descriptive statistics of total aqueous carbon dioxide concentration ($H_2CO_3 + CO_2 + HCO_3^- + CO_3^{2-}$) referred to henceforth as the DIC (total dissolved inorganic carbon) are shown in Table 6. Representative examples of meteogene source water compositions are provided in Table 7. These values are biased since most of the measurements have been made in Western Europe and North America with little work in lower latitudes, Dunkerley (1981) and Drysdale et al. (2003a) providing some of the few exceptions. However, even within Europe, the range of DIC values is large, with a mean and median close to 5 mmol L^{-1}. The variation in DIC can be attributed to pedological, climatic and hydrological factors. Soils vary greatly in their organic content and nutritional status, thus influencing the flora they support and the microbial activity within them. The thickness of the soil cover, and its permeability to water and CO_2 are also important factors in determining the initial levels of DIC in the percolation water. Soil temperature is likely to be significant as many hydrological factors are influenced by it, not least microbial respiration. Measured values of the soil atmosphere CO_2 fall mainly in the range 0.2–5.0 vol% (Brook et al. 1983). Billings et al. (1977)

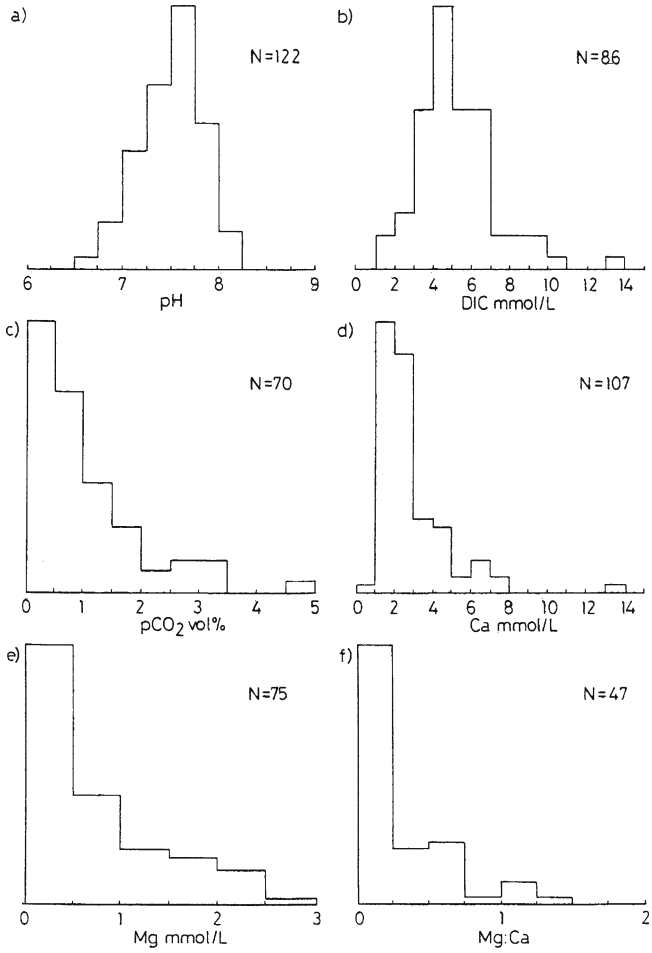

Fig. 32.
Distribution of major ions in meteogene source waters. a) pH; b) total dissolved inorganic carbon (DIC) mmol L^{-1}; c) pCO_2 vol%; d) Ca mmol L^{-1}; e) Mg mmol L^{-1}; f) Mg:Ca ratio. Sources: Barnes (1965); Bayari (2002); Dandurand et al. (1982); Drysdale et al. (2003); Dunkerley (1987); Frisia et al. (2000); Gruninger (1965); Hajek et al. (2002); Hoffer-French and Herman (1989); Kempe and Emeis (1985); Kite and Allamong (1990); Marker (1971); Marker and Casey (1978); Ohle (1937); Pietsch (1984); Pentecost (1992b; 1993 and unpublished); Pentecost and Zhang (2002); Savelli and Wedepohl (1969); Symoens (1949)

Table 6. Descriptive statistics for some major dissolved components of travertine source waters. Sources as for Fig. 32 and 35 plus Edmunds (1971), Lorah and Herman (1988), Pentecost (1999a) and Raymahashay and Chaturvedi (1976)

Determinand		Meteogene	Superambient-meteogene	Thermogene
Temperature °C	mean(N)	10.1(71)	33.2(7)	43.6(57)
	median	9.5	29.4	45.0
	range	4.2–24.3	20.6–50	6–78
pH	mean(N)[a]	7.39(122)	6.97(6)	6.36(44)
	median	7.55	7.26	6.47
	range	6.9–8.15	6.5–7.79	5.8–9.0
DIC mmol L^{-1}	mean	5.22(86)	3.82(7)	33.6(48)
	median	4.89	4.04	26.8
	range	1.48–13.8	1.73–5.5	5.2–97
pCO_2 vol%	mean	1.02(70)	2.37(6)	46.0(28)
	median	0.63	1.30	39.7
	range	0.1–7.8	0.3–9.0	0.8–139
Ca mmol L^{-1}	mean	3.07(107)	8.96(8)	8.9(52)
	median	2.33	10.0	8.0
	range	0.86–15.2	2.3–13.3	0.01–23.7
Mg mmol L^{-1}	mean	0.69(75)	2.91(8)	4.07(47)
	median	0.44	2.81	3.50
	range	0.001–2.74	0.29–5.9	0.44–14.3
Mg:Ca	mean	0.29(72)	0.37(8)	0.54(44)
	median	0.16	0.39	0.43
	range	0.001–1.37	0.24–0.54	0.08–2.60

[a] Geometric mean.

estimate that 60–80% of this carbon dioxide is respired by roots, although a small fraction is adsorbed onto soil and rock surfaces and will not enter the soil atmosphere and percolation water (Adams and Swinnerton 1937). Given open-system dissolution, the equilibrium CO_2 partial pressure in the soil atmosphere should be reflected in the pCO_2 of the emerging groundwaters. With a mean of 1% and range of 0.1–(7.5)% (Fig. 32c) this may be broadly true, but the values are too scattered to provide convincing evidence, and they are complicated by subsurface CO_2 evasion, raising the pH, and lowering the pCO_2 thus mimicking closed-system dissolution. This is probably the main reason why so many of the calculated pCO_2 values range between 0.1 and 1%.

The bedrock and its hydrological characteristics have already been discussed in relation to carbonate dissolution and it becomes apparent that the DIC of emergent groundwaters will be difficult, if not impossible to predict. However, in a study of global soil CO_2 levels,

Table 7. Chemical composition of some travertine-depositing waters. Determinands in mmol L^{-1} unless where stated. *SIC:* calcite saturation quotient; *DIC:* dissolved inorganic carbon; **:* sampling site either uncertain or sampling at source impractical; *nd:* not detected; *tr:* trace. Author's previously unpublished analyses undertaken between 1988 and 1998

	t °C	pH	pCO_2 %	Ca^{2+}	Mg^{2+}	Na^+	K^+	HCO_3^-	SO_4^{2-}	Total S	DIC	SIC	Reference and notes
Meteogene													
Huangousshu, China	–	7.30	0.77	1.63	0.75	–	–	3.31	0.63	–	3.41	0.58*	Yang et al. (1985)
Plitvice, Croatia	7.6	7.67	0.52	1.41	0.97	–	–	5.48	–	–	5.59	1.51	Kempe and Emeis (1985)
Gütersteiner Falls, Germany	8.3	7.18	1.54	2.80	0.06	0.21	0.01	4.77	0.54	nd	5.66	0.94	Author, unpublished
Silver Well, Cheshire, UK	10.5	7.47	0.80	13.0	0.06	5.40	0.03	5.06	13.4	nd	5.64	4.61	Author, unpublished ($CaSO_4$ type)
Waterfall Beck, UK	7.09	7.62	0.39	1.46	0.03	0.16	0.01	2.71	0.10	nd	2.91	1.13	Author, unpublished (annual mean)
Birch Ck, Ca, USA	14.5	7.50	0.7	1.88	1.02	0.57	0.09	4.57	0.97	–	4.95	1.49	Barnes (1965)
Falling Spring Run, Va, USA	14.0	7.01	2.88	1.82	1.17	0.03	0.03	5.74	0.03	nd	7.16	0.95	Hoffer-French and Herman (1989)
Kisanga, Zaire	–	7.70	0.48	0.93	1.19	0.09	0.08	4.15	0.06	–	4.41	1.60*	Symoens and Malaisse (1967)
Crag Cave, Eire	10.4	7.70	0.5	2.29	0.4	0.76	0.04	4.86	0.26	nd	5.17	2.00	Frisia et al. (2000)
Ernesto Cave, Italy	6.5	8.04	0.14	1.32	0.18	0.01	nd	2.93	0.08	nd	3.04	1.70	Frisia et al. (2000)
Invasive meteogene													
Cydach, Dyfed, UK	9.1	8.66	0.02	1,20	0,06	5.60	0.05	1.10	0.04	nd	1.14	2.90	Author, unpublished
Burro Mt, Ca, USA	20.0	11.5	–	1.00	0.01	0.83	0.03	nd	0.01	nd	nd	–	Barnes and O'Neil (1969)
Superambient-meteogene													
Pozza Azulas, Cuatro Cienegas	20.1	7.78	0.43	10.8	4.30	7.50	0.27	3.54	5.46	nd	3.84	19.5*	Author, unpublished
Matlock Bath, UK	20.6	7.77	0–38	2.32	1.15	1.13	0.04	3.98	1.37	nd	4.21	0.94	Pentecost (1999)
Pyramid Lake, Nev, USA	62.0	7.36	0.16	3.25	1.44	54.8	1.59	0.38	3.13	–	0.41	0.37	Galat and Jacobsen (1985)
Warm Springs, Ut, USA	29.4	7.79	0.25	8.04	3.40	250		3.52	3.07	nd	3.24	4.74	Author, unpublished (saline spring)
Orgamox													
Harrogate, UK	14.0	6.53	8.00	12.3	7.1	206	1.8	6.66	nd	5.5	10.4	0.54	Author, unpublished (saline spring)
Thermogene													
Huanglong, China	6.0	6.44	23.9	4.94	0.89	–	–	12.2	–	–	25.1	0.72	Liu et al. (1993)
Bagnaccio, Italy	64.9	6.32	88.0	14.3	6.91	2.08	0.21	17.4	12.9	0.03	31.2	7.34	Author, unpublished
Bagni di Tivoli, Italy	23.0	6.17	81.4	7.3	4.7	3.6	0.49	22.5	5.8	0.41	52.5	1.35*	Pentecost and Tortora (1989)
Hisayoshi, Japan	42.0	5.80	97.9	12.0	5.35	7.8	0.20	8.77	6.9	–	31.4	0.53	Kitano (1963)
Masutomi, Japan	30.0	5.92	139	4.10	0.82	120	3.0	20.9	13.4	nd	61.6	1.04	Kitano (1963) (saline spring)
Ngatamariki, New Zealand	83	7.22	7.8	0.18	0.02	24.2	0.73	7.84	0.47	0.02	8.9	0.76	Mountain et al. (2003). Contains 3.90 mmol L^{-1} Si
Loboru, Kenya	98.5	8.15	0.80	0.03	tr	61.3	1.15	41.9	0.19	–	42.6	8.80	Jones and Renaut (1995) Na-HCO_3^- type
Mammoth Hot Springs, Wy, USA	72.0	6.6	44.3	6.79	2.80	5.6	1.76	13.8	5.22	0.08	20.2	–*	White (1963)

Soil zone CO_2 concentrations, Waterfall Beck catchment 1987-88

Soil type	Mesotrophic brown earth	Oligotrophic brown earth	Rendzina	Rock
Area of catchment %	38	22	35	5
Mean soil pCO_2 vol%	0.69	0.69	0.33	-

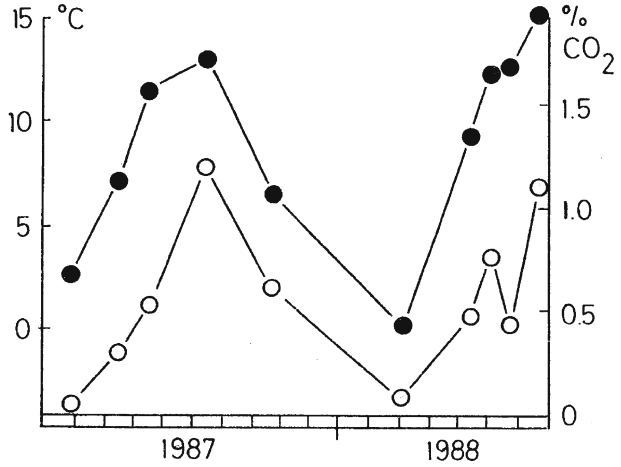

Fig. 33.
Seasonal variation of mean soil % CO_2 concentration (open circles) and air temperature (filled circles) in the Waterfall Beck catchment, Yorkshire Dales, UK. Data are also provided for the individual soil types within the catchment

Brook et al. (1983) found that actual evapotranspiration was the best independent predictor of soil pCO_2, and they provide a world map showing that in general, tropical soils possess the highest pCO_2 values. Drake (1980) had previously given a simple model of soil pCO_2 based solely upon temperature and a similar model predicting pCO_2 in saturated open-system groundwaters. These models provide useful predictive frameworks. The temperature-dependence of the pCO_2 of soil atmospheres is well seen in some data from Waterfall Beck, UK. In the catchment of this stream, three soil types are present under pasture: oligotrophic brown earth, mesotrophic brown earth and rendzina. Soil zone CO_2 was measured at 30 cm depth in all of these soils over a season, using Dräger tubes (Fig. 33). It is clear that the pCO_2 varies seasonally but there were no significant differences between the soil types, despite their different depth and fertility, and the overall weighted catchment mean was 0.53%. The emerging groundwaters in this catchment have a mean pCO_2 of 0.35% suggesting that equilibration with the soil atmosphere was close to completion. Despite the strong seasonality of the soil CO_2, there is only a slight seasonal variation in the DIC or Ca of the emerging groundwater, the former ranging from around 3.3 mmol L^{-1} in summer to 3.0 in winter. In some karst springs, the seasonality is pronounced, often permitting flow-through times to be estimated (Pitty 1968; Rightmire 1978; Kano et al. 1999). In Waterfall Beck, the weak seasonality is probably due to the mixing of groundwaters of different ages. It is not possible to generalise from this one example, since it is the coldest site studied in the UK and hardly representative of the whole. Based upon the knowledge that warmer soils tend to have higher pCO_2 levels, one would expect to see higher DIC values in the source waters and this is borne out, when mean air temperature is plotted against source water DIC (Fig. 34). However, this is not always

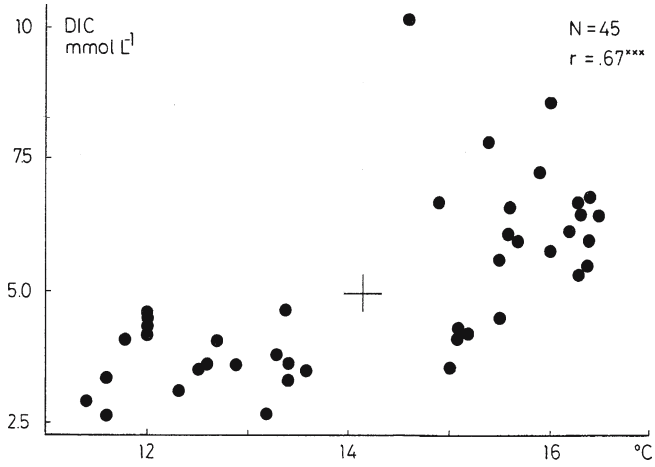

Fig. 34.
Relationship between the total dissolved inorganic carbon (DIC, mmol L^{-1}) in travertine source waters and mean annual air temperature (°C). Centroid marked with a cross (author, previously unpublished)

the case. For example, the karst waters of Puerto Rico have values similar to temperate groundwaters (Troester and White 1986). The reason for this is not understood, but may be influenced by seasonality in the rainfall and soil fertility. Unfortunately, insufficient data are available from the tropics to test these hypotheses further. More support for the influence of temperature on DIC is obtained from data for 45 UK travertine-depositing spring waters (author, unpublished). Here a significant positive correlation ($r = 0.674^{***}$) was found between the DIC and the predicted mean July air temperature. The picture is probably complicated by differences in catchment vegetation types, which is also influenced by altitude. For example, UK catchments at lower altitudes are more wooded, resulting in deeper, often richer and more productive soils, irrespective of the prevailing air temperature. A positive ($p<0.01$) correlation was also found between the calculated springwater pCO_2 and temperature. Jakucs (1977) describes several studies of soil carbon dioxide in relation to site aspect and vegetation. Temperature was found to exert the most significant effect, but the ability of a soil to retain its CO_2 is dependent upon its moisture content and exposure. For example, in the Northern Hemisphere, a north-facing slope experiences lower temperatures and will retain its moisture longer, reducing atmospheric CO_2 transfer. A warmer, south-facing soil will dry more quickly leading to greater CO_2 loss via air circulation, modulating the effect of temperature on soil CO_2 production. Vegetation cover also influences soil CO_2 levels. Forest soils were found to have the highest CO_2 concentrations (ca. 10 vol%) while short grassland may have up to five times less. This is a result of the deeper biologically active soils under woodland and the reduction in wind exposure when compared with grassland. The intensity and distribution of rainfall is a further factor for consideration. Periods of high rainfall have been shown to significantly reduce the soil pCO_2, effectively flushing the carbon dioxide through the soil profile (Rightmire 1978). The soil CO_2 also diffuses out into the epigean atmosphere and this is dependent on soil type and moisture content. While an overall control on soil CO_2 availability to groundwaters is dependent on climate, a complex picture emerges when the above factors are taken into consideration.

The pH distribution for source waters is shown in Fig. 32a. Most waters have a pH between 7 and 8 and within this region, most of the carbon dioxide is present as HCO_3^-. For the average pH of 7.43, just over 90% of the carbon dioxide exists as bicarbonate. pH, the 'master chemical variable', influences the speciation of carbon dioxide and many other solutes, with direct and indirect effects on the biota.

Calcium is the major cation of most non-saline travertine-depositing waters. The mean of 3.07 mmol L^{-1} for meteogene waters (Table 6) is rather more than twice that for the mean bicarbonate concentration which is about 4.8 mmol L^{-1}. Since the carbonate ion concentration is negligible, calcium must be balanced by ions other than those provided by the CO_2 system. Since magnesium is always present, and itself partly balanced by the CO_2 system through the dissolution of dolomite and high magnesian calcite, the ionic imbalance is usually in excess of that indicated above. In some well-studied regions such as the UK, the balance is often made up by SO_4^{2-} and NO_3^- anions resulting from atmospheric pollution (Pentecost 1992b). That calcium is the major cation in most of these waters is not surprising in limestone regions, where other ions, such as K^+ and Na^+ are often in low concentration . The calcium histogram shows a mode close to 2 mmol L^{-1} and it appears that waters depositing meteogene travertine rarely contain less than 1 mmol L^{-1}. A small number of source waters contain calcium exceeding 10 mmol L^{-1}, which is substantially higher than their bicarbonate content. These waters are all of the calcium sulphate type and occur in regions containing evaporites such as gypsum or anhydrite. Calcium sulphate is more soluble than calcium carbonate, and gypsum-saturated waters at NTP contain about 15 mmol L^{-1} Ca. Gypsum dissolution rate is about 15 times that of limestone (Chardon 1992). What is surprising is the apparent scarcity of travertine deposition from such waters through the common-ion effect (Section 2.1). Examples are known from Knaresborough, England and Queyras, France (Brotto 1986) and there must be many more undocumented. The 'global average' of Ca in limestone waters of 1.28 mmol L^{-1} (Wetzel 2001) is less than half the average for meteogene source waters, which may explain in part why travertine deposition is far from a universal phenomenon in karst waters.

The compositions of cave waters are similar to those of the epigean meteogene travertines and examples can be found tabulated in Baker et al. (1998), Frisia et al. (2000) and Fairchild et al. (2000) with some of their data included in Table 7. Both seasonal and spatial variation within individual caves has been observed. It should be noted that source waters in caves are likely to have degassed considerable CO_2 prior to sampling, since in most cases, only slowly-forming drips can be collected. Also, the cave atmosphere pCO_2 is normally higher that the epigean pCO_2 and may vary seasonally.

6.1.2 Magnesium, Sodium, Sulphate and Chloride

These ions may occur in high concentration and influence $CaCO_3$ solubility in the Ca-H-CO_2 system and precipitation of travertine. The magnesium ion is often influential, and its concentration is frequently correlated with calcium. However, magnesium levels fluctuate widely and can rival that of calcium though Ca:Mg ratios less than unity are rarely encountered. The distribution of magnesium in meteogene waters is shown in Fig. 32 where it appears that the element is normally present at low concentration, less than 1 mmol L^{-1}. Levels rarely exceed 2 mmol L^{-1} but this is still insufficient to influence the mineralogy of the precipitated travertine, where Mg needs to approach 10 mmol L^{-1}. The mean Mg concentration in these waters is only slightly higher than the 'global' average for limestone waters of 0.32 mmol L^{-1} (Wetzel 2001). Most meteogene travertine-depositing waters have a molar Mg: Ca ratio less than 0.25 (Fig. 32f) and it rarely approaches unity. Where it does so, it is usually due to dolomite, $CaMg(CO_3)_2$ in the catchment. Dissolution of pure dolomite would provide a Mg:Ca ratio of unity, but calcite is usually a contaminant. The sequential dissolution of rock containing dolomite and calcite is often complex and can result in the formation of subsurface waters supersaturated with calcite (Freeze and Cherry 1979). It would appear that for meteogene waters, the available gas phase CO_2 would be incapable of dissolving sufficient Mg from dolomite to precipitate aragonitic travertines.

Table 8. Minor dissolved constituents in travertine-depositing source waters. Concentrations in μmol L^{-1} unless stated. Mean (range) number of measurements. Excludes invasive meteogene waters

Element	Meteogene	Superamb.-meteogene	Thermogene	Organomox
Al	1.6 (0.4–1.4) 4	0.9(0.9) 1	17 (2–56) 9	–
As	<0.005 () 4	–	41 (7–100) 3	–
Ba	0.84 (0.5–1.5) 3	88 (26–150) 2	0.5 () 1	470 () 1
Be	0.023 () 1	0.02 () 1	–	3.5 () 1
B	63 (4–180) 5	15 () 1	2100 (80–14000) 13	200 () 1
Br	2 () 1	0.9 () 1	27 (0.04–80) 3	350 () 1
Cd	0.015 () 1	–	–	–
Cs	0.001 () 1	0.02 () 1	–	0.4 () 1
Cu	0.01 () 1	0.05 () 1	–	–
F	10 (2–26) 5	25 (0.07–50) 2	250 (120–1600) 4	–
Fe	1.2 (0.1–3) 5	0.3 () 1	38 (0.2–390) 27	–
I	–	0.03 () 1	0.5 (0.001–1) 2	12 () 1
K	100 (2–1900) 45	200 (120–410) 4	2786 (50–19000) 39	1800 () 1
Li	0.2 (0.1–0.4) 6	6500 () 1	1300 (2–10000) 10	40 () 1
Mn	0.1 (0.02–0.3) 4	3.6 () 1	18 (0.01–51) 12	–
Na mmol	0.51 (0.012–2) 73	5.1 (0.03–9.5) 5	16.1 (0.9–85) 34	–
NH_4-N	6 (1.4–18) 7	–	30 (22–38) 2	240 () 1
NO_3-N	65 (1.0–260) 40	8 () 1	15 () 1	–
O_2% satn.	86 (75–96) 2	29 () 1	<2 () 5	–
PO_4-P	2.9 (0.02–4.6) 31	260 (120–410) 6	20 () 1	–
Pb	0.007 () 1	0.02 () 1	–	–
Rb	0.008 () 1	0.007 () 1	–	0.2 () 1
S[a]	–	–	117 (1–355) 11	5500 () 1
Si	119 (14–400) 21	2200 () 1	1333 (320–2850) 10	170 () 1
Sr	21 (0.2–56) 8	14 () 1	140 (1–460) 23	161 () 1
Ti	0.84 () 1	–	1250 () 1	–
V	0.26 () 1	–	–	–
Zn	0.13 () 1	0.6 () 1	0.4 () 1	–
DOC[b]	0.81 () 1	–	1.3 () 1	–
Eh mV	–	–	+110(–280 to +415) 3	–
Specific conductivity μS cm^{-1}	449 (258–747) 27	855 (660–1230) 3	3737 (1800–5900) 12	–

[a] Total dissolved sulphide. [b] Dissolved organic C. *Sources:* Amundson and Kelly (1987); Arana et al. (1979); Barnes (1965); Boyer and Wheeler (1989); Cole and Batchelder (1969); Demovic et al. (1972); Drysdale et al. (2003a); Duchi et al. (1978); Edmunds (1971); Emeis et al. (1987); Emmons and Larsen (1913); Geurts and Watelet (1994); Gruninger (1965); Headden (1905); Herman and Hubbard (1990); Ichikuni (1973); Kano et al. (1999); Kitano (1963); Lang and Lucas (1970); Lorah and Herman (1988); Marker and Casey (1982); Merz-Preiss and Riding (1999); Minckley (1963); Pentecost (1992b; 1993, 1995c and unpublished); Pietsch (1984); Rowe et al. (1973); Savelli and Wedepohl (1969); Sturchio (1990); van Everdingen et al. (1985); Waring (1965) and White et al. (1963); Yoshimura et al. (2004). The OM site is Harrogate, UK.

The distribution of sodium in meteogene waters (Table 8) indicates that this element is rarely a major constituent. Sulphate concentrations are normally subordinate to bicarbonate, and those exceeding bicarbonate are usually associated with evaporites as noted above. Most meteogene waters contain less than 1 mmol L^{-1} sulphate. Chloride is a common anion originating from halite dissolution in evaporites or from marine aerosols and tends to be approximately equimolar with sodium. It may also originate from connate waters trapped in ancient limestones as for example in the superambient waters of Derbyshire, UK (Edmunds 1971).

6.1.3 Calcium Hydroxide Source Waters (Invasive Meteogenes)

This small but interesting group of groundwaters is characterised by a high pH and low DIC. They may be classified into two sub-groups, viz: those associated with serpentinisation and portlandite; and those leaching lime-burning sites. In both cases, the reacting solid is calcium hydroxide and the levels of carbon dioxide in emerging groundwaters range from <1 mmol L^{-1} to undetectable. Carbon dioxide and bicarbonate originally present within the percolating groundwater, reacts with the aqueous OH^- directly often giving rise to subsurface veins of carbonate and is largely removed from the water. The waters frequently emerge close to saturation with calcium hydroxide and with a pH greater than 9. At this pH and above, atmospheric carbon dioxide ingasses often leading to rapid and extensive travertine deposition.

Rocks undergoing low temperature serpentinisation appear to be widely distributed on the Earth's surface but are fairly uncommon. Barnes and O'Neil (1969) describe calcium hydroxide waters from Burro Mountain in California, an alpine ultramafic body that has undergone incomplete serpentinisation. The pH of this water was 11.54 and contained no detectable carbon dioxide (Table 6). Several other examples are known from California (O'Neil and Barnes 1971) the Middle East and Europe (Barnes et al. 1982; Clark and Fontes 1990). Waters contaminated by lime-burning operations have a similar gross composition. It is worth noting that karst waters undergoing closed-system dissolution could theoretically rise with pH values of about 9.0. Under these conditions, atmospheric CO_2 could invade the waters in a similar manner to hydroxide waters leading to travertine deposition. Waters of this type do not appear to have been recorded at the time of writing.

6.1.4 Superambient Meteogene Source Waters

These are distinguished from the ambient meteogenes in possessing temperatures above that of the mean annual air temperature. Their carbon dioxide originates from the soil but their higher temperature can produce a more mineral-rich solution and lead to more rapid CO_2 loss at the surface. Their deep circulation probably results from long contact times with the rock. Their composition would be expected to be seasonally invariant in contrast to most ambient meteogenes. Their origin is similar to that of the cold karst waters, the only difference being the significant increase in temperature resulting from geothermal activity. With an average geothermal gradient of 25 °C km^{-1} water does not need to descend far below the earth to attain temperatures 10–20 °C or more above ambient. Providing the ascent of the water is rapid, little heat is lost until emergence. Superambient travertines are not often reported but they are widely distributed. Some detailed analyses for one UK site is provided by Pentecost (1999a) and other examples from the Himalaya are provided by Raymahashay and Chaturvedi (1976) where quartzites are underlain by radioactive schists responsible for the high heat flow. The best known are the mound springs of the Great Artesian Basin of Australia where spring water temperatures often exceed 40 °C.

The CO_2-Ca-H compositions are similar in composition to ambient meteogenes, but levels of other major dissolved species (Mg, Na, SO_4) tend to be higher (Tables 6, 7) probably resulting from greater water-rock contact. This is supported by the high levels of radioactivity in some waters (De Capitani et al. 1974). Dissolved oxygen levels may be low or even zero, compared with meteogene sources, where dissolved oxygen is 70% or more of atmospheric saturation (Jacobson and Langmuir 1970). Some of the Australian mound springs contain traces of sulphide and therefore devoid of dissolved oxygen, while their alkalinities and Ca contents are similar to those of meteogene waters (Smith 1989).

6.1.5 'ORGAMOX' Waters

The Sulphur Well at Harrogate, UK deposits a small quantity of travertine and may be of this type (Table 6). The high DIC value may include an alkalinity contribution form aliphatic acids, a frequently reported phenomenon in oil field waters.

6.2 Thermogene Source Waters

As previously shown (2.1.2.2) thermogene travertines form from a range of carbon dioxide sources and receive most of their carrier CO_2 from thermally-driven processes. Under high temperature and pressure, aqueous solutions of CO_2 are very reactive and capable of dissolving large amounts of carbonate. Thermal decomposition of carbonate rock at moderate lithostatic pressures releases carbon dioxide attacking cooler rock in the presence of water to provide calcium-rich solutions. The water is largely meteoric in origin according to its isotopic composition, but connate waters, and those resulting from rock dehydration and magma degassing may also be present. Thus both water and gas may come from several sources. On migration to the surface, these gas-enriched solutions cool, but may undergo a series of rapid boiling/condensation phases as the pressure declines. Some will mix with cold meteoric water resulting in further cooling and dilution. They may also undergo exchange reactions with other minerals before emerging at the surface. Such waters will show a wide variation in composition. Here they will be considered as a single group linked by their thermal CO_2 origin.

6.2.1 THE CO_2-Ca-H System

Baseline data on the CO_2-Ca-H system are provided in Fig. 35. They demonstrate the high levels of CO_2 which characterise these waters. Total carbon dioxide concentrations are about an order of magnitude greater than meteogene waters, averaging around 30 mmol L^{-1}, though the range is considerable. This is to be expected through dilution with surface waters. The mean pH of thermogene source waters is one unit lower than the mean meteogene level, and pH values ranging from 6–7 are normally observed. The resulting ten- fold increase in H^+ may in part explain the higher levels of trace constituents such as Cu^{2+} in these waters.

It is likely that some waters particularly high in carbon dioxide have ascended with little dilution. Examples include Terme San Giovanni at Rapolano, Italy and Masutomi, Japan where the associated pCO_2 values approach, or even exceed 100%. There is a significant negative correlation between temperature and the pCO_2 values in these waters ($r = -0.56$, $p < 0.01$), suggesting that cooling rather than dilution is responsible for much of the observed difference in pCO_2. The highest recorded carbon dioxide levels occur at the springs of St. Nectaire in the Auvergne with a value of 65 mmol L^{-1} and an equilibrium CO_2 partial pressure of 64%.

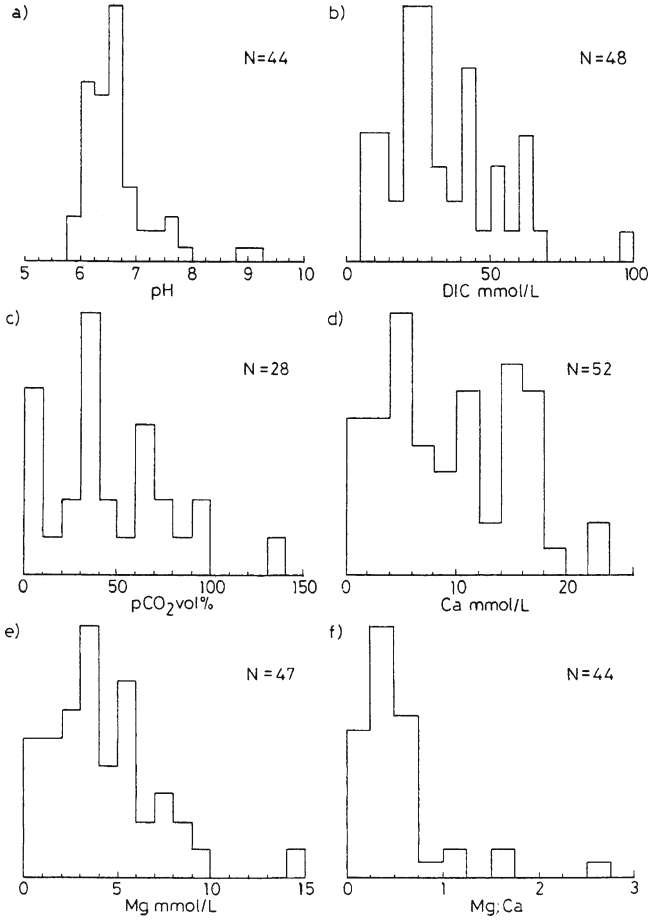

Fig. 35.
Distribution of major ions in thermogene source waters. a) pH; b) total dissolved inorganic carbon (DIC) mmol L^{-1}; c) pCO_2 vol.-%; d) Ca mmol L^{-1}; e) Mg mmol L^{-1}; f) Mg:Ca ratio. Sources: Amundson and Kelly (1987); Cole and Batchelder (1969); Demovic et al. (1972); Dobrol'skiy et al. (1987); Fodor et al. (1982); Geurts and Watelet (1994); Ichikuni (1973); Ishigami and Suzuki (1977); Jones and Renaut (1995); Khoury et al. (1984); Kitano (1963); Liu et al. (1995); Lund (1978); Pentecost (1995c and unpublished); Risacher and Eugster (1979); Waring (1965); White et al. (1957)

The pCO_2 values of thermogene source waters commonly exceed 30%, again an order of magnitude higher than those found in meteogene waters. Much higher CO_2 partial pressures are likely to exist at depth with some subsurface degassing, sometimes leading to formation of vein calcite (Khoury et al. 1984). The emerging waters normally have pH values close to 6.4, with about 50% of the carbon dioxide unionised. Calcium levels are correspondingly high in most of the waters often exceeding 10 mmol L^{-1}, but there are some noteworthy exceptions (Fig. 35d). The hot spring waters at the margin of Lake Bogoria, Kenya, are of the sodium bicarbonate type and contain less than 0.1 mmol L^{-1} Ca, yet they deposit extensive travertines (Jones and Renaut 1995). The DIC values of these waters are sufficiently high to raise the calcium carbonate solubility product for precipitation.

6.2.2 Magnesium, Sodium, Sulphate and Chloride

Magnesium levels are usually higher than those found in meteogene waters, while the molar Mg:Ca ratio does not differ greatly form meteogene waters (Fig. 35e,f). This is presumably because dolomite dissolution is to a large extent controlling the ratio, though not the concentration of these ions of these source waters. It is noteworthy that several waters contain

magnesium in sufficient quantity (c. 10 mmol L^{-1}) to initiate aragonite deposition. Where the Mg:Ca ratio exceeds unity, sources of Mg other than dolomite must be sought. Sodium concentrations are also elevated but most waters contain less than 20 mmol L^{-1} Na, while a small number of springs exceed 100 mmol L^{-1}, e.g. Futamata and Masutomi in Japan (Kitano 1963), and the springs of the Auvergne. These waters approach or exceed the boundary defining saline waters (>5 ppt TDS). Sulphate levels also vary widely and occasionally exceed 20 mmol L^{-1} where they are close to gypsum saturation. Gypsum deposition is common around hydrothermal vents (Waring 1965).

Analyses of the relative contributions of the major cations and anions of thermogene waters indicate that about a dozen sites are close to seawater composition. These include Carlsbad, Pastos Grandes plus several springs in France and Japan, though none of the sites is close to the sea. These waters tend to be depleted in SO_4 and Mg when compared with seawater and their compositions probably reflect solute acquisition from marine evaporites. In some regions such as the Auvergne, many of the dissolved constituents probably arise from recent igneous rocks.

6.3 Minor Components of Source Waters

The concentration ranges of a number of minor elements is shown for the three water types in Table 7. Excepting plant nutrients and oxygen, the concentration of these elements in thermogene waters considerably exceeds those in meteogenes, often by an order of magnitude. This results from more efficient leaching, greater contact times and hydrothermal activity leading to increased reaction rates between rock and water, in addition to the possibility of volatile capture from magma (Kitano 1963). 'Minor' elements often attaining millimolar concentrations in thermogene waters include B, Li, K and Si. Other frequently observed elements in the ppm range include As, F, Fe, Mn and S. Elevated levels of B and F might be taken as indicative of a hydrothermal source but concentrations vary widely and high levels, along with elevated Li also occur in some meteogene waters.

Brines are often found to be poor in K and Si but enriched in Ba, Br, I and Sr. Waters previously noted as similar in composition to seawater have elevated levels of B, Li and Sr but contain low concentrations of several other elements, suggesting that a marine origin is unlikely. Germanium has been reported in travertine where it forms a sol with Ca^{2+} and becomes precipitated. It occurs in solution as *m*-germanic acid and elevated levels are indicative of deep-seated sources (Edmunds 1971). Aluminium has been detected in several waters and in meteogenes is present in amounts similar to other freshwaters. In thermogenes it is higher, attaining levels toxic to some aquatic organisms. Aluminium solubility should be enhanced at pH>9 due to the formation of aluminates and it would be interesting to know whether levels in calcium hydroxide waters are sufficiently high to be detrimental to microbial growth.

Strontium concentration in meteogene waters is similar to that of average river water (Riley and Chester 1971). In the Waterfall Beck catchment, Sr is sufficiently high in the parent limestone to provide the traces dissolved in the source water. As an alkaline earth element, the geochemistry of Sr is similar to that of Ca, but it is rarely found in significant amounts. In thermogene waters it may be much higher. Its solubility is largely controlled by CO_3^{2-} and it is preferentially incorporated into the lattice of aragonite (Section 7.6.1).

A number of transition elements have been detected in meteogene waters. In the 0.45 μm filtered waters of Waterfall Beck, UK, ten elements were detectable using atomic absorbtion spectrophotometry. Of these, Co, Cr, Fe, Mn, Mo, Ni and V concentrations could be accounted for by congruent dissolution of the parent limestone, while levels in the limestone were in-

sufficient to account for the concentrations of Cd, Cu, Ti and Zn. They were presumably derived from the overlying soils, glacial drift and mineral veins in the limestone. Concentrations of Fe and Mn in meteogene waters are low and similar to those encountered in average freshwater. In thermogene waters they are much higher, and the Fe: Mn ratio is lower, possibly reflecting redox reactions, since Fe is more rapidly precipitated as E_h increases. The concentrations of these elements in waters subjected to low pressures and moderate temperatures are controlled by the extreme insolubility of the sulphides. Where sulphide is present, soluble Fe and Mn is extremely low, unless complexed with organic matter. Waters containing in excess of about 100 μmol L^{-1} Fe^{2+} precipitate ochers resulting in ferruginous travertines. Of the remaining transition elements, data are available only for Ti and Zn in thermogene waters. The source waters of Big Horn Springs, Wyoming contain unusually high levels of titanium (quoted in Lund 1996). These springs contain sulphide, and the Ti might exist as the reduced Ti^{3+} ion, since some complexes with this ion are moderately soluble in water. Suspended particulates however are a more likely source. Traces of radium, thorium and uranium have been reported in connection with radiometric dating (Haites 1959; Yong-Lao and Benson 1988). The concentration of uranium has been shown to be correlated with strontium in an Australian stream, and the variation in uranium content linked with stream discharge and the amount of colloidal organic matter (Ihlenfield et al. 2003). A range of other rare elements in meteogene waters is reported by Pentecost (1992b) for Waterfall Beck, UK where concentrations are sufficiently low to have a negligible effect on travertine formation.

Rowe et al. (1973) provide further data for Mammoth Hot Springs, Wyoming. Hot alkaline waters are often rich in silica and often deposit opal-A at vents. Such deposits can be intimately associated with travertines, e.g. Firehole Lake, Yellowstone National Park. The chemical composition of a New Zealand representative, Ngatamariki, is provided in Table 6. Silica is an important nutrient for diatoms and Si-rich waters often contain abundant diatoms often forming large accumulations of diatomite (Weed 1889b). The concentration of silicate increases with water temperature forming the basis of silicate geothermometry.

There are little data pertaining to the major plant nutrients, nitrogen and phosphorus. Total orthophosphate levels are low in virtually all meteogene and thermogene source waters (Table 7) which is to be expected where Ca is high and the pH >6, due to the precipitation of calcium phosphate. High levels are normally only associated with polluted waters where P is associated with organic matter and bacterial mineralisation processes. Much of the 'total' dissolved phosphorus is known to be organically bound though the PO_4 moiety may be liberated by extracellular plant phosphatases. In Waterfall Beck UK, about 80% of the dissolved orthophosphate has been found to be organically bound. During summer, under low discharge, it has been calculated that there is only sufficient P to satisfy the standing aquatic crop (Spiro and Pentecost 1991) but P dynamics are complex since rapid recycling occurs in freshwater ecosystems through nutrient spiralling. Phosphates are powerful inhibitors of carbonate precipitation and are considered further in Section 15.5.3.1. Combined nitrogen likewise occurs at low levels but there are few reports from thermogene waters. Nitrate concentrations, while higher than phosphate (Table 7) might occasionally limit ecosystem productivity, though many cyanobacteria thriving in travertine-depositing streams are capable of fixing atmospheric nitrogen. Nitrite probably occurs at micromolar levels in thermogene waters through nitrate reduction. Ammonia has been detected in trace amounts in small number of meteogene waters and occurs in many hydrothermal waters.

About one third of the thermogene waters so far examined contain detectable sulphide. At pH 7 total sulphide is split almost equally between H_2S and HS^- while S^{2-} only becomes significant at high pH. Below pH 7, the ratio H_2S : HS^- increases approximately ten fold per

unit fall in pH. Hydrogen sulphide is either degassed on reaching the atmosphere or oxidised by microbes and oxygen. Total sulphide levels vary considerably and are sometimes high and accompanied by a well-developed sulphobiota, such as Bagni di Tivoli, Italy where it reaches 0.4 mmol L^{-1}. Sulphides are often found in sulphate-rich thermogene waters (Fig. 35b) and may be derived from them via bacterial sulphate reduction at depth. Isotope studies at Mammoth Hot Springs indicate that here the sulphide arose from the baking of sediments (Leeman et al. 1977). As many sulphate-reducers are thermophiles, both baking and sulphate-reduction is likely to occur. Traces of thiosulphate occur in the Viterbo hot springs where they may be metabolised by chemolithotrophic bacteria. The presence of even trace amounts of S^{2-} influence the solubilities of many metallic elements and is probably an important controlling factor on springwater composition.

Ambient meteogene waters of the open-system type should contain oxygen levels close to saturation but there have been few measurements. The Waterfall Beck springs were found to be 95% saturated but much lower values have been recorded elsewhere. Oxygen levels in the Plitvice springs appear to be substantially below saturation according to the analyses of Kempe and Emeis (1985). The superambient waters at Matlock Bath, UK contain 0.56 mmol L^{-1} (30% saturation) suggesting they remain aerated throughout their 20 year journey to the springs.

There have been few measurements of dissolved oxygen in thermogene source waters. Most thermogenes contain little if any free O_2, since inorganic reductants and microbial activity rapidly remove it. Investigations at Bagnaccio, Italy have shown that the spring waters contain <20 μmol L^{-1} and the other Viterbo springs have been found to contain only traces of the gas using resazurin as indicator. Caldwell et al. (1984) are probably correct in suggesting that the traces observed diffuse into the water from the surrounding rock close to the surface. The ingassing of oxygen into these hot waters is rapid and 80% saturation is achieved in a few minutes at Bagnaccio (Pentecost 1995b). Oxygen levels are important biologically with low values favouring specific groups of microbes and animals thus influencing the travertine fabric. Several downstream studies of oxygen concentration have been made to determine the effects of plant photosynthesis (Minckley 1963; Cole and Batchelder 1969). Other dissolved gases, apart from CO_2 have received scant attention. Noble gas levels are occasionally measured and found to be high in most thermogene and superambient waters (Edmunds 1971) and sources have been suggested based upon their isotope ratios. Since thermogene travertines are frequently radioactive and deeply circulating, their high noble gas content is not surprising.

Dissolved organic carbon (DOC) has been detected in the Viterbo hot spring waters but only in trace amounts. At Bagnaccio, the DOC was found to be 1.3 ppm at source (unpublished). Hydrothermal systems may, however sometimes contain high levels of DOC, depending upon the circulation temperature. A detailed study of the meteogene Plitvice Lakes system by Emeis et al. (1987) gave low values, averaging 0.8 ppm (as C), considerably less than the world average for freshwater. Higher levels (5.6 ppm) have been reported from waters in Slovakia (Hajek et al. 2002).

Two further determinands deserve mention, namely the E_h and electrical conductivity. The E_h, a measurement of the oxidation-reduction potential, would be expected to vary widely on the basis of their varied composition of oxidants and reductants and this is found to be the case. The author measured values as low as –280 mV at the sulphide-rich thermal springs at Bullicame, Italy, with a gradual increase downstream to +80 mV as the water degassed sulphide and ingassed oxygen. Similar variations were found at other Italian sites and were consistent with the measured chemical changes, though many hydrologists remain cautious of interpreting E_h in terms of chemical processes in natural systems. Hajek et al. (2002) found

an average Eh value of –27 mV in some 'tufa fens' of Slovakia, which may explain why these sites had elevated levels of Fe. Some values are also reported for a German meteogene spring by Arp et al. (2001).

Conductivity measurements are useful to detect and semi-quantify downstream changes in dissolved constituents and provide an estimate of calcium or the total dissolved load (Chen et al. 2004). For example, the ionic strength of a solution can be estimated using the relation $I = 1.5 \times 10^{-5} * C$ where C is the conductivity in $\mu S\ cm^{-1}$ (Langmuir 1971). As might be expected, conductivities are highest among the thermogenes and normally in the 1–10 millisiemen cm^{-1} range, while most meteogenes are in the microsiemen range (Table 7). These figures exclude saline waters.

6.4 Saline Waters

Saline waters have been defined as those where total dissolved solids (tds) exceed either 3 g L^{-1} (Williams 1981) or 5 g L^{-1} (Beadle 1974) and the latter figure is used here. Williams notes that saline waters, as defined by him, account for a substantial fraction of the earth's inland waters, and are common, but by no means restricted to the more arid regions of the world. In contrast, 'mineral waters' are defined as having >10 g L^{-1} tds but this term will not be applied here. Hypersaline waters have tds exceeding 53 g L^{-1} (Flugel 1982) though waters exceeding the average seawater salinity (34.7 g L^{-1}) are often referred to as hypersaline. For the purpose of this discussion a saline water will be defined with tds >5 g L^{-1} and a hypersaline water with tds >34.7 g L^{-1}. These waters have been excluded from the above discussion on account of their high ionic strength and varied origins. They are biologically very different from their non-saline counterparts. Increase in salinity is commonly the result of evaporation of freshwaters in endorheic (closed) basins and in such cases the source waters are of low ionic strength. In others areas the source waters themselves may be saline, having leached evaporites or resulted from water-rock reactions at depth. In coastal areas, it is common for seawater to intrude into freshwaters before rising as springs. Travertines with all three types of carrier CO_2 are occasionally found to be saline and some examples are provided below.

Although saline hot springs are frequent worldwide, few appear to deposit travertine, and they have received scant attention. Examples are Utah Hot Springs, Wyoming, the springs at Futamata and Masutomi, Japan (Kitano 1963) the Eregli spring, Turkey (Waring 1965) and some of the Altiplano springs of Bolivia (Risacher and Eugster 1979). The Utah springs are highly radioactive and contain a large proportion of iron oxides. Warm Springs, Utah (Table 6) is probably an example of a saline superambient spring and the deposits appear to differ little from their lower ionic strength counterparts. Deposits of ikaite travertine from the high Arctic originate from a cold saline spring with a water temperature of –2 °C (Omelon et al. 2001). The travertines of Bad Laer, Germany are also believed to have been deposited from a cold saline spring (Hiltermann 1977). Most of the spring waters associated with the travertine mounds of the Australian Great Artesian Basin have a high salinity, and some may be described as saline (Ponder 1986).

Travertines associated with saline waters are more often found in lakes. The best known examples are the Great Salt Lake, Utah, Mono Lake, California, and Pyramid and Walker Lakes in Nevada. The Nevada lakes occur in the large endorheic system occupied by the ancient Lake Lahontan. The salinities of these lakes varies from about 10–100 g L^{-1} and their chemistries are known in varying detail. Pyramid and Great Salt Lake have been well studied limnologically though little attention has been paid to their travertines. Their low DIC values, but high temperature suggest they are derived from superambient waters.

Chapter 7

Mineralogy and Elemental Composition

Almost all travertines consist of the two principal polymorphs of calcium carbonate, aragonite and calcite. The conditions under which these minerals are formed vary according to the chemical composition of the source water, the temperature, pressure and rate of CO_2 evasion. Given the wide range of conditions prevailing in the travertine-depositing environment, the mineralogy of the carbonate is of no small interest, and much can be learned about carbonate mineralogy from travertine deposition. In addition to calcium and carbonate ions, other neutral solute molecules and ions become incorporated into the crystal lattice or trapped as inclusions. They can offer important clues to conditions under which the travertines formed. Hydrothermal waters also contain a high concentration of other solutes that may co-precipitate with the carbonate, forming other minerals. An overall understanding of the mineral composition also requires investigation of foreign particle incorporation, brought by erosion through wind or water, to the site of deposition. These too can provide information about past environments.

Autochthonous and allochthonous travertines often contain different mineral suites. Components other than calcium carbonate may be defined as *accessory* and include authigenic minerals – those formed during and after deposition, and the detrital allochthonous components. Travertines vary widely in their carbonate content but they are often exceptionally pure, with calcium carbonate exceeding 95% by weight. Limestone is usually reserved for rocks exceeding 50% $CaCO_3$ dry weight and this definition is adopted here for travertine.

7.1 Calcite and Aragonite Mineralogy

Travertine consists primarily of crystalline calcium carbonate and to appreciate its physical and chemical properties, some knowledge of the major crystalline forms, calcite and aragonite is desirable. The structure of calcite is simple and can be related to halite which has a face-centered cubic lattice. If the halite structure is deformed by shortening a body diagonal (as opposed to a face diagonal) by 77%, keeping the edges straight, a calcite-type lattice is obtained. The procedure allows bulky carbonate ions to be accommodated while preserving a simple layered structure. The carbonate anion (CO_3^{2-}) consists of a carbon atom surrounded by three equidistant oxygens producing an almost planar equilateral triangle. Four electrons from carbon are shared equally between the three oxygens and the resultant negative charge on the carbonate ion is distributed mainly around the latter. The calcium ions are situated at the centres of octahedra whose corners are occupied by oxygen atoms (Fig. 36a). To obtain this six-fold coordination, the carbonate ions swing around slightly to form an octahedral structure elongated slightly in the direction of the crystallographic (c) axis. Each oxygen atom is placed more or less symmetrically between three contacts, two calcium ions and its own covalently linked carbon. The calcium-oxygen distance in calcite is close to the sums of the known Ca and O ionic radii demonstrating ionic bonding. Because of the size and awkwardness of the large carbonate group

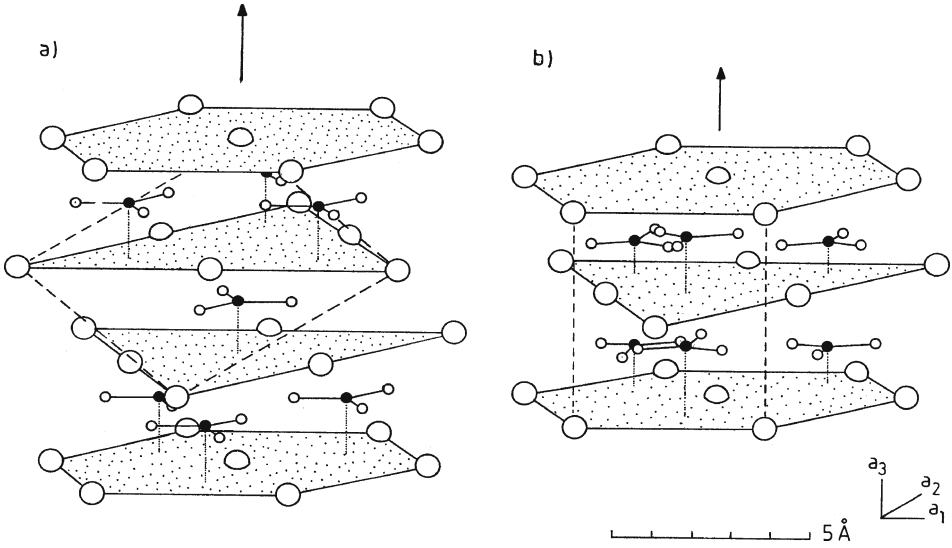

Fig. 36. The structure of calcite and aragonite. a) Calcite; b) Aragonite; Large open circles Ca^{2+}, small open circles oxygen and small filled circles carbon. Arrow shows direction of the c-axis. Planes of Ca^{2+} ions are stippled

there is considerable separation between the oppositely-charged ions and despite the divalency, calcite is a weak crystal with a hardness value of 3.

Aragonite, the other important polymorph of calcium carbonate is more dense than calcite. In common with calcite, layers of cations occur perpendicular to the c-axis but the arrangement of ions is quite different. By means of a minor structural deformation, the architecture of aragonite can be obtained from niccolite (NiAs) where nickel atoms are surrounded by six atoms of arsenic (Fig. 36b). By substituting As with Ca, and slightly corrugating the carbonate groups, aragonite is obtained. In this mineral, calcium ions are surrounded by nine oxygen atoms, but the resulting polyhedron has two orientations with respect to the c-axis. Two oxygens each from three separate carbonate groups are ionically bonded to a calcium atom, and the remaining three oxygen atoms come from another three groups. When viewed away from the c-axis, aragonite is seen to consist of layers of cations separated by two layers of carbonate ions with different orientations. The packing of these ions is slightly more efficient than in calcite leading to the higher density. The difference in packing is also responsible for their differing entropies; 22.2 cal deg^{-1} $mole^{-1}$ for calcite and 21.2 cal deg^{-1} $mole^{-1}$ for aragonite (at NTP), the calcite atoms having a slightly greater degree of movement. Aragonite, which crystallises in the orthorhombic system rarely exhibits identifiable faces in travertine but twinning on (110) is common. There is no three-fold symmetry.

In both minerals, the planar carbonate ions are oriented into flat sheets resulting in strong birefringence, and in both structures, each carbonate is surrounded by six calcium ions. In mixtures these polymorphs can be distinguished using Feigl's chemical test (Davies and Till 1968; Popp and Wilkinson 1983), or bromoform can be used to separate them by their differing density. Differential thermal analysis, and especially X-ray powder diffraction is more accurate and allows estimations in mixtures providing prolonged trituration is avoided, and allowance made for the masking of aragonite traces by quartz (Davies and Hooper 1963). At NTP, the molar Gibbs free energy difference between the polymorphs is due to entropy and calcite is thermodynamically the most stable form at the Earth's surface (Table 9).

Table 9.
Some physical data for calcite and aragonite

	Calcite	Aragonite
Specific gravity	2.713	2.929
Crystal system	Rhombohedral	Orthorhombic
Space group	R-3c	Pnma
Ca coordination	6	9
Optical form	–ve	–ve
Gibbs free energy kcal M^{-1}	–269.78	–269.53
Crystal habit	Rhombohedra, scalenohedra, prism	Acicular, usually twinned

7.2 Occurrence of Calcite and Aragonite in Travertine

Although aragonite is less stable than calcite at room temperature, it occurs widely in nature and is frequently found in hot spring travertines. Numerous laboratory experiments have shown that aragonite is precipitated preferentially from hot water and the limiting temperature lies between 30 and 60 °C, according to experimental conditions (Lippmann 1973; Folk 1994). At lower temperatures, aragonite is normally only formed in the presence of high concentrations of magnesium, when in fact dolomite might be expected to precipitate. Magnesium levels above ~10 mmol L^{-1} appear sufficient to achieve this at room temperature. In Fig. 37, a selection of travertine mineralogies have been plotted against water temperature and dissolved Mg. It would seem from this graph that there is general agreement within these limits, and between 30 and 40 °C, either calcite or aragonite may be formed, irrespective of the magnesium content.

At Mammoth Hot Springs, Wyoming, travertine close to the springs contains >90% aragonite (Sturchio 1990) but calcite begins to form once the water has cooled sufficiently (Friedman 1970). More recent work at this site by Fouke et al. (2000) has shown that at water temperatures >44 °C, only aragonite precipitates, between 30–43 °C, calcite precipitates with aragonite, and below 30 °C, only calcite is formed. In natural situations, large, local differences in temperature lead to interesting variations at hot pool surfaces where calcite may be deposited owing to surface cooling. At Mammoth the spatial distribution of the polymorphs is further complicated by the transport of detrital aragonite to the lower, cooler slopes. Similar phenomena have been reported at other hot spring locations.

Magnesium concentrations in freshwaters rarely exceed 10 mmol L^{-1} and aragonitic travertines are infrequently encountered in cold water, except in situations where it may be concentrated by evaporation. Examples occur in the closed basins of arid regions where evaporation produces saline water high in Mg, such as Mono Lake in California (Scholl and Taft 1964) and in meteogene travertines associated with maritime ultramafic rocks (Flinn and Pentecost 1995). It has also been found in association with the macrophyte *Myriophyllum* in the Plitvice Lakes crusts but its presence there remains unexplained (Stoffers 1975). Since the shells of molluscs are composed largely of aragonite, it is usually present in small quantity in most epigean meteogene travertines. Aragonite deposits are also common in caves, particularly those of warmer climates. In the Carlsbad Caverns of New Mexico, Thrailkill (1971) found that in some drip-waters, evaporation accounted for 40% of the Ca loss to carbonate precipitation, with concomitant magnesium concentration. The increase in magne-

Table 10. Travertine chemical compositions. The $MgCO_3/SrCO_3$ content is calculated on the assumption that all Mg and Sr is present as carbonate

Site/group	Type[a]	$CaCO_3$ %	$MgCO_3$ %	$SrCO_3$ %	Fe ppm	Mn ppm	P ppm[b]	Organic %	Insol. residue %	Reference and notes
Meteogene										
Shuzeng, China	A/C/C	97.9	0.13	–	2430	107	–	1.1	0.7	Pentecost and Zhang (2000)
Waterfall Beck, UK	A/C/C	92.6	0.40	0.01	310	100	125	4.62	2.25	Pentecost (1981)
Itchen River, UK	I/S/C	93.9	0.14	0.01	570	280	340	3.3	2.4	Unpublished (oncoids)
Wateringbury, UK	I/P/C	85.1	0.31	0.07	1300	220	950	2.60	11.90	Pentecost (1993)
S. Germany	–	93.9	0.80	0.25	1200	146	–	–	2.39	Savelli and Wedepohl (1969) mean of 17
Invasive meteogene										
Foel Fawr, UK	A/C/C	99.3	0.20	0.02	60	<20	15	0.18	0.22	Pentecost (1993)
Superamb.-meteogene										
Matlock, UK	A/C/C	95.0	1.30	0.13	80	30	53	2.7	0.92	Pentecost (1999)
Thermogene										
Bagnaccio, Italy	A/M/A+C	94.1	0.34	1.6	135	10	43	0.48	0.15	Pentecost (1995c)[c]
Bagni s. Fillipo, Italy	A/M/A+C	96.0	0.66	1.4	136	74	–	0.14	0.08	Pentecost (1995c)[c]
Bagno Vignoni, Italy	A/C/C	92.4	1.55	1.4	230	34	8	0.8	1.73	Pentecost (1995c)[c]
Futamata, Japan	A/M/A+C	92.6	0.17	0.67	29×10^3	700	–	–	–	Kitano (1963)
Doughty, Co., USA	A/C/C	88.3	2.84	1.65	1400	4800	–	–	2.29	Headden (1905)[d]
Mammoth Hot Sprs, Wy, USA	A/C/A	96.2	1.38	–	–	–	–	–	–	Allen (1934)[c]
Czech Republic	–	94.4	2.25	1.85	13×10^3	1700	110	–	–	Demovic et al. (1972) mean of 38

[a] Type of deposit x/y/z, *x: A* = active, *I* = inactive; *y: C* = cascade/dam, *L* = clastic, *M* = mound, *P* = paludal, *S* = stream crust; *z: A* = aragonite, *C* = calcite.
[b] *P* = acid-soluble inorganic orthophosphate. [c] Contains >2% $CaSO_4$; [d] Contains >2% $BaSO_4$.

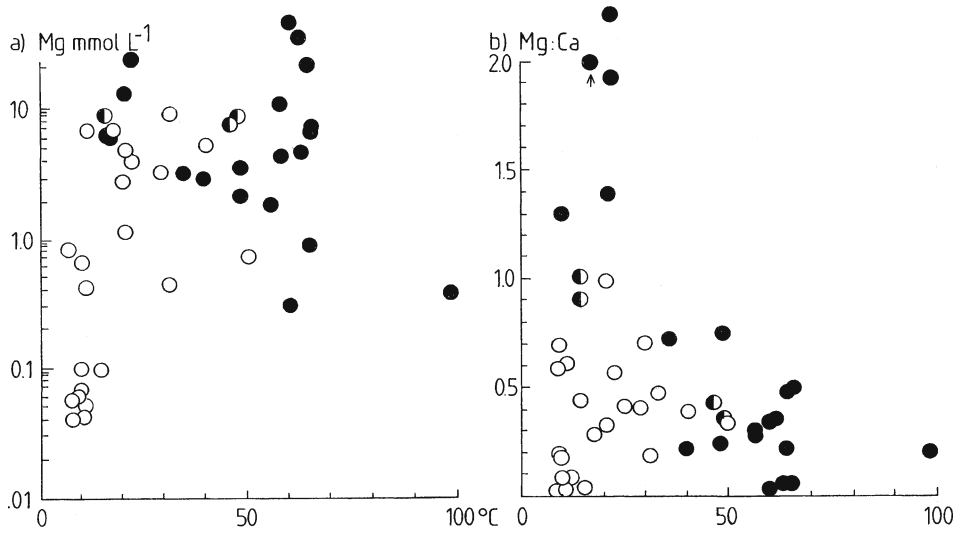

Fig. 37. Calcite and aragonite in travertine in relation to the deposition temperature and magnesium (a) temperature vs magnesium concentration; (b) temperature vs Mg:Ca ratio. Open circles, calcite; filled circles, aragonite; half filled circles, mix of aragonite and calcite. Sources: Amundson and Kelly (1987); Dandurand et al. (1982); Duchi et al. (1978); Folk (1994); Kitano (1963); Liu et al. (1993); Malesani and Vanucchi (1975); Rastall (1926); Risacher and Eugster (1979); Scholl and Taft (1964) and author (unpublished)

sium via evaporation is believed to be responsible for most aragonite deposition in caves. Fischbeck and Müller (1971) found that aragonite precipitation became significant once the Mg: Ca ratio attained ~2.9 and Forti (1980) found that heat from a light bulb was sufficient to cause aragonite deposition in one Italian cave. The rapid diagenesis of aragonite to calcite complicates field relations and it may not always be clear that calcite is the first mineral to be formed.

Most observations suggest that the two important determinants for aragonite formation are water temperature and magnesium, but a more complex picture emerges when other factors are taken into consideration. At least three more could be significant. In a study of Japanese hot springs, Kitano (1963) reported many sites with both calcite and aragonite. At some it was noted that aragonite predominated where the rate of CO_2 evasion was greatest, suggesting that kinetic effects influence the polymorph formed (cf. Lippmann 1973). This could be particularly significant at hot springs, where deposition rates are often high (cf. Chafetz et al. 1991a). An overwhelming abundance of aragonite particles at hot spring vents might also provide seed crystals that would then drift downstream into cooler water, where aragonite may not otherwise be expected. The second factor is the presence of organic matter. There has been much work on the influence of small organic molecules on the deposition of calcium carbonate (e.g. Kitano and Hood 1965; Meyer 1984) and there is no doubt that some substances strongly influence deposition rates, and probably the mineralogy. Numerous investigations of carbonate biominerals (e.g. Murray 1954; Pobeguin 1954; Lowenstam and Wiener 1982) demonstrate the existence of all three polymorphs at room temperature which seem to be independent of Mg concentration. Travertines almost always contain detectable organic matter, but to date there are no clear-cut examples of organic matter directly influencing the polymorph present. Thermal waters often contain strontium, and work in Italy suggests that high levels of this element also favours aragonite deposition (Malesani and

Vannucchi 1975). Work by Duchi et al. (1978) and R. L. Folk has cast some doubt on this observation and they consider that temperature and Mg concentration remain the most significant factors (Folk 1994). Barium has also been suspected in influencing the mineral form (Lippmann 1973) but levels are probably too low in travertine source waters to have a significant effect. Finally, high levels of other solutes, such as Fe^{2+} and SO_4^{2-} are known to influence both the crystal form and growth kinetics, particularly in hot springs. For example, Fe^{2+} inhibits calcite growth at low concentrations (Meyer 1984) and sulphate at concentrations $>10^{-2}$ M favours aragonite formation (Kitano 1962).

Magnesian calcites (calcite with 4–20 mole-% $MgCO_3$) have occasionally been reported from travertine. For example, Adolphe and Rofes (1973) found a stream deposit in France with 13 mole% $MgCO_3$ and some deposits in Mono Lake also contain it (Scholl and Taft 1964). In the Funtana Maore travertines of Sardinia, magnesian calcites up to 5.6 mole% are reported (Caboi et al. 1991). The high values were attributed to their formation from dolomite groundwaters but most travertines contain negligible amounts of magnesian calcite. An X-ray diffraction study of 30 UK travertines revealed only low magnesian calcite (author, unpublished). Barnes and O'Neil (1971) found dolomite $CaMg(CO_3)_2$ in a few Californian travertines derived from ultramafic groundwater sources and traces have been found in some Japanese hot springs (Kitano 1963). There is also some evidence for it in the Central Italian deposits (Folk 1994). Dolomite has also been reported occasionally from caves (Hill and Forti 1997). In these cases, evaporation probably plays a role in its formation. Vaterite, the least known polymorph of calcium carbonate is readily formed from hot calcium bicarbonate solutions in the laboratory but rapidly transforms to aragonite or calcite. It has been detected in some of the opalescent travertine-dammed pools of Huanglong, China, forming a soft white sediment mixed with calcite (Lu et al. 2000).

7.3 Autochthonous Carbonate Minerals Excluding $CaCO_3$

Hydrates of calcium carbonate have been reported in some travertines. Monohydrocalcite, $CaCO_3\ H_2O$ has been found in a few cold caves (Hill and Forti 1997). Ikaite ($CaCO_3 \cdot 6H_2O$) was probably the original mineral forming the 'tufa towers' in the Mono lake area of California (Bischoff et al. 1993; Council and Bennett 1993) and pseudomorphs of ikaite occur in some of the Pyramid Lake towers. This mineral was first discovered in Ika Fjord, Greenland at low temperatures and is known to be metastable, rapidly changing to calcite as temperatures rise. The Mono Lake area is chilled to temperatures sufficient to precipitate ikaite in winter (3–4 °C) and it is probably converted to calcite once the water begins to warm in the spring. A similar process is believed to occur in some unusual travertine-depositing springs of the high Arctic. Apparently perennial springs issue from evaporite deposits of Axel Heiberg Island where the mean annual air temperature is –15 °C. The ikaite appears to form along stream courses during the dark winter months, forming a series of minidams rimmed by evaporite deposits (Omelon et al. 2001). During spring the ikaite reverts to slushy calcite. The travertine is believed to form as a result of CO_2 evasion, but requires further study. Ikaite has also been found rarely in caves (White 1976). These hydrates probably form at low temperature where there is insufficient thermal energy for dehydration.

Hill and Forti (1997) note the rare occurrence of ankerite, $CaFe(CO_3)_2$ and barringtonite, $MgCO_3 \cdot 2H_2O$ in caves. Hydromagnesite, $Mg_5(CO_3)_4\ (OH)_2 \cdot 4H_2O$ is frequently a component of 'moonmilk' and it occurs in the travertines at Salt Lick Spring, California (Amundson and Kelly 1987). Travertines associated with the serpentinisation of ultramafic rocks in

California contain hydromagnesite with nesquehonite $MgCO_3 \cdot 3H_2O$ and hydrotalcite $MgCO_3 \cdot 5Mg(OH)_2 \cdot 2Al(OH)_3 \cdot 4H_2O$ together with a solid solution series of calcium-magnesium carbonate (O'Neil and Barnes 1971). Hydromagnesite is occasionally precipitated in lakes in ultramafic areas, such as Salda Lake, Turkey (Russell et al. 1999). Magnesite $MgCO_3$ may be associated with hydromagnesite and is said to occur around the springs of Lohitsch in Styria (Leitmeier 1909) and in Indonesia and has also been found in the lake crusts of British Columbia (J. Thompson, *pers. comm.*). Thermogene travertines at Hammam Meskoutine, Morocco are reported to contain some strontianite $SrCO_3$ (Daubrée 1888). A radium 'alstonite' (Ba, Ra) $Ca(CO_3)_2$ is reported from a northern Italian travertine by De Capitani et al. (1974).

Carbonates with non-group 2 elements are also known as minor consituents. They include siderite $FeCO_3$ (Kitano 1963) and trona $Na_2CO_3 \cdot NaHCO_3 \cdot 2H_2O$ (Feth and Barnes 1979). A double carbonate, $CaMn(CO_3)_2$ was reported from Yunomata by Kitano (1963).

7.4 Calcite and Aragonite Crystal Habit

Visitors to 'crystal caves' are invariably struck by the beauty and endless variety of forms of calcite crystals. This mineral is renowned for the great number of observable crystal faces. Over 2000 crystal forms of calcite are illustrated in the atlas of Goldschmidt (1913) although few of these are so far known from crystal caves. The earthy appearance of many epigean travertines might suggest an unfruitful source for crystallographers, but the advent of scanning electron microscopy belies this statement and some unique forms have been found. The processes leading to the particular crystal habits found in travertine are for the most part unknown and await investigation.

7.4.1 Calcite

Microscopic observations show that although epigean travertine calcite crystals are frequently elongated in the direction of the c-axis they are usually anhedral. Euhedral crystals are uncommon and normally restricted to cavity linings or fresh travertine surfaces. Of these, the primitive rhombohedron (10–11) is the most frequently observed, at least in meteogene deposits. Complete rhombs are rare, but occasionally seen suspended within algal mucilages (*Chrysonebula*, *Cosmarium*) on travertine surfaces. More often, subhedral rhombs are found on active surfaces, where a sparkling 'sugar crust' sometimes occurs, with crystals 30–150 μm across (Photoplate 13A). 'Sugar crusts' are less common in epigean travertines but often occur associated with the alga *Oocardium stratum* suggesting a degree of biological control (Section 9.2.1). However, epigean spar crusts may form in the virtual absence of algae, in both fast and slow-flowing water and are produced to order in the petrifying wells of the Auvergne, France. Here, the crystal faces are frequently covered in macrosteps (Fig. 38b) with the c-axes parallel to the direction of growth.

Small voids, hollows and joint faces in old travertines provide a rich source of euhedral crystals, which in most cases must be of secondary origin. An SEM study of cavity linings in the Italian hot spring deposits of Rapolano Serre and Bagni di Tivoli by Folk et al. (1985) has revealed many interesting forms. Steep rhombs were most often encountered, whilst the unit rhomb and flat rhomb were rarely seen. Some unique crystal modifications were found. 'Gothic arch' calcite consisted of steep rhombs composed of a series of slabs with raised edges. The combined edges showed convex curvature rising to a point (Fig. 38a). Their curvature was

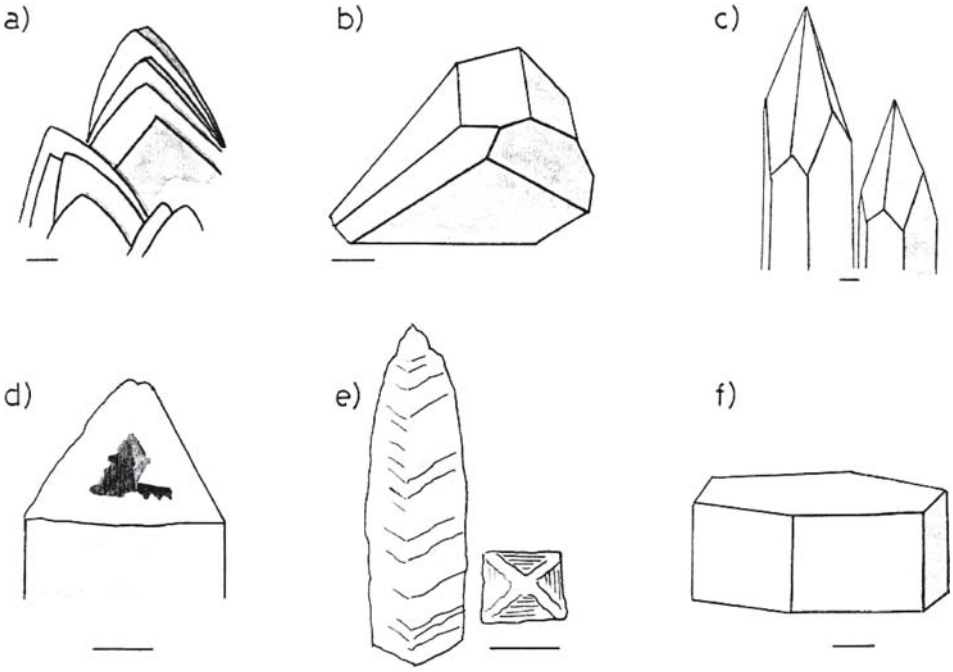

Fig. 38. Illustrations of some calcite crystal habits observed in travertines. a) Gothic arch, bar 20µm (from Folk et al. 1985); b) edge guttered crystal, bar 20µm (from Folk et al. 1985); c) scalenohedra (dogtooth spar), bar 100 µm; d) skeletal calcite, bar 5 µm (from Jones and Renaut 1996); e) thinolite; bar 1 cm (from Radbruch 1957); f) prism with basal pinacoid; bar 50 µm

originally explained by the substitution of carbonate by larger sulphate ions, but this is now thought to be unlikely. Gothic-arch calcite seems to be fairly common in both the cavities and within minidam pools of the Italian travertines and it has also been reported from the Lake Natron travertines (Casanova 1994). In speleothems, much of the columnar calcite fabric is found to consist of crystallites exhibiting the flat (101–4) rhombohedron (Frisia et al. 2000). Busenberg and Plummer (1985) found that sulphate incorporation increases with the crystal growth rate of calcite. Steep rhombs, without gothic-arch type edges were found on the surfaces of *Chara* molds and were possibly formed by circulating waters unassociated with vulcanism. Folk et al. (1985) also describe 'edge guttered' crystals (Fig. 38b) consisting of two sets of rhomb faces. A steep set (f 2 0 –2 1) forms the larger faces while the edges have narrow facets of the reverse rhomb(r, 0 1–1 1), often corroded into irregular spikes.

Large rhombohedra are known from cave travertines. Crystals formed in areas submerged for long periods in the phreatic zone reach the greatest size, and examples exceeding 5 cm in length are known (Hill and Forti 1997). Large crystals are also known from cave pools and the necessary conditions include limited water movement and slow growth resulting from low supersaturation. These authors also mention calcite hopper crystals developing at the surfaces of quiet pools up to 3 cm across.

Scalenohedra, distinguished by their hexagonal outline when viewed end-on, frequently occur in cave travertines, where they are known as 'dog tooth spar' (Fig. 38c). In draperies, Prinz (1908) found scalenohedra developing with their long axes perpendicular to the lower drapery edge. Exceptionally, they may be up to 50 or more cm in length in formerly phreatic

environments (White 1976; Hill and Forti 1997). The conditions leading to the scalenohedral habit are not known, but Sunagawa (1987, p. 553) found that scalenohedra with faces inclined steeply to (0001) were associated with lower temperatures. Scalenohedra are far smaller and less common in epigean travertines. Scholl and Taft (1964) reported them from cavities in the Mono Lake deposits, where they grew up to 150 μm in length and were thought to form in the presence of interfering ions.

Binkley et al. (1980) describe acicular calcite composed of small trigonal prisms from a lacustrine travertine. Trigonal prisms, often with concave faces, occur in the abiotic cement of the Oklahoma and Plitvice travertines (Love and Chafetz 1990; Chafetz et al. 1994). Unusual hollow prisms (skeletal calcite) are described from the hot springs of Kenya and New Zealand by Jones and Renaut (1996) along with skeletal crystals of trona (Fig. 38d). The mechanism of formation is unclear but they probably formed at high supersaturations, perhaps by a mechanism related to the 'Berg effect' described by Sunagawa (1987). Calcite ribbons composed of chains of diamond-shaped plates, 1–2 μm wide are described by (Folk et al. 1985) but their origin is unclear. An unusual form of calcite, termed 'thinolite' (Fig. 38e) occurs in the deposits and lake sediments of Mono Lake, California with well developed prisms, which are composites formed of much smaller crystals (Radbruch 1957). They are probably pseudomorphic after gypsum or ikaite. Small acicular crystals similar to the calcite 'whiskers' of caliche (Klappa 1979) have also been found in Italian deposits, and similar crystals are sometimes found in the UK, perhaps resulting from local desiccation. They have been termed 'needle-fibre calcite' and their occurrence is reviewed by Verrecchia and Verrecchia (1994). Pedley (1987) figures a bladed calcite with *en echelon* twinning, termed 'lublinite' from Caerwys, UK, possibly associated with desiccation. Similar crystals are described from the travertines at Pamukkale, Turkey where they appear to result from desiccation (Pentecost et al. 1997) and fungi may be involved in their formation at some sites (Garnett et al. 2004). The term 'prism' is used fairly loosely in calcite petrography, and often refers to elongate forms without discernable crystal faces. The basal pinacoid {0001} is not commonly observed (Fig. 38f) but may develop under conditions of high carbonate and low calcium activity. Pseudomorphs of calcite are rarely reported from travertine but calcite is sometimes found pseudomorphous after aragonite (Khoury et al. 1984). Calcite (as micrite) replacement of ankerite and siderite was noted in some Israel travertines by Heimann and Sass (1989). The most frequently reported habits are listed in Table 11.

Table 11. Calcite crystal forms reported from travertine

Form	Index	Comments	Reference
Primitive rhomb	10 – 11	Cavity linings	Braithwaite (1979), Schreiber et al. (1981), Pedley (1987)
Flat rhomb	10 – 12	Lining cavities and crusts	Braithwaite (1979), Folk et al. (1985)
Flat rhomb	10 – 14	Crystallites of speleothems	Frisia et al. (2000)
Steep rhomb	20 – 21 40 – 41	Lining cavities and in 'strings', Italy	Folk et al. (1985)
Reversed rhomb	01 – 11	Edge-guttered crystals, Italy	Folk et al. (1985)
Scalenohedron	2131(?)	Mono Lake, Ca, common in caves	Scholle and Taft (1964), Hill and Forti (1997)
Prism	1010(?)	Pisoids and 'ribbons'	Schreiber et al. (1981), Folk et al. (1985)

7.4.2 Aragonite and Vaterite

There have been few petrographic descriptions of aragonite in travertine despite its frequent occurrence. Unlike calcite, aragonite rarely presents large crystal faces, excepting cave anthodites, and the grains are often so small that their form is difficult to describe, even under the SEM. Most aragonitic travertines are characterised by their high porosity and soft texture. The crystals normally occur as minute needles, which may be randomly scattered and loosely interlocked (Sugiyama et al. 1985) or aggregated into spherulites or sheaves.

End-on views of needles from the Mammoth aragonites often reveal the typical hexagonal form, probably representing faces developing from pseudohexagonal twinning on (110), which is common in aragonite, with the c-axis running along the length of the needle. Well-defined faces are rare, but boat-shaped crystals with tapered ends are quite common, and many appear to be formed of composites of much smaller crystals. Khoury et al. (1984) observed aragonite with (010) cleavage and reentrant angles, in the pseudohexagonal prisms of a modern travertine. Crystal-splitting is a common feature of aragonite and is responsible for the formation of aragonite 'sheaves' in the deposits at Mammoth Hot Springs and elsewhere (Pentecost 1990b). Here, a single fusiform aragonite crystal splits distally and the resulting double crystal grows in width more rapidly at the end than in the middle. Further splitting ensues until a sheaf- or dumb-bell shape results (Grigor'ev 1961; Photoplate 13B). In some cave anthodites, aragonite needles up to several mm long make an angle of 60–65° to the main speleothem axis which has been attributed to the prism angle of 63° 48' (Hill and Forti 1997). Although vaterite has been reported from travertines above and below ground, no descriptions of its habit are available from these occurrences.

7.5 The Calcium Carbonate Content of Travertine

Figure 39 shows in histogram form the $CaCO_3$ content of the epigean travertines. Meteogene deposits have a high average $CaCO_3$ content with a median of 92.9% and an upper range of 99.3%. Many travertines thus qualify as limestones of high purity. The frequency distributions are biased towards the authochthonous deposits which by their nature of formation are less contaminated by detrital materials. There have been few measurements of clastic travertines. The histogram depicts data taken from a wide range of sources and it is not possible to further classify all samples in terms of their age as this is not always provided in the literature. If the subset of known active and inactive meteogene deposits is compared, the active deposits are found to have a lower $CaCO_3$ content (mean 91.2%, N = 28) than the inactive ones (mean 94.5%, N = 22). This might be due to the loss of organic matter in the older deposits, but an analysis of variance of the $CaCO_3$ content does not support this hypothesis (F = 5.84, n.s.). Speleothem travertines would be expected to occur in the upper range of these values but data are limited.

The $CaCO_3$ content of thermogene travertines is broadly similar to the meteogenes (Fig. 39b), recording a slightly higher median of 96.1% and an upper range of 99.2%. The two data sets are not significantly different statistically, and again the data range in age from Pleistocene to modern. The $CaCO_3$ content is not shown in relation to the different polymorphs of calcium carbonate as no significant difference is apparent between them. Table 10 provides examples of a range of travertine compositions.

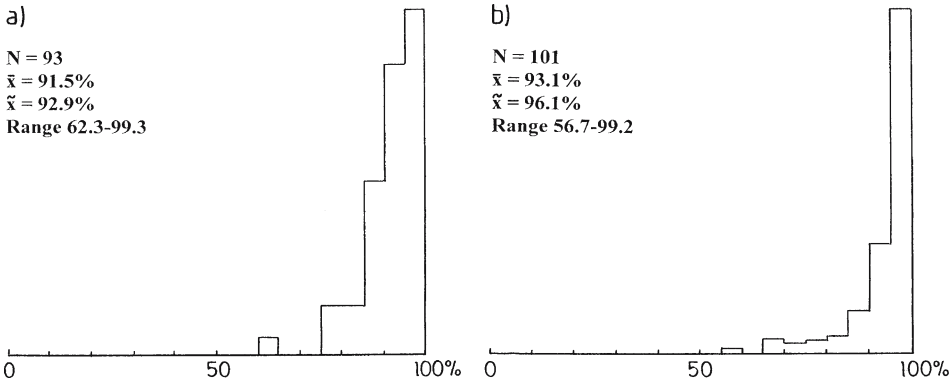

Fig. 39. The calcium carbonate contents of epigean travertines. a) meteogene ; b) thermogene. Sources: Adolphe and Rofes (1973); Allen and Day (1935); Amundson and Kelly (1987); Blaszak (1972); Brown (1939); Buccino et al. (1978); Ferreri and Stanzione (1978); Fritsch and Pantin (1946); Girard and Bordas (1901); Headden (1905); Herman and Hubbard (1990); Ichikuni (1973); Inoue and Iwabuchi (1979); Irion and Müller (1968); Ishigami and Suzuki (1977); Kitano (1963); Klahn (1926); Le Roux (1908); Lindgren (1910); Lookene and Utsal (1971); McFayden (1928); Pentecost (1993, 1995d and unpublished); Pentecost and Zhang (2000); Savelli and Wedepohl (1969); Statham (1977)

7.6 Trace Constituents of Calcite and Aragonite

Small but significant quantities of co-precipitated ions or molecules are frequently found within the precipitated carbonate. They occur in several well-defined locations, namely as fluid or solid inclusions, between lattice planes, at lattice defect sites, or as a substitute for a calcium or carbonate ion. They may also become adsorbed onto the crystal surface. Of these categories, substituting ions furnish the only example studied in any depth. Constraints on ion charge and size mean that only a small number of ions are good candidates for substitution. Since the atomic environment of calcium and carbonate differs in calcite and aragonite, the type of substituting ion and the degree of substitution differ for the two minerals. Aragonite may contain up to 13 mole-% Sr and 2.5 mole-% Pb (Speer 1983), but high proportions of Mg are only found in calcite. Under equilibrium conditions, where heterogeneous nucleation occurs in an open system (Section 10.3.3) it is possible to predict the composition of the solid phase if the solution composition is known by using a partition coefficient (Dickson 1990; Sturchio 1990):

$$^{m}Tr/^{m}Ca_{s} = k \cdot {}^{m}Tr/^{m}Ca_{l} \qquad (7.1)$$

Where Tr is the molar concentration of the trace (i.e. substituting) ion, s = solid phase, l= liquid phase and k is the partition coefficient. For coefficients less than unity, e.g. $Mg_{calcite}$, the ratio of Mg to Ca will be lower in the solid than the solution. The reverse is true for k values >1, meaning that Fe^{2+} will be scavenged from solution, though it should be noted that oxidised Fe and Mn have larger ionic radii and rarely substitute for Ca in calcite. Where diagenesis has occurred, caution must be exercised because open-system conditions are not always applicable, and 'zoned' crystals of variable composition can be formed. Some relevant coefficients are listed in Table 12.

Alkali metals are known to substitute for Ca in aragonite, particularly Na which has a similar ionic radius, but in calcite these metals appear to occupy interstitial positions (Dickson 1990). The amount incorporated has been found to be correlated positively to the crystal growth rate, and this is thought to result from increasing numbers of defect sites formed during rapid growth.

Table 12.
Partition coefficients (k) for some substituting ions in calcite and aragonite at 25 °C

Calcite		Aragonite	
Fe^{2+}	5.0	Mg^{2+}	0.00016
Mg^{2+}	0.03	Sr^{2+}	1.1
Mn^{2+}	10.0		
Sr^{2+}	0.13		

7.6.1 Strontium

The partition of strontium in carbonates has been well studied and several investigations have been made on the Sr content of Italian travertines. Barbieri et al. (1979) mapped Sr concentrations in the Latium deposits. Cipriani et al. (1977) and Duchi et al. (1978) analysed a large number of travertines from central Italy finding up to 9500 ppm Sr in aragonite, equivalent to 1.1 mole-%, and up to 0.5 mole-% Sr in calcite. Transformation of aragonite to calcite via meteoric water circulation led to the precipitation of calcite with a lower Sr content, particularly at depth. Dickson (1990) presents a model of Sr partition in this open system situation. In his model, rainwater percolates an aragonite deposit with a Sr/Ca molar ratio of 0.011, which by coincidence, is that noted above, and dissolves it, precipitating as interstitial calcite further down the profile. Partition theory shows that this recently formed calcite will have a lower Sr:Ca ratio of 0.001. As dissolution of the surface layers proceeds, increasing amounts of this calcite will be dissolved along with the unaltered aragonite with a continuous lowering of the original aragonite surface. The fluid derived from dissolution of the calcite-aragonite mix will be lower in Sr than the initial pure aragonite, because of the dissolved calcite. Consequently the Sr content of the precipitating calcite falls ultimately to around 100 ppm as all aragonite is transformed. Cipriani et al. (1972, 1977) did not find any travertines with such low levels of Sr, but a positive correlation was found between the Sr content and porosity. Such an observation agrees with the partition model, because as aragonite transforms to calcite, porosity declines as a result of calcite infilling. The calcite should contain increasingly less Sr as porosity falls. At Mammoth Hot Springs, the Sr content of the travertine is highest (619–2556 ppm) near the spring vents where aragonite is precipitated, becoming lower where it is partially replaced by calcite in the cooler waters (Sturchio 1990; Fouke et al. 2000). Levels of strontium also depend of the availability of the element in the depositing waters, as discussed by Turi (1986). In Italy, some travertine sequences display large variations in strontium which are thought to reflect element availability within the stratigraphic column.

The range of strontium concentration within travertine is shown in Fig. 40. Levels in calcite are roughly an order of magnitude below aragonite, but analyses of the latter have been few. Many authors either did not state the polymorph analysed, or looked at relict travertines, some of which could have undergone the aragonite-calcite transformation, leaving a calcite with still fairly high Sr levels. In the superambient travertines of Matlock Bath, UK strontium levels are high (Pentecost 1999a). These deposits are of calcite and they contain significantly more Sr than the parent limestone, but the observed values are predicted well by partition theory. The relationship between the strontium content and the proportion of aragonite in travertine is particularly clear in the data of Ishigami and Suziki (1977). They looked at a range of Japanese deposits and their data demonstrate a strong positive correlation between these factors (Fig. 41).

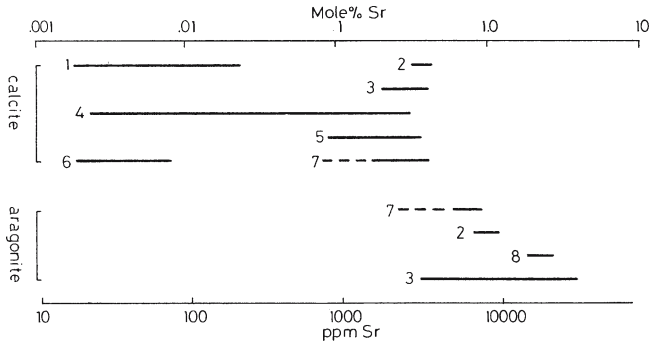

Fig. 40.
Range of strontium concentration in travertines composed predominantly of calcite or aragonite. 1. Irion and Müller (1968); 2. Malesani and Vannucchi, (1975); 3. Kitano (1963); 4. Pentecost (1993); 5. Radtke et al. (1986); 6. Buccino et al. (1978); 7. Cipriani et al. (1972); 8. Richter and Besenecker (1983)

Meteogene (calcite) travertines usually possess fairly low levels of Sr, in the 20–200 ppm range (Irion and Müller 1968; Pentecost 1993), but unusually high values occur in lacustrine oncoids of Lake Constance, Germany (mean 832 ppm) resulting from high groundwater concentrations (Müller 1968). The highest recorded value of 3.8% Sr is from aragonite at Shirahama, Japan (Kitano 1963). To fully test the applicability of the partition equation requires analyses of both rock and water for Sr and Ca and this has rarely been accomplished.

Jacobson and Usdowski (1975) found variable partitioning of Sr for deposits in a German stream, but did not give figures. Irion and Müller (1968) and Cidu et al. (1990) found reasonable agreement between theory and measurement. Applying Eq. 7.1 to the data of Malesani and Vannucci (1975) also gives reasonable agreement between predicted and measured levels but the equation slightly overestimated the amount present. For calcite the results were less satisfactory, there was more Sr present than predicted. This could be accounted for by mineral inclusions of $SrCO_3$. The high Sr values for calcite obtained by Richter and Besenecker (1983) were thought to result from this. Generally, one would expect higher values than predicted, since foreign ions can occupy a variety of sites within a crystal as mentioned above. Ichikuni (1973) observed that the partition coefficients of strontium are increased for both aragonite and calcite if a small amount of Mn has substituted for Ca in the lattice.

In cave travertines, White (1994) demonstrated the partition of Sr in calcite and aragonite, providing an informative composition diagram. The ratios Mg:Ca and Sr:Ca in speleothems and epigean travertines have been used to provide climatic information (see Sect. 13.2).

7.6.2 Magnesium

This element forms a solid solution series with calcite and a wide range of compositions is possible. As noted previously, magnesium does not substitute for calcium to any great extent in most travertines, and high magnesian calcites are rarely encountered. Magnesium levels in the acid-soluble fraction of travertines are shown in Fig. 42. These data show that there are few meteogene travertines composed of calcite which exceed 1% Mg by weight and give a mean value of 0.29 wt% (1.01 mol%). UK deposits average 2300 ppm and Irion and Müller (1968) obtained a range of 240–1060 ppm for travertines of the Schwäbische Alb.

Thermogene travertines consisting of calcite have similar concentrations to meteogenes (Fig. 42b) although few samples have been found where the Mg concentration falls below 0.1% wt, while this is common for meteogenes. Many Italian travertines, undoubtedly of thermogene origin, are in the range 1000–8000 ppm (Ferreri and Stanzione 1978; Buccino et al. 1978; D'Argenio et al. 1983), but the maximum recorded value of

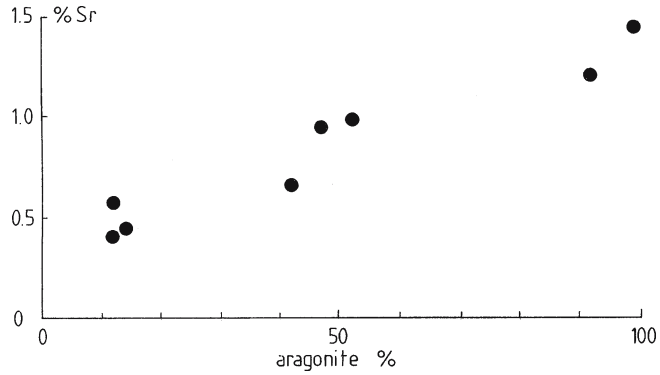

Fig. 41.
Relationship between the Sr and aragonite content of some Japanese travertines. Data from Ishigami and Suzuki (1977)

37,500 ppm (14 mole-%) was found in a meteogene stream deposit of Normandy (Adolphe and Rofes 1973). This carbonate provides a rare and anomalous example of a high magnesian calcite. Buccino et al. (1978) noted that Mg, along with other trace elements, were lower in the cold phytohermal travertines in Italy. Travertines consisting of aragonite have been little studied. In two cases, aragonite deposits were found to contain lower levels of Mg than nearby calcite deposits, namely at Mammoth Hot Springs (Fouke et al. 2000) and in a European cave (Frisia et al. 2002). Considerably higher values have been reported from Japan by Kitano (1963).

Applying partition coefficients for open-system precipitation, to Waterfall Beck, UK a well-studied site with a water containing an average 33 μmol L^{-1} Mg and 1460 μmol L^{-1} Ca, a travertine with 0.07 mole-% Mg should result. In fact the travertine Mg is considerably higher, equivalent to 0.51 mole-% Mg. According to partition theory, aragonite deposits should also contain low Mg concentrations. Even in a water with an unusually high Mg:Ca ratio of 15:24 (Demovic et al. 1972) an aragonite deposit containing just 0.01 mole-% Mg should form. In reality the travertines often contain more. Cidu et al. (1990) found 2.5–5.6 mole-% Mg in meteogene travertines originating from dolomite groundwaters and Kitano (1963) records a Japanese site with >4 mole-% Mg. In a study of travertines deposited from dolomite groundwaters, Klähn (1926) found that little of the Mg in solution was deposited. These results suggest that in most, if not all travertines, Mg occurs other than as a substituting ion. X-ray diffraction data can provide an independent means of assessing the degree of Mg substitution in calcite, but several mole-% would need to be present to provide evidence of this (Goldsmith et al. 1955).

There has been much interest in the partition of Mg in speleothem. Since the partitition coefficients are temperature-dependent, palaeotemperature estimates are possible (Gascoyne 1983). Fairchild et al. (2000) investigated speleothems in two European caves and concluded that the variation in Mg: Ca observed in cave drip-waters could be accounted for by the variable residence times of the groundwater. Cave systems developing in rocks containing dolomite as well as calcite contain drip waters originating from both minerals. Dolomite dissolution is at least ten times slower than calcite dissolution, but the rate depends on the residence time. They also found that the Mg: Ca ratio was higher in the drip-water than expected from the bedrock composition and concluded that there was selective leaching of other Mg minerals. Where aragonite precipitates in the moderately Mg-rich environment of caves, Mg is excluded from the lattice and this is probably the reason that cave aragonites are often found associated with hydromagnesite (White 1982). In epigean travertines, there

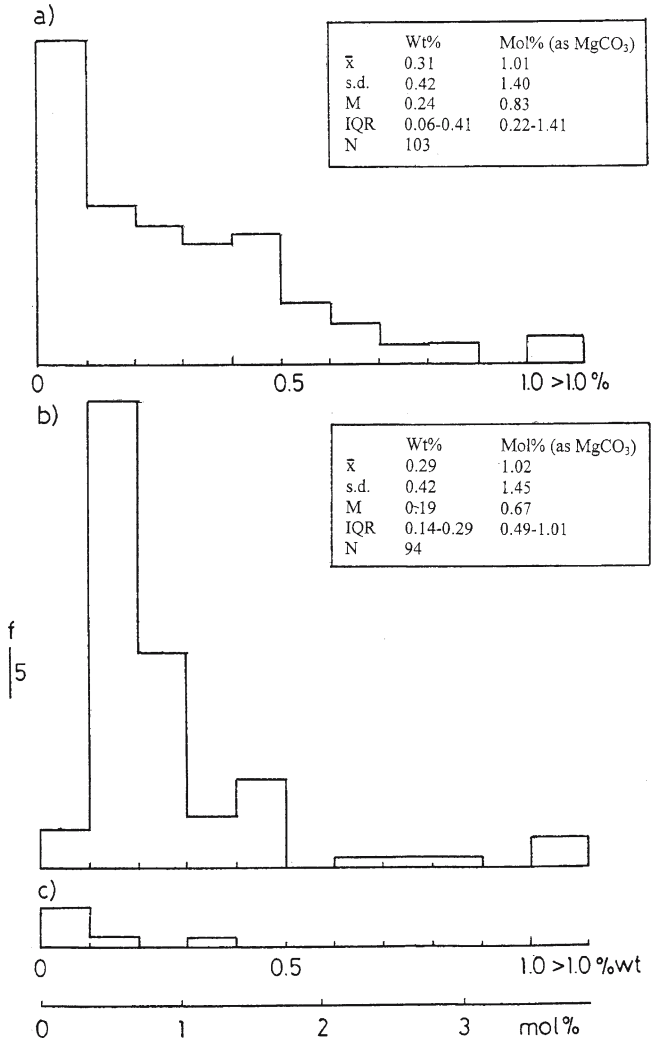

Fig. 42.
Frequency distributions of magnesium in travertine. a) Meteogene deposits of calcite (all types); b) Thermogene deposits of calcite ; c) Travertines composed of aragonite. Sources: Adolphe and Rofes (1973), Amundson and Kelly (1987), Arenas et al. (2000), Blaszac (1972), Brown (1939), Buccino et al. (1978), Cidu et al. (1990), Ferreri and Stanzione (1978), Fouke et al. (2000), Franciscovic-Bilinski et al. (2003), Frisia et al. (2002), Fritsch and Pantin (1946), Girard and Bordas (1901), Headden (1905), Herman and Hubbard (1990), Ichikuni (1973), Inoue and Iwabuchi (1979), Irion and Müller (1968), Ishigami and Suzuki (1977), Kitano (1963), Lookene and Utsal (1971), McFayden (1928), Pentecost (1993, 1995) and unpublished, Pentecost and Zhang (2000), Radtke et al. (1986), Richter and Besenecker (1983), Roberts et al. (1998), Savelli and Wedepohl (1973), Statham (1977). The unusually high value of 14 mol% recorded by Adophe and Rofes has been excluded from the analysis

is some potential for the use of the calcite Mg: Ca ratio as a palaeothermometer, although a better understanding of the form of magnesium within the deposits is clearly desirable (Chapter 13). The incorporation of magnesium into calcite has received much study in terms of the Periodic Bond Chain Model and has been found sensitive to kink site configuration (Paquette and Reeder 1995). Other Group II elements also substitute in the calcite lattice but are rarely recorded. Beryllium has be detected in concentrations up to 15 ppm in some Italian deposits (Dessau 1968) while De Capitani et al. (1974) reported radium in an alstonite as noted above. Much of the Ra was associated with organic matter incorporated in the travertine. A study of barium partition in a meteogene travertine by Caboi et al. (1991) led to the conclusion that this element does not substitute for Ca in the calcite lattice. It does however enter the aragonite lattice resulting in a fall in Ba as aragonite reverts to calcite (Sturchio 1990).

7.6.3 The Alkali Metals

These may substitute for Ca but are more likely to occupy defect sites. They may be present in calcite to the extent of a few hundred ppm (P. Dickson, *pers comm.*). Several authors have detected alkali metals in acid-soluble travertine fractions. Sodium and potassium occur in similar concentrations but a wide range has been recorded for both ions. Buccino et al. (1978) found the greatest range for sodium (7–2941 ppm) in Italian deposits and D'Argenio et al. (1983) obtained a mean of 124 ppm. Similar values were found in the Viterbo travertines (Pentecost 1995c). The greatest range for potassium, 80–5500 ppm was found by Savelli and Wedepohl (1969), but lower values, <8 ppm have also been found (Buccino et al. 1978). The superambient travertines of Matlock Bath, UK contained an average 119 ppm Na and 21 ppm K, slightly less than the parent limestone (Pentecost 1999a). The alkali metals are believed to occupy interstitial positions in the calcite lattice with a frequency of occurrence: Li>Na>K>Rb (Okumura and Kitano 1986). Up to 10.3 ppm lithium has been noted by Ferreri and Stanzione (1978) and Buccino et al. (1978) in Italian deposits. Ferreri and Stanzione (1978) also found traces of rubidium (0–2.3 ppm). There have been no systematic studies relating to calcite and aragonite. Since the concentration of alkali metals is related to the rate of crystal growth (Dickson 1990) further useful work could be done in this area.

7.6.4 Iron and Manganese

Kitano (*pers. comm.*) observed that when Fe levels are high, Mn tends to precipitate with it, but when Fe is low, Mn is incorporated into calcium carbonate. Divalent iron and manganese should be scavenged by precipitating calcite because their partition k-values are greater than unity. Travertine deposition however, usually occurs under oxidising conditions, where divalent iron will be scarce, and little substitution of this element seems to occur. Nevertheless, water-saturated deposits are known with associated organic matter, and the originally oxidised Fe may well be reduced and enter calcite through diagenesis. The Mn^{2+} ion may persist longer under oxidising conditions and could well substitute in the calcite lattice.

Acid-soluble fractions of travertine often contain significant amounts of Fe and Mn, but much of this would come from the dissolution of iron-containing minerals such as limonite (see below). The Fe and Mn content, measured gravimetrically says little about their origin. Irion and Müller (1968) for example, noted that the iron content correlated with increasing acid-insoluble residue, suggesting that this was the principal source of the element. A study, employing two strengths of acid to distinguish between elements originating from the calcite and residual minerals, found that Mn was mainly associated with calcite while Fe was associated with the detrital minerals (Caboi et al. 1991). Travertines are frequently stained with iron where they form from waters possessing low redox potentials as a result of microbial activity as for example in waterlogged soils. A study of the microzonation of travertines rich in iron and manganese has shown that Mn and then Fe was deposited on some Danish calcites, the minerals having been deposited from waters in contact with glacial drift (Villumsen and Grelk 1978). Cidu et al. (1991) using the acid fractionation method concluded that most of the Fe at a Sardinian meteogene site consisted of iron oxides, with up to 0.2 mole-% in the calcite.

Total iron levels have been published for several sites. The range is 20–68,000 ppm, but the upper limit should coincide with the defined boundary between travertine and ocher (see below). Some travertines appear almost white in colour and must contain only traces of oxidised Fe. The majority contain 100–4000 ppm (acid-soluble) and along with traces in organic matter are responsible for the distinctive pale brown hue of most epigean travertines.

The mean Fe content for the meteogene and thermogene travertines reported in Table 10 is 0.16% and 0.26% respectively. The presence of Fe^{2+} in calcite crystals can be tested by staining or cathodoluminescence (Dickson 1966; Machel 1985). Reflectance spectra of speleothems have yielded some useful information on the occurrence of iron and shown that most yellow and brown pigmentation is due to organic contamination (White 1981).

Manganese forms a solid solution series with calcite but is rarely found in large amounts (Kitano 1963). The mean meteogene and thermogene contents (Table 13) are 0.0186% and 0.091% respectively. At Mammoth Hot Springs, Fouke et al. (2000) noted a slight but significant increase in the Mn and Fe content downflow. The presence of Mn-minerals may result in higher proportions. For example at Zerka Ma'in, manganese minerals are zoned with aragonite (Khoury et al. 1984). Several economic deposits of manganese are associated with terrestrial hot springs, and are often intercalated with travertine (Roy 1992). A Spanish meteogene travertine has been reported with pyrolusite, and Mn oxides have been found as dendrites coating calcite crystals in at least two sites (Akdim et al. 1994; Arenas et al. 2000). A wide range of elements were reported from travertines described by the last authors, and a clustan revealed an Mn- and Fe- group of associated elements, possibly derived from different water sources. In some travertines, shrub-like aggregations of iron and manganese occur associated with bacteria (Chafetz et al. 1998).

7.6.5 Phosphorus

This biologically important element has been the subject of intensive research in freshwaters, where its solubility is profoundly influenced by the calcium concentration and pH. Dissolved inorganic phosphorus is present almost exclusively as orthophosphate ions, mainly HPO_4^{2-} derived from triprotic orthophosphoric acid. Laboratory experiments have shown that orthophosphate (P_i) is rapidly adsorbed onto calcite in the pH range 7–9 (House and Donaldson 1985), which is that encountered in most travertine-depositing waters. As the calcite crystals grow from a supersaturated Ca-bicarbonate solution, P_i is incorporated, usually at defect sites. A separate calcium phosphate mineral phase is only observed at high dissolved phosphate concentrations, with $P_i > 20$ μmol L^{-1} (Plant and House 2002), and would not be expected in travertine-depositing waters. The rate of adsorption of P_i is dependent on the ion activity of the solution, and the adsorption isotherm follows the Langmuir model between pH ~7–8.5. For a given P_i concentration, adsorption onto calcite increases with pH in the range 7.4–9.6 but only a fraction of the adsorbed P is incorporated into the lattice with the amount increasing with precipitation rate. At a constant P_i concentration and temperature, the pH and the precipitation rate are important controls on P_i co-precipitation in Ca-bicarbonate waters. One could hypothesise, from these findings, that as a travertine-depositing water evolves from a pH of around 7 at the spring to >8 downstream, that co-precipitation of phosphate would increase to a maximum, then decline as the phosphate was removed in the deposited calcite. This has never been tested, and the situation is likely to be more complex owing to the uptake and cycling of P by the associated biota. A number of spot analyses exist, mainly of meteogene deposits, which contain 8–950 ppm P, with most measurements in the 100–200 ppm range (Demovic et al. 1972; Pentecost 1993). Speleothems appear to contain similar concentrations (Huang et al. 2001). In UK travertines, the mean P content was 210 ppm and is within the expected range for co-precipitation given the low concentrations of P_i in travertine-depositing waters and pH. For example, travertine deposited in an experimental channel had molar Ca:P ratios ranging from 200–2500 dependent on the total P_i in solution and these were considerably higher than the ratios in solution (House et al. 1986a).

Table 13. Elemental composition of travertines presented as ranges in ppm. Mean limestone data are taken from Turekian and Wedepohl (1961). Upper ranges with a > sign indicate a continuous range of compositions as a solid solution series or co-precipitated/detrital mineral assemblages

Element	Average limestone	Meteogene	Thermogene	Element	Average limestone	Meteogene	Thermogene
Al	4200	100–15000	410–8200	Mn	1100	5–1600	8–>3400
As	1	<3–363	150–>1600	Mo	0.4	1–63	<100
Ag	–	to 23	to 2.8	N	–	10–20	–
Au	–	–	to 0.07	Na	400	200–1300	7–2940
Ba	10	2–10000	2–>32000	Nb	–	–	1–8
Be	–	0.05–1.2	1.4–15	Nd	4.7	–	–
B	20	to 50	2–97	Ni	20	4–116	<1–15
Br	6.2	<3–12	–	P	400	8–950	9–220
Cd	0.04	–	–	Pb	1.5–9	<2–31	2–228
Ce	11.5	–	1–126	Rb	3	0.01–31	0.009–284
Cl	150	<80–850	<20–9000	S	1200	240–14000	14–7400
Cr	11	<1–117	<1–146	Sb	0.2	<5–11	[b]
Co	0.1	<1–428	<1–140	Sc	1	<0.5–0.7	<100
Cs	–	0.02–0.04	0.03–0.04	Se	–	<0.3–1.0	–
Cu	4	<0.5–96	4–188	Si	24000	<140–>22000	100–>32000
F	330	–	150–4400	Sn	–	to 30	<100
Fe	3800	46–>4000	<50–>37000	Sr	610	9–>2930	20–14000
Ga	4	–	<1–5	Th	1.7	0.1–0.4	–
Ge	0.2	to 24000[a]	<100	Ti	400	<30–2730	0–3000
Hg	0.04	<0.02–0.08	0.005–1.1	U	2.2	0.4–0.7	<1–>500
I	1.2	–	–	V	20	<2–413	1–100
K	2700	147–5500	8–5500	Y	30	<0.5–71	<1–13
La	–	–	<1–45	Yb	0.5	–	<100
Li	5	<0.05–1.7	<1–10	Zn	15–38	4–680	5–98
Mg	47000	180–>8000	60–>35000	Zr	19	<0.5–192	12–132

[a] 'Orgamox' water.
[b] Reported but without figures.
Sources: Adolphe and Rofes (1973); Allen (1934); Arenas et al. (2000); Blaszac (1972); Buccino et al. (1983); Caboi et al. (1991); Chafetz et al. (1991b); Cipriani et al. (1977); D'Argenio et al. (1983); Das and Mohanti (1997); Demovic et al. (1972); Dessau (1968); Duchi (1976); Duchi et al. (1978); Fabré and Fiche (1986); Ferreri and Stanzione (1978); Fouke et al. 2000; Franciskovic-Bilinski et al. (2003); Frank et al. (2000); Fritsch and Pantin (1946); Garnett et al. (2004); Girard and Bordas (1901); Headden (1922); Herman and Hubbard (1990); Huang et al. (2001); Ichikuni (1973); Irion and Müller (1968); Kitano (1963); Kronfeld (1988); Lindgren (1910); Malesani and Vannucchi (1975); Mawson (1929); Pentecost (1993 and unpublished); Pentecost and Zhang (2000, 2001); Pentecost et al. (2000a); Petrelli et al. (2003); Richter and Besenecker (1983); Savelli and Wedepohl (1969); Suzuki (1978); Van et al. (1973); Zyka (1958); Zyka and Vetelensky (1960).

The average organic matter content of active meteogene travertines is about 4% of the total dry weight (see below). Organic matter contains about 0.1% phosphorus, mainly as covalently-bonded organic phosphates. These compounds are not detected with the standard analytical procedure for P_i, but the mineralisation of organic matter would release P_i, leading to further localised adsorption. For example, the complete mineralisation of a travertine containing 4% organic matter could raise the P_i content of a travertine by about 40 ppm. If the local concentration of P was high enough, hydroxyapatites could also form. In addition, iron (Fe^{3+}) minerals are effective at adsorbing P_i at high pH and could compete with calcite. In UK travertines however, the author found that the acid-soluble P_i content of active and inactive Holocene travertines did not differ significantly, and there was no correlation with the Fe content. Mineralisation was shown to be incomplete, but larger samples and more rigorous analyses are needed to improve our understanding of the relationships between travertines and P_i.

In Waterfall Beck, the author found that the parent limestone contained the same proportion of acid-soluble P_i as the deposits. However, phosphorus undergoes rapid cycling where plants occur and there are probably multiple origins for the P_i. Nothing appears to be known of the relationships between P_i and aragonite in travertines. Phosphorus concentrations are reported for Mammoth Hot Springs where aragonite is replaced by calcite downflow (Fouke et al. 2000), but no significant trend is apparent in the data. Further interactions are to be expected here since many hot spring waters contain an excess of 1 mmol L^{-1} Mg at which concentration this element competes for P_i at adsorption sites (House et al. 1986b). A number of phosphate minerals originating from bat guano and bone beds are known from caves and are occasionally associated with cave travertine (Hill and Forti 1997). Some data on travertine P_i content are provided in Table 13.

7.6.6 Other Elements

Travertines, particularly those forming around hot springs, are sometimes associated with diverse hydrothermally-deposited minerals containing a wide range of elements. Hydrothermal sources are also often rich in volatiles. For example, substantial amounts of fluorite occur in the thermogene travertines of Japan. The fluoride content of aragonite (mean 1903 ppm) was found to be significantly higher than that in calcite (mean 408 ppm) and a negative correlation was found between the pH of the depositing water and the fluoride content of the travertine (Suzuki 1978). Fluorite has also been obtained in small quantity by Emmons and Larsen (1913) and Lindgren (1910) from travertines in Colorado and New Mexico respectively. Minute particles of fluorite have been identified in several thermogene deposits, where they may have been misidentified as 'nanobacteria' (Allen et al. 2000). Boron is a common constituent of thermal waters, and has been found in Japanese travertines in the range 1.6–97 ppm where it appears to be adsorbed onto aragonite and calcite, obeying the Freundlich adsorption isotherm (Ichikuni and Kikuchi 1972). In the travertine mounds of the Pamir Mountains, Tadzhikistan, Ozol (1974) found significant amounts of boron as borax formed through evaporation of a sodium-bicarbonate type water.

Arsenic is often significant in hot spring deposits (Lindgren 1933) but reports from travertine are few. Klähn (1927) mentions its occurrence in Germany, and Clarke (1916) cites an analysis undertaken at Carlsbad with 2.7% As. However, Zyka and Vtelensky (1960) found arsenic to be rare in a large sample of Czech travertines. It has also been noted in a deposit at Vichy, France at a level of 1300 ppm (Girard and Bordas 1901). Arsenic is an important component of the heavily mineralised travertines known from western Turkey (Bernasconi

et al. 1980) where it is associated with several oxides and sulphides of antimony, e.g. dussertite, scorodite and stibnite. Arsenic has also been reported from Italian deposits at levels up to 1600 ppm (Dessau 1968).

Copper is frequently found in traces. Savelli and Wedepohl (1969) noted 7–180 ppm, Ferreri and Stanzioni (1978) 4–37 ppm and Khoury et al. (1984) 47 ppm in modern aragonite travertines and 336 ppm in relict calcite travertines. It has also been reported from Tadzhikistan (Ozol 1974). Speleothems are known where Cu has substituted for Ca in the calcite lattice (White 1981). Zinc occurs in small amounts in epigean travertines (Pentecost and Zhang 2000). Savelli and Wedepohl (1969) found up to 680 ppm Zn in travertines of southern Germany and similar levels are known from a superambient meteogene deposit associated with mineralisation (Pentecost 1999a). Nickel is rarely detected in excess of 20 ppm, but Zyka and Vtelensky (1960) noticed traces in many Czech travertines and it is known from a few speleothems. Another group II element, mercury, occurs in the thermogene travertines of Italy where Duchi (1976) obtained an average of 106 ppb from a large sample. It is not known how the element is dispersed but modern travertines contain the highest concentrations suggesting a degree of post-depositional lability. Mercury is probably deposited from aqueous sulphide complexes and may be associated with the organic fraction of travertine. It is known to be labile in other hydrothermal systems. Cobalt and chromium have been found in similar amounts to zinc (Ferreri and Stanzione 1978). In a chinese speleothem, Li et al. (1997) found that levels of Co and Fe were higher in cold climatic stages, perhaps reflecting lower rates of travertine growth. The travertine at Uncie, Bolivia provides the only known example of an association with a tungsten mineral, wolframite, cited in Waring (1965). In a travertine near Banska Bystrica, Slovakia, up to 2.4% germanium was found by Zyka (1958) and was thought to be deposited from oilfield waters. Formation waters are often highly reducing due to prolonged contact with hydrocarbons and pyrite.

Some travertines are associated with traces of gold and silver. Both Lindgren (1910) and Emmons and Larsen (1913) provide examples of thermogene deposits associated with mineral veins containing 0.02–0.07 ppm Au and 1.4–2.8 ppm Ag. Traces of silver have also been found at Besenova, Slovakia (Zyka and Vtelensky 1960) and in the meteogene deposits encrusting the Nimes Aqueduct in France (Fabré and Fiche 1986). Because of their value in dating travertine, analyses of U and Th are often made. For example, Van et al. (1973) found 0.53–12.37 ppm ^{238}U in deposits from Afghanistan and Kronfeld et al. (1988) report 0.1–0.4 ppm Th from Israel. Using fission track analysis, Bigazzi and Rinaldi (1973) obtained U values of 0.2–0.9 ppm at Bagnaccio, Italy, with highest levels near the source. Much higher levels, exceeding 500 ppm have been found in the Miocene tufas of the Barstow Formation, California (Cole et al. 2004). Uranium is known to form stable complexes with carbonates. Radium was first detected by Headden (1905) in deposits rich in barium, and this element probably occurs in most iron-rich travertines, since ferric hydroxides scavenge heavy elements. Most hot springs are radioactive and probably contain traces of radium, radon, thorium and other decay products of the ^{238}U series. Franciskovic-Bilinski et al. (2003) provide specific activities of the some of the radionuclides of Cs, K, Ra, Th and U from a range of Chinese meteogene travertines. Traces of helium probably exist in most thermogenes, and aragonite should contain detectable amounts of both He and Pb. Lead has been detected in travertine calcite from Jiuzhaigou, China (Pentecost and Zhang 2000) and an average of 655 ppm recorded from the travertines of Matlock Bath, UK (Pentecost 1999a). Lead readily enters the aragonite lattice, but there are no reports of this in travertine, presumably due to the low concentrations of Pb in the source waters. A spectroscopic study of Czech travertines by Zyka and Vtelensky (1960), many of which were associated with hot springs, revealed traces of several other rare ele-

ments including Be, Cd, Ga, Mo, Sc, Sn, V, Yb and Zr. Petrelli et al. (2003) record Ce, Ga, Nb and Y from a range of Italian deposits. In eastern Russia, thermogene deposits have also been found to contain small amounts of Mo and Zr (Zaguzin et al. 1980).

The elemental composition of travertine is provided in Table 13 where it is compared with data for average limestone (Turekian and Wedepohl 1961). Some chalcophile elements, such as Ag, As and Cu occur in higher concentrations in thermogene deposits, compared with average limestone, though the form in which they are present is unknown. Meteogene travertines contain higher levels of Ba than other limestones but no explanation is offered. Regardless of their origin, travertines consist almost wholly of the lithophile elements (Ca, C, O, Mg, Fe, Sr).

7.7 Autochthonous Non-carbonate Minerals

A wide range of minerals may be co-deposited with calcium carbonate. This may be a consequence of carbon dioxide evasion, which changes the pH, or as a result of oxygen transport, which changes the redox-potential. Precipitation also occurs upon rapid pressure and temperature reduction, and evaporation. All of these changes tend to be on a larger scale in thermogene waters, and most of these minerals are encountered in thermogene settings. Numerous minerals are deposited in caves, often associated with calcite but these forms are not considered here and the reader is referred to Hill and Forti (1997) for a comprehensive treatment.

7.7.1 Gypsum

Gypsum is common in evaporating brines and may be found associated with calcium carbonate in playas and the shores of saline lakes. Thinolite (Section 7.4.1) may be calcite pseudomorphic after gypsum in Mono Lake, California. In hot springs, gypsum is usually deposited as a result of evaporation. Bargar (1978) noted it around vents at Mammoth Hot Springs, Wyoming. Malesani and Vannucci (1975) and Pentecost (1995c) noted its occurrence at several thermal sites in Italy (e.g. Bagni di Lucca, Bagni di Roselle, Bagno Vignone) where it makes up to 4% of the travertine dry weight. However, analyses of a large number of other Italian travertines by Ferreri and Stanzione (1978) and Buccino et al. (1983) revealed only traces of $CaSO_4$. Like calcite, the solubility of gypsum decreases with temperature, and this may also lead to deposition around vents. Gypsum forms on travertine cave walls near Banff through the oxidation of sulphide-containing waters (van Everdingen et al. 1985).

7.7.2 Barytes

The deposition of barium sulphate from springs appears surprising considering the extreme insolubility of this salt. However, deposits are well documented from several sites, the best known being Doughty Springs, Colorado (Headden 1905). Here, the deposits contain between 5.4 and 94.6% barium sulphate, the largest proportions occurring in active sites near the springs. Lindgren (1933) noted that CO_2-rich waters can hold moderate amounts of Ba in solution despite the presence of sulphate, and the cooling of barytes-saturated water leads to supersaturation making deposition more likely. Significant amounts of Ba have also been found in a Spanish lacustrine travertine and attributed to a deep groundwater source (Arenas et al. 2000). Brines can hold up to 1.5 mmol L^{-1} barium chloride. On contact with sulphate-rich freshwater, or upon dilution, barytes is precipitated. Anoxic sulphur springs may contain soluble barium hydrosulphide, precipitating as sulphate on oxidation.

7.7.3 Manganese and Iron Minerals

Black deposits of manganese minerals occur in some thermogene travertines, an example being the rim deposits near Firehole Lake, Wyoming. They also occur on a large scale at Cliffroy Mine, New Mexico, Golconda Hot Springs, Nevada and Yavapai, Arizona, (Feth and Barnes 1979). Kitano (1963) reported pyrolusite (MnO_2) and $MnO(OH)_n \cdot H_2O$ from Masutomi, Japan and a hydrous MnO_2 was noted by Ichikuni (1973). Manfra et al. (1976) found Mn deposits associated with Italian travertines at Santa Severa and Civita Castellana but their composition was not determined. A soot-like mineral, birnessite (Mg, Ca, K) $Mn_7O_{14} \cdot 2H_2O$ occurs on speleothems (White 1976) and may also be associated with epigean travertines. The 'black calcites' of the Swabian Miocene travertines contain todorokite associated with graphite (Hanold and Weber 1982).

Traces of iron oxides are sufficient to impart an ochraceous tint to travertine, and the Fe content varies widely. Much of the iron present in travertine is autochthonous, precipitated from solution once groundwaters containing ferrous ions contact the atmosphere, precipitating hydrated ferric oxides. X-ray diffraction reveals that the iron is poorly crystallised and amorphous (Caboi et al. 1991). Sometimes, these amorphous iron oxy-hydroxides assist in the cementation of travertine (Arenas et al. 2000). At the Futamata hot springs, Japan, Kitano (1963) found amorphous iron oxides approximating to limonite, and, more rarely, goethite (FeO OH) the stable form at ambient temperature. By using a spectrophotometric method, he showed that the red deposits equated with Fe_2O_3 and yellow deposits with Fe_2O_3. H_2O. Traces of siderite, $FeCO_3$ occurred there and it is also known from Carlsbad (Lindgren 1933) and Salt Lick Spring, California (Amundson and Kelly 1987). At the latter, the mineral is deposited prior to aragonite and there is some evidence for Fe substitution in the aragonite lattice.

Clarke (1916) briefly described hot spring deposits consisting predominantly of ferric oxides and Lindgren (1933) called these ochers. Klähn (1923) describes some 'iron sinters' containing up to 67% Fe_2O_3 from Germany, and a range of compositions is known (Clarke 1916). The 'travertines' of Salt Lick Spring, California described by Amundson and Kelly (1987) consist of ocher in their upper part grading slowly into travertine below. Spötl et al. (2002) note ocher deposits associated with travertine in the Italian Alps and report briefly on the associated water chemistry. In keeping with the compositional definition of travertine, ocher should be reserved for those deposits containing >50% by weight of limonite and related iron minerals. Ocher is also known from caves. Goethite is considered to be the mineral responsible for occasionally colouring speleothems red or orange (White 1976) and has been found in a spanish thermogene travertine with ferrihydrite and amorphous FeOH (Arana et al. 1979). Iron is deposited prior to calcite in many springs and this is put to use in commercial 'petrifying springs' (Section 17.4.3). In the hot springs of Bath Spa, England, Rastall (1926) described deposits consisting of aragonite, calcite and marcasite. Pyrite is known from the travertine deposits at Wagon Wheel Gap, USA (Emmons and Larsen 1913) at Jemez Springs (Caldwell et al. 1984) and at St Alyre, France (Daubrée 1888). Haematite Fe_2O_3 is thermodynamically unstable under ambient conditions but traces have been found in a Spanish travertine (Arenas et al. 2000) probably owing to its slow hydration rate. Jarosite, $K_2Fe_6 (OH)_{12} (SO_4)_4$ a common secondary epithermal mineral may be associated with some thermogene travertines, but is usually associated with clay minerals and siliceous sinter.

7.7.4 Sulphur

Elemental sulphur often occurs in active hydrothermal deposits as a result of hydrogen sulphide oxidation. At Mammoth Hot Springs, it is found near the vents and also on the cascades (Bargar 1978) and the sulphur content increases downflow at one site from 630–5288 ppm (Fouke

et al. 2000). Considerable amounts have been found in the recent deposits at Bagni di Tivoli, Italy (Pentecost and Tortora 1989) where much sulphur is suspended in the spring waters and it was found as large inclusions in the associated calcite. It has also been found in recent deposits near Viterbo and elsewhere (Demovic et al. 1972; Cipriani et al. 1977), but seems to be short lived, no doubt being oxidised by microorganisms and atmospheric oxygen. Gosse (1820) mentions that the sulphur sublimed in travertine fissures at Bagni san Fillipo was formerly collected and sold. In common with some iron minerals, sulphur may occur as both an allochthonous and autochthonous constituent.

7.7.5 Silica

There has been much interest in siliceous hot spring deposits and they are widespread in geothermal areas. Deposits containing mixtures of opaline silica and calcium carbonate are frequent, occurring in Yellowstone Park in several places. Allen and Day (1935) briefly describe such deposits from Terrace Springs, Firehole Lake, Hillside Springs and Deep Creek Springs. At Terrace Springs the two minerals are segregated in some areas, but well mixed in others. Scalloped silica 'cakes', covered with aragonite needles were reported from Deep Creek Springs. At Steamboat Springs, Nevada and elsewhere, mixtures of calcium carbonate, chalcedony and quartz occur (Becker 1888; Lindgren 1933). Apparently amorphous carbonate crusts containing Mg and Si have been reported from the Lake Bogoria travertines of Kenya by Jones and Renaut (1995). Mixes have also been noted from hot springs of the Auvergne, France (Scrope 1858). Hydrothermal silica is deposited by the cooling and evaporation of Si-rich solutions usually circumneutral in pH and low in Ca. Kitano (1963) mentions silica deposits from Japan and a dark form, termed basanite is known from Italy (Cipriani et al. 1977). Mixtures of travertine and silica occur in several New Zealand hot springs, notably Ngatamariki and Waikite. At the former, calcite is present in thin lenses, up to 1–3 mm long and 0.3 mm wide in a matrix of laminated opal-A (Campbell et al. 2002; Mountain et al. 2003). Here, the calcite content is 10–15% and is probably formed by evaporation. In Yunnan, China, the siliceous sinters appear to be deposited in hydrothermal systems at higher temperatures than the travertine (Meixiang and Wei 1987). Similar deposits are known from the Transbaikal region of Russia (Zaguzin et al. 1980). The formation of siliceous sinters is considered further in Sect. 15.6.

Authigenic silica is also found in meteogene travertines. In the UK, chert has been reported from Pleistocene deposits at Alport, Derbyshire. Shafer and Stapf (1978) found silica in algal filament cavities, and in one case quartz, with undulatory extinction was seen replacing microspar in Lake Constance oncoids. In the lake oncoids of El Mojarral Lake, Mexico, Winsborough et al. (1994) found double-terminated quartz crystals up to 20 μm long which were probably formed from diatom frustules. Heather Viles (*pers. comm.*) also found silica in travertines of the Kimberley district, Northern Australia. Double-terminated quartz crystals have also been encountered in deposits at Caerwys, UK (Jackson 1922) and in the 2000-year old deposits at Gordale, UK. (Pentecost and Zhang, *unpublished*). The thermogene oncoids ('pisoids') of the Bolivian Altiplano contain layers of amorphous silica and quartz (Jones and Renaut 1994). Authigenic quartz has also been reported from a cave travertine where it was thought to have formed at high temperature (White and Deike 1962).

Silica is a common constituent of travertines deposited prior to the Quaternary. Extensive diatom deposits (diatomite) often occur near hot springs (Weed 1889b; Manfra et al. 1976) and travertines, along with marls forming in saline lakes also contain silica (Clarke 1916; Dunn 1953; Feth 1964). The precipitation of quartz in travertine is also reported by Heimann

and Sass (1989) but none of the studies reported here provide detailed information on travertines older than the Quaternary. Thus, the long-term stability of these minerals and their various inclusions is not known.

7.7.6 Other Minerals

Daubrée (1888) described hot spring deposits of Plombieres in the Vosges with fluorite and the zeolites apophyllite and chabazite. These deposits also contain aragonite, calcite and opaline silica. Chabazite, together with mesolite, analcite, stilbite, opal and calcite were also found by Hewett et al. (1928) in the travertines of the Ritter Hot Springs, Oregon. Hydrothermal systems contain a wide range of minerals, both primary and secondary, the latter resulting from hydrothermal alteration of the host rock (e.g. Meixiang and Wei 1987). One invasive meteogene travertine contained volkonskoite, a rare smectite, turning the deposits green (Clark et al. 1991).

The Senator ore deposit in Turkey is closely associated with a siliceous travertine which contains much hydrothermal arsenic and antimony as stibiconite, dussertite and metastibnite (Bernasconi et al. 1980). Evaporite minerals (e.g. trona) are also commonly associated with travertines formed in arid or thermal environments.

7.8 Allochthonous Components

Much of the acid-insoluble residue resulting from a wet chemical analysis of travertine contains mineral grains and organic matter of allochthonous origin. These minerals enter the travertine as erosion or weathering products derived from the soil and bedrock. Most will be water-borne, but there is evidence for wind-borne particulates as well (Pentecost 1994). On occasion, minerals may enter via animal activity. Given their diverse origins, many kinds of minerals are to be expected. Acid-insoluble fractions containing the bulk of this fraction may be found tabulated by Savelli and Wedepohl (1969), Cipriani et al. (1977) and Buccino et al. (1978). They normally comprise 0.2–8% of the travertine dry weight. Sand, silt and clay are common, but there have been few detailed investigations. In clastic, or re-deposited travertines, this detrital fraction is often much higher resulting from admixture with other materials during transport, but again, detailed information is lacking. Paludal deposits, many of which contain a clastic element, are also high in this fraction (Table 10). In caves, those minerals deposited through the process of weathering are termed resistates (White 1976). Resistates enter the cave travertine fabric by flooding or dust-deposition.

Analyses often list a SiO_2 component, but this might include autochthonous silica described above. The SiO_2 content of travertine is often the major component in this fraction, and excluding autochthonous silica-travertine mixes such as those at Yellowstone, it usually varies from 0.01–6% dry weight (Savelli and Wedepohl 1969; Demovic et al. 1972). Cortesi and Leoni (1955) appear to be the only people who have paid much attention to the proportion of mineral types present. In a core from Bagni di Tivoli, they found that quartz made up 30–70% of this fraction, chalcedony (autochthonous?) 4–18% and radiolarian spicules 0.9–3.3%. The latter were derived from the parent limestone, and represent an unusual find considering the instability of organically-deposited silica in travertine. Pentecost (1990d) in a study of suspended particles in Waterfall Beck, UK found that aluminosilicates comprised 54% and quartz 24% of the acid-insoluble fraction. Particles rich in Ba and S were also identified and probably represented barytes eroded from ore veins in the parent limestone.

Levels for aluminium in travertine are usually quoted as Al_2O_3 but its provenance is unclear. Savelli and Wedepohl (1969) give a range of 0.04–4.3% Al_2O_3. Titanium is also occasionally

Table 14. Non-carbonate epigean travertine-associated minerals. Chemical formulae of complex common minerals are excluded

Mineral	Composition	Reference	AU/AL
Analcite	$Na(AlSi_2)O_6 \cdot H_2O$	Hewett et al. (1928)	AU
Apophyllite	$KFCa_4Si_8O_{20} \cdot 8H_2O$	Daubrée (1887)	AU
Barytes	$BaSO_4$	Headden (1905), Tucan (1939)	AL,AU
Bassanite	$2CaSO_4 \cdot H_2O$	Manfra et al. (1976)	AU
Biotite	–	Irion and Müller (1968)	AL
Borax	$Na_2B_4O_7 \cdot 10H_2O$	Ozol (1974)	AU
Brucite	$Mg(OH)_2$	Flinn and Pentecost (1995)	AU
Chabazite	$(CaNa)\ (Al_2Si_4)\ O_{12} \cdot 6H_2O$	Hewett et al. (1928)	AU
Chlorite	–	Bouyx and Pias (1971)	AL
Dussertite	$Ca_3(AsO_4)_23Fe(OH)_3$	Bernasconi et al. (1980)	AU
Epidote	–	Cortesi and Leoni (1955)	AL
Epsomite	$MgSO_4 \cdot 7H_2O$	Spötl et al. (2002)	AU
Ferrihydrite	$5Fe_2O_3 \cdot 9H_2O$	Arana et al. (1979)	AU
Fluorite	CaF_2	Emmons and Larsen (1913)	AL, AU
Glaucophane	–	Cortesi and Leoni (1955)	AL
Goethite	FeOOH	Arana et al. (1979)	AU
Graphite	C	Hanold and Weber (1982)	?
Gypsum	$CaSO_4$	Bargar (1978)	AU
Haematite	Fe_2O_3	Chahida (1988), Korpas (2003)	AU
Halite	NaCl	Waring (1965)	AU
Hyalite	$SiO_2 \cdot nH_2O$	Waring (1965)	AU?
Illite	–	Bouyx and Pias (1971)	AL
Kaolinite	$Al_4Si_4O_{10}(OH)_8$	Irion a. Müller (1968), Fabré a. Fiche (1986)	AL
Limonite	$Fe_2O_3 \cdot nH_2O$	Amundson and Kelly (1987)	AU
Magnetite	Fe_3O_4	Cortesi and Leoni (1955)	AL
Manganite	MnOOH	Villumsen and Grelk (1978)	AU
Marcasite	FeS_2	Rastall (1926)	AL,AU
Mesolite	Na/Ca/Al silicate	Hewett et al. (1928)	AU
Metastibnite	Sb_2S_3	Bernasconi et al. (1980)	AU
Mirabilite	$Na_2SO_4 \cdot 10H_2O$	Feth and Barnes (1979)	AU
Montmorillonite	–	Bouyx and Pias (1971)	AL
Muscovite	–	Heimann and Sass (1989)	AL
Olivine	$(MgFe)_2SiO_4$	Cortesi and Leoni (1955)	AL
Orthoclase	$KalSi_3O_8$	Cortesi and Leoni (1955)	AL
Psilomelane	$Mn_xO_y \cdot H_2O$	Kitano (1963)	AU
Pyrite	FeS_2	Caldwell et al. (1984)	AL,AU
Pyrolusite	MnO_2	Kitano (1963)	AU
Quartz	SiO_2	Shafer and Stapf (1978)	AL,AU
Realgar	AsS	Cortesi and Leoni (1955)	AL
Rutile	TiO_2	Pentecost (1990d)	AL
Scorodite	$FeAsO_4 \cdot 2H_2O$	Bernasconi et al. (1980)	AU
Spinel	$MgAl_2O_4$	Cortesi and Leoni (1955)	AL
Stibiconite	$H_2Sb_2O_5$	Bernasconi et al. (1980)	AU
Stilbite	$(Na_2Ca)(Al_2Si_6)O_{16} \cdot 6H_2O$	Hewett et al. (1928)	AU
Sulphur	S	Cipriani et al. (1977)	AU
Titanite	$CaTiSiO_5$	Cortesi and Leoni (1955)	AL
Todorokite	$(Mn^{4+}Mn^{2+})_8(O,OH)_{16} \cdot 2H_2O$	Harold and Weber (1982)	AU
Trona	$Na_2CO_3NaHCO_3 \cdot 2H_2O$	Ozol (1974)	AU
Volkonskoite	$Ca_3(Cr^{3+},Mg,Fe^{3+})_2(Si,Al)_4O_{10}(OH)_2 \cdot 4H_2O$	Clark et al. (1991)	AU?
Wolframite	$(Fe,Mn)WO_4$	Waring (1965)	AU
Wüstite	–	Franciscovic-Bilinski et al. (2003)	AL

reported. Cortesi and Leoni (1955) found up to 0.5% titanite with rutile in the insoluble fraction at Bagni, Italy. Some rutile also occurs in the Nimes deposits of France (Fabré and Fiche 1986). In Germany, Irion and Müller (1968) found quartz, biotite, kaolinite, montmorillonite, illite and feldspars, thought to come from the parent limestone. Jones and Renaut (1994) found smectite and illite in the acid-insoluble fraction of oncoids from the Bolivian Altiplano, and similar clays occur in the travertine bridges of Turkey (Bayari 2002) and Hungary (Korpas 2003). Ferreri and Stanzione (1978) performed elemental analyses of insoluble fractions and detected many elements including Mg, Sr, Na, K, Fe, Mn, Cu, Cr and Co. An indeterminate fraction of many of these elements would enter solution upon acidification, confounding attempts to apply partition theory to substituting ions in carbonate lattices.

The known epigean travertine-associated non-carbonate allochthonous minerals are listed in Table 14. Most carbonate minerals are also transportable, and when this occurs on a large scale it results in the formation of clastic travertines. Small amounts of parent limestone are also likely to be trapped within travertines. Detrital travertine minerals were used by Casanova (1994) to trace palaeodrainage patterns in the East African Rift. In thermogene travertines, the occurrence of clay may be the result of hydrothermal alteration of the host rock. Traces of uncombined carbon occur in the Latium travertine (Cortesi and Leoni 1955). When the detrital fraction is measured by dissolving the carbonate in acid, then ashing to remove organic matter, the more recalcitrant components such as quartz are unaffected and easily measured. However, reactive minerals such as the Fe and Mn oxides are partially dissolved in the preliminary acidification used to remove the carbonates and will dehydrate on heating so caution must be exercised when making comparisons. Quartz, while unaffected by these methods, is unusual in being both authigenic and detrital, sometimes leading to uncertainties in its origin.

Since thorium is insoluble in water at pH 7–8, its virtual absence in carbonate deposits may be taken as evidence of low allochthonous contamination (Ihlenfield et al. 2003). Thorium is often determined owing to its importance in Uranium-series dating (Sect. 11.1.2).

7.9 Fluid Inclusions

Near infra-red reflectance spectra of speleothems reveal sorbed water in fluid inclusions and crystal interfaces (White 1981) and a considerable amount of information is available on the inclusions as their analysis often allows interpretation of past environments.

Fluid inclusions also occur in surface travertines, and they are often seen in spar cements (Chafetz et al. 1994). Baron et al. (2003) found inclusions in the hot- and cold spring travertines of Italy, Mexico and the UK. Most of the inclusions were less than 5 μm in diameter and at room temperature were single phase and aqueous suggesting that fluids were trapped at temperatures less than 50 °C. Controlled freezing indicated they were all of low salinity (<10 ppt) and probably represented entrapped meteoric water.

Crystal inclusions of several types are described from cave calcites by Kendall and Broughton (1978). They often impart a pseudo-pleochroism to the crystals (ω = mid-brown, ε = colorless). A study of irregular crystal boundaries in cave calcite led Kendall and Broughton to suspect non-competitive crystal growth. An analysis of inclusions suggested development from coalescing syntaxial crystallites at the travertine surface. This would help to explain the frequent occurrence of 'subcrystals' in travertines. These form from crystallites with slightly different crystallographic orientation as a result of lattice mismatching due to substituting ions or other impurities. Slightly curved growth surfaces would result and such surfaces can be frequently seen in larger idiomorphic crystals.

7.10 Organic Matter

Small amounts of organic matter probably occur in all deposits and it is usually a significant component of active epigean travertines, particularly those colonised by bryophytes whose rhizoids and stems may persist for many years in the upper layers of the deposit. While not a 'mineral' component, the organic residue remaining after carbonate dissolution is often quoted in gravimetric analyses. It is not normally practicable to separate the organic components into allochthonous and autochthonous fractions. It may be supposed that the bulk of the organic matter would be autochthonous material derived from the productive biofilm in all but heavily shaded sites, and/or those occurring in densely forested areas where the detrital fraction normally predominates. In this respect, epigean travertines differ from speleothems, whose organic matter is primarily allochthonous and usually present only as a trace constituent. Organic matter is an important component, as it can sequester a wide range of dissolved ions such as phosphate and iron, and also influence carbonate diagenesis. Relict travertines tend to have lower organic matter contents than active travertines due to the decay of the surface biofilm, but the difference is not as great as might be supposed, at least in Holocene deposits. The mean organic content for 10 UK active and inactive travertines was 1.66% and 1.33% respectively (Pentecost 1993), but Pleistocene deposits from the UK have considerably less, those at Alport, Derbyshire being around 0.14% (author, unpublished). The preservation of organic matter in a porous travertine is likely to be much influenced by the availability of oxygen. Where it is excluded, such as in an anaerobic microbial mat, preservation may be prolonged. For example, travertines of the Oligocene Creede Caldera containing 0.24% organic matter are reported by Larsen (1994). Previous work (Pentecost 1985a) identified polysaccharides and NH_2 groups in a 2000 year-old travertine containing 0.37% organic matter while Klähn (1923) had formerly identified cellulose and lignin histochemically. Traces of organic carbon were reported in the Latium travertines by Cortesi and Leoni (1955). In a study of the thermogene Salt Lick Spring travertine of California, Amundson and Kelly (1987) found an average 1.5% and 0.1% organic matter in modern and ancient deposits respectively. The lake travertines of East Africa, most of which date to the Pleistocene, contain an average 1.3% organic matter (Casanova 1994). Some representative examples can be found in the compositions listed in Table 10. A range of carbonate sediments, including travertines have been studied for their amino acid and polysaccharide content in the Plitvice region (Emeis et al. 1987). Active travertines contained about 700 $\mu g\ g^{-1}$ amino acid, dominated by aspartate (18–22 mole-%). Hydrolysis revealed a sugar content ranging from 324 $\mu g\ g^{-1}$ in older travertines to 14808 $\mu g\ g^{-1}$ in active ones, the major components being mannose, galactose and xylose. The total nitrogen content of some Holocene travertine samples was reported by Pentecost et al. (2000a). It averaged 19 ppm as was presumably all of organic origin.

In an investigation of the ancient Delphic Oracle in Greece, de Boer et al. (2001) found traces of ethane and methane in a travertine and attributed their occurrence to entrapment from hydrocarbon-rich fault-guided springs. Ethylene was present in the spring water and was thought responsible for the legendary intoxication of the Pythia.

7.11 Fluorescence and Phosphorescence

Many travertines emit light when irradiated with UV. The fluorescence is usually weak and influenced by other minerals. Fluorescence is higher at 366 nm when compared with 254 nm but similar in character. At 366 nm most meteogene deposits appear dull chocolate-brown in colour and emit little light, though a pale buff glow may be apparent. Travertines containing

aragonite normally differ by emitting a dull purplish glow and this might be used to distinguish the polymorphs. At 254 nm, most travertines fluoresce dull purplish irrespective of their mineralogy. High levels of Fe and Mn result in greatly reduced fluorescence and some samples appear almost black, but speleothems containing traces of Mn^{2+} emit a pink fluorescence (White 1976). The physical environment of these ions is probably important in determining the nature of the phenomenon. Surface growths of phototrophic microbes impart a mottled pink or reddish (rarely blue) tinge, the fluorescence being caused by photosynthetic pigments or their breakdown products. An orange fluorescence probably due to organic contaminants has been detected in speleothems. Some epigean travertines exhibit a short-lived phosphorescence. Epigean aragonitic travertines possess a faint yellow phosphorescence disappearing in about 10 seconds. This is less apparent in calcitic travertines. A number of studies have been made of fluorescence and phosphorescence in speleothems and a range of spectra have been reported (Shopov 1997). In most cases the cause of the luminescence is unknown but may be generated by traces of organic matter and molecular ions.

Stable Isotopes

Mass spectrometers measure the isotope composition of carbonates and water with great speed and accuracy. The ratios of two isotope pairs, ^{12}C, ^{13}C and ^{16}O, ^{18}O undergo discrete changes during biogeochemical cycling allowing inferences to be made concerning their origin and past history. The ratios are expressed in the δ notation providing an expanded scale for the comparatively small differences observed. For $^{12}C/^{13}C$:

$$\delta^{13}C = [(^{13}C/^{12}C)_{sample} / (^{13}C/^{12}C)_{standard}] - 1 \text{ (x 1000)} \quad (8.1)$$

Measurements are made relative to the Vienna Peedee Belemnite standard (VPDB) which has a $^{12}C/^{13}C$ ratio of 88.99 and $\delta^{13}C = 0$. Positive values of $\delta^{13}C$ indicate relative enrichment of a sample with ^{13}C, whilst negative values indicate depletion. Carbonates possess a wide range of values relative to the standard, from approximately –25 to + 15‰ (per mil notation). The ratio of the two oxygen isotopes is expressed in a similar manner, but the standard for water oxygen is based on the Vienna Standard mean ocean water (VSMOW). The oxygen ratio is not so easily derived since ^{17}O is also present. Nor is it quite as precise since the degree of isotopic discrimination is less than carbon. ^{16}O is by far the most abundant isotope at the Earth's surface (99.76%). For carbonates the $\delta^{18}O$ is more conveniently expressed on the VPDB scale. The values are interchangeable, so that a calcite oxygen value on the VSMOW scale is given by:

$$\delta^{18}O(VSMOW) = 1.03086\ \delta^{18}O(VPDB) + 30.86 \quad (8.2)$$

$$\delta^{18}O(VPDB) = 0.97006\ \delta^{18}O(VSMOW) - 29.94 \quad (8.3)$$

Carbonates have $\delta^{18}O$ (VSMOW) values ranging from about 0 to +35‰. Their interpretation is generally less straightforward than carbon isotope values because carbonate oxygen readily exchanges with the oxygen in water molecules. The lightest isotope of any element is the more chemically reactive and makes slightly weaker bonds than heavier isotopes. When a mixture of isotopes undergoes a chemical reaction, each isotope behaves slightly differently and has its own rate- and equilibrium constant (fractionation factor).

$$\alpha_{AB} = R_A/R_B \quad (8.4)$$

Where R_A, R_B is the ratio of the heavy to light isotope in phase A and B respectively. The fractionation factor α is temperature dependent taking the form:

$$\ln\alpha = PT^{-2} + QT^{-1} + R \quad (8.5)$$

Where P, Q and R are empirical constants and T the absolute temperature. At ambient temperatures the first squared term can be neglected. The α values are close to unity and conveniently expressed as isotope enrichment factors ε:

$$\varepsilon_{AB} = (\alpha_{AB} - 1) \times 1000 \tag{8.6}$$

To a good approximation,

$$\varepsilon_{AB} = 10^3 \ln \alpha \tag{8.7}$$

It is important to realise that isotope fractionations only occur when chemical reactions are incomplete. For example, if all bicarbonate is converted to carbonate in solution, no fractionation would be observed since all carbon atoms are converted from one molecular/ionic form to another. Likewise, transpiration of water by plants gives rise to no ^{18}O fractionation as all water passes through the plant. Such changes may occur in closed systems, but the chemical changes occurring during carbonate precipitation are normally 'open' and the reactions do not go to completion. Fractionation is therefore observed. For travertines, fractionations of the isotopes of carbon and oxygen are of particular interest. They provide information about the carbon dioxide source, the physico-chemical conditions of the precipitation event (rate and temperature) and the influence of metabolic processes. In favourable circumstances they provide information on the temperature at which deposition occurred and assist in radiometric dating. Isotope compositions of elements such as hydrogen and strontium and sulphur also provide clues as to the parent carbonate rock and magmatic contributions of volatiles such as S or CO_2.

8.1 Oxygen

The ratio of the stable isotopes of oxygen is of great interest to geochemists and sedimentologists of carbonate rocks. The water in the lithosphere exchanges oxygen atoms with the dissolved carbon dioxide, and where equilibrium is established, the difference between the ratio of isotopes of oxygen in sedimented carbonates and that of the depositing water can be used estimate past water temperatures. Information can also be obtained on rates of evaporation. It is important to establish equilibrium both between water and carbonate oxygen, and the carbonate species themselves before estimates can be made, and this is not always the case, as will be shown below.

8.1.1 The Hydrological Cycle

Before looking at the isotopic composition of carbonates it is useful to briefly review some changes in the oxygen isotope ratio over the hydrological cycle. Formation of water vapour over the ocean leads to a substantial fractionation of the oxygen isotopes because the vapour pressure of $H_2{}^{16}O$ is higher than $H_2{}^{18}O$. The vapour becomes enriched with the lighter isotope compared with seawater. If cloud condenses from this vapour, the reverse process occurs and the cloud will at first be more enriched in the heavier isotope but will still be lighter than the ocean value. In time, the condensate (cloud) will fall as rain. If equilibrium is maintained between the vapour and condensate during rain-out, the isotopic composition of the rain can be described by Rayleigh distillation:

$$R_t = R_o f^{(\alpha-1)} \tag{8.8}$$

Where R_t is the isotope ratio at time t, R_o is the original ratio, f is the fraction of vapour remaining in the cloud at time t and α is the fractionation factor. This process applies only to an open system where the rain immediately leaves the cloud, a reasonable assumption for most precipitation. The outcome of these time-dependent changes of state is that rainfall possesses a wide range of $\delta^{18}O$ values from about –2 to –15‰, the depletion increasing as the cloud is reduced by continued rainout. Precipitation is temperature-dependent and the mean annual $\delta^{18}O$ values show crude correlations with latitude, with poleward ^{18}O depletions. For example much of Canada and northern Europe have mean $\delta^{18}O$ values <= –12‰ with the tropics and subtropics ranging from –2 to –4‰ (Yurtsever 1976). These processes are important because water oxygen equilibrates with carbonate oxygen and may provide information about past climates.

Evaporation of surface waters leaves them enriched in ^{18}O. Unlike condensation, evaporation involves an additional diffusional process further fractionating the isotopes, especially at low humidity. For example, when 80% of a surface water evaporates, both the ^{13}C (of the DIC) and ^{18}O is enriched by about 6‰ (Talma and Netterberg 1983). Two further factors are important in saline waters. These are the reduced water activity and salt hydration which may partially reverse the trend of increasing ^{18}O enrichment with ablation (Tucker and Wright 1990). The significance of these enrichments has not been quantified in saline continental carbonates, but the potential effects need to be recognised.

Travertine-depositing waters are mainly, if not entirely of meteoric origin and possess ^{18}O compositions similar to those found in the local precipitation. Groundwaters however are often slightly enriched in ^{18}O owing to surface evaporation. Thorpe et al. (1981a) working in the UK, found a mean annual precipitation $\delta^{18}O$ of –8.60‰ and in a nearby travertine-depositing stream the mean $\delta^{18}O$ was –8.05‰ demonstrating slight enrichment commensurate with the expected rate of evaporation. In cases where water circulates at depth and is subject to high temperatures and pressures, water oxygen exchange with hot carbonate rock probably occurs (Barnes et al. 1973; Sakai and Matsubaya 1977). This will confound any interpretation of palaeoclimate in the deposited travertines.

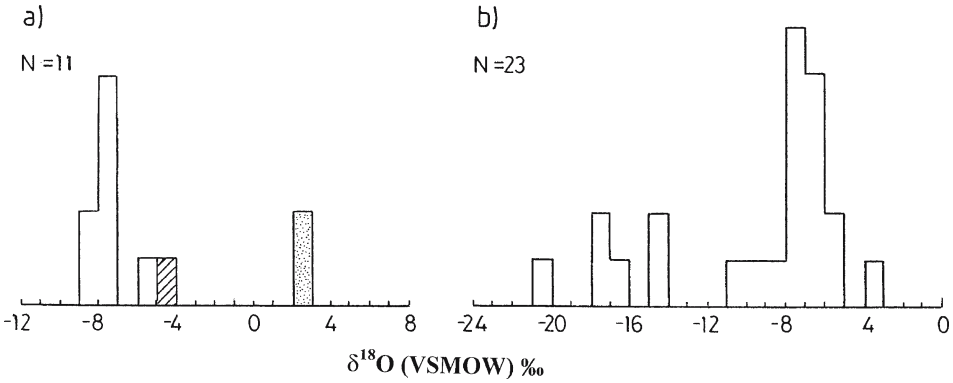

Fig. 43. $\delta^{18}O$ (VSMOW) compositions for travertine source waters. a) Meteogene waters including lakes (stippled) and invasive meteogenes (lined); b) Thermogene waters. Sources: Amundson and Kelly (1987); Andrews et al. (1997b); Baertschi (1957); Barnes et al. (1982); Casanova and Hillaire-Marcel (1992); Chafetz et al. (1991b); Chafetz and Lawrence (1997); Dandurand et al. (1982); Friedman (1970); Fritz (1968); Gonfiantini et al. (1968); Khoury et al. (1984); Lojen et al. (2004); Stoffers and Botz (1994); Thorpe (1981); Usdowski et al. (1979); van Everdingen et al. (1985)

Few travertine-depositing waters have been investigated for their H_2O $\delta^{18}O$, but it is seen that the meteogene and most thermogene waters cluster around –7‰ (Fig. 43), characteristic of meteoric waters for mid-latitudes. Waters from lake-travertine sites have positive values resulting from evaporation. A number of waters depleted in ^{18}O are apparent among the thermogenes from the western United States (e.g. Mammoth Hot Springs) suggesting that here, oxygen exchange has occurred with the country rock. Fritz (1968) suggests that for the Cannstatt waters of Germany, isotopic exchange may also have occurred between the circulating thermal waters and water adsorbed onto clay minerals. Waters from the central Italian springs however, have compositions similar to those expected in local precipitation. The oxygen enrichment factor, $\varepsilon_{(calcite-H_2O)}$ declines from about 32‰ (SMOW) at 10 °C to about 24‰ at 50 °C. At equilibrium, calcite oxygen is isotopically heavier than water but lighter than CO_2(gas). The temperature dependence can be expressed as:

$$1000 \ln \alpha_{calcite-H2O} = (2.78 \times 10^6/T^2) - 2.89 \quad (8.9)$$

Alternatively, an equilibrium deposition temperature (O'Neil et al. 1968; Turi 1986) can be estimated:

$$t(°C) = 16.9 - 4.2(\delta c - \delta w) + 0.13(\delta c - \delta w)^2 \quad (8.10)$$

Where δc is $\delta^{18}O$ (PDB) for CO_2 produced from the calcite using phosphoric acid, and δw is the $\delta^{18}O$ (SMOW) of water (Craig 1965). These relationships have been much used for palaeotemperature estimates. The temperature may be taken as the deposition temperature for calcite, assuming isotopic equilibrium has occurred between water and carbonate. Hays and Grossman (1991) revised (8.10) resulting in slightly lower deposition temperatures for a given δc and δw:

$$t(°C) = 15.7 - 4.36\ (\delta c - \delta w) + 0.12\ (\delta c - \delta w)^2 \quad (8.11)$$

The factor δw is subject to considerable uncertainty in palaeo-waters due to the processes outlined above. Aragonite is 0.6‰ heavier than calcite at 25 °C (Tarutani et al. 1969) and the fractionation is also temperature dependent. A 1‰ fall in the carbonate $\delta^{18}O$ is equivalent to about a 4.5 °C temperature rise under equilibrium conditions.

8.1.2 Oxygen Isotopes in Travertine

Stable isotope data for travertines and allied carbonates are depicted in Fig. 44. The distribution is similar to that provided by Turi (1986) who however plotted single samples, many of which originated from the same deposit. In Fig. 44, data are plotted on the basis of site means rather than individual sample measurements, giving a more revealing pattern. The histograms in Fig. 44a,b and c, and the equivalent histograms in Fig. 46 for $\delta^{13}C$ are each based on more than 500 individual measurements. The epigean meteogene travertines (Fig. 44a) form a tightly bunched group with a median of –7.58‰ (VPDB). Assuming these travertines were deposited from meteoric waters, and at isotopic equilibrium, then deposition temperatures of 12–16 °C obtain. The distribution is skewed to the right as they include a small number of isotopically heavy deposits. Several authors have investigated the variation of $\delta^{18}O$ ($CaCO_3$) in biofabrics. Comparative studies on bryophytes, algae, and chironomid

fabrics taken from the same, or similar travertine-depositing system usually indicate little or no significant difference between them (Müller et al. 1986; Pentecost and Spiro 1990; Andrews et al. 1997a).

When epigean meteogene deposits are compared with speleothem ^{18}O data, the latter are found to be significantly heavier (Mann-Whitney test; $p = 0.015$), the speleothem median being –5.68‰ (Fig. 44b). The variance of the speleothem set is less than that of the epigean set and it is tempting to attribute this to reduced environmental variability within caves. However, this interpretation must be taken with caution since speleothem means tend to be taken from larger data sets and the difference could be largely a statistical artifact.

Invasive meteogene deposits are often depleted in ^{18}O (Andrews et al. 1997b). These unusual travertines form by the reaction of atmospheric carbon dioxide with highly alkaline groundwaters (Section 2.2.1) and the median for the 19 samples analysed was –8.21‰. The ^{18}O depletion results from diffusional phenomena and six of the samples had $\delta^{18}O$ values <–15‰. O'Neil and Barnes (1971) and Turi (1986) argue that the lighter $^{12}C^{16}O_2$ will impinge on the water surface preferentially over $C^{18}O^{16}O$ by a factor $(46/44)^{0.5}$, or about 2%. With an average atmospheric CO_2 $\delta^{18}O$ value of 11‰, the diffusive fractionation will provide CO_2 at the water surface with $\delta^{18}O$ of about –8‰. Unpublished studies of O'Neil, quoted in O'Neil and Barnes (1971) showed that in laboratory simulations, the precipitated carbonate derives 1/3 of its oxygen from meteoric water and 2/3 from the CO_2. This suggests that the travertine $\delta^{18}O$ values should lie around –19‰, close to those shown in Fig. 44.

The thermogene $\delta^{18}O$ values (Fig. 44c) while having a median of –6.95‰, are in contrast, skewed to the left. A distribution-free Mann-Whitney test demonstrated no significant difference between the medians of the thermogenes and meteogenes. Trimming the data to remove the tails gave meteogene and thermogene medians of –7.92 and –6.56‰ respectively, suggesting slightly higher deposition temperatures for the thermogenes, a not unexpected result. However this is probably an oversimplification, since other factors play a part, namely the groundwater composition, the carrier gas generation process and disequilibrium effects. Decarbonation reactions, for example, enrich CO_2 by 5‰ in oxygen (Shieh and Taylor 1969).

The meteogene travertines appear to be slightly depleted with ^{18}O when compared with thermogenes. The long tail to the thermogene frequency distribution is due to the inclusion of travertines formed from ^{18}O -depleted groundwaters (see above). Deposition temperatures calculated for the Lake Turkana thermogene travertines, were found to be considerably lower than the temperature of the rising thermal plume. This led Stoffers and Botz (1994) to conclude that mixing with lake water had occurred prior to carbonate precipitation. The stable oxygen isotope median for the superambient travertines is –7.92‰ ($N = 5$). They are not significantly different from the meteogenes but too few have been analysed to warrant graphical representation.

Data are also provided for lake marls (Fig. 44d) and calcretes (Fig. 44e). Both sets differ significantly from the epigean travertines. The lake marl samples have a median $\delta^{18}O$ of –8.79‰ which is 1.2‰ lower than the epigean meteogene travertine median. The calcrete median of –4.72‰ is nearly 2.9‰ heavier than the epigean meteogenes. It is also statistically significant and probably related to greater water evaporation and the higher rainfall $\delta^{18}O$ at the lower latitudes where calcretes become more prevalent (Talma and Netterberg 1983). While these differences are statistically significant, the degree of overlap is sufficient to prevent any straightforward assignment of individual carbonate samples based solely upon their isotopic composition.

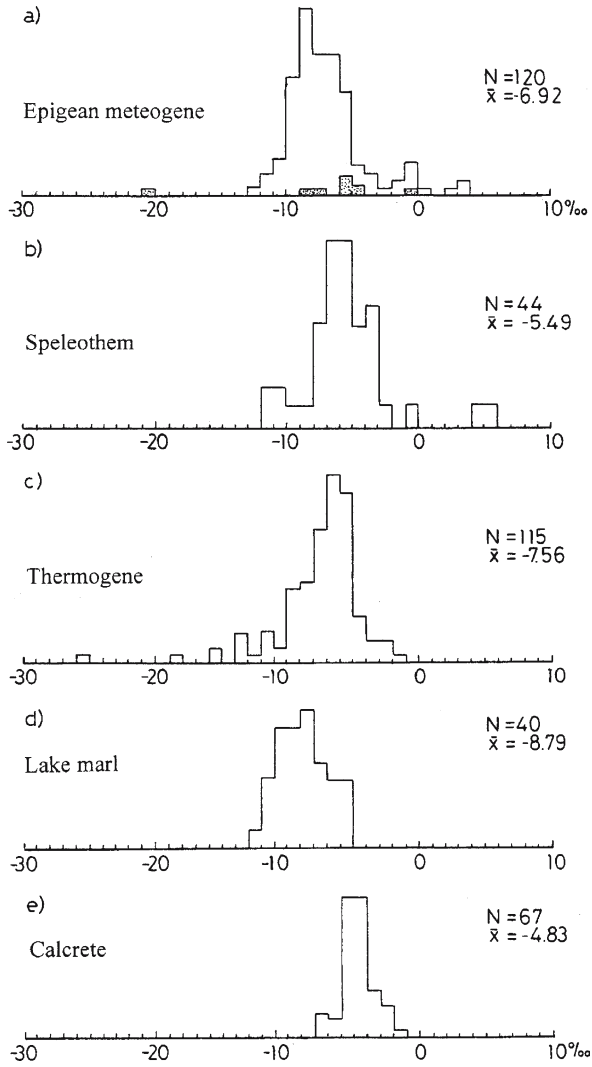

Fig. 44. Distribution of $\delta^{18}O$ (PDB, ‰) of travertine carbonate based upon site/sample averages. a) Epigean meteogene (evasive meteogenes superimposed and stippled); b) speleothem; c) thermogene; d) lacustrine marl; e) calcrete. Sources: Abell et al. (1982); Andrews et al. (1994, 1997a, 2000); Arenas et al. (2000); Arp et al. (2001); Baertschi (1957); Baker et al. (1997); Bar-Matthews et al. (1996); Brancaccio et al. (1986); Buccino et al. (1978); Burns et al. (2001); Cai et al. (2001); Casanova (1986); Casanova and Hillaire-Marcel (1992); Chafetz et al. (1991, 1994); Clark and Fontes (1990); Crombie et al. (1997); Dandurand et al. (1982); D'Argenio et al. (1983); Das and Mohanti (1997); Demovic et al. (1972); Dorale et al. (1993); Duplessey et al. (1969, 1970); Eicher (1976); Fantidis and Ehhalt (1970); Ferreri and Stanzione (1978); Fornaca-Rinaldi et al. (1968); Franciskovic-Bilinski et al. (2003); Friedman (1970); Fritz (1968); Garnett et al. (2004); Gascoyne (1992); Gascoyne et al. (1981); Gradzinski et al. (2001); Hendy and Wilson (1968); Ihlenfield et al. (2003); Kele et al. (2003); Kronfeld et al. (1985); Li et al. (1998); Liu et al. (1997); Linge and Lauritzen (2001); Lojen et al. (2004); Manfra et al. (1976); McDermott et al. (1999, 2001); Müller et al. (1986); Newton and Grossmann (1988); O'Neil and Barnes (1971); Ozkul et al. (2002); Pazdur et al. (1988); Pentecost (1995d and unpublished); Pentecost and Spiro (1990); Richter and Besenecker (1983); Salomons and Mook (1976); Salomons et al. (1978); Savelli and Wedepohl (1969); Spötl et al. (2002); Strong et al. (1993); Thompson et al. (1976); Thorpe (1980, 1981b); Tiercelin et al. (1987); Valero-Garces et al. (2001); Wang (1985, 1986)

8.1.3 Oxygen Isotopic Equilibrium

The first $\delta^{18}O$ measurements from travertine were made by Craig (1953), who looked at a small sample of thermal travertines fromYellowstone. They appeared to be deposited out of isotopic equilibrium but Craig had insufficient data to investigate the phenomenon further. A more detailed study of thermal Italian travertines suggested that isotopic equilibrium between the deposited carbonate and the water was only achieved a hundred metres or so from the springs (Fritz 1965). It was found that the $\delta^{18}O_c$ (carbonate) declined with increasing water temperature. This is consistent with temperature-dependent partitioning of oxygen isotopes between water and carbonate, but there was a pronounced departure from the equilibrium values. At 0 °C, $\delta^{18}O$ (calcite) was almost 2‰ heavier than the equilibrium value at this temperature. A similar observation was made by Gonfiantini et al. (1968) who concluded that equilibrium was only established when the rates of CO_2 degassing and precipitation were reduced, though actual values were not reported. Few of their samples were deposited at equilibrium. Sequential samples taken from the hot springs at Bagnaccio and Bagni san Fillippo, Italy demonstrated downstream ^{18}O enrichment in the travertine which correlated with ^{13}C enrichment. These were ascribed to two separate processes, both time-dependent, namely the progressive cooling of the waters accompanied by some evaporation and the preferential degassing of lighter $^{12}CO_2$. Such effects would be observable during equilibrium precipitation, but non-equilibrium precipitation shifts the isotope relationships to a new line (Fig. 45). At Monte Amiata, a cold spring, Gonfiantini et al. found the highest $\delta^{18}O$ values nearest to the spring followed by a slow decline with distance, resulting from kinetic disequilibrium effects alone. Deposition temperature estimates for these travertines were consistently lower than the measured temperatures by about 12 °C.

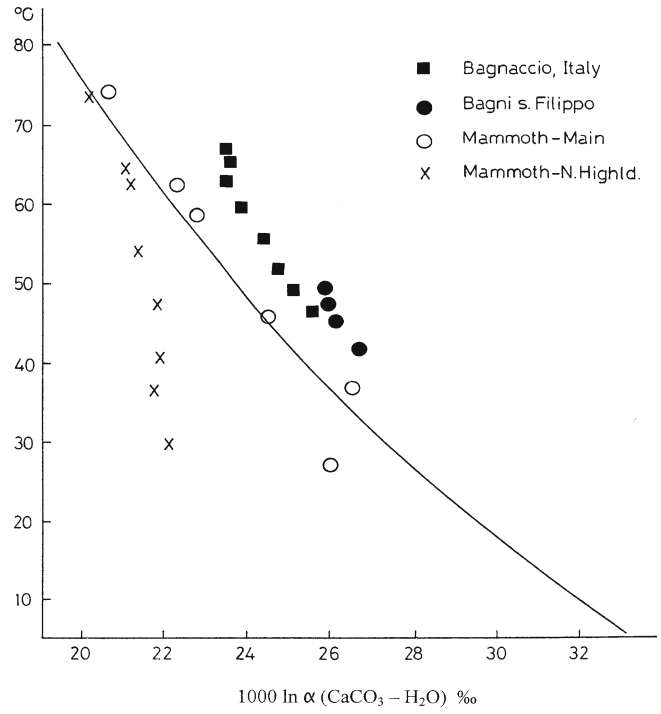

Fig. 45.
$^{18}O/^{16}O$ fractionation between $CaCO_3$ and H_2O vs. water temperature, showing the equilibrium curve and four series of downstream samples taken from travertine-depositing thermogene waters. Data from Gonfiantini et al. (1968) and Friedman (1970). Redrawn after Turi (1986)

Some significant studies were undertaken by Friedman (1970) at Mammoth Hot Springs. Two sites were investigated, Main Springs and New Highland Terrace. Plots of $\delta^{18}O_c$ vs temperature downstream from the springs yielded contrasting results. At New Highland Terrace, the isotope values plotted below the equilibrium line and yielded deposition temperatures 18 °C or more above the measured temperatures (Fig. 45). At Main Springs, almost all of the isotope values fell values fell close to the equilibrium line. This difference may have resulted from the deposition rate being much greater at New Highland Terrace, though again the actual rates were not given. The flow rate at New Highland Terrace was high and Turi (1986) believed that the disequilibrium resulted from a delay in carbonate nucleation. In the above studies, the travertines consist partly or entirely of aragonite whose equilibrium oxygen isotopic composition is enriched by about 0.6‰ over calcite, but shows approximately the same temperature-dependence. Fouke et al. (2000) also studied Mammoth Hot Springs and found that the travertine $\delta^{18}O$ increased downstream from 4.0–8.6‰ and attributed this to evaporation. Spot measurements of temperature in hot springs have a substantial variance owing to changes in solar radiation, air flow and weather patterns. However, the systematic changes observed clearly point to a pronounced disequilibrium at rapidly depositing sites. Most travertine was out of equilibrium downstream and closest to equilibrium near the spring orifice. Further work at Mammoth and other thermogene sites has demonstrated pronounced disequilibrium and systematic downstream changes in travertine $\delta^{18}O$ (Chafetz et al. 1991a; Chafetz and Meredith 1994). These authors point out that those waters issuing from cold springs often warm downstream leading to potential ^{18}O depletions at distance.

Meteogene travertines have been widely scrutinised for stable isotope disequilibrium. At Westerhof in Germany, water and DIC $\delta^{18}O$ showed little variation downstream (Usdowski et al. 1979) but estimates of deposition temperatures were higher than the observed values by about 5 °C. Although the temperature measurements were spot samples, the range of temperatures recorded in the stream (5.6–14.0 °C) still fell outside the estimated average temperature of 15.1 °C. A further study at Roquefort les Cascades showed a similar discrepancy, with estimated deposition temperatures again about 5 °C higher than the observed temperatures (Dandurand et al. 1982). A slight systematic ^{18}O enrichment was traced downstream, possibly attributable to evaporation. The cascade travertines of Waterfall Beck, UK showed a similar temperature discrepancy (Pentecost and Spiro 1990). Studies in nearby Gordale Beck (Thorpe et al. 1981a) demonstrated that according to the criteria provided by Hendy (1969), isotopic equilibrium was established. When a large series of travertine samples taken from European lakes and streams was compared with the predicted $\delta^{18}O$ (H_2O) values, they were also found to be close to equilibrium in most cases (Andrews et al. 1997a). Detailed measurements of streamwater and travertine were conducted in the Arbuckle Mountains, Oklahoma by Chafetz et al. (1991b). They showed that the annual mean water $\delta^{18}O$ of –5.2‰ (N = 139) was in good agreement with the deposited travertines, which even extended to seasonal differences, again demonstrating isotopic equilibrium. Similar results were obtained by Ihlenfield et al. (2003) in Australia again suggesting equilibrium. In contrast, Lojen et al. (2004) in a study of the Krka River system in Croatia, found that isotopic equilibrium was only established at lower water temperatures. When temperature exceeded 12 °C, disequilibrium was the norm. At the time of writing there is no convincing explanation why apparently similar watercourses should display such a range of results. An obvious explanation would be differences in the deposition rate, with the more rapidly deposited travertine showing non-equilibrium effects, but in most of the above studies, deposition rates were not reported. Where they are, the data contradict. The Australian deposits show-

ing isotopic equilibrium having been deposited more rapidly than those of Westerhof where disequilibrium was reported.

Non-equilibrium conditions result primarily from kinetic phenomena. Whilst ionic reactions are almost instantaneous in the carbonate system, the hydration and hydroxylation of carbon dioxide, during which oxygen isotopes undergo exchange, are comparatively slow. For example the half-time for CO_2 hydration ($CO_2 + H_2O \rightarrow H_2CO_3$) is about 20 sec at 20 °C. Also, the deposition rate of the carbonate may outpace the exchange rate of carbonate between the mineral surface and overlying water. As a result of this, disequilibrium is observed during CO_2 evasion and carbonate precipitation. Additionally, downstream temperature changes, evaporation and mineral phase change (e.g. aragonite → calcite) will lead to systematic changes in the carbonate $\delta^{18}O$.

8.1.3.1 Kinetic Disequilibrium Caused by CO_2 Evasion

Turi (1986) noted that during CO_2 degassing, the lighter isotopes would be lost preferentially, leading to ^{18}O and ^{13}C enrichment in the deposited travertine. By considering the rate constants for carbon dioxide hydration and dehydration, and making a number of simplifying assumptions, Hendy (1971) obtained estimates for the chemical and isotopic equilibration times for speleothems in contact with bicarbonate solutions closed and open to the atmosphere. He showed that during rapid (non-equilibrium) degassing, deposited calcite would be enriched in both ^{18}O and ^{13}C, assuming that calcite was precipitated sufficiently slowly that it equilibrated isotopically with the water. He also estimated a degassing rate, which, if exceeded, would result in measurable isotopic disequilibrium. At 10 °C and pH 8, the CO_2 egress in water in contact with speleothem would need to exceed 10^{-4} mol L^{-1} sec^{-1}. This implies that most speleothem calcite would be deposited at equilibrium. Epigean travertine deposition however, differs from speleothem deposition – in the latter degassing invariably occurs under turbulent conditions and theoretical models of turbulent degassing have not been developed. Carbon dioxide evasion rates over short lengths of travertine-depositing streams range from about 10^{-7} to 10^{-5} mol CO_2 L^{-1} sec^{-1} for meteogene deposits and 2×10^{-5} to 4×10^{-4} mol L^{-1} sec^{-1} for thermogenes (Section 10.2). These rates were obtained for pH values at or substantially below 8.0 and at temperatures ranging from 10–55 °C. They indicate that meteogene travertines should be deposited fairly close to equilibrium, while some thermogenes will be deposited out of equilibrium assuming that degassing is the only process leading to disequilibrium.

In cave travertines, oxygen isotopic equilibrium is indeed often observed. Stalagmite $\delta^{18}O$ in particular is used widely as a proxy for Quaternary palaeotemperatures (Section 13.2), and it is normal practice to employ the 'Hendy test' of isotopic equilibrium. This involves identifying a growth layer in the sectioned stalagmite and sampling 10 or more times along this layer from the stalagmite apex to the sides. The $\delta^{18}O$ values are then compared to look for significant trends across the travertine growth layer, and the $\delta^{18}O$ is plotted against the respective $\delta^{13}C$ to look for significant covariance. If no trends are apparent, then isotopic equilibrium is normally assumed. Examples of the employment of this test can be found in McDermott et al. (1999) and Linge and Lauritzen (2001). In practical terms, it is often difficult to sample accurately across growth layers due to the extreme slowness of carbonate deposition causing the layers to be very narrow. In these cases, the stalagmite surface can be used, and if the speleothem remains active, then the usual deposition-temperature test undertaken, often employing an 'equilibrium test diagram' (Thompson et al. 1976; Bar-Matthews et al. 1996; McDermott et al. 1999).

8.1.3.2 Disequilibrium during Carbonate Precipitation

The rate of CO_3^{2-} exchange between water and carbonate mineral can be obtained from the dissolution rate, and is approximately 1–10 x 10^{-7} mol m^{-2} sec^{-1} at 25 °C (Walter and Morse 1985). Crystal growth rate at the travertine surface can be estimated, though it is subject to uncertainties concerning the specific surface area of the growing crystals. Given an average 1–2 μm diameter for travertine calcite crystals, and an approximate spherical shape, a single layer of packed crystals would have a surface area of about 3 m^2 m^{-2}. It is unlikely that the growing travertine surface can be approximated realistically to a single layer of growing crystals since the layer is likely to extend into the deposit. However, it is unlikely to exceed 100 'layers' (c. 150 μm in thickness), because fabrics occurring at this depth below the surface are usually indistinguishable from the bulk material, indicating that primary crystal growth has largely stopped. Growth rate calculations have therefore been made for 1, 10 and 100 crystal layers. Table 15 shows some crystal growth rate estimates for meteogene and thermogene travertines with a porosity of 30 vol% and mean deposition rates taken from Table 22. Inspection shows that meteogene travertines should be deposited under conditions in which isotopic equilibrium is established between the dissolved and solid phase, but will be out of equilibrium for many thermogene travertines, where the deposition rate exceeds 20 mm a^{-1}. The calculations are sensitive to the crystal surface area and if the area is much higher (the mean growing crystal size is smaller) then the crystal growth rate will be lower and isotopic equilibrium may be attained at deposition rates exceeding the above figure.

McConnaughey (1989), in a study of coral calcification, argued that calcium carbonate precipitated out of equilibrium with water is most probably the result of two processes. First, an insufficient rate of exchange between dissolved carbonate (bicarbonate) and the crystal and second, the slow exchange of oxygen between the aqueous carbonate and water. The first process, as shown above, is likely to lead to disequilibrium at high deposition rates. McConnaughey showed that it takes several hours to exchange all three carbonate oxygens with water oxygens. This is due to the slow hydration rate of carbon dioxide in the absence of the enzyme catalase. Although the conditions under which coral calcification takes place differ from travertine deposition in several respects, it appears that during rapid precipitation, both processes lead to disequilibrium and depleted ^{18}O values during travertine formation. Thus there are several competing processes, some of which enrich while others deplete the ^{18}O. The final composition clearly depends upon the magnitude of the processes in any particular system, but the data so far obtained show that enrichment normally outweighs depletion.

Table 15.
Crystal growth rate in a travertine surface consisting of 1–100 layers of 1.5 μm diameter crystals using mean deposition rates of travertine with porosity 30 vol%.

Type	Number of layers	Growth rate Mole m^{-2} sec^{-1}
Meteogene (5 mm a^{-1})	1	10^{-6}
	10	10^{-7}
	100	10^{-8}
Thermogene (200 mm a^{-1})	1	3×10^{-4}
	10	3×10^{-5}
	100	3×10^{-6}

8.1.4 Oxygen Isotopes and Evaporation

Evaporation, as previously noted, gives rise to solutions initially enriched in the heavier isotopes. Such enrichments may be expected to increase downstream from the groundwater source, being particularly noticeable in regions of low relative humidity and in hot springs. Practically all of the thermal deposits investigated show the effect, with downstream increments of 2–6‰. As shown above, kinetic disequilibrium also results in heavier isotope enrichment and this can confuse the picture. It is possible to separate the effects in stream water, by determining the δD, which is particularly sensitive to evaporation. Amundson and Kelly (1987) used δD to show 30% evaporation losses from the thermogene Salt Lick Spring. Chen et al. (1988) report δD values from Huanglong and further work by Yoshimura et al. (2004) demonstrated significant evaporation using $\delta^{18}O$ profiles downstream. Friedman (1970) noted that the deposits of Main Springs, Mammoth were enriched a few per mil downstream, with 25% of the enrichment attributed to evaporation and the remainder to water cooling. Evaporation can also be significant even in cool-temperate meteogene streams. Under conditions of low discharge, where the water film is thin and insolation high, evaporation was shown to approach 30% over a distance of 600 m in Waterfall Beck, UK (Spiro and Pentecost 1991). Cave travertines subject to significant air-flow or low humidity also show evaporation effects in the $\delta^{18}O$, particularly near cave entrances (Frisia et al. 2002; Spötl et al. 2002; Horvatincic et al. 2003).

In lake travertines, evaporation will often be significant. Here disequilibrium can be identified by assuming that the lake waters have a sufficiently long residence time that the isotopes of carbon will be close to atmospheric equilibrium. In this situation, there should be no correlation between oxygen and carbon. If a correlation is found, then disequilibrium probably exists, but there have been no detailed studies to date. Palaeoclimatic studies of the deposits at Lake Turkana, Kenya demonstrated changes in ^{18}O as a response to aridity and thus evaporation (Abell et al. 1982). In Lake Manyara, the $\delta^{18}O$ (H_2O) was found to vary spatially over a wide range and was explained in terms of points of water input and local evaporation (Casanova and Hillard-Marcel 1992). These lake travertines were enriched with ^{18}O by 1–4‰, thought to be the result of evaporation. Similar enrichments are known from Lakes Natron and Magadi and also the Andean lake travertines of Argentina (Valero-Garcés et al. 2001). Travertines deposited from highly saline solutions have not yet been studied in any detail but are likely to provide interesting insights into the precipitation process.

8.2 Carbon

The stable carbon isotopes also undergo fractionation during chemical reactions so that it is sometimes possible to trace the recent history of this element. The modern Vienna Peedee standard (VPDB), taken from marine limestone is defined as zero, and carbon isotope ratios are measured relative to this. Carbon in the gaseous, dissolved and solid state may diverge considerably from zero. Atmospheric CO_2 currently has a $\delta^{13}C$ value of about –7‰, thus depleted in the heavier isotope. Fractionations occur between gas phase CO_2 and the dissolved carbonate species as shown in Table 16.

Compared with CO_2 gas, normally taken as the reference phase, the 'molecule' H_2CO_3* (= CO_2(aq) + H_2CO_3) is slightly depleted in ^{13}C, whilst bicarbonate and carbonate are enriched by about 9‰ at 20 °C. Therefore, the isotopes are unequally distributed between the DIC species. Calcite precipitated in equilibrium with CO_2 gas is enriched by about 11‰ and

Table 16.
Carbon isotope enrichment factors of the aqueous CO_2 system at three temperatures. The factors ϵ_i (‰) for carbon species i given relative to CO_2 (gas). These factors provide values of enrichment (+ve) or depletion (–ve) of carbon in a CO_2 system at equilibrium with CO_2 (gas)

Carbon species (i)	ϵ_i 10 °C	ϵ_i 35 °C	ϵ_i 60 °C
H_2CO_3* (= CO_2 aq)	–1.13	–1.02	–0.93
HCO_3^-	9.62	6.90	4.59
CO_3^{2-}	7.46	5.77	4.44
$CaCO_3$ (calcite)	11.8	9.0	6.81

aragonite by a further 1.8‰ (Rubinson and Clayton 1969). All of these enrichments are temperature-dependent. For example, the isotope enrichment factor $\varepsilon_{calcite-CO2g}$ is given by $1.435 \times 10^6/T^2 - 6.13$ (Bottinga 1968). The factor falls with increasing temperature, to about 7‰ at 60 °C. Carbon dioxide species fractionations are better defined than the oxygen isotopes, the latter being complicated by oxygen exchange with water. As shown in Chapter 2, the carbon sources for travertine carbonate are diverse providing a wide range of isotope compositions. The main sources of carbon dioxide are marine limestones ($\delta^{13}C \sim 0‰$), soil zone CO_2 (~ –15‰) and magmatic carbon (~ –7‰). In lake travertines the aqueous CO_2 phase frequently approaches atmospheric equilibrium providing a carbonate precipitate of $\delta^{13}C \sim +4‰$. Here post-depositional effects might also occur as a result of methanogenesis in lake sediments (Turner and Fritz 1983).

8.2.1 Meteogene Travertine

A considerable literature is available dealing with the $\delta^{13}C$ values of epigean meteogene travertines and several hundred analyses have been published. The distribution of values is summarised in Fig. 46a. All epigean meteogenes have been included and show a well-defined mode at –10‰ with a median of –8.48‰ and standard deviation 3.96‰. If the few lake deposits are excluded then the stream-deposited travertines are found to range from –12 to +2‰ with a median of –8.7‰. The negative values reflect the contribution of soil-respired carbon dioxide, a phenomenon which has been recognised since the earliest investigations (Craig 1953). Values in the region of –10‰ are predicable on the basis of open system dissolution of limestone ($\delta^{13}C \sim 0‰$) by groundwaters charged with soil zone CO_2 with a mean $\delta^{13}C$ value of around –25‰ (Deines et al. 1974). Trends toward higher values may indicate closed-system dissolution, but the magnitude of the effect is dependent upon the soil zone $\delta^{13}C$. A distinction between open- and closed-system pathways requires accurate measurement of the soil zone and bedrock $\delta^{13}C$ (Usdowski et al. 1979) and is best assessed from the DIC rather than the travertine. Higher values also occur as a result of evaporation, CO_2 evasion and photosynthesis as discussed below.

Lake travertines have been less well studied but the $\delta^{13}C$ values are significantly heavier than those of meteogene stream deposits, with a mode of +3.5‰. High values also result from atmospheric equilibration of the carbon dioxide, sometimes accompanied by photosynthetic enrichment and evaporation (Ferreri and Stanzione 1978; Casanova and Hillaire-Marcel 1992). In saline lakes, evaporation may lead to considerable enrichment in ^{13}C. Values up to +16.5‰ have been reported and experimental studies suggest even greater enrichments are possible (Stiller et al. 1985). Invasive meteogene deposits provide a strong contrast in their stable isotopic composition as they are highly depleted in ^{13}C (Fig. 46) ranging from –6 to –34‰ and are significantly different from the meteogenes (M-W test; $p = 0.038$). The depletion is particularly evident in the invasive travertine 'scums' sampled by O'Neil and Barnes (1971). The lowest recorded

value of –33.4‰ was obtained by Clark and Fontes (1990) from calcite nodules growing on a travertine crust in Oman. Here, extensive areas of travertine are associated with ultramafic rocks. The $\delta^{13}C$ values vary widely, according to their provenance and indicate mixing with soil zone groundwaters under less arid conditions. Isotope compositions are reported from laminated Quaternary travertines formed from hyperalkaline groundwaters, 'calcite replaced vegetation' from soil-zone CO_2, and 'fracture' deposits formed within the upper metre of the ophiolite. The latter display a wide range of $\delta^{13}C$ compositions perhaps resulting from the respiratory activities of C3 and C4 plants under different climatic conditions (Fig. 47). Oxygen isotope compositions also show strong depletion for the hyperalkaline deposits with evidence of evaporation in the calcite-replaced vegetation. Industrial deposits forming below lime-burning sites were investigated by Andrews et al. (1997b), and gave similar results. Likewise an industrial travertine forming below a lime kiln in the UK was strongly depleted in ^{13}C (–12.3‰) but without a comparable ^{18}O depletion (unpublished data). The large degree of depletion is explained in terms of the diffusion rates of $^{13}C^{16}O_2$ and $^{12}C^{16}O_2$ as in the case of oxygen discussed above. The relative rate is proportional to the square root of the mass quotient, i.e. $(45/44)^{1/2}$ amounting to about 1%. Applied to the atmospheric CO_2 which had $\delta^{13}C$ of –7‰, the travertine $\delta^{13}C$ value would be about –17‰, in reasonable agreement with most sample averages (Barnes and O'Neil 1971; Turi 1986). The more extreme values still require explanation.

Most of our knowledge of meteogene stable carbon isotopes comes from speleothems. The median speleothem $\delta^{13}C$ from Fig. 46b of –8.6‰ is only slightly lower than the epigean meteogene travertines and is not significantly different statistically. The standard deviation of these samples (2.26‰) is considerably lower than the epigean meteogenes (4.15‰), and the reduced variability perhaps reflects the more equable climates and lower deposition rates in caves as noted with oxygen. However, since the data sets comprise a wide range of data means and single values, this point should not be too strongly emphasised. There is a substantial body of information on the variation of the $\delta^{13}C$ in Quaternary cave travertines. As with oxygen, the data have been used to assist in the interpretation of palaeoenvironments. Although it would appear that the $\delta^{13}C$, like the $\delta^{18}O$ is usually deposited at or close to isotopic equilibrium, differences have been observed, both between adjacent speleothems (Wang Xunyi 1986; Baker et al. 1997) and different fabrics (Frisia et al. 2000). The sampling of a range of speleothems, using closed caves has been recommended by Bar-Matthews et al. (1996). Based upon the evidence obtained from different speleothem fabrics, Frisia et al. (2000) recommended the Hendy equilibrium test be expanded to include petrography and the calcite saturation index of the drip-water. Baker et al. (1997) in a study of the speleothems of Stump Cross Caverns, UK, found that many samples were more enriched in ^{13}C than expected and suggested that degassing of groundwater within the aquifer or short residence groundwater may have been responsible.

Lake marl and calcrete carbonates are both enriched with ^{13}C when compared with meteogene travertines (Fig. 46e,f respectively). The mean and median lake marl $\delta^{13}C$ is significantly higher than the epigean meteogene values (Fig. 46) and has a lower variance. This can be explained by a combination of factors: CO_2 exchange with the epigean atmosphere, and a more predominant evaporation and photosynthesis component. The lower variance may be explained by the more equable temperatures and hydrodynamics of lake systems. The median for the calcretes figure lies between that of marl and travertine. The difference is also significant statistically and largely reflects greater evaporation and CO_2 exchange.

Few epigean superambient deposits have been studied and they yield contrasting results. The high $\delta^{13}C$ of the DIC at Bath Spa, UK has been attributed to ^{13}C fractionation following incongruent dissolution over a long period within the water circuit (Edmunds and Miles

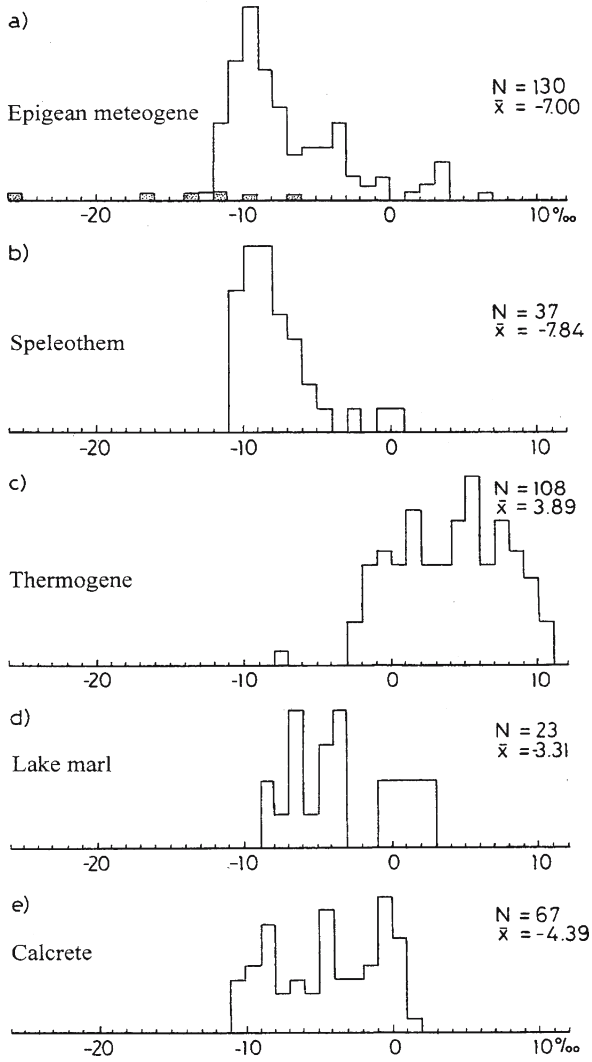

Fig. 46. Distribution of $\delta^{13}C$ (PDB, ‰) of travertine and allied carbonates based upon site/sample means. a) Epigean meteogene (invasive meteogenes superimposed and stippled); b) speleothem; c) thermogene; d) lacustrine marl; e) calcrete. Sources: Andrews et al. (1994, 1997a, 2000); Arenas et al. (2000); Arp et al. (2001); Baertschi (1957); Baker et al. (1997); Bar-Matthews et al. (1996); Benson 1978; Brancaccio et al. (1986); Buccino et al. (1978); Cai et al. (2001); Casanova (1986); Chafetz et al. (1991, 1994); Clark and Fontes (1990); Craig (1965); Crombie et al. (1997); Dandurand et al. (1982); D'Argenio et al. (1983); Das and Mohanti (1997); Demovic et al. (1972); Dorale et al. (1993); Fantidis and Ehhalt (1970); Ferreri and Stanzione (1978); Fornaca-Rinaldi et al. (1968); Franciskovic-Bilinski et al. (2003); Friedman (1970); Fritz (1968); Garnett et al. (2004); Gascoyne (1992); Gascoyne et al. (1981); Gonfiantini et al. (1968); Gradzinski et al. (2001); Kele et al. (2003); Kronfeld et al. (1985); Liu et al. (1997); Linge and Lauritzen (2001); Lojen et al. (2004); Manfra et al. (1976); McDermott et al. (1999); Müller et al. (1986); Newton and Grossmann (1988); O'Neil and Barnes (1971); Ozkul et al. (2002); Pazdur and Pazdur (1988); Pazdur et al. (1988); Pentecost et al. (1990); Pentecost (1995d and unpublished); Pentecost and Spiro (1990); Richter and Besenecker (1983); Salomons and Mook (1976); Salomons et al. (1978); Savelli and Wedepohl (1969); Spötl et al. (2002); Strong et al. (1993); Thompson et al. (1976); Thorpe (1981); Tiercelin et al. (1987); Usdowski et al. (1979); Valero-Garces et al. (2001); Vita-Finzi, (1974); Yoshimura et al. 2004)

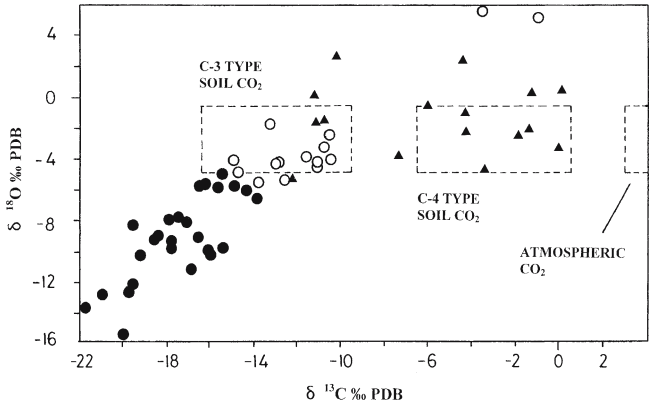

Fig. 47.
Stable isotope contents of Quaternary travertines from the northern Oman ophiolite, with superimposed equilibrium fields for two soil CO_2 types and atmospheric CO_2. Full circles; laminated invasive meteogene travertine, open circles; 'calcite replaced vegetation' from soil-zone CO_2; triangles; fracture-calcites (see text). Redrawn and simplified from Clark and Fontes (1990)

1991). High values (5.7‰) are also recorded in the Manitou Springs travertine, Colorado (unpublished data). The superambient travertines at Matlock Bath, UK possess a mean $\delta^{13}C$ of –6.71‰ suggesting little water-rock reaction during the estimated 20 year residence time of this water (Pentecost 1999a). This wide range of values probably reflects differences in groundwater-rock reactions. High temperatures, deep circulation, and long residence times would be expected to enhance exchange processes. Detailed geochemical data from a range of these groundwaters is needed for a greater understanding of the isotope compositions. 'Orgamox' deposits, as stated previously (Chap. 2), could result from organic matter oxidation, fermentation and decarboxlyation. Methane and its oxidation products are usually characterised by substantial ^{13}C enrichment (Bottinga 1969) while decarboxylation and oxidation should provide a DIC similar to that observed under karst soils. The sulphide-rich orgamox waters of Harrogate Spa, UK have a $\delta^{13}C$ of –11‰, consistent with the oxidation of organic matter accompanying sulphate reduction.

8.2.2 Thermogene Travertine $\delta^{13}C$

Thermogene deposits display a similar range of $\delta^{13}C$ values to the meteogenes, with a standard deviation of 3.73‰ (Fig. 46c) but they are displaced to more positive values, the median being 4.3‰, which is nearly 13‰ higher than the median for the meteogenes. The difference is highly significant statistically (M-W test; $p < 0.0001$) largely reflecting non soil-zone carbon sources, including water-rock reactions, and also the enrichments encountered in travertine formation during rapid CO_2 evasion. There is no well-defined mode, but 90% of the travertines fall within the range –1 and +10‰. In most cases, the carbon dioxide is believed to originate from limestone decarbonation reactions (Turi 1986; Pentecost 1995a) but a magmatic component may also be significant (Yoshimura et al. 2004) and there is also a strong likelihood of water-rock exchange reactions as mentioned above. Some of the lighter travertines of this group will have formed from mixed hydrothermal-surface waters whilst others probably reflect a dominantly magmatic origin for the carrier CO_2.

8.2.3 Modelling Downstream Changes

In common with oxygen, the carbon isotope composition of travertines and their associated waters changes downstream. As the evasion of carbon dioxide progresses, the lighter molecules are lost preferentially, leaving the gas in solution enriched in ^{13}C, and progressive

downstream enrichments in ^{13}C tend to be observed at increasing distances from source. The isotope composition of the DIC has been modelled using Rayleigh fractionation by Usdowski et al. (1979) subject to a number of simplifications regarding the time-dependent speciation of the DIC. This group observed a 1‰ rise along the flow path and provided a model for the isotopic composition of the DIC in the absence of calcite precipitation:

$$\ln (c_T/c_{T,0}) = ((1/\alpha_T) - 1) \ln (M_T/M_{T,0}) \quad (8.12)$$

Where c_T, $c_{T,0} = {}^{13}C/({}^{13}C + {}^{12}C)$ at the beginning and end of the degassing phase respectively, $\alpha_T = \alpha_f x_f + \alpha_b x_b + \alpha_d x_d$, where α is the isotope fractionation factor and x the mole fraction for f (dissolved $CO_2 + H_2CO_3$); b (dissolved HCO_3^-), and d (dissolved CO_3^{2-}). M_T, $M_{T,0}$, are the sums of the $^{13}C + {}^{12}C$ at the beginning and end of the degassing phase respectively. The model adequately described the DIC isotopic composition for travertine-depositing streams in Germany prior to the calcite deposition phase, where α_T closely approximates α_b, (Usdowski et al. 1979; Dandurand et al. 1982; Michaelis et al. 1985). It is also applicable to some thermogene systems in the United States (Amundson and Kelly 1987; Fouke et al. 2000). In travertine deposits, systematic enrichments over distance are also known, but the isotope composition is less well predicted due to disequilibrium and other effects. Working with a meteogene travertine system in Germany, Michaelis et al. (1985) found that the Rayleigh fractionation model showed a marked departure in the calcite-depositing section of flow. A kinetic model was subsequently developed for this system. It assumes that calcite precipitation begins immediately after a critical activity of CO_3^{2-} is attained and takes the form:

$$\delta^{13}C - \delta^{13}C^0 = (X - 1)\, 10^3 \ln (N/N^0) \quad (8.13)$$

The superscript o indicates the initial value/concentration, $N = [HCO_3^-]$ and X represents a combined isotope partition coefficient. A good fit of this model was obtained for the Westerhof stream. In common with the DIC, the $\delta^{13}C$ composition of travertine frequently increases downstream, reflecting the preferential degassing of the lighter isotope (e.g. Gonfiantini et al. 1968; Pentecost and Spiro 1990; Chafetz and Lawrence 1994). However, this is not always the case as Fritz (1965) reported downstream depletions. Furthermore, the isotopic composition of the travertine is not always predicted successfully from the equilibrium composition of the DIC.

8.2.4 Disequilibrium and the 'Metabolic Shift'

Gonfiantini et al. (1968) found that some Italian thermogene travertines were enriched by about 2‰ above their equilibrium $\delta^{13}C$ values. In contrast, Dandurand et al. (1982) found that meteogene cascade travertines were depleted by about 2‰ from their equilibrium position. The difference between the DIC ($\sim HCO_3^-$) and $CaCO_3$ (calcite) should be +2.3‰ (Emrich et al. 1970) whereas it was in fact close to zero. At another meteogene site, Michaelis et al. (1985) also found that the observed difference between the DIC and travertine was close to zero indicating depletion of ^{13}C in calcite. In other cases, the travertine $\delta^{13}C$ has been found to be variable (Chafetz et al. 1991b) or apparently close to equilibrium with the DIC (Amundson and Kelly 1987). Overall, epigean travertine ^{13}C tends to be deposited out of equilibrium with the DIC. In a study of isotope disequilibrium in speleothem, Hendy (1971) showed that rapid CO_2 evasion would lead to a ^{13}C enrichment of the carbonate that would be correlated to ^{18}O enrichment. This certainly seems to be the case in some thermogene

sites such as those investigated by Gonfiantini et al. (1968) but is not always observed. Increasing the precipitation rate appears to decrease the ^{13}C enrichment (Turi 1986, p.217) as does an increase in temperature, and the phase transition calcite-aragonite, both of which affect isotope fractionation. Michaelis et al. (1985) also believe that the reason the Güterstein travertines were depleted in ^{13}C was rapid calcite precipitation. Chafetz and Lawrence (1994) found that downflow ^{13}C in the DIC increased more rapidly than the ^{18}O in a number of thermogene systems, and that the travertine ^{13}C increased more slowly than the DIC ^{13}C. This was also noted by Friedman (1970) and is attributed to a combination of non-equilibrium processes and temperature effects. Aquatic plant photosynthesis leads to enrichment of the DIC in ^{13}C as this isotope is discriminated against in CO_2 reduction. Since plants are almost always present in travertine-depositing streams, photosynthesis will make some contribution to the travertine isotope composition. The phenomenon has been given the sobriquet *metabolic shift* by McConnaughy (1989). Most studies have shown the effect to be negligible, but on warm, sunny days, when discharge is low, it may become significant. In a diel study of the DIC of Waterfall Beck, UK, Spiro and Pentecost (1991) found that 10% of the stream DIC was fixed by aquatic plants within 24 h. This affected the DIC $\delta^{13}C$ giving a 4‰ increase during the day. Although the stream was investigated during an atypical period of drought, it showed that photosynthetic activity can have a pronounced effect on the DIC and by implication, travertine formation. The travertines of this stream are not greatly affected by photosynthetic activity overall, but deposits formed around discrete algal colonies, which make up a fraction of the travertine (most is deposited around a moss framework) did show a significant increase in $\delta^{13}C$ over the bulk travertine. This was also attributed to photosynthesis (Pentecost and Spiro 1990). Evidence of photosynthetic activity comes mainly from diel or seasonal measurements. Fritz (1968) first reported on the seasonal laminae in Pleistocene deposits at Cannstatt, Germany which contained lower ^{18}O values in the presumed summer layers but no systematic variation in ^{13}C. Chafetz et al. (1991b) found that ^{13}C was higher in both the DIC and travertine of two Oklahoma meteogene systems during the spring and summer, probably due to photosynthesis. Amundson and Kelly (1987) found some evidence for photosynthesis in a Californian thermogene spring during a diel investigation of the DIC and diel changes in the Huanglong Ravine, China indicate some photosynthetic contribution to deposition (Yoshimura et al. 2004). Most investigators however, have failed to detect a significant effect in flowing systems (e.g. Usdowski et al. 1979; Fouke et al. 2000; Lu et al. 2000). In lakes, the situation is different because the water usually has a residence time measurable in weeks or months, rather than in minutes or hours, allowing a greater fraction of the DIC to be utilized by plants. In a study of the Pleistocene travertines of Lake Turkana, Abell et al. (1982) found that both $\delta^{13}C$ and $\delta^{18}O$ values oscillated in laminated samples, but attributed this to variations in aridity rather than photosynthesis. The ^{13}C - enrichment of the Lake Manyara rift travertines have been partly explained by photosynthetic activity (Casanova and Hillaire-Marcel 1992). However, some of this DIC enrichment is thought to have resulted from hypolimnic fermentation.

Some investigations have focussed on detecting differences in the $\delta^{13}C$ between fabrics within the same travertine-depositing system. A study of mixed clastic/backfill and cascade deposits at Caerwys, UK revealed no significant differences between the $\delta^{13}C$ values (Pentecost and Spiro, unpublished). Müller et al. (1986) looked at a range of moss and algal travertines, including oncoids from the Schwäbische Alb, Germany. Though based mainly on single samples, the stable isotope differences between them were minimal and did not reveal a metabolic shift. Andrews et al. (1997) found no significant differences in the $\delta^{13}C$ values of several microbial carbonates, but did find an altitude effect. Deposits at high altitude had

$\delta^{13}C$ values 2–6‰ higher than lowland sites and this was attributed to thinner soils and a smaller soil zone CO_2 component.

While most studies have focused upon the bulk travertine carbonate, carbon and oxygen isotope ratios have occasionally been measured on minor constituents. For example, the organic (mostly algal) fraction $\delta^{13}C$ ranged between –31.9 and –34.2‰ for samples collected in the Krka River, Croatia (Lojen et al. 2004). Similar values have been found for travertine-associated bryophytes (Pentecost 2000). The carbonate valves of an ostracod, *Psychrodromus olivaceus* were found to be consistently heavier in ^{18}O and ^{13}C when compared with the bulk travertine and the difference attributed to vital effects (Garnett et al. 2004).

8.3 Sulphur, Strontium, Lead and Lithium

Many elements exist as a mixture of stable isotopes. Those of low mass in Periods 1–3 are especially useful owing to their abundance and large differences in mass (e.g. H,C,O). Others include S and Si and all fractionate when undergoing chemical transformations. With modern mass spectrometry, the ratios of elements with higher mass can be measured routinely, greatly extending possibilities for understanding the origins and reaction paths of elements involved in carbonate sedimentation. Among these are lead and some of the heavy elements of Period 7 used in uranium-series dating.

8.3.1 Sulphur

Sulphur occurs in travertine mainly as sulphate or the free element and often occurs in sufficient quantity for measurement of the $^{34}S/^{32}S$ ratio ($\delta^{34}S$) relative to the Cañon Diablo meteorite (CDT). An investigation of central European travertines by Savelli and Wedepohl (1969) provided $\delta^{34}S$ values ranging from +12 to +21‰. The sulphur source was identified as Permo-Triassic evaporite sulphates that occurred at considerable depth within the region. Evaporite sulphate was also implicated in a similar study of Czech travertines, with $\delta^{34}S$ values ranging from +20.5 to +31‰, where however, the carbon dioxide sources were more diverse (Demovic et al. 1972). At Mammoth Hot Springs, sulphide is present in the springwater in common with many other thermogene sites. The $\delta^{34}S$ values for H_2S and S were found by Leeman et al. (1977) to be –3.0 and –8.4‰ respectively which are somewhat depleted in relation to magmatic sources (+0.7 to +2.6‰). This was interpreted at the result of rock baking combined with bacterial activity, although other explanations are possible. In contrast, the sulphate $\delta^{34}S$ was higher (+20.5‰) suggesting a marine evaporite source. Work by Fouke et al. (2000) at Mammoth demonstrated that the water $\delta^{34}S$ varied little downstream and no evidence of metabolic S pathways could be identified on the travertine. Investigation of a travertine at the Cave and Basin Hot Springs, Alberta using $\delta^{34}S$ as a marker, (Van Everdingen et al. 1985) suggested that bacterial activity was responsible for sulphide production. The sulphide ($\delta^{34}S$ –6.6‰) was then oxidised by the atmosphere to form sulphuric acid which attacked the travertine to form gypsum ($\delta^{34}S$ –5.2‰).

8.3.2 Lead, Strontium and Lithium

Analysis of heavy isotopes provides further information on the sources of these elements in the hydrological system. Leeman et al. (1977) analysed a number of travertines, siliceous sinters and thermal waters in the Yellowstone Caldera, Wyoming. The $^{87}Sr/^{86}Sr$ ratio for a water sample taken at Mammoth Hot Springs was 0.7111 with the travertines providing a similar ratio. The

results from both Sr and Pb indicate that the source rocks occurred locally and included rhyolite tuffs, lavas and possibly magmas, along with calcareous sediments. The Sr isotope ratios in the Mammoth waters varied little downstream (Fouke et al. 2000). Similar studies have been used to determine the provenance of solutes leading to speleothem formation (Verheyden et al. 2000). For the lead isotopes, bivariate plots obtained from the ratios, $^{206}Pb/^{204}Pb$ and $^{208}Pb/^{204}Pb$ are useful in the interpretation of provenance. The results for Yellowstone indicate a mixed volcanic/sedimentary source for this element. Extensive studies have been undertaken on the strontium content and isotope composition of the central Italian travertines in an attempt to identify the rock sources (Barbieri et al. 1979; Turi 1986). The $^{87}Sr/^{86}Sr$ values for the travertines ranged from just below 0.708 to 0.7125 with a mean around 0.709 suggesting for most of them, a local sedimentary source of limestone, marl and evaporite. A high ratio for the Palidoro travertine, and some sites in southern Latium indicates leaching from local volcanics. Many of the above measurements were undertaken on travertines that had undergone diagenesis, leading to some uncertainty of the interpretation (Turi 1986). Higher strontium isotope ratios, in the range of 0.72–0.78 were found in epigean travertines and speleothems from an alpine site in Italy and attributed to the radiogenic metamorphic rocks giving rise to the deposits (Spötl et al. 2002).

Preliminary work on the lithium isotope composition of the Mono Lake thermal springs and associated travertines has been undertaken by Tomascak et al. (2003). The thermal springs giving rise to the travertine towers were found to be isotopically light, and there was no evidence of Li fractionations in the travertine.

Chapter 9

Organisms Associated with Travertine

Rocky, soil-free surfaces are not usually recognised for the richness of their biota. Plants have few opportunities to root and water may be scarce, resulting in a sparse flora of a few hardy cryptogams, providing scant food and shelter for animals. However, few rocks can match travertine in its range of hardness or texture and the source waters are chemically diverse. Consequently, actively accreting surfaces often support a surprisingly rich biota which in turn influence the form and structure of the accreting deposits. If inactive travertines, with their associated regoliths and soils are included then this diversity is further increased. A detailed study of the latter communities is not possible in a book of this size, but brief reference will be made to them. The communities and ecosystems present on active deposits have not been described systematically. Several hundred plant and animal species have been recorded, but taxonomic lists are rarely informative in isolation. Of more interest are the communities themselves, the ways in which the organisms interact with each other, cope with and influence the deposition process, how the systems evolve, and what determines their stability or succession. Much is to be learned about ecosystems in general by the study of these comparatively simple, and sharply delimited travertine communities.

9.1 Prokaryotes

The prokaryotes form a well-defined group of organisms distinguished by their simple cellular organisation. They are subdivided into two domains, the Archaea and the Bacteria. The former, discovered late in the 20th Century, are superficially similar to the Bacteria, but lack murein in their cell walls, and have a well-defined genetic constitution (Woese et al. 1990). Bacteria are well represented, and frequently dominate the flora of active travertines. Those performing oxygenic photosynthesis are known collectively as the cyanobacteria and are of particular interest owing to their ability to precipitate carbonates through uptake of carbon dioxide. Many other kinds of bacteria occur, particularly in sulphide-rich thermal springs and in both groups, laminate or bushy stromatolitic structures may be found. Stromatolite-building organisms are thought to be among the first to colonise the planet (Section 15.4) and travertines are therefore of particular interest to palaeobiologists and astrobiologists.

Travertine bacteria have so far been found in 21 taxonomic units (Fouke et al. 2003) but the number is certain to grow as new molecular methods of identification are applied. Little is known about many of these forms and still less about their influence over travertine formation. However, they are found in considerable numbers. At Mammoth Hot Springs for example, up to 6.5 x 10^4 bacteria per mm^3 of travertine have been recorded (Pentecost 1990b) and at a Japanese site, viable counts of 2.1 x 10^8 cells g $^{-1}$ have been found (Yoshimura et al. 1996). Bacteria are sometimes evident in large numbers as revealed by the scanning electron microscope (e.g. Durrenfeldt 1978; Pitois et al. 2001).

Owing to their small size, and generally rapid growth rates, the bacteria are primary colonisers, and found in highest numbers at or near the travertine surface (Photoplate 14A). Occasionally, they are the only colonisers, and their metabolic products can influence the precipitation of calcium carbonate. The Archaeota are well-known extremophiles, often occurring in acidic or sulphide-rich hot springs, hypersaline waters and in anaerobic waters (Stetter 1996). They do not yet appear to have been identified in travertine deposits *per se*, but they have been detected among deposits of iron at Calcite Springs, Yellowstone (Reysenbach et al. 2000). Although some sub-groups of the Archaeota, such as the methanogens would not be expected to be significant in travertine-depositing environments, genera capable of using sulphur as terminal electron acceptor (e.g. *Pyrodictyum*), are likely to occur in sulphide-rich thermal travertines.

Molecular studies conducted in the past few years are shedding new light on the distribution and diversity of microbes worldwide. Methods employing 16S rRNA sequencing are now commonplace and have resulted in the detection of a huge range of otherwise unculturable taxa. While their phylogeny can often be predicted from the base-sequences, their metabolism and ecological requirements cannot be ascertained with any precision. Owing to the potential importance of photosynthesis in travertine deposition, groups containing photosynthetic bacteria have been considered separately below.

9.1.1 Photosynthetic Bacteria

These bacteria fall into two categories, the 'anoxygenic phototrophs' ('classical' photosynthetic bacteria but currently classified as phototrophic proteobacteria) and the oxygenic phototrophs (cyanobacteria). The distinction can cause confusion because some cyanobacteria are capable of anoxygenic photosynthesis, but the groups are otherwise biochemically and genetically distinct. Anoxygenic phototrophs contain bacteriochlorophylls and special carotenoids and water never serves as electron donor.

These bacteria are known from sites containing dissolved sulphide. *Chromatium*, a coccoid purple bacterium, is abundant in the travertine-depositing waters at Bagni di Tivoli, Italy (Pentecost and Tortora 1989) where it forms a layer 2–5 mm thick at the travertine surface and also covers most of the benthos of Lago delle Collonelle. SEM observations show cells growing upon and apparently within crystals of calcite, sometimes forming a layer below mats of the cyanobacterium *Oscillatoria formosa* (= *Phormidium inundatum*). The springs contain high levels of sulphide (0.3 mmol L^{-1}). Other Italian sulphur springs, not necessarily depositing travertine e.g. Lagi di Vescovo, Terme de Cotilia also possess dense growths of *Chromatium*. Cohn (1864) first described a red *Palmella* from Bagni di Tivoli, which was probably *Chromatium*. The occurrence of these bacteria in the Italian springs appears to be controlled by water temperature, and the level of dissolved sulphide. For example, they are present near the orifices of the cooler sulphide springs of Bagni san Fillipo at a temperature of 32 °C and with sulphide at 30 μmol L^{-1}, but absent from the hot-springs of Viterbo, whose temperatures range from 40–63 °C but with similar sulphide levels. In the hot springs of Yellowstone however, a thermophilic *Chromatium* growing at 50 °C has been found on the travertine terraces of Mammoth Hot Springs (Madigan 1986). These bacteria are not found in the absence of sulphide and it appears that when sulphide falls below about 10 μmol L^{-1} and oxygen rises to around 100 μmol L^{-1}, they are outcompeted by other phototrophs. Species of the green sulphur bacterium *Chlorobium* have also been isolated from enrichment cultures of *Chromatium* from some Italian springs

(Pentecost 1995b) and two further *Chlorobium* taxa and one of *Pelodictyon* have been identified at Mammoth based upon 16SrRNA sequences (Fouke et al. 2003). Castenholz (1989) described a filamentous phototrophic green non-sulphur bacterium *Chloroflexus aurantiacus* from several thermal springs, including Mammoth Hot Springs, Yellowstone. *Chloroflexus* is often found associated with cyanobacteria at temperatures of 30–72 °C where it forms an orange-yellow undermat a few mm in thickness. The bacterium forms dense tangles of narrow filaments, often less than 1 μm in diameter with indistinct cross-walls. Giovanonni et al. (1987) describe the ecophysiology of *Chloroflexus* at Mammoth Hot Springs (Photoplate 1E) and demonstrate the cycling of sulphur within the mat. *Chloroflexus* also occurs as salmon-pink mats encrusted with travertine in the hot springs of Viterbo where both oxygen and sulphide are present (Pentecost 1995a). Several physiological strains are known, some of which survive at low temperatures where only traces of sulphide are present. *Chloroflexus* appears to be largely heterotrophic where associated with cyanobacteria, obtaining its carbon from these organisms. Where sulphide is present, and cyanobacteria absent, sulphide-dependent photoautotrophy occurs. A little known but related bacterium, *Heliothrix oregonensis* is also likely to occur on thermal travertines (Fouke et al. 2003).

9.1.2 Non-photosynthetic Bacteria

This section includes bacteria of great diversity, divided into more than 20 divisions in the 10th edition of Bergey's Manual (Boone et al. 2001). They are grouped below according to their metabolism (Table 17).

9.1.2.1 Sulphur-oxidising Chemolithotrophic Bacteria

The bacteria of this section have the ability to oxidise reduced sulphur compounds. Water containing more than about 15 μmol L^{-1} total sulphide usually contain species capable of sulphide oxidation, using the free energy for metabolism. They do not necessarily require sources of exogenous reduced carbon (chemolithoautotrophy) and are capable of reducing carbon dioxide in the absence of light. These 'colourless sulphur bacteria', are a diverse assemblage of microbes.

Two bacteria appear to be widely distributed. The best known is *Thermothrix thiopara*, found as white streamers in thermal sulphide waters of the United States (Caldwell et al. 1984). This taxon has been found at the sulphide-oxygen interface in Jemez Springs, New Mexico and on the travertines of Yellowstone National Park (Farmer and Des Marais 1994a; Allen et al. 2000). It has a pH range of 5.9–7.9 and an optimum growth temperature of 72 °C. Sulphide levels were around 30 μmol L^{-1}, but oxygen was also present at Jemez Springs. *Thermothrix* is a facultative autotroph and work by Kieft and Caldwell (1984) has shown that sulphuric acid generated during sulphur oxidation contributes towards travertine weathering. More recent work at Mammoth Hot Springs suggests that here at least, some forms of *Thermothrix* has been misidentified, and another member of the Aquificiales is present (Fouke et al. 2000). Apparently similar, but unidentified bacteria occur in the central Italian hot springs. At lower temperatures (below about 40 °C), species of *Thiobacillus* occur, and have been isolated at one site (Table 17). Some bacteria, e.g. *Beggiatoa* and *Pseudomonas* oxidise sulphur, but are incapable of obtaining energy from the process. *Beggiatoa* is sometimes found in abundance in sulphide-containing waters, such as those of Saturnia, Italy and

Table 17. Bacteria associated with travertine. Note that taxa listed under Fouke et al. (2003) are based on close matches of 16s rRNA sequences

Division/phylum	Taxon	Traditional grouping	Site/temperature/comments	Reference
α-proteobacteria	*Acidomonas methanolica*		Mammoth Hot Springs/18–38	Fouke et al. (2003)
	Agrobacterium tumefaciens	Gram negative rods	France/unusual site for sp.	Caudwell (1987)
	Brevundimonas		Mammoth Hot Springs/35–55	Fouke et al. (2003)
	Caulobacter		" /38–55	"
	Hyphomonas jannaschiana		" /35–59	"
	Isosphaera pallida	Budding bacteria	Mammoth Hot Springs (40–55), Pamukkale (20–30)	Giovannoni et al. (1987); Pentecost et al. (1997)
	Porphyrobacter		Mammoth Hot Springs/38–55	Fouke et al. (2003)
	Rhodobacter sphaeroides	Phototrophic bacteria	" /18–59	"
	Rhodopseudomonas	"	Bagni di Tivoli/23	Pentecost and Tortora (1989)
	Rickettsia spp.		Mammoth Hot Springs/38–55	Fouke et al. (2003)
	Rubrimonas cliftonensis	Phototrophic bacteria	Mammoth Hot Springs/35–59	"
	Thiosphaera	S-oxidising chemo-lithotroph	Central Italian springs/40	Pentecost (1995b)
β-proteobacteria	*Hydrogenophaga palleronii*		Mammoth Hot Springs/35–59	Fouke et al. (2003)
	Janthinobacter lividum	Gram negative rod	Falls Creek, Oklahoma/10	Pentecost and Terry (1988)
	Leptothrix ochracea	Sheathed bacteria	Several European meteogenes/10–20	Hevisi (1970); author unpublished
	Thermothrix thiopara	S-oxidising chemo-lithotroph	Jemez Springs, NM/70	Caldwell et al. (1984); Allen et al. 2000
	Thiobacillus thiooxidans	" "	Central Italian springs/40	Pentecost (1995b)
	T. thiopara	" "	Central Italian springs/23–40	Pentecost (1995b)
γ-proteobacteria	*Acinetobacter calcoacetus*	Gram negative rods	Rio Mesquites, Mexico/20	Pentecost and Terry (1988)
	Beggiatoa	Gliding bacteria	Mammoth Hot Springs; Saturnia, Italy/30	Copeland (1936), author unpublished

Table 17. *Continued*

Division/phylum	Taxon	Traditional grouping	Site/temperature/comments	Reference
γ-proteobacteria	*Chromatium minutissumum*	Purple phototrophic bacteria	Central Italian springs/23–55	Pentecost and Tortora (1989), Pentecost (1995b)
	Erwinia	Facultative anaerobic rod	Velka Chuchle, Czech R./10	Pentecost and Terry (1988)
	Macromonas bipunctata		British caves	Danielli and Edington (1983)
	Pseudomonas spp.	Heterotrophic gram negative rods	Numerous meteogene deposits/10–20; Mammoth Hot Springs/35–59	Adolphe a. Billy (1974); Caudwell (1987); Pentecost a. Terry (1988); Fouke et al. (2003)
	Stenotrophomonas maltophila		Mammoth Hot Springs/35–59	Fouke et al. (2003)
	Vibrio	Facultative anaerobic rod	Luxembourg	Pentecost and Terry (1988)
δ-proteobacteria	*Bdellovibrio bacteriovorus*		Mammoth Hot Springs/35–59	Fouke et al. (2003)
	Desulphovibrio cf. *thermophilus*	Sulphate-reducing bacteria	Central Italian springs/20–40 Mammoth/38–55	Pentecost (1995b); Fouke et al. (2003)
Aquificiales	*Hydrogenobacter thermophilus*		Mammoth	Allen et al. 2000
Gram positive bacteria	*Actinomyces*	Non-sporing rods	Bagni di Tivoli, Italy; Vietnam/23. Requires confirmation	Glazek (1965); Pentecost and Tortora (1989)
	Bacillus cereus	Endospore formers	France	Billy (1975)
	Bacillus subtilis		Mammoth	Allen et al. 2000
	Bacillus sp.	"	UK meteogenes/10–15	Pentecost and Terry (1988)
	Dictyologlomas thermophilum	Firmicutes/Low G+C	Mammoth Hot Springs/69–73	Fouke et al. (2003)
	Lactobacillus sanfranciscensis	Uncertain affinity	Mammoth Hot Springs/38–55	"
	Listeria	Endospore formers	Falls Creek, Oklahoma/10	Pentecost and Terry (1988)
	Paenibacillus larvae	Firmicutes/Low G+C	Mammoth Hot Springs/35–59	Fouke et al. (2003)
	Thermoanaerobacter ethanolicus	Non-sporing rod	Firehole Lake, Wy/68	Wiegel and Ljungdahl (1981)

Table 17. *Continued*

Division/phylum	Taxon	Traditional grouping	Site/temperature/comments	Reference
BCF bacteria	*Dyadobacter fermentens*		Mammoth Hot Springs/35–59	Fouke et al. (2003)
	Flectobacillus major		Mammoth Hot Springs/35–73	"
	Flexibacter elegans		" /38–55	"
Planctomycetales	*Pirellula staleyi*		Mammoth Hot Springs/35–59	"
	Planctomyces		" /65–71	"
Flavobacteria	*Flavobacterium*	Heterotrophic rods	France?	Adolphe and Billy (1974)
Green sulphur bacteria	*Chlorobium chlorovibrioides*	Green Sulphur bacteria	Central Italian springs/23–40	Pentecost and Tortora (1989); Pentecost (1995b)
	C. ferroxidans		Mammoth Hot Springs/65–71	Fouke et al. (2003)
	C. limicola		" /38–55	"
	C. tepidum		" /38–55	"
	Prosthecochloris aestuarii		" /35–59	"
Green non-sulphur bacteria	*Chloroflexus aurantiacus*	Green non-sulphur bacteria	Mammoth Hot Springs/30–72; Central Italian Springs/35–59	Castenholz (1989); Pentecost (1995b); Fouke et al. (2003)
	Heliothrix oregonensis		Mammoth Hot Springs/38–55	Fouke et al. (2003)
	Pelodictyon luteolum		" /38–55	"
	Roseiflexus castenholzii		" /38–55	"
Deeply branching bacteria	'*Aquificiales* pBB'		" /69–73	"
Spirochaetes	*Leptospira fainei*		" /38–55	"
Thermus group	*Thermus brockianus*		" /38–55	"

Mammoth Hot Springs, Wyoming. Members of the genera *Achromatium*, *Beggiatoa* and *Thiothrix* may be responsible for travertine dissolution by forming sulphuric acid in some warm sulphur springs according to Hubbard et al. (1990).

Cave systems have long interested microbiologists, but there is little to report from the travertines. Moonmilks, composed of hydromagnesite have long been suspected to be formed at least in part by bacteria (Hill and Forti 1997). Work by Danielli and Edington (1983) showed that the cave bacterium *Macromonas bipunctata* was capable of precipitating calcium carbonate in the laboratory and may contain carbonate inclusions.

9.1.2.2 Heterotrophic Bacteria

These microbes require a source of reduced carbon and occur in a wide range of phylogenetic groups. The carbon source may be the excreted product of another organism, or the organism itself. The most abundant are gram-negative rods and cocci. For example, numerous isolates of *Pseudomonas* (γ proteobacteria) were obtained from a range of travertines by Pentecost and Terry (1988). Pseudomonads are notable for the range of substrates catabolised and they are common aquatic organisms, inhabiting aerobic environments. They are also known to occur on limestone surfaces to which they adhere strongly (T. F. Preece, *pers. comm.*) although the significance of this is unknown. The calcified cyanobacterium *Rivularia* (Section 7.2.3) also contains these bacteria (Caudwell 1987). Endospore-formers have also been isolated, and species of *Bacillus*, e.g. *B. stearothermophilus* can grow at high temperatures. Some filamentous bacteria, e.g. *Leptothrix* are often found in enrichment cultures for travertine cyanobacteria and occur abundantly at sites in the UK where much allochthonous iron is present (unpublished observations). Actinomycetes have been reported, but as yet, tests on isolates have not been undertaken. Facultative anaerobes are sometimes found and include *Erwinia* and *Vibrio*. Travertine surfaces are bound to contain small anaerobic niches where organic decay is in progress, even in the absence of sulphide, and isolates capable of anaerobic growth are readily obtainable. At Firehole Lake, Yellowstone, an interesting but little studied site, an anaerobe, *Thermoanaerobacter ethanolicus* has been isolated and described by Wiegel and Ljungdahl (1981). Pentecost and Terry (1989) isolated *Coyrnebacterium*, *Enterobacter*, *Micrococcus* and *Staphylococcus* from a piped source at Carlsbad, Czech Republic, and they were thought to be contaminants of human origin.

Budding bacteria have been found among cyanobacterium mats by Giovannoni et al. (1987). *Isosphaera pallida* consists of chains of cells 2–2.5 μm in diameter, showing gliding motility. The chains occur in oxic environments at a temperature of 40–55 °C and pH 7.8–8.8. *Isosphaera* has been found in thermal springs of the USA, Europe, and Turkey (Pentecost et al. 1997) but few of these deposit travertine. Their close association with cyanobacteria suggests that the latter provide the energy source. Other bacteria probably occurring in considerable numbers, but as yet unrecorded include, in thermal sites, the aerobic decomposers *Thermus*, *Thermoleophilum*, *Thermomicrobium* and the anaerobes *Thermobacteroides* and *Thermoanaerobium* (Ward et al. 1987). Hot alkaline waters in the United States sometimes contain *Clostridium thermohydrosulfuricum*. Species of mesothermic *Flexibacter*, which often attack cyanobacteria, might also be expected.

9.1.3 Cyanobacteria

Since the publication of Ferdinand Cohn's pioneering work at Tivoli (Cohn 1862), the cyanobacteria have occupied an important position on account of their significance

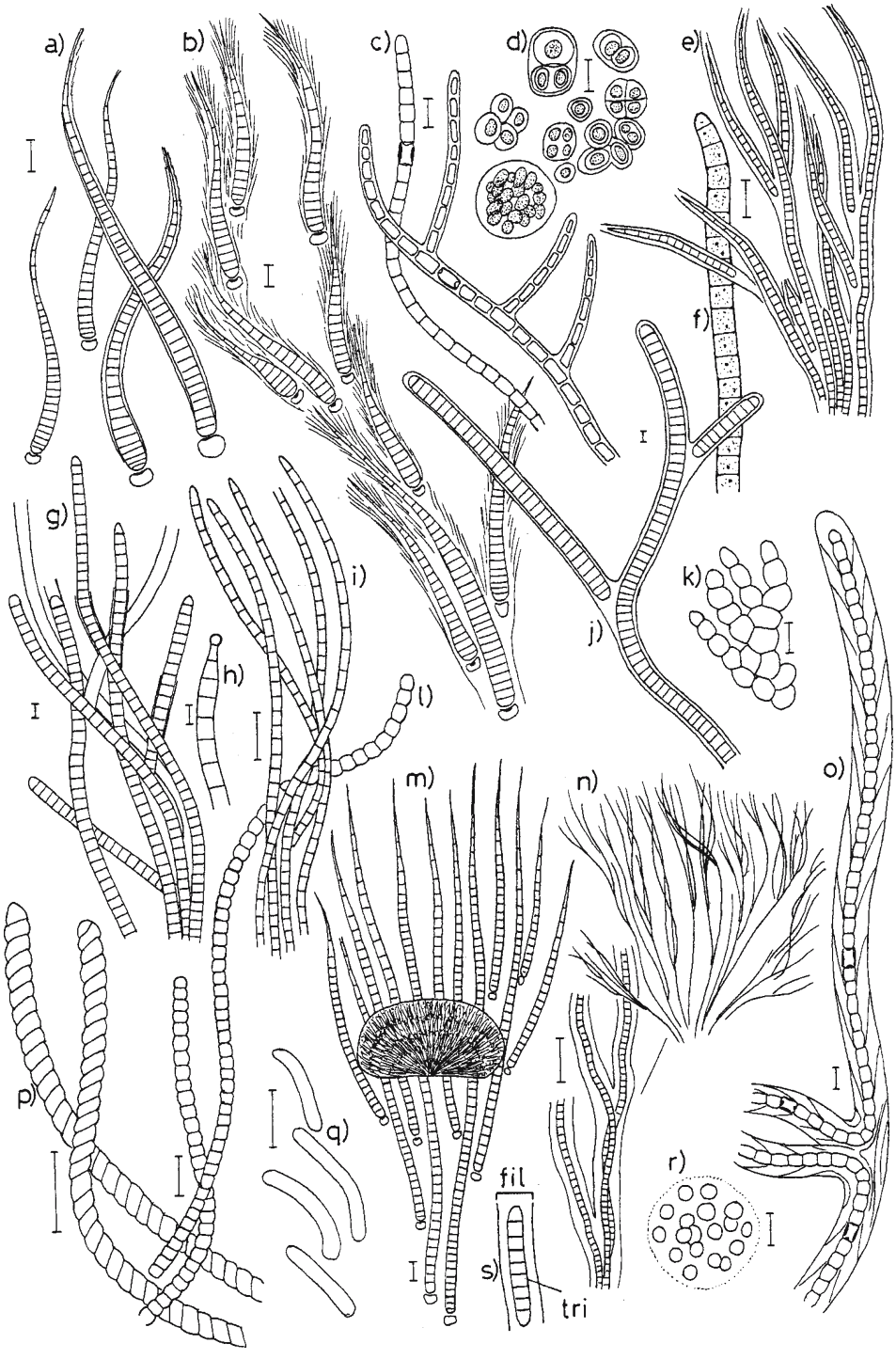
a)
b)
c)
d)
e)
f)
g)
h)
i)
j)
k)
l)
m)
n)
o)
p)
q)
r)
s)
fil
tri

in certain kinds of travertine formation. Several members of the group are widely distributed, and often dominant on actively growing travertine surfaces. This is presumably because these organisms are among the few which thrive in hot, sulphide-containing waters, and many species tolerate a wide range of light intensities, high pCO_2 and survive desiccation well (Castenholz 2002). Filamentous, non-heterocystous cyanobacteria, belonging to Subsection III ('Oscillatoriales') are well represented, and occur in a wide range of waters. Recognition of the group is not difficult, but identification to species presents problems. All cyanobacteria possess chlorophyll-a, with one or more accessory pigments, which can render their colour *en masse* anything but green. Extracellular pigments may also be present. While many other bacteria can be isolated from their environment, purified and then tested with a wide range of media and substrates, the cyanobacteria respond reluctantly to these techniques. Their growth rates are low, and once purified, there are few simple tests available to aid identification. This has led to a dichotomy among cyanobacterium taxonomists. The identification of cyanobacteria was traditionally based upon morphological characters, a line that has been all but abandoned by other bacteriologists. More recent investigations of genetic relatedness of cyanobacterium strains through DNA base composition, DNA-DNA hybridisation, (Rippka et al. 1979) and 16S rRNA sequencing are beginning to resolve these difficulties (Wilmotte and Herdman 2001). Molecular taxonomy will lead to a more logical, phylogenetic classification, but there is still a long way to go, and morphological characters are unlikely to be abandoned entirely. Ultimately, a detailed understanding of the DNA-relatedness and the genetic constitution of cyanobacteria will permit a much greater understanding of their physiological and ecological requirements. These should ultimately provide definitive answers to two nagging questions: are certain taxa cyanobacteria unique to the travertine-depositing environment, and is their ability to 'calcify' genetically determined? For the time being we remain saddled with a morphological system which though in some ways undesirable, is still useful in distinguishing the basic forms.

A review by Castenholz (2002), based on morphological and molecular data, divides the cyanobacteria into five subsections, corresponding to the five fairly well defined classical 'orders'. This system is followed here, though unfortunately, a number of the important travertine-associated forms do not fit comfortably within this scheme at the generic level. It has been decided therefore to conserve the older 'classical' names of these organisms until they can be placed correctly using their 16S-rRNA or other sequences. Many form-genera and form-species have been obtained from active travertines and an attempt to synthesise the available information is given below. Early floras are provided by Prát (1929), Pia (1933), Copeland (1936), Golubic (1957) and more recently by Pentecost and Whitton (2000) and Pentecost (2003a). Illustrations of the commoner forms are provided in Fig. 48.

◀ **Fig. 48.** Illustrations of the commoner travertine cyanobacteria. a) *Calothrix parietina* Thuret; b) *Dichothrix gypsophila* (Kütz.) Bornet showing complex, feathery sheaths; c) *Fischerella thermalis* (Schwabe) Gom. with a trichome of the form *pseudanabaenoides*; d) *Gloeocapsa punctata* Kütz.; e) *Homoeothrix crustacea* Woron.; f) *Oscillatoria formosa* Bory; g) *Phormidium calcareum* Kütz. showing the terminal calyptra; h) *P. incrustatum* (Näg.) Gom.; i) *P. tenue* (Menegh.) Gom.; j) *Plectonema tomasianum* Born.; k) *Pleurocapsa minor* Hansg. em. Geitler; l) *Pseudanabaena catenata* Lauterb.; m) *Rivularia haematites* (D.C.) Ag., filaments and colony section; n) *Schizothrix fasciculata* (Näg.) Gom., filaments and small colony; o) *Scytonema myochrous* (Dillw.) Ag.; p) *Spirulina labyrinthiformis* Gom.;q) *Synechococcus lividus* Copeland; r) *Synechocystis* (*Aphanocapsa*) *endolithica* (Erceg.); s) cyanobacterium trichome (tri) and filament (fil). Bar 5 μm

9.1.3.1 Subsections I (Chroococcales) and II (Pleurocapsales)

These cyanobacteria are to be found on a wide range of travertines. Colonies of *Synechocystis* and *Aphanocapsa* are common but easily missed on account of their small size. On remora that remains dry for much of the year, species of *Gloeocapsa* are widely reported, especially forms with pigmented sheaths, e.g. *G. kützingiana*, *G. punctata* and *G. sanguinea*. These algae are often responsible for the dark, almost black scurfy crusts of the remora of South-East Asian travertines such as those of the Guilin tower karst and the Kimberley travertines of Australia (H. Viles, *pers. comm.*). Cox et al. (1989) describe an Australian cave where speleothem deposition is attributed to a species of *Gloeocapsa*. Members of the order are often found associated with deposits in saline lakes. *Aphanothece packardii* forms huge encrusted 'biostromes' consisting of flat-topped mounds, ridges and ring structures in Great Salt Lake, Utah (Carozzi 1962). The reef-like structures bordering Green Lake, New York State appear to owe their existence in part to a planktonic *Synechococcus* which nucleate calcite and gypsum in the epilimnion (Thompson and Ferris 1990) after which it is transported by an unknown mechanism to the littoral. These deposits are not travertines in the strict sense, but are included on account of their similarity to other littoral deposits. In thermal waters such as Mammoth Hot Springs, *Synechococcus* is often the only cyanobacterium occurring >60 °C. Some species (*S. lividus* and *S. minervae*) also occur with pool aragonites at lower temperatures (Pentecost 1990b) while *Chroococcus minutus* occurs on the lower slopes of the Egerszalók thermogene mound in Hungary. Budding cyanobacteria (Chamaesiphonales) such as *Chamaesiphon* have been reported from a few German deposits (Gruninger 1965; Arp et al. 2001) but are not apparently associated with carbonate deposition.

Members of the order Pleurocapsales form ill-defined, irregular filaments. *Pleurocapsa* is widely distributed on meteogene travertines in Europe and frequently reported (Golubic and Fischer 1975; Ordoñez and Garcia del Cura 1983; Krumbein and Potts 1979; Arp et al. 2001). An unusual deposit occurs in Lake Van, Turkey, where *Pleurocapsa* forms a dark aragonite-encrusted biofilm over submerged travertine towers (Kempe et al. 1991). *Entophysalis deusta* a well-known stromatolite-former, has been found on the Mono Lake travertine mounds by Scholl and Taft (1964), perhaps due to its frequent association with waters of high salinity. *Hyella fontana* is an occasional endolith of European travertines and has been noted by Gruninger (1965), Pentecost (1991b) and Arp et al. 2001. The last authors noted several further indeterminate endoliths in a German deposit.

9.1.3.2 Subsection III (Oscillatoriales)

The filamentous, non-heterocystous cyanobacteria are among the most frequent colonisers of active travertine surfaces but the taxonomy of the group is in a highly unsatisfactory state. The number of 'form' species is fortunately small, but provides plenty of problems. Included are seven form genera, of which three, *Oscillatoria, Phormidium* and *Schizothrix* are of significance. The presence of absence of a loose extracellular polymeric layer termed the sheath is important in identification to the level of genus. The sheaths of these species are usually more clearly developed and are often densely encrusted with carbonate. The trichome (Fig. 48s), defined as the filament devoid of its sheath, shows little active motility. Several species of *Phormidium* are widely distributed on travertine and largely confined to it. Three are common, and probably cosmopolitan on meteogenes. *P. incrustatum* is the most abundant of these (Photoplate 14B), occurring throughout the Northern Hemisphere, where it often forms almost pure, dark blue-green growths, particularly in shaded situations (Arp et al. 2001; Pentecost 2003b). The trichomes are

found within the surface layers and surrounded by an encrusted mucilaginous sheath down to a depth of 3 mm or more (Photoplate 14C). An investigation of the distribution of *P. incrustatum* near Urach, Germany has shown that here at least, the species is partially endolithic, occasionally penetrating and dissolving away the travertine. A separate taxon, *Phormidium favosum,* is sometimes used for this form. Examination of material from some UK sites has shown that trichomes can grow out of the travertine crust, losing the mineralised sheath at their extreme apices, and forming spike-like projections. Similar observations were recorded by Gruninger (1965) for *Lyngbya aerugineo-caerulea* which is probably a synonym of *P. incrustatum*. Here the deposits were illustrated and described as *nadelstein*. *P. incrustatum* has also been observed growing in tangled unencrusted masses on travertine surfaces in Europe and the United States during winter. Nodular deposits containing the species have been described from UK streams by Fritsch and Pantin (1946). These forms are widely distributed in Europe and further described by Freytet and Plet (1991, 1996) from France. Kann (1973) reviewed the classical taxonomy of the carbonate-encrusted species of *Phormidium* and reduced the group to two taxa, *P. incrustatum* and *P. calcicola*, the latter distinguished only by the presence of a small apical enlargement termed a calyptra. This form-species is often associated with *P. incrustatum* and may be merely a growth-form of the latter (Pentecost 2003b). *P. foveolarum, P. martensiana* and *P. valderianum* are also similar to and associated with *P. incrustatum*, and distinguished mainly by their cell diameters (Table 18). All of the above-mentioned *Phormidium* species are more correctly assigned to the form genus *Lyngbya*, but in view of the current taxonomic fluidity, there is little point in making new combinations at this stage. Frequency distributions of trichome diameters taken from travertine sites often demonstrate distinct populations of *Phormidium*, (e.g. Pentecost et al. 1997) but there is substantial inter-site variation.

Phormidium laminosum is a well-known hot spring alga, frequently found on travertine. It is common in the central Italian hot springs and also occurs widely at Yellowstone. This species normally forms superficial dark green mats in spring channels at temperatures of 30–55 °C (Pentecost 1995a,b). At Pamukkale, Turkey the species forms thick finely laminate mats that become encrusted with calcite, sometimes associated with *P. ambiguum* and *P. valderianum*. Walter et al. (1976) describe *Phormidium* conophytons from Jupiter Terrace, Mammoth Hot Springs, which show features in common with ancient stromatolites.

Oscillatoria is distinguished from *Phormidium* by its sheath-free trichomes showing continuous gliding motility. The species are found as superficial mats on travertines and are often common in sulphide-rich, thermal waters. They are most often observed as dark, non-calcified mats. *O. formosa* has been found in the Italian hot springs, including those of Bagni di Tivoli where it forms extensive benthic mats (Pentecost and Tortora 1989). *O. amphibia* and *O. geminata* are narrower forms inhabiting similar niches. Species of *Oscillatoria* have not been observed as calcified colonies, presumably owing to the lack of a well-defined sheath. *Pseudanabaena catenata* is similar but distinguished by its small barrel-shaped cells. It is occasionally found forming radiating fascicles in stream crusts or oncoids or living free in thermal waters (Pentecost 1990b) and closely-matched 16S rRNA sequences have been detected at Mammoth Hot Springs (Fouke et al. 2003).

Schizothrix is distinguished traditionally on sheath characters although these are variable and often unreliable in identification. *S. fasciculata* builds nodules up to 5 mm in diameter containing large numbers of fine radiating trichomes, often in well-lit fast flowing streams (Photoplate 14D). An orange-brown pigmentation is usually well developed, and consists of intracellular carotenes probably serving as photoprotectors. Experiments employing radioisotopes demonstrated that in this community, the species could exist photoautotrophically to a depth of 2 mm in the travertine, which coincided with depth of occurrence (Pentecost

Table 18. Morphological and environmental characters of the commoner Oscillatoriales known from active travertines. ± indicates that the character may or may not be present

	Sheath >1 µm wide	Sheath simple single	Sheath compound	False branching	Continuous motility	Trichome helical	Trichome width 0.4–1 µm	Trichome width 1–2 µm	Trichome width 2–4 µm	Trichome width 4–6 µm	Trichome width 6–8 µm	Trichome width >8 µm	Cells barrel-shaped	Calyptra present	Nodular encrustations	Laminar encrustations	Endolithic	Temperature regime 0–30 °C	Temperature regime 30–50 °C	Temperature regime >50 °C	Sulphide tolerant (>15 µmol L^{-1})
Leptolyngbya perforans	±	−	+	±	−	−	+	+	−	−	−	−	−	−	−	−	+	+	+	−	
Lyngbya martensiana	+	+	−	−	−	−	−	−	−	−	+	−	−	−	+	+	−	+	−	−	
Oscillatoria amphibia	−			−	+	−	−	−	+	−	−	−	−	−	−	−	−	−	+	−	
O. formosa/terebriformis	−			−	+	−	−	−	−	+	−	−	−	−	−	−	−	+	+	−	
O. geminata	−			−	+	−	−	−	+	−	−	−	−	−	−	−	−	+	+	−	
O. subtillisima	−			−	+	−	+	−	−	−	−	−	−	−	−	−	−	+	+	−	
Phormidium ambiguum	−			−	−	−	−	−	−	+	−	−	−	−	−	−	−	+	+	−	
P. calcareum	±	+	−	−	−	−	−	−	+	+	−	−	−	+	−	−	−	+	−	−	
P. foveolarum	±	+	−	−	−	−	−	+	−	−	−	−	−	−	+	+	−	+	−	−	
P. incrustatum	±	+	−	−	−	−	−	−	−	+	−	−	−	−	+	+	±	+	+	−	
P. laminosum	−			−	±	−	+	−	−	−	−	−	−	−	−	−	−	+	+	+	−
P. tenue	−	+	−	−	−	−	−	+	−	−	−	−	−	−	+	+	−	−	+	−	
P. valderianum	±	+	−	−	−	−	−	−	+	−	−	−	−	−	+	+	−	+	−	−	
Plectonema phormidioides	+	+	−	+	−	−	−	−	−	−	+	−	−	−	−	+	−	+	−	−	
P. tomasianum	+	+	−	+	−	−	−	−	−	−	−	+	−	−	−	−	−	+	−	−	
Pseudanabaena catenata	−			−	+	−	+	+	−	−	−	−	+	−	−	−	−	+	+	−	
Schizothrix fasciculata	+	−	+	±	−	−	+	+	−	−	−	−	−	−	+	−	−	+	−	−	
S. lateritia	+	−	+	±	−	−	−	+	−	−	−	−	−	−	−	+	−	+	−	−	
Spirulina labyrinthiformis	−			−	+	+	+	−	−	−	−	−	−	−	−	−	−	+	+	+	+

1978). *Schizothrix* is one of the most frequently encountered and colourful cyanobacteria of meteogene travertines (Photoplate 3C). Phycobilin- and phycoerythrin-rich strains of *Schizothrix* can sometimes be found which colour shaded travertine surfaces red or blue-green respectively. This pigmentation is related to light intensity with the red forms occurring in darker situations, but sheath pigments also often occur, giving rise to a range of tints. *S. lateritia* is also widespread and distinguished mainly on the occurrence of calcified laminate rather than nodular mats. *Leptolyngbya (Schizothrix) perforans* differs only in the endolithic habit, clearly seen by the penetration of limestone bedrock beneath travertine crusts. *Plectonema* is known by its falsely-branched filaments and has been found on a range of deposits, from the mounds of Mono Lake, California (Scholl and Taft 1964) to desert springs (Krumbein and Potts 1979) and waterfalls (Wallner 1934b).

Species of *Spirulina* often form dark green mats in sulphide-rich thermal waters. Often, they are associated with *Oscillatoria* and are normally unencrusted. At Bagnaccio, Italy these mats develop at the edges of the stream channels at temperatures of 40–54 °C and sulphide concentrations of approximately 5–30 μmol L^{-1}, forming a conspicuous green border (Pentecost 1995b). They occur at lower temperatures at Mammoth Hot Springs but their distribution appears related more to chemical (S, O_2) than physical factors. Several other Oscillatoriales are known. The 'classical' taxa of thermal (mostly thermogene) travertines have been reviewed recently (Pentecost 2003a).

9.1.3.3 Subsections IV (Nostocales) and V (Stigonematales)

The filamentous heterocystous cyanobacteria, although less common on travertine than the Oscillatoriales, include several interesting calcified forms. The form genera of the Rivulariaceae are distinguished mainly by their degree of false-branching. At least two species produce calcified button-like colonies that coalesce to form glistening brown mats. *Rivularia haematites* forms dark shiny brown or green buttons 1–20 mm across and is mostly found in exposed travertine flushes but with a markedly patchy distribution which may be associated with the availability of organically-bound phosphate (Whitton 1987). It is a noteworthy taxon as crystals of microspar are deposited within the mucilaginous sheaths (Photoplate 14E) contrasting with the closely related *Calothrix* and *Dichothrix*. Laminated crusts are formed by *Calothrix* and *Dichothrix*, and species of the former are common on travertine stream-crusts, including oncoids. *Calothrix* frequently behaves as an endolith, but carbonate-depositing activity has also been shown (Pentecost 1989). Some taxa occur in thermal sulphide springs. *Dichothrix* is known from oncoids, stream crusts and from more massive deposits and can become dominant as in the coastal travertines at Augusta in Western Australia. The species are more often found in warm regions. The Rivulariaceae as a whole appear to be slow-growing (Pentecost 1987, 1989; Caudwell et al. 2001) but measurements are lacking for tropical sites.

Smaller pale-buff coloured colonies of *Homoeothrix* are sometimes encountered and distinguished from *Rivularia* by the lack of heterocysts. Several forms occur on travertine and their taxonomy reviewed by Komarek and Kann (1973). The button-like or nodular colonies are normally heavily calcified, but, in common with *Rivularia*, they are not found in hot or sulphide-rich waters. The colonies often fuse laterally to form tiny ledge-like crusts (Pentecost 1988a; Winsborough et al. 1994). Although *Homoeothrix* should strictly belong to the Oscillatoriales, the affinities of the species seem closer to the Rivulariaceae.

A small number of falsely-branched cyanobacteria without tapered ends (Scytonemataceae) can be significant colonisers, particularly in areas prone to desiccation. *Scytonema myochrous* forms dark mats on damp travertines throughout the world but is rare in permanently flowing

water. Thunmark (1926) found evidence of growth laminae and heliotropism in this species on travertine. Other unusual travertine morphologies have been found in Laguna Grande, Cuatro Cienegas, Mexico and are associated with this genus. *Tolypothrix*, distinguished by its mode of branching, is common in flowing water, but it is unusual to find the species encrusted, at least in Europe.

A notable feature of most of the cyanobacteria forming calcified, hemispherical cushions with a radiating structure of trichomes is the frequent formation of primary sparite as opposed to micrite (Section 3.1.1). Cushion-formation is normally the result of false-branching in cells embedded in a mucilaginous sheath, suggesting that the sheath mucilage influences crystal size.

The 'true-branching' heterocystous cyanobacteria (Stigonematales) are less often encountered. *Fischerella thermalis* (*Mastigocladus laminosus*) a well known thermophilic cyanobacterium is sometimes associated with travertine and was first described from the travertines of Carlsbad (Cohn 1862). The taxon is polymorphic and exists as several strains, some of which are sulphide-intolerant (Castenholz 1973, 1989) perhaps explaining its rarity at sites such as Mammoth Hot Springs. Species of the related *Stigonema* are also occasionally reported from moist meteogene travertines (e.g. Powell 1903).

9.2 Eukaryotic Algae

The eukaryotic algae are divided into several phyla distinguished by their cytology and biochemistry. They are a diverse group of mainly microscopic plants and most are cosmopolitan. On travertine, they are often found associated with cyanobacteria, but usually tolerate less shade and are rarely found in water with a temperature exceeding 45 °C. Their growth is often more rapid in the warmer parts of the year, and then, they will frequently overgrow cyanobacteria. Numerous species have been collected from travertines, but insufficient is known of their ecology to draw much inference concerning their distribution or preferences. They are considered under their respective phyla.

9.2.1 Chlorophyta (Green Algae)

A diverse assemblage, but few of the thousands of described species are found regularly on travertine. However a small number demonstrate some notable adaptations. Green algae are rarely encountered in sulphide-rich waters, and thermophiles are rare. The majority belong to three orders, the Charales, Chaetophorales and Zygnematales. About a quarter of the approximately 20 species known from travertine are regularly encrusted with calcite and become incorporated into the deposits. The remainder are short-lived attached forms which colonise rapidly but are readily lost. Common members are illustrated in Fig. 49(b–h).

Fig. 49. Illustrations of some characteristic eukaryotic algae of travertines. a) *Audouinella* sp.; b) *Chara vulgaris* L.; c) *Chlorotylium cataractarum* Kütz.; d) *Cladophora glomerata* (L.) Kütz.; e) *Dilabifilum printzii* Tschermak-Woess; f) *Gongrosira incrustans* (Reinsch) Schmidle; g) *Oedogonium rufescens* Wittr. with oogonia; h) *Oocardium stratum* Näg. branched colony and single cell enlarged; i) *Vaucheria geminata* (Vaucher) de Candolle with two oogonia; j) *Achnanthes minutissima* Kütz. showing valve and girdle view (right); k) *Amphora ovalis* (Kütz.) Kirchn.; l) *Cymbella cistula* (Ehr.) Kirchn.; m) *Denticula tenuis* Kütz.; n) *Diatoma hyemalis* (Roth.) Heib.; o) *Epithemia argus* (Ehr.) Kütz.; p) *Gomphonema olivaceum* var. *calcareum* (Cleve) Cleve; q) *Mastogloia smithii* var. *lacustris* Grun.; r) *Navicula cari* Ehr.; s) *Nitzschia dissipata* (Kütz.) Grun.; t) *Rhopalodia gibba* (Ehr.) O. Müll. a) Rhodophyta; b-h), Chlorophyta; i), Xanthophyta; j–t), Bacillariophyta (diatoms). Except for c), h) and i) the cells are shown without their chloroplasts. Bar 10 μm ▶

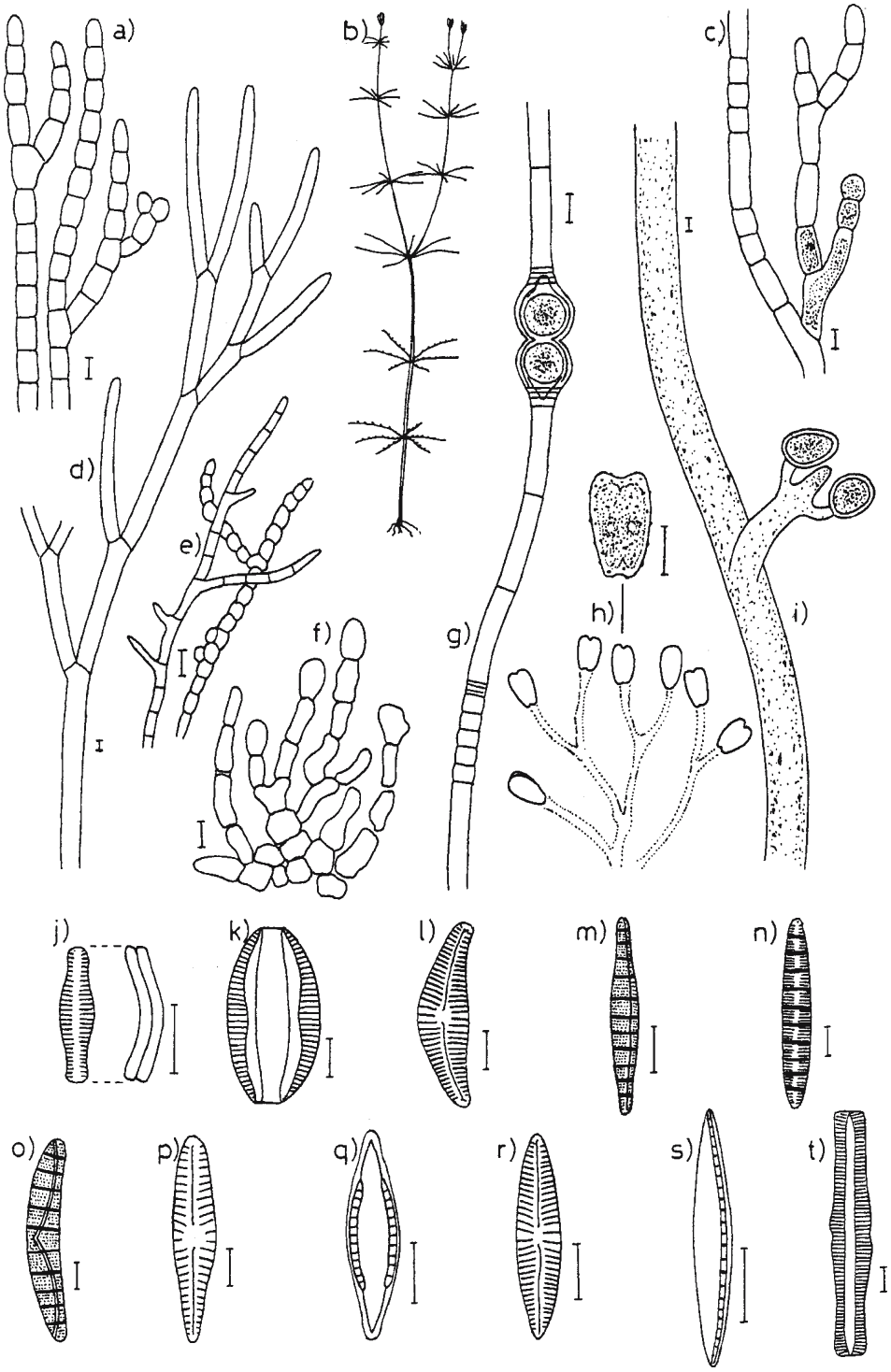
a)
b)
c)
d)
e)
f)
g)
h)
i)
j)
k)
l)
m)
n)
o)
p)
q)
r)
s)
t)

9.2.1.1 Zygnematales

These algae include the desmids, a well-defined sub-order (the Desmidiineae) whose cells possess a deep median constriction and are often elaborately ornamented with spines or nodules. Only two of the many desmid genera, *Cosmarium* and *Oocardium* are well known from travertine. Several species of *Cosmarium* have been reported by Thunmark (1926) and Stirn (1964) and occur mainly as loose periphyton associated with bryophytes or cyanobacteria. Wallner (1935a) described the growth of two weakly encrusted species, *C. nitidulum* and *C. granatum* from the moss *Eucladium* growing on a German travertine. A form closely resembling *C. nitidulum* but with a greater length-to-breadth ratio (1.75 opposed to 1.23 in the type) is characteristic of sheltered travertine seeps in northern England where it forms a green, weakly calcified slime during early summer. *Cosmarium laeve* occurs in the cooler thermogene waters at Pamukkale, Turkey (Pentecost et al. 1997) and at Egerszalók, Hungary. However, the most interesting desmid is *Oocardium stratum* which occurs exclusively on active meteogene deposits (Wallner 1933; Pavletic and Golubic 1956; Pentecost 1991c). *Oocardium* is a colonial desmid whose cells develop at the ends of bifurcating mucilage tubes. The cells all occur at approximately the same level, forming small green cushions 0.2–5 mm in diameter. The median cell constriction is oriented perpendicular to the colony surface and in side view, the cells frequently appear tapered toward their lower end with their walls covered in fine punctae (Fig. 49h). Methylene blue staining reveals an apical tuft of 'prism' mucilage (Wallner 1935b) but the most interesting feature of *Oocardium* is the manner in which it is encrusted with calcite. The colonies are completely encased in large crystals of sparite of characteristic form, easily recognisable in ancient travertines (Photoplate 15A), with only the tips of the cells protruding. Frequently, crystal faces are clearly discernable and pockmarked with innumerable perforations, each occupied by a cell (Photoplate 13C). The association of *Oocardium* with sparry calcite is common, resulting in a scintillating pale green 'sugar crust'. Other forms of colony are known with less clearly discernable crystal faces, with the mucilage tubes which support the cells beautifully calcified forming an open coralloid structure. Wallner (1933) was the first to recognise these forms, and described a further species, *O. depressum* with slightly larger and fatter cells, though later work by Golubic and Marcenko (1958) suggests that there is little to justify a further species. The calcification process in *Oocardium* has not been studied in detail. Crystalline continuity through large areas of colony is apparent but the selective calcification of mucilage tubes has not been investigated. It may be significant that the mucilage tubes of diatoms may also become calcified and it would be interesting to know why the calcite fails to grow over the colonies and entomb them. Field observations suggest that young colonies provide a crystallisation centre for calcite but the colonies may not have much control over crystal formation. The *Oocardium* cells may be seen to protrude only slightly beyond the crystal surface so that calcification could provide some protection from abrasion. The species usually occurs in fast flowing water, which lends some support for this. Where flow rates are below about 0.3 m s^{-1}, colonies develop as cushions, but as flow increases, they seem to coalesce and form a smooth crust (Wallner 1933). In parts of Bavaria, *Oocardium* is found on iron-rich travertines and the upper and exposed parts of the cell walls are sometimes found encrusted with iron oxides. The association between desmids and iron deposition has long been recognised and a certain concentration of available iron is perhaps critical to its establishment and growth. When colonies of *Oocardium* were placed for a few days in almost static water, Wallner (1935b) found that the cells came out of their tubes and formed a mucilaginous growth on the travertine surface, termed a *'Freistadium'*. He concluded that under stagnant conditions, some cells would detach and move away to allow the establishment of new colonies (*'Wanderstadium'*).

Oocardium occurs worldwide and is locally common in parts of Germany and the United States. In France it is frequently associated with bryophytes (Freytet and Plet 1991). There are several records from the tropics and it is found as far as 55° N in Sweden. The species seems to be more common in warm-temperate regions, and is rare in Britain, where it is known from just two sites in Yorkshire (Pentecost 1991c). Even on a small scale, *Oocardium* has a patchy distribution and may be locally so abundant that other algae are almost excluded. Large stretches of some Bavarian streams are coloured green by it. The exact positioning of the cells with respect to the deposits suggest that rates of crystal growth and of mucilage tube extension are critical to its development. Travertine associated with *Oocardium* has a characteristic microstructure recognisable in old deposits providing there has been little diagenesis. Substantial deposits are reported from Bavaria (Wallner 1933), Virginia (Mathews et al. 1965) and China (Pentecost and Zhang 2000). *Oocardium* is exceptional in being one of the few algae known exclusively from travertine. Filamentous Zygnemales are common on travertine but are rarely incorporated into the fabric. They include taxa belonging to the genera *Mougeotia*, *Spirogyra* and *Zygnema*. *Spirogyra olivascens* has been found at Krka Falls, Croatia (Golubic 1957) and *S.* aff. *mirabilis* on the Blanche Cup mound spring of Australia (Ling et al. 1989). The rare *Debarya polyedrica* has been reported from a Chinese travertine (Skuja 1937). All of these filamentous algae are also known from non travertine-depositing waters.

9.2.1.2 Charales

Charales are poorly represented on travertines in fast-flowing water, as they require a soft medium in which to establish. They are most often found in the boggy hollows of crons, in travertine-dammed lakes or slow muddy seeps and here they may be common. Two species are frequently recorded in Europe: *Chara foetida* and *C. vulgaris* (van Oye 1937; Pentecost 1991a). *Chara* is also known from the cooler waters of thermogene sites such as Viterbo and Mammoth Hot Springs (Copeland 1936) and as fossils at Bagni di Tivoli (Folk and Chafetz 1983) and many other sites, particularly in China. These algae are important marl-formers and their remains are often common in marl lakes (Section 15.1.1.1).

9.2.1.3 Chaetophorales and Other Orders

Most of these Green Algae, excepting *Chlorotylium* and *Gongrosira* are 'ephemerals' on travertine. Among the Chaetophorales, *Chlorotylium cataractarum* is an occasional branched cushion-former that although poorly known, appears to be closely associated with travertine and usually encrusted (Fig. 49c). There are records from the United States e.g. Doe Run, Kentucky (Minckley 1963), Germany (Stirn 1964) and Croatia (Golubic 1957). The alga is characterised by its alternating long and short cells but is otherwise similar to the much commoner *Gongrosira*. Of the remaining species, the rare *Dilabifilum printzii* is one of the more interesting, consisting of irregularly branched filaments arising from a parenchymatous base, usually encrusted and easily mistaken for *Gongrosira*.

Gongrosira forms small green encrusted colonies and apt to be mistaken for *Oocardium* in the field, though not in thin section. The species is unusual in being at least partially endolithic (Pentecost 1991c). Richly branched filaments form compact cushions found throughout the world (Fig. 49f). Printz (1964) recognised 10 encrusting species, but the taxonomy is currently confused. *G. incrustans* with slightly swollen terminal zoosporangia is widely recognised but other species probably occur on travertine. *Gongrosira* crusts are sometimes a major component of travertine deposits (Blum 1957; Golubic and Fischer 1975).

At Cuatro Cienegas, Mexico, some streams contain large nodular 'bioherms' consisting of a massive *Gongrosira* travertine (Pentecost 1988b) with lacustrine *Gongrosira* oncoids and lake crusts in the same region. Straggling mats of *Oedogonium* (order Oedogoniales) are common on travertine cascades during warm weather but rarely become encrusted possibly due to their rapid and quickly terminated growth. There are reports of *Oe. plagiostomum* var. *gracilis* (Emig 1917); *Oe. rufescens* (Golubic 1957) and *Oe. australe* (Pentecost 1991b). *Microspora floccosa* (Klebsormidiales) was found growing as 'pseudostalactites' from the nose of the Uracher Waterfall by Gruninger (1965). The order Cladophorales contains one common travertine alga, *Cladophora glomerata*. It occurs as coarse wrinkled mats and may become extremely abundant in areas of high flow. The filaments are often lightly encrusted with calcite. The species is particularly common in sewage-polluted water, which may account for its current dominance on the Cascatelle of Tivoli, Italy. It is thought to be sensitive to dissolved iron (Blum 1957). A closely related alga, *Rhizoclonium* is recorded from some Arizona travertines (Malusa et al. 2003).

9.2.2 Diatoms

Diatoms were among the first algae to be recognised on travertine (Porter 1861) and have long been known as a significant component of the flora (Meunier 1899). Diatoms have a silicon requirement and travertine-depositing waters always appear to contain adequate supplies of this element (Section 6.3). They occur in a wide range of habitats and some species tolerate high levels of sulphide. Others are moderate thermophiles, though incapable of living at temperatures much exceeding 40 °C (Stockner 1967). They are found growing directly upon travertine or as epiphytes on the associated bryophytes and macroalgae such as *Cladophora*. Most investigators have contented themselves with the publication of species lists accompanied by brief ecological notes. Examples are Kindle (1927), Hevisi (1970), Lang and Pierre (1974) and John et al. (1982). According to Murray (1895), E. Grove prepared an unpublished list of over 100 species from a Canadian lake containing travertine crusts. Ecological work has also been undertaken, employing multivariate methods (Iserentant 1988) and quantitative sampling (Davis et al. 1989; Pentecost 1991b; 1998). As a result, the diatom flora of active travertines is moderately well known, comprising more than 160 species. The commoner taxa, several of which are illustrated in Fig. 49 are listed in Table 19. None is known to be restricted to travertine, but some deposits are so densely colonised with diatoms that their frustules make up a significant proportion of the surface material. Of the 51 taxa listed in Table 19, all have been recorded from meteogene deposits and 32 from thermogenes. This difference is due in part to the greater amount of attention applied to the former, but it also appears that many thermogenes contain either smaller numbers, or fewer diatom species. This will be in part due to their water temperatures often exceeding 40 °C. Owing to the popularity of diatoms among microscopists, the generally clear species limits, and wealth of literature, more can be said about their ecological requirements than algae belonging to most of the other phyla. The majority of records come from lake and stream crusts and travertine cascades but there has been a lack of systematic sampling, and it would be premature to attach too much ecological significance to the statistics at present. Many taxa have been classified according to their nutrient status and their pH tolerance, and these data are listed in Table 19. 'Alkaliphils' are species whose growth optimum exceeds pH 7. They are well represented, and account for about half of the total listed in the table. All but one of the remainder are either 'pH indifferent or 'circumneutral' species and include many diatoms with a wide ecological amplitude. This is a common phenomenon among diatoms as many species may be found in a wide range of environments. Some taxa are more ecologically demanding, but there are

none known only from travertine deposits. While at species level most of the taxa are well-circumscribed, the higher taxonomic levels are currently confused due to differing schools of thought concerning key characters. This will no doubt clarify as molecular analyses advance, but in discussing the species here, a conservative view has been taken. The diatoms can be subdivided into three major groups. Most species belong to the raphid pennate diatoms. These forms possess silica frustules in the approximate shape of a boat, with a pronounced longitudinal slit termed the raphe along the valve faces. The raphe and associated pores are important as they secrete mucilage that can provide a nucleation site for calcium carbonate, and also allow the diatom to move and adhere to the travertine surface. There is also a group of non-raphid pennate diatoms, and finally the centric diatoms, with a cylindrical, often petri-dish form.

9.2.2.1 Raphid Pennate Diatoms

There are several important travertine genera. The genus *Cymbella* is well represented with nine species listed in Table 19. The genus is subdivided into subgenera dependent on morphology of the frustule and form of the mucilage secretions. Only two of the species form structural mucilage; *C. minuta* where mucilage forms a long tube in which the cells are aligned, and *C. lanceolata* where it forms an attachment stalk or peduncle. Most of the remaining species have an almost symmetric form reminiscent of the genus *Navicula*. Most of these taxa are pH-indifferent and tolerate a wide range of water types. They are often extremely common on meteogene travertines. The genera *Didymosphenia* (Photoplate 15B) and *Gomphonema* (Fig. 49p, Photoplate 3B) are also well represented and all of the species produce a mucilaginous peduncle for attachment. They are distinguished on the frustule shape and the wedge-shaped cells, as seen in girdle view, are common in travertine preparations, and can occur in huge numbers attached to the travertine surface. The most 'closely associated' travertine species is probably *Gomphonema olivaceum* var. *calcareum*. This diatom produces extensive mucilage in the form of branched stalks many times the length of the cells that often become calcified (Winsborough and Golubic 1987).

Considering the huge size of the genus *Navicula*, few species are regularly encountered on travertine. Most characteristic is *N. cari,* a medium-sized lanceolate species belonging to the sub-genus *Navicula*. It is a plant of wide ecological range but not usually found in large numbers, often associated with the related forms *N. tripuncata* and *N. viridula*. Other genera structurally related to *Navicula* include *Brachysira*, *Caloneis*, *Diploneis* and *Rhoicosphenia*. The species occur in small numbers, and often as epiphytes on the associated travertine flora. The majority are actively motile as are members of the large genus *Nitzschia*. Species of *Nitzschia* are almost ubiquitous on travertine but usually subordinate to other diatoms. Several of the recorded species have a wide ecological amplitude. Two interesting genera belong to the Epithemiaceae, viz. *Epithemia* and *Rhopalodia*. They are more local in their distribution but noteworthy for their accociation with oligotrophic calcareous waters and ability to fix nitrogen. *R. gibba* has also been shown to positively influence calcite deposition in a UK travertine (Pentecost 1998).

The above diatoms contain a raphe on each valve of the frustule, but another group contains a raphe on one valve only. The group includes the important travertine genus *Achnanthes*. One species, *A. minutissima* is by far the commonest and is the most frequently recorded travertine diatom (Photoplate 13D). It is a small alga, often present in huge numbers, but does not appear on deposits formed from sulphide-rich waters. The remaining species listed in Table 19 are much less common although *A. lanceolata* is often recorded on account of its distinctive appearance. The related genus *Cocconeis* with oval frustules is also a common alkaphil and most often found as an epiphyte of travertine bryophytes.

Table 19. Diatoms frequently recorded from active travertines. Travertine types: ca cascade; d dam; lc lake crust; m mound; sc stream scrust. pH range: aci 'acidophil'; alk 'alkaliphil'; ind 'pH-indifferent/circumneutral'. Nutrient status of taxa: e eutrophic; m mesotrophic; o oligotrophic

Taxon	Meteogene	Thermogene	Travertine type	Nutrient status	pH range
Achnanthes exigua Grun.	X	X	lc, m	m, o	Alk
A. lanceolata (Breb. ex Kütz.) Grun	X		ca ,d, lc sc	m, o	Alk
A. minutissima Kütz.	X	X	ca,d,lc,m,sc	m, o	Alk
A. thermalis (Rabenh.) Schrenf.	X	X	d, lc, sc	m, o	Alk
Amphora coffaeformis (Ag.) Kütz.	X	X	m	m, o	Alk
A. ovalis (Kütz.) Kütz.	X		ca, lc, sc	m, o	Alk
Brachysira vitrea (Grun.) Ross	X		sc	o	Ind
Caloneis alpestris (Grun.) Cleve	X	X	d, lc, sc	o	Alk
C. bacillum (Grun.) Cleve	X	X	ca, d, m, sc	o	Ind
Cocconeis pediculus Ehr.	X		ca, lc	m, o	Alk
C. placentula Ehr.	X	X	ca d, lc, sc	m, o	Alk
Cymatopleura solea (Breb.) W. Sm.	X		ca, lc	e, m	Ind
Cymbella affinis Kütz.	X	X	ca, lc, m, sc	o	Alk
C. cesatii (Rabenh.) Grun.	X		lc, sc	o	Aci
C. cistula (Ehr.) Kirch.	X	X	ca, d, lc, sc	e, m, o	Ind
C. cymbiformis Ag.	X	X	ca, d, lc, sc	m, o	Ind
C. helvetica Kütz.	X		ca, lc	E, m, o	Ind
C. laevis Näg. ex Kütz.	X		ca, lc	o	Alk
C. lanceolata (Ehr.) Kirch.	X		ca, lc	m, o	Alk
C. microcephala Grun.	X	X	d, sc	m, o	Ind
C. minuta Hilse ex Rabenh.	X	X	ca, d, lc, sc	o	Ind
Denticula elegans Kütz.	X	X	ca d, m	m, o	Alk
D. tenuis Kütz.	X	X	ca, d, lc, sc	e, m o	Alk
Diatoma hyemalis (Roth) Heib.	X	X	d, sc	m, o	Ind
D. vulgaris Bory	X	X	ca, lc, m, sc	e, m	Alk
Diploneis elliptica (Kütz.) Cleve	X		ca, lc, sc	o	Ind
D. oblongella (Näg. ex Kütz.) Ross	X	X	ca, sc	o	Ind
Epithemia argus (Ehr.) Kütz.	X		lc, sc	m, o	Alk
Eunotia arcus Ehr.	X	X	ca ,d, sc, lc	o	Alk
Fragilaria virescens Ralfs	X	X	ca, d, lc	e, m, o	Ind
F. ulna (Nitzsche) Lange-Bert.	X	X	ca,d,lc,m, sc	m	Ind
Gomphonema acuminatum Ehr.	X	X	d, lc ,sc	e, m, o	Ind

Table 19. *Continued*

Taxon	Meteogene	Thermogene	Travertine type	Nutrient status	pH range
G. angustatum (Kütz.) Rabenh.	X	X	ca, d, lc, sc	m, o	Alk
G. angustum Ag.	X		ca, sc	o	Ind
G. olivaceum var. *calcareum* (Cleve) Cleve	X		ca, sc	o	Alk
G. parvulum (Kütz.) Kütz.	X	X	d, sc	e, m, o	Alk
G. truncatum Ehr.	X		ca, lc	e	Ind
Mastogloia smithii var. *lacustris* Grun.	X	X	d, lc, sc	o	Alk
Meridion circulare (Grev.) Ag.	X	X	ca, sc	m, o	Alk
Navicula cari Ehr.	X	X	ca, lc, m, sc	e, m, o	Ind
N. cryptocephala Kütz.	X		sc	e, m	Ind
N. cryptotenella Lange-Bert.	X		ca	e, m, o	Alk
N. pupula Kütz.	X	X	lc, m	m	Ind
N. tripunctata (Müll.) Bory	X		ca, lc, sc	e, m, o	Alk
N. viridula (Kütz.) Ehr.	X	X	lc, m, sc	m	Ind
Nitzschia amphibia Grun.	X	X	d, lc, m	m	Alk
N. dissipata (Kütz.) Grun.	X	X	ca, lc	e, m, o	Alk
N. palea (Kütz.) W. Sm.	X	X	ca, lc, m	e, m, o	Ind
N. sinuata (Tyhw. ex W. Sm.) Grun.	X		ca, lc	m	Ind
Rhoicosphenia abbreviata (Ag.) Lange-Bert.	X		ca, lc, sc	m, o	Alk
Rhopalodia gibba (Ehr.) O. Müll.	X	X	ca, lc, m	o	Alk

9.2.2.2 Araphid Pennate and Centric Diatoms

These diatoms are not well represented although species of *Fragilaria* often occur in small numbers. Fan-shaped colonies of the calcicolous diatom *Meridion* are frequent on meteogene deposits. Centric diatoms are notably scarce partly due to the fact that the majority of species are planktonic. However, they have been found on travertine dams, where some of the planktonic lake flora has probably been incorporated. There is also a group of common fluviatile centrics. *Melosira varians* is a well known species from European waters but has not yet been recorded from travertine, perhaps because it tends to be associated with eutrophic, phosphate-rich streams.

9.2.3 Other Eukaryotic Algae

Chrysonebula holmesii (Chrysophyta) forms extensive blooms on several UK travertines. This alga has an exceptionally restricted distribution, currently known only from this area, and usually in travertine-depositing waters. *Chrysonebula* resembles the more frequent *Hydrurus foetidus* and like it, develops only in water below 20 °C. Another member of this phylum, *Phaeodermatidium rivularis* has been found among crusts of *Gongrosira* at Gütersteiner, Germany (Gruninger 1965).

Violet-pigmented filaments of *Audouinella* (Rhodophyta) are sometimes found growing on the surfaces of oncoids and stream crusts in the shaded watercourses of Europe. Some of the species are thought to be part of the life cycle of the macroscopic red alga *Batrachospermum* and are sometimes termed the '*Chantransia*' stage of this genus. *Auduoinella chalybeia* occurs at Urach (Stirn 1964). It is widespread in Britain and also known from the United States (Blum 1957). The species forms well-defined cushions and is pollution sensitive according to Edwards and Heywood (1960). Other Red Algae occasionally found on travertine include *Bangia atropurpurea* and *Lemanea fluviatilis*. Both require turbulent water. Gibert et al. (1983) noted a red alga at a thermal site in the Auvergne, but its identity is uncertain.

Several species of *Vaucheria* (Xanthophyta) form characteristic convex tufts on cascades and travertine dams and are described by Wallner (1934). Growth of this alga in England is most rapid in the spring prior to leaf-break. The tufts become rapidly encrusted (Photoplates 7E, 15C) and are frequently fossilised as characteristic colonies and they can play a major part in the formation of travertine dams (Section 4.1.4). *Vaucheria* is a common filamentous alga superficially resembling *Cladophora* though paler in colour and unbranched. The most frequently recorded species are *V. geminata* and *V. sessilis* though *V. debaryana* is also known (Emig 1917; Stirn 1964; Pitois et al. 2001). Both filaments and reproductive organs become encrusted (Kolkwitz and Kolbe 1923) but it is not known how this affects reproduction. In addition, the taxonomy of the group is difficult and there appear to be a number of overlapping forms. The species are frequent in semi-shaded sites, and in contrast with *Cladophora* they are often found on iron-rich travertines, especially cascades.

A small number of flagellate algae from diverse phyla may occur in thermogene travertine pools. At Mammoth Hot Springs, Fouke et al. (2003) detected close 16S rRNA sequence matches for the chloroplasts/mitochondria of *Chrysodidymus synuroides*, *Cyanophora paradoxa*, *Mesostigma viride* and *Nephroselmis olivacea*.

9.3 Fungi and Lichens

Aquatic fungi should be common on active travertines but there have been no systematic studies. Members of the Saprolegniales are the best known aquatic fungi and can be isolated from meteogene travertines when these are incubated with sterile hemp seeds (unpublished observations). Fungal hyphae are common in decalcified travertines and on rare occasions may be encrusted with carbonate in subaerial sites (Schneider 1977). Tilden (1897) noted the ascomycete *Pseudohelotium granulosellum* growing on cyanobacterium crusts near the Mississippi, but could not account for its presence. It has not been recorded from travertine since and may have developed from encrusted wood. Another unidentified ascomycete with an encrusted fruit body is figured and described from a German site by Arp et al. (2001). Small tubular structures composed of radiating calcite prisms are occasionally observed in petrographic sections of travertine where they have been placed under the form genus *Microcodium* (Hartkopf-Fröder 1989). They are thought to represent calcified mycorhiza and are common in some calcretes. Fungi are common in caves and have occasionally been implicated in speleothem formation (Went 1969).

Aquatic lichens are a characteristic feature of many flowing waters but they are rare on travertine probably due to their slow growth rates. One encrusting species *Thelidium microcarpum* has occasionally been found on the deposits of North Yorkshire, UK (Pentecost and Fletcher 1974). Its presence suggests that it is a fast-growing opportunist developing during periods of low accretion. Two foliose lichens, *Peltigera venosa* and *Solorina saccata* occur on the Grand Cron, Belgium (Verhulst 1914) but these species are unlikely to survive on active deposits. The lichenflora of inactive travertines is known to be rich, but has never been systematically documented.

9.4 Bryophytes

In the streams and rivers of the cool and temperate regions of the Earth, bryophytes abound. Active travertines are often festooned with these plants and their remains become incorporated into the deposits, often providing distinct and recognisable fabrics. They are rarely associated with hot spring deposits though their tolerance to high water temperature and dissolved sulphide has been little investigated. The association between bryophytes and travertines has often been expounded upon. Townson (1797) first described bryophyte remains from old travertines in the Gerecse Mountains of Hungary and several accounts of travertine bryophytes followed (Schauroth and Zerrenner 1851; Unger 1861; Cohn 1864; Eulenstein 1866).

Steep gradients and cascades are favoured by mosses adapted to withstand high shear stresses. They are equipped with adpressed leaves, long wiry stems, and abundant rhizoids providing good anchorage. If parts of the mat are torn away, re-growth soon occurs from stem or rhizoid bases entombed in the underlying deposit. In regions of less turbulent flow, where discharge is low and often reduced to seepage, large bryophyte cushions can develop, forming small hummocks or mounds. In these communities, cushions are maintained moist by capillarity and travertine begins to encrust the lower stems providing a degree of stability leading to increasing diversity. The high density and small size of bryophyte leaves provide a large surface area. For example, the surface area of *Palustriella* (*Cratoneuron*) *commutatum* was found to average 12 cm^2 cm^{-2} leading to enhanced evaporation and evasion of carbon dioxide (Pentecost 1991b). This assists travertine formation, and the fine meshwork of leaves provides shelter for invertebrates. A similar process, aided by capillarity, can often be seen on the lips of travertine dams, where bryophytes assist in raising the dam height (La Touche 1913; Lang and Lucas 1970). A small group of bryophytes, including *Didymodon* (*Barbula*) *tophaceum*, *Eucladium verticillatum*, *Hymenostylium recurvirostrum* and *Southbya tophacea* are closely associated with active meteogene travertines but there are no species occurring exclusively on these deposits, at least in Europe and North America.

9.4.1 Mosses

Over 200 species of bryophytes have been recorded from travertine worldwide and the majority, about 80%, are mosses. Several deserve special mention due to their prevalence and influence on carbonate deposition (Table 20). *Palustriella (Cratoneuron) commutata* is the most frequently recorded travertine-associated moss in Western Europe, and may be found throughout the northern hemisphere (Photoplates 1D, 2A,15D). It is a pleurocarp, consisting of a main axis and a variable number of side branches growing all in the same plane. The extent and form of the branching is variable and dependent upon the habitat and this has resulted in the description of several varieties. The specific epithet refers to 'change' or 'alteration' – a reference to its frequent encrustation. *Palustriella commutata* var. *commutata* possesses dense feathery branches often accompanied by a dull reddish tomentum while in the var. *falcata*, the branching is less regular with the main axis and branches often curved to one side, with the tomentum lacking. In both varieties, the leaves are bent over to one side and gradually taper to sharp points. They posses a strong nerve which ends near the leaf apex and the leaves have a toothed margin. Stem leaves are slightly larger than branch leaves. In the var. *commutata*, the stem leaves measure about 1–2 mm in length, while the branch leaves typically measure around 0.7–1 mm. The var. *falcata* has larger leaves giving the plants a more robust appearance, with stem leaves 1–3 mm in length and less strongly toothed. Some bryologists consider these differences in leaf size and shape significant, but there is consid-

Table 20. Frequently recorded travertine bryophytes of China (C), Europe (E) and North America (N). Travertine types: *ca* cascade; *d* dam; *lc* lake crust; *m* mound; *p* paludal; *sc* stream crust/seepage

Family; (a) acrocarp, (p) pleurocarp	Taxon	Travertine morphology	Distribution
Musci			
Amblystegiaceae (p)	*Amblystegium tenax* (Hedw.) C. Jens	ca	N,E
	Calliergon cuspidatum (Hedw.) Kindb.	ca	E
	Campylium stellatum (Hedw.) J. Lange and C. Jens	ca, d	E
	Cratoneuron filicinum (Hedw.) Spruce	ca, d	C, E. N
	Drepanocladus aduncus (Hedw.) Warnst.	ca	E, N
	Hygrohypnum eugyrium (Schimp.) Broth.	ca, sc	C, N
	Palustriella commutata var. *commutata* (Hedw.) Ochyra	ca, d, m, p, sc	C, E
	P. commutata var. *falcata* (Brid.) Ochyra	ca	E, N
	P. commutata var. *virescens* (Schimp.) Ochyra	ca	C, E
	Scorpidium scorpidioides (Hedw.) Limpr.	p	E
Bartramiaceae (a)	*Philonotis calcarea* (Br. Eur.) Schimp.	ca, m, p	E
	P. fontana (Hedw.) Brid.	ca, p	C, E, N
	P. speciosa (Griff.) Mitt.	ca	C
Brachytheciaceae (p)	*Brachythecium rivulare* Br. Eur.	ca, sc	C, E
	B. rutabulum (Hedw.) Br. Eur.	ca	E
	Cirriphyllum crassinervium (Tayl.) Loeske	ca	E
	Eurhynchium swartzii (Turn.) Cum.	ca	E
	Orthothecium rufescens Br. Eur.	ca, m, p	E
	Rhynchostegium riparioides (Hedw.) C. Jens	ca	E
Bryaceae (a)	*Bryum creberrimum* Tayl.	ca	E, N
	B. gemmiparum De Not.	ca	E
	B. pseudotriquetrum (Hedw.) Schwaegr.	ca, m, p	C, E, N
	B. setchwanicum Broth.	ca	C
	B. turbinatum (Hedw.) Turn.	ca	C, N
Catascopiaceae (a)	*Catascopium nigritum* (Hedw.) Brid.	ca, sc	E
Fissidentaceae (a,p)	*Fissidens adianthoides* Hedw.	sc	E
	F. crassipes Br. Eur.	ca	E
	F. grandifrons Brid.	ca	C
	F. taxifolius Hedw.	ca, sc	C, E
	F. viridulus (Sw.) Wahlenb.	ca, sc	E

Table 20. *Continued*

Family; (a) acrocarp, (p) pleurocarp	Taxon	Travertine morphology	Distribution
Meesiaceae	*Amblyodon dealbatus* (Hedw.) Br. Eur.	p	E, N
Mniaceae (a)	*Plagiomnium rostratum* (Schrad.) Kop.	ca, sc	C, E
	P. undulatum (Hedw.) Kop.	ca, sc	E
Pottiaceae (a)	*Barbula constricta* Mitt.	ca	C
	Didymodon. spadiceus (Mitt.) Limpr.	ca	E
	D. tophaceus (Brid.) Lisa	ca, sc	C, E, N
	Eucladium verticillatum (Brid.) Br. Eur.	ca, sc	E
	Gymnostomum aeruginosum Sm.	ca	C, E, N
	G. aurantiacum (Mitt.) Jaeg.	ca	C
	G. calcareum Nees and Hornsch.	ca, sc	C, E
	G. subrigidulum (Broth.) Chen.	ca	C
	Hymenostylium recurvirostrum (Hedw.) Dixon	ca, sc	C, E, N
	Hydrogonium williamsii Chen	ca	C
Thamniaceae (p)	*Thamnobryum alopecurum* (Hedw.) Nieuwl.	ca	E
Hepaticae			
Aneuraceaea	*Aneura pinguis* (L.) Dum.	ca, p, sc	C, E
Anthocerotaceae	*Anthoceros punctatus* L.	sc	C
Conocephalaceae	*Conocephalum conicum* (L.) Dum.	ca, sc	C, E
Geocalycaceae	*Cheiloscyphus polyanthus* (L.) Cords.	ca	E
Jungermanniaceae	*Jungermannia atrovirens* Schleich.	ca	C, E

erable overlap and variation. The varieties occur in contrasting habitats. Rich green to orange-brown mats of the var. *commutata* occur as cushions in small springs, seepages and boggy areas where the water flow is only moderately turbulent or laminar. The plants grow with their bases submerged and the cushions remain moist by capillarity. In highly turbulent water, the var. *falcatum* predominates. Here it is common for the entire plant to be submerged, forming dense dark green mats on cascades or fast-flowing streams. Under a flow rate of 2 m s^{-1} at Whitewell, UK this variety showed a modification, with all the branches curved away from the region of greatest shear (Photoplate 15D). Shearing stresses therefore influence the growth habit of this moss and a continuum of forms can be recognised from areas of gradually increasing water flow. This observation, coupled with the variability of leaf characters raises doubts about the validity of the varieties as separate entities, though cultivation experiments conducted by Bell and Lodge (1963) suggest that such differences can be conserved. Another doubtfully distinct form, the var. *virescens* often occurs with the var. *falcatum*. It is distinguished by its less strongly curved leaves and the presence of 'bristles' (leaf nerves denuded of their laminas) on the branches.

A structurally similar moss, *Cratoneuron filicinum* often occurs intermixed with *Palustriella* and is distinguished by its more slender form and marked differences in the leaf structure. It is a widespread pleurocarp and the third most frequently reported species in the UK. *Rhynchostegium riparioides* (Photoplate 15E) is another pleurocarp confined to fast-flowing waters, where it is often associated with *P. commutata* var. *falcata*. In Waterfall Beck, *Rhynchostegium* tends to grow in areas of permanent fast flow and is sensitive to drought. Though common on cascades in Britain it appears less so on the continent. Its growth and productivity is similar to that of *P. commutata* var. *falcata*. *Brachythecium rivulare* is a species normally found in the 'splash zone' and subject to regular drying. This plant along with a number of others, although associated with, and often growing upon travertine, usually remains free of encrustation. *Brachythecium* however, has been found associated with ferruginous travertines in the United States (Taylor 1919) and encrusted in Luxembourg (Symoens and Van der Werff 1951). Other aquatic pleurocarps include species of *Cinclidotus* and *Fontinalis* normally associated with circumneutral, rather than alkaline waters, tending to occur above areas of deposition. *Camplyium*, *Drepanocladus* and *Scorpidium* are often found in boggy areas and may contribute to travertine mound formation with the acrocarp *Philonotis fontana*. These mosses are also common, and sometimes significant marl-formers in calcareous fens (Clapham 1940). Weed (1889c) found *Drepanocladus aduncus* growing at 35 °C on thermogene deposits at Yellowstone, but bryophytes as a whole are uncommon on these deposits, at least close to their water source.

A number of acrocarpous mosses are also characteristic of European and North American travertines. While the majority of species are cushion-formers, many are closely associated with pleurocarps. Two taxa, *Didymodon* (*Barbula*) *tophaceus* and *Eucladium verticillatum* are practically synonymous with travertine formation. *Eucladium* is one of several mosses with short, upright, little-branched stems protruding just 1–2 cm above active travertine surfaces, especially in seepages subject to low illumination (Photoplate 16A). It is readily distinguished microscopically by its leaf structure. The moss is widely distributed and known almost exclusively from travertine. Some forms of *Eucladium* are able to grow in areas of temporary inundation with fast-flowing water where they produce thin carpets with the stems bent in the direction of flow. It also grows on travertine at cave entrances. An interesting ecological account of *Eucladium* is provided by Dalby (1966). Berner (1949) recorded this species from thermal springs at Aix en Provence growing in water at 20–30 °C. *Didymodon tophaceus* is more robust than *Eucladium*, forming similar but darker cushions, generally in brighter, more exposed situations. Useful microscopical characters are the recurved leaf margins and the elongate cells overlying the nerve. It is a widely distributed moss in the Northern Hemisphere. Like *Eucladium* it is practically confined to travertine where it may grow submerged, though more often in the splash or capillary zone. It is common at Plitvice, Croatia and often grows on dams (Lang and Lucas 1970). Dense, dark green cushions of *Gymnostomum* and the closely related *Hymenostylium* sometimes form small travertine mounds associated with crons or shaded cliffs. *H. recurvirostrum* forms dark cushions in northern England with a high stem-packing density and here it is a characteristic species of travertine cliff seepages. It is characterised by having some of the marginal cells in mid-leaf appearing elongated. *Gymnostomum* also occurs on the Coal River Springs dams in northern Canada (Geurts et al. 1992). Species of this genus are often significant colonisers of remora in the tower karsts of southeast China. All of the above acrocarps belong to the large family Pottiaceae consisting of small mosses with strongly nerved leaves. This family contains most of the travertine-associated bryophytes, and many taxa have been recorded from Asian deposits.

Among the other acrocarps listed in Table 20, *Philonotis* and *Bryum* deserve mention. Emig (1917) described *Philonotis calcarea* from the deposits at Turners Falls, Oklahoma but Wilson and Guest (1961) redetermined the plants as *P. fontana*. Both species occur on travertine in Britain, though rarely encrusted, and their waxy, water-repellant leaves probably account for their general lack of travertine deposition. Species of *Bryum* are also common on paludal deposits and crons. *B. pseudotriquetrum* is widespread throughout Europe and a typical species of boggy travertine seeps (Photoplate 2B). It grows on the Plitvice dams and also occurs in the United States (Flowers 1933). This moss is often associated with *Philonotis*. *B. ventricosum* forms substantial cushions on sheltered cascades and is common on the terraces below the Gütersteiner Falls in Germany.

Some of the most detailed work on the travertine bryophytes has been undertaken by Zhang Zhao-hui in China (Zhang 1993, 1996, 1998; Zhang and Pentecost 2000). As a result, the travertine flora of this region is at least as well known as Europe allowing inferences to be made about the biogeography of the species and their relationship with the deposits. Approximately 60 species of travertine-associated bryophytes are recorded from China, the majority of which are mosses. In contrast with Europe, the most important taxa belong to the genera *Bryum* and *Fissidens*, although a few European species such as *Cratoneuron filicinum* are widespread in China. On the large cascade travertines and dams of Guizhou and Sichuan, the pleurocarps *Bryum setchwanicum, Fissidens grandifrons* and *Hydrogonium ehrenbergii* are often dominant, while seepages are frequently colonised by *Gymnostomum aurantiacum* and *G. subrigidulum* (Pentecost and Zhang 2000). China shares about 50% of its travertine bryophyte flora with Europe but some well-known European species such as *Eucladium verticillatum* are notably rare. The contrasting flora has been attributed to differences in rainfall duration and intensity and the proximity to tropical lowland floras (Pentecost and Zhang 2002). Where rainfall is seasonal, as in many parts of China, watercourses are often reduced to a trickle during the dry seasons and much of the associated flora is desiccated. Resistance to desiccation is an important ecological factor controlling bryophyte distribution.

In a series of papers by Pant and co-workers, several additional travertine-associated mosses are recorded from Uttar Pradesh, India (Parihar and Pant 1982; Pant and Tewari 1984, 1988). These include *Hymenostyliella involuta*, *Hydrogonium javanicum* and *Hyophila ehrenbergii*. *Vesicularia montagnei* (Hypnaceae, Photoplate 16B) is a common form which appears to inhabit the niche occupied by *Eucladium* in Europe. *Barbula inflexa* has been described from dams in the Shan States of Burma (La Touche 1913).

9.4.2 Liverworts

These plants are not as well represented on travertines as mosses. Conditions are probably too harsh for most species as few are adapted to life in turbulent waters. Most liverworts are delicate cryptogams and nourished by capillarity, but there are exceptions. They are most frequently found in damp sheltered niches and often found overgrowing mosses. The most frequently reported European hepatic is *Pellia endiviifolia* (Photoplate 16C), often occurring in hollows on cascades. This is the only European thallose liverwort that appears regularly in areas of deposition, where it may be incorporated into deposits. *Conocephalum conicum* and *Marchantia polymorpha* are also large thallose hepatics that sometimes become encrusted (Klahn 1923). The former is common in Europe on travertines subject to desiccation. Other liverworts are often associated with the moss *Eucladium* and include *Riccardia multifida*, *Aneura pinguis, Preissia quadrata* and the rare *Southbya tophacea.* Leafy liverworts are rarely

reported from active travertines and most occur in the capillary zone of seepages and paludal deposits at high latitudes/altitudes. For instance, *Plagiochila asplenioides* is a taxon usually associated with oceanic woodland, which has been observed encrusted by Berner (1949). Another unusual example is provided by *Jungermannia atrovirens*. This plant grows closely adpressed to cascade travertine in flows exceeding 1 m sec^{-1} in Waterfall Beck, UK. In China, other leafy species have been reported. They include *Plagiochasma rupestre,* often found on remora liable to desiccation, and *Anthoceros punctatus.* The latter is an uncommon plant that grows in damp, sheltered travertine hollows and is notable for its symbiotic association with nitrogen-fixing cyanobacteria.

9.5 Tracheophytes

Vascular plants are often encountered on active travertines, but since they are less closely involved with the precipitation process, they have received less attention. However, several ferns, herbs and trees are frequently associated with meteogene deposits worldwide, though none is known to be confined to this habitat.

9.5.1 Lycopods, Horsetails and Ferns

Representatives of these groups have been found on travertine but they rarely dominate the vegetation and are usually uncommon. Lycopods are the least frequently recorded and occur among moist moss cushions, usually upon crons. *Selaginella selaginoides* has been found in England at several northern sites (e.g. Holdgate 1955). Parihar and Pant (1982) report *S. chrysocaulos* from northern India. The horsetails are more frequently found. *Equisetum palustre* occurs in the boggy hollows of crons and paludal deposits in northern England. Ferns are more often recorded though they are usually absent from depositing sites. They occur on deeply shaded seepages or regions of moist mossy travertine. *Adiantum capillus-veneris* is widespread on this substratum, being found in India (Parihar and Pant 1982), South Africa (Marker 1973), Sicily (Privittera and Giudice 1986), Turkey (Pentecost et al. 1997), the UK (Hyde et al. 1978) and China. Species of *Asplenium* are also widespread, at least in Europe, and include *A. ruta-muraria*, *A. trichomanes* and *A. viride* (Verhulst 1914; Gruninger 1965). Other occasional species are *Thelypteris robertiana* (Pevalek 1935) and *Cystopteris fragilis*. *Phyllitis scolopendrium* is occasionally found growing on actively accreting cascades and dams in wooded regions, such as Gütersteiner, Germany and Cwm Nash, Wales. Most of these ferns are more characteristic of sheltered limestones and would not be expected in areas of regular inundation.

9.5.2 Gymnosperms and Angiosperms

Most active meteogene travertines possess some rooted vegetation though these sites are not generally favourable for their establishment. Elevated water temperature and turbulent flow may limit the flora, but higher plants survive wide-ranging conditions and they often flourish in water-saturated ground. Many plants have however been recorded from active paludal travertines where the drainage pattern is braided and marshland is widespread.

Most information concerns the angiosperms but gymnosperms also occur. For example, *Picea abies* and *Pinus* were noted by van Oye (1937) on the Belgian crons. Flowering plants usually dominate paludal deposits. Herbaceous species are well represented while woody

plants tend to be uncommon, at least on active sites. This is often due to the fact that depositing sites shift rapidly in comparison to the life span of a tree. By the time a seedling has grown to maturity, the site of deposition may have changed, leading to alteration of water availability and the ground flora. This is one reason why it is sometimes difficult to designate regions of active deposition in relation to the flora. A survey of the recorded European angiosperm flora shows that about 56% consists of dicotyledonous plants of which only a small proportion are trees. These include *Acer pseudoplatanus* which sometimes grows upon active cascades though it is not normally regarded as a wetland species and *Sambucus niger* which grows upon active dams and cascades in parts of Britain and Germany. *Fraxinus excelsior* and species of *Salix* have also been recorded. In Sichuan, China, extensive areas of woodland are sometimes found on active travertines, such as the Zhaga Water Forest near Jiuzhaigou (Photoplate 16D).

The extant flora is surprisingly poor when compared with the fossil flora (see 12.1) although for fossils, many may have grown outside the area of active deposition and then been washed in. Shrubs such as *Ligustrum vulgare* are rare on active depostis but there is a great diversity of herbaceous plants. Frequently recorded species in northern Europe are *Angelica sylvestris*, *Caltha palustris*, *Chrysosplenium alterniflorum*, *Cirsium palustre*, *Epilobium hirsutum*, *Eupatorium cannabinum*, *Geranium robertianum*, *Mentha aquatica*, *Parnassia palustris*, *Petasites hybridus*, *Urtica dioica* and *Veronica beccabunga*. One of the most common plants is *Eupatorium cannabinum* which is widespread in all kinds of wooded European wetland (Photoplate 16E). *Geranium robertianum* is also found regularly growing upon mossy cascades throughout Europe. *Pinguicula vulgaris* is an insectivorous species closely associated with travertine seeps in the UK.

Monocotyledons are also frequent, particularly rushes and sedges. In Europe, *Juncus articulatus*, *J. effusus* and *J. subnodulosus* are widespread in open marshes, as are the carices *Carex flacca*, (Fig. 14b) *C. lepidocarpa*, *C. panicea* and *C. pulicaris*. Other plants belonging to the Cyperaceae include *Blysmus compressus*, *Eriophorum angustifolium*, *E. latifolium*, and *Isolepis setacea*. Grasses are widespread on open sites but rarely dominate the flora. In the tufa fens of Slovakia, Hajek et al. (2002) observed that *Carex distans* and *Juncus inflexus* were associated with sulphate-rich waters. Other noteworthy species are *Agrostis tenuis*, *Brachypodium pinnatum*, *Deschampsia cespitosa*, *Molinia coerulea* and *Sesleria albicans*. The last is abundant on the small crons of Yorkshire where it occupies the slighly drier surfaces on the summits of miniature moss-built dams characteristic of these deposits (Fig. 14b). Boggy sites may be colonised by the Orchidaceae. Several species have been observed on the Belgian crons (van Oye 1937); *Dactylorchis incarnata*, *Epipactis atrorubens*, *E. helleborine*, *E. palustris* and *Gymnadenia conopea*. The travertine Orchidaceae of lower latitudes are practically unknown, but Parihar and Pant (1982) provide some information on the cascades of northern India.

9.6 Travertine Plant Ecology

The relationship between plants and their environment is a challenging topic. Unravelling the factors responsible for observed plant distributions is an absorbing yet often frustrating task. An accreting surface provides continuously new areas for colonisation and also presents problems to plants- such as the possibility of rapid burial or waterlogging. However, adaptations have evolved enabling some of them to exist for long periods on accreting surfaces. Adaptation to burial is found among the bacteria, algae and bryophytes. Several cyanobacteria and algae occur as endoliths and may bury into travertine of their own accord.

9.6.1 Plant Communities and Water Relations

9.6.1.1 Bacteria and Algae

A number of communities have been described from active travertines but there have been few objective investigations employing modern analytical techniques. This is unfortunate as it prevents statistically valid conclusions from being drawn concerning the influence and relative importance of the controlling factors. The most detailed bacteriological study to date is that of Fouke et al. (2003) who investigated several sites at Mammoth Hot Springs using molecular methods. Samples were taken from five depositional facies: vent, apron and channel, pond, proximal slope and distal slope. Universal bacterial primers were used to identify 553 partial and 104 complete gene sequences and 221 distinct taxa were recorded, though most are at present un-named. The principal finding was that each of the facies had distinct bacterial assemblages. The vent facies, where water temperature and dissolved sulphide was highest had a preponderance of Aquificiales and a lower phylogenetic diversity than the 'apron and channel' facies below. Particular attention was paid to the pond facies where bacteria were reported from 17 of the current 18 bacterial divisions. Here the β-proteobacteria were well-represented. These were also common on the proximal slope along with many taxa of unknown affinity, while the distal slopes had many representatives of the α-proteobacteria. The communities had few taxa in common and it was suggested that this resulted from the different environmental conditions. Water chemistry and temperature changed continuously downstream, while a range of distinct travertine fabrics were observed dependent upon the same parameters and flow characteristics. The fabrics provide their own, distinct microniches, while the bacteria themselves influence the fabric in some areas and are themselves influenced by the deposition rate. There was little evidence of microbial drift, though this probably occurs. This large data-set is also revealing when compared with the limited 'classical' data of the few other travertine sites listed in Table 17. For example, species of *Pseudomonas* and *Thiobacillus* so widely recorded from the European sites were almost absent at Mammoth.

Of much interest are the specific inter-relationships between these organisms and their environment. Availability of new organic substrates is likely to increase downstream as more microbially-synthesised molecules are produced by a greater diversity, and probably, greater abundance of bacteria. Are these substrates utilised by an ever-increasing diversity of microbial taxa downstream? Are suites of microbes adapted to a specific range of temperature, pH and dissolved sulphide? The answer to both is probably a qualified 'yes' but too little is as yet known about the taxa identified. Molecular methods while providing important insights into bacterial communities do not currently provide us with information on absolute numbers of viable organisms and there is always the possibility that DNA is not extracted efficiently from all types of cell.

Among the algae (including here the cyanobacteria), several encrusting associations have been described. Early descriptions are given by Butcher (1946), Fritsch and Pantin (1946) and Blum (1957) the last recognising two associations, namely, a 'permanent' *Homoeothrix-Gongrosira* association, and a more ephemeral *Phormidium-Schizothrix-Auodinella* association. Encrusting communities are also described by Pentecost (1982, 1990a), Freytet and Plet (1996) and Pitois et al. (2001). A study undertaken by Iserentant (1988) describes the diatom communities associated with *Palustriella* and bare travertine from Belgium. Multivariate analysis revealed three diatom communities, two associated with bryophytes and one with the travertine surface. Pentecost (1991b) found that *Palustriella* and *Rhynchostegium*, whilst possessing many algal epiphytes in common, contained markedly different numbers of some

species and attributed this to differences of leaf shape and architecture. However, there were no well-defined communities on the travertine surface and the algal floras of particular bryophyte species were found to vary substantially from place to place.

A number of diatom associations have been observed. Winsborough and Seeler (1984) noted a preponderance of species with internal septa on travertine (e.g. *Diatoma, Epithemia, Mastogloia*) that may be more able to withstand changes in osmotic pressure associated with desiccation. This could be significant where there is rapid evaporation such as stream margins or remora. However, diatoms are normally uncommon on surfaces receiving infrequent immersion. Diatom-rich meteogene travertines have been investigated by Winsborough and Seeler (1984) and Winsborough and Golubic (1987). They contain several rarely recorded taxa. Some appeared characteristic of specific types of travertine deposit in Mexico and Germany; *Gomphonema olivaceum* var. *calcareum*, *Amphora katii* and *Nitzschia denticula*. Another diatom widely associated with travertines is *Mastogloia smithii* var. *lacustris*. An investigation of Waterfall Beck, a UK hill stream containing much travertine in its lower reaches showed that several species were casuals, having washed onto deposits from above (Pentecost 1991b). An example is *Cocconeis placentula*, a common epiphyte. This study showed that among the diatoms, *Achnanthes minutissima* was volumetrically the most important, followed by *Navicula tripunctata*, *Fragilaria virescens*, *Cymbella minuta* and *C. delicatula*. Diatoms colonising these cascade travertines consisted mainly of attached forms (*Achnanthes*, *Cymbella*, *Diatoma*, *Fragilaria*) while gliding forms (*Navicula*, *Nitzschia*) sheltered within the associated moss cushions.

Thermogene sites have been investigated briefly by Stockner (1967) and Lang and Pierre (1974). Thermal waters vary so much in ionic strength that many interesting forms are to be expected. In the oxygen-depleted sulphide-rich waters of Bagni di Tivoli, Pentecost and Tortora (1989) found abundant diatoms, including *Navicula* cf. *halophila* and *Nitzschia communis*. The Suio travertines of Italy had *Achnanthes minutissima* and *Nitzschia frustulum* growing up to 48 °C, an unusually high water temperature for the group. Héribaud (1920) and Fournier et al. (1966) provide large lists of fossil diatoms associated with the Auvergne travertines. The thermogene travertines of Carlsbad, along with many others, are also associated with rich diatom deposits (Sprenger 1930).

Algae, along with bryophytes and tracheophytes can be grouped into life-forms according to their relationship with the substratum and their structure (Fig. 50a–e). The majority of taxa may be classified as adpressed and creeping forms, consisting mainly of diatoms. These algae rarely calcify, but creep along the deposit surface or among bryophytes and larger algae. Attached forms, also including a large number of diatoms are well-represented. Species forming calcified cushions, while conpicuous and common, are few in number.

9.6.1.2 Bryophytes and Tracheophytes

There have been several descriptions of travertine bryophyte associations. Phytosociological relevés are provided by Gams (1932), Walther (1942), Symoens et al. (1951), Poelt (1954), Privittera and Giudice (1986), Frey and Probst (1974) and Couderc (1977) for travertines colonised by *Palustriella* and *Eucladium*. The paper by Poelt is the most informative for those ecologists interested in such classifications. Although unsupported by direct measurements, simple observation shows that water availability, duration and impact are important factors governing the distribution of the travertine flora. A study of cascade travertines in the Schwäbische Alb led Gruninger (1965) to describe plant associations in terms of the water regime, i.e. the flowing regime, an inner and outer 'spray zone', a trickling water zone, damp and dry zones.

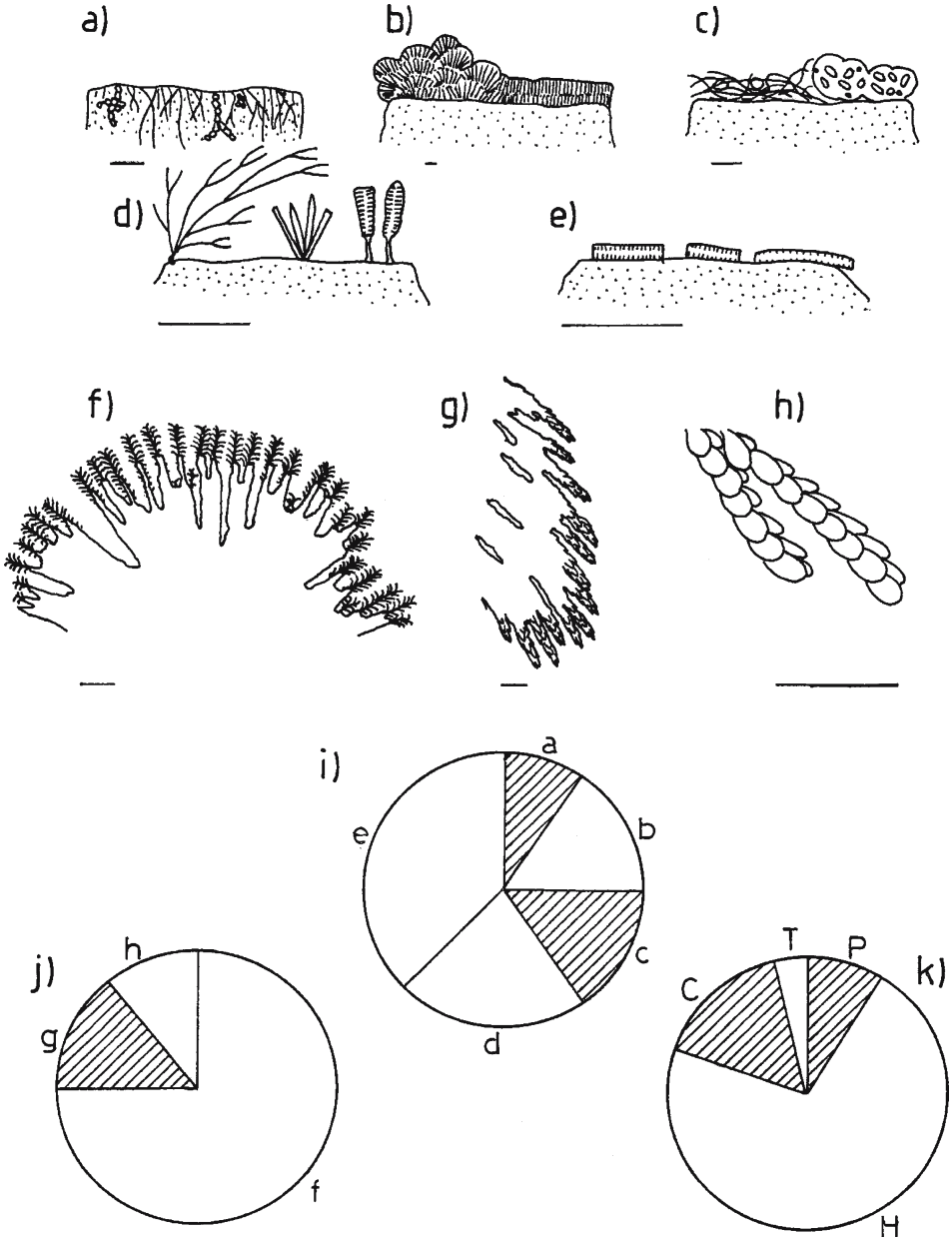

Fig. 50. Plant life-forms on travertine. Algae: a) endoliths; *Gongrosira*, *Schizothrix*,b) encrusted forms; *Oocardium, Phormidium, Rivularia*, c) superficial mats and cushions; *Chrysonebula, Oedogonium*, d) basally attached forms; *Cladophora, Gomphonema*, e) adpressed and creeping forms; *Cocconeis, Navicula*. Bar 50 µm. Bryophytes: f) capillary cushions and mats; *Eucladium*, g) flow-moulded cushions; *Rhynchostegium*, h) adpressed forms; *Jungermannia atrovirens*. Bar 5 mm. Below: Pie charts showing relative proportions of life-forms as taxa on European meteogene travertines (with same lettering as above): i) algae: a, 9%; b, 15%; c, 10%; d, 22% and e, 44%; j) bryophytes: f, 74%; g, 14%; and h, 12%. k) tracheophytes: C, chamaeophytes, 17%; H, hemicryptophytes, 71%; P, phanerophytes, 8%; T therophytes, 4%

The physical impact of water descending cascades also affects plant communities. The force is often sufficiently great to entirely inhibit the growth of bryophytes, which are replaced by encrusting/endolithic algae. The plants themselves act as sponges, retaining water for long periods during dry seasons. This is evident in partially encrusted mats of the cyanobacterium *Scytonema* (Parihar and Pant 1982) and the mosses *Eucladium* and *Gymnostomum*. The significance of flow was also investigated by Pitois et al. (2001) who found that cyanobacterium biomass increased with current speed in the River Eaulne, France. The importance of water relations had already been recognised by Symoens et al. (1951) and Pavletic (1957) and undoubtedly many previous observers and could be today categorised into a range of aquatic, mesic and xeric habitats. The great majority of travertine bryophytes are perennial hygrophiles, living permanently under water or wetted by capillarity. Water is drawn up into the plants by the close ranks of leaves and tomentum, and the bulk of their nourishment is presumably obtained in this way. These species usually lack the long hair-points usually associated with long periods of desiccation, but a considerable number possess papillose cell walls which may be an adaptation to reduce water loss when the leaves are dry and inrolled. Adaptations to temporary, rather than extreme desiccation are apparent in *Didymodon tophaceus.* This is one of the least papillose species in the genus and is often seen in a partially dried out state at the sides of cascades, but rarely remains dried for months on end, as in some other members of the genus. The bryophyte flora of travertine can be broadly classified into three life-forms, namely capillary-nourished cushions, flow-moulded cushions and adpressed mats, the latter occurring in high flow regimes (Fig. 50). In terms of species numbers, most taxa form cushions.

Of higher plant communities little is known apart from a few European studies. Association analysis was used by Frey and Probst (1974) to identify seven species groups on some German deposits including one typical of beech (*Fagus*) forest and a *Eupatorium-Molinia* association. Pietsch (1984) described several associations along a watercourse and found that the vegetation varied with distance downslope and with microtopography. A *Caricetum davallinae* developed on the small topographic highs, while a *Molinietum coeruleae* was found in the wetter depressions. Hajek et al. (2002) used ordination to demonstrate the importance of water chemistry in fen development, including the travertine fens of Slovakia. Analysis of plant life-forms based on the travertine literature indicates that helophytes (herbs with perennating buds lying in wet sediment) far outnumber other forms such as the chamaeophytes and phanerophytes (trees and shrubs).

9.6.2 Diversity

The floristic diversity of some travertine-depositing sites appears to be high. Of the 57 plant taxa recorded from the cascade travertines of Waterfall Beck, UK, 17 were cyanobacteria, 5 green algae, 25 diatoms and 8 bryophytes (Pentecost 1991b). The richness of the community is due in part to its instability permitting continuous recolonisation of sloughed surfaces whilst retaining areas which had stabilised and matured for several years. Even sheltered sites may be species rich. Fjerdingstad (1957) recorded 32 algae, mostly cyanobacteria and diatoms from an encrusted well in Denmark while Boyer and Wheeler (1984) found in excess of 20 higher plant taxa associated with paludal deposits. A comparative study of French and English travertines colonised by bryophytes demonstrated that species-richness was related to site size and heterogeneity (Pentecost and Zhang 2002). In contrast, Pitois et al. (2001) found that calcite stream crusts of northern France were low in biodiversity and suggested that this could affect salmon-spawning.

Travertine dam formation is responsible for increasing the range of habitats for both plants and animals although there have been no detailed comparative studies. Formation of dams results in stretches of slack water and soft sediment promoting the establishment of macrophytes such as *Chara*. These, in turn provide a food source and shelter for a range of aquatic invertebrates and fish increasing the diversity of the system.

9.6.3 Light, Water Chemistry, Temperature and Pollution

These play an important but largely undetermined role in the ecology of aquatic lower plants. There have been few measurements of irradiance in travertine-associated communities. It is known that many cyanobacteria prefer low light levels and are found predominanly under dense vegetation. For instance *Phormidium incrustatum* often completely covers travertine surfaces in the wooded valleys of Western Europe. Under strong illumination, this species is less prevalent and often replaced with bryophytes. At Shelsley Walsh, UK a travertine mound developed on a wooded slope created an open glade leading to bryophyte colonisation which in turn influenced the fabric and morphology of the deposit (Pentecost et al. 2000a). *Schizothrix* species are usually more frequent under high illumination, but Allen (1971) describes an encrusted low-light community from Wales that appeared to exclude other associated algae. In deep calcareous lakes, a 'low light' phycoerythrin-rich cyanobacterium community termed the 'Rotbunte Tiefenbiocoenose' occurs (Kann and Sauer 1982; Winsborough et al. 1994) but there is as yet no known travertine equivalent. Studies on *Rivularia* populations in the UK suggested that light was more important than temperature for growth in upland streams (Livingstone et al. 1984). Most 'ephemeral' algae need higher illumination levels, e.g. *Cladophora glomerata* and *Oedogonium* overgrow encrusting communities during summer (Minckley 1963; Pentecost 1991b).

Several studies have been made on the influence of light on bryophyte communities. Pavletic (1955) and Matonickin and Pavletic (1962) in their investigations at Plitvice noted the prelavence of light-demanding species such as *Rhynchostegium riparioides* and *Palustriella commutata*, and the latter seems to be replaced by *C. filicinum* in more shady areas. Shaded habitats also support *Eucladium verticillatum*. This moss is often found in abundance on underhangs of cascades and dams and Dobat (1966) describes forms from cave entrances where phototropic remora may develop. It also occurs in the 'lamp flora' of caves. *Fissidens crassipes* is another low-light species. In Europe, deeply shaded sites support few bryophytes whilst the cyanobacteria flourish but data on light levels are lacking. A survey of the European tracheophyte list showed that most species (48%) preferred exposed positions, while 17% were shade-demanding and the remainder (35%) presumed indifferent.

The influence of temperature is poorly documented. Several algae from Waterfall Beck, an upland hill stream were noted as low-temperature forms by Pentecost (1991b), such as *Caloneis alpestris* and *Didymosphenia geminata*, but the cyanobacteria appear to be cosmopolitan for the most part. Obvious effects of temperature occur in the flora of hot springs where gradients are high and the effect on the microbial populations easily seen, though it may be complicated by the chemical changes taking place downstream. Only prokaryotes can survive temperatures exceeding 62 °C (Ward et al. 1987) and eukaryotes are generally only common below 40 °C. The influence of temperature is demonstrated in the Viterbo hot springs where mats of *Chloroflexus* occurred immediately below the vents followed by the filamentous cyanobacteria *Phormidium* and *Spirulina*. In cool-temperate streams, the growth of the cyanobacteria *Rivularia haematities* and *Homoeothrix crustacea* was positively correlated with stream water temperature and little growth occurred during winter (Pentecost 1987b;

1988a). Temperature undoubtedly affects bryophyte growth. Furness and Grime (1982) found the maximum growth of the travertine moss *Brachythecium rivulare* occurred at 15 °C. Bryophytes only become abundant when water temperature is below 35 °C. A study of their geographic distribution showed that the *Palustriella commutata* extended to more northerly latitudes than *Eucladium verticillatum* in Europe suggesting that temperature was an important factor (Pentecost and Zhang 2002).

Travertine-depositing waters undergo rapid compositional changes as a result of CO_2 evasion and carbonate precipitation. These changes probably influence the flora but discovering which, if any factor, is involved has proved elusive as many changes occur at once, i.e. pH, Ca, DIC, temperature and the speciation of dissolved phosphate. The hydrogen ion concentration can fall by an order of magnitude over a few metres of flow and is most likely to influence the biota. A significant correlation was obtained between the abundance of the cyanobacterium *Schizothrix calcicola* and pH in Waterfall Beck (Pentecost 1982). Cyanobacteria that utilize bicarbonate in preference to carbon dioxide might be expected to become more numerous as the pH rises. Pollution of waters with phosphates is particularly detrimental to travertine-depositing systems as these are very low in dissolved phosphorus and possess a flora adapted to these levels. *Phormidium incrustatum* stream crusts have disappeared from several rivers near Cambridge, UK as a result of agricultural eutrophication (nitrate-N and phosphate-P exceeding 6 and 1 ppm respectively) and dredging. Edwards and Heywood (1960) found that pollution by domestic sewage destroyed calcite crusts on gastropod shells in the UK whilst the eukaryotic algal flora remained largely unaffected. In a study of some streams in south-east France, Casanova and Lafont (1986) found that calcium carbonate precipitation was inhibited when the phosphate concentration exceeded 0.05 ppm (1.6 μmol L^{-1}). Acid industrial effluents have taken their toll with the destruction of the Little Conestoga oncoids of Pennsylvania. The associated cyanobacteria disappeared while the green alga *Gongrosira* remained in a morphologically altered state (Golubic and Fischer 1975).

9.6.4 Succession and Seasonality

The accretion of the travertine surface provides special problems for plants which may limit the flora to specialised forms, analogous to that of dune plants, and the adage 'rolling stones gather no moss' is no more aptly applied than to oncoids. Despite this, the environment sometimes permits sufficient stability to allow a climax community to develop. Plant succession has been studied in both paludal and cascade travertines allowing some general conclusions to be made.

Most work has been devoted to the flora of travertine cascades. Work on the Belgian crons by van Oye (1937) suggested two lines of succession, one beginning with the desmid *Oocardium stratum* and the other with *Palustriella commutata*. It would appear that here, hard *Oocardium* crusts become invaded by cyanobacteria, followed by mosses, grasses, herbs and trees. In the other, *Palustriella* first forms a friable crust colonised by further mosses, then grasses, other herbs and trees and the distinction lies in the physical nature of the starting material. The climax vegetation consists of deciduous woodland, but this develops only upon inactive deposits. There is clearly a need to distinguish between succession on active and inactive sites, where the climax vegetation may be very different. Succession of bryophytes on travertine dams is also discussed briefly by Pavletic (1955) and Matonikin and Pavletic (1962).

Pant and Tewari (1984) describe plant succession on some Indian cascade deposits beginning with cyanobacteria, followed by diatoms, bryophytes and finally herbs. A study on Waterfall Beck began in 1980 with the diversion of the stream over a clean limestone ledge

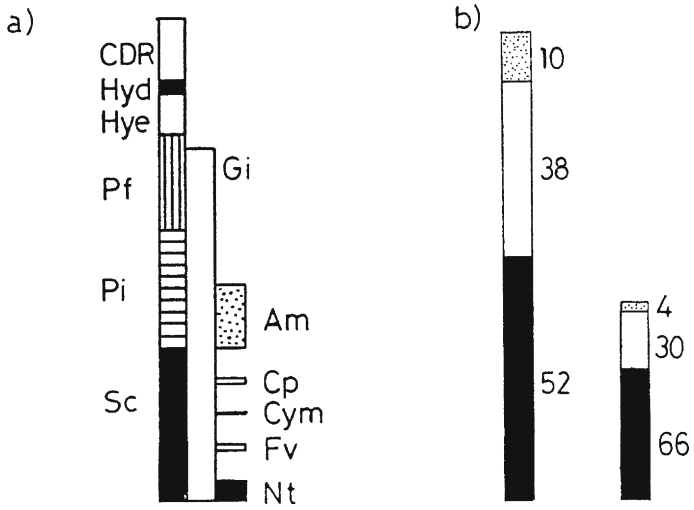

Fig. 51. Relative biovolumes of algae in active meteogene travertine averaged over one year, Waterfall Beck, UK (from Pentecost 1991b). a) Biovolumes of individual species/species groups on travertine surface. Left bar: cyanobacteria; middle bar: green algae; right bar: diatoms. Am *Achnanthes minutissima*; CDR *Calothrix/Dichothtix/Rivularia*; Cp *Cocconeis placentula*; Cym *Cymbella* spp.; Fv *Fragilaria virescens*; Gi *Gongrosira incrustans*; Hyd *Hydrococcus*; Hye *Hyella*; Nt *Nitzschia* spp.; Pf *Phormidium favosum*; Pi *Phormidium incrustatum*; Sc *Schizothrix calcicola* agg. b) Relative biovolumes of travertine-encrusted (left) and limestone bedrock (right) algal communities in Waterfall Beck. Black, cyanobacteria; white, green algae; stippled, diatoms

to follow travertine formation and the plant succession. This investigation showed that the pioneer phototrophs were cyanobacteria and diatoms. The first colonists were *Schizothrix calcicola, Achnanthes minutissima, Cocconeis placentula, Denticula tenuis* and *Gongrosira incrustans* followed in two years by the bryophytes *Palustriella commutata* and *Cratoneuron filicinum*. Total species richness stabilised within two years followed by a small increment to 40 taxa after 16 years and the pattern of change for both algae and bryophytes was similar. During the study, 15 cm of travertine was deposited. Pitois et al. (2001) in a study of artificial substrata in a French stream found that a non-encrusted pioneer community with *Cocconeis placentula* and members of the Chroococcales was overtaken by filamentous encrusted cyanobacteria (*Phormidium*, *Rivularia*). In the Saline River, Blum (1957) observed colonisation of fresh surfaces by the cyanobacterium *Homoeothrix janthina* within eight weeks, suggesting it is a pioneer and similar rates of colonisation by other cyanobacteria have been noted on cleaned substrates in England. Winsborough et al. (1994) showed that lake travertines also have diatom pioneers. The succession on active cascades appears to occur quickly and usually progresses no further than the bryophytes. This is to be expected in an environment subject to high shear stress and periodical floods causing local erosion. Fine sediments rarely remain in place for long and soil formation is impossible.

The succession on paludal deposits is quite different. Here, the flow of water is sufficiently slack to allow accumulation of fine sediments allowing a greater range of life forms to flourish. Despite this, there has been little work on the flora, though calcareous marshes in general have received considerable attention. Clapham (1940) provides an early account of succession in calcareous fens where travertine may develop, but is concerned primarily with the transformation of shallow open waters to fenland. Of the few paludal deposits investigated it appears that the first photosynthetic plants to appear are again the algae, but these are

soon followed by mats of cushion-forming bryophytes such as *Palustriella commutata*, *Drepanocladus* and *Scorpidium*, to be followed by a wide range of helophytes, especially *Carex* and *Juncus* species. Tussock and mound-like forms soon develop leading to a differentiation of the flora as some species can now occupy the capillary-zone or even exist above it. An interesting example of this occurs on Great Close Mire in Yorkshire, where travertine-encrusted cushions of *Hymenostylium* and *Palustriella* support the calcifuge moss *Racomitrium lanuginosum* that presumably receives moisture and nutrients exclusively from rainfall. Thus a miniature 'raised bog' system develops, whose water relations and nutritional requirements bear no relation to the underlying vegetation and groundwater.

The seasonality of some plants also deserves mention, particularly in relation to travertine growth laminae (Section 3.2.6). Several algae are markedly seasonal such as the small diatom *Achnanthes minutissima*, which is much more numerous in winter than summer in Waterfall Beck, UK (Pentecost 1991b). Growths of *Vaucheria* occur mainly in spring or late summer (Marker 1976) and may be abundant on the crests of travertine dams. Algal overgrowths are commonly observed in European streams as a response to seasonality or changing water conditions (Wallner 1934a).

9.6.5 Biomass and Growth

Biomass measurements of plants have been few owing to the practical difficulties of measurement encountered in flowing waters. A study of Waterfall Beck provided estimates of biovolume for all of the common aquatic plants (algae and bryophytes) and showed that 82% of the biovolume consisted of the mosses *Palustriella commutata*, *Cratoneuron filicinum* and *Rhynchostegium riparioides* (Pentecost 1991b). The green alga *Oedogonium* forming superficial and seasonal blooms accounted for 11% followed by *Plectonema*, *Mougeotia* and a range of encrusted species. These data are for the entire stream, about 35% of which is encrusted with travertine. Bryophytes therefore dominate the flora of Waterfall Beck. The biovolume of the algal community on the travertine (excluding moss epiphytes) was also determined (Fig. 51a) and it can be seen that *Gongrosira incrustans* was most abundant, followed by *Phormidium favosum*, *P. incrustatum* and *Schizothrix calcicola* agg. Overall, cyanobacteria accounted for just over half of the total algal biovolume while diatoms made only a minor contribution. When compared with the flora of limestone free of travertine further upstream, the biovolume was found to be considerably higher on the travertine (Fig. 51b) suggesting that the carbonate was stabilising the algal biofilm and perhaps pro-

Table 21. Plant biomass on meteogene travertines as chlorophyll-a. Standard deviations in parentheses

Site	Community	Chlorophyll-a mg m^{-2}	Reference
Artificial stream channel, UK	*Chamaesiphon*, *Lyngbya*, *Gongrosira*	200	Marker and Casey (1982)
Waterfall Beck, UK	*Phormidium*, *Schizothrix*, *Gongrosira*	68 (56)	Pentecost (1991b)
" "	*Palustriella commutata*	427 (160)	" "
" "	*Rhynchostegium riparioides*	534 (148)	" "
Cowside Beck, UK	*Schizothrix*	40	Pentecost (1992c)
Seine Basin, France	*Phormidium*	200	Pitois et al. (2001)

tecting algae from grazing. Algae epiphytic on the mosses were also studied and although abundant in terms of numbers, their combined biovolume was only about 2% of the moss biovolume. Biomass measurements as chlorophyll-a are also available (Table 21). The moss chlorophyll levels were found to be high, exceeding maximum chlorophyll cover in terms of theoretical light absorption, but levels in the encrusted communities are considerably lower presumably due to the absorption of light by travertine.

Growth rates of some travertine algae and mosses are also available. Measurements of encrusted colonies of *Rivularia*, *Homoeothrix* and *Gongrosira* have been made in Waterfall Beck and fall in the range 0.4–2.2 mm a^{-1} (Pentecost 1987, 1988a,b). Wallner (1935c) reported a growth rate of 5 mm a^{-1} for *Oocardium* in Germany though it appears to be less than this in the UK. Growth measurements of the two main varieties of *Palustriella commutata* have also been undertaken. Tagged specimens of *P. commutata* var. *commutata* were found to have average rates of less than 2 mm a^{-1} in Yorkshire, UK (Pentecost 1987) compared with 40 mm a^{-1} for the var. *falcata*. Differences in nutrient availability may be responsible since the former was wetted by an intermittent seepage while the latter grew in continuously flowing water. In the springs at Matlock Bath, the same species grew at a rate of 70–80 mm a^{-1} and attributed to the warm spring water (Pentecost 1998). *Rhynchostegium* growth in cascades is similar whilst other 'capillary zone' mosses such as *Eucladium verticillatum* and *Hymenostylium recurvirostrum* grow slowly, at 2–4 mm a^{-1}. In Britain, the insectivorous plant, *Pinguicula vulgaris* is often associated with these slow-growing moss cushions, further suggesting nutrient limitation. In Kent, UK the hepatic *Conocephalum conicum* was found growing up to 0.18 mm per day on damp travertine. Growth rates of *Brachythecium rivulare* and *Philonotis fontana* were reported by Furness and Grime (1982) and found to be similar to a wide range of terrestrial species. They were not collected from travertine although they are frequently found growing upon it. Magdefrau (1956) measured a rate of 1 cm a^{-1} for *Bryum ventricosum* on a German deposit. The productivities of these communities are discussed further in Chapter 10.

9.7 Fauna

Travertine provides food in the form of encrusted algae and detritus as well as shelter for animals and some interesting associations have been observed. In common with most other shallow fresh waters, the fauna is dominated by invertebrates, with the insects and snails well represented. This section concentrates on those animals having a close association with the deposits, though some consideration is given to animals found in travertine-depositing waters but having no particular relation to it. There are no known chordates closely associated with travertine but a few, notably man, have altered groundwater characters and watercourses, often to the detriment of travertine formation. Man's influence will be taken up later (Section 13.3).

9.7.1 Protozoa

Members of the protozoa occur on active travertine but are little known. Thunmark (1926) noted two testate rhizopods, *Difflugia olliformis* and *Euglypha* sp. from deposits in Sweden and protozoa were recorded from Hungary by Hevisi (1970). The rhizopod *Centropyxis* cf. *aculeata* was observed by the author on a UK deposit associated with the moss *Didymodon tophaceus*. The tests were constructed mainly of the diatom *Achnanthes minutissima* and were free of encrustation.

9.7.2 Metazoa

Among the Pseudocoelomates, the rotifer *Philodina* and nematodes *Cylindrolaimus* and *Labronema* were noted from Falling Springs, Illinois (Davis et al. 1989). Endolithic nematodes are closely associated with cyanobacteria in stream crusts. In the UK, crusts colonised by *Phormidium incrustatum* had between 77 and 1460 nematodes cm^{-2} while a *Schizothrix/Homoeothrix* crust from Waterfall Beck had 210 cm^{-2} (unpublished data).

A variety of worms can be found in active travertines and the associated vegetation. Their porous nature provides shelter for the lumbricid *Eiseniella tetraedra* and the oligochaete *Pristina osborni* (Durrenfeldt 1978; Davis et al. 1989). Numerically however, the Nematoda predominate. The triclads *Dugesia*, *Polycelis* and *Planaria* have been encountered (Durrenfeldt 1978) though Minckley (1963) mentions the avoidance of *Dugesia* in carbonate-depositing areas. Leeches also appear to be scarce among travertine, but they have been observed in the Pine River, Michigan (Leonard 1939). As predators and semi-parasites of molluscs they might be expected to be more widespread. Despite their value in palaeoecology we know little of the extant travertine-inhabiting Mollusca. In areas of turbulence, few molluscs would be expected, but elsewhere, the abundance of calcium, vegetation and the high humidity should attract many species. A limited and specialised fauna sometimes occurs in fast-flowing stretches, where the river limpet, *Ancylus* (Fig. 52a) has occasionally been reported (e.g. Matonikin and Pavletic 1962). Adjacent mossy fringes and quiet pools often support other aquatic taxa. The author has seen the pulmonate gastropod *Lymnaea peregra* grazing damp travertines in England, and these areas are also attractive to terrestrial snails such as *Cepaea*. Durrenfeldt (1978) often found *L. (Radix) balthica* associated with a travertine-depositing stream in Germany. The more equable marsh environment however provides greater shelter and here, a wide range of freshwater and terrestrial Mollusca may be encountered. The aquatic gastropods *Lymnaea* and *Bithynia* are often well represented, frequently occurring with the lamellibranchs *Pisidium* and *Sphaerium*. The last often inhabit calcareous muds in deep, permanent water. Encrustation of mollusc shells appears to be common and is not exclusively a post-mortem effect. Deposits building on the shells of *Lymnaea* and *Potamopyrgus* have been described and analysed by Warwick (1953) and Weiss (1970). Aquatic molluscs would presumably find difficulty in removing these deposits and in some cases this may explain their scarcity in rapidly depositing sites. A number of terrestrial pulmonates live in wet or marshy areas and are loosely associated with some travertines, yet have little if any contact with the material when alive. Several species of *Carychium*, *Vertigo* and *Zonitoides* live on marsh vegetation and are common in old deposits. They will be considered further in Section 12.2.2. Invasive meteogene waters, originating from calcium hydroxide dissolution may be lethal to molluscs, as slaked lime is used to control their numbers. Several crustaceans have been recorded, but like the worms and triclads, none show preference for travertine-encrusted areas. The freshwater shrimp *Gammarus* is widely recorded from the more sheltered waters and may become abundant (Durrenfeldt 1978). I have recorded *G. pulex* in excess of 5000 m^{-2} in the detritus-rich waters of the Fleinsbrunnenbach, Germany. With such numbers, large accumulations of faecal pellets occur and cover the travertine to depths of several centimetres. These crustaceans feed upon travertine algae in addition to suspended detritus. Other crustaceans appear to be less in evidence, but include *Crangonyx* (Minckley 1963) and *Asellus*. The latter is a common animal of freshwaters generally but apparently scarce on travertine. However, Minckley found the cavernicole *A. stygius* sheltering among travertine slabs in Kentucky. In Montezuma Well, a travertine mound spring in the USA, Cole and Watkins (1977) described a new amphipod *Hyalella montezuma*.

Water-filled depressions often provide unique habitats in remote regions conducive to speciation and endemicity. Crayfish remains are occasionally encountered in old deposits. These crustaceans would find cavernous travertines eminently suitable for feeding and shelter but there are no modern records. Several large crustaceans occur in the Australian mound springs including the Yabbie (*Cherax destructor*).

The Ostracoda are common travertine fossils but we know little about their life on active sites. These animals prefer still waters with some vegetation and detritus and may be expected to be common in paludal sites and standing water (Fig. 52b). For example in the cold upland paludal travertine at Tarn Moor, UK, *Candona candida, Ilycyprus bradyi* and *Ilyodromus olivaceus* were recorded (Preece and Robinson 1982). These authors found that travertine-depositing habitats were of low diversity when compared with non-depositing lakes and streams. Characteristic species also occur in springs. Blanchard (1903) noted ostracods living up to 51 °C in the waters of Hamman Meskoutine, Algeria. In the 'pulpit basins' of Pamukkale, Turkey, *Heterocypris incongruens* was found in abundance at temperatures of 20–30 °C (Pentecost et al. 1997).

The Chelicerates are mainly terrestrial animals but water mites (Hydracarina) are widely distributed in freshwaters where they parasitise a range of other aquatic organisms during their larval stage. Of the numerous forms, only *Hygrobates* appears to have been recorded from travertine streams (Durrenfeldt 1978). Some specimens were found to be encrusted with calcite.

9.7.2.1 Uniramia-Hexapoda (Insects)

Of all invertebrates inhabiting freshwaters the insects are usually by far the most important in terms of their diversity, travertine providing no exception. Insect larvae are highly adaptable and able to exploit most freshwater habitats. In common with other invertebrates, rapidly depositing sites are normally avoided and these include most thermogene travertines, though insects are among the few animals occasionally found around hot springs. A number of highly specialised insects have made travertine their home and use the deposits for camouflage and protection. These peculiar adaptations have attracted the attention of entomologists and there is now a moderate literature on the subject. Particular attention has been been paid to those Diptera belonging to the sub-order Nematocera such as *Lithotanytarsus*, *Oxycera* and *Pericoma*. There are also many insects appearing as casuals with no particular association with travertine. It is probable that for the travertine-associated invertebrates as a whole, the casuals greatly outnumber the 'specialists', since numerous species are known to inhabit a range of water types. There are likely to be many as yet undiscovered forms, particularly in the tropics, where travertines have scarcely been investigated for their invertebrates.

The Hemiptera (bugs) are common freshwater invertebrates but neither larvae nor adults have yet been recorded from deposits, but several Coleoptera have been taken. Elmid beetles appear to be widely distributed but infrequent. Both Leonard (1939) and Minckley (1963) note their scarcity among stream crusts, the latter recording *Optioservus* and *Stenelmis*. Thienemann (1934) noted *Hydraena polita* and Bertrand (1950) records *Deronectes delarouzii* and *Riolus* sp (Fig. 52c). A small riffle beetle, *Microcylloepus formicoideus* has been described from Travertine Springs in Death Valley, California where it occurs with a rich benthic fauna, though its relationship with the deposits was not investigated (Shepard 1990). Beetles, although good swimmers, usually prefer slow-flowing water and would not be expected in areas of rapid flow where most travertine is deposited. Plecoptera (stoneflies) seem to fare better. Species of *Baetis* have often been noted and may be abundant (Fig. 52d). The nymphs

inhabit slack waters with detritus, being poor swimmers and they are known to feed on travertine algae. Other stoneflies include *Leuctra*, *Nemoura* and *Protonemura* (Thienemann 1934; Durrenfeldt 1978). Minckley (1963) found two travertine-encrusted species in Kentucky, *Isogenus subvarians* and *Paragnetina media*, but it is not known if the deposits are used for camouflage.

The Ephemeroptera contain both swimming and burrowing nymphs, neither of which would be expected to be suited to travertine. Ide (1935) mentions them in an encrusted section of the Mad River, Ontario and *Ephemera simulans* was abundant in Doe Run, Kentucky (Minckley 1963). Species of *Ephemera* burrow in muds and gravel. Leonard (1939) recorded *Ophogomphus* (Odonata) from the Pine River and *Sialis* (Megaloptera) has been noted in Germany. Both animals are more at home among vegetation and detritus but will colonise cobbles and gravel where some shelter is provided.

Several caddis fly larvae (Trichoptera) find travertine a suitable substratum and a number of families are represented. Net-building caseless genera such as *Hydropsyche* (Hydropsychidae), *Philopotamus* (Philopotamidae) and *Polycentropus* (Polycentropidae) are sometimes common in Europe. The nets are built to collect suspended food particles, and retreats are also constructed for protection. Caseless larvae that do not build silk nets may also be common such as *Rhyacophila* (Durrenfeldt 1978) and develop typically among travertine fragments or bryophytes in flowing water. The tubular galleries of *Tinodes* (Psychomyidae) are a frequent site on British travertines where they produce a serpentine pattern on the travertine surface in spring and summer (Fig. 52e). *Tinodes* is another larva known to be associated with and possibly feed on *Phormidium* filaments, and they are believed to secrete acids capable of dissolving the surrounding carbonate (Edington and Hildrew 1981). In Venezuela, Paprocki et al. (2003) have described a new species of caseless caddis, *Smicridea travertinicola*, whose silk nets and retreats result respectively in travertine accretion and erosion. In Australia, net-building caddis-fly larvae are abundant and significant in travertine formation in some regions. In the Barkly karst of northern Australia, larvae of the genus *Cheumatopsyche* (Hydropsychidae) build extensive nets and retreats in fast-flowing sections of the travertine-depositing streams. Encrustation of the silk is rapid leading to swift accumulation and preservation of the structures (Drysdale 1999; Drysdale et al. 2003b).

Cased caddis belonging to a wide range of families are also known and include *Agapetus*, *Beraea*, *Helicopsyche*, *Oecitis*, *Mystacides*, *Silo* and *Stenophylax*. Ricker (1934) noted that the cases may be made of wood and sand, but travertine fragments are also used. In the Pine River, Michigan, the bulk of the fauna consisted of *Agapetus* (Leonard 1939). Minckley observed that the cases of *Agrayle multiplicata* were heavily encrusted in travertine. This is a common phenomenon in Western Europe sometimes leading to entombment of the larvae. The larval stages of caddis flies are thus well represented on meteogene travertines worldwide, and their silk nets probably act as traps for carbonate detritus and perhaps also nucleation sites of calcite. Most of the travertine-inhabiting species are probably univoltine (one life cycle per year) and may provide a useful record of travertine accumulation (Leggitt and Cushman 2001).

Many Diptera also possess aquatic larvae. They are among the most frequently recorded aquatic insects and arguably the most interesting of the travertine-associated fauna. Larvae belonging at least ten dipteran families have been recorded from Europe and North America. Blackfly larvae (Simulidiae) are a common sight on travertine cascades during summer (Fig. 52g). The larvae occur in the fastest flowing stretches and are attached by a disc covered in small hooks. Minckley suggested that encrustation helped in their attachment, but they are capable of living on all kinds of rock surface in fast-flowing water. These larvae may

represent the sole invertebrate fauna of travertine cascades as they can withstand high shear stresses. In Australia, Drysdale et al. (2003b) noted their occurrence in high-impact areas unsuitable for other insects. Tiny larvae of the Chironomidae have achieved some prominence in travertine sedimentology owing to their influence on the microfabric. Though far from ubiquitous, these tube-dwelling larvae show clear evidence of their former existence in the formation of well-defined feeding burrows each summer. The porosity of the associated travertines can reach 70% (Szulc 1983). In Montezuma Well, 30 taxa of the biting midge family Ceratopogonidae were recorded by Blinn and Sanderson (1989) though they were not stated to be associated with deposition. However, a small number of forms are characteristic of travertine-depositing sites, in temperate, sheltered valleys. They were first described from Russia by Bajaranus (1924) and later studied in detail by August Thienemann in Germany. Most attention has been devoted to *Tanytarsus emarginatus*, a species first described by Goetghebuer (1933) from material sent by Thienemann. In the same year, Thienemann renamed the larva *Lithotanytarsus* on the basis of its calcified nets (Thienemann 1933) followed by more detailed studies of its biology (Thienemann 1934), ecology (Thienemann 1936), and distribution (Thienemann 1950). The larvae are small, measuring up to 5 mm long and 0.3 mm wide in their final instar (Fig. 52i). They spin a serpentine tubular net on the travertine surface that soon becomes encrusted. The tubes are often found together in great numbers with individual tubes commonly 15 mm long and 0.3–0.6 mm wide. The larva hatches from eggs laid by the adult in late summer and slowly develops over winter. By the end of April they obtain maturity, and the tubes become noticeable. In Germany, the larvae pupate during May, leaving their tubes in June. *Lithotanytarsus* larvae often recolonise the same travertine year after year, providing a characterisitic lamination, with a highly porous tubular layer developing in the spring. They feed upon microbes and are frequently found associated with *Phormidium incrustatum* and diatoms of the genus *Navicula* (Thienemann 1934). They may also be associated with the desmid *Oocardium stratum* (Wallner 1936). This chironomid has a palearctic distribution, and in Bavaria, where it was first studied, lives in waters of 8–10 °C. The species is widely distributed, though often local in the streams of southern Germany (Bavarian and Franconian Alps) and in Lower Saxony (Danische 1950). It is also known from streams in Belgium (Symoens 1955), France, Switzerland and Russia, but not so far from Britain or Scandinavia.

Thienemann (1935) described a related chironomid, *Rheotanytarsus* which occurs in similar sites and may be associated with *Lithotanytarsus*. This genus is notable for the form of its nets, which have a series of arms extending from a central tube (Fig. 52h). Carthew et al. (2002) found that one species, *R. flabellatus* Glover was a major net builder in the Gregory River, Australia. Many other chironomid larvae have been found on travertine, frequently in association with *Lithotanytarsus*. In Europe, these include *Brachydiamesa streinbeckii, Brillia* sp., *Camptocladius pusillus, Eudactlyocladius* sp. *Eukiefferiella alpestris, E. lobifera, Micropsectra acuta,* and especially *Trichocladius bituberculatus* (Thienemann 1936). McMillan and Zeissler (1986) noted the frequent occurrence of *Stempellina* spp. and in North America, Ricker (1934) recorded *Chironomus* and *Pentaneura* from marl crusts in the Mad River, Ontario.

Larvae of the moth flies (Psychodidae) are among the most intriguing of all travertine-inhabiting insects so far discovered (Photoplate 2B). Members of one genus, *Pericoma* are provided with specialised scythe-like setae on their abdominal segments that may become selectively encrusted with a thin layer of travertine. Several of the many *Pericoma* species seem to be encrusted, and non-encrusted species are also found occasionally among deposits. The larvae inhabit the margins of travertine-depositing streams, often living among mosses such as *Palustriella commutata*, leafy detritus and algae, feeding on decaying vegetation.

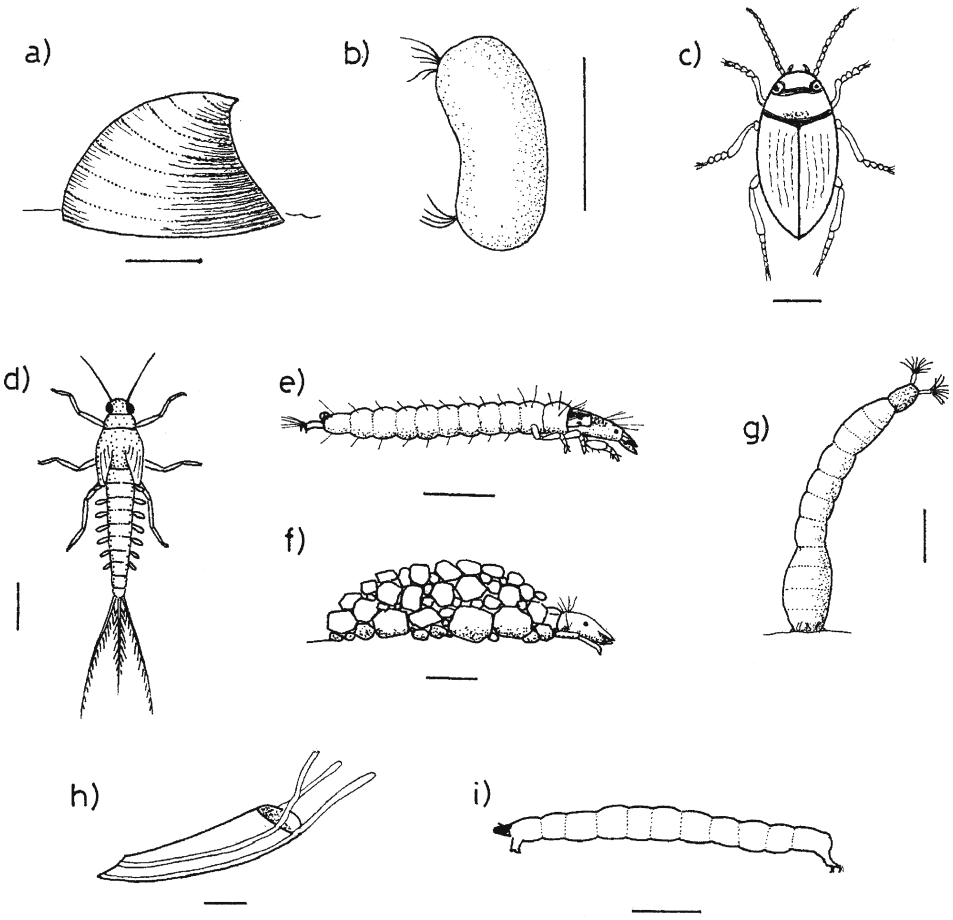

Fig. 52. Examples of invertebrates living in travertine-depositing systems. a) *Ancylus fluviatilis* (River limpet, Gastropoda); b) *Candona* (Ostracoda); c) *Deronectes* (Coleoptera); d) *Baetis* nymph (Ephemeroptera); e) *Tinodes* larva (Trichoptera); f) *Agapetus* larva in case (Trichoptera); g) *Simulium* larva (Diptera); h) silk retreat of *Rheotanytarsus* (Diptera); i) *Lithotanytarsus* larva (Diptera). Bar 1 mm

Feuerborn (1923) was the first to describe the encrustation in detail and suggested that travertine reduced the rate of desiccation of the larvae, allowing them to colonise a wider area. Experiments conducted by Krüper (1930) showed that the deposits were not secreted, but precipitated from solution. Further investigations by Durrenfeldt (1978) revealed details of the deposits using scanning electron microscopy and suggested that bacteria play a part in the process. The deposits of some taxa form only on the modified, scythe-shaped setae of the dorsal abdominal segments. Durrenfeldt suggested that the modification of the setae allowed *Pericoma* to live in rapidly depositing environments unsuitable to most other insects, by directing the deposition away from vital areas such as the eyes and respiratory tracts. It was also suggested that the travertine may serve a protective or defensive role. P. Withers (*pers. comm.*) considers that the setae trap the carbonate, and the deposits reduce predation through cryptic camouflage. The genus *Pericoma* includes several European species with encrusted larvae measuring up to 5 mm in length, well-known representatives being

P. calcilega, *P. incrustans* and *P. trifasciata*. The species are distinguished by the number and arrangement of setae on the segments, and structure of the anal siphon. Two taxa, *P. calcilega* and *P. trifasciata* appear to be widely distributed in Europe, but at least 14 are known in the 'trifasciata' group in Europe and North Africa. Vaillant and Withers (1993) suggest that microspeciation has occurred in the group owing to the isolation of suitable habitats and describe ten European taxa. The related *Phyllotelmatoscopus* (*Telmatoscopus*) *decipiens* also has an encrusted larva (Vaillant 1991). At least three other genera of moth flies have been found associated with travertine. *Atrichobrunnettia* has beenfound in flat marshy areas, as has *Sycorax* (P. Withers *pers. comm.*). Larvae of *Saraiella*, an alpine genus are also encrusted and occur in trickling water. Larvae of *Oxycera* (= *Hermione*) may also be encrusted. The latter belong to the Stratiomyidae, and rosettes of calcite growing directly upon the cuticle are figured and described by Durrenfeldt (1978).

Pentecost and Tortora (1989) found that an Italian thermogene travertine at Bagni di Tivoli was densely colonised by larvae of the brine fly *Ephydra*. Another closely related fly, *Paracoenia beckeri* is endemic in these waters and its biology is described by Giordani Soika (1956). The larvae form small vertical cavities in the dense, sulphur-encrusted travertines at temperatures of 25–28 °C. At present it is uncertain if the larval cavities are excavated or the result of encrustation but they occur in huge numbers in these oxygen-depleted waters. The adult flies feed upon the photosynthetic bacterial mats and scums growing over the travertine and upon the water, and are not currently known from any other thermogene site. Another species, *Ephydra hians* is abundant on the Mono Lake deposits, California (Herbst and Bradley 1993).

Other dipterans have been reported from travertines from time to time but they are probably casuals with no strong association. They include larvae of the Tipulids *Antocha*, *Dicranota* and *Pedicia* (Leonard 1939; Durrenfeldt 1978), *Atherix variegata* (Rhagionidae: Leonard 1939), *Thaumalea* (formerly *Orphnephila*; Thaumaleidae: Bertrand (1950), *Atrichopogon* (Ceratopogonidae), and *Dixa* (Dixidae). In Wales, *Hilara maura* (Empididae) has been seen flying above the travertine dams of Cwm Nash, but the larvae were not associated with the deposits.

An interesting account of the influence of invertebrates on the travertine fabric in a tropical environment is given by Humphreys et al. (1995). They found an abundance of Trichopteran and Dipteran larvae colonising dams in Madang Province, Papua New Guinea. Fourteen species of Trichoptera from eight genera were recorded including *Cheumatopsyche*, *Chimarra* and *Tinodes*. The larvae were found as several instars and most of the species were strainers, catching organic food particles in silk nets. Eight genera of Chironomidae including *Microtendipes* and *Rheotanytarsus* were widely distributed on the deposit with a Lepidopteran larva belonging to the family Pyralidae. The caddis net-spinning larvae were mostly confined to the dam overhangs where the water flow was reduced. The Pyralidae have also been noted from an Australian site where spray falls from cascades (Carthew et al. 2002).

9.7.2.2 Vertebrates

Excepting man, few vertebrates influence travertine formation. Fish, reptiles, amphibians and birds are all found in the vicinity of deposits from time to time. While fish are seldom evident, it should be noted that large travertine dams would act as effective migratory barriers, potentially isolating fish populations, though this factor does not appear to have been investigated with reference to travertine formation. However, some of the remote Australian mound springs have some noteworthy endemic faunas. The impounded waters of these springs are inhabited by endemic fish including *Craterocephalus dalhousiensis* with

an atyid prawn *Caridina thermophila*. Lesser animals include the isopod *Phreatomerus* and some unusual copepods. Ponder (1986) provides a review of the distribution and discovery of these animals.

Among other vertebrates, the fire salamander (*Salamandra salamandra*) is a well-known and colourful amphibian of the Schwabische Alb travertines (Photoplate 2A), though hardly restricted to them. The only animal likely to influence travertine formation is the beaver (*Castor fiber*) whose remains have occasionally been found in deposits (e.g. Lyell 1829; Steiner 1977). Beavers build lodges and small dams along streams and could provide foundations for a travertine encrusted structure (Goudie et al. 1993). Though beavers have been observed along travertine-depositing streams (Minckley 1963), build-ups on beaver dams do not seem to have been recorded. It should be noted that herds of large animals, drinking from streams, also have a destructive influence through trampling and eutrophication (cf. Emig 1917).

9.7.3 Ecology of Animals

Active travertine surfaces provide a source of food and protection for animals, but also present problems from encrustation as noted above. High rates of deposition (1–10 cm a^{-1}) provide a potentially hostile setting, and most thermogene deposits possess a depauperate fauna consisting only of brine flies, the adults of which may land on water but are not immersed in it. High temperature also poses a risk and animals are normally absent from hot springs >50 °C (Ward et al. 1987). It has been seen that some specialised groups have overcome some of these problems and others have made use of travertine as cryptic camouflage. A range of niches is colonised and include bryophyte cushions, superficial algal mats, bare travertine, endoliths, cavernicoles and detritus-rich clastic deposits. Most animals seem to prefer the slimy growths of algae of active travertines, where the algae and biofilm provides food, but several of these niches need further investigation. Bryophytes for example are often colonised by chironomids, nematodes and ostracods but have never been systematically studied.

For invertebrates, a general distinction can be made between shredders, collectors and scrapers and the two latter categories are well represented on travertine. Predators have been little recorded but certainly occur. Another distinction can be made between active and passive feeders, the former using *in situ* material and the latter using food drifting downstream. In a detailed study of Doe Run, Kentucky, Minckley (1963) found that the majority of species living in the travertine-depositing sections were active feeders utilising algae and organic detritus. He provided trophic spectra for a number of taxa and found that the mean density of 1560 animals m^{-2} was lower than non-depositing sections, reflecting the scarcity of plant material. At one site, 44% of animals were Ephemeroptera, 36.6% Diptera and 13.3% Trichoptera. The biomass, excluding shrimps and molluscs was 4.3 g m^{-2} and the Trichoptera at 37.1% made the greatest contribution. The main factors influencing animal numbers are similar to those of plants and include nutrition, temperature, water availability and flow rate.

The detrital component of the organic matter available for invertebrate food is usually classified into two forms, coarse particulate organic matter (CPOM) and fine (FPOM). Invertebrate taxa often specialise in the form of detrital food taken, though it is often found that food type varies with the life history of the larva and may change significantly over time. Major sources of CPOM are leafy of woody detritus washed into the system and allochthonous sources such as fragments of aquatic macrophytes include reeds, and particularly bryophytes. In some travertine systems, bryophytes should make a major contribution, but their stems upon emtombment in calcite are made unavailable as food. Detached cushions of bryophytes with their epiphytic algae may eventually settle and compost within dam pools and provide

a useful food source, though this is also prone to encrustation. Much of the FPOM is formed from the faeces of invertebrates feeding on CPOM. Flow will be an important factor where there are dams, since much of the fine particulate organic matter (FPOM) will be trapped upstream, leading to a decline of collector invertebrates downstream.

The river continuum concept (RCC) of Vannote et al. (1980) may be usefully applied to travertine systems. The RCC predicts that the proportions of shredders, collectors and grazers will vary with the type of food source available and their position in the fluvial system. In a first-order wooded stream, high CPOM inputs from the riparian vegetation would cause sufficient shading to reduce the travertine biofilm. In an exposed thermogene system, extensive biofilms would develop, attracting grazers but CPOM would be in short supply, providing the physico-chemical environment was suitable. However, in the lower reaches, FPOM released by the grazers could support collectors such as *Hydropsyche*. A food web with examples of functional feeding groups for a temperate travertine-depositing stream is illustrated in Fig. 53.

The retention of nutrients in a lotic system influences both biomass and diversity. Nutrient-spiralling – the sequential uptake and release of nutrients by biota down a stream gradient, is influenced by the ability of the stream system to retain organic matter. For example, in a stream containing a sequence of travertine dams, organic matter will tend to accumulate, resulting in tight spirals, delaying nutrient loss, but so far the effects of dams on streams have not been investigated in terms of nutrient retention. Interesting comparisons could be made on dammed and non-dammed sections, although the effects of differing flow regimes and sediment characteristics would need to be taken into account.

Factors affecting animal diversity in streams have been reviewed by Giller and Malmqvist (1998). Streams containing a wide range of substrate sizes (silt, sand, cobbles and boulders) and

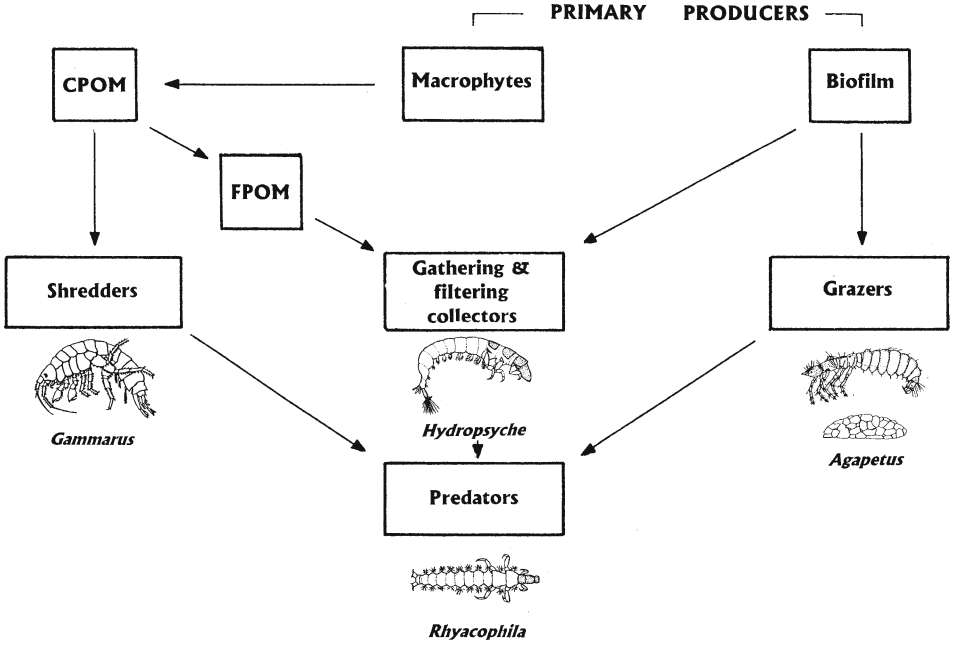

Fig. 53. Food web and functional feeding groups in a meteogene travertine system, illustrated with examples of invertebrates recorded from these environments. CPOM, coarse particulate organic matter; FPOM, fine particulate organic matter

larger obstacles tend to have greater diversity owing to an increase in the type of microflow patterns, cavity sizes and opportunities of plant growth. More complex surfaces tend to have a wider range of species and can act as refugia. For example, bryophyte cushions may contain 15 times more invertebrates per unit area than bare riffle areas (Hynes 1970). Obstructions such as dams also give rise to leaf packs that have been shown to attract invertebrates, potentially increasing diversity. Travertine systems would therefore be expected to contain a wide range of invertebrates. When investigating such areas, seasonality is obviously important, and the largest numbers of animals are normally found in spring and summer prior to emergence. The seasonal flow regime is also a factor. Streams can be classified as permanent, intermittent and episodic, the latter with unpredictable flow patterns. The frequency of drying periods in streams is of great importance to aquatic organisms, since many will not tolerate desiccation, while others require a suitable reproductive and dispersal strategy to permit colonisation.

In arid regions, where watercourses or groups of watercourses are distant from one another, island biogeographic theory should be applicable (Giller and Malmqvist 1998), where species richness is a non-linear function of the area of water surface. However, for some of the mound springs of Australia, an increase in area of an individual spring did not change the species diversity, but diversity did increase with the spring number, with clear conservation and management implications (Ponder 1986).

Deposition Processes

Waters giving rise to travertine deposits undergo rapid chemical change. Typical groundwater residence times are measured in months or years, yet travertine can be precipitated almost instantaneously when groundwaters contact the epigean atmosphere. For a typical cool-temperate cascade travertine, such as that developing in Waterfall Beck, UK, the groundwater residence time is about 3 months, while the transit time is just 5–10 minutes, during which the bulk of the travertine is deposited. Thus the water residence time is about 10^4 times the precipitation time. With prolonged periods of water-rock contact, spring waters usually emerge at or close to chemical equilibrium, while the rapid precipitation process is characterised by disequilibrium. This chapter is concerned with the processes involved with carbon dioxide loss downstream and the resulting precipitation of calcium carbonate. The rate of loss is dependent upon many factors, few of which exert a predictable, regular influence downstream. This is a consequence of the morphological irregularity of natural watercourses compounded by surface and subsurface water losses and gains downstream. 'Model' streams are hard to find, and those few approaching the ideal have only been partially investigated. Factors germane to atmospheric CO_2 loss include the concentration of molecular CO_2 in the groundwater, water and air temperature, water turbulence, depth and discharge. The loss of carbon dioxide shifts the equilibrium position of calcium-bicarbonate groundwater to the right (10.1) leading to travertine formation.

$$Ca^{2+}\ 2HCO_3^- \rightarrow CaCO_3 + H_2O + CO_2 \qquad (10.1)$$

Calcium carbonate however is rarely, if ever precipitated stoichiometrically, and complete precipitation may only occur over months or years. By this time, the depositing water may have so altered chemically that precipitation is no longer possible. The kinetics of calcium carbonate nucleation and crystal growth also require consideration in addition to the influence of photosynthetic plants as a carbon dioxide sink. We begin by looking at the rate of deposition of travertine, in a search for temporal and spatial patterns upon which models of the process may be built and compared.

10.1 Travertine Deposition Rates

Rates of calcium carbonate deposition are useful for dating travertine layers, investigating the effects of seasonality and testing hypotheses involving gas transport, nucleation, crystal growth and photosynthesis. Travertines are the most rapidly deposited natural calcium carbonates known to form direct from solution, providing a convenient experimental system.

A useful expression of rate is given in terms of numbers of molecules deposited per unit area (L^{-2}) per unit time (T^{-1}) but this is infrequently used and rates are most often expressed

as LT^{-1}. The disadvantage of the latter is that it takes no account of the deposit density. This may vary substantially, even at a single site and should always be borne in mind. Other methods have also been used, such as the rate of loss per unit volume of water (e.g. mole kg^{-1} s^{-1}) or the total annual mass loss for a complete travertine-depositing system (kg a^{-1}). Overall rates expressed in this form are useful in assessing the likely accumulation periods for particular sites.

Rates of deposition have been estimated using several methods. Direct methods involve placing suitable substrata in the water body and measuring accumulation over time as a difference in mass. This is possible once the $CaCO_3$ content has been determined and is the only suitable method for determining mass increments with any accuracy. Care must be exercised as some surfaces require 'ageing' before they accept the deposit, and others may be inhibitory. Copper poses a particular problem. Lack of deposition on copper has been taken as evidence for biological control of travertine deposition, but in the low ppm range, copper ions are inhibitory to inorganic precipitation (unpublished data). However, copper may become co-precipitated with calcite in caves, and under some conditions rates may exceed those of other apparently inert materials (Chibowski et al. 2003; Lojen et al. 2004). For this reason it is best avoided. An alternative is to place a marker stick or tube in the deposit and measure the upward growth avoiding substrate effects. All of these methods are subject to significant loss due to damage, washout and even theft (e.g. Porter 1861). Another method is to use the travertine itself. The author once marked oncoids with a bright plastic stud to aid retrieval and measured deposition rates as a mass increment (Pentecost 1989). Sprinkling carborundum dust or ocher directly onto the travertine surface followed by sectioning is another useful method. Other techniques include the use of a micro-erosion meter (e.g. Drysdale and Gillieson 1997) which has proved useful in determining rates with a high spatial resolution.

Indirect methods involve counting growth laminae, or estimating rates from water analysis at two or more fixed points on the water body and employing a mass-balance calculation. Many travertines display growth laminae. There are several kinds (Fig. 7) and they can often be demonstrated as seasonal, displaying thick summer layers and thinner winter layers. They provide the potential for investigating travertine deposition in considerable detail in wooded stream valleys where irradiance is sufficiently low to inhibit bryophyte growth. Bryophytes disrupt laminae, but may themselves be used to monitor deposition by the direct method, and occasionally grow as discrete annual layers. Thermogene travertines also possess growth laminae, often recording diel variations and the accumulation rates of clastic deposits have been measured on occasion. There are obvious difficulties here since phases of erosion will often be included in the overall rate. Where growth has been continuous over a long period, pollen- or radiometric dating is possible. The latter is often used to obtain estimates of speleothem growth. Even historical records can be useful, especially where dated excavations or buildings are available.

10.1.1 Meteogene Rates

Most of these measurements have been made in cool-temperate climates but there are few detailed investigations. Most are 'spot measurements' whereas deposition profiles are more informative but less often obtained. A number of studies have concentrated on particular fabrics allowing some comparisons to be made. For example there have been a series of studies on several types of cyanobacterium deposit, mainly in Western Europe. They show that the cyanobacteria are often associated with slowly accumulating deposits with rates of 1–3 mm a^{-1} being most often observed (Table 22). Rates obtained from oncoids colonised by cyanobacteria range from 0.14–5.8 mm a^{-1} and fall within the overall range for stream crusts. Measurements on the travertine-encrusted green alga *Gongrosira* showed that both growth and depo-

sition was positively correlated with water temperature (Pentecost 1988b). There are too few measurements to compare them statistically with cyanobacteria. However, the Xanthophyte *Vaucheria* appears to be associated with more rapid deposition (mean 14.7 mm a^{-1}).

Bryophyte travertines have significantly higher deposition rates that those associated with algae, with a mean of 24 mm a^{-1}. They also have a wider range of growth rates. The greater rates are probably related to the large surface areas of bryophyte leaves and stems. In general, it appears that where bryophytes occur, the travertine deposition rate is comparable to the growth rate of the plants themselves. This may be attributed to photosynthesis to some extent, but is more likely due to the observation that bryophytes can only survive where their growth is at least equal to the deposition rate, otherwise they become smothered and die. This is less true of algae, many of which are endolithic.

Many published records of deposition do not mention the associated flora. Deposition rates for travertines where the biota were not recorded appear to be higher than those for cyanobacteria with a mean of 5.51 mm a^{-1} and are thus intermediate between those colonised by algae and those with bryophytes. Most of the data relating to epigean meteogene travertines are from cascades or stream crusts where both turbulence and deposition rates would be expected to be high. Rates from other travertine morphologies have been obtained from radiocarbon dating of Holocene sequences. Paludal deposits from the UK have mean rates of 0.48 mm a^{-1}. Similar deposits in Belgium and France ranged more widely, from 1–26.5 mm a^{-1} and probably included clastic material (Geurts 1976). Deposits from Ddol in North Wales, consisting largely of dam-filled clastics, had a mean rate of 6.5 mm a^{-1}. Deposition rates of clastics are likely to be

Table 22. Summary statistics for travertine deposition rates

	Range mm a^{-1}	Mean mm a^{-1}	Standard deviation mm a^{-1}	Mean mm a^{-1} solid $CaCO_3$	Mean mmol cm^{-2} a^{-1}
Epigean meteogene (all)	0.04–48	5.28 (N=55)	6.32	2.16	5.86
Cyanobacteria-associated	0.04–7.0	2.38 (N=16)	1.99	1.00	2.72
Eukaryotic algae assoc.	0.42–48	9.08 (N=5)	11.1	3.40	9.25
Bryophyte assoc.	0.6–20	8.7 (N=7)	6.06	2.17	5.89
Speleothem[a]	0.002–0.90	0.027 (N=8)	0.020	0.027	0.073
Thermogene[a]	1.0–1000	202 (N=16)	194	93.6	254
Lake marl[b]	–	2.0	–	–	–
Marine limestone[c]	–	1.0	–	–	–

[a] Means of these sets have been trimmed to remove effects of extreme values.
[b] Kelts and Hsu (1978).
[c] Tucker and Wright (1990).
Sources: Baker et al. (1998); Bargar (1978); Chafetz and Folk (1984); Dorale et al. (1993); Dreybrodt (1988); Drysdale (1999); Drysdale and Gillieson (1997); Durrenfeldt (1978); Emeis et al. (1987); Folk et al. (1985); Geurts (1976); Gewelt (1986); Gruninger (1965); Guo and Riding (1992); Harmon et al. (1975); Heimann and Sass (1989); Irion and Müller (1968); Jacobson and Usdowski (1975); Jehl (1983); Kerney et al. (1980); Kitano (1963); Limondin-Lozouet and Preece (2004); Liu et al. (1995); Lu and Li (1992); Magdefrau (1956); McDermott et al. (1999); Meyrick and Preece (2001); Newton and Grossman (1988); Ohle (1937); Pazdur et al. (1988); Pentecost (1978, 1987b, 1995c, 1998 and unpublished); Preece and Day (1994 and unpublished); Salomon (1986); Schnitzer (1974); Statham (1977); Stirn (1964); Twenhofel (1939); Wallner (1935b); Weed (1888); Weijermars et al. (1986).

among the most variable owing to the nature of the deposition process. The lowest deposition rates are found in the speleothems, although these also vary considerably and overlap with the epigean travertines. There are few data for superambient deposits and none for invasive-meteogenes. The limited data for the superambients suggest that they are higher than those of ambient meteogenes.

10.1.2 Thermogene Rates

Comparatively few measurements have been made but most attest to the rapid accumulation of these travertines. The data, mainly from Mammoth Hot Springs, Wyoming, the central Italian springs and Huanglong, China are summarised in Table 22. The range is 1–1000 mm a^{-1} with a mean of around 200 mm a^{-1}. At Mammoth Hot Springs, rates range from 153–584 mm a^{-1}. It is unfortunate that the maximum recorded rates lack detailed information on both site location and water chemistry. They may be overestimates based upon short-term studies and for this reason, truncated averages are provided in Table 22. It can be seen that thermogene deposition rates are at least ten times as high as meteogene rates. The difference is due largely to the far greater concentrations of carbon dioxide and calcium in most of the source waters.

Table 22 also provides some comparative data on the deposition rates of other marine and freshwater carbonates. Travertines are seen to be among the most rapidly deposited carbonates on the Earth's surface. The average meteogene deposition rate is considerably higher than both the rate of marine carbonate sedimentation, and freshwater marl deposition. Thermogene deposits appear to be unrivalled in their rapid rate of precipitation.

As previously mentioned, deposition measured in LT^{-1} while convenient, is unhelpful as it is not readily translatable into a flux of ions to the depositing surface. Reasonable estimates of the flux are obtainable if the travertine porosities are known. In several studies, this has been determined, and in others, it can be estimated with reasonable precision at least in cases where the travertine type has been specified. With this information, deposition rates can be obtained as both mm a^{-1} for 100% $CaCO_3$ and as mol cm^{-2} a^{-1}. The available data are summarised in Table 22 and show that the mean thermogene flux rate is nearly 45 times the mean meteogene rate.

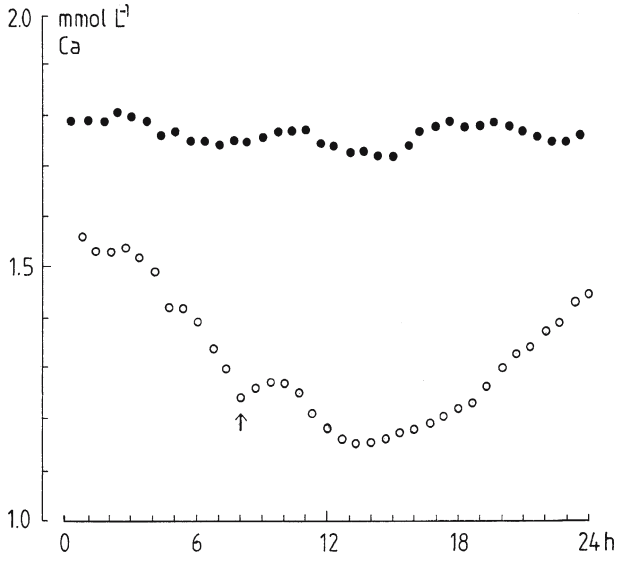

Fig. 54.
Daily variation in travertine deposition as a decline in Ca^{2+} between two sampling stations along Waterfall Beck, UK under conditions of low flow. Top station (filled circles) close to spring, shows little overall variation. Bottom station (open circles), 616 m downstream, shows a decrease in Ca with a maximum corresponding to maximum irradiance and water temperature around midday. The small dip (arrow) corresponds to a morning irradiance peak prior to cloud cover signifying a temporary increase in photosynthesis. Discharge fell slightly during the study, but did not influence the overall pattern of calcium loss. Data presented as 3-point running averages, redrawn from Spiro and Pentecost (1991)

10.1.3 Temporal Variation

10.1.3.1 Daily (Diel) Rates

It has not proved possible so far, to directly measure deposition rate changes on an hourly basis, although studies based on periods of 20–50 h have proved feasible. However, short-term changes can be inferred from mass-balance calculations along a section of stream. Diel variations in dissolved calcium show that in travertine-depositing streams, precipitation in the daytime is usually greater or equal to that at night. For example, In Waterfall Beck, UK, daytime deposition was twice as high as during nighttime, with a total of 3.2 kg calcite deposited along a 600 m length of stream within 24 h (Spiro and Pentecost 1991). The difference was attributed to a combination of photosynthetic activity and increased water temperature, both of which elevate the calcite saturation index and assist CO_2 removal (Fig. 54). The above measurements were made during an exceptionally dry period. Normally, the effects of photosynthesis on travertine deposition in this system are much less. Diel variations in conductivity have also been detected in several Australian streams using data-loggers (Drysdale et al. 2003a,c). In their second paper, temperature differences of up to 11 °C were detected resulting in greater degassing and an increase in calcium carbonate deposition of up to 100 mg L^{-1}. Precipitation was also significantly

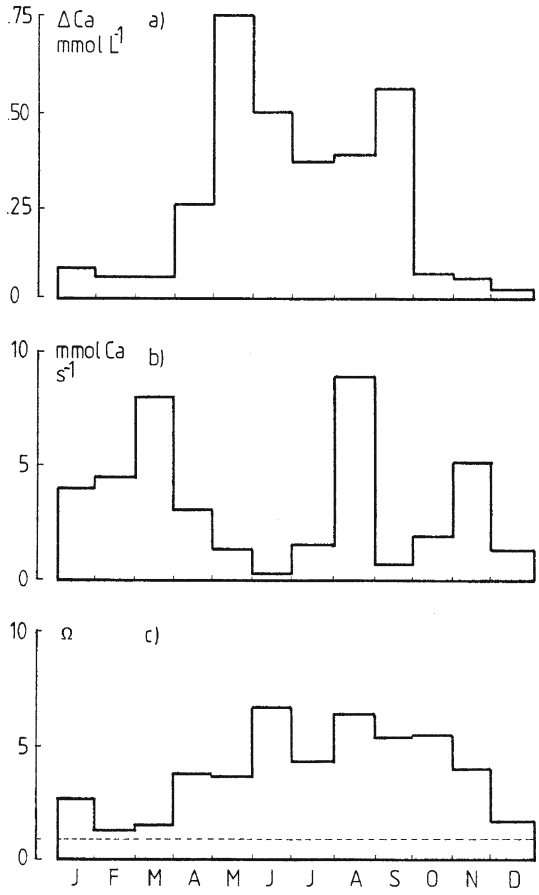

Fig. 55.
Seasonal variation in some chemical parameters of Waterfall Beck, UK. a) The difference in Ca^{2+} concentration (ΔCa) in water at the top (spring) and bottom (616 m) sampling station. b) Calcium loss between the same stations in mmol Ca^{2+} s^{-1}. c) The calcite saturation quotient Ω at the lower sampling station (on travertine). Based upon monthly spot samples for 1989

correlated to temperature. Another, less detailed study was conducted on the thermogene waters of Bagno Vignoni, Italy (Pentecost 1994). Calcite deposition was 35% higher during the day than the night, and again attributed to a combination of solar heating and photosynthesis. Variations in the daily rate have also been inferred from the existence of daily laminae in thermogene travertines (e.g. Chafetz and Folk 1984), see Section 3.4.2.

10.1.3.2 Seasonal Rates

The recognition of seasonal growth laminae goes back to Cohn (1864) and Bradley (1929). Tertiary oncoid laminae of 0.1–2 mm were subsequently measured by Weiss (1969) and interpreted as seasonal. The rates are similar to those of oncoids growing today. Wallner (1936) found that Bavarian chironomid travertines grew fastest in the summer andMinckley (1963) observed that oncoids in Doe Run, Kentucky grew most rapidly in the spring and early summer. Durrenfeldt (1978) found that cyanobacterium travertines also grew fastest at this time, and Geurts (1976) found that in the Bois d'Hautmont, Belgium, deposition was maximum in the spring but did not correlate with the period of maximum calcite supersaturation. Merz-Preiss and Riding (1999) found that deposition rates on artificial substrates in a small German stream were higher in summer than in winter, attributing this to algae that provided nucleation sites.

A series of investigations was carried out on the growth rates of travertine-associated algae in the 1980s by the author. Oncoids encrusted with the cyanobacterium *Calothrix* in northern England were found to grow most rapidly in the period July to September which corresponded to the period of maximum water temperature (Pentecost 1989), (Table 22). Growth of the cyanobacterium *Rivularia* was maximum during the summer at four sites and minimal in the period January to March and again growth was correlated to water temperature (Pentecost 1987b). The same phenomenon was observed for the encrusted green alga *Gongrosira* (Pentecost 1988b) and the cyanobacterium *Homoeothrix crustacea* (Pentecost 1988a). Seasonal variation may also be deduced from examination of changes in water chemistry downstream. They demonstrate generally higher rates during summer. In Fig. 55a, seasonal data are presented for Waterfall Beck and show a substantial increase in calcium loss from water during the spring and summer. The total loss of calcium per unit time however does not show a seasonal trend (Fig. 55b) owing to the higher winter discharge. A similar study conducted on a sequence of travertine dams in a wooded catchment also failed to reveal a seasonal trend (Pentecost et al. 2000). Systematic variations in the stable carbon and oxygen isotope compositions of travertine also indicate seasonal variations in the deposition process (Fritz 1968; Chafetz et al. 1991b).

Long term deposition rate changes have been deduced by examining growth laminae on deposits of the Nimes Aqueduct, France. Here, there appears to be a correlation between lamina thickness and the solar cycles of 11, 80 and 90 years (Fabré and Fiche 1986). These deposits represent the longest known continuous epigean lamina sequence, spanning about 400 years. Much longer sequences are known from speleothems, where the laminae result from variations in the hydrology (e.g. Tan et al. 1999). Measuring rates of longer periods of time requires other, less reliable techniques but may be accomplished in the absence of laminations. Geurts (1976) obtained accumulation rate estimates for some Holocene Belgian valley deposits (Table 22) based upon biostratigraphy. A maximum rate of 26.5 mm a^{-1} was estimated for the Boreal period (Table 22). Lookene and Utsal (1971) estimated maximum deposition of 1.5 mm a^{-1} in the Atlantic period. Valley deposits usually contain thick sequences that can accumulate rapidly during flood. Since erosion surfaces are also common and often difficult to detect, they should be borne in mind when interpreting the figures.

10.1.4 Lateral Variation

Lateral changes have been studied in few streams and much remains to be learned. Problems arise on two fronts; long stream sections with autochthonous travertine are uncommon, and within any section, hydrodynamic and hydrochemical variations occur due to breaks in slope and incoming tributaries. Given the variation in travertine morphologies around and below springs, prediction of deposition rates is fraught with difficulties although some general trends may be established. In laboratory degassing experiments using calcite-seeded spring-water from travertine-depositing streams, carbonate deposition was at first zero, then climbed to a maximum and fell, as the water pCO_2 fell to atmospheric values (author unpublished). Similar results were obtained by Dian Zhang et al. (2001) using limestone tablets in an experimental system. Although these results are only valid for streams where turbulence, temperature and other hydrological characters remain constant, natural systems often show the same trend.

A study of deposition rates in a small German stream, the Fleinsbrunnenbach by Heather Viles and the author showed a slight but significant increase in deposition with distance. Rates were obtained by measuring the couplet width of seasonal laminations and converted to mass per unit area using porosity data. The results indicated considerable local variation but did not correlate positively with average stream gradient. Growth rates of oncoids were significantly less than those of travertines attached to the stream beds. In the same stream, Merz-Preiss and Riding (1999) recognised three zones relating to travertine deposition; spring-resurgence, precipitation and precipitation-decline, the latter being inferred as there is no evidence for it in the Fleinsbrunnenbach owing to its disappearance underground. They also note how groundwater recharge downstream can augment the system, leading to a further round of precipitation. In Japan, a meteogene deposit where precipitation occurred over a distance of 460 m showed maximum deposition in the middle reaches based upon chemical analysis. The thickness of the deposit was maximum about 25 m from the source, the difference being attributed to erosion (Kano et al. 1999).

Thermogene deposits often show maximal deposition close to the source resulting in mound formation. For example Fouke et al. (2000) found that deposition rates at Mammoth were about 30 cm a^{-1} proximal to spring emergence, falling to less than 5 cm a^{-1} distally using stainless steel washers as substrates. The geometry of some mounds could perhaps be used to measure centripetal deposition rates, but irregular water-spreading on the mound surface complicates the modelling process. Mound springs usually have a small discharge (<10 L s^{-1}) though the mound-form itself is more a reflection of local topography, hydraulic head, and the carbonate saturation state.

At the thermogene spring of Le Zitelle, near Viterbo, Italy, deposition rates were obtained by placing aluminium discs at a range of distances from the source and weighing the accumulated travertine after three days immersion (Fig. 56a). Here the stream gradient is low and without major breaks in slope and a linear rise in deposition is apparent from source to a distance of 160 downstream where an incoming stream recharges the system. At another thermogene site, Bagno Vignoni, where the waters cascade over a steep travertine mound, the deposition rate was maximum 60 m below the outfall (Fig. 56b). This point corresponded with a break in slope at the edge of the mound, with precipitation declining thereafter until the waters entered a pond. The rates of these thermogenes are, unsurprisingly, much higher than those of meteogene waters, approaching 0.75 mm d^{-1} (c. 25 cm a^{-1}) for Zitelle and 0.34 mm d^{-1} (c. 12 cm a^{-1}) for Vignoni.

Table 23. Deposition rates expressed as kg d^{-1} for some travertine systems

Site/travertine type	Deposition rate kg d^{-1}	Notes	Reference
Meteogene			
Checa Terrace, Spain	10.1	Exposed, moss-dominated	Weijermars et al. (1986)
Fleinsbrunnenbach, Germany	10	Small shaded stream	Pentecost and Viles (unpublished)
Fossil Springs, Arizona	11900	Strong flowing, arid region	Malusa et al. (2003)
Plitvice Lakes, Croatia	27000	Large lake system	Kempe and Emeis (1985)
Shelsley Walsh, UK	2.5	Large deposit, small stream	Pentecost et al. (2003)
Shirokawa, Japan	16	Small stream	Kano et al. (1999)
Waterfall Beck, UK	3.2	Small system, drought conditions	Spiro and Pentecost (1991)
Thermogene			
Bagno Vignoni, Italy	100	Small thermal spring	Pentecost (1995c)
Hamman Meskoutine, Algeria	2000	Large system	Urbain (1953)
Huanglong, Sichuan, China	4300	Extensive system of lakes, dams and shoals	Yoshimura et al. (2004)

10.1.5 Amounts Deposited over Time

Estimates of the total quantity of calcium carbonate deposited over a given time are useful for estimating the age of travertine deposits and inferring changes in the rate over long periods. For example, the Holocene cascade deposit at Shelsley Walsh, UK was estimated as >7500 tonnes, yet the modern stream system was found to deposit less than 3 kg per day (Pentecost et al. 2000a). Therefore it must be assumed that deposition was much greater in the past. Some additional estimates are shown in Table 23. Rates vary both according to the areal deposition rate and the spring discharge.

10.2 Carbon Dioxide Loss from Emerging Groundwaters

With the exception of invasive meteogene deposits, formed by the reaction of atmospheric CO_2 with OH^-, atmospheric CO_2 loss is almost always the major driving force for travertine deposition. High levels of dissolved CO_2 have been shown to be present in most travertine-depositing source waters (Chapter 6) and several attempts have been made to understand the dynamics of CO_2 loss in these systems. One of the earliest was that of Emig (1917) who used the phenolphthalein alkalinity method to demonstrate the occurrence of free CO_2 changes, attributing them to temperature differences in an Oklahoma stream. Klahn (1923), Ohle (1937) and Symoens (1949) made similar measurements in Europe but the earliest useful quantitative data originated in the United States (Barnes 1965; Cole and Batchelder 1969). These studies provided valuable information on the loss of molecular CO_2 from travertine-

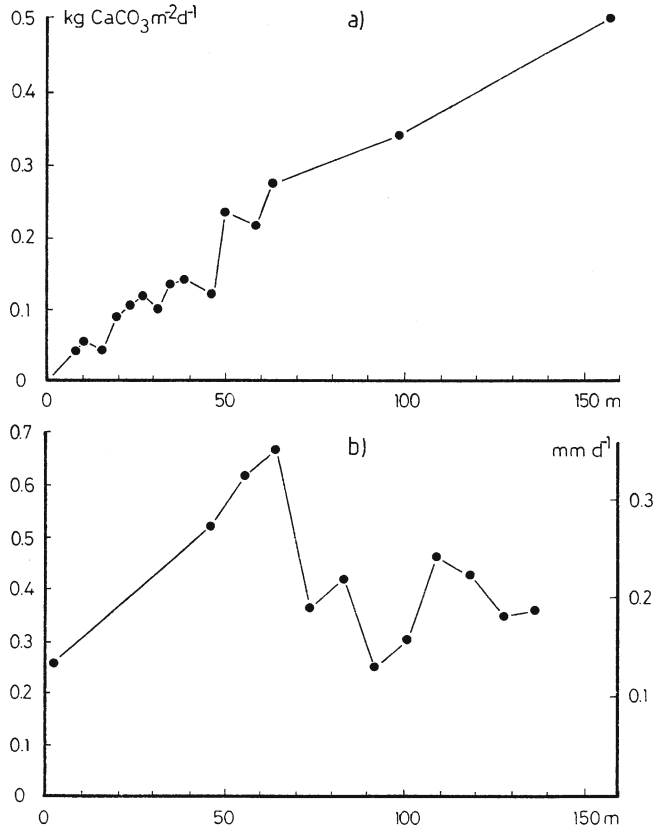

Fig. 56.
Lateral changes in calcium carbonate deposition rate for two Italian thermogene waters. a) Le Zitelle, Viterbo showing linear increase with distance from source; b) Bagno Vignoni, Siena, showing a maximum at the first break in slope on the travertine mound (from Pentecost 1994)

depositing waters and made some estimates of the evasion (de-gassing) rate. More detailed studies on gas evasion and precipitation rates were obtained in the 1970s, particularly from Usdowski's group in Germany on the Westerhoff stream, and during the same period in the UK at Waterfall Beck by the author. Evasion rates have also been investigated by Janet Herman's group in Virginia and more recently in China by Wolfgang Dreybrodt, Liu Zaihua and David Dian Zhang. Most of this work has focused on precipitation at the solid-liquid interface and the evasion of carbon dioxide has received less study.

The epigean atmosphere currently contains about 0.037 vol-% CO_2, at least an order of magnitude below the equilibrium partial pressure present in most travertine source waters. Emergent groundwaters spontaneously degas their excess carbon dioxide. Because CO_2 loss from water does not alter the charge balance, alkalinity remains constant and the CO_2-system readjusts leading to an increase in pH downstream. The escape of CO_2 leads to the consumption of H^+ and HCO_3^- (10.2) and an increase in CO_3^{2-}.

$$H^+ + HCO_3^- \rightarrow CO_2 + H_2O \qquad (10.2)$$

Aqueous carbon dioxide concentration is conveniently expressed in terms of its equilibrium partial pressure, the pCO_2. This facilitates comparison with the atmospheric CO_2 concentration. The pCO_2 is obtained from (10.3).

$$pCO_2 = \{HCO3^-\}\{H^+\} / K_1 K_H \quad (10.3)$$

Where the curly brackets stand for the ion activities, K_1 is the first dissociation constant of CO_2 and K_H is Henry's Law constant at the given temperature and pressure. Since pCO_2 values are wide-ranging and small they are often expressed as their logarithms.

The rate of transfer of a dissolved gas from water to atmosphere depends upon the concentration difference between the phases and the rate at which the gas can be transported to the liquid film in contact with the atmosphere. While this topic has been studied intensively in the sea and some lakes, there has been little work on carbon dioxide in flowing waters. Several models describe the transfer of carbon dioxide across the water-atmosphere boundary. In the absence of turbulent motion in both water and atmosphere, the static film model (Stumm and Morgan 1996) is considered appropriate. Here, transport is diffusion-controlled across the thin non-turbulent layers of gas and liquid at the interface. The rate of diffusion is proportional to the concentration gradient across the liquid layer as this offers by far the greatest resistance to diffusion, diffusivities in gases being c. 10^4 times greater than in water. The flux of gas is described by Fick's Law (10.4).

$$F = k (C_* - C_o) \quad (10.4)$$

Where C_*, C_o are the concentrations of molecular CO_2 across a boundary layer and k is a temperature-dependent transfer coefficient. For most waters, $k = 5 \times 10^{-3}$ cm s^{-1} to a good approximation. Under static conditions, the variables of interest become the concentration difference of CO_2 across the boundary layer, the surface area, temperature and surface impurities. In thin water films, the boundary layer is equated with the water depth.

In flowing water the situation is more complex because the boundary layer thickness is not readily obtainable. Turbulence is induced in streams by the roughness of the stream bed, and to a lesser extent by interactions between the water surface and flowing air. Air flow becomes progressively more important as the water becomes deeper, as in lakes.

Several models have been proposed for turbulent waters. Most are based on the concept of surface renewal where the liquid in contact with the atmosphere is continuously replaced with fresh liquid as a result of turbulence. Some of these models are appropriate for shallow streams and in all, the transfer coefficient k, is proportional to the square root of the diffusivity. This contrasts with the stagnant film model where k is equal to the diffusivity divided by the boundary layer thickness. In the surface renewal models, the flux has a complex relationship with turbulence, but of interest here is the model of Tsivoglou and Neal (1976) where k is expressed in terms of turbulent energy dissipation. Work by Pankow et al. (1984) has shown that the gas transfer coefficient, is proportional to $(D_m s)^{1/2}$ where D_m is the molecular diffusivity and s the surface renewal rate. The renewal rate can be shown to be approximated by u/h where u is the average stream velocity and h the stream depth (O'Connor and Dobbins 1958). The situation for dissolved carbon dioxide is complicated by the slow dehydration reaction whereby bicarbonate is converted into CO_2 which could retard evasion under conditions of strong turbulence (Pankow et al. 1984). In addition, experimental studies used to model the transfer rates of gases are conducted using a vertical oscillating grid. This permits rates to be obtained with a minimum of surface water disturbance. Under natural conditions, surfaces are rough, spray and bubbles form, and rates are found to be much higher than those predicted by the above model (Roberts 1984).

Carbon dioxide evasion rates can be determined directly by measuring the loss of gas between two points along a stream then expressing the loss as a function of water mass or

surface area per unit time. This can be achieved by measuring the alkalinity and pH on replicated samples. Rates are most conveniently obtained by choosing two points 10–100 metres apart along a stream section of approximately uniform depth, gradient and width with minimal surface-roughness of the water. Measurements performed in the 'clear zone' (the area close to the spring prior to the deposition of calcium carbonate) capture the rapid evasion phase, avoid the complications of carbonate deposition but considerably reduce the number of potential sites, especially for thermogene waters. The author has measured a small sample of European waters in this manner and the evasion rates are listed with some relevant hydrological data in Table 24. The measurements neglect photosynthesis and are thus likely to overestimate the evasion, but biological activity is rarely significant in these situations (see Section 11.8.4). Large differences are apparent between meteogene and thermogene waters but inspection of the correlation matrix provides only one significant association, namely that between the areal evasion rate (column 3) and the mean water temperature ($p = 0.01$). Lu et al. (2000) found a positive relationship between the CO_2 evasion rate and flow velocity. They obtained a rate of 250 μmol m^{-2} s^{-1} at a Chinese site with a maximum flow velocity of 2 m s^{-1} and extrapolated a rate of 27 μmol m^{-2} s^{-1} at velocity 0 m s^{-1}, but the mean pCO_2 was not recorded. Their data imply a linear relationship between evasion rate and turbulence. Transfer rates were also obtained by Herman and Lorah (1988) and Hoffer-French and Herman (1989) in meteogene Virginia streams. In the latter, it was found that evasion rates peaked in cascade

Table 24. 'Instantaneous' carbon dioxide evasion rates from the 'clear zones' 10–100 m in length, of some travertine-depositing waters. Westerhof data calculated from Usdowski et al. (1979), the remainder unpublished data of author from measurements made between 1990 and 2000

Site	Mean temperature °C	CO_2 evasion rate μM m^{-2} s^{-1}	CO_2 evasion rate μM L^{-1} s^{-1}	Mean pCO_2 (%)	Flow velocity m s^{-1}	Discharge L s^{-1}
Meteogene						
Fischbrunn, Franconia, Germany	9.7	7.0	6.5	0.75	0.67	0.4
Fleinsbrunnenbach, Schwäbische Alb, Germany	8.5	29.0	2.9	0.93	0.37	7.7
Harrietsham, Kent, UK	14.6	11.0	0.8	0.16	0.4	11.2
Pommelsbrunn, Franconia	8.5	8.9	1.0	0.21	0.35	2.5
Slade Brook, Gloucs., UK	9.6	5.6	13.2	0.99	0.44	18.0
St. Victore, Peisey, France	5.7	30.0	1.5	0.33	0.57	1.6
Westerhof, Germany	10.0	8.0	–	0.29	–	4.0
Means	*9.51*	*14.2*	*4.32*	*0.52*	*0.47*	*6.49*
Thermogene						
Bagni di Vignoni, Italy	40.8	800	370	3.65	0.69	3.2
Bullicame, Viterbo, Italy	56.0	890	20	10.4	0.16	2.7
Reotier, Queyras, France	21.0	1170	68	1.04	0.41	2.7
Means	*39.3*	*953*	*153*	*5.0*	*0.42*	*2.87*

sections (to 4.2 μmol L^{-1} s^{-1}) where the water was most turbulent. This rate was obtained in a travertine-depositing section but is close to the mean value obtained for the clear sections above (Table 24). The general lack of correlation between the hydrological factors in this table reflects the limited number of measurements, the high variability of stream sections and difficulty in obtaining measurements, but flow velocity is clearly important since high rates of CO_2 loss have been recorded from a number of sites. Srdoc et al. (1986) also report that maximum CO_2 exchange occurred on cascades using the ^{14}C content of the DIC.

A useful measure closely related to turbulence is the shear stress, τ (Eq. 10.5).

$$\tau = \rho g R S \tag{10.5}$$

Where ρ = water density, g the acceleration due to gravity (981 cm^{-1} s^{-2}), R the hydraulic radius, usually equated with water depth (cm) and S the stream gradient. Hoffer-French and Herman (1989) found a strong correlation between the shear stress and CO_2 evasion in a Virginia stream but no correlation was obtained in some of the Italian thermal springs (Pentecost 1995c). Here however, the flow was not contrasted on cascading sections.

As noted above, estimates for transfer rates of CO_2 require knowledge of boundary layer thickness in the case of the 'static' model. Relationships exist between mean velocity and the solid/liquid boundary layer and can be used to gauge the onset of turbulence (Smith 1975). In the mean velocity range 0–5 cm s^{-1}, the solid/liquid boundary layer is approximately 5–30 mm in thickness. These measurements are characteristic of seepage waters, including those flowing over travertine minidams and suggest laminar flow. In the mean velocity range 10–100 cm s^{-1}, typical of the stream sections listed in Table 22, the boundary layer thickness falls below 3 mm, demonstrating a turbulent flow regime. Surface-renewal models of CO_2 evasion have yet to be applied in these situations. Application of the more simple but less appropriate stagnant boundary model to the clear zone of Waterfall Beck, UK yields a rate of 8 μmol m^{-2} s^{-1} giving an estimated surface film thickness of a few hundred micrometres. This is applicable if it is assumed that the surface water film is in equilibrium with the atmospheric CO_2 concentration of $10^{-3.5}$ atm. and the turbulence is constant along the section (Gislason 1989). Further work using the same model has been undertaken on some of the Italian thermogene sites (Pentecost 1995). Here, the situation was complicated by calcium carbonate precipitation as deposition began at source. However, downstream CO_2 transfer coefficients ranged from 66–360 cm h^{-1} and were consistent with moderately turbulent flow although the surface film is unlikely to be at atmospheric equilibrium owing to the high bulk CO_2 concentration.

The variation of pCO_2 downstream is of interest as it is a sensitive indicator of chemical change and the approach of atmospheric equilibrium. Profiles of three meteogene and one thermogene water are shown in Fig. 58. The two profiles illustrated in Fig. 58a show an initially steep descent followed by a section where the pCO_2 is almost invariant and most of the travertine is deposited. In Fig. 58b an approximately exponential decline is suggested (cf. Srdoc et al. 1986a), but it is interesting to note that the short lengths of rapid CO_2 loss in the lower sections are associated with travertine-encrusted cascades. In c) a hot spring profile demonstrates extremely rapid and approximately exponential evasion with travertine deposition along the entire length of the section. These upper stream sections have been equated with first-order kinetics (Jacobson and Usdowski 1975). Dian Zhang et al. (2001) correlate this rapid degas stage with bicarbonate conversion to CO_2 using H^+. Similar profiles to a) have been published by Dandurand et al. (1982), Michaelis et al. (1985), Dian Zhang et al. (2001) and Drysdale et al. (2003c) from other streams and in none of them does the pCO_2 attain atmospheric equilibrium. The closest approach is that of Waterfall Beck (Fig. 58a) where the

pCO_2 declines to about 1.2 times the atmospheric equilibrium value before it joins a larger non-depositing stream. Here, the average journey time from spring to stream is about 15 minutes. In this stream there is negligible allochthonous organic carbon input. Where this is significant, subsequent decay of the organic matter and the production of CO_2 may prevent complete CO_2 drawdown in the water.

Downstream sampling is dictated by the nature of the terrain and limitations of the analytical techniques. Precision is insufficient to provide useful data over extremely short lengths of stream, yet travertine-depositing waters with their numerous cascades often demand them. Investigation of small scale features where turbulence and water velocity is locally high are of interest with respect to both CO_2 evasion and calcium carbonate deposition but much remains to be done. Cascades are particularly interesting and challenging in this respect. Dian Zhang et al. (2001) provide a useful summary of the processes leading to gas exchange on cascades. Two kinds of water flow are identifiable; the plunging jet on steep gradients, and slope flow on more moderate ones. In the plunging jet, the bulk of the water separates from the stream bed and undergoes free-fall while in slope flow, water remains in contact with the bed. In both types, three fundamental processes lead to enhanced gas evasion; internal pressure reduction, turbulence increase, and surface area increase. Pressure reduction occurs as a result of the Bernouilli effect and is proportional to the water velocity (Chen et al. 2004). Where velocity increases suddenly, such as the lip of a dam or waterfall, rapid pressure reduction occurs and will promote bubble formation. Dian Zhang et al. (2001) observed bub-

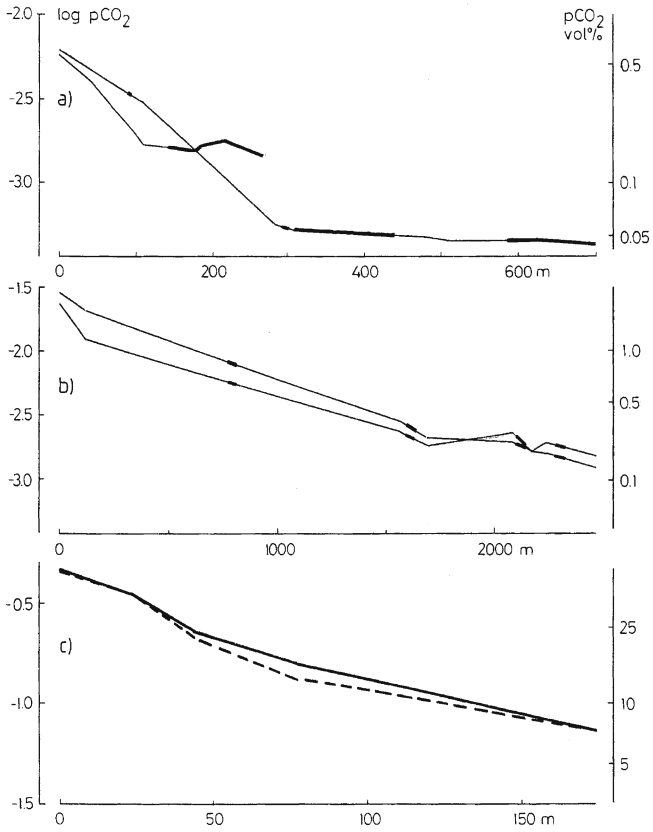

Fig. 57.
pCO_2 profiles along travertine-depositing streams. a) Waterfall Beck, UK, mean of seven runs (long line), and Westerhof stream, Germany, mean of two runs (short line). b) Falling Spring Run, Virginia showing two sampling runs. c) Bagnaccio, Italy. Full line daytime, broken line nighttime. Thickened lines show areas of major travertine deposition. The abscissa in a) and b) represents the atmospheric equilibrium line. Note differing scales for the axes in a)–c). Partly redrawn from Usdowski et al. (1979), Herman and Lorah (1987) and Pentecost (1995c)

bles with diameters of 0.2–3 mm forming in this way. Turbulence increase is also the result of water acceleration as the stream gradient increases. This begins at the dam/waterfall lip and continues in plunging jets until the terminal velocity of the water packet is reached or the water contacts the base of the cliff. During free-fall, turbulence will be maintained by strong air flows and the breaking and uniting of water columns. This type of flow is sometimes termed 'shooting' and can be distinguished by a Froude number from the more frequent 'streaming' flow on lesser gradients. On more moderate slopes, surface irregularities will have a significant effect on turbulence leading to thorough mixing. Turbulence reduces the diffusion boundary layers between solid/liquid and liquid/gas, promoting gas evasion. Surface area increase is an obvious outcome of the plunging jet where the water separates from the stream bed. Complete separation is rare, and a thin layer of water is usually maintained in contact with the substratum further increasing the area of liquid exposed. Area is also increased when the water surface becomes irregular due to turbulence and hydraulic jumps. Chen et al. (2004) showed that under static conditions, both CO_2 evasion and calcite precipitation is directly proportional to the liquid-gas surface area. Bubble formation is particularly significant in this respect. While pressure reduction remains a factor, air entrainment caused by the trapping of gas in the irregular water surface, air trapped at hydraulic jumps and that resulting from substratum irregularities are likely to be more important (Fig. 58). Bubbles may also form as the result of photosynthetic oxygen production. Anti-bubbles might also form in turbulent regimes though their significance is unknown. Cavitation is mentioned as a gas-transfer process by Lambert (1955) and this has also been shown as a potential eroding force by Dian Zhang et al. (2001). Spray formation is probably important as well. This results from bubble collapse, water impact and separation, forming small spherical droplets where gas evasion will be rapid. For example, Droste (1997) found that CO_2 reduction in water droplets reached 70–90% in 2 seconds, while Dian Zhang et al. (2001) emphasise the significance of spray in some jet-flow experiments. The effects of surface area increase probably outweigh all other factors and their importance was recognised long ago (Eulenstein 1866). Chanson and Cummings (1996) found a 100-fold increase in the air-water interface for turbulent water falling down a gentle slope.

Much of the potential energy of stream water must be converted on cascades to a surface area increment. For example, the potential energy of the springwater at Waterfall Beck, UK, is about 1.4×10^7 erg g^{-1} relative to the stream base which is sufficient to increase its area from 6×10^{-4} m^2 to 19 m^2. It is unlikely that anything like that increment is achieved owing to frictional and other losses, but it emphasises the potential for surface area increment in turbulent waters. Other factors also deserve mention. Friction will increase water temperature it flows downhill also increasing gas evasion but this could be masked by evaporation. On stream beds where the water forms a trickling, often laminar layer, gas exchange can be enhanced by the presence of plants. Mosses are well-known colonisers of cascades (Chapter 9) and the complex network of moss leaves and stems provide a large surface area as previously noted. On mossy cascades with a free-plunging water jet the result will be vastly increased CO_2 evasion.

The rate of CO_2 evasion in cave drip-waters has aroused considerable interest. Early work by Roques (1964) determined rates from hanging drops. Most speleothem formation occurs from thin films of water under conditions of laminar flow, where in theory, the diffusion boundary layer would extend throughout the film. However, water sampling for analysis is often difficult in caves, and the cave air CO_2 composition is frequently variable and cannot be assumed to be that of the epigean atmosphere. In some caves, increased concentrations of cave atmosphere CO_2 have been found near the floor owing to its high density. In the flowing water of caves, minidams have been the subject of several enquiries. In some flow

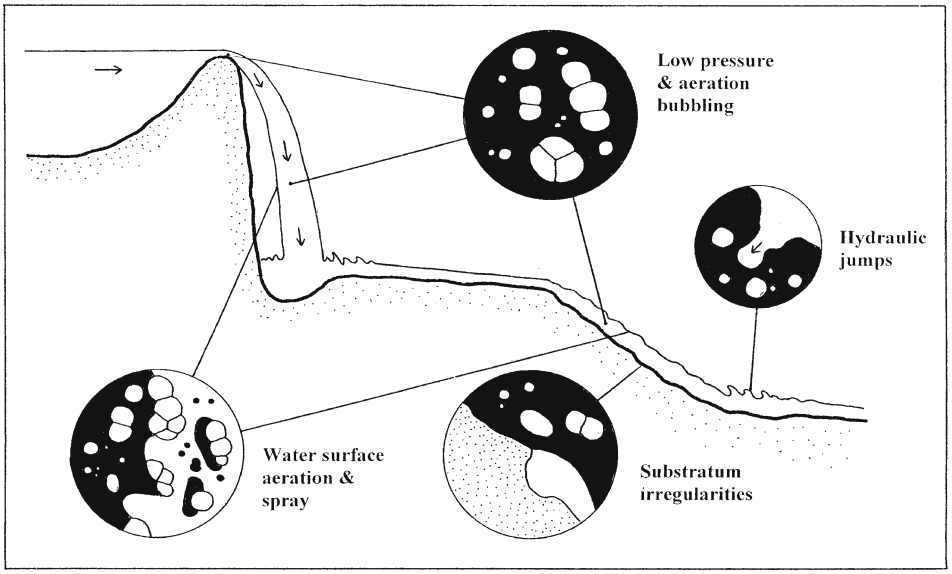

Fig. 58. Bubble and spray formation on a free-plunging dam/waterfall (left) and a slope (right). After Dian Zhang et al. (2001)

regimes, regular alternations of laminar and turbulent flow can be envisaged as the water runs through the quiescent pools then suddenly passes over the crests of dams. Varnedoe (1965) pointed out that this pattern would be self-perpetuating, with enhanced CO_2 evasion and calcite precipitation at the crest sites resulting from pressure reduction and turbulence. Similar situations would occur in many epigean travertine dams, but in minidams, the flow may not always be sufficient to become turbulent. Even in these situations, a change in velocity occurs over the dam lips leading to surface renewal and pressure reduction.

The role of evaporation in CO_2 transfer is important in some caves, particularly those in arid regions. For example in the Carlsbad Caverns of New Mexico, evaporation is believed responsible for up to 40% of the cave carbonates (Thrailkill 1965). Evaporation is probably important in the formation of some epigean travertines, especially at low latitudes or in hot springs with many authors suspecting or demonstrating its involvement, e.g. Branner (1911), Kitano (1963), Van Everdingen (1969), Butzer et al. (1978), Schreiber et al. (1981), Dunkerley, (1987), Newton and Grossman (1988), Wright (2000) and Ihlenfield et al. (2003). Downstream temperature changes will also be significant. Solar warming of cool springwaters will increase the evasion rate, while the cooling of thermal waters has the reverse effect (Lorah and Herman 1988).

Finally, the effects of freezing require mention. Streams often freeze over during winter and the process excludes dissolved salts, most of which concentrate in the unfrozen water resulting in a depressed freezing point. Calcium carbonate precipitates may become trapped among plants once the temperature rises. Thin, laminated travertine-like deposits are sometimes found on the soles of glaciers and attributed to freeze-melt sequences (Hallet 1976), sometimes forming delicate horizontal 'stalactites' pointing downstream. Ford et al. (1970) have suggested that pressure reduction on the glacier sole may supersaturate the water with calcite leading to precipitation on seeds of glacial flour. The deposits may be distinguished by their $\delta^{18}O$ and $\delta^{13}C$ signatures which are often strongly fractionated (Clark and Lauriol 1992; Strong et al. 1993).

Calcareous crusts have long been known from the undersides of buried stones. They are composed of a thin, often knobbly layer of calcite and are occasionally laminated (Cailleux 1965). They seem to be widespread in cold regions such as Queen Elizabeth Islands (Bunting and Christensen 1980) but also occur in many parts of Europe including Britain, France and Hungary, where they may be relicts from a colder period. Some experiments suggest that freezing is needed (Cailleux 1965) though Bunting and Christensen (1980) believe evaporation of soil water is the cause. The freezing of cave waters usually results in the deposition of calcite as a cryptocrystalline form termed 'lublinite' and in rare cases it can aggregate into microscopic cave pearls (Viehmann 1963).

10.3 Saturation Indices and Nucleation

The processes involved in the transformation of solvated calcium and carbonate ions into the minerals calcite and aragonite is complex, and the literature devoted to the topic is substantial. In essence, the process can be divided into two stages: 1) the formation of a solid nucleus from the dissolved ions and 2) addition of ions to the nucleus to form crystals of calcium carbonate. Both processes are dependent on the chemical composition of the solution, its temperature and pressure. For both nucleation and crystal growth, the solution must be supersaturated with respect to the precipitating mineral phase. This is a prerequisite and a topic of considerable importance. The level of supersaturation is always made with reference to the product of the ion activities in question and the mineral phase. The ions here are Ca^{2+} and CO_3^{2-} and the phase is calcite, though for some studies, the more soluble, but unstable aragonite may be referred to.

The nucleation of the calcium carbonate polymorphs follows the well-established rules of most other insoluble salts. Of the two main processes of nucleation, homogeneous and heterogeneous, only the latter is thought to be important in dilute aqueous solutions, since the former requires solute supersaturations too high to be realised under most natural conditions of carbonate precipitation. Heterogeneous nucleation results from the attachment of ions to a pre-existing substrate. Substrates may be either suspended in the medium or fixed at either the air/water or solid/water interface. The nature of the substrate has been little studied, but it is thought that attachment of ions occurs preferentially at active sites and may be accompanied by a degree of lattice matching between substrate and nucleus. For example, there is known to be a good match between polyaspartate and calcite owing to the coordination of calcium atoms parallel to {001} with the aspartate carboxyl groups (Sikes and Wierzbicki 1995). At Plitvice, Emeis et al. (1987) suggested that algae-excreted aspartate could act as a calcite template, initiating travertine formation. More complex templates involving humates have also been shown to nucleate both calcite and aragonite (Ferguson et al. 1978).

For a nucleating particle, the free energy of the interface between the solid and its surrounding phases is considered to be the most important factor. This energy term is the sum of the free energy of the interface (proportional to area) and the free energy liberated by each precipitating unit volume (i.e. ionic 'bond' formation) of solid phase (proportional to volume). In the case of a simple nucleating particle the total free energy is found to rise to a maximum value corresponding to the energy barrier to nucleation. To effect nucleation, the activation energy barrier must be surmounted. It is usually of the order of 20 kJ $Mole^{-1}$ and may be equated with the solution supersaturation. During nucleation, calcium and carbonate ions must undergo a dehydration step, since each ion is surrounded by a hydration shell

of about ten water molecules (Lippmann 1973). During the early stage of nucleation, which may involve no more than about 20 ions, partial dehydration may result in the formation of a poorly crystallised solid. As dehydration proceeds via the constant bombardment of the surface with ions and water molecules, a more regular solid results. The energy barrier for heterogeneous nucleation is lower than that for homogeneous nucleation, and substrates capable of forming nuclei are thought to be ubiquitous in most natural waters. Before considering nucleation further, it is necessary to provide definitions of calcium carbonate saturation indices.

10.3.1 Calcium Carbonate Saturation Indices

Barnes (1965) used a saturation quotient in a study of the travertine-depositing Birch Creek as IAP_c/K_c where IAP_c stood for the sample ion activity product for calcite and K_c the equilibrium ion activity product at the same temperature. The same index has been used widely in theoretical and hydrochemical studies, often being referred to as Ω. Values of $\Omega > 1$ indicate supersaturation. Langmuir (1971) defined a saturation index S_c as:

$$S_c = \log (IAP_c/K_c) \tag{10.6}$$

The use of a logarithmic transformation has some theoretical advantage, and also reduces the variance of these measurements, which is often large. For undersaturation, Sc values are negative, and positive for supersaturation, as with SI. The relative supersaturation, $\Omega - 1$ also finds applications in kinetic studies (Kazmierczak et al. 1982). Both S_c and Ω are in wide use.

Several alternative methods have been proposed to measure calcium carbonate saturation. Picknett (1964) and Brunskill (1969) advocate the measurement of dissolved Ca and/or pH in water samples before and after addition of a calcite suspension. Changes in pH will provide an estimate of the saturation state of a water independent of its alkalinity and have the advantage of *in situ* temperature control. Disadvantages are potential lack of accurate pH determination with meters that are susceptible to condensation and comparisons are difficult to make with theoretical indices. In addition, the equilibrium period for the calcite suspension may be extended which is often inconvenient in field-based studies. The author used this technique in Waterfall Beck and found a reasonable correlation between it and Ω but it was laborious and time-consuming (Pentecost 1988a). It could prove useful in hypersaline or high sulphate waters. In these cases, some equilibrium constants are less well known due to complex formation and ion pairing (e.g. Wigley 1971; Dreybrodt et al. 1992) leading to uncertainties in the computation of Ω. It should be noted that the precision of Ω itself is subject to a number of errors at it is sensitive to the pH determination required for its calculation. Field pH measurements are usually quoted with a precision of 0.1 pH units and it is unrealistic to expect anything better in most situations.

Working with this figure, and an 'average' meteogene springwater with DIC, Ca and SO_4 precisions of 0.01, 0.04 and 0.025 mmol L^{-1} respectively, a Monte-Carlo run of 20 Ω determinations gave a precision of 0.32 for Ω =1.5. The accuracy will be somewhat less when uncertainties in the equilibrium constants and activity corrections are taken into account. The loss or gain of mass in a mineral sample may also be used to assess calcite saturation. Herman and Lorah (1988) suspended calcite rhombs in cages and measured their difference over a known period, but mechanical erosion may also lead to errors.

10.3.2 Calcite Saturation Indices for Travertine-depositing Waters

A considerable amount of data are available for saturation indices in cave and epigean waters. It will be useful to distinguish between Ω values for the emergent source waters and those taken from waters flowing over the travertine itself. In most cases, emerging source waters are close to saturation, while those taken from above the travertine surface are usually supersaturated with respect to calcite. Figure 59 provides statistics from travertine depositing waters both at source and on the travertine surface. More information is available for meteogene waters, where for the springwater the mean Ω is 2.07 (Fig. 59a), somewhat above the saturation (equilibrium) level for calcite and the data are positively skewed. The median value of 1.44 is closer to unity but a number of samples are clearly supersaturated at

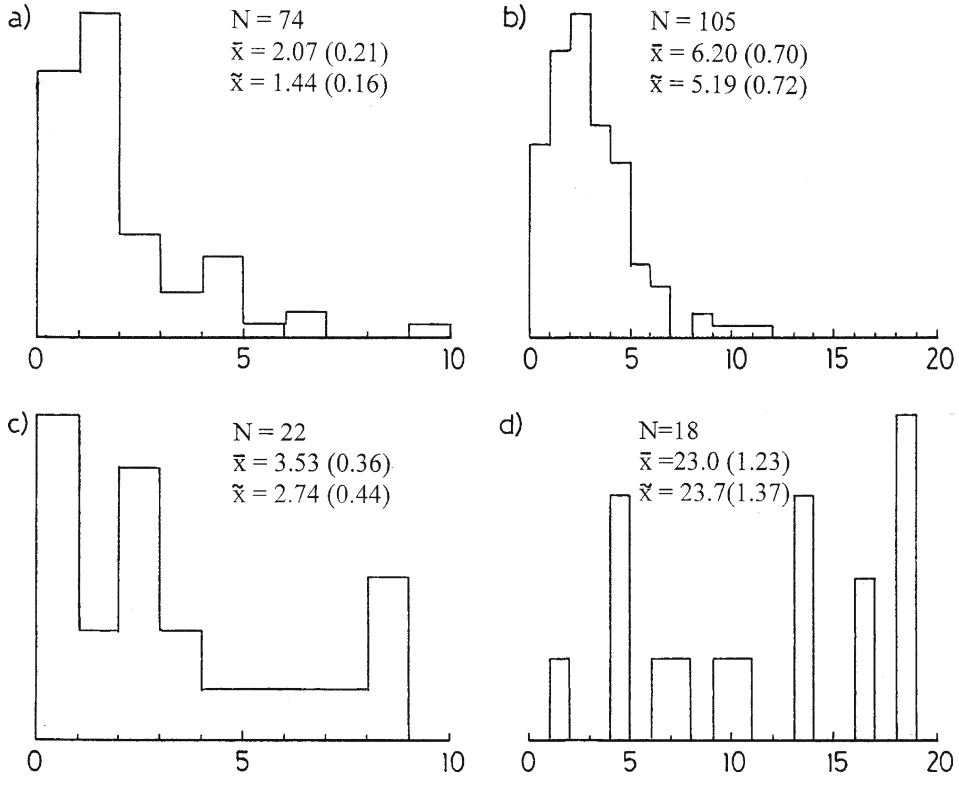

Fig. 59. Distribution of calcite saturation indices (Ω) for travertine-depositing waters. The values in parentheses are for the logarithmic form of the index (S_c). a) meteogene spring waters; b) meteogene waters on travertine surfaces; c) thermogene spring waters; d) thermogene waters on travertine surfaces. Sources: Arp et al. (2001); Barnes (1965); Chafetz et al. (1991a); Cole and Batchelder (1969); Dandurand et al. (1982); Dian Zhang et al. (2001); Drysdale and Gale 2003; Drysdale et al. (2003); Dunkerly (1987); Duchi et al. (1978); Fairchild et al. (2000); Frisia et al. (2000); Geurts (1976); Geurts and Watelet (1994); Gonzales et al. (1992); Herman and Hubbard (1990); Hoffer-French and Herman (1989); Holland et al. (1964); Horvatincic et al. (1989); Ichigami and Suzuki (1977); Jacobson and Usdowski (1979); Jones and Renaut (1995); Kano et al. (1999); Kempe and Emeis (1985); Kerr and Turner (1996); Khoury et al. (1984); Kirby and Rimstidt (1990); Li et al. (1993); Lorah and Herman (1988); Lund (1978); Malusa et al. (2003); Merz-Preiss and Riding (1999); Mountain et al. (2003); Pentecost (1992b and unpublished); Raymahashay and Chatuverdi (1976); Risacher and Eugster (1979); Steidtmann (1936); Symoens (1950); van Everdingen et al. (1969); Viles and Pentecost (1999); Yoshimura et al. (1996); Zhang Jie (1993)

source. This is probably caused by subsurface degassing of groundwater since at some sites, the waters rise through caves or thin rubbly soils allowing a degree of atmospheric circulation (Kano et al. 1999). Fewer data are available for thermogene springs and the graph shows a higher mean supersaturation of Ω =3.53 (Fig. 59c). Again the histogram is skewed, due to subsurface degassing which is more pronounced for waters with a high pCO_2 rising rapidly from depth.

Values taken from waters flowing over travertine are shown in Fig. 59b. The meteogenes show a positively skewed distribution with a mean Ω of 6.2 and a mode of 2–3. Few values exceed Ω = 7 and 90% fall within the range 0.5–7. Thermogene values tend to be higher and with a greater variation (Fig. 59d). Over 50% of the thermogene values exceed 12 and occasionally attain 40 or more, approaching the realm of homogeneous nucleation. Superambient waters, few of which have been measured, have values intermediate between the meteogenes and thermogenes.

Several saturation index/quotient profiles may be found in the literature. One is shown in Fig. 60 for a well-studied German stream. At the spring, the waters are already supersaturated though most of the travertine is deposited on the steeper sections about 175 m downstream. As the waters evolve, Ω initially undergoes an approximate linear increase with distance but then rises and peaks 200 m from the source at c. 20, declining thereafter. The fall is probably the result of calcite precipitation removing Ca^{2+} and releasing H^+ (Fig. 60c). The dissolved calcium profile is also shown and suggests that most calcite is deposited once Ω has risen to about 15 and continues while Ω falls to about 10. This unimodal pattern is to be expected but is not always observed especially where there are multiple water sources. For example, it was found in only two of the five stream profiles obtained by Drysdale et al. (2003c).

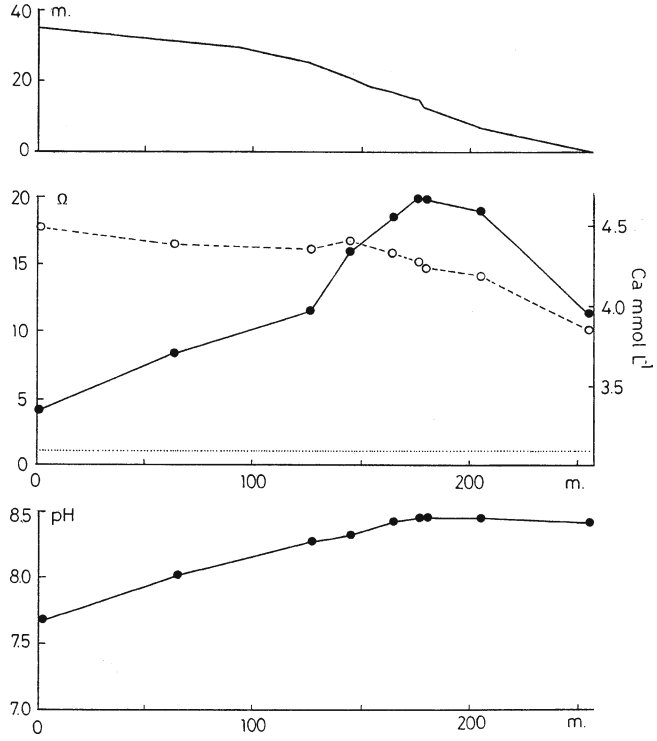

Fig. 60.
Downstream changes in the travertine-depositing Westerhofbach, Germany. Above: stream profile. Centre: profiles of the calcite saturation quotient Ω (solid line) and dissolved calcium (broken line). Dotted line represents calcite saturation level. Below: pH. Redrawn from Dreybrodt et al. (1992)

Cave waters are not plotted separately but the available data suggest that in general, these waters do not supersaturate to a high degree. Data from some North American and European caves taken from pools, speleothem drips and surfaces have most Ω values in the range 1.5–4 (Fairchild et al. 2000; Frisia et al. 2000) but values in the range 7–18 were obtained by Holland et al. (1964) and Gonzalez et al. (1992). The lower supersaturations perhaps reflect a reduced degassing rate into an atmosphere frequently elevated in CO_2 in the virtual absence of turbulent flow.

Invasive meteogene waters such as those associated with lime-burning and serpentinization have not been investigated in terms of their saturation state. The rapid rate of deposition in some of these waters suggests that high supersaturations are attained following atmospheric CO_2 ingress. In the presence of much magnesium however, the supersaturation will be reduced at high pH owing to the formation of $MgCO_3$ ion-pairs.

The supersaturation necessary to promote the precipitation of calcium carbonate is of particular interest from both a practical and theoretical standpoint. A number of values have been suggested for calcite on the basis of observation on natural calcite-depositing systems. The value is usually taken as that measured in the bulk phase where travertine is first deposited in a stream. As noted previously, a good number of streams possess a clear zone where the onset of deposition can be identified. In these sites it is possible to estimate the saturation state required for precipitation (Table 25). The resulting values vary somewhat, but the average is around $\Omega = 6$. Considered in terms of calcite nucleation, a critical supersaturation is a function of the activation energy required for the formation of a crystal nucleus. Experimental work does not indicate a precise value because heterogeneous nucleation may occur on a wide range of surfaces, each with its own surface energy value. The surface energy is an important component of the activation energy so may vary according to the nature of the surface. In addition, the role of nucleation in travertine formation, once crystal growth has started, is subject to a number of uncertainties as indicated below.

The saturation index is related to the energy of the system through the relationship $\ln \Omega = \Sigma_i \Delta\mu_i / RT$ where $\Delta\mu_i$ is the change in chemical potential of the i'th ion from solute to incorporation into the crystal lattice (House and Donaldson 1985). Calcite supersaturations have also been interpreted as a 'free energy excess' through the relationship: $\Delta G = -RT\ln \Omega$ (Dandurand et al. 1982; Michaelis et al. 1985). For meteogene travertines, ΔG is found to be around -5 KJ mol^{-1}. These values are less than the experimentally-determined activation energy of 39 KJ mol^{-1} (Kazmierczak et al. 1982).

Some data on the seasonal variation in Ω for travertine-depositing waters, above the travertine surface are available. In a pioneering study of some Virginia stream travertines, Steidtmann (1936) observed year-round supersaturation with a maximum in winter. Merz-Preiss and Riding (2001) found that the index also reached its highest value in winter for a small German stream. In Waterfall Beck, the supersaturation reaches a maximum of 5–7 in summer, and is close to the equilibrium value (1.0) in winter (Fig. 55c) although deposition occurs throughout the year. In a Japanese stream, Kano et al. (1999) also found that supersaturation values peaked in summer. Variation at source implies changes in chemical composition as described in Chapter 5 for meteogene travertines but seasonal variations downstream are more difficult to account for since several independent variables are likely to be involved such as discharge and temperature. Increasing the temperature increases the saturation index leading to potentially higher rates of deposition although this was clearly not the case in the Fleinsbrunnen above. In hot springs, cooling is the norm, reducing the supersaturation downstream (Van Everdingen 1969). Regular, daily variations have been reported for some Australian meteogene streams using data-loggers (Drysdale et al. 2003a) where it is linked to changing water temperature.

Table 25. Critical supersaturations reported for calcite deposition in freshwaters

Critical supersaturation Ω_c	Site	Reference
4 – 6	Berkeley karst streams, Australia	Drysdale et al. (2003c)
> 6	Fleinsbrunnenbach, Germany	Merz-Preiss and Riding (1999)
10	Huanglong, China	Liu et al. (1995)
5 – 7	Plitvice travertine system, Croatia	Horvatincic et al. (1993)
10	Roquefort-les-Cascades, France	Dandurand et al. (1982)
3 – 4	Waterfall Beck, UK	Author, unpublished
> 3.2	Japanese streams	Kano et al. (1998)
5	Marl lakes	Kelts and Hsu (1978)

10.3.3 Heterogeneous Nucleation and Crystal-Trapping

Heterogeneous calcite nucleation on foreign substrates appears to be the dominant nucleation process occurring in travertine-depositing systems. Supersaturations are too low to allow homogeneous nucleation, although secondary nucleation on calcium carbonate probably occurs and will be discussed later. The substrates responsible for heterogeneous nucleation are unknown, but knowledge of the types of surfaces likely to be present provides some clues. These substrates have a variety of origins, as summarised in Fig. 61. Heteronuclei may be found in suspension, or at the atmosphere- and benthos-water interfaces. Allochthonous particles in suspension and at the water surface originate from the atmosphere, groundwater and through erosion. Autochthonous particles originate from within the system and include the phytoplankton and zooplankton of lakes and the microbe/moss biofilm of the benthos. Bacteria are ubiquitous and often found associated with suspended particles and the benthos and are potentially important in the nucleation process.

There have been many *in vitro* studies of calcite nucleation from filtered metastable solutions in the range Ω 1–50 (e.g. Reddy 1986, 1988, 1995). They have demonstrated that in the range Ω 5–7, typical of that of most meteogene waters, nucleation is not observed within the first 24 hours unless stirring is introduced, when it falls to about 20 minutes whereas at higher supersaturations, nucleation is almost instantaneous. This induction time, t_I has been found useful in comparing nucleation under different conditions and Reddy distinguished *labile* solutions where it is very rapid, and *metastable* where it is slower. Most travertine-depositing solutions fall into the metastable category. The rate of particle production, measured in particles $mL^{-1}\ s^{-1}$ and equated with the nucleation rate (R_N) has been found to be inversely proportional to the induction time, and log R_N is roughly proportional to Ω (Reddy 1986). High supersaturations (>= 10) were used in this study. At Ω = 10, R_N ranged from about 5–60, so at Ω values typical of meteogene travertines (Ω ~ 5) the rate will be extremely low and unlikely to exceed 10 particles $mL^{-1}\ s^{-1}$. If these *in vitro* studies apply to the travertine-depositing environment, they have important implications for calcium carbonate deposition. Such a low nucleation rate shows that in fast-flowing streams, nucleation will be extremely slow. In the case of epigean travertines, the benthos is normally covered with a biofilm of algae, bacteria and bryophytes and it within this biofilm that nucleation would be expected. The travertine biofilm has been shown to be biologically diverse with much of the flora encrusted with calcium carbonate. Micrite

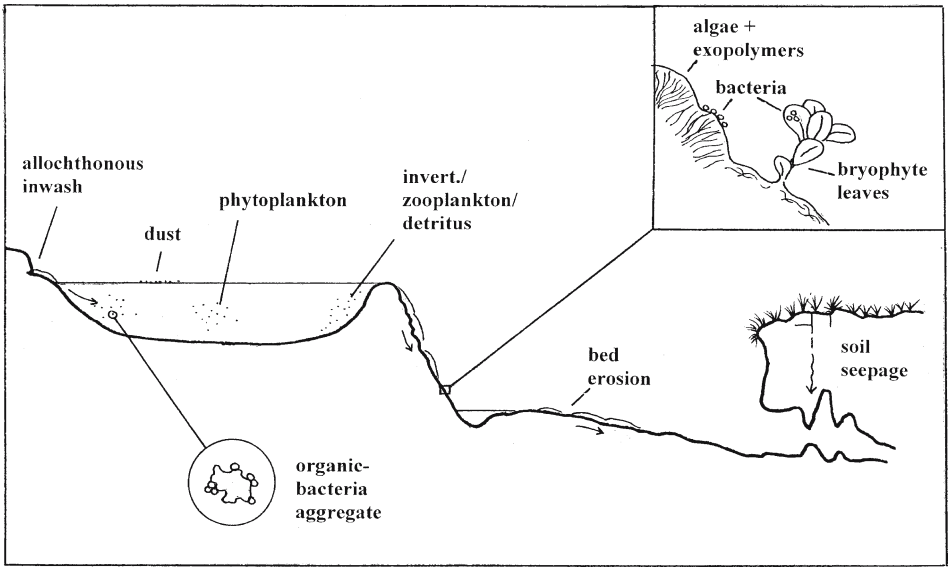

Fig. 61. Sources of heteronuclei for calcium carbonate deposition in travertine-depositing systems

is commonly associated with algae, particularly cyanobacteria (Section 9.2.3) where it is believed to be a primary deposit. The persistent occurrence of calcite crystals in the micrite size range suggests that each small crystal has grown around at least one nucleation centre. At a North Wales site, the author obtained measurements on the growth of the cyanobacterium *Schizothrix fasciculata* and obtained estimates of crystal size. This permits an estimate of nucleation rate since the deposit was entirely of micrite. At this location the mean crystal size was close to 2.5 μm, the porosity 50% and the growth rate 0.66 mm a^{-1}. This translates into a surface nucleation rate of 4000 cm^{-2} min^{-1}, far in excess of the experimental values quoted above, particularly with reference to the calculated Ω values of 5.3–9, which were maintained throughout the year. These are probably typical rates of micrite formation in the UK algal deposits, and suggests that nucleation in the biofilm is strongly influenced by the surrounding microenvironment. The frequent association of micrite with microbes may be related to the inhibition of crystal growth post nucleation. Lebron and Suarez (1996) found that organic matter inhibited crystal growth at lower concentrations than nucleation. Thus, if traces of inhibitors are present, nucleation might proceed, but crystal growth is soon arrested as inhibitors bind to the mineral surface, resulting in micrite formation.

Within the laminar boundary layer, adjacent to the photosynthesising biofilm, supersaturation is likely to rise well above the turbulent bulk water level (see below) and organic surfaces may provide highly favourable environments for nucleation, if not for crystal growth. It can be concluded that nucleation of the solid calcium carbonate phase at supersaturations below about 30 is mainly heterogeneous, since the rate of formation of nuclei is otherwise too slow to account for the observed precipitation rates. At the high supersaturations existing in some thermogene waters, the possibility of homogeneous nucleation from a labile solution must be considered. Whether precipitation is homogeneous or heterogeneous, or a combination of both, precipitation is rapid and sometimes gives

rise to an initially unstable phase of carbonate such as vaterite (Lu et al. 2000). Reddy (1988) describes five phases of solid $CaCO_3$: calcite (stable anhydrous); aragonite, vaterite (unstable anhydrous); $CaCO_3$ mono and hexahydrate (unstable hydrates) and amorphous, linking them by their differing solubilities and showing how they may interconvert as the milieu changes from labile to metastable. While amorphous $CaCO_3$ is yet to be reported from travertine its existence appears likely under high supersaturations where it would rapidly revert to the anhydrous forms.

While heterogeneous nucleation would be expected to be the main initiator of the solid phase, three further processes may be responsible for travertine growth: secondary nucleation; surface nucleation and particle trapping. Trapping will be considered later but secondary nucleation is unlikely to be important, at least in meteogene deposits (Kazmierczak et al. 1982). It might result from microattrition of dendritic crystals (Nancollas 1979; Reddy and Gaillard 1981) and could however be expected in rapidly-depositing aragonitic travertines such as those at Mammoth Hot Springs. Surface nucleation occurs on crystal planes either due to the loss of a growth step or surface inhibition. It may be a common phenomenon, but as Reddy (1995) remarked, it is difficult to characterise crystal growth as it is often accompanied by nucleation.

Nucleation is not necessary for the initiation of travertine formation if sources of calcium carbonate are already present in the environment. Crystal growth may proceed directly on dislocations or steps present in an allochthonous calcite source. Small particles of calcite are probably ubiquitous in karst waters, resulting from turbulent flow, particle transport from the soil zone and direct atmospheric deposition (Lorah and Herman 1988). The trapping of calcite by algae, bryophytes and invertebrates is discussed by Casanova and Lafont (1986), Emeis et al. (1987) and Drysdale and Gillieson (1997). In a one-year study of Waterfall Beck, UK, the author found an average of almost 25% $CaCO_3$ in the total suspended load of this stream, amounting to 0.22 ppm (Pentecost 1990d). Calcite particles were found in the spring water and their quantity increased downstream, presumably due to erosion of the limestone bedrock and travertine deposits. The particle diameters had a mode of 1.5 μm, but extremely small particles of 0.2 μm or less would have passed through the filter employed. Using the 1.5 μm mode as an average, the Waterfall Beck waters must contain at least 50 particles of calcite per mL. Calculations show that the trapping and binding of this material at the travertine surface would account for a negligible proportion of the travertine accumulating there. However, small crystals trapped at the water-biofilm and water-atmosphere interface could provide suitable growth centres for the travertine. For particles less than 0.1 μm in diameter, the forces of molecular bombardment can overcome the repulsive potential energy barrier between the biofilm and the suspended particle leading to adhesion (Pentecost and Riding 1986). Although particles of this size range have not been detected, they probably exist providing the water is sufficiently supersaturated with respect to the mineral phase, preventing their dissolution. Minute particles could easily result from the evaporation of fine spray on cascades, and may even be responsible for the 'spray tufa' sometimes seen at the edges of cascades (Dian Zhang et al. 2001). The trapping of allochthonous calcite at the travertine surface therefore appears likely but cannot be easily distinguished from heterogeneous nucleation and it may well contribute to the high nucleation rates necessary for micrite formation noted above. Because travertine deposition appears to occur at a 'critical supersaturation' where Ω is considerably higher than unity one might reasonably ask why travertine formation does not begin immediately Ω exceeds unity. If trapped calcite exists, then crystal growth should proceed, albeit slowly, once supersaturation begins. Perhaps the precipitation

rate at $\Omega \sim 1$ is so slow that erosion and dissolution events prevent buildups, or traces of inhibitor or occluding biofilm reduce the deposition rate almost to zero (cf. Lebron and Suarez 1996). In deep cave systems, some of the famous 'crystal caves' are believed to have formed at extremely low calcite supersaturations (Hill and Forti 1997). This is clearly an area requiring further research that would lead to a better understanding of the important initial stages of travertine formation.

Calcite must also occur in travertine-dammed lakes, kept in suspension by turbulence and Brownian motion. The turquoise colour of the lakes and pools of Huanglong and Jiuzhaigou, China (Photoplate 3B) are probably due at least in part to the light-scattering effects of sub-micron sized particles of calcium carbonate.

10.3.4 Apparent Onset of Nucleation in Streams

The length of the clear zone in meteogene streams is presumed to be correlated with the time required for gas evasion to increase the calcite saturation index to a critical value. Since the evasion rate is dependent largely upon the initial pCO_2, the surface area and turbulence of the emerging water, commensurate variations are to be expected. Some of these are explored in Fig. 62 where the clear zone is plotted against the discharge (Fig. 62a) and the average gradient (Fig. 62b). In both cases, significant correlations result, positive in the former, and negative in the latter. Thus springs with a large discharge and gentle gradient possess long clear zones. Transit times for most of these zones were not determined, but for Waterfall Beck, a representative example with a clear zone of 70 m and a gradient of 6°, the transit time is about 100 seconds. Some of the scatter in the data will result from the differing water chemistries and bed geometries of these streams. Drysdale et al. (2003c) came to a similar conclusion with reference to the position of travertine-depositing systems in general, suggesting that higher discharge streams deposit their travertine at greater distances from their source.

Once the supersaturation has reached a 'critical value', deposition commences. This is presumably accompanied by nucleation, although this is not always necessary as explained above.

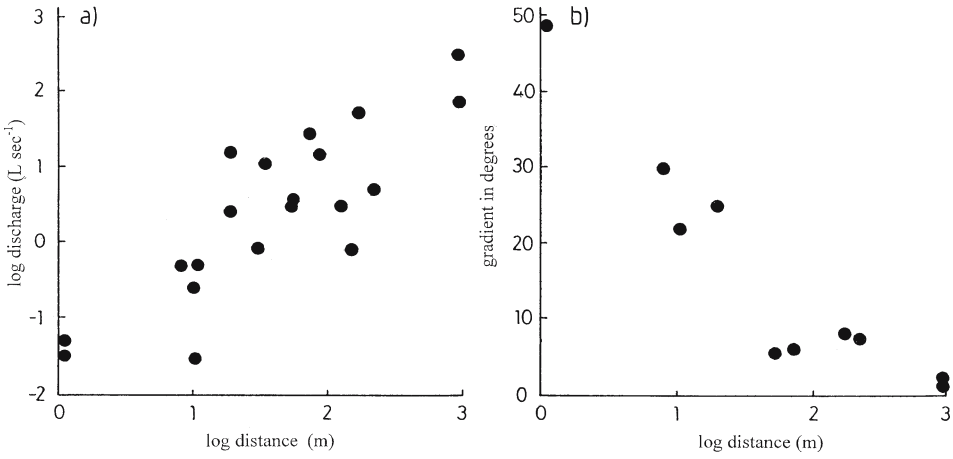

Fig. 62. Relationship between the clear zone in meteogene springs, measured in metres with a) spring discharge and b) clear zone average gradient. Based mainly on original observations in Western Europe

10.4 Crystal Growth

Travertine formation results from crystal growth in a supersaturated solution. Understanding the growth process is challenging since the chemical conditions at the crystal surface cannot be ascertained by direct analysis. Crystal growth from solution proceeds in up to five stages (Brady and House 1995): 1) diffusion of components to the growing surface; 2) adsorption; 3) diffusion across the surface; 4) reaction at a high energy (kink) site and 5) incorporation into the lattice. In the case of calcite and aragonite the crystal growth components are Ca^{2+} and CO_3^{2-}. Both ions have associated water molecules, and a dehydration step must precede their incorporation into the crystal lattice as in the case of nucleation (Nancollas 1979). The whole process must be accompanied by a decrease in the free-energy of the system and probably takes place within a few nanometres of the surface. Although ion-by-ion incorporation has not been observed, atomic force microscopy and crystal growth kinetics have permitted some understanding of the growth process on an atomic scale. A study of the step dynamics of the (1 0 – 1 4) cleavage plane of calcite indicates the direct addition of ions from solution onto a step region (Gratz et al. 1993). This contrasts with crystal growth from atomic vapours where surface diffusion is important, and is explained in terms of the surface charge mosaic on this calcite crystal plane. The same mosaic is believed responsible for the cleavage of calcite along (1 0 – 1 4).

Crystal growth usually proceeds along steps in the crystal surface and steps are a common feature of calcite crystals (Davis et al. 1995). Ions are added preferentially to re-entrant angles (kinks) of the step as they possess a high binding energy (Zhdanov 1965), permitting it to advance across the crystal face. One a step has reached the edge of a crystal, ion incorporation is no longer favourable and growth is stopped. To continue, new steps must form. To form a new step, nucleation on the smooth crystal face may occur, or a deformity resulting from a foreign inclusion could provide the necessary irregularity to initiate a step. These growth processes are the basis for two important crystal growth models. In the first, spiral growth steps are formed by screw dislocations and growth may continue indefinitely without the need for further nucleation. In this process there is no nucleation energy barrier to be overcome and growth may proceed at low supersaturations (Gratz et al. 1993). Some evidence for screw dislocations in thermogene travertines has been found by Folk et al. (1985) but these probably relate to diagenetic forms where secondary growth has occurred at low supersaturation. The columnar calcites of speleothems are also believed to form from the spiral mechanism (Frisia et al. 2000).

At higher supersaturations another growth mechanism is possible. In the VKS Model (Sunagawa 1987), growth occurs upon a crystal interface through the formation of two-dimensional nuclei to which ions may be added on the resulting step. Growth relies upon continued nucleation on the crystal face. A critical supersaturation is required which may be as low as 2 Ω (Dove and Hochella 1993) and this is clearly a potential mechanism for travertine crystal growth. However, in other *in vitro* studies, (e.g. Paquette and Reeder 1995) the spiral mechanism has been observed at much higher values. At supersaturations >>10 a third process known as adhesive-type growth could occur leading to the formation of rough crystals with ill-defined faces. The distinction could be important in determining the crystal growth rate as a function of the supersaturation. Sunagawa (1987) notes that for the spiral mechanism, the rate is proportional to the supersaturation, whereas for the two-dimensional model, the rate is proportional to supersaturation raised to some power *n*.

Some idea of the frequency with which ions interact with the surface can be gained through estimates of the impingement rate. For a meteogene travertine in contact with water containing an average 3 mmol L^{-1} Ca^{2+}, approximately 1.2 x 10^6 ions contact any growth site per second (Meyer 1984). With estimates of the lattice layer rate, it can be seen that fewer than one in

Table 26. Calcite lattice layer and impingement rates for travertines. Estimates based upon mean deposition rates, mean travertine porosities and mean dissolved Ca and for a unit surface area of travertine calcite. The impingement rate is based upon mean Ca values from Fig. 35

Travertine type	Mean deposition rate corrected for porosity mm a^{-1}	Lattice layer rate for unit surface layer min^{-1}	Impingement rate of nutrient ions at a growth site $\times 10^{-6}$ ion s^{-1}
Speleothem	0.19	1.5	1.2
Meteogene (epigean)	2.7	21.5	1.2
Thermogene (epigean)	182	1450	3.6
Thermogene maximum	675	5400	–

3 x 10^6 ions ends up adsorbed and enters the lattice, the remainder returning to the solution (Table 26). For thermogene travertines the impingement rate is somewhat greater owing to the higher calcium concentration and temperature.

Estimates of the rate of crystal growth can be obtained from observed deposition rates and the volume occupied by $CaCO_3$ in the calcite crystal. The molecular area of $CaCO_3$ is 20.1 x 10^{-20} m^2 $molec.^{-1}$ (House and Donaldson 1985). With average rates of deposition of travertines, and taking into account their porosities, the lattice layer rates can be calculated (Table 27). These rates assume a unit surface area of calcite, i.e. the surface area of crystal exposed in 1 cm^2 travertine is taken as unity. This is unrealistic since the depositing surface will be uneven, and with a porous material there is opportunity for crystals to grow in all directions and the rates listed must be regarded as maximum values. The actual crystal surface area available for growth is unknown. It is likely to be at least ten times the unit area, in which case the lattice layer rates will be at least ten times lower than those shown. They may be even lower, since the specific surface areas of calcite (as micrite) is known to be high. An *Oscillatoria* tufa was found to have a specific surface area ranging from 0.7–2.4 m^2 g^{-1} (Irion and Müller 1968), and a sample of micrite from Waterfall Beck, UK had a value of 4.25 m^2 g^{-1}. If crystal growth continues to a depth of 0.5 mm below the travertine surface, the lattice layer rate would fall by a factor of at least 1000 in Table 27.

The irregularity of most travertine calcite crystals, particularly those of micrite indicate the occurrence of numerous small faces and a high surface area. The reasons for this heterogeneity are unknown. Since speleothem crystals tend to be larger and more regular, it may be connected to the number of heteronuclei and the lower rate of calcite growth. Kendall (1993) has drawn attention to the importance of the CO_2 gradient above the crystal surface and the surface topography. Where thin films of water are involved, flow is laminar with a steep gradient of CO_2 resulting from calcium carbonate deposition. The growth of large isolated crystals above the general surface is inhibited by obstruction of flow in a thin film leading to the formation of numerous small crystallites as observed on speleothems. Where the water is deeper, but slow-flowing, the CO_2 gradient is lower, obstructions divert less flow, and larger crystallites can develop, becoming dendritic at high supersaturations.

Calcite is deposited from aqueous solution and in all cases, water molecules close the crystal surface exist within a boundary layer ($\in$) where all molecules enter and leave by diffusion. The thickness of the boundary layer is a function of the prevailing hydrodynamic conditions as for CO_2 evasion. In thin films of thickness 1 mm or less, the boundary layer will equate with the film thickness, but with deeper layers of water, the boundary layer varies according the rate of flow. In rapidly flowing water, the boundary layer can be reduced to a thickness of a few micrometres. Several empirical relationships exist allowing the prediction

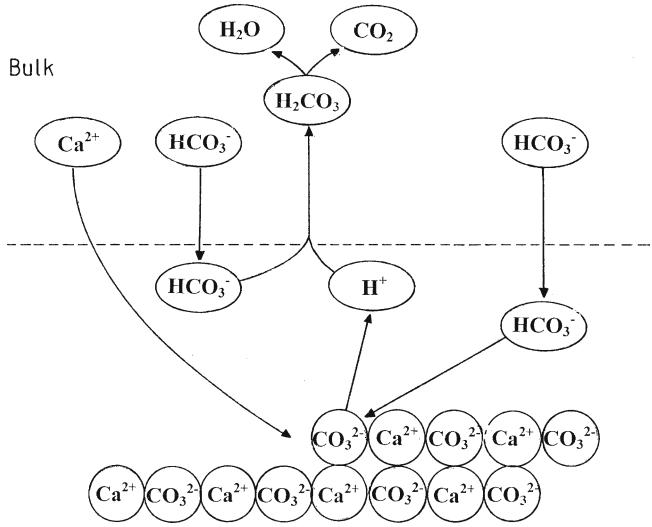

Fig. 63.
Diffusive transport of ions from the bulk solution to the calcite crystal surface during crystal growth. Diffusion occurs within the diffusion boundary layer (broken line) where ions enter the crystal lattice on the calcite cleavage plane at a monatomic step. The process is shown as the reverse of calcite dissolution (after Dreybrodt 1988)

of $\in$. It may also be obtained experimentally by measuring the rate of gypsum dissolution (Opdyke et al. 1987). This method has been shown to relate well to theory and is useful in complex hydrological systems encountered with most epigean travertines. However it is not always convenient to use since several days may be needed to assess the dissolution rate, and the geometry of the growing travertine surface may be too irregular to simulate. In this case, a theoretical method can be applied.

During precipitation, ions enter the boundary layer by diffusion where some Ca^{2+} and CO_3^{2-} are removed as they attach to the growing calcite surface. This leads to an activity gradient within the layer unless diffusion is more rapid than the surface reaction (Brady and House 1995 p.285). A gradient also exists for other ions of the CO_2-system, since CO_3^{2-} is linked through rapid ionic reactions with bicarbonate and H^+, itself linked to a much slower reactions involving the hydration/dehydration of CO_2. The chemical gradients occurring within the layer during precipitation are therefore complex and not readily computable. The processes occurring in the boundary layer during precipitation are summarised in Fig. 63. They neglect any complex formation, which is acceptable for most evasive meteogene waters excepting those containing high SO_4.

10.4.1 Models of Crystal Growth and Precipitation Rate

Several attempts have been made to provide empirical models of the $CaCO_3$ flux to the calcite surface. Experiments on the precipitation of calcite from pure solutions of the Ca-CO2 system by Nancollas and Reddy (1971) led to a precipitation rate (R) relationship of the form:

$$R = k_r (\Omega - 1) \tag{10.7}$$

Where the constant k_r incorporates the calcite solubility product constant K_c. The rate is seen to be proportional to the relative supersaturation (Ω – 1) at a given temperature. A detailed analysis by Sturrock et al. (1976) provided a more accurate relationship of the form:

$$R = -k\,[(\{Ca^{2+}\}\{CO_3^{2-}\})^{0.5} - K_c^{0.5}]^2 \tag{10.8}$$

The equation, known as the Davies-Jones model, was found to be valid for a wide range of initial conditions and lent support to the hypothesis that precipitation rates are largely surface-controlled. Meanwhile, studies of calcite dissolution rates by Plummer et al. (1978) led to the relationship:

$$R = k_1\{H^+\} + k_2\{H_2CO_3^*\} + k_3 - k_4\{Ca^{2+}\}\{HCO_3^-\} \quad (10.9)$$

The constants k_1-k_4 are functions of the reaction temperature. This relationship is termed the Plummer-Wigley-Parkhurst (PWP) model. As written it is a dissolution reaction with the k_4 term a back-reaction denoting precipitation. The flux F, of Ca^{2+} can be obtained with this equation using estimates of the ion activities at the surface, owing to the stoichiometry imposed by one Ca^{2+} ion for every CO_3^{2-} ion. Precipitation can be regarded as the reverse of dissolution and the experimental results indicated that the surface reaction mainly involves Ca^{2+} and HCO_3^-:

$$Ca^{2+} + HCO_3^- = CaCO_3 + H^+ \quad (10.10)$$

The solvated hydrogen ion is lost from the surface and enters solution. House (1981) compared the Nancollas-Reddy, Sturrock and PWP models using laboratory experiments and found reasonable agreement with the latter two. Reddy et al. (1981) found generally good agreement with the PWP model. Accordingly, Dreybrodt (1988) suggested that the PWP model was the best of those currently available for predicting precipitation rates, pointing out its generality in both calcite dissolution-and precipitation phenomena. Alternative models have also been described involving a deposition term proportional to $\{Ca^{2+}\}\{CO_3^{2-}\}$ (Brady and House 1995).

Buhmann and Dreybrodt (1987), Dreybrodt (1988) and Dreybrodt and Buhmann (1991) have developed precipitation models relevant to karst water systems employing the PWP model under a range of hydrodynamic conditions. The models are used in conjunction with rates of diffusion relevant to static film and turbulent systems for a range of temperatures and pCO_2 values. Most of this work relates to thin films relevant to speleothem formation but a model is also provided relevant to travertine formation in turbulent waters. For thin films up to 0.5 mm in thickness and with the pCO_2 at air equilibrium, the flux, F, was obtained as:

$$F = \alpha\,(Ca^{2+}{}_{eq} - Ca^{2+}{}_{d}) \quad (10.11)$$

Where α is a quantity dependent upon T and pCO_2. $Ca^{2+}{}_{eq}$ is the concentration of calcium at equilibrium in mmol L^{-1} and $Ca^{2+}{}_{d}$ the concentration in the film. Using this model, precipitation rates were found to increase with increasing temperature and film thickness up to about 0.5 mm. Rates fell with increasing pCO_2, but the temperature effect was more significant. At film thickness >>0.5 mm, turbulence is often important, especially in flowing water. Turbulence affects diffusion rates, often to a degree where the turbulent regions may be considered to have equal solute concentrations throughout. Since molecular diffusion is increased by turbulent eddies, precipitation rates can increase by up to an order of magnitude under turbulent flow when compared with laminar flow or stagnant conditions. Dreybrodt (1988) provides a model including a turbulent layer up to 50 cm in thickness, covering most travertine-depositing regimes. Based on the PWP equation, this model demonstrated that the flux increased in a non-linear fashion with increasing layer thickness up to about 50 cm. Little increase in flux was apparent above 50 cm. At the temperature used

(20 °C), a theoretical maximum deposition rate of around 19 cm a^{-1} $CaCO_3$ was obtained for a $Ca^{2+}{}_d$ of 12 mmol L^{-1}. This is in reasonable agreement with the measured deposition rates of thermogene travertines, bearing in mind their porosity of around 25% (Fig. 5) and the fact that water temperature is often somewhat greater than 20 °C. This model does not take into account the diffusion boundary layer (DBL) which inevitably exists between the bulk turbulent solution and the surface of the travertine. The presence of this layer reduces the flux of ions, and the reduction is related to its thickness, in turn depending upon the hydrodynamics of the system. For example, studies in the Yorkshire Dales, UK have shown that moss growth and travertine deposition is rapid on waterfalls (c. 9 mm a^{-1}) where there is a continuous supply of water. In seepages with low, but continuous flow, moss growth and deposition is much less and in one study ranged from 0.56–3.7 mm a^{-1} (Pentecost 1987). These differences may well be caused by turbulence. Dreybrodt (1988) provides another model accounting for the DBL. Using this approach, a Nernst Layer model was employed of the form:

$$F = D_m/\in (C_{eq} - C_b) \tag{10.12}$$

Where C_b is the concentration in the turbulent core, $\in$ the thickness of the boundary layer and D_m the molecular diffusion coefficient. The boundary layer thickness may be estimated by theory using standard hydrodynamic factors, or by using an experimentally determined rate of gypsum dissolution. Application of this model has demonstrated that the precipitation rate increases as the pCO_2 falls, and more significantly, increases as the depth of the turbulent layer increases and $\in$ falls (Fig. 64).

Increase in deposition rate with turbulence has been noted earlier and has been related to PWP models at three sites. Lorah and Herman (1991) investigated deposition rates in Falling Spring Creek, Virginia and found that the experimental rates were often considerably higher than rates calculated using the PWP model, although the DBL had not been taken into consideration. It was suggested that part of the discrepancy may have been due to underestimation of the travertine surface area. A similar study on the Westerhof stream in Germany by

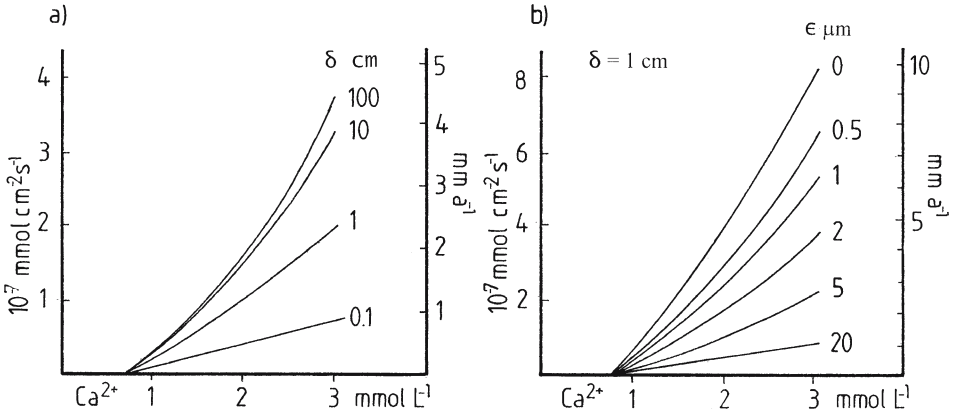

Fig. 64. Predicted precipitation rates of calcium carbonate for an open system using the layer model of Buhmann and Dreybrodt. a) Precipitation rate as a function of the calcium concentration in the bulk solution (abscissa) and the thickness of the turbulent water layer (δ). Curves for pCO_2 0.1 vol% at 10 °C and with a diffusion boundary layer $\in$ of 5 µm. b) Precipitation rate with δ fixed at 1 cm and $\in$ ranging from 0–20 µm. Curves for pCO_2 0.03% and 10 °C. The precipitation rates are given as mmol cm^{-2} s^{-1} on left ordinate and as mm a^{-1} solid $CaCO_3$ on right ordinate. Curves redrawn from those given by Buhmann and Dreybrodt (1987) and Liu et al. (1995)

Dreybrodt et al. (1992) found that the PWP model predicted deposition rates about ten times higher than actual rates obtained from marble tablets. For this site, the gypsum dissolution method was used to obtain estimates of 10–30 μm for the thickness of the DBL, and when the model was modified, satisfactory agreement with the field data was obtained. At Huanglong, China, a thermogene site consisting of a series of travertine dams, Liu et al. (1995) found that the turbulence model was in reasonable accordance with the precipitation rates obtained from marble tablets. It was also found that the deposition rates at the crests of minidams was higher by a factor of 4–5 compared with the quiescent intervening pools. Similar results were found for a series of dams in the UK by Viles and Pentecost (1999). A further study on meteogene dams resulted in similar conclusions (Bono et al. 2001). Dam crests would be expected to experience high flow rates with greater turbulence and therefore a reduced value of $\in$. It will be recalled earlier that the hypothesis of Varnedoe (1965) suggested a laminar-turbulent transition but placed emphasis on CO_2 evasion via pressure reduction rather than Ca/CO_2 transport to the travertine surface.

Complications may arise at pCO_2 levels in excess of c. 1 vol% and as $\in$ increases (Dreybrodt and Buhmann 1991; Liu and Dreybrodt 1997). Experiments of calcite dissolution rates using rotating discs have shown that under these conditions, the slow reaction $CO_2 + H_2O = H^+ + HCO_3^-$ may become rate-limiting within the DBL. The reverse reaction is also rate-limiting for calcite precipitation, and precipitation rates fall below those predicted for instantaneous reactions. Although the slow hydration of CO_2 has been known for many years, and its effects predicted, Liu and Dreybrodt also demonstrated its existence through the use of the enzyme carbonic anhydrase. When this enzyme was added to the experimental system, increases in dissolution rate were observed under the conditions described above. It leads one to speculate on the possible role of this enzyme in the free state in travertine-depositing systems.

A related problem is the form of speleothems, in which there has been much interest, and their relationship to the rate of supply of calcite-supersaturated solutions. Based upon the assumption of a known and constant supply of precipitant, Franke (1965) obtained the relationship:

$$d = 2\sqrt{c_0 q/\pi Z} \tag{10.13}$$

Where d is the equilibrium stalagmite diameter, c_0 is the calcite available for deposition, q is the flow rate of solution and Z is the vertical rate of growth. Curl (1973) showed that the above model is appropriate for a rapid flow regime. An alternative 'slow flow' mass balance model yielded a minimum stalagmite diameter of about 3 cm, close to measured values. Using the thin film model of deposition, Dreybrodt (1988) found that with slow drip rates, where it may be assumed that all of the calcium is deposited before the next drip arrives, stalagmites of about 4 cm diameter should result. Higher drip rates require a more complex expression to account for the mixing of drops, and both deposition rate and diameter increase with drip rates. Under high drip rates, diameters of 30 cm or more are predicted with the model.

Buhmann and Dreybrodt's model has also been applied to speleothem deposition rates and compared with actual rates through measurements of annual couplets. Using a static film model, Baker et al. (1998) found that for two of the three sites studied, the predicted rate obtained from the model was in reasonable agreement with the measured rates. Similar results were obtained by Genty et al. (2001). However considerable variation in the drip rates of water onto stalagmites leading to uncertainty in the estimation of long-term deposition rates prompted these workers to suggest that detailed studies should be made where palaeoclimatic information is sought.

10.5 Travertine Deposition and Discharge

Theory and experiment demonstrate that the rate of calcium carbonate deposition depends on several variables, particularly temperature, chemical composition and the stream hydrodyamics. In general, deposition will be higher in moving water because both the evasion of CO_2 and the diffusion of ions to the precipitating surface will increase. It is also of interest to explore the effect of varying discharge on the deposition rate. Neglecting for the present, the effects of photosynthesis, it would be of interest to determine how increase in discharge will change the rate of flow, water depth and thus turbulence.

It has already been noted that the deposition rate changes as water depth increases. If a diffusion boundary layer model is to be employed, the effect of increasing water flow clearly depends upon the initial and final water depths (Fig. 65). For a slot-like stream, increase in discharge does not change the surface area of the flow. If the original flow was a thin water film about 1 mm in thickness, then a ten fold increase in depth increases the precipitation rate about three-fold. If the original depth was 10 cm and it doubles, the precipitation rate increases only slightly. If the stream is not slot-like then the water surface area will increase with discharge and the effects are more complex. The greater surface area will also enhance CO_2 evasion and there will be a greater area available for precipitation. Under these conditions, one might reasonably expect to see more carbonate precipitation than the case of a slot-like stream. The above argument has tacitly assumed that a discharge increase will not affect the rate of water flow which itself influences deposition rate via boundary layer thickness changes. Clearly this is not the case, particularly with trickles where the frictional component of the benthos will be considerable. For a 'model' stream of fixed gradient with width >> depth, and under conditions of turbulent flow, the mean velocity is proportional to $\sqrt{h}$ (h = water depth), and the discharge approximately proportional to $h^{2/3}$ (Woodburn 1932; Smith 1975). For example, doubling the depth of a slotted stream from 10 –20 cm would result from an approximate threefold increase of discharge. Increasing discharge therefore increases the rate of flow but in a non-linear fashion. This increase in flow will reduce the thickness of the boundary layer $\in$, also increasing the precipitation rate.

It would appear therefore, that in general an increase in deposition rate is to be expected with an increase in discharge although the exact rates cannot be predicted as it is dependent upon stream geometry. This is a neglected topic in travertine hydrogeology although Kano et al. (1999) in their investigation of the Shirokawa travertine of Japan did report such a correlation. However, Drysdale and Gillieson (1997), Drysdale et al. (2003a) and Ihlenfield et al. (2003) found the reverse. Deposition increased as discharge fell in some Australian streams. There are several processes that could lead to a reversal of the 'expected' relationship. For instance, a significant fall in discharge of a meteogene stream will result in more rapid warming of the groundwater leading to greater CO_2 evasion and evaporation. In an arid climate with low air humidity this could be important. In addition, where travertine-dammed pools abound, the residence time of the water in the pools will increase under low discharge allowing more time for CO_2 evasion. If rates are measured on artificial substrates, increased discharge will lead to more vigourous erosion, with the possibility of erroneous conclusions based upon unknown losses. Also, the effects of photosynthesis may become significant when discharge falls, a topic to be discussed later. These factors, among others are summarised in Table 27.

Table 27. Positive discharge effects on meteogene travertine deposition in streams

Low discharge	High discharge
Photosynthesis more significant due to limited DIC	Greater dissolved chemical load for precipitation
Reduced erosion	Increased flow velocity will reduce the diffusion boundary layer, increasing precipitation
Proportionately greater evaporation	Increased turbulence promoting CO_2 loss
Insolation warms water promoting CO_2 evasion and increases the calcite supersaturation	Increase in water surface due to edge flooding, frothing and splashing promotes CO_2 loss and increases crystal growth area
Where discharge varies over short periods (days, weeks) the Ca and DIC will tend to increase due to the longer groundwater residence time ('base flow')	

10.6 Inhibitory Effects

Mention has been made above of the possible effects of inhibitors on travertine deposition. For example Liu et al. (1995) suggest that the slight reduction of observed rates of deposition compared with those predicted by the models of Dreybrodt and Buhmann could be explained by the inhibition of calcite deposition by Mg^{2+}. They cite a study by Reddy (1986) who found a significant reduction in the calcite growth rate in the presence of Mg^{2+} in the millimolar range, but the necessary levels of Mg are only encountered in some saline and thermogene waters. A wide range of other cations may also interfere (Meyer 1984). Orthophosphate is another potential inhibitor and according to Casanova and Lafont (1985) could inhibit precipitation at concentrations as low as 0.05 ppm. The seasonal variation of P in speleothem is also thought to be of potential significance in cave calcite precipitation (Huang et al. 2001). Organic phosphates such as ATP are also active (Meyer 1984) and may enter a watercourse as a result of biological degradation. Sulphate may also interfere (Brady and House 1995). Other natural substances can also inhibit crystallization by adsorption. They include the ubiquitous humic and fulvic acids (Morse 1983; Lebron and Suarez 1996) and the extracellular polymeric substances of cyanobacteria (Kawaguchi and Decho 2001). The humic and fulvic acids have been deemed responsible for the lack of travertine deposits in a number of UK limestone streams draining areas of blanket bog (Pentecost 1992b), although humates, as noted above could also nucleate calcium carbonate. An experimental study by Lebron and Suarez (1996) demonstrated inhibition of calcite crystal growth at dissolved organic carbon levels as low as 0.05 mmol L^{-1} and inhibition of nucleation at around 0.3 mmol L^{-1}. The inhibition of calcium carbonate deposition in the sea has long been suspected to result in part from the adsorption of fatty acids and other substances associated with algal biofilms (Bathurst 1976). There are clearly plenty of candidates for calcite crystal growth inhibition in the natural environment, and there is some evidence for inhibitory effects. The problem will be addressed further below. Artificial inhibitors of calcite precipitation are discussed in Chapter 15.

10.7 Biological Processes

There are many reports of biological activity influencing travertine formation, ranging from the direct precipitation (and dissolution) of calcium carbonate, to control over its fabric and structure. The latter have already been discussed (Chapters 3 and 9), and in this section the focus will be upon the precipitation and dissolution of travertine by organisms.

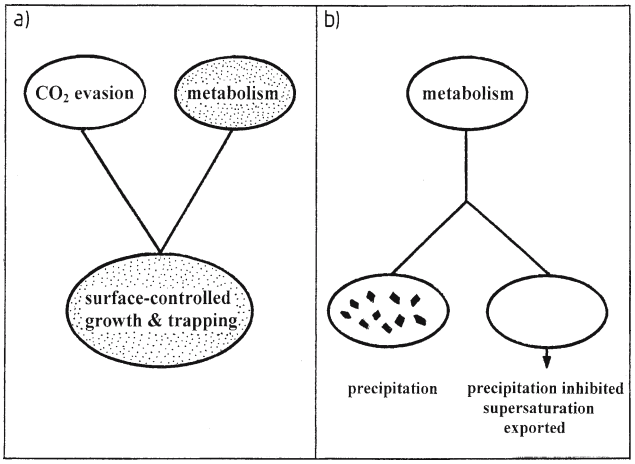

Fig. 65.
Relationships between biogenic and inorganic precipitation within algal/bacterial colonies and the effects of inhibition. a) Calcium carbonate supersaturation is sourced by both CO_2 evasion and metabolism. In an algal/bacterial colony, both processes feed into surface-controlled growth and/or trapping within the colony. Stippled areas indicate a biological influence. b) Supersaturation sourced in metabolism can only result in precipitation within a colony if nucleation/growth inhibitors are absent (left). In their presence, the supersaturation will be exported (right)

It has long been recognised that calcium carbonate precipitation can result from biological activity. A walk along the seashore will reveal numerous examples in the marine arthropods and worms, as well as in sponges and corals. Calcified plants are less often encountered but are known among the algae. They include the marine genera *Corallina* and *Halimeda* and the freshwater alga *Chara*. The algae and bryophytes in particular are major colonisers of travertine and among the former there are some calcified freshwater species.

In plants it is widely assumed that photosynthesis drives calcification. In many cases this has been reasonably well demonstrated but it is by no means well established in all groups, even within the marine environment where most of the research has been done. Carbonate should be deposited with a 1:1 stoichiometry with photosynthetic carbon dioxide uptake from a calcium bicarbonate type water (Eq. 2.1). Several algae have been found to calcify with this stoichiometry (Pentecost 1990c and references therein), providing support for this hypothesis. Other metabolic processes also result in the precipitation of carbonates. For example, deposition can occur through nitrate uptake and metabolism, bacterial sulphate reduction and methanogenesis (Castanier et al. 2000). This type of deposition may also be described, along with photosynthesis, as 'metabolic'.

Plant and microbial surfaces may also provide favourable sites for calcium carbonate nucleation or particle-trapping, providing a nucleation or growth site (Section 10.4.3) where the bulk solution is supersaturated with a carbonate mineral phase. They may excrete biopolymers containing repeated sequences of carboxyl groups permitting the epitaxial growth of a mineral phase. This precipitation process may be described as 'surface-controlled'.

It is therefore evident that both metabolism and evasion of CO_2 can result in mineral supersaturation which can feed into a surface-controlled process where organisms are present. That this is a sequence of events rather than a synchronous 'all or nothing' process is often unappreciated in the literature with the effects of metabolism confused with surface-controlled precipitation via CO_2 evasion. Another important but neglected factor is the influence of nucleation/crystal growth inhibitors of biological origin. There is increasing evidence for the existence of these substances in algae (Kawaguchi and Decho 2001) and they may be widespread in organisms as a whole. Thus, while metabolism may provide a source of calcite supersaturation, a nucleation inhibitor could prevent the formation of calcite within the photosynthesising biofilm and the supersaturation may be exported to the bulk phase or an adjacent region where inhibitors are absent (Fig. 65).

The role played by organisms in travertine deposition is therefore manifold, and several processes may act in consort, either aiding precipitation or preventing it. The opinion of travertine researchers on this topic is divided. Of the 48 senior authors found expressing a view in the literature over the past 40 years, 26 stated or implied that abiotic processes are the dominant mechanism, and 14 each thought that either photosynthesis and/or surface-controlled/trapping processes were dominant or at least relevant to travertine formation.

In this section the evidence for metabolism, with emphasis on photosynthesis as a mechanism of travertine deposition is explored. It is examined with other processes leading to the encrustation of plants with calcium carbonate in an attempt to determine the significance of the process and its implications. It is instructive to divide the travertine-associated plants into three groups: the non-photosynthetic bacteria; the photosynthetic bacteria and algae; the bryophytes/higher plants. For, although the processes have much in common, they differ in detail.

10.7.1 Non-photosynthetic Bacteria

While microbes have frequently been shown to cause mineralisation, and often with good reason (Lowenstam 1990) their implication in travertine formation remains controversial. Folk (1994) in a study of the Central Italian thermogene travertines provided a series of high-resolution scanning electron micrographs showing rounded bodies interpreted as nanobacteria. The bacteria occurred on both aragonite and calcite at Le Zitelle and were intimately associated with these minerals. The aragonite needles, aggregated into sheaves and spherulites were often tipped with subspherical bodies. The needles were parallel-sided, and mostly 0.1–0.4 μm in diameter with the nanobacteria slightly larger. Since bacterial cells usually have negatively-charged walls (Beveridge 1989), Folk argued that calcium ions would be attracted to the wall surface and be concentrated there. This would raise the $\{Ca\}\{CO_3\}$ ion product leading to supersaturation and carbonate precipitation. Since the bacteria sit atop aragonite needles, he argued that the crystals would build up from the tips thus explaining their parallel-sides. Similar bacteria were seen on calcite where a different mechanism was envisaged. Nanobacteria colonised the entire calcite surface, allowing, as before, the calcium ions to be concentrated close to the crystal surface to be incorporated there. In this case, the bacteria are not displaced by crystal growth as in aragonite, but divide, with the lower cells becoming engulfed by calcite and incorporated into the crystal fabric.

Several objections can be raised against these mechanisms. For example, bacterial division would have to be carefully synchronised with crystal growth and the subsequent growth direction for new spherulites and sheaves would frequently oppose that predicted by the 'keimauslese' hypothesis described by Lippmann (1973). Travertine deposition at Le Zitelle is extremely rapid, up to 3 mm per day. Folk calculated that each spherulite took about 10 minutes to grow. This is probably a reasonable estimate and if correct provides a further reason to doubt the mechanism. Estimates of approximately 900 aragonite needles per spherulite can be made from Folk's figures. If we start with a single bacterium dividing to produce the first needle, a total of 10 divisions is required to produce 900 needles each with its own bacterium. The doubling times of well-studied bacteria such as *E. coli* are known to be a minimum of about 20 minutes. The time is required for completion of the complex process of DNA replication and protein synthesis. Nanobacteria, if they exist, may divide more quickly than this as they are smaller, but it stretches the imagination to believe that they would replicate in the 60 seconds required by this model. In fact, if spherulites evolve from sheaves, two separate bodies result, so that the number of bacteria would have to be doubled again.

Most bacterial cells have negatively-charged surfaces and it is doubtful if their short range and low charge density would be sufficient range to affect the local supersaturation. A further objection can be raised with reference to the thermodynamic properties of the Zitelle waters. According to Folk's own chemical data, the waters of Le Zitelle within the area sampled are highly supersaturated with respect to both aragonite and calcite ($\Omega > 20$) so there is no need for it be raised further by the mechanism proposed. Folk's bacteria would also need to be resting, rather than attached to the (001) aragonite face. If attached by mucilage, diffusion of ions would be retarded. If they were merely resting upon the tips of the needles they would be physically unstable. In the size range 0.1–0.4 μm, Brownian motion would soon dislodge these bodies and their integrity would be lost.

At the same time Folk was investigating the Italian travertines, Katherine Terry obtained with me a series of bacterial isolates from travertines in other parts of Europe. We conducted a number of bacteriological tests and for each isolate we took the equivalent of 500 cm^2 of cell surface, washed it free of nutrient broth and added it to metastable solutions of calcium bicarbonate at pH 6.3 (Pentecost and Terry 1988). We then aerated the flasks to simulate CO_2 evasion and looked for signs in precipitation. In our calcite controls (no bacteria) we found clear evidence of calcite precipitation, but none was found in any of the 44 isolates tested. While the isolation procedure would have been selective, these experiments demonstrate that a wide range of taxa (11 genera were identified) were not conducive to surface-controlled growth of calcite. Observations of fresh travertine surfaces by Arp et al. (2001) and Pitois et al. (2001) have also shown a lack of calcification around bacterial colonies. Together these studies show that a wide range of travertine bacteria do not play a significant role in surface-controlled travertine growth. Not all bacteria behave in this way. A filamentous *Thermothrix* was found to nucleate aragonite at Mammoth Hot Springs (Farmer and Des Marais 1994a) and there is some evidence that non-filamentous bacteria may participate in the formation of a particular type of aragonite spherulites where they occupy a central position, with the needles growing away from the centre (Pentecost 1990b; Guo and Riding 1992). These observations by no means negate metabolic processes leading to supersaturation. In fact many of Katherine's isolates showed positive for base production. The bases included ammonia and ammonia production is a likely process in the travertine biofilm. Its overall significance however is hard to gauge. Ammonia production requires a nitrogen source, normally protein or a breakdown product. Protein will be present in the organic matter fraction of the biofilm, but the amount converted to ammonia is unknown. It is likely to be a small fraction of the total nitrogen present. Values could be estimated using microelectrodes, but the overall effect on carbonate deposition would be difficult to determine. It it probably small when compared with photosynthesis since nitrogen is about five times less abundant than carbon in organic matter.

During our visits to the sulphur springs of Bagni di Tivoli in the early 1990s, Paulo Tortora and I collected samples of photosynthetic bacteria from sulphur scums and travertines. The bacteria were purified in the laboratory so that single strains could be investigated. Our older cultures of *Chlorobium chlorovibrioides* were found to contain colonies of extremely small cells in the range 0.3–0.4 μm. The cells were found later to represent a stationary phase, probably responding to nutrient stress in the culture medium, a phenomenon that has been reported before (Pentecost 1995b). Structures of the same size have been reported from boiling springs by Jones and Renaut (1996). Although cells of this size were not found in our travertine samples, they are among the smallest bacteria isolated from travertine. Bearing this in mind, some fresh travertine was collected from Bagnaccio, one of the Viterbo group and immediately fixed in buffered glutaraldehyde to preserve the organic structures. We then decalcified with EDTA, stained and impregnated the samples with resin and examined ultrathin

sections with an electron microscope. A day was spent searching for signs of nanobacteria among the 'normal' bacteria in the samples, but no candidates were found. This helped confirm my initial doubts about the existence, or at least significance of extremely small (<0.2 μm) organisms in travertine.

Others have also expressed doubts about their existence. For example, a report of DNA in nanobacteria was found to be based on a flawed procedure (Abbott 1999). Structures, below 50 nm in size, also interpreted as nanobacteria by Folk at Le Zitelle could be either etching artefacts or caused by non-living organic contaminants (Kirkland et al. 1999). A study at four thermogene travertine sites using electron microscopy (Allen et al. 2000) showed the presence of minute rounded particles of opaline silica and flourite in the same size range as nanobacteria. The particles were often associated with bacterial polysaccharides but organic matter was not detected within them. They considered that these particles were associated with microbial exopolymer production but were unlikely to have been the mineralised remains of microbes. It is also possible that the inorganic pseudofilamentous silica-carbonate structures synthesised by Garcia-Ruiz et al. (2003) could be mistaken for nanobacteria. Such structures could form during the chemical changes occurring during sample desiccation. Small spherical growths of calcium carbonate also form in the presence if high concentrations of alkali metals such as Na (Wilken 1980). Concentration would occur as specimens dried through evaporation. It can be concluded that as yet, there is no convincing evidence for the existence of nanobacteria in travertine.

10.7.2 Photosynthetic Microbes

Photosynthetic microbes are major primary producers in travertine-depositing systems as they colonise surfaces unfavourable to more structurally complex plants. They can also grow in waters too hot for other plants and those containing dissolved sulphide that is toxic to most other forms of life. Algae, including the cyanobacteria, and also the photosynthetic bacteria are referred henceforth as the microflora since they are conveniently treated together. Unlike the bryophytes, some members of the microflora undergo calcification that shows a considerable degree of structural control.

Chafetz and Guidry (1999) described regular alternations of travertine shrubs and silt-sized micrite aggregates from several thermogene travertines of Italy and elsewhere. They considered the cycles to be annual, implying that shrub growth was seasonal and linked to a growing season. Seasonality of growth is usually associated with favourable light and temperature conditions. In hot springs, light would be the main variable linked with growth, implying the influence of seasonal photosynthesis by microbes. UV-flourescence microscopy of thin sections of shrubs demonstrated the presence of organic matter, and although direct evidence of microbes was scant it was concluded that microbes were responsible for shrub formation. However, in a previous study of the aragonite shrubs at Mammoth Hot Springs, the author failed to find convincing evidence for significant microbial influence of shrub formation (Pentecost 1990b). Shrubs were collected from the minidam pools at Canary Springs and examined for signs of microbial precipitation. Only on rare occasions were aragonite crystals seen to have developed on microbial surfaces. Bacterial numbers were estimated as 0.6–1.7 x 10^5 mm^{-3} and the organic carbon content of the travertine was low (mean 0.54% wt). Stoichiometric calcium carbonate precipitation as a result of photosynthesis would be negligible. Chafetz and Giudry (1999) believe that the associated microbes acted as catalysts for calcium carbonate precipitation in these shrubs, although details of the mechanism were not provided. This might occur, but it fails to explain why bacteria, ubiquitous as they are,

should catalyse shrub formation only at certain times. Shrub formation should occur throughout the season, even when the bacteria were not actively dividing if surface catalysis is responsible. In addition, the exposed aragonite surface, exhibiting favourable crystal growth planes, should provide at least as good a nucleation/growth surface as the bacterial surfaces, since the bathing solutions are highly supersaturated with respect to aragonite. At Minerva Terrace, shrub bacterium numbers translate into a surface area of about 5 cm^2 cm^{-3}, assuming an average cell diameter of 1 μm. This compares with a total travertine surface area of almost 3 m^2 cm^{-3}, as measured by gas adsorbtion, a difference of more than three orders of magnitude. Even given the uncertainty involved with bacterial counts which probably gave an underestimate, precipitation directly onto aragonite should predominate. To suppport their case, Chafetz and Guidry argued that bacterial metabolism can be likened to that of a human being. A human, over a lifetime consumes a vast amount of energy as food when compared with its mass. Therefore large amounts must be returned to the environment, influencing its chemistry. This is a fallacious argument when applied to bacteria. Most of the carbon (at least 50%) entering a photosynthetic microbe is normally stored or used in growth. The remainder is used for metabolism, the end product of which, for a photosynthetic microbe, is largely carbon dioxide and water. When the former is returned to the environment, it will dissolve, and not precipitate aragonite.

Although some kind of bacterial influence over shrub morphologies, such as those of the Italian sulphureta is highly probable, precipitation is more likely to be influenced by the presence of extracellular polymeric substances (EPS) rather than the organisms themselves. It is also possible that the EPS is largely responsible for the flourescence of shrubs under UV light.

In the cyanobacteria, calcification has been shown to occur in several genera. Again the 'mucilage' (EPS) is involved. In *Phormidium incrustatum*, perhaps the commonest travertine-associated species, calcite is deposited within the mucilaginous sheath or at the sheath surface. In *Rivularia*, precipitation is also observable within the outer layers of the sheath (Caudwell et al. 2001). Microenvironments can be envisaged simulating semi-enclosed spaces (cf. bryophytes, below), as for example where the trichomes form parallel bundles, enclosing narrow tubes of water, or where the filaments cross each other. This has been explored in *Phormidium* where cross-over points are common (Pentecost 1995d) and may well provide early crystallisation centres for calcite.

Among the travertine diatoms, some have been shown to calcify their stalks. For example, Winsborough and Golubic (1987) and Winsborough (2000) describe calcification in *Gomphonema* and *Pleurosira* respectively. It is also recorded in an unidentified species by Pedley et al. (1996) and in *Didymosphenia geminata* (Photoplate 15B). More often, diatoms are found to be loosely associated with irregular micrite grains, probably associated with mucilage, although statistical analysis revealed that at one site *Rhopalodia gibba* was closely associated with micrite grains (Pentecost 1998). This is not always the case however. For example, Arp et al. (2001) noted that some moss surfaces with abundant diatoms were almost free of deposits.

Lowenstam (1986) distinguishes two forms of biomineralisation: biologically controlled and biologically induced. In biologically controlled calcification, crystal growth is controlled by an organic matrix to form regular and well-defined mineralised structures. In many cases the structures can be shown to provide a means of support or protection for the organism. In biologically induced calcification, there is no control over the crystal form, but metabolic activities of the organism lead to calcite precipitation, often in the immediate vicinity. The distinction is usually made on the basis of microscopic observation of the organism and its style of mineralisation. There is a wide range of mineralisation mechanisms described in the literature but few have been identified in the freshwater algae. Good examples of biologically

controlled calcification are scarce, and on travertine confined to a few green algae (*Chara, Oocardium*) and possibly some diatoms (*Gomphonema*). Even here however, the level of organisation is low and their *raison d'être* unclear. Biologically induced calcification is probably much more common as for example in the cyanobacteria. However in species such as *Rivularia* some degree of control is apparent and the calcified colonies are probably protected from water shear and perhaps grazing. Photosynthesis has also been shown to precipitate at least some of the calcite in *Rivularia*. However in other travertine cyanobacteria, the significance of photosynthesis has not been explored. In the case of the green alga *Oocardium*, photosynthesis probably plays little part in the calcification of its mucilage tubes yet the mineralisation is under structural control. Clearly, the terms 'biologically induced' and 'biologically controlled' are open to interpretation and should not be too strictly applied in the examples above.

There has been considerable interest and speculation concerning the role of cyanobacterial EPS in the nucleation and growth of calcite crystals. Merz-Preiss and Riding (1999) suggest that deposition within the EPS may be restricted to high pH environments where photosynthetic HCO_3^- transport is favoured. They cite some evidence for this and suggest that OH^- export could lead to localised precipitation.

It has also been noted that some algae of travertine-depositing streams are not associated with calcite. For example, colonies of the cyanobacterium *Nostoc verrucosum* grow in Waterfall Beck but show no sign of mineralisation. *Nostoc* produces copious EPS and it is likely that a nucleation or crystal growth inhibitor is produced by this organism. Algae such as *Nostoc*, will photosynthesise and their effects on the water may then be felt at a site distant from that plant, probably downstream. Arp et al. (2001) speculate that travertine cyanobacteria produce EPS rich in carboxylate groups under times of stress. The type of stress was not discussed but would include nutrient limitation and high irradiance. Epitaxial growth of calcite on carboxylate-rich surfaces would then lead to a higher rate of nucleation during these periods leading to the observed differences in travertine fabric.

It is apparent then, when considering photosynthesis and its effects on travertine formation that calcite may be formed *in situ*, where inhibitors are absent, or deposited at distance where they are present, either in other parts of the colony or further downstream. Different calcification styles might reflect different uptake mechanisms of carbon dioxide and different fabrics result from a variable EPS biochemistry. A summary illustration is provided in Fig. 66. Here, an algal colony surrounded by a bulk solution with a pH of ~ 8.0 and alkalinity of ~ 4 mmol L^{-1} in equilibrium with calcite is considered. These conditions are similar to those of many travertine-depositing waters although they would normally be supersaturated with respect to calcite. The figure is divided vertically to include situations where EPS calcification occurs, and situations where inhibitors prevent it. On the left, calcification occurs in the EPS and three mechanisms are shown for the uptake of carbon dioxide into the cytoplasm with EPS carbonate precipitation. The illustration accounts for situations where the uptake of carbon dioxide into the cytoplasm is either passive (CO_2) or active (HCO_3^-). There is evidence for both processes in the algae (Bhaya et al. 2000). If uptake is passive then carbon dioxide diffuses into the cytoplasm from the EPS and the simple mechanism shown in Fig. 66a operates. In Fig. 66b carbon dioxide in the EPS reacts with water to produce bicarbonate and H^+. This is one variant of active ion uptake and requires the co-transport of an anion (HCO_3^-) with a cation (Na^+ or H^+) to maintain electroneutrality. Path c) is a variant where a bicarbonate ion is taken up into the cytoplasm and a hydroxyl exported. Hydroxyl is generated by intracellular carbonic anhydrase. The exported hydroxyl then reacts with another bicarbonate ion and a calcium ion in the EPS to form calcite and water. There is

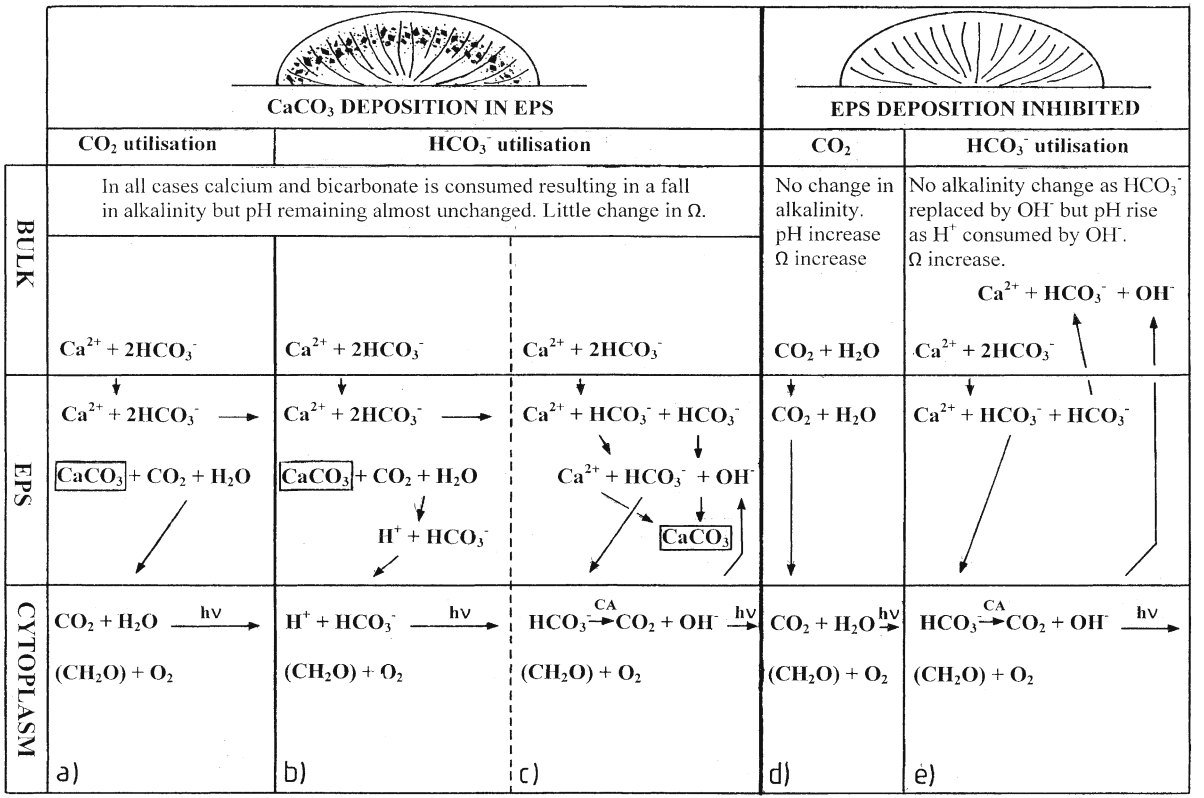

Fig. 66. Chemical processes associated with algal photosynthesis within the bulk solution, EPS and algal cytoplasm. Two scenarios are shown both with a bulk solution of pH ~ 8.0 and an alkalinity ~ 5 meq L^{-1} at equilibrium with calcite ($\Omega = 1$). On the left, calcium carbonate is deposited within the EPS of a button-shaped algal colony, illustrated above. The removal of bicarbonate and Ca^{2+} results in minimal change to Ω in the bulk, irrespective of whether HCO_3^- or CO_2 is utilized by the algae. On the right, calcium carbonate is not deposited within the colony owing to the presence of inhibitors. Here, the bulk may undergo a significant chemical change and Ω increases. Note the alternative pathways for HCO_3^- utilisation where calcification occurs and the involvement of carbonic anhydrase (CA) in some pathways. See text for further details

some experimental evidence for this mechanism in members of the green algae and cyanobacteria, though it should be noted that other mechanisms are possible such as the co-transport of Ca^{2+} or Na^{+}. In all of these cases, there is little change to the bulk medium. Calcium and bicarbonate ions diffuse into the colonies and become fixed. The alkalinity of the bulk falls but the pH and Ω remains little changed. Where calcium carbonate deposition is inhibited within the EPS, changes in the Ca-CO_2 system differ, as shown on the right of Fig. 68. Molecular CO_2 in the bulk diffuses through to the cytoplasm and is reduced during photosynthesis (Fig. 66d). In the case of active bicarbonate uptake, calcium and bicarbonate ions diffuse into the EPS (Fig. 66e) and the bicarbonate/hydroxyl port(s) operate as in c) above. The net result in the bulk is the same, hydrogen ions are consumed and both pH and Ω rise. This results in calcite supersaturation in the bulk with the potential for biological travertine formation downstream.

Several mechanisms therefore provide the same overall result but there are complications. For example it has been assumed that the source of the Ca and DIC is the bulk solution, but this fails to take account of any diffusion from *below* the colony. Here, respiratory carbon dioxide from decaying biofilm could supplement that available in the bulk, and up to half of the incoming DIC could be sourced from this zone, providing the upwards diffusion rate greatly exceeded the infiltration rate. Its significance remains unknown. Second, the simplifying assumption for the bulk to be at calcite saturation is rarely met. Travertine-depositing waters are almost invariably supersaturated with calcite, with the potential for spontaneous calcite precipitation in the absence of biological activity. This does not negate the effects of photosynthesis, but makes interpretation of biological events almost impossible in the light of the uncertainty of the critical supersaturation for crystal growth in complex organic microenvironments.

At least two approaches can assist with an understanding of the microenvironment within an algal colony and its likely impact on the bulk. One can obtain estimates using known CO_2 uptake rates by algae, or one can probe algal colonies with microelectrodes to determine some of the relevant chemical parameters. For example, using representative mean meteogene data for depositing waters of DIC 4 mmol L^{-1}, Ca 2.9 mmol L^{-1} and pH 7.8, a theoretical upper pH limit when all CO_2 has been removed from water by evasion and photosynthesis can be determined (Talling 1976). For the above composition the limiting pH is 11.9. No measurements approaching this value have ever been made over evasive meteogene travertines. This is partly due to the difficulty of measuring pH within the laminar layer, but more importantly, diffusion of DIC from the turbulent layer above would normally ensure that this limit was never reached. However, assuming no initial loss of CO_2 to calcite precipitation and a linear decline of DIC with the pH increment, Ω values exceeding 50 are soon reached (at c. pH 9.0) demonstrating the potentially high supersaturation which can be attained from photosynthesis. Even higher pH values have been obtained within photosynthesising colonies of the cyanobacterium *Rivularia* using a pH microelectrode (author unpublished). These colonies precipitate calcite and are often found upon travertine. At present however, there is no reliable method to probe colonies to obtain reliable DIC estimates using microelectrodes, so the calcite saturation state within them remains indeterminate.

Using the same average water composition, it is possible to estimate the thickness of the layer of static water that would be exhausted of its DIC using a photosynthesising biofilm within one day. If it is assumed that all of the DIC is obtained only from this layer, and a mean net production rate of 0.5 g C m^{-2} d^{-1} used (see below), the layer thickness is close to 1 mm. Thin, static films of water should therefore be strongly influenced by photosynthesis in the biofilm. Thin static films however, also degas their excess CO_2 in a matter of minutes.

10.7.3 Bryophytes and Higher Plants

Travertine-associated bryophytes in meteogene waters are significant primary producers and their photosynthetic activity must influence water chemistry and travertine formation. The effects of photosynthesis will vary according to the hydrological regime, three broad categories of which are recognisable: complete inundation, capillary flow as a result of evaporation and capillary flow from spray and water drops (Fig. 67).

Where bryophytes are completely submerged, the carbon dioxide required for photosynthesis is obtainable only from the surrounding water. Removal of CO_2 therefore alters the carbonate system in the usual way and promotes precipitation. Fully submerged bryophytes such as *Jungermannia atrovirens* have a prostrate growth form and must receive most CO_2 directly from the water, but most species prefer to grow as emergents, with their photosynthetic parts in the capillary zone. For example, in a Europe-wide study of travertine bryophytes, 86% of the 200 sampling units contained only emergent bryophytes (Pentecost and Zhang, *unpublished*).

For emergents, two broad categories are recognisable (Fig. 67b,c). Where seepage occurs only from below the cushions, water rises up the bryophyte stems and leaves by capillarity. Flow is induced by evaporation and calcium carbonate is precipitated. A small experiment was conducted on the common travertine-associated moss *Palustriella commutata* to determine the rate of ascent of water by capillarity. A moss plant, suspended in dilute India Ink at a temperature of 15 °C, air flow of 0.5 m sec^{-1} and relative humidity 70% showed a rise of about 3 mm and 0.8 mm min^{-1} along the main axis and leafy side branches respectively. Given that a thin layer of water (c. 0.1 mm) equilibrates its carbon dioxide with the atmosphere in a few seconds (Dreybrodt 1980), it is clear that rapid gas exchange would occur close to the base of the stem. Any subsequent loss of CO_2 in the capillary water due to photosynthesis would be replaced primarily by atmospheric carbon dioxide. Under capillary flow, it would therefore appear that photosynthetic deposition of calcium carbonate would be limited and deposition, as a result of gas evasion, confined largely to the stem base. This would explain the frequent occurrence of travertine build-ups around the stem bases of *Palustriella* and other travertine mosses. The importance of evaporation under capillary flow has been demonstrated in another study of bryophytes in the UK. Here cylindrical samples of moss plus travertine were set up as miniature lysimeters. The samples were placed in open plastic containers allowing seepage water to pass through the travertine beneath while the cylinders could be removed at regular intervals for re-weighing to measure water loss by evaporation.

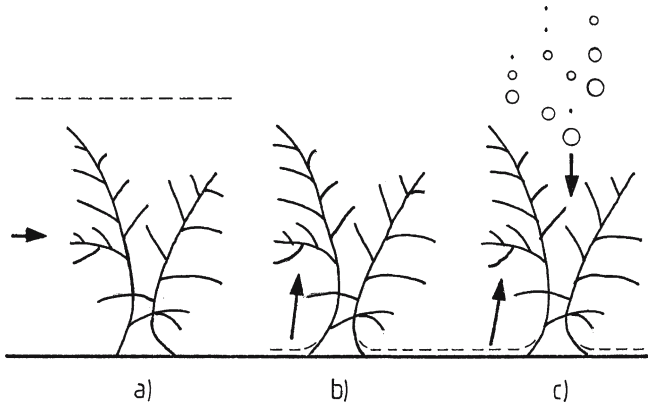

Fig. 67.
Water-flow regime for travertine bryophytes illustrated with *Palustriella commutata*. a) complete inundation; b) capillary flow from below; c) capillary flow from below and water drops from above. Arrows show direction of water flow, broken line represents water level

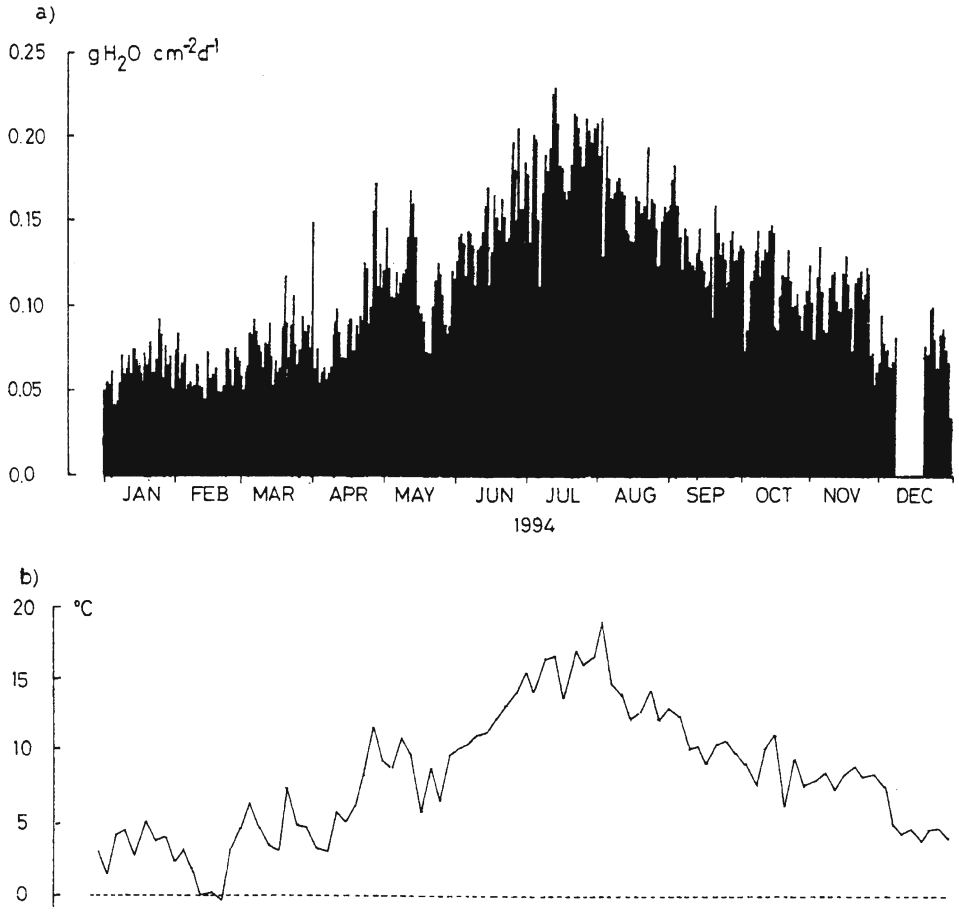

Fig. 68. Predicted evaporation rates and air temperature at a moss-covered travertine surface subject to seepage water at Gordale, UK during 1994 (From Pentecost 1996)

Net photosynthesis was estimated by the growth rate of the moss and the amount of travertine deposited by a direct measure of the deposition rate. By this means, it was estimated that between 6–12% of the travertine was deposited as a result of photosynthesis, 10–20% through evaporation and 70–80% through CO_2 evasion (Pentecost 1996). Evaporation was measured throughout the year and related to air temperature (Fig. 68). The photosynthetic component is a maximum figure since it assumes that all of the fixed carbon originated from the water, and this is unlikely as explained above. In this example, the bryophytes were growing below an overhang and received negligible precipitation.

In the majority of cases, bryophytes will receive precipitation and this will set up a flow in the opposite direction. Raindrops will probably dissolve some of the deposited calcite and perhaps re-deposit it below through evaporation. Further evidence of evaporation is the frequent occurrence of small travertine beads about 1 mm in diameter at the tips of moss stems and leaves prone to desiccation on overhang sites. Presumably the evaporation rate is highest at the extremities, leading to the formation of rounded and localised accumulations of carbonate.

In a study of the stable isotopic composition of bryophyte organic carbon, it was found that travertine-associated bryophytes obtained some of their carbon from the atmosphere since the bryophytes most persistently in contact with the springwater had the lowest $\delta^{13}C$ values (Pentecost 2000).

Close observation of bryophytes in areas of turbulent flow, such as cascades shows that capillarity alone is normally confined to the wet stream margins, and bryophytes closer to the stream centre receive trickles and splashes of water from above (Fig. 68c). In this, the second case of capillarity, the flow of water along a bryophyte stem is more complex and a net flow down the stem is likely. Under these circumstances evaporation is less significant and photosynthetic activity is probably enhanced. The phenomenon frequently occurs on waterfalls. On the great cascades of Jiuzhaigou, China, Pentecost and Zhang (2000) found evidence for photosynthetic precipitation of calcium carbonate in three bryophytes, *Bryum setchwanicum*, *Gymnostomum subrigidulum* and *Fissidens grandifrons*. In all of these species, the leaves fold over to form a semi-enclosed space similar to that found in some of the marine calcifying algae such as *Halimeda* (Fig. 69a). In *Halimeda*, these spaces allow carbon dioxide to be removed by photosynthesis while retarding its ingress from the external medium. Structurally, this confinement should promote precipitation on bryophyte leaves although its significance is likely to be limited for emergent bryophytes owing to the much greater rate of diffusion of CO_2 in air when compared with water. It requires further study and it is worth noting that the leaf anatomy is unlikely to have evolved for the purpose of depositing carbonate, as these bryophytes are cosmopolitan in distribution, occurring in a range of water types. It is also worth mentioning that some travertine-associated bryophytes such as *Philonotis calcarea* possess waxy, water-repellent leaves where capillarity is altogether inhibited.

Bryophytes are often colonised by algae and the biomass of the latter can exceed that of bare travertine. For example, in Waterfall Beck, the mean annual biovolumes of epiphytic algae on the bryophytes *Palustriella commutata* var *falcata* and *Rhynchostegium riparioides* amounted to 0.69 and 1.82 $mm^3\ cm^{-2}$ respectively, whereas the average for travertine free of

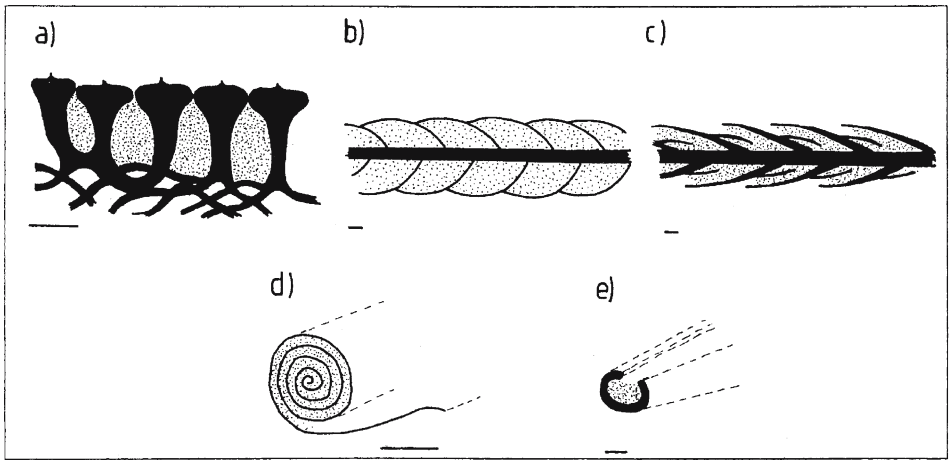

Fig. 69. Structural similarities between marine calcified algae and three travertine-associated bryophyte genera. Plant tissue filled, intercellular space (ICS) stippled. Bar 50 μm. a) section through the marine alga *Halimeda*; b) stem and leaves of *Bryum setchwanicum*; c) stem and leaves of *Fissidens grandifrons*; d) section through the marine alga *Padina*; e) leaf tip of *Gymnostomum subrigidulum*. From Pentecost and Zhang (2000)

bryophytes was 0.52 $mm^3\ cm^{-2}$ (Pentecost 1991b). The bryophyte biovolumes per unit area were 50–100 times higher than their algal epiphytes. In common with bryophytes and bacteria, algal colonies can provide a large surface area for the nucleation or trapping of calcite. This is noticeable in the large, dense growths of *Vaucheria* on travertine dams, and on *Rhizoclonium* colonising artificial substrates (Malusa et al. 2003).

Mention must also be made of the possible role of aquatic macrophytes and other organisms. Most macrophytes only thrive on soft or rubbly substrata where they can root. In travertine-depositing systems these are usually found only in lentic areas where fine sediments can be deposited such as pools and lakes. Here, calcifying species such as *Chara* (an alga) and *Potamogeton* deposit calcite on their leaf surfaces via photosynthesis. Their overall contribution is probably small, unless large and shallow lake systems are present. Surface-controlled deposition may also occur, mediated in part by algal and bacterial epiphytes. Dense swards of macrophytes also act as a baffle, trapping suspended material. The silk nets of insect larvae have been shown to play a similar role.

10.7.4 Photosynthesis and Respiration

The productivity of travertine plant communities is of significance both ecologically and geochemically. Photosynthesis of aquatic species provides an important sink for carbon dioxide and that may lead directly to travertine deposition. Unfortunately, data for travertine-depositing systems are limited (Table 28). Most primary production measurements are given as hourly or daily rates making annual estimates speculative. Only two streams, Waterfall Beck and the Ohanopecosh Hot Springs have seasonal data permitting an estimate of the annual rate. The productivity of Waterfall Beck is overall, fairly low and probably attributable to the cool temperate climate with an average stream temperature of 10 °C. There are clear differences between the productivities of the bryophyte and algal communities in this stream, the former being the most significant but it must be borne in mind that a proportion of bryophyte photosynthesis is direct from the atmosphere. Data for hot springs are sparse and much needed considering the controversy over the significance of photosynthesis within them. The Ohanopecosh measurements indicate a high carbon fixation rate. These could rival CO_2 evasion rates in a meteogene system, but thermogene waters rise with high dissolved CO_2 levels, so the effects are diluted out.

Productivity of paludal travertines was investigated by Boyer and Wheeler (1989) who made net production estimates in short fen vegetation associated with travertine in England obtaining standing crop increments of around 140 $g\ m^{-2}$ during the six-month growing season. Phytometer experiments and chemical analyses suggested that these sites were phosphorus-deficient. Taken as a whole, the production rates for travertine- depositing streams appear to be wide-ranging. The low productivity measurements are probably a combination of phosphorus limitation, cool climate and the generally poor macrophyte flora. More observations are needed before any sound conclusions can be made. Only in the case of Waterfall Beck, are sufficient data available to assess the effects of photosynthesis on travertine formation. Using our 1989 hydrochemical and discharge data, the total amount of carbon dioxide lost to the atmosphere from this stream is estimated as 3.36 $kg\ m^{-2}\ a^{-1}$. The mean carbon dioxide fixation rate by photosynthesis is 0.1 $kg\ m^{-2}\ a^{-1}$. Looked at in this way, photosynthetic uptake of CO_2 is around 3% of the degassing rate. An independent estimate can be made based upon the downstream loss of calcium providing an overall deposition rate with an assumption of a 1:1 ratio of photosynthesis:calcium carbonate deposition. The best estimate of $CaCO_3$ deposition in the Beck is 6,400 $kg\ a^{-1}$ giving an estimated photosynthetic

contribution of 13%. This discrepancy is doubtless due to the uncertainty of the estimates used, but overall it indicates a minor role for photosynthesis. A further line of evidence also points to the comparative insignificance of photosynthesis. Dian Zhang et al. (2001) and Chen et al. (2004) cite measurements of O_2/CO_2 gas exchange for 18 common algal species in the range 0.005–0.7 mmol m^{-2} s^{-1} while their lowest CO_2 degassing rates on cascades were at least an order of magnitude greater than this. An indicator of significant photosynthesis (*sensu* meteogene travertine forming potential) in freshwaters is a pH value > 9. In almost all freshwaters, these values are associated with an extremely low pCO_2 in the water, well below that in equilibrium with the atmosphere. This CO_2 'drawdown' is accomplished by algal photosynthesis but has not, to my knowledge been reported in evasive travertine-depositing systems. Where turbulence is high, CO_2 exchange masks the increase in pH, but in slow-flowing reaches such as dam pools, it should occur if photosynthesis is significant. This criterion is not of course valid in invasive travertine-depositing streams, where high pH is the result of inorganic OH^- production.

The above estimates from Waterfall Beck are based upon net production and thus account for losses resulting from plant respiration. As the biota become buried in the deposit, they are entombed and decay. One would therefore expect to find a zone of decomposition where carbon dioxide is liberated by microbial oxidation of the accumulated organic matter. This

Table 28. Net primary production rates in travertine-depositing systems

Location	Main phototrophs	mg C m^{-2} d^{-1}	g C m^{-2} a^{-1}	Method/comments	Reference
Hants, UK	*Phormidium incrustatum*, Diatoms	600	–	O_2 balance, summer rate	Marker and Casey (1982)
Cowside Beck, UK	*Schizothrix coriacea*	280	–	$^{14}CO_2$, seepage	Pentecost (1992c)
Cowside Beck, UK	*Scytonema*	92	–	$^{14}CO_2$, seepage	" "
Cwm Nash, UK	*Phormidium incrustatum*	100	37	Growth rate, shaded site	Author unpublished
Priory Mill, UK	*Phormidium incrustatum*	85	31	Growth rate, shaded stream	"
Waterfall Beck, UK	*Gongrosira incrustans*	30	–	Growth rate	Pentecost (1991b)
" "	*Homoeothrix crustacea*	100	–	Growth rate	" "
" "	*Schizothrix fasciculata*	60	–	$^{14}CO_2$, 15 °C	Author unpublished
" "	*Palustriella commutata*	520	190	Growth rate	Pentecost (1991b)
" "	Entire community	270	100	Various	" "
Montezuma Well, Arizona	*Potamogeton*	880	–	Oxygen balance, warm spring	Cole and Batchelder (1969)
Ohanapecosh, Washington	*Phormidium*, *Schizothrix calcicola*	2200–4200	306	Oxygen balance, 37 °C in flume	Stockner (1968)

source of CO_2 may percolate down into the travertine reducing the saturation quotient potentially leading to dissolution, or may migrate upwards providing an additional source for photosynthesis, or even enter the bulk solution. If all the organic matter produced in the system is subsequently consumed, then it could be argued that the overall effect of metabolism on travertine deposition is zero, providing all of the 'photosynthetically' precipitated carbonate is re-dissolved by the liberated CO_2. Waterfall Beck has a negligible allochthonous organic carbon input, but in afforested catchments, organic carbon inputs as leaf packets may be high and in these cases, the subsequent decay of this organic matter within the travertine-depositing system may lead to substantial CO_2 inputs, raising pH and possibly leading to local travertine dissolution. It is unlikely that all of the organic matter produced is consumed, but we have no data with which to compare.

Travertine Dating

Two dating methods have been widely applied to travertine; the decay of unstable isotopes, and biostratigraphy. Methods involving the measurement of isotopes have met with most success, and biostratigraphic methods usually rely upon radiometric calibration. The decay of isotopes ^{14}C and ^{234}U have been used most extensively and can date deposits up to 30 and 400 Ka respectively. Other isotopes may also be used but all of the methods are prone to error caused by the presence of contaminants or to diagenesis (Schwarcz 1990). Most reliable dates are obtained from autochthonous deposits, but even these may possess contaminants in sufficient quantity to prevent reliable dating. Chronostratigraphic methods can be used for deposits containing a recognisable fossil assemblage or archaeology, but comparatively few travertines are datable by this means. Other techniques such as electron spin resonance and thermoluminescence have found occasional use. Physical methods are preferable, and often provide the only means of age estimation.

11.1 Radioisotopes

A large number of naturally occurring radioactive isotopes have the potential for dating rocks. The choice depends upon their abundance, the assumed age of rock to be dated and their relationship to the formation process of the rock. Recently, interest has been confined almost entirely to the Quaternary, where suitable isotopes are few. Of potential value is ^{14}C as it is incorporated directly into the carbonate and originates from the atmosphere, but the decay rate is such that dating is only possible within the past 50 Ka. Other widely used isotopes are those of the uranium-series. These can be used to date travertines over a much greater time span.

11.1.1 Radiocarbon

The isotope ^{14}C has a half life of 5730 years and forms continuously in the atmosphere by the interaction of cosmic rays with molecules of nitrogen. It is customary to date Holocene and Late Pleistocene sediments in 'radiocarbon years before present (B.P.)' calculated from the modern atmospheric ^{14}C level. It was originally assumed that the atmospheric ratio of the common isotope ^{12}C to ^{14}C had been constant over time but this is now known not to be the case. More accurate measurements based upon the decay of ^{234}U and dated tree rings have shown that radiocarbon dates underestimate the true date. The difference amounts to about 10% for dates of 10 Ka B.P. To overcome this problem, radiocarbon dates are usually calibrated using master tree-ring curves. Dates are therefore referred to either as 'calibrated' or as RCY (radiocarbon year) dates. A further complication is the presence of additional atmospheric ^{14}C resulting from nuclear bomb tests after 1950. Radiocarbon dates are nevertheless invaluable as they provide a relative measure of age, against which the strata and their fossil assemblages may be compared.

Since travertine consists of calcium carbonate an obvious source of datable mineral carbon appears to be available. However it has been seen that the carbon originates from diverse sources and its dating is rarely straightforward. An alternative is to date organic matter contained within the travertine but this can also give rise to problems if the material originated from aquatic plants. If travertine is to be dated using ^{14}C then the sources of carbon must be known. The only available metric is the current concentration of ^{14}C in the atmosphere. If the epigean atmosphere can be shown to be the only source of carbon, then dating is straightforward and the level of ^{14}C in the sample gives a direct measure of the age of the sample. Travertines formed solely from atmospheric CO_2 are comparatively few in number. They include the invasive meteogenes formed from calcium hydroxide groundwaters and some lake travertines such as those forming in alkaline waters. Examples are the Oman ultramafic travertines which have provided a palaeoclimatic reconstruction over the past 30 Ka (Clark and Fontes 1990) and the deposits of Daba Siwaqa in Jordan (Clark et al. 1991). Direct travertine dating has been used to elucidate the history of Lake Lahontan, Nevada but

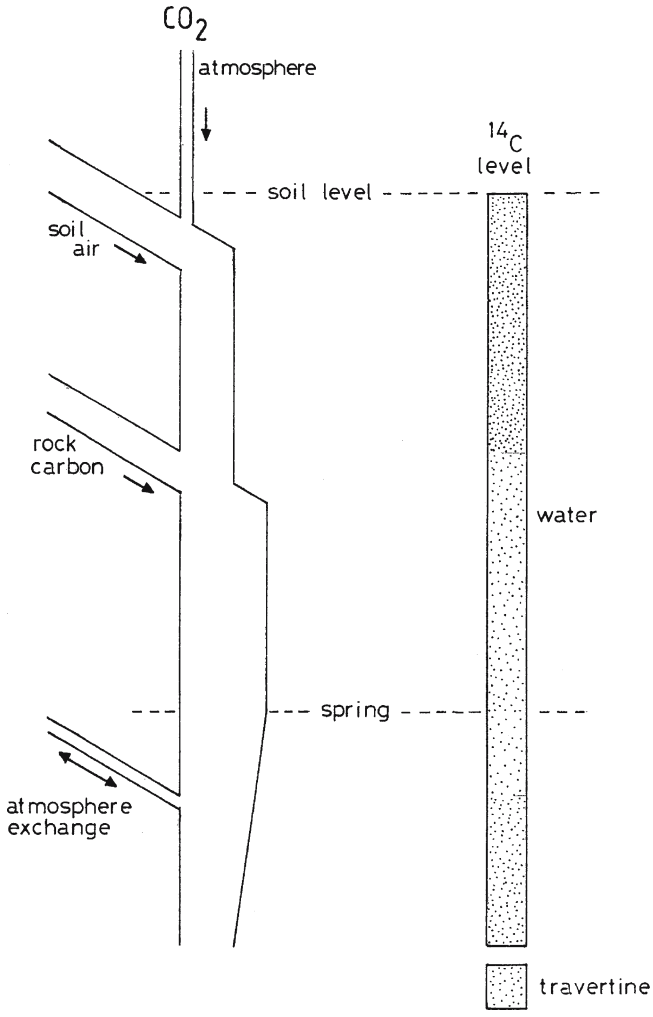

Fig. 70.
Diagram illustrating the inputs of carbon dioxide in groundwater, $^{14}CO_2$ activity and meteogene travertine deposition. Left: CO_2 contributions to groundwater, line thickness showing relative concentration; right: $^{14}CO_2$ level shown by density of stippling and effect of dilution by dead carbon from limestone dissolution

with mixed results (Benson 1978; Benson and Thompson 1987). It was argued that the error introduced by bedrock dilution (see below) was cancelled by fractionation of ^{14}C into the travertine. Where the precipitation rate is sufficiently low that atmospheric ^{14}C equilibrates with the depositing water, direct dating is also possible. This most often occurs in caves and may be possible where there is supporting stable isotopic data.

Most meteogene travertines have formed from waters which have been in contact with a soil atmosphere. The carbon dioxide respired by roots and soil microbes possesses a $^{14}C/^{12}C$ ratio similar to that of the epigean atmosphere (Srdoc et al. 1986a) but the aggressive percolation water continues to dissolve limestone which usually contains negligible ^{14}C to form the calcium bicarbonate solution necessary for travertine formation. The respired ^{14}C is diluted by 'dead' carbon prior to the deposition of travertine. One might expect a 50:50 dilution of 'active' carbon by 'dead' carbon but measurements do not demonstrate this, activities being in the range 60–90% rather than 50%. This phenomenon is best explained by additional exchange of ^{14}C between the groundwater and ground air present in the hydrological system, and kinetic factors (Usdowski et al. 1979; Srdoc et al. 1986b). Further $^{14}CO_2$ exchange occurs between atmosphere and springwater prior to travertine deposition. The overall effect of these processes is to provide a radiometric age considerably greater than the true 'radiocarbon age'. A number of techniques have been used to circumvent these problems. One is to measure the ^{14}C level in the travertine currently forming. If it is assumed that the groundwater chemistry has remained constant over time, then the 'modern' date can be used to correct dates from older parts of the same deposit. This also assumes that the process of deposition has occurred under the same conditions and the source water has flowed overground for the same distance and for the same time prior to deposition, which would be too much to expect in most systems (cf. Srdoc et al. 1983). If for example, an older travertine had been deposited further from the source, there would be more opportunity for atmospheric $^{14}CO_2$ input providing a travertine more enriched with ^{14}C. This would result in a later date, so that the travertine would appear younger than it actually was (Fig. 70). The above method cannot be applied where deposits are no longer active, or where the activity is so restricted as to provide an unrepresentative sample. In these cases, 'empirical dilution factors' have been used to correct the ^{14}C activity of the atmosphere. These may be found by measuring the ^{14}C activities of groundwaters in the same location, or at least in the same climatic province. They also find use in the dating of groundwaters. The dilution factor q is defined in an exponential decay equation:

$$A_s = A_0 q \exp(-\lambda t) \tag{11.1}$$

Where A_s is the travertine (or groundwater) ^{14}C activity; A_0 = ^{14}C activity of the atmosphere at the time of travertine genesis; λ = the decay rate constant ($\log_e 2/t_{0.5}$) 1.2097×10^{-4} a and t = sample age in years (Vogel 1970; Thorpe et al. 1981b). The quotient A_s/A_o is often expressed as 'percent modern carbon' (pMC or pM).

Rearranging (11.1) gives:

$$t = -1/\lambda \ln (1/q \cdot A_s/A_o) \tag{11.2}$$

As an example, suppose a travertine sample gave a ^{14}C activity of 36.5 pMC and q = 0.85. Then t = −8267 ln (1.25 x 0.365) = 6.487 Ka. The factor q is usually quoted as a fraction or percentage. Vogel (1970), found q to be 0.85 ±0.05 whilst Geyh (1970) obtained values between 0.85 and 0.90 for groundwaters forming speleothems in central Europe. Thorpe et al.

(1981b) applied a q value of 0.85 ±0.05 to correct a range of UK travertine dates and found the values were consistent with dates obtained from associated organic materials. The method has been applied to the dating of old travertine dams at Plitvice (Srdoc et al. 1980) and several sites in the UK (Thorpe et al. 1981a,b; Pentecost et al. 1990). Further measurements on a large number of Plitvice samples gave a mean q-value of 0.85 but the variance was such that an error up to 1 Ka could be expected (Srdoc et al. 1982). Genty et al. (1999) also obtained data supporting this value of q. Detailed investigations of karst springs in the former Yugoslavia and the Czech Republic revealed seasonal variations in springwater ^{14}C amounting to ±10% and significant, so far unexplained differences between springs that exceeded 10% (Krajcar-Bronic et al. 1986; Horvatincic et al. 1989).

When carbonate is precipitated from a bicarbonate solution at equilibrium, a degree of isotopic fractionation occurs, as is the case with ^{13}C (Chapter 8). Thus 'q' values obtained from groundwater and travertine are not the same quantity. However, fractionation under equilibrium conditions is small (<0.1 pMC) and is often neglected assuming that equilibrium deposition has occurred (Krajcar-Bronic 1992). Many measurements of A_o have been made on modern travertines. Krajcar-Bronic et al. (1992) measured the ^{14}C activity in recent, pre bomb-test travertines and obtained the ratio of this activity to that of wood deposited at the same time and obtained modern A_o values between 77.0 and 77.8 pMC.

The exchange of $^{14}CO_2$ between atmosphere and stream water has received much attention. A case study is provided by the Korana River in Croatia which originates as a karst spring and flows across several cascades and travertine-dammed lakes over a length of 15 km (Srdoc et al. 1986a). A steady increase in the ^{14}C activity occurs downstream together with a decline in the DIC as evasion and photosynthesis deplete the carbon reservoir (Fig. 71). Small fluctuations were caused by inputs of other karst waters. A model of the system is provided by Srdoc et al. (1986a). For much of its length, the rate of change of the DIC ^{14}C activity in the Korana River was found to be proportional to the difference between the atmospheric partial pressure of CO_2 (p_{atm}) multiplied by its ^{14}C activity (A_{atm}), and the CO_2 (aq) partial pressure (p_{aq}) multiplied by its ^{14}C activity (A_{aq}) at a distance of l km downstream:

$$d(p_{aq}\, A_{aq})/dl = k\,(p_{atm}\, A_{atm} - p_{aq}\, A_{aq}) \tag{11.3}$$

Integration yields:

$$A_{aq} = (1/p_{aq})\,(A_{atm}\, p_{atm} - (A_{atm}\, p_{atm} - F_o)\, \exp\text{-}k\delta l) \tag{11.4}$$

Where $F_o = A_{oaq}\, p_{oaq}$ represents values at the start of the river section and δl is the distance between the beginning and end of the river section. The exchange coefficient k varies according to water turbulence. In the Korana River, k reached its maximum value on the cascades (0.635 km^{-1}) with its lowest value in slow meandering sections (0.0016 km^{-1}). A more complex model was developed taking into account additional ^{14}C contributions from respiring biota. This is important in the Korana River system since the dammed lakes contain a well-developed aquatic flora. A complete validation of the model remains to be established but good agreement was found with measured values (Krajcar-Bronic et al.1992). Implementation of the models however will be difficult in watercourses experiencing rapid changes in turbulence and they are only applicable in reaches where there is no appreciable change in the aqueous CO_2 concentration. An alternative method for estimating the ^{14}C activity of groundwaters interacting with carbonate rock is to solve mass-balance equations based upon the ^{13}C contents of the carbon sources. The respired soil CO_2 has a $\delta^{13}C$ value of around

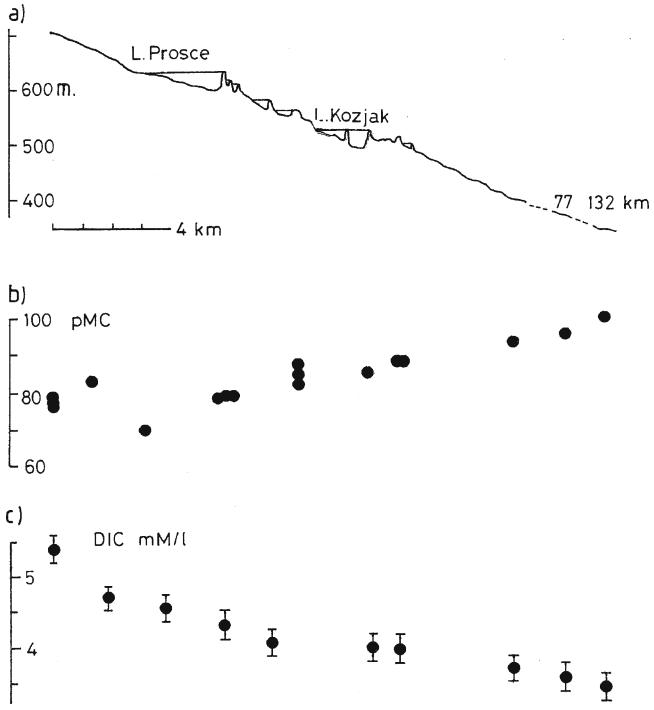

Fig. 71.
The Korana River, Plitvice, Croatia showing the ^{14}C activity and total CO_2 content downstream. Redrawn after Srdoc et al. (1986a). a) Korana River profile, with exaggerated vertical scale; b) ^{14}C activity in water and travertine samples downstream; c) Total CO_2 (DIC) content of water

–25‰, whilst most marine limestones have values of around zero. Measuring the $\delta^{13}C$ values of groundwater enables the proportion of dead carbon to be estimated and the necessary correction applied. Thorpe et al. (1981b) provide a mass-balance model to predict the ^{14}C activity of groundwater:

$$A_o = \{ \delta^{13}C \text{ (springwater)}/ -25\} \text{ 100 pMC} \quad (11.5)$$

This model, which is only applicable to a closed hydrological system, was further explored by Wigley (1975) in terms of the $\delta^{13}C$ values of the springwater, bedrock and groundwater where the system changes from an open to a closed system. Much carbonate dissolution occurs within and just below the soil horizon where the process is usually accepted to be 'open', i.e. with dissolution taking place in an essentially infinite CO_2 gas phase of approximately constant composition. Although sections of groundwater pathways are likely to be closed, open-system pathways tend to predominate in the majority of karst regions and the ^{13}C models often tend to underestimate the dead carbon contribution, resulting in younger than expected dates (Thorpe et al. 1981b).

Pazdur and Pazdur (1986) approached the dilution problem by emphasising the difference between the uncorrected radiocarbon age of the travertine and the 'true' radiocarbon age determined from contemporaneous organic carbon. This difference they call the 'apparent age' or T_{app} but it would perhaps be more appropriately labelled δT as the difference between two age estimates. Using a q value of 0.85, δT is approximately 1300a. They have suggested that some of the variation in δT is caused by bedrock type and the form of the carbonate precipitated. Furthermore, a correlation between δT and the $\delta^{13}C$ value of the precipitated carbonate is apparent, at least at some sites, leading to the suggestion that there

may be a useful linear relationship between these variates (Pazdur 1988). When the model was applied to some well-studied cascade travertines in the UK (Pentecost et al. 1990), δT turned out to be 3.04 ±3.5 Ka, a range too wide to be of any value in dating these deposits. The experience gained by application of all the above models is their limited application. They certainly provide useful descriptions of particular hydrological systems but lack generality and should be used with caution.

The ^{14}C activity of thermogene travertines has been little researched. There is little incentive to do so since the soil-derived CO_2 is much diluted by thermal CO_2. The thermal, and possibly thermogene travertines near Banja Luka in the former Yugoslavia yielded ^{14}C activities of 1.9–13.2 pMC (Srdoc et al. 1987) but their geochemical characteristics are not known. Such levels, however, suggest that superambient deposits may occur at these sites. Modern travertines and source waters may be a more profitable source of enquiry. Combined ^{14}C and ^{3}H activity could provide useful information on groundwater age, and in favourable situations an estimate of the atmospheric CO_2 contribution.

A further complication to ^{14}C dating is the presence of 'bomb ^{14}C' in the atmosphere (Krajcar-Bronic et al. 1992). This gives higher than normal atmospheric ^{14}C levels and its presence is readily detected in modern terrestrial vegetation, as well as the atmosphere. Some bomb carbon enters the soil where it has been detected in the upper layers (Horvatincic et al. 2002). It contributes to ^{14}C activity of modern travertine and several studies have confirmed its presence, e.g. Thorpe et al. (1981a). Krajcar-Bronic et al. (1992) found that levels in water and deposits of the Korana River system were slightly elevated during the 1970s and 80s but were not as great as expected. It was concluded that pre-bomb carbon stored in the soil profile was diluting the more recent thermonuclear additions. Bomb ^{14}C has also found use as a dating marker for recent speleothems (Genty et al. 2001).

Dating of associated organic carbon can provide a useful check on the initial ^{14}C activity of the travertine. It is assumed that despite some organic decay which inevitably proceeds post-burial, that there is no exchange of carbon between the organic matter and the surrounding deposit, though this does not appear to have been tested. The source of the organic carbon must also be established. Aquatic plants utilize CO_2 directly from water containing a significant fraction of dead carbon giving modern pMC values as low as 65 (Srdoc et al. 1980). Semi-aquatic mosses such as *Palustriella commutata* also demonstrate the effect, with a pre-bomb A_o of 72.8 pMC being reported by Krajcar-Bronic et al. (1992). Terrestrial vegetation such as buried tree branches provides the most satisfactory source of 'calibration' carbon. Ombrotrophic peats are also useful as they are occasionally found intercalated with paludal travertines. The 'hard water effect' resulting from dilution with dead carbon may be detected by the $\delta^{13}C$ values of the organic carbon. It will be higher than that of terrestrial vegetation owing to dilution with limestone-derived carbon. Considerable use of organic carbon markers has been made in dating deposits of the former Yugoslavia (Krajcar-Bronic et al. 1992). Dates have also been obtained from the organic residues of travertines which would contain both allochthonous and autochthonous organic matter (Caran et al. 1995; Winsborough et al. 1996).

Contamination of autochthonous travertines with allochthonous carbonates is a recognised problem (Srdoc et al. 1986b; Horvatincic et al. 1993). Samples of the Eemian Gradina Kozjac travertines were found to be contaminated by modern carbonate by the application of fractional dissolution (Srdoc et al. 1987). When Holocene travertine samples were dated using both ^{14}C and U/Th, Srdoc et al. (1986b) found that the less porous deposits gave the most reliable dates. Minute particles of parent limestone occur in karst groundwaters (Pentecost 1990d) and invariably become a component of travertine. A possible way to reduce errors introduced by these allochthons is to sample the dripstone forming on the roofs of

overhangs found under travertine cascades. Allochthonous particulate matter should be negligible, having been filtered out and trapped in the overlying deposits though it might conceivably be dissolved and redeposited. A potential difficulty, which does not seem to have been addressed is the comparatively slow rate of deposition of these dripstones. The environment is non-turbulent and the depositing water film may remain in contact with the atmosphere sufficiently long to take up significant quantities of atmospheric ^{14}C. Dates from dripstones may thus be expected to yield younger ages than the bulk. The dating error is in the opposite direction to that imposed by inclusion of dead allochthonous carbonate. A preliminary study comparing dripstones with associated dam travertines revealed no clear-cut differences in dates (Srdoc et al. 1987).

When anomalous AMS carbon dates of charcoal were obtained in an English Holocene deposit, Meyrick and Preece (2001) obtained further measurements from remains of the land snail *Cepaea nemoralis* whose shell carbonate is believed to contain negligible dead carbon. The resulting dates were more consistent with the molluscan biostratigraphy of the sites than the charcoal.

Speleothem dating using ^{14}C is subject to the same uncertainties as epigean travertine and has been used mainly to check the seasonality of stalagmite growth laminae (Gewelt 1986; Baker et al. 1998; Tan et al. 1998). Most carbon dating in caves is undertaken on organic material of known provenance such as bone collagen using the AMS method. This technique employs a mass spectrometer to measure the ^{12}C:^{14}C ratio and can handle sample sizes down to a few milligrams.

11.1.2 Uranium Series

Traces of uranium occur in all natural waters as the uranyl ion (UO_2^{2-}) forms stable soluble complexes with carbonate and phosphate. Fission track analysis has shown that most uranium is trapped within the carbonate lattice rather than at crystal boundaries (Schwarcz 1980). The isotope ^{234}U decays with a half-life of 75 Ka to sparingly soluble ^{230}Th. Isotopes of thorium occur in karst waters in traces but the amount co-deposited with travertine is thought to be negligible (Harmon et al. 1980; Schwarcz 1990), most of it being adsorbed onto surfaces of clay minerals (Schwarcz 1980) or ferric hydroxides. Such deposits must be avoided, and the potential exists for thorium and uranium to leach and contaminate otherwise 'clean' carbonates. For example Clark et al. (1991) found evidence of uranium loss by natural travertine dissolution. Measurements of ^{234}U and ^{230}Th in clean carbonates should provide a means of age determination. Dates with excellent reproducibility are now obtainable in the range 5–350 Ka using mass-spectrometric techniques (Li et al. 1989). Allochthonous particles must be avoided as much as possible since they will contain some ^{230}Th leading to an underestimate of the age. Since most travertines contain a few percent detrital material, the selection of samples is crucial. Fortunately, detrital thorium can be detected as it occurs with ^{232}Th, but corrections are sometimes difficult and may not be very reliable. Deposits with $^{230}Th/^{232}Th > 10$ have been considered acceptable for dating by Livnat and Kronfeld (1985) though corrections are still required.

Most travertines contain 0.5–5 ppm U and are datable using alpha-spectrometric or mass spectrometric methods. The former require about 10 g of material, but the latter only a few milligrams offering clear advantages in selectivity of clean material. As with ^{14}C, dripstone, or well crystallised deposits have yielded the most reliable results. Dense, sparry travertines appear to be less contaminated with allochthonous material than micrite. Several studies provide favourable comparisons between U/Th dates and esr dates (Gaida and Radke 1983; Hennig et al. 1983a).

The direct dating of speleothem calcite with U/Th is almost always the method of choice, and numerous dates have been obtained using this technique. Speleothems are often of well-crystallised calcite containing little allochthonous material, and tend to yield more reliable dates than the epigean travertines (Gordon et al. 1989).

11.1.3 Other Radioisotopes

The possibility exists for dating travertine with ^{231}Pa which has a similar half life to ^{234}U. The problems associated with this are the same as those for U/Th dating and the U content of the travertine must exceed 1 ppm (Schwarcz 1990). The ratio ^{234}U/^{238}U approaches unity with increasing sample age and this could also be used to provide a date estimate back to about 1 ma. A method is described by Schwarcz (1990). On a smaller time scale, the decay of ^{226}Ra which has a half-life of 1600 a, can be used for dating Holocene deposits. This isotope is one of the products of the decay of ^{238}U. The ratio ^{228}Ra/^{226}Ra was determined for a series of core samples from the Mammoth Hot Spring travertine giving dates reasonably consistent with expectation, based upon known deposition rates (Sturchio 1990). A more complex treatment was applied to a Holocene travertine from the Hell Grottoes of Switzerland where the dates indicated maximal deposition during the Atlantic period (Eikenberg et al. 2001).

Incorporation of allochthonous particles may be advantageous if these are derived largely from volcanic eruptions. For example, beds of potassium-rich tephra are often encountered in the Pleistocene travertines of Italy (Manfra et al. 1976) where they have provided potassium/argon dates. Dates can be obtained for deposits in the range 40 Ka->100 Ka. Possibilities also exist for dating more recent deposits using ^{210}Pb.

11.2 ESR and TL Dating

Electron spin resonance (ESR) and thermoluminescence (TL) can be used to date carbonates. The techniques measure the amount of damage in carbonates as a result of cosmic radiation and localised radioactivity. The method is based on the assumption that when a calcite crystal is first formed, it possesses no trapped or metastable electrons, but the number of these electrons increases with time from localised radiation sources (Grün et al. 1988; Grün 2001). There have been few attempts to date travertines as yet but the techniques gave consistent results when applied to the Pleistocene deposits of Weimar-Ehringsdorf (Grün et al. 1988) and of Jordan (Clark et al. 1991). Speleothem can also be dated by this method (Debenham and Aitken 1984). Unfortunately many epigean travertines appear to be unsuitable due to the presence of acid-insoluble impurities, particularly those containing Mn, where there may be difficulties obtaining a stable signal. Optically stimulated luminescence on quartz crystals, some of which were subject to heating from a fire, was used to date a travertine on the Tibetan Plateau (Zhang and Li 2002).

11.3 Palaeomagnetism

For Quaternary deposits, palaeomagnetism may be used to establish a date range. Prior to 720 Ka the Earth's magnetic field was reversed and remnants of this field are detectable in carbonates containing traces of detrital magnetite. In speleothems it has been used to detect the Brunhes/Matuyama reversal at c. 750 Ka, but large amounts of material are required compared with radiometric dating (Latham and Ford 1993). Vernet et al. (1984) and Lantos (2004) report the reversal in a French and a Hungarian travertine respectively. Schwarcz (1990) suggests that dates could also be obtained by measuring the secular variation of the magnetic field in deposits though this has yet to be attempted.

11.4 Amino Acid Racemisation

This technique is based upon the racemisation of L-amino acids to the D-forms which is time-dependent in bone, shell and organic matter (Bowen et al. 1989). Shells, in particular, are often abundant in travertines and could provide useful dates for Pleistocene deposits. The method is not as reliable as radiometry since racemisation is a function of temperature and also perhaps the depositional environment. Contamination by exogenous amino acids may occur for example. Nevertheless, useful corroborative data has been obtained by analysing the organic matter of speleothems (Lauritzen et al. 1994) and for allochthonous travertines it may provide the only means of age estimation.

11.5 Seasonal Lamination

Short sequences of travertine can often be assigned a relative date by counting annual growth laminae (Chapter 5). This method has been used to estimate an accumulation period of 900a for a travertine at Ehringsdorf, Germany (Magdefrau 1956) and it has also been applied to deposits of the Nimes Aqueduct, France. Caution is required since laminae may reflect other periodicities such as daylength or seasonal rainfall. In speleothem, which has been well studied in this respect, lamination is often seasonal. Tan et al. (1999) found a series of 2246 layers in a Chinese stalagmite caused by variation in the organic matter content. Radiometric dating suggested the couplets were seasonal, but hiatuses and some biannual couplets were observed. Another long sequence was found by Genty (1993) which was shown to be annual on the basis of ^{14}C dating.

11.6 Chronostratigraphy

Chronostratigraphic dating has been applied to the Plio-PleistoceneTaung travertines of Bophuthaswana by the careful comparison of vertebrate assemblages and dated extinctions (McKee 1993a). Distinct molluscan assemblages have been found in the United Kingdom by Kerney (1977) and Kerney et al. (1980) who described a series of biostratigraphical assemblage zones which could be used to provide approximate dates to deposits within the UK Holocene (Chapter 12). The system works reasonably well in lowland England but appears to be inapplicable further afield. Distinct assemblages have also been recognised in Pleistocene travertines (e.g. Mania 1978) where they are more useful as biostratigraphic markers than providing secure dates. Pollen analysis can likewise provide an estimated date, but complications are introduced by the selective preservation of grains. All methods rely on suitable radiometric calibration. The potential exists for plant macrofossils and other faunal groups to provide markers but they are all likely to suffer the disadvantage of limited geographical range.

In parts of Europe deposits of soot over the past 200 years follow a predicable pattern and have been used to date recent lake sediments (Renberg and Wick 1985) and there is potential to date epigean travertine using the same technique.

Chapter 12

Palaeobiology and Biostratigraphy of Quaternary Travertines

The high deposition rates of epigean travertines result in the rapid burial of biota trapped at the surface. Because of this, preservation of structure may be good and travertines have long been known as a rewarding source of fossils. There are three common types of travertine fossil: organic remains, impressions and encrustations (Table 29). Organic remains can be subdivided into the hard structural components of bone and shell and softer materials such as wood, seed and pollen. The latter, excluding pollen, are normally only found in waterlogged sites where the exclusion of oxygen has retarded decomposition. Impressions consist of moulds enclosing organic remains that have decayed away and build-ups around plant materials (encrustations). Encrustations to a degree are complementary to impressions but may provide sufficient external detail to allow identification of the encased biota. Certain cascade encrustations for example are diagnostic of the moss *Palustriella* (*Cratoneuron*) *commutata*. The processes of decay and fossilisation have received little attention in travertine despite their amenability for study. Large fragments of wood are common in modern aerobic stream crusts of northern Europe and appear to persist up to 20 years or more but encrusted leaves decay rapidly with all traces of organic matter lost within a few years. Conditions near the travertine surface, although water-saturated appear to be highly oxidising. Alkaline conditions presumably suit a wide range of bacterial decomposers and many of the heterotrophic bacteria isolated from modern travertines presumably represent part of this flora. In more stagnant waters, such as marshes, travertine deposits often contain layers of peat with well preserved plant remains, often indicative of more acidic, ombrotrophic phases. Thus the potential for preservation is variable, even within one deposit. True petrifactions, while common enough in other sedimentary facies, are uncommon in travertine and the processes in this rock have not been studied (see Section 17.4.3). Massive forms of travertine are often devoid of planes of weakness, frustrating attempts to split the material along contemporaneous layers to recover intact fossils. Where bedding planes exist however, the palaeontologist may be rewarded with excellent impressions of plants and animals. Leaf impressions may be sufficiently detailed as to preserve the outlines of the epidermal cells and on rare occasions, birds feathers may also be found. Indurated travertines such as those used for building sometimes reveal well preserved bones, but good material has also been obtained from softer, poorly consolidated strata deposited in marshy environments or clastics, and in caves. Such deposits are the richest source of fossils and are particularly favoured by molluscan biostratigraphers but a number of travertine forms are notably poor in certain types of fossil. Cascade and dam deposits do not provide a suitable environment for fossil emplacement, as most loosely attached forms would be simply washed away, though they often contain abundant plant encrustations preserved *in situ*, such as bryophyte cushions. Back-fills of dams however provide an excellent environment for preservation of fauna in a soft matrix. Hot spring mounds possess a poor fauna, though remains of bacteria

Table 29. Fossil forms in travertine

Type	Examples	Morphologies/facies	Special conditions
Mineralised parts	Bone and teeth Shell *Chara* oospores	Paludal and lake-fill deposits, travertine caves	Reduced turbulence to avoid abrasion and cominution
Non-mineralised-parts	Wood/peat Seeds Pollen and spores Insect parts	Paludal and clastic deposits. Pollen has been recovered from most types	Waterlogging- preserving organic structures in Holocene deposits
Moulds and burrows	Leaves and twigs Feathers Insect wings Invertebrate burrows	Cascades, dams, stream crusts and paludal deposits	Fine-grained matrix and rapid deposition
Encrustations	Grass and reed Twigs and branches Bryophyte cushions Algae	Cascades, dams. stream crusts, littoral deposits of lakes	Rapid deposition, normally in fast flow
Petrifaction	Twigs, algae	Stream crusts	Unknown and rarely recorded

and algae may be abundant. The hot, sulphide-rich waters are unsuitable for higher life forms but as the waters cool and enter more marsh-like regimes, a rich fauna may be preserved.

Travertine fossils may be usefully divided into autochthonous and allochthonous components. Into the latter category belong the Vertebrata, most of the Mollusca and many of the plants, especially the microspora. The 'catchment' area for many of these fossils may extend for several hundred metres outside the depositing zone and provide valuable information on the surrounding environment making travertine a useful source of information for palaeoenvironmentalists and palaeogeographers. Travertines occur throughout the fossil record, but most palaeontological interest has centred on Quaternary deposits. Fossils recorded in older travertines will be considered briefly in Chapter 14.

12.1 Fossil Flora

Travertines contain a rich flora consisting of leaf impressions, encrustations around moss cushions, twigs and seeds, and pollen. Of these, leaf impressions normally provide the most valuable record, since they frequently permit identification to species, and record vegetation living upon, or in close proximity to the deposit. Knowledge of the flora, particularly of the trees, can be used to construct, or reinforce palaeoenvironmental evidence obtained from other sources, such as the fauna or oxygen isotope record. However, extrapolation of climatic conditions from modern plant communities is not foolproof. West (1964) found that vegetation communities of the Pleistocene often consisted of different combinations of extant species than today, making palaeoclimatic interpretations equivocal. Woodward (1987) argues that climate controls the geographical distribution of plants. Temperature, in particular, has been found to be the most important factor controlling the distribution of some common European trees. For example, the distribution of *Pinus sylvestris* is restricted to regions where the absolute minimum temperature is less than –22 °C, with a heat-sum of less than 2800 day-degrees. In Europe, the northern limits of perennial plants, such as trees, seem to be determined both by winter climate, particularly the absolute minimum temperature, and the cli-

mate of the growing season. In contrast, annual species appear to be limited only by the growing season climate (Woodward 1988). For the southern range limit in the Northern Hemisphere however, the growing season climate is the most important. These observations must be taken into consideration, if climate is to be inferred from the fossil flora. Numerous investigations of the Quaternary flora leave no doubt that dramatic changes of vegetation have occurred as the continental ice volume waxed and waned. Travertine floras have played a small but important part in unravelling the complex changes that took place during the period. Lower plants are also found as fossils, but their distributions tend to be less restricted than those of flowering plants. Nevertheless they can provide useful information on site water relations, illumination, and occasionally on rates of deposition. Leaf impressions however are the most visually impressive remains found in deposits. The matrix is often sufficiently fine grained to preserve imprints of individual epidermal cells.

12.1.1 Pleistocene Flora

Most of our knowledge concerning Pleistocene travertine floras comes from Europe. The occurrence of plant impressions in the Italian travertines has been widely observed but there are few detailed investigations. In a study of the Fiano Romano deposits of Lazio, Clerici (1887) listed 11 angiosperms including the Judas tree (*Cercis siliquastrum*), box (*Buxus sempervirens*) and laurels (*Laurus nobilis* and *Planera ungeri*). The deposits date to the Middle Pleistocene (Manfra et al. 1976) and indicate temperate forest cover similar to that occurring in the region today. *Laurus nobilis* is also a common fossil in the Pleistocene deposits of Malta (Zammit-Maempel 1977), where it is thought to be indicative of a cooler climate than that of today (Pedley 1980). Vernet et al. (1984) found numerous leaf impressions in some of the Tarn Valley travertines of France which could be correlated with a mammalian fauna and indicated a Mediterranean-type interglacial climate. In Hungary, over 200 plant taxa have been identified in the travertine deposits, largely from leaf impressions (Skoflek 1990; Korpás 2003).

Several interglacial German sites have been studied intensively, particularly for their early human fossils and associated fauna. The Ilm valley contains three important sites, Taubach, Weimar and Ehringsdorf, where travertine has been quarried for building over many centuries (Section 17.2). The Ehringsdorf locality contains abundant plant impressions which includes remains of algae, fungi, bryophytes and higher plants. The Lower Travertines contain impressions of several trees including *Pinus sylvestris* and *Betula verrucosa*. Of particular interest is the presence of *Thuja occidentalis* which does not currently occur in the region, and requires less severe winters than those experienced in the region today (Magdefrau 1956). Impressions and molds of crab apples (*Malus sylvestris*) have also been uncovered here, and their occurrence is possibly the result of human activity. The Upper Travertine, separated by the Pariser Loess band contains a similar flora plus *Tilia cordata* and a basidiomycete fungus, *Lentinus diluviali*. The deposits date from the Middle Pleistocene (Hennig et al. 1983). Two other important interglacial travertines occur in this part of Germany. Bilzingsleben is a site where a series of travertines form a terraced 'staircase' on the River Wipper. The earliest terraces, Bilzingsleben I and II are probably of Holsteinian age (Schreve and Bridgland 2002) and contain ten angiosperms, including *Buxus sempervirens*, *Picea abies* and *Rhododendron* sp. (Harmon et al. 1980). The Eemian (Last Interglacial) Burgtonna site has yielded leaf impressions of 26 taxa including some thermophiles now occurring further south (Vent 1978). They include the Mediterranean Maple, *Acer monspessulanum* and the medlar *Mespilus germanica*, species characteristic of temperate deciduous forest plus several Atlantic species such as the fern *Phyllitis scolopendrium*, and the trees *Acer campestre* and *Fraxinus excelsior*.

This flora indicates a climate slightly warmer than that of today. The quarries at Cannstatt, near Stuttgart have yielded many interesting fossils. Leaf impressions of the trees *Corylus avellana*, *Juglans paviaeformis*, *Populus alba*, *P. freesii* and *Quercus mamuti* occur, but the most interesting find is the wing-nut, *Pterocarya fraxinifolia*, a species which now occurs much further south in Europe (Photoplate 18A). Bertsch (1927) believed that the flora is representative of a climate 2–3 °C warmer than that of Stuttgart in the mid 20th Century. The deposits appear to have been formed during two brief phases corresponding approximately to the previous two interglacials (Reiff 1955; Hennig et al. 1983). Nearby, at the Stuttgart-Untertürkeim quarry, Schweigert (1991) described a rich temperate forest flora with Mediterranean elements from an Eemian travertine including the honeysuckle tree (*Lonicera arborea*). In England, Bramwell and Shotton (1982) also found impressions of *Acer monspessulanum* in cave entrance deposits of presumed Ipswichian (Eemian) age. Further afield, plant impressions have been reported in deposits from northern and southern Africa (Butzer and Hanesn 1968; Peabody 1954).

There are also many records of lower plants from Pleistocene travertines, but few reliable identifications. Remains of algae including cyanobacteria are abundant in thermogene deposits, especially those of Italy (D'Argenio et al. 1983) and the United States. Thick beds of diatomite are often found close to such travertines (Weed 1889b; Manfra et al. 1976) and Devoto (1965) showed that lacustrine diatom deposits were formed during a cold phase of the middle Pleistocene. In the Auvergne, France, Héribaud (1920) provided extensive lists of diatoms associated with thermogene travertines, some of which probably date to the Pleistocene. Other thermogene travertines of probable Quaternary age were investigated by Winsborough (2000) and found to contain about 130 diatom taxa. A range of facies was studied and members of the genera *Achnanthes*, *Navicula* and *Denticula* were well represented. Deposits attributed to the desmid *Oocardium stratum* have been uncovered in the Tanagro Valley (195–240 Ka) by Buccino et al. (1978). Charophyte oospores (gyrogonites) have often been noted (e.g. Cannstatt, Ehringsdorf) and undoubtedly record temporary lacustrine conditions, probably in travertine-dammed lakes as they do today. Boros (1925) described encrusted moss cushions from several Hungarian deposits. He recognised *Didymodon (Barbula) tophaceum* and *Eucladium verticillatum* along with the alga *Vaucheria*. Well-preserved bryophyte cushions occur in the Ehringsdorf deposits (Magdefrau 1956) and include *Cratoneuron glaucum*, *Eucladium verticillatum*, *Hymenostylium recurvirostrum* and *Rhynchostegium riparioides*. Annual growth layers could be recognised in some areas, providing an estimate of the deposition rate. Impressions of the hepatic *Conocephalum* have also been found in some French travertines (Rytz 1934; Edwards 1936). When preservation is good, microfungi have been identified on leaf impressions (Fischer 1956). The palynology of these travertines is less well known, in part due to pollen grain corrosion. Pollen spectra have not been reported from any of the major interglacial sites of Germany or the UK, but its presence has been noted in some Hungarian and German deposits (Kovanda 1974; Brunnacker et al. 1982). It has also been observed in a Chinese travertine thought to date from the late Pliocene (Zhang et al. 1990).

12.1.2 Holocene Flora

Plant impressions are again common, but have been little studied. One of the earliest investigations was undertaken at Kiffis, near the French-Swiss border, where Fliche (1894) identified a number of trees, including *Laburnum* which is currently restricted to the warmer parts of southern Europe. The flora also included more northern elements such as *Frangula alnus*, but taken as a whole, it indicated a considerably warmer climate than today and the

deposits probably date to the Atlantic 'climatic optimum', (5–7 Ka). At Weilheim, Germany, a travertine dated to the same period (c. 5 Ka) contained the thermophiles *Tilia platyphyllos* and *Ulmus laevis* (Herrmann 1957). Several travertines of southern France are known for their rich flora. In the Vis Valley, deposits of Atlantic age contain *Laurus nobilis* whilst Subboreal travertines at Huveaune possess a coniferous flora (Vernet 1984). At St. Antonin, 31 plant taxa were identified by their impressions and charcoal fragments including *Acer monspessulanum* and *Quercus pubescens* (Ali et al. 2003). The flora was seen to change as a result of human exploitation. An interesting travertine-flora occurs at Soko Banja in the former Yugoslavia where Markovic (1951) uncovered a rich Holocene site with abundant beech leaves (*Fagus sylvatica*) and fruits preceded by a period of mixed deciduous forest. The travertine complex at Caerwys, Wales contains a rich arboreal flora (Bathurst 1954), the most abundant trees being hazel (*Corylus avellana*) and willow (*Salix* spp.). Beech has also been recorded suggesting a date during or later than the Atlantic period. In Western Europe, several deposits have yielded numerous cypselas of *Eupatorium cannabinum* which are highly resistant to decay. This herb is common on active boggy travertines in open woodland. Seeds of several other herbaceous plants were found in waterlogged deposits in Kent (Kerney et al. 1980) also indicating an open habitat during the first stage of deposition following the last ice age. Further north, Nordhagen (1921) describes the travertine flora of Gudbrandsdalen which includes *Dryas octopetala*, a well-known arctic-alpine herb. While European sites have received most attention, a number of sites have been studied further afield. Dzhanelidze (1969) records impressions from a site in the Caucasus, and seven plant taxa have been identified from the Hula Valley deposits of Israel (Heimann and Sass 1989). They are also known from a number of North African travertines.

Several palynological studies have been undertaken with varying degrees of success. Geurts (1976) made a detailed investigation of five valley tufas in Belgium. Pollen diagrams were used to determine the age of the deposits and obtain some idea of their rate of accumulation. The results showed that deposition began in the Preboreal and the deposition rate attained a maximum in the Boreal, after which it declined. A further investigation of the pollen spectra related some of the temporal variations to changing weather patterns (Geurts 1988). Work on currently forming Belgian stream crusts demonstrated that the seasonality of pollen production, the 'pollen calendar' could be detected in the travertine layers, but it was not found in the older valley deposits (Geurts 1976). In England, Kerney et al. (1980) and Preece et al. (1984) found evidence for differential pollen preservation in Holocene travertines and advised caution in the interpretation of travertine pollen spectra. They found many grains broken or badly corroded though some distinctive forms could be recognised. Pollen of the genera *Corylus*, *Alnus*, *Tilia* and *Pinus* together with lycopods and ferns appeared to the most resistant, while pollen of *Quercus*, along with that of many herbs seemed to be susceptible to decay. Alkaline environments are widely regarded as having poor pollen preservation potential, and the degree of preservation is unpredictable. In Kent, Kerney et al. (1980) were able to identify only 30–60% of grains encountered. At a Scottish site, Preece et al. (1984) had difficulty in finding 200 grains for the standard count, and analysis proved impossible at one Welsh locality. This contrasts with a site near Oxford, UK, where Preece and Day (1994) found corrosion rates as low as 5–35%, permitting the construction of detailed pollen spectra and they then compared them with the molluscan biostratigraphy. Some travertines are associated with layers of peat, and these often yield more satisfactory results (Groschopf 1952; Couteaux 1969; Villumsen and Grelk 1978). Work by Fritz (1976) provided pollen diagrams showing major vegetation changes during the Holocene. Dublanski et al. (1983) record pollen from some Russian sites.

Remains of lower plants also occur frequently as fossils, mainly as encrustations. Herrmann (1957) records the bryophytes *Palustriella commutata* and *Eucladium verticillatum* from the deposits at Huglfling, Germany, together with the alga *Oocardium*. A statistical analysis of bryophyte morphology was used to identify species on abandoned cascades in Yorkshire, UK (Pentecost 1987), which included *Palustriella commutata*, *Gymnostomum* spp. and *Eucladium verticillatum*. The first named is ubiquitous on British Holocene cascade deposits (Pentecost et al. 2000a). Remains of algae as encrustations are often abundant, but have not been studied in depth. Coccoid bacteria are figured from a moss travertine by Gradzinski et al. (2001b).

12.2 Fossil Faunas

Travertines have been the source of some of the most spectacular and important fossil finds of the Quaternary era, despite the generally non-fissile nature of the rock. Weakly consolidated paludal deposits are easily sampled with a hand-corer and sieving often reveals a large and varied collection of gastropod shells, ostracods and bone fragments. Numbers are often sufficiently high to allow detailed biostratigraphic analysis of the faunas, providing insights into environmental change. The fossils are often visible in natural sections and soon attracted the attention of palaeontologists. The often massive meteogene and thermogene dam and cascade travertines yield their faunas more reluctantly. These fossils have mainly come to light during quarrying operations and are responsible for the discovery of the famous Taung primate and some of the important interglacial faunas of Central Europe. They have provided a wealth of information on the European mammalian fauna and its distribution during the Pleistocene. The calcareous matrix, and rapid rate of deposition provides an excellent preservation medium for fossils.

12.2.1 Invertebrates Excluding Mollusca

Diverse invertebrate fossils occur in Quaternary travertines, but only one group has received much attention apart form the Mollusca, -the Crustacean class Ostracoda. These small shell-inhabiting creatures occur in a wide range of aquatic and marshy habitats and are used as stratigraphic markers in marine and freshwater sediments. Only the two-valved carapace survives burial and this frequently separates into its components, especially in high-energy regimes. Identification of ostracod valves can be difficult. Some species display strong sexual dimorphism (e.g. *Candona* spp.) and valve size can vary considerably from site to site. Also, many extant species characters are taken from the unpreserved soft parts of the body. In common with the Mollusca, a number of species occur in specific habitats and are adapted to burrowing, crawling or swimming, according to the depth of water and nature of the sediment and may provide evidence for past hydrological conditions. Some species are characteristic of cold climates such as *Nannocandona faba*, while a few occur in much hotter water (Chapter 9). They are good indicators of water salinity but this is not usually a significant variable in travertine-depositing environments. They are normally extracted from unconsolidated travertines with an 0.5 mm sieve. Numbers recovered vary greatly but may reach 300 valves kg^{-1} (Preece 1979). J. Robinson (in Kerney et al. 1980) pointed out that most ostracods provide more information on springwater temperature rather than the prevailing climate. Detailed work has been undertaken on the ostracod faunas of two Pleistocene travertines in Germany. These are the Eemian site at Taubach, where 26 species have been recovered (Diebel and Pietrzeniuk 1977, 1978) and Burgtonna with dominant taxa *Cyclocypris laevis*, *Ilyocypris bradyi* and *Potamocypris wolfi*. The faunas are characteristic of cold calcium-rich springs of

low salinity. These authors provide a table comparing the German Pleistocene and Holocene faunas and they show many similarities. Eemian deposits at Condat, France contained eight species (Preece et al. 1986a) one of which, *Ilyocypris schwarzbachi*, is extinct. It was a crenophil fauna containing only one swimming taxon, *Ilyocypris gibba*. In a study of Italian lacustrine sediments containing travertine layers, Devoto (1965) found a stenotherm ostracod fauna indicating deposition under cold conditions (12–15 °C).

Holocene travertines often contain ostracods. Diebel and Pietrzeniuk (1975) describe in detail the fauna of deposits at Bad Langensalza in Germany. It included *Ilyocypris bradyi* an abundant species that occurred as a range of forms thought to be a reaction to low salinity. The fauna is dominated by cold crenophil ostracods such as *Ilyocypris inermis*, *Ilyodromus olivaceus* and *Potamocypris wolfii* and dates to the early Holocene/Late Glacial. In Kent, Kerney et al. (1980) showed, using quantitative measurements of valve articulation and species composition, that travertine deposition began in a low-energy marshy environment, followed by periods of flooding and flushing and then returned once again to quiet conditions. British sites contain a varied fauna, but species numbers at any one site are generally low (5–6) when compared with lakes and streams, and the Central European Pleistocene faunas. Ostracods characteristic of boggy travertine-depositing springs include *Eucypris pigra*, *Ilyodromus olivaceus* and *Psychodromus olivaceus* plus the difficult genus *Candona* whose species burrow and are normally restricted to marshes (Kerney et al. 1980; Preece and Robinson 1984). More mobile taxa characteristic of open, quiet waters are sometimes found and include members of the genus *Potamocypris*, *Ilyocypris* and *Limnocythere bradyi* (Preece and Robinson 1982; Preece et al. 1986a).

Remains of other crustaceans are rarely reported, though some, such as the amphipod *Gammarus* are common on active deposits. Lohest and Forir (1904) however, found fragments of the crayfish, *Astacus fluviatilis* at Hoyoux, Belgium. Tubes and cases of fly larvae are frequently reported in the Late Pleistocene deposits of France (Edwards 1936). They have also been found in Wales (McMillan and Zeissler 1986) and Germany. Cases of caddis flies are occasionally abundant. The narrow curved cases formed by members of the family Leptoceridae are frequently found in British Holocene deposits (Keen 1989) and are indicative of shallow open water. Delicate wing impressions of adult caddis flies belonging to the Limnephilidae have also been recovered from a British Holocene cave travertine (Rhodes 1954). Remains of coleoptera, which have been found to be of so much value in palaeotemperature estimates, are rarely noted in travertine but often occur in the associated marls and clays. Elytra of *Carabus* have been found in the Burgtonna travertine however (Mania 1978). Other invertebrates have been discovered in unexpected ways. An insect living on beech trees is known from a medieval deposit in France (Vernet 1986) and impressions of alder (*Alnus*) leaves in a pre-boreal travertine were found to be covered in lesions caused by the mite *Phytoptus laevis* (Pentecost 1986). The same mite was identified from deposits in Sweden (Kurck 1901) with another insect, *Otiorhynus ovatus*. Several enigmatic fossils continue to confound palaeontologists, such as the *Taubachia* of Ehringsdorf (Zeissler 1977a) (Fig. 72a,b).

12.2.2 Mollusca

Most of the animals of this highly successful phylum possess shells of calcium carbonate and have a high calcium requirement. Active travertine-depositing sites are among the most calcium-rich environments in freshwaters and when well vegetated, they supply adequate food and shelter for these animals. Consequently, certain travertines contain a rich molluscan fauna.

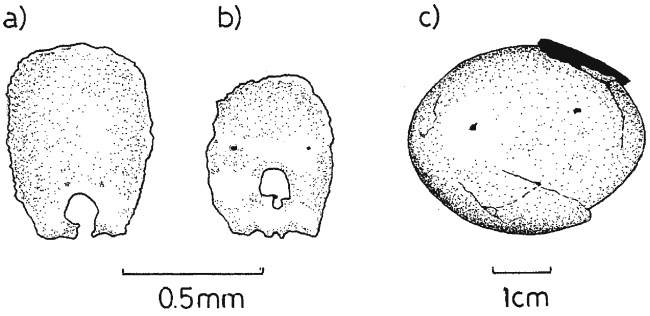

Fig. 72.
Fossils of the Ehringsdorf travertines, Germany. a) *Taubachia taubachensis* Zeissler (from Zeissler 1977a); b) *T. vimariensis* Zeissler; c) A duck's egg from the Taubach deposits (redrawn from Jánossy 1977)

The shells of molluscs provide many taxonomic characters and these are to a large extent preserved after burial. Both aquatic and terrestrial molluscs are found in deposits but the majority belong to the Gastropoda (snails) which are largely surface-dwelling animals requiring a good deal of moisture to maintain their body fluids. Most species feed on decaying vegetation or algae, though some are carnivorous. Malacofaunas preserved in travertines can give valuable clues to the former local environment. The shells will not have travelled far, and are usually representative of the travertine fauna and its immediate surroundings. Frequently it is possible to distinguish the autochthonous fauna of aquatic and obligate marsh species from the terrestrial fauna that has been washed in from adjacent ground. Faunas containing these two elements provide most information about past conditions. Loose, poorly consolidated deposits forming in marshy areas provide the best material for study as the molluscs can be readily extracted by sieving and they provide one of the best preservation media, often in long sequences extending for thousands of years making them ideal for study (Meyrick and Preece 2001). More massive lithified deposits are generally unsuitable for extraction but they often contain abundant remains. Overall, the Mollusca are thought to be better indicators of habitat rather than climate, but changes in their diversity has often been correlated with temperature (Jones and Keen 1993). During the Pleistocene their slow evolution means that they are of little value in chronostratigraphy.

12.2.2.1 Pleistocene Mollusca

A number of Pleistocene faunas have been studied, revealing much about the prevailing climate and local vegetation. Again, most current knowledge comes from the Eemian and Holsteinian (penultimate interglacial) deposits of southern and eastern Germany. The Ehringsdorf deposits contain a rich fauna with 96 gastropods and nine bivalves (Zeissler 1975). The Lower Travertines of Ehringsdorf, which are currently thought to be pre-Eemian (c. 225 Ka), contain 63 species including *Discus rotundatus*, *D. ruderatus*, *Oxychilus cellarius* and *Iphigena plicatilis*. The fauna is representative of a temperate forest environment but is succeeded by a cooler, drier phase, the loess-rich 'Pariser' horizon with intercalations of travertine containing some Atlantic Mollusca, e.g. *Azeca menkeana*, *Cepaea nemoralis* and *Truncatellina costulata*. The Upper Travertines again contain a different fauna but herald return to more equable conditions (Zeissler 1969, 1975; Blackwell and Schwarcz 1986). It is noteworthy that no Mollusca indicative of cold climates were recovered from these travertines and the whole sequence is believed to represent climatic variations within a single interglacial period. Distinct assemblages, presented as faunal spectra, also occur in the Taubach deposit nearby, originally thought to date from the same period (Zeissler 1977b) but now believed to be Eemian (Schreve and Bridgland 2002). The earliest travertines at Taubach

contain a cool climate fauna with *Discus ruderatus* followed by a warmer forest fauna including species of *Belgrandia*. The persistence of an arctic fauna may have resulted from the slow migration of more thermophilic taxa into the region. The fauna was classified into a number of ecological groups such as 'moderately damp semi-shade' and 'Ubiquisten'. The Eemian Burgtonna site has yielded 102 taxa (Mania 1978) which could be placed into eight faunal groups or phases. The first four represent a period of maximum species richness within the interglacial, characterised by a forest fauna including a number of exotic southern and eastern forms. Phase 3 contained the richest fauna (85 taxa) including southern and continental species such as *Cepaea vindobonensis*, *Helicogona banatica* and *Truncatellina strobeli*. The fauna is contemporaneous with some thermophilic plant impressions, e.g. *Acer monspessulanum*. Deterioration in the climate then becomes apparent, and phase 5 includes open ground Mollusca such as the steppe species *Pupilla triplicata* with a return to milder conditions during phases 6–8. Mollusca have also been examined at Bilzingsleben (probably Holsteinian) where thermophilic taxa occur, e.g. *Azeca schulziana*, *Belgrandia margianta (germanica)* and *Zonites verticillus* along with *Theodoxus serratiliniformis*.

At Cannstatt in Germany, a warm interglacial fauna is also known (Geyer 1920) and a similar fauna, containing abundant *Belgrandia* and *Truncatellina* occurs in two Danube Valley sites of the Schwäbische Alb (Dehm 1951) and may be contemporaneous with Bilzingsleben. The travertines of Tata, Hungary have yielded a rich Molluscan fauna and demonstrate at least one phase of climatic deterioration. An early warm phase (Eemian) was indicated by the occurrence of species such as *Mastia bielzi*, *Pomatias elegans* and *Soosia diodonta*, followed by cooler conditions with *Pupilla sterrii* and *Succinea oblonga* (Krolopp 1969). Dominance curves were established for the commoner fossils and a number of aquatic thermal species were found associated with the warm springs, e.g. *Fagotia acicularis*, *Theodoxus prevostianus* and the endemic *Belgrandia tataensis*. Other Hungarian interglacial Molluscan faunas are described by Kovanda (1974) with a review by Krolopp (2003).

There have been few detailed investigations in French travertines despite their abundance and potential. The deposits at Condat, Dordogne, have been shown to be interglacial in age with some locally extinct species such as *Belgrandia marginata* and *Daudebardia brevipes* included in the temperate fauna (Preece et al. 1986a). The former is a well known climatic optimum indicator. In the Tarn Valley, Peyre, *Ceciliodes acicula* and *Jaminia quadridens* were associated with a rich mammalian cool climate fauna (Vernet et al. 1984). In the Durance Valley, some travertines yielded *Rumina decollata*, a mollusc typical of the Mediterranean Eemian interglacial (Magnin et al. 1991). In Italy, Settepassi and Verdel (1965) and Devoto (1965) found a cold-temperate fauna in the Liri Valley travertines with a radiometric date of 368 Ka. In southern England a few sites of limited extent have yielded interesting finds. At Hitchin, deposits yielded over 40 species including *Platyla similis* (*Acicula diluviana*) (Fig. 73) and *Ruthenica filograna*, both extinct in Britain, though *Ruthenica* still occurs in central Europe. The fauna probably developed during the Eemian interglacial (Kerney 1959). A similar fauna, containing *Lyrodiscus* was later exposed at Icklingham (Kerney 1976) but U/Th dating suggested it was much older (Holyoak et al. 1983). At Marsworth, a travertine contained leaf impressions of *Acer monspessulanum* associated with temperate woodland Mollusca (*Azeca goodallii*, *Clausilia bidentata* and *Discus rotundatus*) and dated to 140–170 Ka, probably representing a warm stage (interstadial) between the Eemian and Holsteinian interglacials (Green et al. 1984).

Despite the large numbers of available isotopic and other dates, it is still not possible to associate the majority of Pleistocene faunas and their associated travertines with a particular climatic period with any certainty (Jones and Keen 1993).

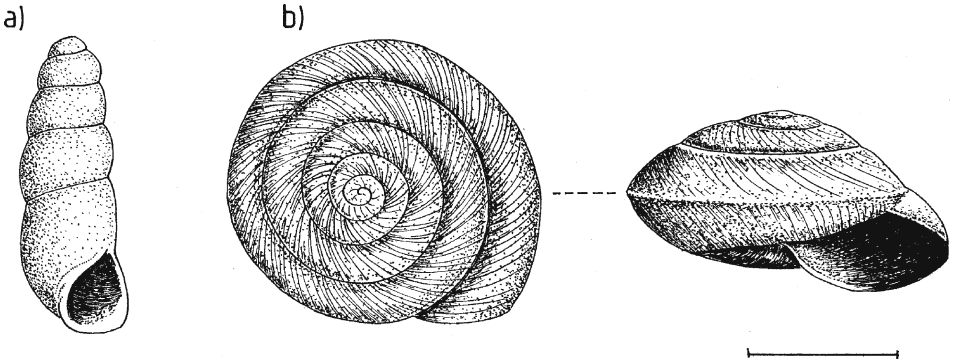

Fig. 73. Examples of Pleistocene Mollusca recovered from European travertines. a) *Platyla similis* [*Acicula diluviana*], b) *Helicogona banatica.* Bar 2 mm

12.2.2.2 Holocene Mollusca

Most of our knowledge of Holocene Mollusca comes from northern Europe. There are a number of reasons for this, which are in part historical. The extant Mollusca are not very numerous in the region, amounting to about 300 species due to the comparatively cool climate and effects of the last glaciation (Kerney and Cameron 1979). Collecting has been fairly intense for well over a century and knowledge of the fauna is good. Consequently the ecological preferences and biogeography of the species are reasonably well known, allowing fossil assemblages to be interpreted with some degree of confidence. In southern Europe, and many other parts of the world, although the terrestrial malacofauna is richer, knowledge of the species is generally insufficient to apply techniques currently available in northern Europe.

Mollusca have been recognised in Holocene travertines for over 200 years. Perhaps the earliest published record of a travertine fossil snail fauna is from the UK Midlands (Morton 1706). Lyell (1829) listed 21 species from a deposit in southern England. Taxonomic lists have grown over the years, but it was not until the 1930s that the assemblages began to be investigated more critically. At the time of printing, in excess of 60 sites have been investigated in Europe, mainly from France, Germany, Hungary, the Czech Republic and the British Isles. Data from the more detailed investigations of Holocene travertine biostratigraphy are summarised in Table 30. In many cases, the deposits were not found to persist to the present day, an observation that will be taken up in Chapter 13.

In Britain the pioneering work by Kennard and Kerney provided detailed knowledge of the extant Molluscan fauna. This was applied to the Holocene assemblages obtained from two travertine sites in southern England (Kerney et al. 1980) and resulted in the designation of four species groupings characteristic of particular habitats: aquatic species, swamp species, terrestrial 'A' and terrestrial 'B' (Fig. 75). The aquatic species include the pea mussels,

Fig. 74. Examples of Late Pleistocene-Holocene molluscs frequently recovered from European paludal travertines and grouped by environment. a-c) low temperature/glacial open ground environments; a) *Columella columella*, b) *Discus ruderatus*, c) *Eucobresia nivalis*. d-f aquatic species; d) *Bithynia tentaculata*, e), *Lymnaea peregra*, f) *Pisidium casertianum*. g-i) marsh species; g) *Carychium minimum*, h) *Oxychilus alliarius*, i) *Vertigo antivertigo*. j-m) terrestrial 'A' species; j) *Cochlicopa lubrica*, k) *Nesovitrea hammonis*, l) *Punctum pygmaeum*, m) *Vitrea crystallina*. n-q) terrestrial 'B' species; n) *Acanthinula aculeata*, o) *Carychium tridendatum*, p) *Clausilia bidentata*, q) *Ena obscura*. Bar 2 mm

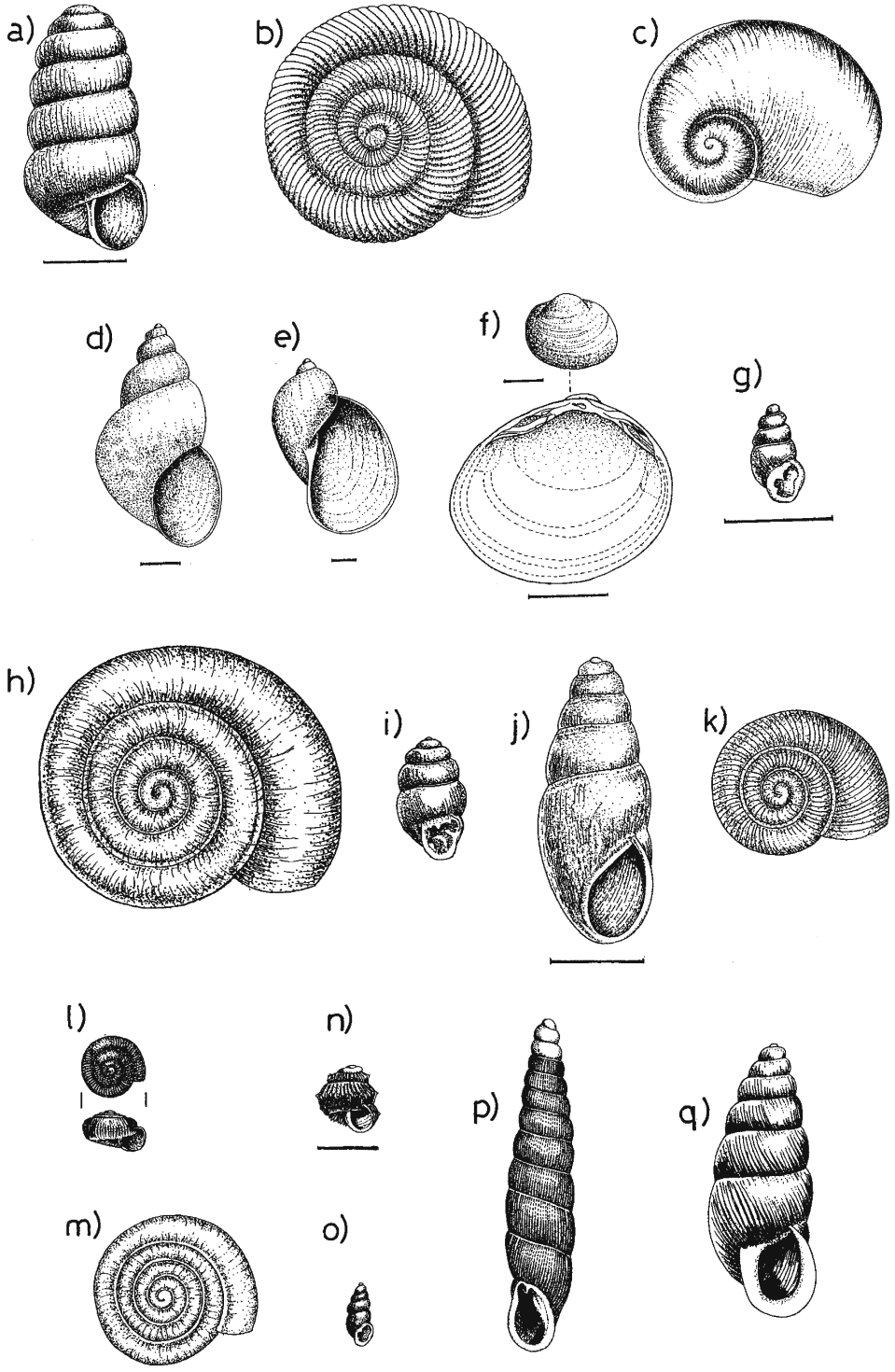
a)
b)
c)
d)
e)
f)
g)
h)
i)
j)
k)
l)
n)
p)
q)
m)
o)

Table 30. Holocene sites with data on Molluscan biostratigraphy

Site name and location		Comments	Reference
Austria	Fendels, 47.05 N, 10.40 E	Eroding terrace to 0.85 ka, medieval forest fauna, ceased on deforestation	Huckreide (1975)
Belgium	Tourinnes la Grosse, 50.47 N, 4.45 E	Fauna dominated by *Clausilia*, *Discus* and *Trichia*. Marsh environment in woodland, dating to c. 2 ka	Soens and Gullentops (1969)
Bulgaria	Svischtov, 43.37 N, 25.20 E	Site underlain by sub-boreal clay. 18 taxa includes the aquatic *Lithoglyphus naticoides* spreading into W. Europe	Petrbok (1935)
Eire	Newlands Cross, 53.21 N, 6.45 W	Paludal with 48 taxa showing transition from open ground to closed hazel woodland and evidence of forest clearance, active 9.7–7 ka	Preece et al. (1986b)
	Roscrea, 52.58 N, 7.47 W	Paludal site with peat and many terrestrial taxa. Began c. 7–8 ka and ceased c. 3.2 ka	Preece and Robinson (1982)
France	Meyrargues, 43.38 N, 5.32 E	Ordination showed climatic change from steppe to open forest, grassland and closed forest, with maximum deposition under forest	Magnin et al. (1991)
	St. Germain-le-Vasson, 49.06 N, 0.22 W	Rich fauna beginning 9.7 ka and ceased by 4.2 ka. Open marsh followed by woodland fauna	Limondin-Lozuoet and Preece (2004)
	Vauvenargues, 43.33 N, 5.36 E	Thick clastic sequence with maximum deposition in the boreal. Forest and steppe taxa found	Del Giovine (1986)
Germany	Bad Laer, 51.57 N, 9.05 E	Began c. 8 ka with Atlantic maximum. Saline springs	Hiltermann (1977)
	Eggloffstein, 49.42 N, 11.15 E	Began in boreal and ceased in dub-boreal. 44 taxa including *Monacha incarnata*. Overlain by colluvium	Brunnacker and Brunnacker (1959)
	Kloster-Mühle, 49.51 N, 6.36 E	Open ground *Succinea/Oxyloma* fauna succeeded by a brief aquatic phase followed by woodland, 9.7–4.3 ka	Meyrick (2003)
	Niedervogelsgang, 50.57 N, 13.59 E	Late-Glacial to early Holocene with 37 taxa including *Carychium minimum* and *Vallonia costata*.	Mathe (1982)
Luxem-bourg	Direndall, 49.41 N, 6.06 E	An early catholic assemblage succeeded by a forest optimum fauna. Deposition lasted from c. 10–0.9 ka	Meyrick (2000)

Table 30. *Continued*

Site name and location		Comments	Reference
Poland	Dobrzyn, 51.26 N, 19.20 E	Late Glacial to Holocene with 17 taxa including *Helix pomatias*	Brykzynski and Skompski (1979)
	Pradnik Valley, 50.06 N, 19.57 E	Diverse fauna indicating three phases of deforestation begninning 9.8 ka. Two distinct assemblages with richest fauna during climatic optimum	Alexandrowicz (1988a)
	Pieniny Mountains, 49.25 N, 20.24 E	Malacospectra indicate transition from steppe to closed forest	Alexandrowicz (1988b)
	Tatra Mountains, 49.15 N, 19.57 E	Dendrogram of assemblages with relict glacial taxa. Deposition ceased in sub-Atlantic zone	Alexandrowicz (1988b)
Spain	Rio Henares, 41.01 N, 2.41 W	Deposit overlain by silt and noteworthy for lack of open-ground to closed forest succession, c. 6.2–5.2 ka	Preece (1991)
Turkey	Bursa, 40.11 N, 29.04 E	Thermogene deposit with 16 taxa indicating warm, humid climate	Pfannenstiel and Forcart (1957)
United Kingdom	Blashenwell, 50.37 N, 2.04 W	Rich paludal and terrestrial fauna notable for occurrence of the calcifuge *Zonitoides excavatus*	Preece (1980)
	Caerwys, 53.15 N, 3.18 W	Largest UK deposit with Late Glacial to late Holocene fauna. Periods of forest clearance apparent and evidence of lateral variation in fauna	McMillan and Zeissler (1986); Preece et al. (1982)
	Folkestone, 51.05 N, 1.11 E	Early Holocene, beginning 9.3 ka with *Pisidium tenuilineatum*	Kerney et al., (1980)
	Inchrory, 57.10 N, 0.14 W	Rich shade-demanding flora with apparent lack of marsh species. Most deposition 9.7–6 ka	Preece et al.. (1984)
	Letchworth, 51.58 N, 0,14 W	30 taxa including the extinct *Vertigo parcedentata*. Damp ground with rushes indicated	Kerney (1955)
	Sidlings Copse, 51.46 N, 1.15 W	Open marsh conditions succeeded by *Corylus* woodland. Deposition 9.3–5.1 ka, terminated by changing hydrology or human activity	Preece and Day (1994)
	Totland Bay, 50.40 N, 1.32 W	Sequence of swamp and terrestrial taxa suggesting closed forest at Atlantic optimum	Preece (1979)
	Wateringbury, 51.16 N, 0.29 E	Swamp fauna with few aquatics, showing change from low- to high-energy flow regime. Began prior to 8.47 ka but much reduced by 2 ka	Kerney et al. (1980)
United States	Winchester, VA, 39.11 N, 78.12 W	List of mainly terrestrial taxa with deposition between 8.8 and 1.5 ka. Mollusca up to 10% deposit mass	Giannini (1990)

(*Pisidium* spp.) and the water snails (*Lymnaea* spp.). These are molluscs that live most or all of their lives under water and require permanent pools. Swamp species are less readily defined but include a number of characteristic forms, namely *Carychium minimum*, *Vertigo antivertigo, V. genesii, V. moulinsiana, V. angustior*, *Zonitoides nitidus* and members of the genera *Oxychilus* and *Succinea*. The terrestrial species were divided into two broad groups. The terrestrial 'A' group includes snails with a wide ecological range, found in both wet open areas and damp woods. Characteristic members include species of *Cochlicopa*, *Columella*, *Punctum*, *Vitrina*, *Vitrea*, *Nesovitrea*, *Euconulus*, *Arianta* and *Cepaea*. Terrestrial 'B' snails have more exacting requirements and live mainly in damp shaded deciduous woods. These include *Carychium tridentatum*, and species of the genera *Aegopinella*, *Acanthinula*, *Ena*, *Clausilia*, *Macrogastra* and *Platyla*. In a north German site, Meyrick (2003) recognised six broad groups; open ground; shade-demanding, catholic, marsh, aquatic and subterranean. The latter, represented by a single taxon, was excluded in subsequent analyses. The shade-demanding species were the most numerous, followed by the catholic, marsh and aquatic species. By plotting the relative abundance and diversity of these groups it is possible to follow changes in local vegetation patterns throughout the period of deposition. A series of biostratigraphical assemblage zones has also been recognised in Holocene sequences of southern England (Kerney 1977; Kerney et al. 1980). They demonstrate how molluscan assemblages can be used to interpret changes in the environment (Table 31) and how they may be related to vegetation and climatic periods (Fig. 76). Following deglaciation, zones *y* to *d* demonstrate migration of species into the revegetating ecosystem, followed by the gradual loss of arctic-alpine forms such as *Columella columella*, *Catinella arenaria* and *Vertigo genesii*. Zones *b*, *c* and *d* contain a more diverse assemblage of woodland and marsh snails than exists today in Britain, possibly the result of human deforestation. Zones *e* and *f* represent communities occurring in regions of intense human activity. In zone *f*, *Helix aspersa* appears as an introduction into Roman Britain. These zones are fairly well defined in southern England, but not always so clearly recognised in other parts of the country or abroad (Meyrick and Preece 2001). This results from interruptions in deposition, phases of erosion, climatic effects caused by aspect, altitude and latitude or possibly a reduced human influence on the landscape.

Table 31. Molluscan biostratigraphical assemblage zones proposed for Holocene travertine deposits in southern England (Kerney 1977; Kerney et al. 1980)

Zone	Definition of zone
y	First appearance of a molluscan fauna, dominantly of *Pupilla*, *Vallonia* and *Vitrina*
z	Periglacial assemblage with expansion of *Pupilla* and *Abida*, plus *Vallonia*, *Trichia* and *Columella columella*
a	Decline of bare soil species (*Pupilla*), and expansion of terrestrial group 'A' species, appearance of *Aegiopinella*, *Carychium* and *Vitrea*
b	Woodland fauna, expansion of terrestrial group 'B' species, *Aegiopinella* spp., *Carychium tridentatum*. *Discus ruderatus* characteristic
c	Woodland fauna, expansion of *Discus rotundatus*, suppression of *D. ruderatus*
d	Woodland fauna, expansion of *Oxychilus cellarius*, *Acicula*, *Leiostyla* and *Spermodea*
e	Open ground fauna, decline of shade-demanding 'B' species, re-expansion of *Vallonia*
f	Open ground fauna as in zone e, but with appearance of *Helix aspersa*

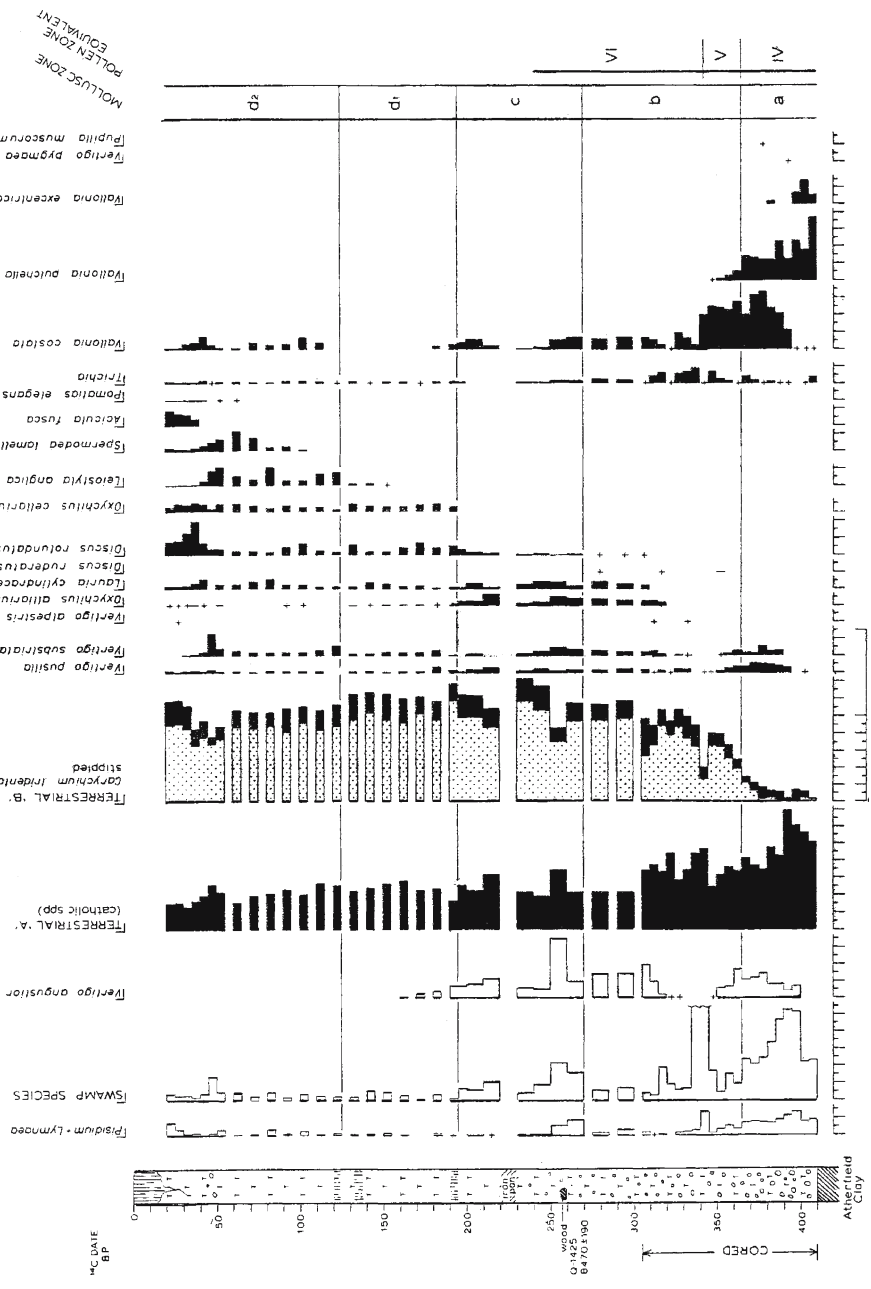

Fig. 75. Molluscan diagram for the Holocene travertine at Wateringbury, UK. From Kerney et al. (1980), Fig. 5, p.26 with permission from the Royal Society

Fig. 75. Molluscan diagram for the Holocene travertine at Wateringbury, UK. From Kerney et al. (1980), Fig. 5, p.26 with permission from the Royal Society

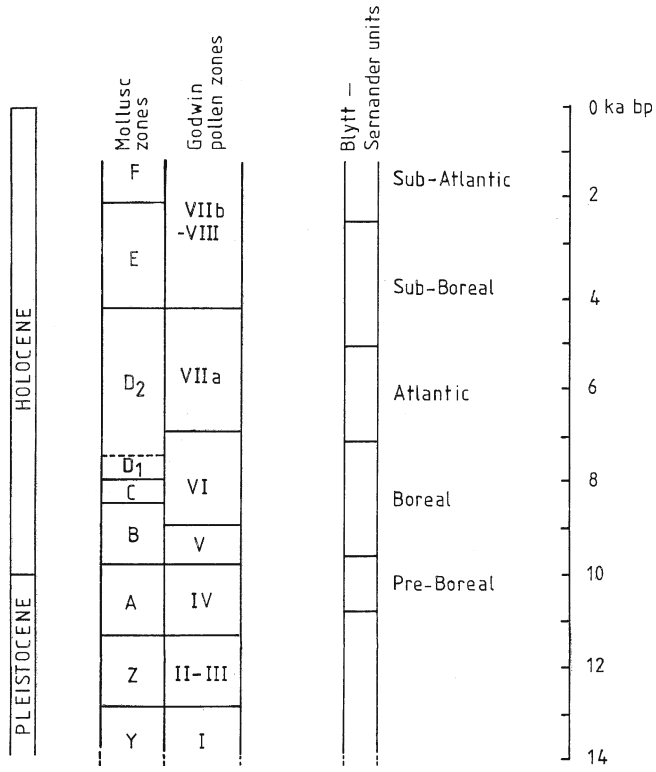

Fig. 76.
Temporal relationships between the molluscan biostratigraphic zones of Kerney et al. (1980), the classical Godwin pollen zones, climatic zones and radiocarbon ages for the Late Glacial-Holocene travertine sequences of Southern England. Note that the sequences are subject to some uncertainty in terms of their absolute ages

12.2.3 Vertebrate Faunas Excluding Primates

Travertines are no less rich in their vertebrate remains than in their Mollusca. Fine, base-rich sediments provide an excellent preservation medium for bone by inhibiting bone mineral dissolution. The potential for rapid deposition also helps to maintain intact skeletons particularly in low-energy lacustrine sites. Some large vertebrates might find themselves trapped in paludal deposits with potential scavengers unable to approach the sinking body. Occasionally, animals may seek refuge from predators in such marshy ground. Early man certainly lived near, and often upon a number of travertine deposits and may have hunted game sheltering in the associated marshland vegetation. Once more, most of our current knowledge of vertebrate faunas comes from Europe, through chance excavations, and from large travertine quarries, many of which have been operating for centuries. The most notable of these is the series of quarries in the Ilm Valley, Germany, where excavation, mainly by hand, has yielded one of the richest known Pleistocene faunas, with over 28 species recorded from the Ehringsdorf travertine alone. Cave travertines are also a major source of Pleistocene vertebrate fossils. Caves are used as dens by hyaenas, bears and other large mammals and remains of themselves, together with their prey are sometimes found embedded in flowstone deposits such as those of Victoria Cave, UK (T. C. Lord, *pers. comm.*). There is insufficient space to consider caves in general here, but it should be noted that caves and cavities in epigean travertines have been the source of major finds. In France, Vernet et al. (1986) found a cavity used as a hyaena den which included over 20 species of Pleistocene

vertebrates. Interpretations based upon the faunas are subject to less certainty than the invertebrates but supply invaluable additional information. Many vertebrates travel great distances during migrations and give little information on local conditions, but can provide useful regional data on climate and vegetation.

12.2.3.1 Pleistocene Faunas

The Ilm Valley travertines of Germany (Ehringsdorf, Taubach) have yielded a wide range of vertebrates that include reptiles, amphibians and birds (Fig. 73c). The deposits formed from warm springs at the edge of a graben. They are not particularly extensive and their comparative richness has not been explained. Among the most notable finds are several extinct large mammals: *Coelodonta antiquatis* (woolly rhino), *Dicerorhinus hemitoechus*, *D. kirchbergensis* (rhinos); *Mammuthus primigeneus* (woolly mammoth); and *Paleoloxodon antiquus* (straight-tusked elephant). The species of *Dicerorhinus* and *Paleoloxodon* are characteristic Northern European interglacial fossils and there are widely distributed finds dating to the Eemian and pre-Eemian interglacials to which the bulk of the Ilm Valley deposits are thought to belong. The woolly mammoth and woolly rhino however, are adapted to cold and fed on low tundra-type vegetation (Stuart 1991). Their presence in the travertine itself appears anomalous and they may belong to strata within a sequence that heralds cold conditions. These mammals have not been found in other Pleistocene travertines where the large mammal faunas are generally typical of temperate woodland in keeping with interglacial conditions of Northern Europe, including several species of deer (e.g. *Capreolus capreolus*, *Cervus elaphus*), horses (*Equus* spp.) and the wild boar (*Sus scrofa*). The occurrence of reptiles is especially noteworthy and indicative of warm conditions through part of the year. The present distribution of the European Pond Tortoise (*Emys orbicularis*) has demonstrated that the Eemian interglacial, and indeed periods during the current interglacial were significantly warmer than at present (Jones and Keen 1989). Other animals are believed to have been so widely distributed that they provide no information on climate (e.g. the bison, *Bison priscus* and wolf, *Canis lupus*). Finds of the extinct Giant Deer *Megaloceros giganteus* are noteworthy as they are also common in the Holocene marl lakes of Eire (Stuart 1991). Lake marls often accumulate in close association with travertine, and marl-like sequences are known from a number of the German quarry sites. Nearly 20% of the recorded vertebrates belong to the Carnivora, an unusually high proportion. Data on the absolute abundance of animal finds are unavailable so it would be unwise to speculate on the reasons for this.

12.2.3.2 Holocene Faunas

The vertebrate faunas of postglacial travertines are species-poor when compared with Pleistocene deposits. Only about a dozen taxa have come to light in Europe compared with more than 50 in the Pleistocene. Even accounting for the loss of 12 extinct species, the difference remains significant, though perhaps an artefact resulting from the huge amount of work undertaken at the German quarry sites. Despite this apparent paucity, small-mammal bones are frequently associated with Mollusca and sieve-out with them. Among the commonest is the rodent *Clethrionomys glareosus*, one of the most widely distributed extant European voles, with a preference for open shrubby ground, and the common shrew, *Sorex araneus*. The most frequently reported large mammal remains are from the red deer (*Cervus elaphus*) another widely distributed European species with a preference for open woodland. Fish have also been recorded (Meyrick 2003).

12.2.4 Primates

In 1924 Reginald Dart was presented with a small skull by R. B. Young which had been found among the rubble of the Buxton Lime Works at the edge of the Kalahari Desert in the district of Bophutatswana. Careful examination showed that it was not human, yet it appeared to possess a number of human characters. He described the find as *Australopithecus africanus* (Dart 1926) and it was soon hailed as the missing link between man and the apes. After much discussion among anthropologists it became the one of most significant fossil discoveries of the century, and soon sparked off controversy. At the time, humans were thought to have evolved in Asia, but the new find questioned this view and anthropologists began to flock to South and East Africa. The quarry at Buxton yielded few further remains of *Australopithecus* but additional finds of adult *Australopithecus* have been made in South African caves. *A. africanus* (Fig. 77, inset) is not currently considered to be part of the direct evolutionary line between these apes and *Homo*. He was an upright walker and probably evolved from earlier *Australopithecus* forms such as *A. afarensis* but the link with this species currently appears to be tenuous (Wood 2002). The Taung travertines occur at the edge of the Ghaap (Kaap) Escarpment, the eastern rim of an extensive dolomite plateau (Fig. 77) where intermittent streams flow across the slope break. The deposits, though of limited extent were sought for lime, but little now remains. Detailed mapping revealed at least four depositional sequences correlating with pluvial periods during the Pleistocene (Peabody 1954). The travertine consists in the main of cascades with some cemented rudites. Evaporation probably aided their formation (Butzer 1978). Travertine is still forming at the site, below the Taba Sikwa spring. The deposits were named chronologically as the Thabaseek, Norlim, Oxland and Blue Pool Travertines (Peabody 1954). The skull, that of an infant, was found in the upper part of the Thabaseek deposit, thought to be of Early Pleistocene age, the earliest of the four deposits at the site, though this chronology has been disputed (McKee 1993b). The two earliest travertines were also the most extensive and appear to correlate with the gravels and terraces of the Vaal River. Unfortunately, quarrying operations have destroyed most of the site. It is probable that the skull came from a breccia-filled travertine cave, which were widespread in the deposits. These caves were initially thought to be solutional phenomena, thus postdating the travertine (Peabody 1954; Vogel and Partridge 1983) but later excavations have shown them to be primary caves formed beneath cascades (McKee 1993b). Soon after the *Australopithecus* discovery, Hrdlicka (1925) found a similar infilling in the Thabaseek travertine containing the bones of baboons and other vertebrates. The deposits were also formed in a primary cave adjacent to, but not contemporaneous with the *Australopithecus* cave (McKee 1993b). The faunal assemblage was used to provide an early to mid-Pleistocene age for the deposits. Later $^{234}U/^{238}U$ dates of 764 and 942 Ka have been obtained for the Norlim and Thabaseek travertines respectively (Vogel and Partridge 1983) and were consistent with dating by thermoluminescence (Vogel 1985), though these dates are now thought to be unacceptably young (Tobias et al. 1994). More recent excavations in the vicinity of the first discovery have shed further light on both the depositional environment and the age of the Taung skull (McKee 1993a,b). Further information on the fauna of the nearby Hrdlicka site has come to light including the discovery of *Parapapio broomi* and *Procavia antiqua*. A detailed analysis of the time ranges of the Taung fauna and comparison with other fossil sites in South Africa indicate an age of 2.5 – 2.6 Ma for the Hrdlicka site and a slightly earlier age of 2.6–2.8 Ma for the Taung *Australopithecus*. In the Norlim Travertine, Black Earth Cave yielded two forms of *Homo* along with a range of other mammal bones suggesting a hyaena den. Further discoveries were made at quarries south of Buxton. Stone-age artefacts were found at Witkrans and numerous plant impressions at Thoning.

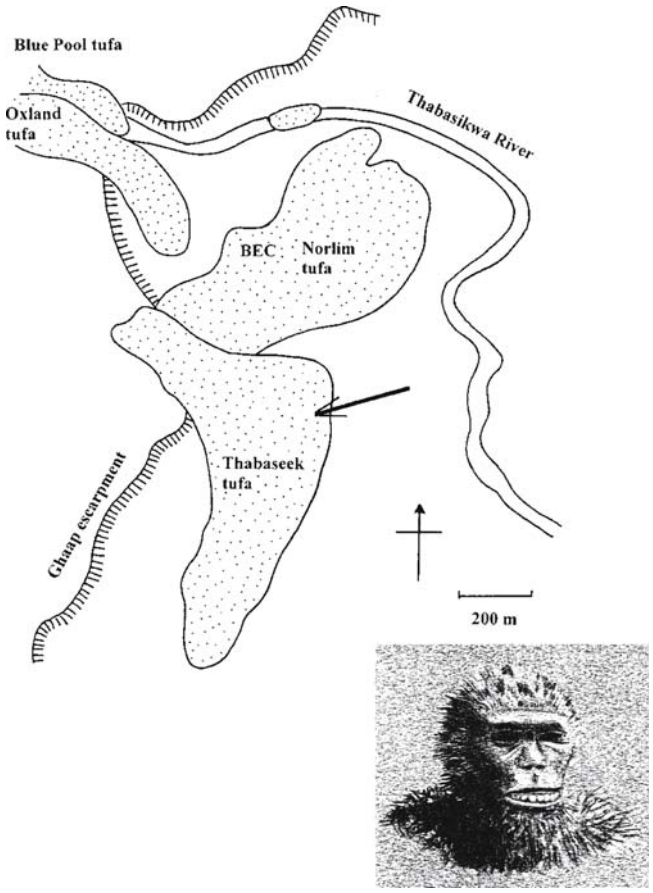

Fig. 77.
Reconstruction of the Buxton travertines in South Africa. The Taung hominid, Dart and Hrdlicka deposits were found at the arrow point. BEC Black Earth Cave. Travertine stippled. After McKee (1993b). Inset shows *Australopithecus afarensis* reconstruction

Hominid remains have been discovered in several European travertines most of which were also being quarried for stone or lime. One of the most notable sites is at Vértesszöllös in Hungary. Here, a layer of travertine 12 m in thickness rests upon the fifth (Gunz) river terrace of the Tata River (Fig. 78). The upper part of this travertine contained a Lower Palaeolithic industry. The travertine sequence lies upon a marginal flood plain sequence of the Tata River and appears to have accumulated from upwelling warm waters issuing from the edge of a subsiding graben (Pécsi 1973). The industry was discovered by Pécsi in an intercalated loess mud in 1962. Travertine formation must have postdated terrace development and began within an interglacial as it overlies typical glacial sequences. Since the finds occurred in a loessic layer it is thought that they correlate with the humid Mindel anaglacial period. Isotope dates suggest an age >350 Ka with a minimum of 162/+73/−22 Ka using U series methods (Pécsi 1973; Schwarcz and Latham 1984). The remains include a cranium fragment of *Homo erectus* with other mammalian bones and stone tools and suggest activity over several millenia in the vicinity of the warm springs (Pécsi 1973; Kretzoi and Dobosi 1990; Dobosi 2003). Use was made of abandoned dam basins where the drop wall provided shelter from the elements. Nearby, the footprints of humans and other mammals have been preserved in a layer of lime-mud. Other early human finds have come to light in the Hungarian quarries at Dunaalmas, Tata and Obuda-Kiskelli where palaeolithic implements were

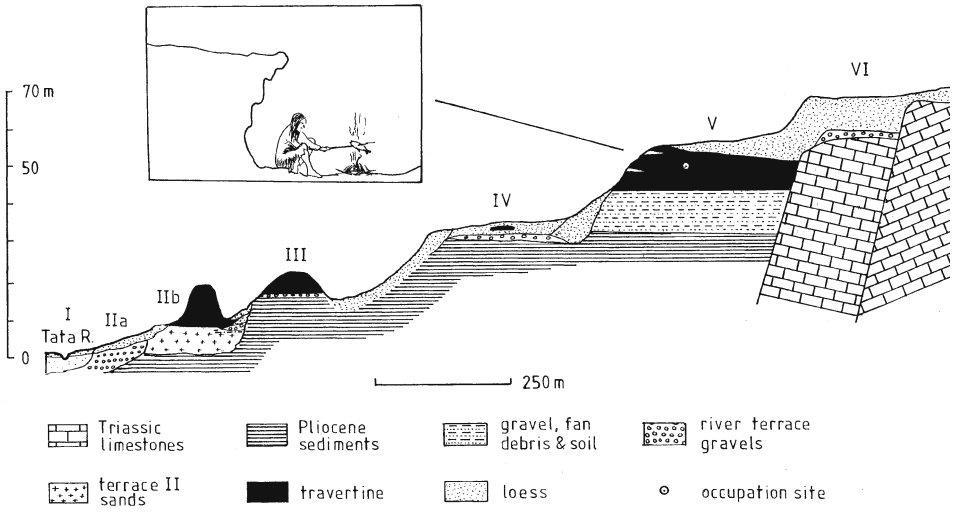

Fig.78. The Vertesszöllös occupation site, Hungary. (Redrawn and modified from Pécsi 1973)

recovered. A notable collection of pebble tools has also been uncovered at Eiserfey, Germany where the travertine has been dated to the Mid-Pleistocene (Brunnacker et al. 1982). At Millau, France, charcoal and other evidence of human occupation has been found in a travertine sequence dating to at least 240 Ka (Ambert et al. 1989).

In a Pleistocene river terrace near Bilzingsleben, Germany a sinkhole developed in the underlying limestone. The gravel depression filled with water and accumulated a sequence of marls, silts, and travertines during the penultimate Polish Lubline Interglacial, 245 ± 45 Ka. The depression was subsequently quarried for marl and in 1818 yielded the skull of an archaic form of *Homo sapiens*. The precise location of the find was uncertain but further fragments of worked flint were found with a rich flora and fauna (Glazek et al. 1980; Harmon et al. 1980) together with palaeolithic notched bones. In the same region, quarrying at Burgtonna revealed human bones in the 17th Century which later sparked a fierce debate between the actualists and the diluvianists (Kahlke 1978). This travertine was deposited from calcium sulphate waters derived from gypsum lenses in the underlying Keuper beds during the last interglacial. The springs were probably active at the same time as warm springs deposited travertine in the Ilm Valley. The celebrated Ilm deposits at Ehringsdorf contained, in their lower levels, hominid remains with apparent isotopic ages in excess of 350 Ka (Blackwell and Schwarcz 1986) corresponding to an interglacial preceding the overlying Eemian travertines. Further remains have been uncovered at Kartstein where the oldest travertine sequence contains primitive pebble tools that appear to date from the Middle Pleistocene (Brunnacker et al. 1982).

The Italian travertine quarries are among the largest and oldest in the world, and have, not surprisingly also yielded interesting finds. At Muracci, solutional depressions in the travertines subsequently became filled with Pleistocene sediments that include Aurignacian flint tools and pottery of the late Bronze Age (Segré and Ascenzi 1956). The Ferentino quarries revealed human skulls (Cacciamali 1892) in a Mid- to Late Pleistocene deposit. In Israel, there is also evidence of human activity in the Early Pleistocene, with valley deposits and spring mounds yielding Mousterian artefacts (Schwarcz et al. 1979). Travertines clearly pro-

vide a profitable source of human remains . Jones and Keen (1989) note that Lower Palaeolithic man seemed to favour waterside habitations but the reasons are likely to be manifold. At travertine sites, clean water, caves and the presence of game are probably important factors.

Postglacial travertines also provide much evidence of human activity and occupation. In Provence, France, neolithic remains are frequently found associated with deposits. D'Anna and Courtin (1986) found eight sites in Var but provide no explanation. In Wales, the remains of a Mesolithic flint industry were discovered upon a small island in a boulder clay hollow within which travertine was accumulating (Clark 1938). Flints of the same culture had previously been found at Blashenwell, Dorset (Reid 1897), and Evans and Smith (1983) comment on the frequent occurrence of Mesolithic finds in UK deposits. At Zerka Ma'in, Jordan, implements have also been discovered.

Climate, Man and Travertine

Interest in the climate of our planet, and the extent to which humankind is changing the biosphere has never been as great as at present. Climate influences all Earth surface processes and travertine formation is no exception. Though travertine is unusual in that its precipitation can be observed in detail, the effects of climate upon its formation remain largely conjectural, principally because of the large number of variables affecting deposition, and the comparatively long periods of time necessary for the completion of meaningful experiments involving climate change. At present, it is only possible to make generalisations concerning climate and much scope remains for further experimentation and observation.

Human activity of various kinds has affected carbonate deposition. Among the most spectacular is the pollution of water with industrial and domestic wastes. However, agricultural practices over several thousand years have had an accumulative effect on travertine formation in many parts of the world.

13.1 Travertine Deposition in the Quaternary

A considerable number of radiometric dates are available for Quaternary travertines. Many of these have been analysed by Hennig et al. (1983b) for the Pleistocene where travertine development is discussed in relation to climate. Their histogram depicting the frequency of error-weighted travertine dates over the past 300 Ka has been redrawn in Fig. 79, together with the oxygen isotope record of a deep-sea core. The epigean travertines show a bimodal distribution of travertine formation, with peaks corresponding to the previous two interglacials. Few Holocene travertines were included, hence the lack of a third, more recent peak. Of particular interest is the lack of dates during the period 20–40 Ka B.P. for both epigean travertine and speleothem, corresponding approximately with the previous glaciation whose maximum is estimated to be at 22 Ka. Data obtained from cave travertines are broadly similar. The Last Cold Stage, of approximately 100 Ka duration also includes a number of short, warmer periods where speleothem deposition is known to have occurred. The most obvious peak (115–125 Ka) is that corresponding closely to the last interglacial (113–127 Ka), during oxygen isotope substage 5e. Frank et al. (2000) found that the Cannstatt thermogene travertines were deposited over short periods of a few thousand years during the two interglacial sub-stages at 99.8 Ka and 105.9 Ka (marine isotope stage 5.3). These periods are thought to represent times free of permafrost in that region. Soligo et al. 2002 U/Th dated travertines in the Velino Valley, Italy and found that travertines corresponded to warm humid periods in the marine isotope stages 5, 3, and 1 and similar results were obtained in the Granada Basin, Spain (Martín-Algarra et al. 2003).

Travertines dating to >130 Ka are subject to greater errors in precision and accuracy, but there does appear to be a maximum corresponding to the penultimate interglacial of isotope

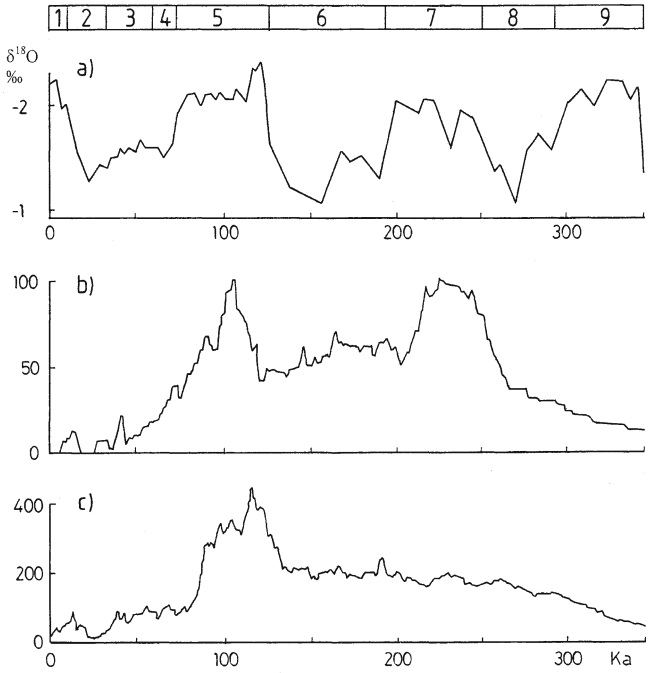

Fig. 79.
Quaternary travertine deposition (redrawn after Hennig et al. (1983). a) Oxygen isotope record of deep-sea core V28–238 and oxygen isotope stages for comparison. b) Frequency of U-series error-weighted dates for epigean travertines. c) Frequency of U-series error-weighted dates for speleothems

stage 7. A histogram published by Gascoyne (1992) using additional speleothem data, provides further support for this. Another study of NW European speleothem dates by Baker et al. (1993) pointed out that aridity during an interglacial will reduce speleothem growth and provided evidence for this by comparing it with the oceanic isotope record. Cemented rudites (slope breccias) provide a similar pattern. They were noted by Gradzinski et al. 2001) to form only in interglacial periods, and during the Holocene climatic optimum in the Czech Republic. In China, Sweeting et al. (1991) reported several U-series dates from Tibetan travertines where they appear to record previous interglacials.

At lower latitudes the relationship between travertine formation and interglacials is not always so evident. For example in the Grand Canyon, Arizona, Pleistocene travertines date to the glaciations, when more humid conditions permitted travertine growth (Szabo 1990). Similar findings were obtained for the Caatinga travertines of Bahai, Brazil, (Auler and Smart 2001). Zhang and Li (2002) found a fireplace on a thermogene travertine of the Tibetan Plateau dated to c. 20 Ka, near the height of the glacial maximum where the mean air temperature was estimated to have averaged –1 to –3 °C. They suggest that the slightly warmer environment near the springs would be more conducive to habitation, but the climate must have been extremely harsh at the time. In Egypt however, Crombie et al. (1997) identified travertine formation with pluvial periods corresponding to interglacial maxima using U/Th dating.

Several attempts have been made to identify the period of maximum travertine deposition during the Late Glacial and Holocene. Data for British speleothems (Fig. 80a) suggest a maximum between 6–7 Ka B.P. during the early Atlantic period. An analysis of ^{14}C dates for British epigean travertines provided equivocal results but suggested travertine deposition reached a maximum between about 5–9 Ka (Pentecost 1993). A larger sample, including data from Europe indicated widespread deposition between c. 4–10 Ka (Vaudour 1986; Goudie et al. 1993). Another large European sample suggests a maximum between 8–9 Ka (Fig. 80b)

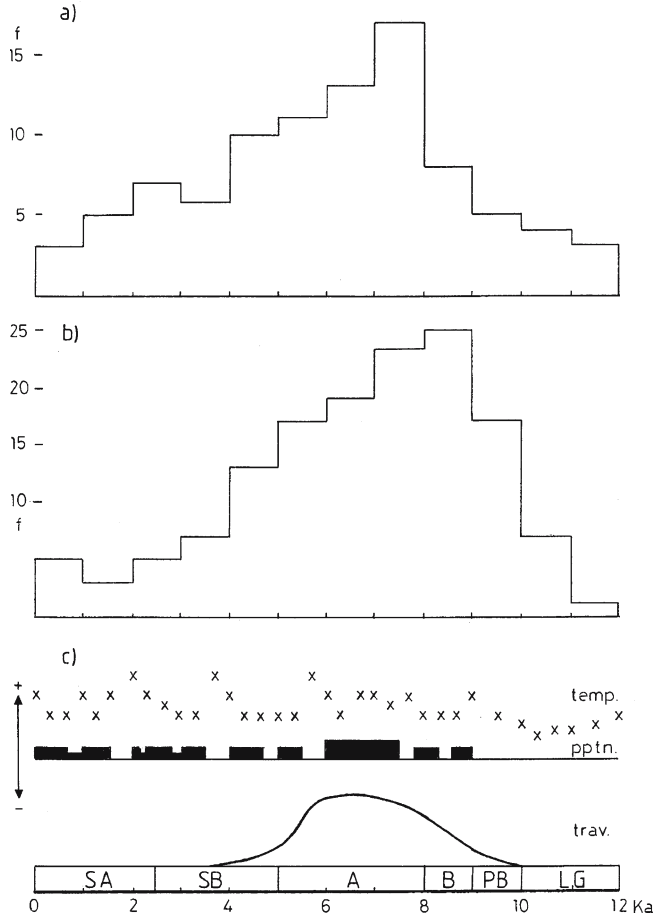

Fig. 80.
Travertine deposition in the Holocene. a) Frequency distribution of speleothem dates in the British Isles (after Gascoyne 1992). b) Frequency distribution of epigean travertine dates in Western Europe. Data from Hartkopf-Fröder et al. (1989), Meyrick (2000, 2003), Meyrick and Preece (2001) and Pentecost (1995a). c) Development of the Hell-Grottoes travertine, Switzerland with trends in air temperature and precipitation. A, Atlantic period; B, Boreal; LG, Late Glacial; PB, Preboreal; SA, subatlantic; SB, Subboreal. After Eikenberg et al. (2001)

which corresponds to the Boreal period. This is also the period Geurts (1976) identifies with the maximum rate of travertine deposition in Belgium. In the UK, the Boreal represented a time of moderate to low precipitation accompanied by gradual warming. Forests of pine and birch were widespread, forest soils were developing and humans were spreading into the more remote northern and western areas. In China, a Holocene peak is also apparent during the period 5–10 Ka, but the available data are limited (Pentecost and Zhang 2001).

Dramis et al. (1999) propose that the deposition of travertine early in interglacial periods is higher than later in those periods. This is based upon the recognition that the low conductivity of aquifer rock leads to a delayed warming of groundwater. Bedrock cooled during a glaciation may take thousands of years to warm during a succeeding interglacial. It was hypothesised that the cooler rock would increase the solubility of carbon dioxide in water, resulting in greater degassing and more travertine deposition early in interglacial periods. Although difficult to test, it is apparent that travertine deposition does occur early within interglacial periods and may be extensive. The Boreal period in the UK commenced about a thousand years after the ice sheets finally melted. Since soil development often takes several hundred years following re-vegetation it is conceivable that the frequency of travertine dates in this period is related to soil formation rather than increased CO_2 solution in cold

rock, through the two might act in consort. Several examples of deposition in late Glacial times are also known. Spötl et al. (2002) observed travertine deposition in the Italian Alps soon after the Bølling period, a time of rapid warming. The eventual warming of bedrock during interglacials led to Soligo et al. (2002) suggesting that the decline of travertine occurrence after 5 Ka in some areas was also due to this.

The histogram of Fig. 80b should be compared with the data from a Swiss site (Eikenberg et al. 2001) (Fig. 80c) where the maximum period of deposition is placed firmly in the Atlantic. This period, identified as the postglacial 'climatic optimum', is associated with closed forests in the lowlands, mature forest soils with high precipitation and temperatures similar or slightly higher than those experienced in Europe today. However, the large amount of data obtained from the Plitvice Lakes travertines tells a quite different story (Srdoc et al. 1983). Here, the travertine maximum seems to have occurred much more recently at about 1 Ka. The frequent association of travertine with peat led Srdoc et al. (1986b) to speculate its decay would raise the groundwater pCO_2 in, leading to further travertine deposition. Peat is found associated with paludal and dam travertine worldwide, but the conditions under which it is formed are not always clear. Large-scale peat formation normally occurs during periods of climatic deterioration, rather than amelioration (Jones and Keen 1993).

While the Atlantic period in Britain represents the Holocene climatic optimum, this may not have been the case in other parts of Europe (Huntley and Prentice 1988). Evans (1972) notes that during pluvial episodes, such as that of the Atlantic, water tables will tend to rise which could lead to increased travertine deposition. Further support for travertine formation under equable climates comes from the biostratigraphic record. Much of the detail has been discussed already in Chapter 12, where it is clear that the fossils contained in most travertines were representative of a well-vegetated, frequently forested environment. Forests rarely develop when the mean July air temperature falls below 10 °C (Jones and Keen 1993).

Although radiometric data provide useful information, it should be noted that many dates only provide spot samples taken from individual deposits, and do not necessarily indicate the time of maximum deposition. The overall pattern however certainly suggests extensive travertine formation during the Boreal-Atlantic period in Western Europe. It is easy to understand why travertine formation increased at the beginning of the present interglacial, as the ice retreated and the soils matured but rather more explanation is required to account for the decline to the present day. According to the data shown in Fig. 80, the reduction began during the Atlantic period. Goudie et al. (1993) named this the 'late-Holocene tufa decline', pointing out the likely effects of changing climate and increased human activity. The decline is not just based on travertine dates. There is abundant evidence in Britain of inactive sites, now completely dry and covered in mature woodland (e.g. Pentecost and Lord 1988, Pentecost 1993). At the Shelsley site, measurements of spring discharge and water chemistry have shown that deposition at current rates could not possibly be responsible for the known Holocene travertine mass (Pentecost et al. 2000), and there are several, similar examples in the UK. However, the 'tufa decline' has been challenged by Baker and Simms (1998) who argue that the number of active sites has been underreported in some areas of the UK, and that the true rate of current formation could be considerably higher than supposed. It is not just a question of site number however, but their size and activity. Sites are indeed numerous in some parts of the country, but in areas which have been studied in detail, such as the Yorkshire Dales, while the number of sites is certainly well in excess of 100, the quantity of travertine deposited is extremely small in the majority of cases. Large associated inactive masses of travertine, often obscured by terrestrial vegetation and later soils attest to an earlier period of more extensive deposition. Other explanations for the decline are taken up in Section 13.4.

13.2 Climate and Travertine Deposition

A region's climate is defined by its prevailing atmospheric conditions, the most important of which is air temperature. Changes in temperature affect almost all of the physicochemical properties of matter. In a complex, multiphase system, such as a soil or vegetation, it is therefore difficult, if not impossible to identify which particular property undergoes the most significant change as temperature is altered.

A considerable number of climatic indicators exist in travertine deposits. Gascoyne (1992) lists eight potential indicators for speleothem, all of which are relevant to the epigean travertines. These indicators, plus the fossil fauna are shown in Table 32. Some (growth laminations, micro- and macrofossils) have already been discussed. Here I shall concentrate on geochemical methods and how they can be used to provide information on past rainfall and temperature.

The stable isotope record has been used widely to seek evidence of climatic change in travertine deposits, after the successes scored with speleothems and lake marls. In Oman, direct ^{14}C dating of invasive meteogene travertines allowed reconstruction of the climate over 35 Ka (Clark and Fontes 1990). The characteristic stable isotope signature of travertines developing under arid conditions could be distinguished from those formed in the presence of soils, which implied much wetter conditions.

Pazdur and Pazdur (1988) examined four sites in the Cracow Uplands of Poland and obtained $\delta^{13}C$ and $\delta^{18}O$ profiles from the calcite. They noted temporal trends in several profiles and attributed these to changes in air temperature during the Holocene. They concluded that warm and humid periods occurred from 3–4.5 Ka and 5–8.6 Ka, with maximum deposition between 8.1–8.6 Ka. Thus travertine deposition was apparently favoured at submaximal temperatures. In the UK, Andrews et al. (1994) found that variations in the $\delta^{18}O$ record of up to 1‰ were due to changes of ^{18}O in the rainfall induced by changes in air temperature. They also found that there was a general lowering of the $\delta^{13}C$ as $\delta^{18}O$ rose, suggesting a greater soil

Table 32. Potential climatic indicators in datable meteogene travertine deposits (adapted from Gascoyne 1992)

Indicator	Potential palaeoclimatic significance
Growth laminations	Low rates of deposition indicate cool or arid conditions. High rates indicate moist, warm conditions
Internal stratigraphy	Possible sudden climatic change resulting in growth hiatus, colour or fabric change
Variation in calcite ^{18}O	Change in water ^{18}O content and /or deposition temperature: rainfall; air temperature; evaporation
Variation in calcite ^{13}C	Change in ^{13}C of source water and/or calcite precipitation process: soil or change in plant flora and/or productivity; evaporation; temperature
Strontium isotope ratio	Palaeohydrology and temperature
Variation in ^{2}H of fluid inclusions	Change in ^{2}H due to varying climate
Pollen and other fossil plant content	Indicates surface vegetation type, especially the latter
Fossil fauna, especially Mollusca and vertebrates	Surface vegetation type. Isotope record provides further clues to climate variation
Organic content	May indicate surface vegetation type or changes in soil type
Variation in trace element content	Changes in water composition and/or deposition temperature

CO_2 component during warmer periods. These preliminary studies suggest that the stable isotopic record may provide a useful method for interpreting palaeoclimates. However, not all profiles from epigean travertines are so readily interpreted. Pentecost and Spiro (*unpublished*) obtained two well-constrained ^{14}C-dated profiles for the travertines of Caerwys, North Wales but failed to find any meaningful correlation between the isotope values and the climatic changes known to have occurred during the period of deposition. Stable isotope profiles from travertine dam systems in Spain by Andrews et al. (2000) led them to conclude that deposition under turbulent regimes such as cascades was more likely to provide useful palaeoclimatic information than the hydrodynamically variable systems found associated with travertine-dammed lakes. Garnett et al. (2004) found a significant correlation between the $\delta^{13}C$ of a UK Holocene travertine and the Mg:Ca and Sr:Ca ratios, suggesting that their secular variation reflected changes in groundwater characteristics such as residence time, probably bearing indirectly on the climate. These ratios also reflect residence times of speleothem-depositing solutions (Verheyden et al. 2000). Thus, isotope values must be selected and interpreted with care, and are best considered as a backup rather than an absolute indicator of climatic change. For example, an increase soil CO_2 contribution to groundwater, which has the potential to lower the overall $\delta^{13}C$, could be offset by increased aquatic photosynthesis, which will raise the DIC $\delta^{13}C$. This may be further complicated by a change in vegetation type, from say, C3 to C4 plants. The carbon of C4 plants is isotopically heavier than C3 plants so an increase in C4 vegetation would probably increase the soil carbon dioxide $\delta^{13}C$ (Cerling and Quade 1993; Dorale et al. 1993; Bar-Matthews et al. 1996) and this would find its way into the groundwater. Even C3 plants, if water-stressed tend to have more positive $\delta^{13}C$ values (Ehleringer 1988). As a result, carbon isotope signatures are less easily related to climate than oxygen.

More progress has been made with the stable isotope geochemistry of speleothems. Cave systems provide a more stable environment for calcite precipitation, particularly in regions distant from cave entrances, where the atmospheric pCO_2, air temperature and humidity change little over the season (Horvatincic et al. 2003). Isotopic equilibrium is more likely to be achieved when deposition rates are sufficiently low to provide extensive, unbroken records, permitting long-term high-resolution studies (Dorale et al. 1993).

Subtle changes in travertine morphology and position in response to rainfall have been suggested by Drysdale et al. (2003a). They note that during periods of high discharge, travertine would be deposited further from source so that the positioning of deposits downstream may provide evidence for pluvial periods. Carthew and Drysdale (2003) found dated travertine incisions of 1.5–1.6 Ka probably corresponded with a pluvial period based upon palaeoweather data. At other times the travertine accreted in the stream. Pedley et al. (1996) also found that some travertine dam morphologies and fabrics vary with the climatic setting. Temperature influences the distribution of organisms and animals are particularly sensitive to this, especially certain insect groups such as the chironomids, though these are not well-represented taxonomically on travertine. Krolopp (2003) observed that the size of the mollusc *Bithynia tentaculata* varied with water temperature and used it to estimate the deposition temperature of a Hungarian deposit.

Soil properties are particularly important when considering meteogene travertines but are less significant for thermogenes. Thermogene deposits are nevertheless sensitive to changes in air temperature. Extreme cold prevents infiltration of water by freezing, blocking the hydrothermal circuit. Sturchio et al. (1994) for example, found that the positions of the thermogene travertines of Wyoming were profoundly affected by Pleistocene glaciations which altered the hydraulic head. The positions of speleothems in cave systems may also provide

clues to the prevailing climate. Pluvial periods lead to raised water tables often leading to speleothem formation at higher elevations in caves. The dating of some high-level travertines in a Brazilian cave, Toca da Boa Vista, demonstrated the existence of a pluvial maximum during the last glaciation (Auler and Smart 1997).

The mean air temperature is normally correlated to soil temperature and can be used to give an estimate of regional soil conditions, which may then be related to travertine formation. For example, in the Alps, meteogene travertines are found up to an altitude of about 1400 m, corresponding to a mean air temperature of 5 °C (Chardon 1992). Meteogene deposits become increasingly scarce as one proceeds from southern to northern Europe and they are rare above 65°N, where the mean air temperature is almost everywhere below 5 °C. Within Europe, a significant correlation ($p < 0.05$) exists between the recorded thickness of European meteogene travertines and the mean air temperature (Pentecost 1995a). For example, in Waterfall Beck, UK, the downstream loss of calcium is significantly correlated ($p < 0.01$) to mean water temperature over the seasons. In addition, travertine deposition in this stream is negligible when the mean water temperature falls below 4 °C (equivalent to a mean air temperature of about 6.5 °C). Thus, there is good reason to suppose that mean air temperature, averaged over a month or more, is providing a crude measure of the travertine deposition rate.

Rainfall is arguably an equally important climatic factor affecting deposition. Sufficient rain is necessary to maintain groundwater flow and provide a carrier for the dissolved carbon dioxide. Many of the Earth's regions are too arid and possess negligible groundwater for travertine, though some possess 'fossil' groundwater originating from earlier pluvials.

The effects of rainwater are less readily assessed than temperature. As rainfall increases, the soil infiltration rate should rise to a maximum value. Any further increase would simply result in overland flow that might have detrimental effects caused by flooding and erosion. Also, if infiltration continues at a high level for a protracted period, soil respiratory activity will probably fall, closed system dissolution would increase, and the total CO_2 in the infiltrating water may be diluted out. All of these processes would tend to reduce travertine deposition, but the intensity and duration of rainfall needed to produce such effects is unknown and would vary with both terrain and soil type. It would seem therefore, that increasing rainfall would tend to increase travertine formation initially, but excessive rainfall may be detrimental.

In order to assess the combined effects of rainfall and temperature on modern travertine formation, the limestone regions of Europe were classified by Pentecost (1995a) into six zones characterised by their mean annual temperature and rainfall. It was argued that, within the region, travertine deposition would be at a maximum where mean annual air temperature ranged from 15–20 °C and rainfall exceeded 500 mm a^{-1}. Such regions are of small extent in Europe, occurring mainly along the Mediterranean seaboard. The zones were correlated with travertine deposition within the region, as the largest meteogene deposits occurred in zones 4–6 while deposits were scarce in zone 1.

Taking the world as a whole, these zones require modification to account for the high rainfall and temperatures of the tropics. About 4% of the continents are covered with carbonate rocks (Balazs 1977) and Fig. 81 provides a classification of the world's limestone regions into seven zones A-G. Zone A includes all regions with a mean annual air temperature less than 5 °C and/or <200 mm annual precipitation and includes all of the Earth's cold and arid regions. None would be expected to contain significant active meteogene travertines. It is evident, from the legend of Fig 82 that almost half the Earth's exposed limestone falls within this zone. In Eurasia, the zone descends as far as latitude 30°N in the elevated Tibetan plateau. Almost half the area of North America also falls within this zone. Zone B (5–15 °C, 200–2000 mm rainfall) covers most of Europe but further east there are few areas due to increasing continentality. Zone B

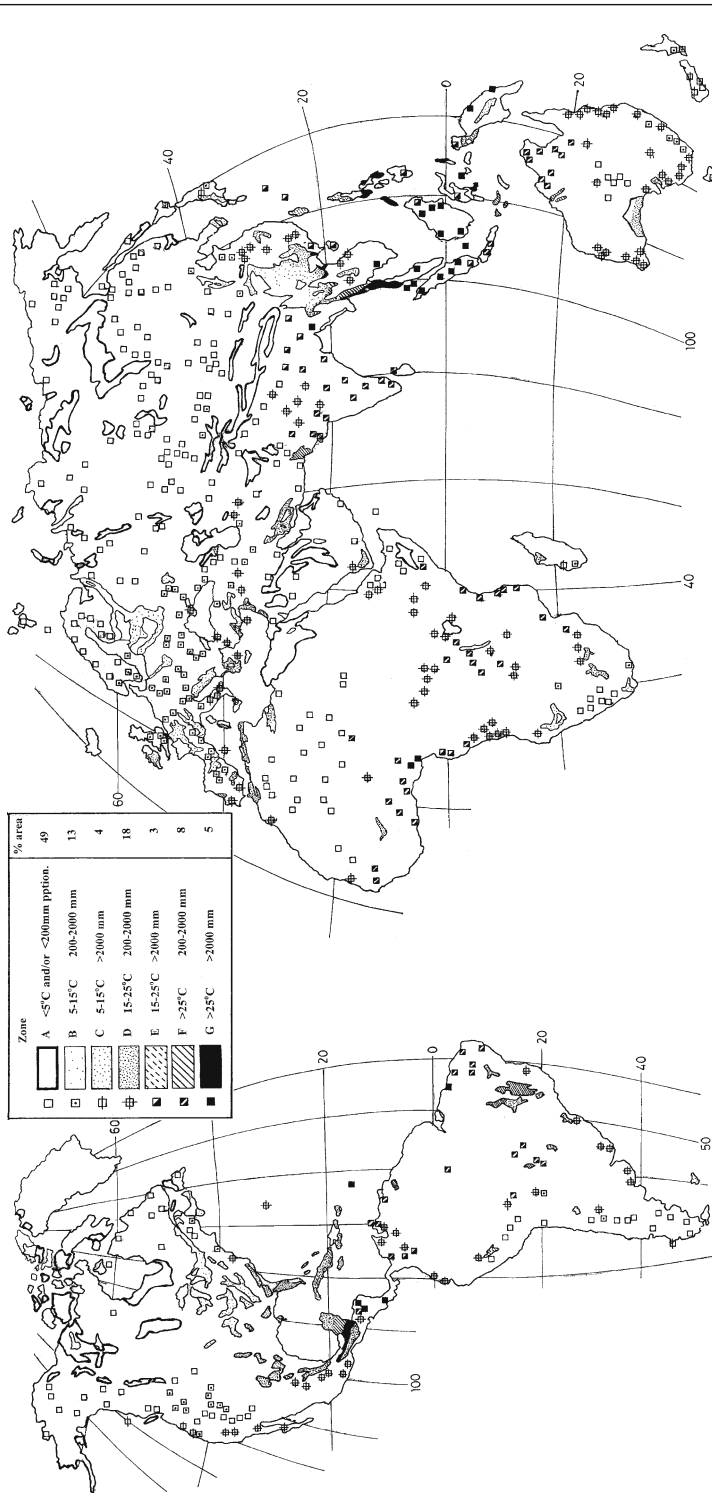

Fig. 81. Main regions of limestone outcrops in the world classified into zones A-G according to the mean annual air temperature (°C) and annual precipitation (mm). Small areas of limestone (<c. 25000 km^2) are shown as coded squares. The relative areas of the zones are given in the legend on the map

also occurs in parts of China, and at higher latitudes of the southern hemisphere – southern Africa, southern Australia and New Zealand. Some of the more mountainous regions of the western United States also belong to zone B and travertine deposition is widespread throughout these regions. Zone C (5–15 °C, >2000 mm) has a more restricted distribution and occurs in Europe along the Dalmatian coast, Italy and the western coast of North America. Zone D (15–25 °C, 200–2000 mm) skirts the Mediterranean coast, covers much of Iran, a small part of Yemen, and considerable areas of China. Many of the Australian limestones lie in this zone and in North America it occurs in most of the southern states and throughout Mexico. Zone E, with the same temperature range as D but higher precipitation, has, like zone C a restricted distribution, including parts of Indonesia, Burma, India and Colombia. The hottest regions (>25 °C) are included within the final two zones. Zone F (200–2000 mm rainfall) is widely distributed in the tropics but covers fairly small areas of limestone; parts of tropical Africa, Central and South America, southern India and northern Australia. Zone G (>2000 mm rainfall) with the most extreme temperature and rainfall occurs in two main regions, Indonesia/Malaysia and Central America. The former is the most extensive, and includes the region containing the world's largest cave systems. Areas within zones F and G should contain the most extensive active meteogene travertines along with well-developed karst if rainfall and temperature act in consort. Many do, but much of zone G occurs in remote, little investigated terrain. It includes the Palawan and Mindoro Islands (Philippines), Sumatra and Borneo in the East, and southern Mexico, Guatemala, Honduras and the Bahia State of Brazil in the Americas. Travertines are certainly known from most of these areas, but little has been written about them. The best known of these high zone sites are the provinces of Guizhou and Yunnan, China, where both epigean and cave travertines are very extensive (Pentecost and Zhang 2001).

While maps of this type could prove useful for travertine 'prospecting', topographic factors also need to be considered. Moderate to high relief is necessary for the development of perched water tables and the steep gradients needed for rapid degassing and carbonate precipitation. Most of Cuba, Florida and Yucatan, all in Zones D and E, are too flat to permit the extensive development of epigean travertines.

Meteogene travertine formation is dependent upon soil characteristics, as previously noted. Drake (1980) obtained a linear relationship between mean annual air temperature and soil pCO_2 whilst Brook et al. (1983) provide a world map of soil CO_2 and found that the best predictor of was actual evapotranspiration, which is itself a function of rainfall and temperature. They showed that the soil pCO_2 is on average higher in the tropics than elsewhere. Applying soil CO_2 data to limestones on a global scale yields a pattern almost identical to that shown in Fig. 82, based on rainfall and temperature.

13.3 Human Influence

It has already been pointed out that human activity often occurred close to sites depositing travertine (12.2.4). Human influence on travertine deposition, and within entire river catchments, has been profound over the past 5000 years. Much of the decline in travertine deposition, which has been well documented in Europe can be blamed on humanity. Goudie et al. (1993) list 26 hypotheses relating to travertine decline, 17 of which are either directly or indirectly related to human activity (Table 33). Those relating to deforestation, drainage and pollution (water and atmospheric) would seem the most important.

Deforestation in various forms has been practiced by man for millenia, and its impact on the hydrological cycle has been considerable, ever since the use of controlled burning. The

rate of deforestation in Europe accelerated during the late Neolithic and Bronze Age (3 Ka B.P.) when more efficient lumbering tools became available. In Europe, deforestation has continued more or less unabated to the present time, where less than 5% of the original forest cover exists over large areas. Removal of tree cover and replacement with arable crops can reduce travertine deposition in at least ten ways, as outlined by Goudie et al. (1993). These authors provide a conceptual model of the travertine-forming potential before and after deforestation (Fig. 82). Factors recognised as influencing the process are listed below in roughly decreasing order of importance:

1. Exposure of bare soil and loss of forest cover leads to soil erosion and increased turbidity in rivers and streams. The suspended particles abrade travertine surfaces and damage attached biota, they also reduce aquatic photosynthesis and smother invertebrates, and may therefore remove travertine and destroy the biological framework. Evidence for increased suspended load has been found by comparing the compositions of modern and old travertines in Britain and Germany (H. Viles, *unpublished*).
2. Increase in discharge results from reduced interception and evapostranspiration leading to more frequent flooding, including physical damage and burial of deposits by alluvium. Hubbard and Herman (1990) suggest that burial of some deposits in Virginia over the past two centuries has resulted from this. Urbanisation and ditching of deforested areas exacerbates the problem. Evapotranspiration models suggest a 10% fall in stream discharge when 50% of a catchment is covered with forest (Hornung and Reynolds 1995).
3. Removal of forest cover will affect the soil atmosphere and lead to an overall decline in the soil CO_2. Goudie et al. (1993) provide a model of the likely changes which will occur once a forest is felled and replaced by scrubland or grass. Soil CO_2 will initially rise as the roots of the felled trees decay in the soil profile but will then decline. Recolonisation with scrub or grass will replenish the soil organic matter, but if the area is cropped the soil CO_2 will remain overall, lower than it was under forest. Increased runoff with deforestation will further reduce the concentration of CO_2 in the groundwater leading to reduced travertine deposition.
4. As erosion proceeds, soil cover is reduced providing less soil CO_2 to the groundwater.
5. Removal of forest from floodplains will make them prone to channel migration and erosion.
6. Podsolisation and acidification of soils often follows intense grazing and/or burning leading to nutrient leaching, reduced soil productivity and reduced soil CO_2.
7. Studies in the Hubbard Brook Catchment in the USA (Likens et al. 1970) have shown that a large rise in groundwater nitrate follows deforestation. This could lead to a change in the aquatic flora by altering the N:P ratio and affect the travertine framework.
8. Removal of trees exposes running water to direct sunlight, increasing water temperature. This has been demonstrated in the Hubbard Brook Catchment and may lead to floristic changes, an increase in the CO_2 evasion rate and more rapid travertine deposition as observed by Drysdale et al. (2003b). Clearfelling of riparian vegetation increases stream temperature maxima by 6–7 °C according to Gray and Edington (1969).
9. Increasing light will favour the growth of mosses and macrophytes leading to alteration of the travertine fabric.
10. Removing trees may reduce the potential for travertine dam construction because some develop on log jams (Viles and Pentecost 1999).

Table 33. A summary of human influence on travertine deposition (modified from Goudie et al. 1993)

Cause	Effects	Influence on travertine formation
Discharge-related		
Deforestation and urbanisation	Increased flow, flooding	±
River regulation	Erratic discharge	–
Water abstraction and drainage	Lowering of water table, stream loss	–
Chemical change		
Acid deposition	Soil acidification	–
Deforestation	Nutrient release	±
Deforestation	Root loss in soil	–
Deforestation	Increased light	+

The seven negative effects could outweigh the three positive ones, though there is as yet little direct conclusive evidence of travertine reduction following deforestation. For example, Ali et al. (2003) found in a French Holocene deposit that extensive exploitation of the forest occurred during the period 6–4.6 Ka with replacement of forest species and spread of *Juniperus* and *Rubus ulmifolius*. This was evidenced in the travertine flora resulting from farming activities – but it did not appear to affect travertine deposition itself. However, several biostratigraphic studies of travertine do suggest a negative effect of deforestation. Meyrick and Preece (2001) found that for sites in Northampton, UK, deposition started at about 10.3 Ka but had ceased by 6 Ka with the decline attributed to forest clearance. At the German Kloster-Mühle site, Meyrick (2003) found that deposition began around 9.7 Ka and ceased sometime earlier than 4.4 Ka. Forest clearance or subsequent erosion of the more recent layers was the suggested cause.

In Australia, Carthew and Drysdale (2003) found that incision of a deposit has occurred in the past 150 yr and attributed it to the impact of European settlement and land clearing. Erosion of fluvial travertines has also been reported in China. In the Beishuihei River, Guizhou much of the travertine is scoured and pitted and the Stone Village dam is breached by small caves. The dams of Xiangxekong are also eroding and show little sign of active deposition (Pentecost and Zhang 2001). Both sites occur in areas of increasing rural populations and have been subject to recent deforestation/water management but there is no direct evidence of human intervention. It should be pointed out that a number of detailed studies on European sites have failed to identify a cause for the decline in deposition (e.g. Limondin-Lozouet and Preece 2004) and other as yet unidentified factors could be involved in at least some of these sites.

Water pollution has also caused damage. One of the best documented cases is that of the Little Conestoga Creek, Pennsylvania (Golubic 1973; Golubic and Fischer 1975) where acidic industrial pollution had destroyed many of the stream crusts. The microalgae associated with the deposits were formerly described by Roddy (1915). These were growing normally at the turn of the 20th Century, but during the period 1966–69, deposition had almost ceased and fewer algae showed signs of encrustation. In England, stream crusts have disappeared from several areas. In one well documented case Edwards and Heywood, (1960) found that

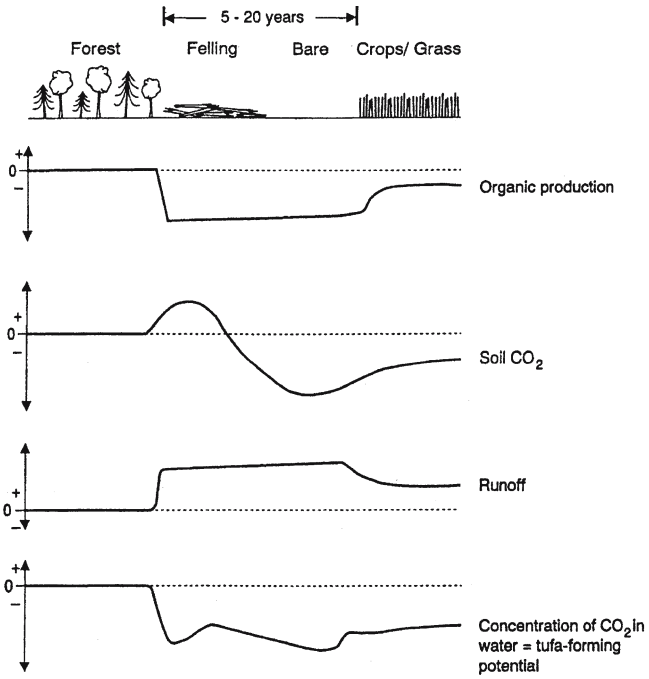

Fig. 82.
A conceptual model of the tufa (travertine)-forming potential of a region that has been deforested then planted with crops (from Goudie et al. 1993, with permission)

crusts had disappeared completely below a sewage outfall but remained healthy above it. Interestingly, the algal flora, consisting of the diatom *Cocconeis* and red algal '*Chantransia*' stage of *Batrachospermum* appeared unaffected by the pollution. Lake Kosjac, Plitvice is also affected by eutrophication owing to inadequate sewage treatment (UNEP 2004). A number of other currently active sites are known to receive varying amounts of organic pollution but appear, at least on casual inspection to be unaffected. These include the deposits along Falls Creek, Oklahoma (Pentecost 1990a), and the thermogene deposits at Pamukkale, Turkey. Mine drainage and leaching from spoil tips are serious sources of water pollution but there are no reported effects on travertine deposition. Ironically, certain industrial wastes such as calcium chloride and slaked lime give rise to travertine formation (see Section 15.5), but it is unlikely to attract a diverse biota and such deposits are often unsightly.

Pollution via acid rain is widespread in the Northern Hemisphere but its effect on travertine deposition is difficult to assess. In the Yorkshire Dales, where many small travertine deposits occur, Pentecost (1992b) found that sulphate in groundwaters balanced a proportion of the calcium ions and could have been responsible for dissolution of up to 10% of the carbonate bedrock. This may not affect travertine deposition *per se* but might have long term effects on soil acidification and biological activity. In the Czech Republic, where the effects of acid rain and water pollution are locally severe, travertine deposition appears to have been reduced in some streams.

Several other human activities adversely affect travertine. The widespread pumping of groundwater for domestic and agricultural use has had a profound effect by lowering water tables and reducing spring discharge. Pumping has lowered the water table in the Chalk aquifer south of London to such an extent that seawater intrusion has occurred. Several small streams have disappeared and no longer deposit travertine. At Plitvice, concerns have been raised about the removal of Lake Kosjak water for domestic and industrial use (UNEP 2004). Huge

irrigation and water transfer schemes have affected the great karst springs feeding the world's largest deposit of travertine in Antalya. The water is now channeled and the deposition of travertine is negligible. In the Great Artesian Basin of Australia, many of the mound springs are no longer active, in some cases owing to the diversion of water for other purposes (Ponder 1986). Ditching and drainage of karst water has been deemed responsible for the loss, or severe reduction of travertine deposition in several parts of Britain (Pentecost 1990a). Trampling also causes problems. Delicate structures are easily destroyed by both domestic stock and people. Some paludal deposits in England have been damaged by intensive grazing of stock, which is widely practiced in the country. At Pamukkale, Turkey, attempts have been made to reduce damage by requesting visitors to remove their shoes, but the pulpit basin pools are heavily used and the deposition processes within them have been disturbed. Major losses of cave speleothem have also been reported by cavers resulting from collectors, accidental damage or deliberate despoilation. Overall, it is seen than human activity is deleterious to travertines both active and inactive.

13.4 The Conservation of Travertine

Travertine-dammed lakes generate millions of dollars every year from tourism. They are the prime attraction at Huanglong, Jiuzhaigou in China, Pamukkale in Turkey and Plitvice in Croatia. Travertine formations are also major attractions at Yellowstone Park, Wyoming and Kakadu, Australia. All of the above belong to World Heritage Landscape Sites which totalled 149 in 2003. They receive considerable protection from damage and pollution, with implemented management plans. Other World Heritage Sites include parts of Rome, Paestum and Taxila where travertine has been used extensively as a building material. Other larger areas are recognised nationally such as the Witjira National Park in Australia, set up to for the Australian mound springs (Zeidler and Ponder 1989). Their conservation, along with other lesser sites throughout the world is cause for concern as pressures associated with the tourist industry increase. For example, in 2003, tourist numbers at Huanglong, Jiuzhaigou and Plitvice were 800,000, 500,000 and 350,000 respectively and rising (UNEP 2004). Yellowstone National Park received over 3 million visitors in the same year. Concerns at the major sites are focussed upon traffic management (human and vehicular), the built environment and water pollution (Ivandic and Klavic 1996). Well-managed sites such as Huanglong provide waymarked boardwalks allowing tourists to see the sites in comfort without touching the travertine surface. At all of the travertine world heritage sites except Pamukkale, bathing in the lakes and pools is banned and at several, visits are supervised by guides. Increasing visitor numbers have forced China to improve access roads both within and outside the park boundaries resulting in some loss of habitat and forest disturbance by noise and pollution. Large travertine-depositing systems have an associated fauna attracted to the lakes for food and water and include the Giant Panda, wolves and bears, all at risk from increased disturbance. At most of these sites, building is strictly regulated, preventing the erection of hotels close to the travertine areas. Hotels are a particular problem if built within the travertine catchment since effluent may infiltrate the groundwater. Phosphates are a potential problem unless tertiary treatment plant is installed. At Pamukkale, some buildings were altered to reduce problems of eutrophication despite current tourist numbers of almost 1 million per year. In China and Yellowstone there are strict controls on building within the park boundaries, but adjacent development is likely to increase.

Other concerns include illegal logging and fishing (Jiuzhaigou, Plitvice), quarrying (Huangguoshu) and development of tourist-associated industries. All of the World Heritage Sites

excepting Pammukale have low resident populations, but with a ready supply of cash-endowed visitors, souvenir and other markets could expand out of control as visitor numbers increase, leading to an expansion of the local resident population, land clearance and strip development.

The conservation of travertine extends beyond the preservation of dramatic visual effects. Pentecost et al. (2000b) drew attention to the inactive deposits that share noteworthy geological features such as cave systems and unique fossil assemblages. In the UK, several of the more significant inactive sites have protection with Sites of Special Scientific Interest (SSSI) status. They include Caerwys and Ddol in North Wales with their large fossil dam complexes and associated molluscan faunas. On continental Europe similar schemes protect active and fossil sites such as the 'crons' of the Ardennes. EC Directive 92/43/EEC, Annex 1 (Conservation of Natural Habitats) specifies petrifying springs with tufa formation as a priority habitat type.

These habitats are noteworthy for their unusual plant and animal communities, previously described in Chapter 9. Taken as a whole, travertine is seen to be a limestone with high conservation status.

Travertines and Their Fossils: Archaean to Pliocene

Travertines are usually associated with, and originate from older limestones. Their occurrence in the geological record might therefore be expected to show a correlation with limestone abundance throughout Earth's history. Since most limestones are marine in origin, a long period could elapse between the original limestone sedimentation and reprecipitation as a freshwater carbonate.

The earliest known limestones occur in the Archaean, where they are rare and considerably altered through diagenesis. It is clear that limestones are not commonly encountered until crustal thickening in the late Archaean allowed the development of platforms suitable for extensive carbonate precipitation (Walter 1983). A few semi-quantitative attempts have been made to assess the amount of carbonate sediments laid down in the Earth's history. Ronov (1964) estimated the relative abundance of limestones and dolostones (Fig. 83a) which demonstrates a rapid increase that begins in the late Proterozoic and continues to the present day. A more detailed analysis covering the past 600 Ma (Kazmierczak et al. 1985) suggests large long term fluctuations in limestone production associated with high sea stands, the most notable being the extensive deposition of pelagic carbonates in the late Cretaceous. A cumulative curve based on Kazmierczak's original data is shown in Fig. 83b, indicating an increasing trend in sedimentary carbonate production over time. Another significant factor for past travertine (and limestone) formation is the atmospheric CO_2 concentration. This is known to have varied in the past, from high levels during the early Proterozoic down at least to the Devonian. In the absence of soils, the resulting aggressive rainwater would dissolve substantial amounts of carbonate, but evasion would be retarded by the high atmospheric CO_2. Meteogene travertines were probably uncommon, and terrestrial carbonate production may have been restricted to evaporite deposits, possibly aided by algal photosynthesis. Evasion from thermogene waters would have also been retarded if not entirely inhibited in the early Proterozoic.

Of relevance to thermogene travertine production are temporal variations in terrestrial vulcanism since the two are often closely associated in the Quaternary. Volcanic activity has not been constant over time and terrestrial vulcanism is often associated with major orogenic cycles, but so far, no such relationship has been found with travertine formation during these earlier periods. Given the decline in carbonate rock and increase in atmospheric CO_2 with time, travertine should occur with decreasing frequency back through the geological record and this is apparent from the information currently available. However, characters used to identify early travertines, namely their fabric, fossils and isotope geochemistries become increasingly obscured through time by diagenesis. Furthermore, atmospheric and geological conditions in the earliest period of Earth's history are little understood and travertine-like rocks may have formed under conditions that no longer exist on the planet.

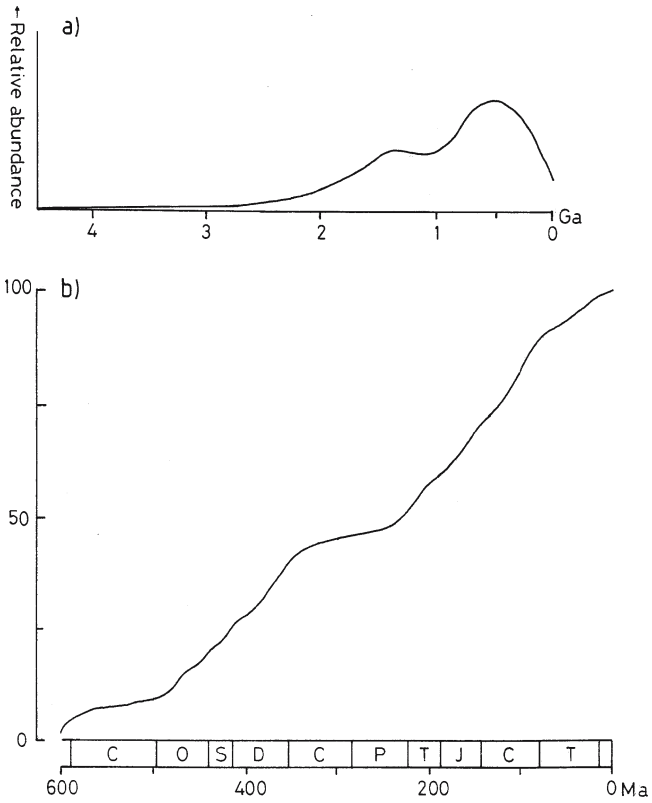

Fig. 83.
Carbonates in the Earth's crust over time. a) Relative abundance of carbonates including dolomite (after Ronov 1964); b) cumulative relative abundance of carbonate rocks during the Phanerozoic, based upon a curve of Kazmierczak et al. (1985)

The study of ancient travertines can lead to insights into palaeohydrology – areas of groundwater recharge and palaeoflow directions (Ordoñez and Garcia del Cura 1983), the recognition of local topographic highs for recharge and sources of carbonate rock. It remains a potential source for early microbial fossils on Earth and other celestial bodies (Chapter 16).

14.1 Archaean and Proterozoic Travertines

It would be valid to question the notion that any convincing travertine has been found in the Archaean, a long and important period of Earth history. Archaean carbonates are rare and comprise no more than 1% of total sediments deposited in this eon (M. Tucker in Tucker and Wright 1991). Most of the carbonate is dolomite whose provenance is still a matter of debate. Many dolomites contain stromatolites- organosedimentary carbonates thought to be formed under the influence of prokaryotes, particularly cyanobacteria – the predominant life forms existing at the Earth's surface at the time. While most stromatolites appear to have been formed in the marine intertidal, some were almost certainly freshwater forms and include the fluvial and lacustrine travertines. The lack of marine indicator fossils at this time makes the identification of freshwater sediments particularly difficult.

Three Archaean and two Proterozoic lacustrine stromatolite/travertine formations are documented. These are, in order of age, the Fortescue Group (2.77 Ga), the Ventersdorp Group

(2.64 Ga) the Pechanga Belt (2.2 Ga), the Rocknest Formation (2.2–1.8 Ga) and the Murky Formation (1.86–1.3 Ga).

Cherty limestones occur at several horizons in the Australian Fortescue Group and are believed to represent accumulations in shallow freshwater lakes and ephemeral ponds (Walter 1983). Evidence of shallowing is provided by prism cracks and the associated shales contain rare element levels consistent with a freshwater environment. Bulbous stromatolites occur through a thick succession and are variable in form, occasionally showing divergent branching. Laminae are present and consist of dark-light couplets from 15–160 μm in width.

Lacustrine stromatolites and ooids have been found intermittently in coarse alluvial sequences in the Ventersdorp Group of South Africa (Buck 1980). Intermittent braided streams deposited conglomerates and gravels and during drier periods ephemeral pools allowed the development hemispherical, dolomitic and cherty stromatolites with finely crenulate laminae. The nodules measured up to 5 cm in diameter and were thought to form through the activities of cyanobacteria. There was active vulcanism during part of the period, but no evidence of hot spring activity. The stable carbon isotope composition averaged –2.87‰ and suggests a non-marine origin.

Small (1–10 cm) travertine mounds, crusts and pisoids have been identified in the Kuetsjärvi Formation within the Pechenga Greenstone Belt of northern Scandinavia (Melezhik and Fallick 2001). They date to c. 2.2 Ga, and consist of a range of dolomite fabrics, some of which have become silicified. In places the travertines consist of 1–5 mm thick dark-light couplets and in others, shrub-like layers occur. Isotopic evidence suggests that the dolomite is primary, in which case the deposits have no modern analogue. They appear to have formed from thermal springs close to a playa lake in an arid climate.

Although completely dolomitised, the Rocknest deposits of Canada contain well-preserved sedimentary structures permitting an interpretation of the depositional environment (Hoffmann 1975). The younger strata contain arborescent stromatolites 1–2 cm in thickness and described as 'tufa-like'. They are interpreted as low-lying supratidal algal flats and marshes. These locations are currently only known today as travertine-depositing where there are associated hot springs or groundwater seepages. More often they are rapidly evaporating regimes supporting hypersaline stromatolites and/or calcretes such as those so well studied in the Bahamas. During the Proterozoic there were no significant land plants and any soils would have developed largely from mats of bacteria, so meteogene travertines would not have occurred under conditions as they exist today.

Alluvial fan deposits embedded with large tabular carbonate concretions have been described from the Great Slave Craton in the Canadian Shield (Hoffman 1976). The masses consist of closely packed branched columns that coalesce to form a range of rounded concretions. They are thought to be lacustrine in origin, and externally resemble the modern lake-edge 'travertines' of Cuatro Cienegas, Mexico. They were considered by Schäfer and Staf (1978) to represent the oldest known lacustrine stromatolites.

Late Proterozoic travertines are also reported from south Karelia in Russia. Here, they have been found associated with mineral veins near basaltic volcanic centres and probably have a hydrothermal origin. The travertines occur associated with jasper, in small bodies up to 3.5 m in thickness (Svetov 1974). Most of these occurrences suggest lacustrine settings and the evidence for travertine as defined in Chapter 1 is scant. Large thermogene deposits have not been encountered but may exist, since the existence of earlier sediments is not a prerequisite. The calcium could be sourced from an igneous rock containing abundant Ca-feldspars.

14.2 Palaeozoic and Mesozoic

Few freshwater carbonates have been identified in the early Palaeozoic. Fannin (1969) describes travertine-like rocks from granite joints up to 50 cm in thickness in the Devonian Old Red Sandstone in Scotland. Fabrics include layers of 'bushes' and 'trees'. The rock probably represents part of a lake shore deposit but a marine origin could not be discounted. More convincing lacustrine deposits were found by Donovan (1973), from the same formation, and consist of dolomitic laminae up to 8 cm thick. They were interpreted as deposits from a lake of variable salinity. Travertine-like rocks are also known from the Old Red near Achvarasdale and Reay in Scotland. A mineralised travertine of Lower Permian age occurs at Karniowice in Poland in the Slawkow Graben where it is locally associated with ores of copper and nickel (Zakrzewski 1984). The deposits crop out along a narrow escarpment about 3 km in length and contain abundant leaf impressions (Lipiarski 1971) and a molluscan fauna (Panow 1936). Szulc and Cwizewicz (1989) describe several lithological units including continuous sheets and many lens-like masses with well-preserved algae (*Chara*, '*Cladophora*' and *Rivularia*) and their primary biofabrics. Presumed annular couplets occur in places with regular carbon and oxygen isotope fluctuations. In the Upper Trias of Sully Island, South Wales, Leslie et al. (1992) describe travertine mounds up to 1 m in thickness associated with palaeosprings issuing from the Carboniferous Limestone. Fabrics include floe calcite, shrubs and pisoids suggesting a thermal origin.

From the Jurassic onwards, more information is available. Small mounds of lacustrine travertine surround the stumps of silicified trees at Lulworth, England (Perry 1994, Photoplate 18D) while probable thermogene deposits occur in the early Jurassic of the Hertford Basin, Connecticut. (Steinen et al. 1987). The deposits are exposed in a quarry face, up to 5.5 m in thickness but laterally discontinuous. They consist of an open cellular calcite framework, partly infilled with carbonate spherulites with geopetal fabrics, suggesting an original dip of about 45°. The travertine has undergone considerable diagenesis with local infills of quartz, chalcedony and dolomite. 'Algal clots' were noted but there were no clearly identifiable organic remains. The occurrence of small spherulites (c. 0.1 mm diameter) consisting of radial calcite fibres was given as evidence for a thermal origin. The deposits were associated with basalts suggesting contemporary volcanic activity.

In the early Cretaceous deposits of Valencia, Spain, Monty and Mas (1981) describe oncolites from lacustrine facies showing similarities to modern lake oncoids. The deposits formed in a graben which also include remains of charophytes and ostracods with molluscan debris. The oncoids ranged from 1–10 cm in diameter and are of two types. One consists of superposed micrite films built upon a knobbly nucleus with laminae 0.1–1 mm thick. The second type possesses finer laminae with a sequence of spongy filamentous and dense layers interpreted as the result of alternating growths of different filamentous cyanobacteria, or some form of seasonal activity. The occurrence of miliolids in some of the lower strata suggest occasional marine incursions into a shallow marl lake. They could represent the earliest recorded freshwater oncoids in the geological record. Small mounds of travertine have also been reported from the Lower Cretaceous lacustrine Baum limestone of Oklahoma (Swartz 1990). A travertine of similar age, associated with mineral deposits is reported from southeast Mongolia by Verzilin and Kalmykova (1989). Late Cretaceous oncoids have been described by Weiss (1969) from Arizona. They possess well-defined laminations and again closely resemble modern freshwater forms. In France, Freytet and Plaziat (1982) found Upper Cretaceous travertines containing structures reminiscent of chironomid larva tubes. The great marine transgression of the late Cretaceous reduced land area and elevated water tables, undoubtedly leading to a fall in freshwater carbonate production.

14.3 Paleocene to Oligocene

The earliest travertines include the deposits at San José de Itaborai, Brasil, which extend over an area of 1 km^2. The deposits are mainly clastic and contain a rich molluscan and vertebrate fauna including a marsupial *Eobrasilia coutoi*. They are of Paleocene age and are thought to be lacustrine, possibly associated with a thermal source (Machado 1967). Another interesting site is that at Sézanne, France where a Thanetian spring deposit originating from the Chalk contains a rich flora indicative of a hot, humid climate (Saporta 1868; L'Apparent 1964). The deposits cover an area of about 0.2 km^2 and represent an ancient cascade complex, now heavily indurated and showing inversion of relief. The flora, obtained from exceptionally well preserved leaf impressions, exceeds 90 species including *Sassafras primigenia* (Fig. 84), *Vitis sezannensis* and two hepatics, *Marchantia sezannensis* and *M. gracilis*. It is noteworthy that *Marchantia* species are occasionally found on modern cascade travertines (Section 9.5.2). The fauna includes Mollusca (e.g. *Clausilia*, *Physa*, *Pupa*), the crustacean *Astacus edwardsi* and a reptile, *Simoedosaurus*.

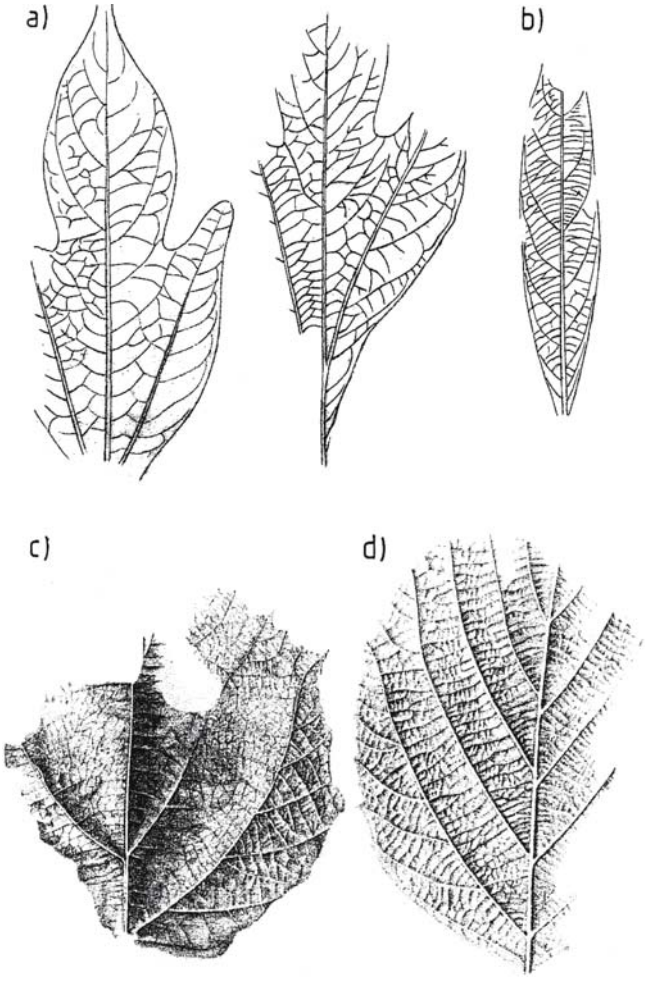

Fig. 84.
Leaf impressions from the Sézanne travertine. a) *Sassafras primigenia*; b); *Laurus assimilis*; c) *Grewiopsis anisomera*; d) *G. credneriae*. From Saporta (1868)

The Eocene Green River Formation is without doubt the best-documented sedimentary unit of the period containing a wide range of lacustrine travertines. The formation represents sediments deposited from the ancient Lake Gosiute which occupied a large part of what is now Wyoming. It had a maximal area of about 40,000 km^2 and formed part of a larger lake complex that spread into Utah and Colorado, and represents the world's largest known lacustrine deposit (Eugster and Hardie 1978). The deposits accumulated over a period of c. 4 Ma during the middle Eocene under a warm-temperate or subtropical climate (Surdam and Wolfbauer 1975). Their nature indicates deposition in an endorheic basin subject to rapid changes in salinity and shore geometry. Sediments are divided into three stratigraphic members, named, from oldest to youngest, the Tipton Shale Member, Wilkins Peak Member and the Laney Shale Member (Fig. 85). The Tipton Shales represent a freshwater episode, and is the smallest unit. This is followed by shrinkage of the lake and the deposition of large quantities of trona in the Wilkins Peak Member. Finally, a more mesic environment returned and freshwater muds were deposited as the Laney Shale Member. Littoral travertines occur at a number of horizons, where they form important markers. Two occur in the Tipton Shale Member, with a further dozen in the overlying Laney Shales (Bradley 1964). The stromatolitic travertines were first recognised by Bradley (1929) who mapped some of them in Sweetwater Co. A fossil alga, *Chlorellopsis coloniata* was described from them. At the base of the Tipton Tongue (Tipton Shales Member), Bradley (1974) described an *Oocardium* algal tufa which closely resembles the modern *Oocardium* deposits of Europe, though the structures are ten times larger in the fossil material and may be unrelated to the modern

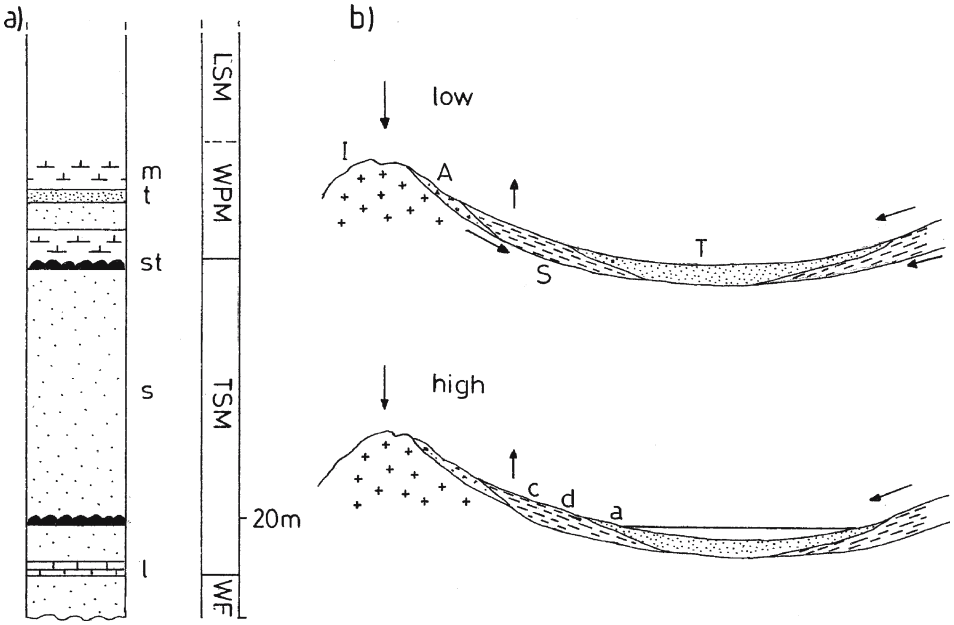

Fig. 85. Stratigraphy of the Green River Formation, Wyoming. a) Section showing the main units; LSM Laney Shale Member; TSM Tipton Shale Member; WPM, Wilkins Peak Member; WF Wasatch Formation. L Limestone; M marlstone; S Oil shale and mudstone; ST stromatolitic travertine; T trona. After Surdam and Wray (1976). b) A playa-lake model of the sequence and high- and low-lake stages showing relationships between hydrology and sedimentation: H, alluvium; I, igneous and metamorphic rocks; S, sandstone; T, trona. Superficial deposits: a, algal deposits at lake margin; c, calcite; d, dolomite. After Surdam and Wolfbauer (1975)

O. stratum. *Oocardium* is a lotic desmid, not known from modern lake shore deposits, but the occurrence of caddis fly cases at the same location (Bradley 1924) indicates the presence of freshwater. Near the base of the Laney Member, extensive reefs composed almost entirely of caddis fly cases have been described in detail by Leggitt and Cushman (2001). In the Tipton Shales, Surdam and Wolfbauer (1975) note that the first appearances of cryptalgal fabrics correlated with a dramatic decrease in abundance of other lacustrine fossils suggesting that the algae proliferated in the absence of grazers as the salinity of the water rose. Travertines also appear to have been forming during Wilkins Peak time. Calcite and dolomite muds were being deposited at the lake margin, along with calcretes and cemented talus. One of the carbonate sources has been shown to be detrital travertine forming around basin springs and in ephemeral streams. The stromatolitic travertines are associated with ooliths, pisoliths and casts of evaporite minerals, indicating a near-shore environment, and periods of high salinity. Where best developed, they form isolated, dome-shaped bodies with internal lamination, forming layers up to 1 m in thickness, but of great lateral extent. As the lake margin receded toward Wilkins Peak time, travertine deposition migrated toward the centre of the lake, but become less evident as salinity further increased. Surdam and Wolfbauer (1978) argue that Lake Gosiute represented a shallow playa-lake complex whose margins responded rapidly to changes in rainfall and evaporation (Fig. 85). Parallels have been sought with modern Deep Springs Playa, California (Jones 1965) which consists of a core of lacustrine saline crust surrounded by calcitic and dolomitic muds.

Other lake travertines are known from this period in the United States: oncoids dating from the early Eocene of Arizona are described by Weiss (1969) and series of thin deposits of Late Eocene age are known from the Chadron Formation of South Dakota (Evans 1999). They consist of oncoidal and other clastic deposits but are most noteworthy for their dam remnants, the dams being up to 60 m wide and displaying a range of microfabrics. The springs giving rise to these deposits were associated with faulting, fold axes and palaeovalleys. Lake reefs have been found in the Upper Eocene deposits near Kinik, Turkey, formed around a

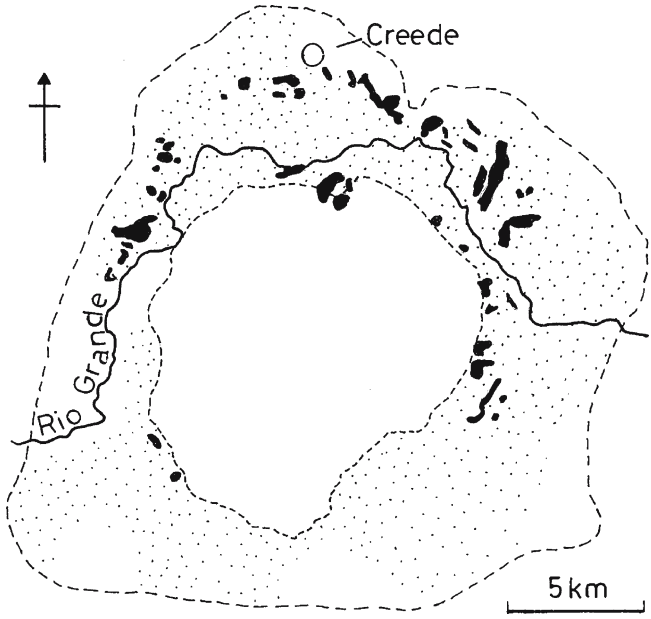

Fig. 86.
The Oligocene Creede Caldera, Colorado. Tuffs, pyroclastics and latite rocks stippled; other volcanic rocks, blank; travertine, black. Redrawn after Larsen (1994)

Schizothrix-like cyanobacterium (Varol et al. 1984). Lacustrine oncoids, with gastropod nuclei occur associated with thin laminar travertines at Big Bend, Texas (Collinsworth and Rohr 1986). Similar deposits are known from southeast France (Moulin 1966). Here, some fabrics indicate deposition around higher plants, bryophytes and algae in a paludal environment. In the Guarga Formation of the Spanish Pyrenees, Nickel (1983) describes oncoids in fining-upwards sequences. They resembled those currently forming in small streams, growing on sticks and display plenicinct growth patterns. The oncoids averaged about 2 cm in diameter and sections sometimes revealed tufted filaments reminiscent of the cyanobacteria *Rivularia, Scytonema* and *Phormidium*. A fibrous or bladed calcite cement with acicular terminations lined the cavity walls and formed a crust around the woody fragments. A later equant microspar sometimes replaced an earlier cement. Diagenesis appears to have reduced grain size in some areas, whilst enlarging it in others. A schematic model is provided for the oncoid morphologies encountered. A thermal travertine is known from the Palm Park Formation, New Mexico, where seasonal accumulations have been demonstrated through stable isotope profiling (Chafetz et al. 1991b).

There are few reports of travertine from the Oligocene. Perhaps the most celebrated site, for the fossils it contains, is the Geilston Bay Quarry in Tasmania (Tedford et al. 1975). The spring-deposited travertine accumulated under humid, subtropical conditions beneath a layer of basalt, which interrupted deposition and was dated radiometrically to 22.4 Ma, close to the Miocene-Oligocene boundary. The deposits are noted for their rich flora, and the occurrence of an early marsupial, *Ngapakaldia* in the associated clays. Further lacustrine travertines occur at Limage dated to the late Oligocene (Bertrand-Sarfati et al. 1966). The Late Oligocene Creede Caldera of Colorado contain layers of travertine which interfinger with volcanic sediments and outcrop over a wide area. The travertine occurs as irregular stromatolitic masses with occasional relict terraces and sheets in a wide arc from Spar City to Wagon Wheel Gap (Fig. 86). The caldera lake underwent large changes of salinity and there is evidence of hydrothermal discharge into the lake from the travertine-depositing springs developing along caldera faults (Steven and Ratté 1965; Larsen 1994).

14.4 Miocene and Pliocene

Some interesting travertine-like deposits occur in the Miocene Ries meteorite crater of Germany. The deposits form marginal buildups 7 m high and 15 m in diameter and larger, irregular mounds. The reefs are full of fine calcareous tubes, belonging to an extinct green alga, *Cladophorites incrustans* (Riding 1979). Nodular mounds including peloidal and skeletal carbonate sand and are thought to have developed in a saline lake as sublacustrine spring mounds (Arp et al. 1998; Pache et al. 2001). The deposits contain 'sickle-cell' shaped voids, thought to be characteristic of saline lake deposits. Changes in the lake level caused temporary emergence and finally burial and diagenesis of the reefs, with aragonite dissolution and dolomite precipitation. Also within the crater, a lake travertine dating to15 Ma has been found to contain a rich vertebrate assemblage with excellent preservation, including bones of amphibians, reptiles, birds and mammals (Heizmann and Fahlbusch 1983). The lime-rich Molasse of southern Germany contains oncoids with the remains of cyanobacteria (Rutte 1954). Further afield, in the Eastern Rift of Africa, travertine crusts dated to 10.5 Ma were noted by Casanova (1994).

Travertines apparently deposited from thermal waters are known from several regions. In the Schwäbische Alb, Germany, volcanic activity throughout the Miocene led to deposition of the Böttingen Marble. The deposits possess a flora indicative of a warm-temperate climate

(Gregor 1982) and possess a rich arthropod fauna (Westphal 1959). The fabric of a similar deposit is described by Koban and Schweigert (1993) and contained floe calcite, encrusted gas bubbles and shrubs. Other thermal deposits include the fault-controlled deposits in central Afghanistan which are still active (l'Apparent 1966), the manganiferous (thermogene?) travertines of the Pilanes Formation, Baja California (McFall 1968) the diatomite-associated travertines of Kamchatka (Grechin 1972) and the tufa mounds of the Barstow Formation, California (Cole et al. (2004).

In Pliocene times, the global climate cooled and the first evidence for the current ice ages appeared. The land masses assumed much their present form though there was also a large marine transgression. Deposits of travertine are known from many areas, and in some, a more or less continuous sequence can be traced up to the present day. Link et al. (1978) note stromatolitic travertines and oncoids in the Californian Ridge Basin Group. The oncoids consisted of micrite laminae and contained algal filament molds and were considered to represent a near-shore facies. Pliocene deposits also occur elsewhere in the state (Hunt and Mabey 1966). In Argentina, a racoon, *Cyonasua groebii* has been described from travertines

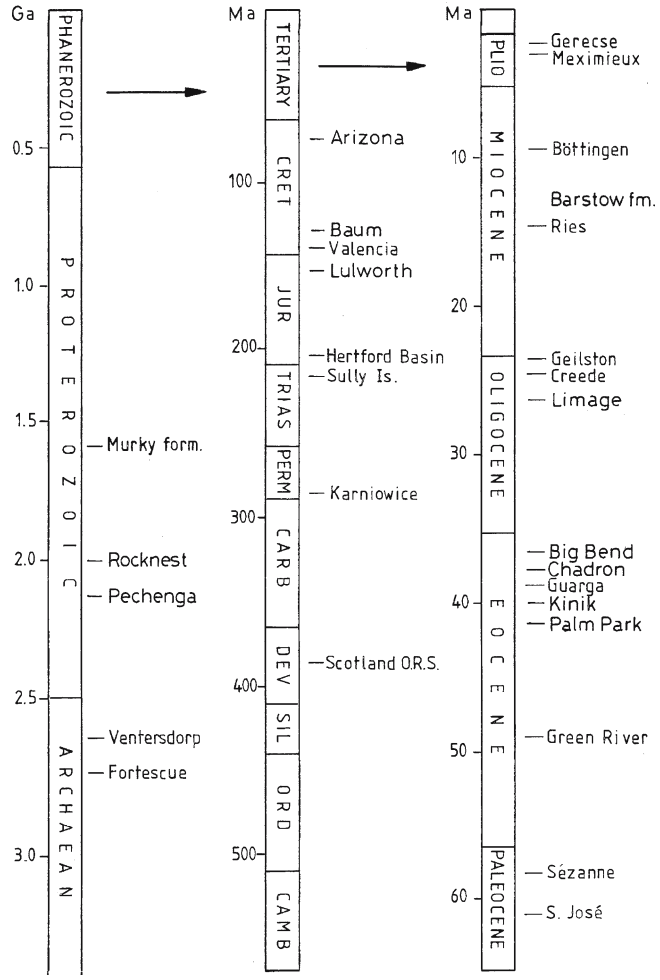

Fig. 87.
Chronology of some travertine and travertine-like occurrences in the pre-Quaternary geological record

of this period (Kraglievich and Reig 1954). Most Pliocene travertines so far reported represent fluvio-palustrine accumulations. The early plateau travertines of Egypt probably belong here (Butzer and Hanesn 1968) and in Morocco, Pliocene travertines are extensive in the Saiss Basin (Ahmamou et al. 1989). They are also known from Algeria (Julian and Martin 1981). In Hadar Lake, East Africa, oncoids have been dated to 3.5 Ma (Casanova 1994) and Pliocene travertines are also known from the Lake Bogoria area of the African Rift. The hominid-bearing cascade travertines of South Africa discussed in Section 12.2.4 also belong here. Ivanova (1946) found four travertine layers in the Caucasus Mountains, the earliest of which was upper Pliocene. In France, Pliocene valley deposits occur at Meximieux and contain a flora indicative of climatic cooling (Pomerol 1973). Travertine complexes are also known from Montouliers and Murviel, Languedoc, in a region containing over 100 Quaternary sites (Fabré 1986).

In Turkey, the world's largest deposit of travertine at Antalya (ca 600 km^2) is thought to date from the late Pliocene (1.5–2 Ma). Burger (1990) interprets the deposit as a series of large infilled travertine dams within a small graben. Up to eleven large terraces associated with the dams form a stepped-landscape down to the Mediterranean Sea. A later study by Glover and Robertson (2003) identifies two major terraces, the upper associated with a large lake-fill with dam and the lower with a period of marine erosion, now exposed by uplift following the glaciation. Some of the deposits contain plants such as *Parrotia persica*.

Another noteworthy site, considering its altitude is Aqqikkol Lake on the Tibetan Plateau which contains a rich flora thought to date from the late Pliocene (Zhang et al. 1990). Other occurrences include the extensive deposits of the Gerecse Mountains, Hungary, where the travertine forms a series of mounds along a horst fault (Pécsi et al. 1982) and form a discontinuous sequence until the present day. Intensely karsified thermogene deposits occur at Spis, Slovakia (Vitek 1973).

Figure 87 provides a summary of travertine occurrences within the geological record. Of these, about 50% are thought to represent lacustrine deposits, while the remainder are divided equally between fluvial/palustrine and hot spring deposits. Oncolitic facies predominate at about 20% of sites, most of which are lacustrine. The predominance of lacustrine forms may be related to their higher preservation potential. Many of the lake deposits were found in regions subject to long term subsidence in horst and graben terrain. Such deposits are more likely to become buried and preserved by overlying sediments, whilst fluvial dams and cascades, by their nature occur in rapidly eroding sites and are rarely preserved. Surface-cemented rudites are hardly recognised, but cemented fans are known from the margins of the Green River Formation. Cementation of older rudites however, often occurs a long time after burial, leading to problems of interpretation. A search for further well preserved Proterozoic travertines would be rewarding as an investigation of their isotopic and fossil composition could throw light on their formation processes and the associated biota give information on the local environment.

Related Sediments and Industrial Deposits

Although travertine is a widely distributed continental carbonate, other carbonate deposits are equally, if not more significant. These include the lacustrine marls or 'lake chalks' and the calcretes, the latter deposited mainly through evaporative processes. Often, examples of all three limestones can be found together, and in some cases, it is difficult to decide where one type begins and the other ends. Along tropical coastal margins, travertine-like accumulations of beachrock are often observed, where most of the carbonate is precipitated under the influence of seawater. There are also industrial deposits of calcium carbonate, formed in hot water pipes and boilers, some of which are closely allied to travertine. They result in pipe blockages and energy loss in industrialised countries entailing considerable costs. Finally, the siliceous sinters of hot springs frequently form mounds, terraces and cascades and are often associated with travertine. Here they are briefly compared and contrasted with them.

15.1 Lacustrine Marl

These deposits are characterised by their fine, soft, crumbly texture and paucity of framework or fenestral porosity. Porosities range from about 45–60% in recent marls, dependent upon the degree of compaction. They are formed in lentic waters of variable depth and a range of types can be distinguished according to the origin of the carbonate. Authigenic marls are usually associated with aquatic plants, especially charophytes and phytoplankton and appear to be largely the result of plant photosynthesis. Deposits may also result from inorganic or physical processes such as sediment transport, evaporation or degassing. Marls are found in water bodies which range from fresh to hypersaline (>300 ppt). They range from <1 cm to >30 m in thickness and can exceed 100 km^2 in area. Some are unstratified, while others possess regular varve-like layers that may, or may not be formed annually. They normally consist of calcite, but aragonite (Müller 1971), monohydrocalcite (Kelts and Hsu 1978) and vaterite have been recorded (Rowlands and Webster 1971). Lake marl is sometimes referred to as 'chalk', a term best avoided owing to its confusion with the pelagic Cretaceous chalks of marine origin. Marl however, is often applied to sediments containing a large proportion of clay, and is not necessarily lacustrine in nature. Kelts and Hsu (1978) classified freshwater carbonates into two groups based upon their geological setting, 1) deposits of brine layers or playas in arid regions and 2) deposits in fresh- or brackish lakes in humid regions. Here, the marls have been classified into four broad categories (Sections 15.1.1 to 15.1.4).

15.1.1 Biogenic Marls

Included here are the bioclastic carbonates of Kelts and Hsu (1978), consisting largely of the remains of calcified aquatic plants, mainly algae. An ecologically important group of algae, the Charophyta, grow attached to soft lake sediments where they often become encrusted in carbonates making a major contribution to the lake sediments. A less well-known group of planktonic freshwater algae also calcify and contribute towards the sediments.

15.1.1.1 Benthonic Chara Marls

Sediments formed mainly by deposition of calcite on benthic plants, especially *Chara*, with smaller contributions from submerged angiosperms such as *Potamogeton*. Photosynthetic activity is known to play a part in their formation (McConnaughey et al. 1994). These marls are found in lakes, ponds and marshes of low to moderate salinity. They are formed only in shallow waters since *Chara* rarely grows at depths exceeding 20 m. The deposits are easily recognisable as they contain abundant *Chara* fragments including the uniquely sculpted oospores whose calcified fossils are termed *gyrogonites* (Photoplate 17A). The deposition rate of *Chara* marl is comparable to that of the meteogene travertines, of the order of 1–15 mm a^{-1}. They are often unstratified, fine grained and pale in colour and they are widely distributed in Europe and North America. *Chara* marls are often found associated with travertines. They may even occur to a limited extent on cascades such as 'crons' where small water pools develop, but they are more often found in travertine-dammed lakes whose depths rarely exceed 20 m. Such deposits occur at Antalya, Turkey, (Burger 1990); Welheim, Germany (Herr-mann 1957); the Liri Valley, Italy (Devoto 1965) and in many other places. Occasionally, encrusted *Chara* is rapidly sealed by a layer of travertine or mud before it disintegrates into marl. The form of the plant is then preserved in its growing position, to provide a delicate 'honeycomb' structure sometimes sold as a curio in China (Photoplate 17B).

15.1.1.2 Planktonic Marls

Several planktonic algae nucleate or trap calcium carbonate and ultimately become incorporated into sediments. Dense crops of phytoplankton are capable of severely depleting lake water of carbon dioxide leading to calcium carbonate supersaturation and the formation of 'whitings' (Strong and Eadie 1978; Koschel et al. 1983; Thompson 2000). Thus the carbonate may be biologically controlled or biologically induced (Section 10.8.2). Interesting examples of biologically-controlled deposition are described for the cyanobacterium *Synechococcus* by Thompson (2000) and the green algae *Coccomonas* and *Phacotus* by Müller and Oti (1981). They are well-characterised by their calcified microfossils. These marls and those formed from whitings are often 'varved' forming annual layers sandwiched between carbonate-poor sediments laid down in winter (Brunskill 1969).

15.1.2 Abiogenic Marls

Calcium carbonate is one of the first minerals to separate when lake water evaporates. In most cases, the carbonate is first deposited as low magnesian calcite while the water becomes progressively enriched with magnesium which may ultimately result in the depsition

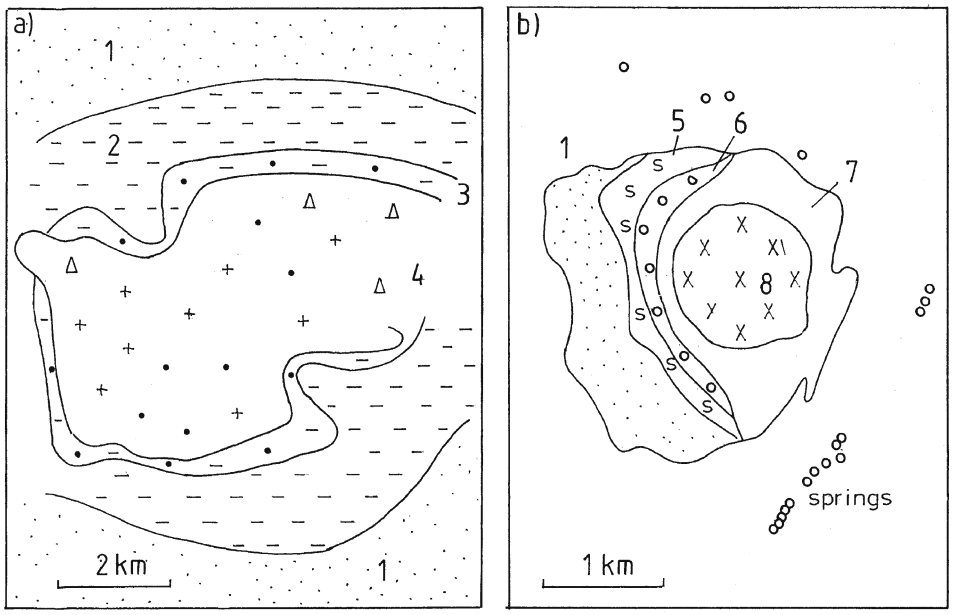

Fig. 88. Playa lake mineral zonation. a) Minerals deposited on the surface of Saline Valley Playa, California. After Hardie (1968); b) Deposits of Deep Springs Playa, California, modified from Jones (1965). 1, calcite/aragonite; 2, gypsum; 3, gypsum and glauberite; 4, glauberite, mirabilite and halite; 5, dolomite; 6, gaylussite; 7, thenardite 8, burkeite

of protodolomite or magnesite. After carbonate, gypsum is frequently formed so mixtures of the two can occur as for example in the Dead Sea (Neev and Emery 1967). Further processes occur in the sediments of this lake, where sulphate reduction leads to the consumption of gypsum and precipitation of more carbonate as calcite. Precipitation of calcium carbonate can also occur in some playas via capillary evaporation. The carbonates often form an outer rim in playa lake deposits, encircling deposits of more soluble salts, as in the Saline Valley Playa (Hardie 1968; Fig. 88a) and Deep Springs Playa (Jones 1965; Fig. 88b). During evaporation, some degassing of carbon dioxide may be expected, but if the waters are alkaline, this will be negligible. Nesbitt (1974) quoted in Eugster and Hardie (1978) calculated that all the alkaline earth carbonate deposited in the Basque Lakes of British Columbia could be accounted for by precipitation with negligible degassing. Most saline lakes probably contain layers rich in calcium carbonate. The Great Salt Lake, Utah, one of the world's largest examples contains great quantities of calcite, as do many fossil Pleistocene lakes, such as Searles Lake, California.

Marl lakes at high latitudes would not normally be expected to have an elevated salinity and the effects of evaporation on precipitation are likely to be minor. This was found to be the case for Malham Tarn in the UK (Coletta and Pentecost, *unpublished*). However, a detailed study of the carbon budget for this lake did reveal that the evasion of carbon dioxide was substantial and likely to contribute to calcite supersaturation and marl deposition. In Malham Tarn, the uptake of carbon dioxide by *Chara* photosynthesis was found to almost equal the amount lost by atmospheric evasion. Similar observations have been made in the Plitvice Lakes of Croatia by Emeis et al. (1987) where surface degassing also occurs.

15.1.3 Clastic Marls

These deposits occur where there is a large input of suspended carbonates, such as the glaciated limestones of the Northern Calcareous Alps (Sturm and Matter 1972) and Lake Huron, Canada (Thomas et al. 1973). A number of European lakes possess Late Glacial sediments consisting largely of these marls which formed during deglaciation to be replaced later by biological marls or other types of sediment. They are usually distinguished by their stable carbon and oxygen isotope values, which are typical of marine limestones (Kelts and Hsu 1978). They are often structurally distinct, consisting of recognisable limestone fragments and 'rock flour'. Some travertines are also readily eroded by water and form beds of marl behind travertine dams. Their secondary nature can usually be identified by their isotopic signature, structure and setting.

15.1.4 Other Marls

A considerable number of marls do not readily fall into the above categories but nevertheless cover extensive regions of the low-lying tropics and sub-tropics. Many are associated with cyanobacteria, but the role these microbes play is at present uncertain, despite a substantial literature on the subject. They include the extensive deposits of the Florida Everglades, a marsh-fen environment containing abundant cyanobacterium mats. The deposits are formed during periodic flooding and occur as thin beds over large areas. Merz and Zankl (1993) have shown that cultures of the cyanobacteria are capable of precipitating calcium carbonate under laboratory conditions. Freshwater algal carbonates are also widespread in the Bahamas, and have been widely studied on Andros Island (Monty 1976). In Lake Fryxell, Antarctica, laminated calcites have been found associated with the benthic cyanobacterium *Phormidium frigidum*. The waters have a high alkalinity and the cyanobacteria are thought to be involved in calcite precipitation (Wharton et al. 1982).

15.2 Calcrete

Calcrete was a term originally applied by Lamplugh (1902) for deposits of calcium carbonate cementing clasts in a cool temperate near-surface environment, but this is not what is generally understood by the term today. A current definition of calcrete is given by Wright and Tucker (1991), modified from Goudie (1973) and Watts (1980) as:

> a near surface, terrestrial, accumulation of predominantly calcium carbonate, which occurs in a variety of forms from powdery to nodular to highly indurated. It results from the cementation and displacive and replacive introduction of calcium carbonate into soil profiles, bedrock and sediments in areas where vadose and shallow phreatic groundwaters become saturated with respect to calcium carbonate.

Calcretes thus form under a range of conditions, but the majority are associated with soils subject to a prolonged moisture deficit. Calcretes cover up to 13% of the total land surface (2×10^7 km^2) mostly as low magnesian calcite, but high magnesian calcite, aragonite and dolomite are also known (Watts 1980; Wright and Tucker 1991). The classification of calcretes is complex, much of the difficulty arising from the separate approaches taken by soil scientists and sedimentologists, but Wright and Tucker (1991) who provide a thorough review, suggest four useful schemes based on morphology, development, hydrology and microfabric.

The morphological classification recognises nine types of pedogenic calcrete ranging from calcareous soils containing small carbonate grains and patches of needle-fibre calcite to

boulder/cobble calcrete consisting of dense hardpans fractured and partly dissolved by rhizobrecciation. This parallels a common developmental phase for pedogenic calcretes where Machette (1985) recognised six stages beginning with thin, discontinuous coatings of carbonate on pebbles or soil particles and a total carbonate content of 2% up to a strongly indurated mass with >75% $CaCO_3$. The complete process can take thousands of years (Wright and Tucker 1991). Carlisle (1983) classified calcretes according to their hydrology into five groups in relation to the water table. It was observed that some calcretes develop within or below the capillary fringe many metres below the soil surface. Classification based upon the microfabric has been proposed by Wright (1990) who recognised two end-members termed alpha- and beta-calcrete. The alpha-calcretes consist of dense micrite/microspar containing crystallaria (calcite-filled cracks), floated, etched and exploded skeleton grains, large euhedral crystals, crystal size mottling and displacive growth structures. They are thought to be largely the result of physico-chemical processes and show much evidence of volume expansion during emplacement leading to 'grainified' brecciation and are frequently found in silica-rich hosts. The beta-calcretes are dominated by biogenic features, thought to be mostly fungal and algal, which include needle-fibre calcite, microbially-formed tubes, alveolar septa, and rhizocretions (Fig. 89) and occur more often in carbonate-rich hosts. Riding (2000) also uses the term 'microbial calcrete'. Nodular structures termed glaebules are frequently found in calcretes. Their origin is unclear but they may be concentrically laminated and resemble oncoids (Brewer 1964). Pisoids are also found (Hay and Reeder 1991) as well as peloids, both possibly of faecal origin. Calcretes form from a range of processes, of which direct evaporation and evapotranspiration must play a major role. However, degassing of CO_2 from the soil surface could play

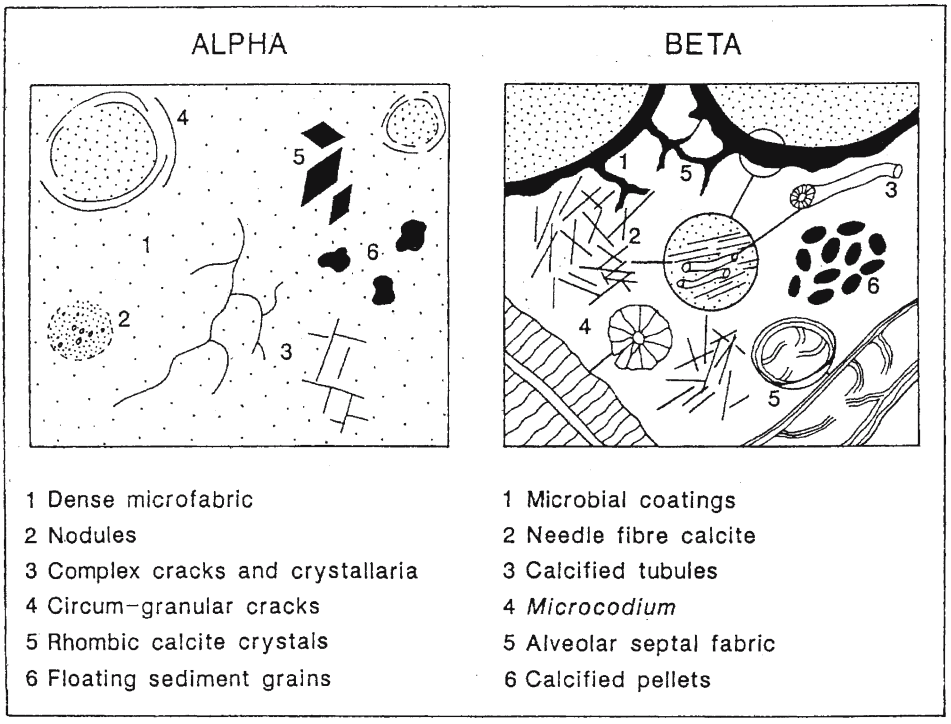

Fig. 89. Petrographic characters of α and β calcretes. From Wright and Tucker (1991) with permission

some part as well as plant activity (Goudie 1996). The common ion effect is believed to be a significant process around playas, where gypsum is present. Plants have been suspected of playing several important roles. Soil microbes, particularly fungi appear to promote precipitation by providing a suitable nucleation surface, possibly aided by calcium excretion (Phillips et al. 1987) and the bacterial conversion of calcium oxalate into calcium carbonate (Verrecchia et al. 1993). Rhizocretions – deposits of pedodiagenetic carbonate surrounding plant roots are commonly recognisable, particularly in the earlier stages. Non-rooted plants may also have an important contribution to make. Algae, common on many soil surfaces, remove carbon dioxide and promote deposition much as they do in lakes and streams (Krumbein and Giele 1979). Stable isotope studies have shown that there is considerable variability in $\delta^{13}C$ (see 8.2) and indicate that in most cases the major source of carbon dioxide is the soil.

There are several calcium carbonate sources for calcrete. Evaporation of water from the capillary fringe overlying groundwater was long thought to be the most important ('per ascensum' model of Goudie 1973) but calcium salts can also accumulate on the surface and move downwards ('per descensum'). Surface accumulations result from wind-blown dust, evaporating rainwater and marine aerosols. Over many years, substantial quantities may be added to the soil then move down through the soil profile. Calcretes forming on non-carbonate bedrock or well above the water table are formed in this way. Calcretes can also develop through re-solution and/or secondary precipitation in existing carbonates, as for example in the solution and redeposition of aragonitic limestone of the Edwards Plateau, Texas (Rabenhorst and Wilding 1986). Travertines may also undergo such a process as has been shown by Burger (1990).

Certain deposits formed within the vadose and phreatic zones have been referred to as 'groundwater calcretes' (Wright and Tucker 1991; Alonso-Zarza 2003). In the Wahiba Sands, Oman, large areas of alluvial fan gravels have been cemented by carbonates to depths exceeding 200 m (Maizels 1987) and similarly large areas are known from Australia. The deposits form as groundwater seeps slowly downslope and becomes progressively enriched in salts. Precipitation results from the common ion effect, degassing, and evaporation or a combination of these and occurs both within and below the capillary fringe. The deposits often form around topographic highs where the groundwater approaches the surface, facilitating evaporation. Carbonate growth can be both replacive and displacive and can lead to inverted relief (Reeves 1983).

In the UK, surface- and subsurface-cemented boulders and breccias have been reported widely (Pentecost and Lord 1988; Pentecost 1993). Most date to the Holocene and a petrographic study by Strong et al. (1993) found meniscus cements of sparite and micrite and a delicate fibrous calcite associated with roots and rootlets (rhizocretions). Owing to the cool temperate climate, evaporation is unlikely to have played a major part in their formation. Pentecost (1993) classified the surface-cemented forms as travertine on the assumption that CO_2 evasion from a soil-CO_2-enriched groundwater was responsible for cementation. Strong et al. suggest that deposits forming in the subsurface were infiltrated with CO_2-rich waters from a vegetated soil, but did not detail the process. They noted that the current water table was well below the calcrete horizon suggesting their formation during either a wetter climate, or that cementation occurred well above the water-saturated zone. Similar deposits occur where cave- and epigean travertine-depositing waters flow over cobbles and scree, and they may result in travertine dams, but fibrous calcite does not normally occur in this setting. Distinguishing epigean deposits from these subsurface 'clast' calcretes could be problematic in the geological record, although the presence of fibrous calcite and of rhizocretions would point to a subsurface origin.

15.3 Coast Deposits

A range of travertine-like carbonates occur in coastal environments and some, such as beachrock are widely distributed between latitudes 35°N and 35°S (Scoffin and Stoddart 1983). A considerable variety of deposits are described in the literature but their origins, by and large are not well understood. The best known forms are beachrocks. This term applies to carbonate-cemented intertidal clastics. Grain size may range from fine silt to cobbles, but sand-sized particles are most frequently recorded. The cemented grains may themselves be composed of carbonate such as ooids or calcified algae fragments but siliciclastic material is equally common. Beachrock is often a highly resistant layer confined to the upper tidal and supralittoral of moderate to high energy shorelines. The deposits rarely exceed a few metres in thickness but may be extensive on tidal flats. Often, they form a series of low, landwards-facing ledges which impound small areas of water at low tide. Submarine cementation giving rise to 'hardgrounds' is also well known in shallow tropical waters subject to stong tidal currents (Dravis 1979). Beachrock cement consists of aragonite or high magnesian calcite and isopachous fringes, meniscus- and gravitational cements are the most frequently encountered forms (Scoffin and Stoddart 1983). Cementation is believed to form just below the beach surface. Further up the beach, where meteoric water may be present, cements of low magnesian calcite are sometimes encountered.

The origin of beachrock cement is uncertain. Evaporation within the intertidal zones of tropical shores is intense and is the most likely cause. There is stable isotopic evidence for seawater evaporation in some of the Bahamian beachrocks (Beier 1985). There appears to be no correlation between beachrock occurrence and rainfall, and the interstitial waters of beachrocks have salinites up to four times higher than seawater also indicating high rates of evaporation (Ginsburg 1953). Schmulz (1971) concluded that lithification occurs close to the water table, where marine and groundwaters mix. It is unlikely that the simple mixing of these waters would normally give rise to precipitation through a common ion effect alone, and degassing of carbon dioxide could be significant. Hanor (1978) for example, conducted experiments showing that groundwater degassing would occur when the tide recedes leading to measurable precipitation rates. Cyanobacteria and other algae often colonise beachrock in profusion and may supply some carbonate through photosynthesis (Beier 1985; Tucker and Wright 1990) but there is no conclusive evidence for this. Some remarkable cemented aeolianites are described from the coasts of Madagascar resembling travertine minidams (Battistini 1981). The structures show evidence of biocorrosion and are presumably a type of beachrock. Other noteworthy cemented aeolianites are known from calcareous dunes of the Western Australian coast, where erosion sometimes reveals entire calcified bushes of landplants (M. E. Gilham, *pers. comm.*).

Quaternary 'beachrocks' are also known from temperate latitudes and are widespread in the British Isles, occurring on the Isle of Wight, the Gower and Portland West Beach, Dorset (Davies and Keen 1985). They consist of carbonate-cemented pebbles and sands and appear to have formed in the vadose zone at, or near the upper shore and most are more realistically classified as cemented rudites as described in Chapter 4. Degassing of meteoric waters, aided by the loose and porous nature of the material is probably responsible for such deposits. Similar crusts are widespread below coastal dunes and are known from South Harris, Scotland (Photoplate 17C) and Lleyn in North Wales. Inland equivalents would be referable to calcrete as noted above, and the distinction between calcrete and beachrock in general can only be made on the basis of location, as it appears that the presence of seawater is incidental to beachrock formation, unless the cement mineralogy is considered. This is reinforced by

the occurrence of beachrock around some marl lakes. Resistant layers of cemented oncoids and shells occur along the shore of Ore Lake, Michigan closely resemble their marine counterparts. Mineralogically, the cements are readily distinguished, being composed entirely of low magnesian calcite, but here the degassing of groundwater is the most likely cause, as evaporation is negligible (Binckley et al. 1980). Other forms of coastal carbonate are known. Høeg (1929) described unusual carbonate deposits developed on the Island of Malmo, Norway consisting of superficial crusts above and below high tide. They have a laminated structure similar to travertine, but their origin is unknown. The travertines of Shetland, UK also provide examples of deposits forming under the influence of sea spray, if not seawater itself (Flinn and Pentecost 1995).

Several marine-floor deposits of calcium carbonate resemble travertine in some respects but are clearly not the result of atmospheric CO_2 evasion. The occurrence of ikaite chimneys has already been noted (Section 7.3). Mention should also be made of calcite mounds resulting from hydothermal activity in the shelf sea of Mexico (Canet et al. 2003). These deposits, consisting of fine-grained and radial-fibrous calcite, may result from microbial methanogenesis.

15.4 Industrial Deposits of Calcium Carbonate

The accumulation of carbonates on metal and other surfaces to form 'lime scale' and 'fur' is of great concern to industry, incurring considerable cost in terms of pipe and screen blockage, boiler deterioration, and the loss of heat-exchange capacity. Ever since people have attempted to transport water by pipes and channels the problem must have arisen. Those channels transporting thermal water were especially vulnerable. The travertine canals at Pamukkale have already been noted and similar problems no doubt occurred at Bullicame and Bagni di Tivoli, Italy and along the aqueduct at Nimes (Fabré and Fiche 1986). The early remedies can only be guessed but presumably consisted of no more than hacking away at the material until flow was restored. The extensive use of pipe-work for water distribution did not begin until the 19th Century and it soon became apparent that 'furring' would be a problem where hard waters were concerned. A gradual reduction of water pressure, leading ultimately to the complete cessation of flow is a sure sign of pipe blockage by furring. The only solution was pipe replacement, an expensive and often difficult task. Water companies were aware of the problem and early attempts of alleviation were made by chemically altering the composition of water either by blending or addition of chemicals to reduce the pH. Serious problems were also encountered where large volumes of water were heated in boilers. Precipitation was accelerated, and the deposits may contain a range of minerals including calcium carbonate, silicate and sulphate. The blockage of hot water flowing through pipework has been of concern in geothermal fields and oil rigs for many years. The problem is by no means confined to water supply. Boats used on hardwater lakes frequently have their hulls encrusted with carbonates, increasing friction and fuel consumption.

The term 'water hardness' was originally used to measure the capacity of a water to precipitate soap, caused by dissolved Ca, Mg and occasionally Fe. The water industry recognises two types: *Temporary hardness* is that produced by bicarbonates, and is removable by boiling; *permanent hardness* is that due to sulphates, especially $CaSO_4$ which remain in solution and cannot be removed by heating alone. Industry employs 'degrees of hardness' (dh) equivalent to one part $CaCO_3$ by weight per 100,000 of water. Today, the term 'total hardness' is defined as the quantity of dissolved Ca and Mg expressed in terms of milligrams per litre $CaCO_3$.

15.4.1 Deposits in Wells, Pipes and Boilers

Well screens, and slotted borehole linings frequently accumulate deposits of calcite that may lead to complete blockage. Deposition is believed to result from pressure reduction during drawdown by pumping. Sometimes, deposition may extend a short way into the rock or gravel filling leading to cementation further reducing flow (Summers 1972). One measure used to combat the problem is acidisation. A tonne or so of hydrochloric or sulphamic acid is dropped down the hole to dissolve the carbonate, but the remedy may be short-lived (Howsam 1990). Reduced pumping rates also alleviate the problem. A form of electrochemical carbonate deposition is also possible. As steel casings become corroded, electric current is generated. Those parts of the casing acting as a cathode experience increased pH leading to deposition. The problem may be connected with a streaming potential and can be reduced using stainless steel mesh with fibreglass casings.

The water distribution systems of the developed world consist largely of 2–50 cm diameter pipe composed of steel or polythene. The amount of underground pipe-work is substantial. In the London, UK region alone it exceeds 31000 km in length. The older steel pipes are particularly prone to blockage and corrosion caused by the deposition of calcite and iron oxides. Carbonate deposition is usually associated with hard water regions containing limestones in the catchment. Corrosion of steel pipe can be exacerbated by hard water as the roughened surface resulting from corrosion appears to favour calcite nucleation. However, corrosion is eventually reduced as the carbonate layer builds over the unprotected steel, inhibiting access of oxygen to the metal (Kiuru 1980). Furring has also been used deliberately to reduce toxicity from lead plumbing (Schock 1989). In all cases the bore of the pipe is reduced and roughened leading to reduced flow, problems with turbidity and ultimately complete blockage (Photoplate 17D).

The cause for the deposition of calcite in water distribution systems can vary. It will naturally depend upon the nature of the raw water, its subsequent treatment and storage and the design of the distribution system. In parts of the London area for example, hard anoxic groundwater is pumped from a confined limestone aquifer and is aerated to remove ferrous iron. It is subsequently filtered and transported to a series of service reservoirs and water towers. The distribution path can be many kilometres in length and the water, rising close to calcite saturation, loses carbon dioxide during the initial aeration and storage in the service reservoirs and towers. Without further treatment, the water would enter the remaining pipework slightly supersaturated with respect to calcite with the potential for precipitation. A series of pressure and temperature shifts will also occur as the water moves from the aquifer to the customer's taps leading to further changes in the calcite saturation state.

Further physico-chemical changes occur once the water is released from the tap. Old tap washers permit calcite deposition from drips due to further CO_2 evasion and evaporation in sinks and baths. If the water is heated, the effect is more dramatic, particularly with boiling which expels most of the aqueous carbon dioxide. The result in kettles is the familiar 'fur' of aragonite and iron oxides.

Boilers come in two forms: low pressure, often small units used in domestic appliances and central heating; large high pressure systems used in paper mills, wood pulping and the food industry. In the latter, the high temperatures require make-up water for steam loss, which can lead to concentration of solutes and serious scaling. Cooling towers are used as heat exchangers, allowing heat to escape through the evaporation of water. In the West, they represent the major use of industrial water in power stations and heavy industry. As the water re-circulates, the solutes become concentrated leading to the precipitation of carbonates. In both boilers and cooling towers, a major concern with scaling is the reduced efficiency of heat exchange resulting from the added thickness of the containing wall and its lower heat conductivity.

Desalination using reverse osmosis also faces scaling problems. As the saline water is forced through a semi-permeable membrane under high pressure, concentration gradients build on the saline side leading to supersaturation and precipitation. Problems with scaling have also been noted in connection with boating on hard water lakes. In the UK this has prompted research into the associated organisms and their response to calcification inhibitors (Heath et al. 1995).

15.4.2 Quarrying and Construction

Burning for lime which involves the conversion of limestone to calcium oxide has been practised for at least two millenia and used for mortars and neutralising soil acidity (Williams 1989). In the UK, demand peaked in the late 18th and early 19th Centuries as a result of the Agrarian Revolution and the Napoleonic Wars, leading to a wheat shortage. Extensive tracts of land are currently contaminated with slaked lime, some of which enters watercourses and deposits an invasive meteogene travertine. The resulting waters are noteworthy for their high pH, (often >10), and lack of vegetation. The best known site in the UK is that at Pen-wyllt quarry, Foel Fawr in Wales. This travertine has been investigated petrographically (Braithwaite 1979) and its geochemistry has been reported (Andrews et al. 1997b). A similar stream runs below Brook Bottom Springs, Derbyshire (Ford and Pedley 1992). Bauxite processing in Jamaica results in the discharge of caustic liquors and on entering hard-water streams, lead to similar deposits (Andrews et al. 2001).

Lime mortars and concrete often set with incomplete reaction. Some of the remaining calcium hydroxide is then available for dissolution by rainwater, transport and precipitation with atmospheric carbon dioxide. This accounts for the frequent occurrence of travertine-like sheets and pendants on the undersides of concrete bridges and tunnels worldwide. The rate of dissolution may be high judging by the lengths of pendants on Victorian brickwork tunnels in the UK, and the deposition rate may be in excess of 1 cm per year. The development of vertcial travertine minidams is widespread where rainwater seeps out of stonework of UK railway bridges. In London, small minidam pools have developed below regular drip-points on the concrete South Bank Centre, constructed in 1950. Schwedt (1987) notes an 'Eifelmarmor', a deposit forming in a Roman aqueduct thought to be due to mortar redeposition. Despite its general undesirability, the phenomenon is presumably too insignificant to have provoked remedial research.

15.4.3 Remedies

A large industry has developed to combat the problem of scaling using a range of inhibitors. There are several key issues for a successful inhibitor; cost; toxicity and other environmental concerns; ability to work at high/fluctuating temperature and pressure; non-interaction with other additives such as biocides and finally, non-corrosive effects. In addition there is a need to find the optimum dose for a particular system.

15.4.3.1 Chemical Inhibitors of Scaling

Scaling can be reduced chemically using two methods. The water may be pretreated to change the chemical composition, or an inhibitor of scaling may be introduced. The simplest pretreatment is acidification to remove alkalinity and adjust the pH so that corrosion is also minimised. This is widely practiced in industry, particularly for cooling tower water. Numerous water-softening techniques are also available as pretreatments. There are many scaling

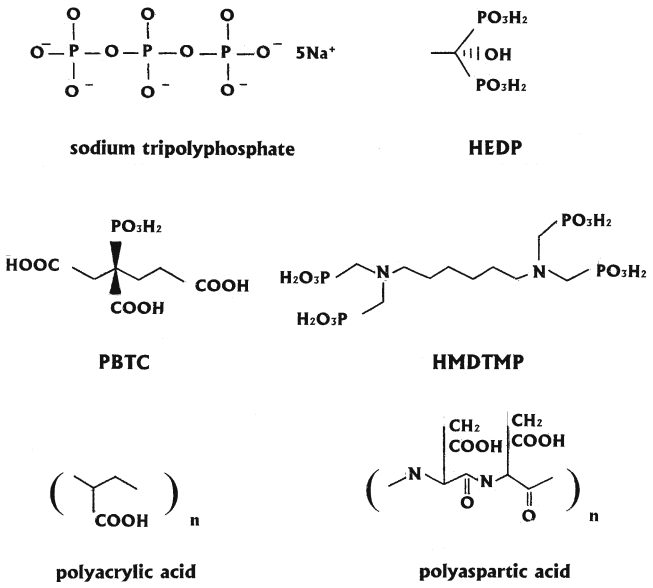

Fig. 90.
Structures of some inhibitors of calcium carbonate scale formation. HEPD, 1-hydroxyethylidene-1,1-diphosphonic acid; HMDTMP, hexamethylene-N,N,N',N'-diamine tetramethylenephosphonic acid; PBTC, 2-phosphonobutane-1,2,4-tricarboxylic acid

inhibitors and a substantial literature is devoted to their mode of action, their merits and demerits. Inhibitors can be divided into four main categories (Table 34): metal ions; compounds of phosphorus oxyacids (organic phosphonates and inorganic/organic phosphates), and polycarboxylic acids.

A wide range of metallic ions either inhibit the precipitation of calcium carbonate or alter the crystal habit. Meyer (1984) lists 14, with iron, zinc and cerium being the most effective. Iron, zinc and copper at ppm levels are often added to industrial waters to reduce scaling, bacterial growth and corrosion. Traditionally, condensed inorganic phosphates were used as inhibitors, owing to their cost-effectiveness. Examples include sodium tripolyphosphate (Fig. 90) which is active well below 1 ppm concentration and sodium polymetaphosphate (Calgon, $Na(PO_3)_x$). Their ease of conversion into orthophosphate and uptake by algae, leading to eutrophication makes them undesirable for most large-scale water treatment. Hypophosphorus acid, H_3PO_3, is a lower oxyacid of phosphorus that forms a wide range of ionisable aliphatic organic compounds, the phosphonates, several of which find use as scale inhibitors (Fig. 90). One of the simplest and best known is HEDP (1-hydroxyethylidene-1,1-diphosphonic acid). Unfortunately, the phosphonates also have the potential to cause eutrophication. Under some conditions they may precipitate calcium phosphonates, encouraging further scaling (Perez and Zidovec 1995). A number of phosphorus-free polymeric organic compounds are known and have been exploited. They include several polymeric carboxylic acids such as polymaleic acid and polyacrylic acid. Polyacrylic acid is used in the molecular weight range of 2000–3000 but there are some environmental concerns on account of its limited biodegradability, and its reactivity towards silicates may reduce its effectiveness (Perez and Zidovec 1995). However, it has been a popular scale inhibitor on owing to its low cost.

Inhibitors containing ionisable groups such as COOH and H_2PO_3 are believed to be effective due to their adsorption to the carbonate surface, reducing nucleation or crystal growth. For example, Nancollas (1979) found that for inhibitory concentrations of phosphonates (10^{-6} M) in contact with experimental calcite seed crystals, less than 1% of the crystal surface area would be covered. He concluded that the inhibitor was bound to active sites, consistent with a screw-

Table 34. Some commercial inhibitors of calcium carbonate industrial scales

Category/substance	Concentration for inhibitory activity (ppm)	Comments	Reference
Metallic ions			
Cu^{2+}	0.5	Effective at low alkalinities	Katz and Parsiegla (1995)
Fe^{3+}	0.5	Effective at high alkalinities	" "
Mg^{2+}	5–20	Aragonite formation	
Zn^{2+}	0.5	Effective at low alkalinities	Katz and Parsiegla (1995)
Inorganic orthophosphates			
Sodium tripolyphosphate	0.001	Potential eutrophication problem	Meyer (1984)
Polyphosphonates/organic phosphates			
HEDP	2.5	Widely used. May form secon-dary phosphonate scales	Davis et al. (1995)
HMDTMP	10	Inhibits both amorphous and crystalline $CaCO_3$	" "
Phosphocitrate	0.1	Also corrosion prevention	Sallis et al. (1995)
Polycarboxylic acids			
Polyacrylic acid	0.5	Used at c. 2500 MW. Low biodegradation	Davis et al. (1995)
Polymaleic acid	1.0	Less effective at high pH	Perez and Zidovec (1995)

dislocation mechanism of crystal growth. Small anions such as the lower molecular weight phosphonates have a high affinity for cationic regions on crystal surfaces, and it is thought that polyanionic inhibitors act in part owing to spatial matching of their ionisable groups with crystal cation binding sites. Using molecular modelling, polyaspartate has been found to exhibit directional binding on calcite. Polyaspartate (Fig. 90) showed strong stereospecific matching on (1 –1 0) (Sikes and Wierzbicki 1995). The selective adsorption of polyaspartate molecules leads to directional growth and is believed to be important in matrix-mediated biocalcification. The polymer has also been shown to have inhibitory activity (Wheeler et al. 1988).

Inhibition is not the only means by which scaling problems may be overcome. By altering the crystal morphology, producing irregular and mal-formed crystals, the scale may be more readily disrupted and removed mechanically. A number of compounds have been shown to do this, including alkali metal ions and polymaleic acid (Wilken 1980; Carrier and Standish 1995).

15.4.3.2 Physical and Physico-chemical Inhibitors

Small-scale problems can be overcome by providing a good nucleating surface so that precipitation is diverted from important components such as heating elements of kettles. For example, a ball of wire wool placed within a kettle offers considerable protection. Pre-treatment of water with softeners can be achieved using inexpensive ion-exchange materials such as zeolite. Many zeolites can exchange Na^+ and K^+ for Ca^{2+} and Mg^{2+} and are used for this

purpose in washing powders, reducing the likelihood of scaling and improving the washing process. Large-scale water-softening is also undertaken at water-treatment works.

There is considerable interest in electromagnetic technology for inhibiting the deposition of carbonates. The method requires the installation of a simple, fairly inexpensive device without the use of chemicals and their environmental concerns. Electromagnetic/electrostatic water treatment is currently an expanding business. The aim is to subject flowing water to a strong magnetic field by a device attached to a pipe. The equipment is used for 'single pass' flows and recirculating systems, but the latter appear to give a better response (Anon 2003). Results have been mixed, but success in reducing scaling, removing old scale and loosening of the deposits have all been reported. The mechanism however is not fully understood, and neither is it always effective. Three hypotheses have received serious consideration (Anon 2003). Coey and Cass (2000) found that drawing hot water through a static magnetic field of 0.1 T altered the mineralogy of the deposit by changing the aragonite/calcite ratio. They suggest that traces of iron may form clusters of paramagnetic FeOOH which then serve as heteronuclei for aragonite. Aragonite forms a looser scale than calcite, and is therefore removed more easily. Another hypothesis proposes that a strong magnetic field will break some of the water hydrogen bonds. This could influence ion hydration, altering the nucleation process, though the details are obscure. Finally, it has been observed that when colloidal silica is present, the electric double layer of the particles will be distorted under the influence of a magnetic field leading to the adsorbtion of Ca and Mg ions, thus removing them from solution (Szkatula et al. 2002). The calcium-rich particles may then nucleate calcium carbonate, carrying it away in suspension rather than forming scale (Anon 2003). These studies are clearly of fundamental interest and may eventually lead to a much clearer understanding of the nucleation of calcium carbonate in natural waters.

15.5 Siliceous Sinter

Deposits of opaline silica are probably of more frequent occurrence around hot springs today than are travertines. The deposits are usually referred to as siliceous sinter, or just sinter, though the latter has been used as a more general term. However, *sinter*, incorporating the silicon atomic symbol, is an apposite term. Hot water under high pressure is capable of dissolving large quantities of silica as monosilicic acid, $Si(OH)_4$. Typical values for sinter-depositing waters are 150–350 ppm as SiO_2 (2.5–5.8 mmol L^{-1}). Upon cooling, the acid polymerises to form cyclic polymers and then nanospherules (Iler 1979). Ostwald ripening results in the formation of spherules of opal-A up to 0.5 μm in diameter. Evaporation and pH change also promote silica deposition. At acid pH, the polymerisation and nucleation of silica is inhibited owing to the lower deprotonation of monomeric silicic acid, as shown by Mountain et al. (2003). Several forms of opaline silica exist, and most recently-formed sinter consists mainly of opal-A (SiO_2. nH_2O). The silica is deposited on all objects with which the water is in contact and is often finely laminated. In some cases, laminations may record individual eruptions, as in the case of geysirs, or they may be related to the growth of phototrophic microbes. Close to vents, where the temperature often exceeds 70 °C sinter is usually referred to as *geyserite*, a bladed or laminate form, originally thought to be deposited entirely abiotically. Sinter formed at lower temperatures is often more obviously associated with microorganisms such as cyanobacteria and flexibacteria. In common with the travertines, a wide range of morphologies exist for silica deposits (Photoplate 17E). They include mounds, ridges, cascades, dams, crusts and a wide range of micromorphologies such as spheroids, 'pisoids', spikes, bumps and microstromatolites, but there is no universal classification (Jones

and Renaut 2003). Kerr and Turner (1996) describe in detail the famous White Terrace of Rotomahana, destroyed by a volcanic eruption in 1886.

An association of sinter with photosynthetic microbes has been noted since the 19th Century. It was originally thought that the microbes were passive inhabitants, living in hot sulphide-rich waters gaining energy from light and the springwater milieu. More recent studies employing electron microscopy demonstrate that at least some microbes provide nucleation centres, allowing the silica to become deposited first in the sheaths and capsules of the bacteria, then later within the cytoplasm (Cady and Farmer 1996). Schultze-Lam et al. (1988) found that Icelandic *Chloroflexus* was silicified in this manner, and a similar process occurs in the cyanobacteria *Calothrix* and *Fischerella* (Konhauser et al. 2001). Replacement of organic matter by silica is also believed to occur (Jones and Renaut 2003). Nucleation is thought to be aided by hydrogen-bonding between sugar OH groups in the EPS and the silicic acid groups, sometimes with Fe^{3+} cation-bridging (Konhauser et al. 2003). The process differs from calcite mineralisation, where it is only the outer cell layers that are usually affected by mineralisation. The pervasiveness of silicification should lead to good preservation of fine structure and potentially good fossilisation. A well-known example is provided by the Rhynie Chert of Scotland where many fossils have been discovered (Trewin et al. 2003). The degree of preservation of some the more complex fossil plants in the silica is remarkable, but cytoplasmic details appear to have been lost. The Drummond Basin geyserites of Australia have yielded microbial fossils (Walter et al. 1996) as have the Palaeoproterozoic Gunflint Cherts, though the origin of the latter is uncertain (Knoll and Walter 1996). Overall, preservation in silica is likely to be more complete than in calcite (Konhauser et al. 2003). Opal-A is not stable under Earth-surface conditions and is transformed into a variety of other minerals; chalcedony, cristobalite and quartz (Campbell et al. 2001; Lynne et al. 2003). After diagenesis, little of the original fabric may remain. For opal-A it has also proved difficult to distinguish the primary encrusting fabric from the later cements (Jones and Renaut 2003). In addition, intraclasts of opal-A are frequently found, so the process has not proved easy to follow. Silicification is not dependent upon plants, since all objects tend to become encrusted, though they are clearly capable of providing nucleation templates and can be responsible for the final fabric, in a similar manner to travertine.

Sinter can be deposited at rates exceeding 3 cm a^{-1} close to vents, but is usually around 0.5–5 mm a^{-1} (Campbell et al. 2002; Mountain et al. 2003). The latter report a deposition rate of 350 kg m^{-2} a^{-1} in a drain from Wairakei Power Station, New Zealand and found that the rate of growth was correlated to the silica supersaturation. For a comprehensive review of siliceous sinters the reader is referred to the special issue on the sedimentology of hot spring systems published in the Canadian Journal of Earth Sciences (2003).

Extraterrestrial Travertine

The constituent elements of calcite are common in the universe and there is no reason why travertine should be unique to Earth. Nevertheless, the conditions needed for Ca^{2+} and HCO_3^- ions to be transported and the CO_2 degassed do constrain the temperature and pressure fields to those spanning a narrow range, and require the existence of an epigean CO_2 partial pressure lower than that generated below ground. A process to regenerate the carrier solution, such as a hydrological cycle is also desirable but not essential. The combination of processes is probably unique to Earth within the Solar System today. It may not have been so in the past, and is likely to exist within other solar systems. In the absence of a sustained hydrological cycle, travertines could form when liquid water is forced to the surface by gas pressure at depth resulting from localised heating. This might conceivably result from vulcanism or a meteor impact mobilising solutions and forcing chemical change at the surface. There is plenty of evidence for travertine formation associated with vulcanism and some for hydrothermal activity around large impact craters on Earth, but we do not have experience of these processes in the complete absence of a hydrological cycle. For this we can only surmise.

The search for hydrothermal deposits on other bodies in the Solar System has high priority for those seeking evidence for extraterrestrial life (Farmer and Des Marais 1994b; Allen et al. 2000; Bishop et al. 2004). On Earth, they provide an environment for extremophiles – microorganisms capable of surviving high temperatures and an absence of molecular oxygen (Stetter 1996). It has been seen that travertine deposits can provide such an environment, and by entombing their biota, they provide potential sites for extraterrestrial microbial fossils. Travertines in particular, received attention when supposed fossilised bacteria were discovered in calcite globules of the Martian Allan Hills Meteorite (McKay et al. 1996).

Thermogene and invasive meteogene deposits will be those most likely to be encountered in other parts of the Solar System. They are independent of a soil-respired carbon source and can be generated by non-biological processes as described in Chapter 2. Given a source of carbon dioxide, water and calcium ions, some means is required to mobilise this mixture so that it flows to the planet's surface where the carbon dioxide can be degassed. In the presence of a hydrological cycle, water is returned to the ground and the process may be maintained for prolonged periods, perhaps millions of years. The presence of permanent groundwater also permits a hydrothermal circuit to operate through convection and artesian flow. Where a cycle cannot be maintained in its entirety, the water makes a one-way trip and artesian flow is not possible. Water, as a volatile molecule can be driven to the surface by other means if a thermal circuit is inoperable. An adjacent heat source can force water and other volatiles laterally or to the surface by generation of pressure. Obvious sources are vulcanism via radiogenic heating and large meteor impacts. Compositional and environmental constraints must also be considered. All of the Solar System planets will contain the elements necessary to form a travertine-depositing solution but the distribution of the necessary compounds on some makes their existence near the surface most unlikely.

16.1 Vulcanism

The surfaces of the five outer planets of our Solar System are too cold to permit the existence of liquid water, and they are believed to consist largely of liquid and/or solid hydrogen and methane. Some of their satellites are however more rocky in nature. Meteor impacts, tidal heating and ice-vulcanism are methods whereby local heating could allow liquid water at the surface, as is likely on Jupiter's moon Europa. Deposits of salts have been predicted along the large fractures of this moon's surface and the existence of travertine-like deposits are a possibility, where warm CO_2-rich waters might reach the surface for short periods. However there have been suggestions that sulphuric acid occurs in the icy surface in which case travertine formation is unlikely. Kargel (1991) believes that brines also exist below the surface of some bodies such as Ganymede, in which case earlier calcium carbonate deposits may exist. Despite these intriguing possibilities too little is currently known about these moons to speculate further.

On Earth, thermogene travertines are frequently associated with continental plate margins where hot CO_2-rich solutions find their way to the surface. Vulcanism is frequently associated with these activities (Fig. 91) but is not essential. Given this association on Earth, similar processes on the neighbouring rocky planets would be worthy of investigation. Of the inner planets, Mars has received the most attention, largely because of the accessibility of its surface to Earth-based observation and its surface temperature which is more similar to Earth than any other planet. Mercury and Venus have much higher surface temperatures with the latter obscured by a dense atmosphere. Unlike Earth, these planets have little or no surface water, so that hydrothermal activity today is likely to be negligible and hydrothermal circuits non-existent. All three planets show evidence of past vulcanism but much of this appears to have occurred early in the history of the Solar System, when their internal temperatures were much higher than today. Mars is thought to be a one-plate planet (Francis 1993) and being considerably smaller than Earth is unlikely to have supported much vulcanism through plate movements. The huge shield volcanoes of Tharsis Montes are thought to have been formed over convective 'hot spots' in the mantle and are unlikely to have been active for a long period. There is little evidence at present of plate tectonics on Mercury but it probably occurred on Venus where there is much evidence of vulcanism.

Well-known oceanic hot spot volcanoes on Earth include the Hawaiian, Galapagos and Cape Verde Islands, none of which have extensive hydrothermal activity, at least on land, and travertines have not been reported. Continental hot spots fare little better, although their magmas are more varied as their basalts often assimilate continental lithosphere (Francis 1993). The best studied is the Snake River Plains Province of the United States which includes

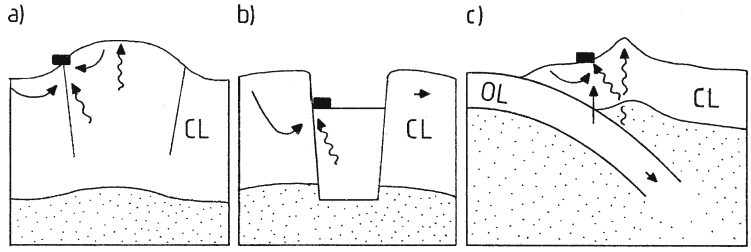

Fig. 91. Travertine, vulcanism and plate tectonics. a) hot spot volcano and associated hydrothermal activity; b) rift ;c) continental margin volcano. Short arrow shows plate movements; curly arrow, CO_2 flux; long arrow, water flow. Asthenosphere stippled, CL continental lithosphere, OL oceanic lithosphere. Black boxes show position of thermogene travertine formation

Yellowstone and the Mammoth Hot Springs travertines. However, most of these hot springs are acidic and Si-rich. Hydrothermal activity around two large hot spot volcanoes in North Africa, Emi Koussi and Jebel Marra is very limited, but that may be due to the arid climate. Hot spot volcanoes may not therefore represent prime sites for extraterrestrial travertines. In rocks of basaltic composition on Earth, travertines are known but are not particularly common or extensive, and may only become significant where a variety of rock types, particularly carbonate sediment are in juxtaposition.

The majority of volcanic activity on Earth results from continental drift. Where oceanic crust subducts into the mantle, it is dehydrated at depth and the resulting volatiles reduce the melting points of the rocks above. The magmas rise and form chains of volcanoes 100 or so km above the subducting plate. The well-known thermogene travertines of Italy and also those of Japan are an indirect result of this activity. Other volcanoes develop along extensional zones such as rift valleys and there are many examples of travertines associated with crustal extension, with or without volcanic activity. In this context, a rare type of carbonate-containing magma termed carbonatite should be noted. Although there is only one known active carbonatite lava in Tanzania, older carbonatites in the African rift are associated with travertines. The apparent lack of plate tectonics on the other rocky planets bodes ill for this type of hydrothermal activity. The situation is made even less likely in the absence of oceans that probably provide a large proportion of the ascending volatile material, and maintain the hydrological cycle. Despite this pessimistic scenario, smudges of possible hydrothermal deposits have been observed in images of Mars near the volcano Apollinaris Patera. If caliche-like materials are abundant in the martian 'soils' there is a ready source of carbonates awaiting dissolution and precipitation providing the right hydrological process come into being. The past existence of near-surface and surface water is given credence by the appearance of large, probably water-cut channels, close to the volcano Elysium Mons and many other places on Mars (Carr 1996). Vulcanism could conceivably mobilise a frozen regolith leading to water flow and carbonate precipitation but too little is known concerning the amount of water likely to be released and its longevity at the surface.

If the volcanoes of the extraterrestrial rocky planets are not going to provide the right conditions for travertine formation then other sources of heat need to be sought. These may be provided by large meteor impacts.

16.2 Meteor Impacts

The huge craters of the Moon attest to the intensity of bombardment to which bodies of the Solar System have been subjected in the past. Since the launch of space probes in the 1970s by Russia and the United States, similar craters have been found on most of the other rocky bodies of the Solar System. Detailed studies of returned lunar samples have led to the conclusion that most of these large impacts occurred within a billion years of the Moon's formation. The impact of large meteors onto a solidified crust must have generated high temperatures, often sufficient to vaporise the rocks and to spread material within a wide radius of the impact. Depending upon the planet's gravity and density of the atmosphere, the falling material will retain some of the impact heat, forming a blanket that may be many metres thick immediately outside the crater. The images of some craters indicate fracturing of the upper crust. Fragmentation and brecciation by impacts is thought to have formed a mega-regolith up to several km in depth on planets such as Mars. On Earth, many impact craters have now been recognised, despite their being rapidly assimilated into the landscape by erosion, weathering or burial. The heat generated by large impacts is known to have caused

the melting and fracturing of rocks on Earth although much remains to be discovered about impact phenomena. Larger impacts would be expected to generate heat over long periods, leading to hydrothermal activity. Osinski (2003) records evidence of hydrothermal activity around about 70 of the Earth's 170 known craters. Detailed work has been carried out at the 24 km diameter Haughton Crater, Canada where 70–100 billion tonnes of rock was displaced 23 Ma ago. Hydrothermally altered rock has been found in the vicinity of the crater though travertine was not reported. Osinski cites estimates of the sustainability of hydrothermal activity around craters, with several thousand years for a 7 km crater and almost a million years for a 250 km crater. He has also provided a conceptual model of the process (Fig. 92). At the centre of the impact, much of the crust is melted, perhaps of a depth of several hundred metres, while hot ejecta are spread over a wide area. This partially melted material could form an impervious layer close to the impact. The impact also causes a series of concentric faults or fractures and these could provide pathways for water and other volatiles to reach the surface. Hydrothermal minerals would be expected within and above these fractures as water is heated at depth and then rises to escape. Since the surrounding land will generally be higher than the impact area, a pressure-head will assist in forcing water to the surface. Providing a continuous supply of water is available, large hydrothermal deposits could be formed covering many square kilometres such as those of central Italy. However, there are no extensive travertines associated with Earth's impact craters as far as this author is aware. The Miocene Ries Crater contains some travertine mounds and they are believed to be formed from sublacustrine springs, but there appears to be no evidence of associated hydrothermal activity. Some thought also needs to be given to invasive processes. If calcium carbonate exists near the surface of a planet, the high temperature of an impact could lead to decarbonation to form calcium oxide. This highly reactive compound will remove water and carbon dioxide from even a low-pressure atmosphere to form a travertine-like material on the surface.

Several highly reflective areas have been identified on the surface of Mars, the best known being the 'White Rock' in an unnamed crater in Sabaea Terra. Measuring 18 x 15 km, it has been variously interpreted as a layer of chloride/sulphate evaporite or a lens of magnesium carbonate deposited from a groundwater seepage (Forsythe and Zimbelman 1995; Russell et al. 1999). Calcium carbonate is likely to be present among the reflective minerals, and

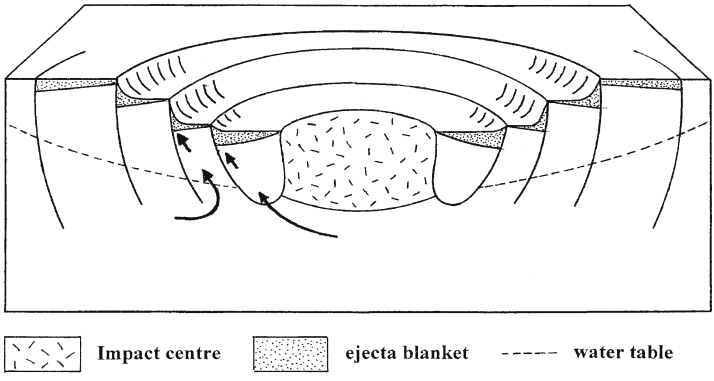

Fig. 92. Diagram of an impact crater with diameter 5–100 km with vertical scale much exaggerated. Concentric faults surround the impact and provide a route for hot migrating solutions after impact (arrows). Ascending water is guided along fault scarps through an otherwise poorly pervious partially melted impact centre and ejecta blanket, where travertine could be deposited along with other hydrothermal minerals at the surface (redrafted after Osinski 2003)

travertines of the same areal extent occur on Earth but their true origin is unlikely to be settled until the rock is examined by a lander. Possible lacustrine carbonates have also been identified on the floor of Melas Chasma (McKay and Nedell 1988).

Travertines, along with other hydrothermal deposits are capable of harbouring and entombing the simplest of Earth's organisms. It is for this reason, more than any other, that the search for hydrothermal deposits on other planets has been given serious attention. From what has been said before, it is apparent that if such deposits are found, they will probably be of great antiquity. On Earth, all travertines older than about 100 Ma have undergone substantial diagenesis. This can wipe out all traces of former microbial activity. Silica, another common hydrothermal deposit is in general a better preservation medium and will probably yield more reliable information. Silicified travertines could be of particular interest as they may contain a wider range of preservation environments. For example, Melezhik and Fallick (2001) found traces of organic matter in partially silicified travertine-like deposits dating to 2.2 Ga. Although no fossils were reported, the silicification of ancient travertines needs more study since potentially good fossil preservation may result. Small spheres of silica have been found associated with biofilms in several thermogene travertines and might provide evidence of extraterrestrial microbial activity (Allen et al. 2000). On some planets however, intense diagenesis may never have occurred. For example, if travertines did form on Mars early in its history when there was some liquid water present, there may have been insufficient water to cause rainfall. Percolation of water through an inactive travertine is an important mediator of travertine diagenesis on Earth. Also, without plate tectonics, the deposits would not have been deeply buried and subject intense heat and pressure. Without these processes, travertines could perhaps exist in an almost unaltered state close to the planet's surface.

Surface hydrothermal minerals may also act as 'traps' for subsurface microbes. With the realisation that microbes exist hundreds of metres below the Earth's surface, it is just possible that the same could happen on Mars and perhaps some of the moons of Jupiter. On Mars, the cryosphere is thought to extend down to several kilometres from the surface. Below this, there may be a narrow zone where liquid water exists. Juvenile gases such as CO_2, NH_3 and SO_2 may provide energy for chemolithotrophs to exist there. The prospects of finding life at this depth are slim but travertines and siliceous sinters could preserve these forms as they are swept to the surface by plumes of warm water resulting from impacts or vulcanism. Scarps may provide natural outlets as the unmelted cryosphere forms a perched water table (Fig. 93). At the planet's surface, the microbes may mutate and become adapted to solar radiation during the inevitable decline in gaseous nutrient flow and temperature.

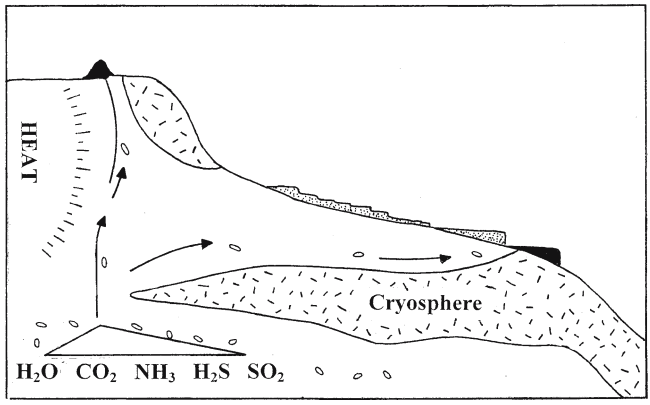

Fig. 93.
Mechanism for microbe migration from a wet zone existing below a cryosphere. The cryosphere is breached by the heat generated from an impact or volcano so that volatiles carrying bacteria are able to reach the surface. The microbes (small ovals) are then trapped in surface hydrothermal deposits (active, black; fossil, stippled)

Utilisation of Travertine

Practically all of the materials found at the Earth's surface have been of service to man, and travertine is no exception. Despite its scarcity, travertine is much valued as a building and decorative stone and has been exploited on numerous occasions and in many locations. Its use in building results from a combination of strength with lightness by virtue of its high porosity. This porosity also provides low thermal conductivity, good sound insulation and easy cutting, in common with many of the characteristics of the modern 'breeze block'. Extensive neomorphism of the crystalline matrix of travertine often provides a material with all-round strength without planes of weakness. As a decorative stone, the denser travertines have found preference and when polished reveal intricate patterns in soft brown tones pleasing to the eye and of infinite variety. Surfaces are easily worked, take a fine polish and are used extensively for both internal and external decoration. Quarried blocks with uncut faces find use in garden and aquarium decoration where they provide an excellent rooting-medium for alpine plants. Although few sculptors have favoured travertine for their work, it is a material well suited to particular styles. Of particular interest is its use in the making of bas-reliefs and encrustations at 'petrifying springs'. Clastic travertines have been much utilised as a form of soil sweetener as it may be applied directly to the land. Here the use of travertine is explored over the centuries as both an artistic and structural medium, beginning with the means by which it is extracted from the ground.

17.1 Quarrying Methods

The history of travertine quarrying is as old as its utilisation but little is known of the ancient methods of extraction. Travertine as 'onyx marble' was used widely by the Egyptians and blocks may have been removed using a metal saw, abrasive wire and water-soaked wedges. The same methods were probably used for the more massive Italian deposits by the Etruscans and Romans. Some of the earlier techniques are described by Schmid (1972). In the 19th Century, a special rake or 'krahlause' was used to extract travertine in south Germany where blocks of 80 x 30 x 30 or 40 x 30 x 30 cm were hewn for building. Another method of extracting crude blocks was by washing out. This was used at the Hofer Tufffsteinwerk at Wiesensteig, Germany but sawing has now replaced all of these methods, at least in developed countries. Removing porous varieties with dynamite has not proved successful since the blast energy is dissipated by the porosity and made ineffective (Kirby and Rimstidt 1990). The methods currently used in the huge quarries at Bagni di Tivoli, Italy are fairly typical of those used elsewhere for the more massive, thermogene traver-

tines, and may well bear some connection to the techniques used centuries or even millenia ago. At one of the largest quarries, Cave Bruno Poggi, the travertine is taken from three or four benches each 10–15 m in height by stoping. The rock is cut stepwise from each bench in large slabs to the thickness of the bench (Photoplate 18.B) by first drilling a series of vertical holes about 5 cm in diameter and c. 1 m apart. Water is run into the holes and they are wet-cut vertically using a portable diamond wire saw to a depth of about 2.5 m. Cutting out a single block takes about a day. Blocks are cut through from the upper bench and the side and may be up to 6 m high, about 1.5 m thick and 3–4 m wide, weighing up to 90 tonnes at this stage, though smaller blocks, weighing about 20 tonnes are the norm. After cutting through, these monoliths are supported only by their base and are detached by pushing them over with the aid of winches so they fall on their side. This is a critical stage, as further splitting may occur though losses appear to be small. From the quarry floor the blocks are lifted by crane to the cutting yard, where most of the material, which is destined for facing work, is sliced into thin slabs measuring about 200 x 300 x 3 cm each taking about 50 minutes to cut with a reciprocating saw. Most travertine at the present time is used as a decorative cladding and is graded, filled and polished at the quarry prior to sale. Loss through flaws is common, but the wastage at the quarry is not quantified. At this site, the travertines have been proved to a depth of 40 m. There is little overburden, just a few metres of karstified travertine, immediately below which the best quality material is found. In 1990, the quarry employed 120 people of whom 35 were directly employed in quarrying. About 20 blocks, each weighing 20 tonnes were removed each day. The area surrounding Bagni di Tivoli has around 40 active quarries with a workforce of about 2500. All of the quarries are of the plain type, requiring water extraction, but hillside quarries, cut into the sides of travertine mounds are numerous in Italy. There are many other travertine quarries in Italy, both in use and abandoned. In Lazio alone there are at least 50 quarries in operation, notably those of Bagni di Tivoli, Canino (used for road metal) and Fiano Romano. The last has been in use since Roman times and noted for the quality of its stone. Some, such as those at Palidoro are known for their mammalian faunas (Section 12.2.3).

At the much smaller Wiesenstieg Quarry mentioned above, meteogene travertines were won on a small scale by cutting out blocks with a 2 m circular saw mounted on a railway at the quarry edge. The travertine was, until recently, cut through vertically and horizontally to release small blocks weighing a few tonnes, which were then transported to the workshop. Here, the blocks were also cut with a circular saw into slabs 35 mm thick or into building blocks of variable size, for small local contracts. In 1992, this quarry employed only three people and was about to close due to lack of trade.

Removal of clastic travertines for liming and road metal has also been popular. In this case, cutting is not required and the material can be removed with mechanical excavators, such as a pan scraper and front-end loader (Giannini 1990). Sometimes conveyer belts have been used in conjunction with crushing and screening (Sweet and Hubbard 1990).

Several anecdotal accounts exist describing the quarrying of travertines that later harden on exposure to air (e.g. Leland 1538). The author experimented with this but found the results unconvincing, and it may be that exposure to the elements merely washes away the softer parts, revealing more resistant building-quality fragments. Dissolution and re-precipitation of minute calcite crystals is known to occur through water percolation, leading to consolidation under favourable conditions (3.3.2), but this must be weighed against frost damage in those northern latitudes where the phenomenon has been reported.

17.2 Mechanical and Physical Properties

The variable mechanical properties of travertine have already been alluded to. Many clastic deposits readily disintegrate in the hand while others display exceptional strength and durability and are much valued as a building stone. Both the strength and weakness of travertine, such as its tendency to split if stood on end, have been recognised for a long time (Vitruvius c. 10 B.C.; Plinius c. A.D. 50). Information on the mechanical and physical properties of travertine is sparse and available only for those materials used in construction. Some relevant information for thermogene travertines, with some comparative data on other building stones taken from Vallardi (1982) is presented in Table 34. These examples demonstrate considerable variation among the travertines. The stronger Romano Oniciato sample compares well in compressive strength with Carrara marble but is inferior to granite. It is however inferior in tensile strength when compared with the marble. These travertines also share a higher water absorption capacity and are inferior with regard to impact and abrasion. Their coefficients of thermal expansion are also markedly higher than marble, though this remains unexplained. Less information is available for meteogene travertines. Bayari (2002) quotes tensile strengths of 0.4–1.2 kg cm^{-2} for 'spongy' and 'plant rich' young travertines respectively. Older travertines provided values as high as 2 kg cm^{-2}. These measurements are far lower than those provided for the thermogene travertines in Table 35.

Some useful but apparently unquantified properties of the more porous travertines are their low specific gravities, their thermal and sound insulation properties and their ability to evaporate water. These have occasionally been exploited in specialised building applications.

C. Kelsall (*pers. comm.*) observed that travertine, at least in the UK is mainly used for interior decoration. Used externally, unfilled travertine, particularly slab, is vulnerable to rainwater penetration and freeze-thaw disintegration, though it provides a good adhesion base for mortar bonding. In cities the holes attract dust and crusts of gypsum may develop via sulphur dioxide emissions leading to shabbiness (Török 2004). For this reason, travertines are frequently filled with calcium carbonate- or tinted polyester resins. After polishing, the overall appearance, durability and strength is often improved. Even so, filled travertine paving is vulnerable to damage by stiletto heels and is often avoided for this reason.

17.3 Building and Exterior Decoration

Dense travertines of low porosity are well-suited to building. While their formation results in weaknesses along lines of bedding and lamination, their strength is often increased by cementation and the presence of structural elements provided by plant growth developing across this bedding, reducing planes of weakness. The surface of travertine and its soft brown colour is aesthetically pleasing and may be enhanced by polishing and filling. As a result, travertine is a much-valued building material.

17.3.1 Pre-Roman Use

Travertine has undoubtedly been used for building since the earliest times as it often occurs close to human habitation (see 13.3). Some of earliest examples of stone masonry date from the 1st Dynasty of Egypt, c. 3200 B.C. (Emery 1961) and use was made of crudely fashioned travertine blocks in the prehistoric navetas of Minorca dating to about 1500 B.C. The Estruscans made some use of it in the town wall of Perugia (Blake 1947). In Hungary, excavation of an early

Table 35. Mechanical and physical properties of thermogene travertines. From Vallardi (1982)

Sample	Compression breaking load kg cm^{-2}	Breaking load after freezing	Coefficient of imbibition %	Ultimate tensile strength kg cm^{-2}	Impact test, fall height cm	Thermal linear expansion 10^{-3} mm $°C^{-1}$	Frictional wear test (realtive)	Specific gravity	Modulus of elasticity kg $cm^2 \times 10^{-3}$
Romano Oniciato, Tivoli	1153	1132	7.30	146	29	60	0.72	2.44	–
Romano Montemerano, Grosseto	577	506	30.4	104	29	44	0.3	2.23	–
Range, nine Italian samples	577–1268	506–1311	4.3–30.4	104–155	26–41	44–63	0.25–0.72	2.2–2.56	505–659
Mean, nine Italian samples	1044	988	11.7	131	33	52	0.40	2.42	565
Carrara marble	1202	1212	1.10	227	57	29	0.20	2.71	–
Granite	1735	1536	2.75	154	80	72	0.87	2.66	–

Bronze Age cemetery at Békásmegyr (c. 1000 B.C.) yielded a cut travertine slab with evidence of quarrying activity in the same region (Dobosi 2003). Some well-executed reliefs in travertine and basalt survive from the Neo Hittite Period (950–850 B.C.) from Carchemista, Turkey and may be seen in the Ankara Museum. In the Greek City of Paestum in Italy travertine was used extensively in the building of the temples. The oldest, known as the Basilica dedicated to Argive Hera was built in the mid 7th Century B.C. and has large fluted columns. The Temple of Neptune, a large building measuring about 60 x 30 m is considered one of the finest of all Greek temples dating to c. 450 B.C. and has a magnificent series of Doric columns (Guido 1972). Also in Italy, stands the early Etruscan Arch near Perugia, a large and impressive structure built largely of travertine. Analyses of the trace element geochemistry using fuzzy logic enabled Petrelli et al. (2003) to conclude that the travertine was obtained locally, possibly at the nearby Santa Sabina quarry. The Persians apparently used facing stones of onyx marble, a form of travertine, for some of their buildings (Merrill 1903) and the Greek city of Taxila near Rawalindi, Pakistan is partly built of it (Ford and Pedley 1992). Similar marbles have been quarried more recently in Austria such as the Laaser Onyx, a polished speleothem (Unterwurzacher 2002).

17.3.2 Roman Buildings 200 B.C.–A.D. 455

17.3.2.1 Bridges, Temples and Other Large Structures

The Romans were the first people to use travertine on a large scale. Much of the following has been drawn from Blake (1947, 1959) who has provided a detailed description of building materials of Rome up to A.D. 96. The earliest known employment of travertine blocks by the Romans is in the Arco d'Augusto, Perugia where it was employed in the ornamental town gate, believed to date to the late 2nd Century B.C. It found use somewhat later in the Ponte della Badia at Vulci (1st Century B.C., Photoplate 19A). In Rome, travertine voussoirs were used in the Pons Mulvius (109 B.C.) which crossed the Tibur just above the ancient city, though it had been employed earlier as chippings set in concrete in the Metellan Temple of Castor (117 B.C.). This would imply that stones were being worked at the time somewhere in Rome. At the Tullianum (c. 100 B.C.) it found occasional use as a doorframe or window casing. The hard-wearing qualities of the Tivoli travertine were also appreciated, as it was used for paving near the Curia by Julius Caesar (45 B.C.). An important bridge, the Pons Fabricius, crossed the Tibur at the small navicular island known as the 'Ship of Aesculapium' which was originally faced with travertine blocks fastened with iron cramps. It was also used in the facade and corbelling of the bridge itself, but this no longer exists. The work may have been carried out as early as 62 B.C. Other early uses are known from two approximately contemporary buildings, the Temple of Juno Sospita and the Temple of Janus (c. 90 B.C.). Travertine was used for the podium and architrave of the latter and parts of the column piers and entablature in the former, but due to extensive rebuilding, precise dates cannot be given. In none of these buildings is travertine used to the exclusion of other materials, and its choice may have been primarily for decoration. Other early uses were in the Ionic temple near the Tiber (c. 50 B.C.), where it was used in the podium, the stylobate, architrave and columns and the Tabularium (78 B.C.) where it was used for arches, bases and capitals, and in the Forum Julium (c. 46 B.C.). It also found limited use in the lower tier of the Pantheon (25 B.C.). An interesting early use was in the Roman sewerage system.

The Temple of Aedes Spei, in the Forum Holitorium (31 B.C.) is considered by Blake to represent a climax in travertine use, as almost the entire structure is composed of it, though

now incorporated into the wall of a church. The weakly fluted columns (Photoplate18C) six of which remain, are still entire, though cracked in places across the grain, and measure approximately 3.7 m high and 60 cm in diameter. The columns are interesting in that they are cut lengthwise along the bedding, but the fallen roundel in the left foreground has been fashioned with the bedding horizontal, a more common practice, though these might belong to another building. Such standing columns, although more able to withstand lateral stresses, would be less reliable under compression, though they have certainly stood the test of time. Their use in this form may have been experimental, or an attempt to simulate fluting. The capitals are simple and support an architrave with small imposts and a series of square-cut slots, perhaps of later date. The frieze is missing, along with most of the stylobate. During the same period, the elegant arch of the Porta Tiburtina (c. 5 B.C.) was built of travertine, and it had also been used for arches in the Porta Mugonia, the Forum Romanum, the Theatre of Pompey (55 B.C.) and the Theatre of Marcellus (13 B.C.). Around the same time, many porticoes were built of travertine and in some cases, travertine was used exclusively in areas of stress, such as the Basilica Aemilia (14 B.C.) in the springing of the vaulting and pillar foundations, while the bulk of the structure was built of softer Anio tufa. Other examples of this are to be found in the temples of Divus Julius (c. 35 B.C.), Castor (A.D. 6) and Concord (A.D. 10) and the Forum of Augustus. Use of travertine increased significantly during the Augustan (27 B.C.–A.D. 12) and later periods, but it must have been an expensive material, being difficult to extract and dress. The nearest quarries, at Bagni di Tivoli, allowed direct transport by boat to Rome, a distance of about 37 km, so it must have been cheaper than marble, which came from much greater distances. Marble however, soon replaced travertine as a purely decorative material, even in the Augustan period, where the growing wealth of the empire was used to import fine marbles from northern Italy and Greece. In later times, the use of travertine at points of stress decreased as Roman experience with concrete developed (Blake 1947). Travertine continued to be used extensively as a construction material in the first century. During the early first century, few buildings employing much travertine have come to light. Small quantities were used in the Carcer (c. A.D. 40) built by Nero, and the arch at Spoleta (A.D. 23). It had also been used for porticoes in a number of shops and bazaars, and continued in use for paving. During the reign of Claudius (A.D. 54–68) it was used widely in buildings, as in the Doric capitals and corbelling in the Grandi Horrea at Ostia and found wide use in the Domus Aurea. A little later, rusticated blocks were employed in the precinct of the deified Claudius (c. A.D. 60). Its use in arch construction continued, particularly for the keystones of bridges and other points of stress, most notable being the Claudian aqueducts. For example, near the Via Nazareno it was used for the cornice below the conduit, for imposts and keystones, and sometimes for the entire entablature. In Ostia it was sometimes used for the first flight of stairs in large private houses and in doorways (Meiggs 1973). In Rome the Porta Prenestina (now P. Maggiore) is an impressive travertine gateway carrying the Aqua Claudia and Aqua Anio Novus over two roads. This rugged structure was built in A.D. 38 and the travertine attic still bears inscriptions of three Roman emporers (Photoplate 19B). During this time, travertine also found use in the dam at Subiaco, and in several Roman canals. After the fire of A.D. 64, there was much reconstruction in Rome and travertine was widely employed. The Templum Pacis, built c. A.D. 75 and once considered one of the finest buildings in Rome, appears to have had a travertine corbel, but was mainly of marble. However, in one of the most exceptional buildings of all time, the Amphitheatrum Flavium (Colosseum) great use was made of travertine. This structure, built over many years, was started by Vespasian around A.D. 70 and opened, unfinished, after his death in A.D. 80. The building consists of a huge oval shell with axes of 188 and 156 m. The massive outer wall

was built of a series of piers and arches and within, a series of galleries, linked by steps provide accommodation for 50,000 people. Below the arena is a complex substructure now open to view with the vaults built largely of pumice to reduce weight. The facade of the Colosseum is of travertine blocks, some measuring in excess of 1 x 1 x 1.5 m. Those of the fourth (uppermost) storey may come from another source and were probably added at a slightly later date. The arches above the peripheral corridors were also of travertine, as is much of the substructure, combined with concrete. Many of the travertine blocks are held together with iron cramps set in lead. Within the facade, a series of travertine piers to the top of the second storey bears the weight of the upper galleries. Originally, the facade may have been painted or locally faced with marble. Large travertine keystones can be seen in parts of the substructure (Fig. 94) where the travertine bedding was sometimes used vertically, perhaps for decoration although more likely to yield under compression when laterally positioned (Fig. 94, left). Much of the stone is undressed. The substructure, used to hold animals, contain huge travertine corbels supporting posts and some of the barrel-vaulting, with much of this being surrounded by brickwork. The main structure was apparently built in haste as the travertine was not always used with advantage (C. Clelia, *pers. comm.*). A number of less famous buildings and walls dating to the same period included either travertine facing, foundations or capital bases, examples being the Templum divi Vespasiani (c. A.D. 80), the Temple of Diana, the Arch of Titus and the Aedes Caesarum.

During the following centuries, until the sack of Rome in 455, use of travertine continued but on a diminished scale. Little if any is found in extant constructions after 150. For example the Tomb of Hadrian (138) was constructed of marble, brick and concrete, as was the Forum of Trajan. The great baths of Caracalla (216), Diocletian (298–306) and the massive Basilica of Constantine (306–312) were all built almost entirely of brick-faced concrete.

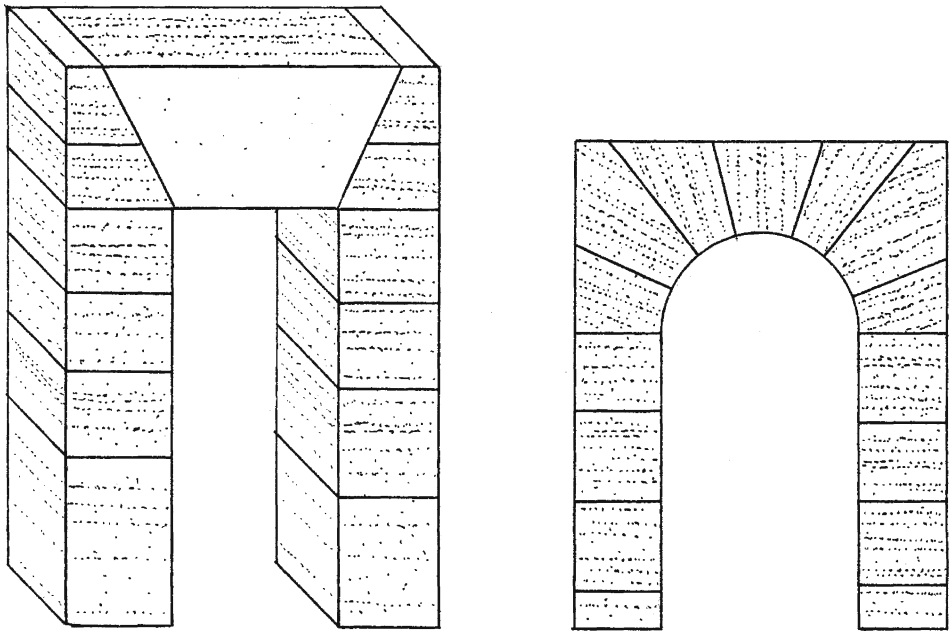

Fig. 94. Use of travertine in the Colosseum vaults showing the form of the keystones and their relationship to the travertine bedding

Villa Adriana (A.D. 117–138), a huge complex of large buildings, is remarkable for the sparing use of travertine, being built almost entirely of volcanic tufa and brick, yet is situated just 3 km from the great travertine quarries at Tivoli. Since the economy was in good shape at the time, it can only be supposed that travertine was out of fashion or not to Hadrian's liking. Why travertine fell in popularity is unknown but at Ostia, just west of Rome it appears to have been used widely in the 2nd Century. Marble continued in use on a fairly large scale, so fashion, rather than cost may be the reason. As Roman expertise in concrete and brick building advanced, the use of massive stone supports for arches and other stressed areas also declined. The use of travertine in building was not restricted to Rome, and examples can be found in buildings in many parts of Italy where travertine was close at hand. Examples include the Terme Taurine, Civitavecchia and at Vulci where it was used sporadically in the town walls dating from the 4th–5th Century. It was also used occasionally at Pompeii (Hull 1872).

At Hierapolis, Turkey, great use was made of it, to the exclusion of most other materials (Cramer 1987). A reason is not hard to find, since the city was founded on the great travertine mound of Pamukkale, which later entombed much of it. Travertine was employed as huge blocks in the monumental buildings over a long period after its foundation in c. 190 B.C. A good example is the theatre (Photoplate 19C) rebuilt after the earthquake of 17 A.D. Here as in Rome, the masonry was largely of travertine while the decorations were sculpted in marble with great skill. On the Main Street, near the Domitian Gate, are a few columns of free-standing travertine. With the grain set vertically, the weakness of the rock is well exposed. In no other city has the use of travertine been so extensive. In Hungary, many examples have come to light with travertine use in secular buildings, aqueduct pillars and milestones, and some evidence of quarrying operations (Dobosi 2003).

In Britain, the Romans made use of travertine despite the scarcity of good quality material. The one remaining Pharos (lighthouse) at Dover (1st Century) is the best-preserved British example (Photoplate 19D). It was built of small poorly dressed travertine blocks measuring about 30 x 10 cm interposed with tiles every seven courses, the whole cemented with mortar. The tower stands 18.9 m high, the lower 13 m being Roman. The walls measure 3.6 m at the base with a rubble core. Window architraves consist of thin travertine slices interposed with tile, presumably to add strength and reduce fragmentation. The travertine was probably obtained from the Dover valley about four kilometres away. Nearby at Folkestone, the walls of the Roman villa were initially built entirely of travertine, but other materials were incorporated at a later date (Williams 1971). Travertine was used in 16 of the 154 Roman sites documented by Williams (1971) from southeast England but only at the aforementioned was it used extensively. At other locations it had been used for quoins (Maidstone and Silchester), the lining of a hypocaust (Richborough) as voussoirs (Pulborough) and sparingly in structures associated with Hadrian's Wall in the north. At Aylburton, Gloucestershire, a temple dedicated to the deity Nodens (A.D. ~300) contains many crudely-worked travertine blocks in the superstructure. Elsewhere in England, Williams mentions its use in vaulting. This selective use probably reflects the scarcity of suitable material. Masonry is not widely found in Britain until the second half of the second century, but travertine appears to be one of the first materials used, both in the Dover Pharos, and in buildings at Cobham in Kent (Williams 1971).

17.3.2.2 Roman Tombs

Around Rome may be seen many Roman tombs, both above and below ground. Although a law forbade burial within the city walls a few exceptions were permitted. An early example is provided by the tomb of Bibulus (60 B.C.) which had a travertine facade. The Pyramid of

Cestius (c. 12 B.C.) was also partly faced with it. An unusual example, by the Porta Maggiore, is the large tomb of Marcus Vergilius Eurysaces which is entirely of travertine and embossed with a decorative frieze showing breadmaking and thought to date from the Augustan period (Photoplate 19B). Of the same period is the tomb of Caecilia Metella on the Via Appia, also travertine-faced. Tombs employing travertine can also be found from the first century and in a number of columbaria, such as the Columbarium Via Taranto (A.D. 54–68). At Hierapolis, Turkey, the great necropolis contains hundreds of finely decorated tombs all of local travertine dating from the early first Century (Photoplate 19E). Travertine tombs are also known from Fratin, Belgium, and elsewhere (Couteaux 1969).

17.3.3 The Dark Ages to the Renaissance, A.D. 455–1550

17.3.3.1 Europe Excluding the United Kingdom

In Italy the use of travertine continued for building after the fall of the Roman Empire, but in common with the rest of Europe, structures built between the 5th and 10th Centuries are rare, and as far as the author is aware, have not been surveyed comprehensively for their stonework. In Belgium, Couteaux (1969) comments on its use during the 'Dark Ages', presumably continuing in the Roman fashion. It was used in many medieval churches in southern Belgium, including the 12th Century abbey at Orval. Schmid (1972) mentions the use of travertine in Germany in the 11th Century. The Steinrinne Quarry, Bilzingsleben has been in operation since the 12th Century (Glazek et al. 1980) and early examples of stonework are known from the Teutoberger Wald (Hiltermann 1977). The Stadtchurch, Geislingen (1424–1428) is a Gothic building constructed mainly of travertine, including the mullions, and the gateway to Tübingen castle, c. 1600 is built largely of local travertine, including the vaulting. Its use continued in Italy though little appears to have been published on the matter. Riccetti (1988) mentions it in the construction of Orvieto Cathedral in the 13th Century.

In France, Paillet (1986) notes its use for walls and quoins at St Bonnet (1156–1160) near Nimes and in the 12th Century chateau at St. Hilaire-le-Vieux. According to Blot (1896) it has been used extensively in France, and in medieval churches of the former Yugoslavia (Srdoc et al. 1987).

17.3.3.2 The United Kingdom

In the UK the most notable early example of this period is the church of All Saints at Brixnorth, Northampton. This early Saxon building, the finest of its kind in England, was built in a wide range of materials, including a small amount of travertine, of unknown but presumably local provenance. The church was probably built around A.D. 750 by King Ethelbald of Mercia, though some argue for an earlier date. The original structure followed the form of a Basilica and suggests Italian or Syrian influence. Travertine was used sparingly in the simple pillars supporting the apse, the voussoirs for one of the apse windows and the surround of one of the tower and stair turret windows. There is also an occasional quoin block and some facing in the tower and stair turret. The latter is believed to be a 10th Century addition. There are also a few travertine fragments incorporated into the wall of the 13th Century Lady Chapel so there were several periods of travertine use. Of interest is the use of Roman tiles in the nave arches which implies that Roman materials were being re-used by the Saxon builders and it is therefore possible that the travertine has also been re-used. The occurrence of thin travertine slices in the apse window arch however, suggests that if there was re-use, then the blocks would have needed re-cutting.

The use of travertine in buildings may therefore be either functional or merely a 'convenience' material locally at hand. The 7th Century tower of St Mary in the Castle next to the Dover pharos (Photoplate 19C) contains travertine fragments but these were probably incorporated at a later date. Fragments have also been uncovered in the Norman work of Canterbury Cathedral. Here travertine was used at an early period in the vaulting of the Great Dorter (1070–1091) as large undressed blocks cemented with a coarse mortar.

In the following centuries good examples of travertine use may be found in the churches at Moccas (c. 1130), Hanley William (c. 1180) and Shelsley Walsh, Herefordshire (12thC.), all of which are built almost entirely of local travertine (Photoplate 20A). A significant use was in the vaulting of several cathedrals. At Canterbury it was used in the choir vaults after the fire of 1174 and also in Gloucester and Worcester Cathedrals, and Bristol in the 13th Century. This may be a throwback to a Roman discovery though vaulting design had changed radically since then. Certainly the more porous travertines are good low density building materials but they are usually concealed behind stucco in these churches so the construction details are obscured. At Rochester the crypt vaulting consists of travertine slabs with intervening stretchers of another limestone close to the supporting pillars. A sample of vaulting from Gloucester cathedral shown to the author, was 5–6 cm in thickness. More massive vaulting can be seen above the library of Wenlock Priory. This vaulting probably dates from the 13th Century when the church was enlarged. There is also some earlier travertine vaulting (c. 1150) spanning the Chapter House about 25 cm in thickness. Travertine vaulting was also used in the 15th Century Lady Chapel and the Great Church of Glastonbury Abbey. Travertine is scattered in the walls of the latter and also in the town where it has probably been re-used. Fragments can be seen on Glastonbury Tor, perhaps remnants of the early church destroyed in the earthquake of 1275.

Though travertine is found most frequently in the ecclesiastic buildings of England during this period, it found occasional use in secular buildings. It can be seen in the Norman vaulting of Kenilworth Castle, Warwickshire (1123), a huge edifice otherwise built entirely of sandstone though the vaulting is no longer in place. Berkeley Castle, Gloucestershire is another example where travertine, quarried from Dursley has been used extensively in the curtain wall, keep wall and some window surrounds dating to the 12th C. Its employment here continued into the 20th Century with renovation of the castellations and the vaulted gate, providing a rare modern example in this context (Photoplate 20A).

Use in private buildings during this period is rare. The chimney-breast of the Lion Inn, Clifton on Teme, built partly of dressed travertine blocks, is thought to date from the 12th Century.

17.3.4 Europe 1551–2000

Travertine has been used increasingly in the latter part of this period to modern times. In the 'Second Empire' period of construction in the late 19th Century, examples are often found, such as its use in the Ministry of Justice Building, Paris. However there are plenty of early works, several of which are famous attractions. For example in Italy, Bernini (1598–1680) used travertine with great effect in the piazza colonnade and gate of St Peter's Basilica, Vatican City, Rome. Work on the piazza began in 1656. It was bordered by two huge free-standing colonnades of travertine and its form was likened by Bernini to the outstretched arms of the Church welcoming the faithful. This unique form is thought to have been inspired by the Roman Sanctuary of Fortuna Primigenia at Palastrina. Travertine statues of saints, executed by Bernini's followers surmount the colonnade. The Spanish Steps, built in 1726 by Francesco de Sanctis are also constructed of travertine. Walls of travertine along the Tiber at Rome (the Lungotevere) built during the same period have been investigated for their plant communities in relation to biodegradation (Bellinzoni et al. 2003).

In more recent times, travertine has been used widely in the Schwäbische Alb, Germany. Schmid (1972) provides a distribution map of its use in buildings and notes particular examples such as the Pfullinger Hall (1903). Urach Railway Station (c. 1940) provides a late example of German travertine use prior to its rapid demise as new and cheaper building materials became available.

Travertine chippings have been found in early Roman fillings but were little used as concrete aggregate presumably because it was too highly valued (Blake 1947). Some recent attempts at reviving this by binding travertine aggregates in cement have been made at Wiesenstieg, Germany, where building blocks and pipes have been made, but the market failed.

In England travertine use in churches had almost stopped by the 18th Century but it may be found in a few private houses, the most noteworthy being Marl Cottage at Dunsley, Derbyshire (1810) built entirely from a local source (Photoplate 20B). Other examples include Rose Cottage, Alport (1688) partly built of it, several Tudor chimney-breasts in Clifton on Teme, at Kilnsey Hall, Yorkshire (17th C), and the Lodge at Shelsley Walsh, a complete late 19th Century example. At Matlock Bath, Derbyshire there are several Victorian structures built largely of local travertine, including the Pavilion and the rusticated grottoes surrounding the thermal springs (Fig. 95). The mapping of travertine use in Matlock Bath demonstrates how locally the use of this material was, with practically none found beyond the old town limits (Fig. 96).

In the 20th Century imported travertine has been used in many modern city buildings throughout the world. In London, examples include the internal facing at Picadilly Underground Station, Senate House, the new British Library and Broadgate Circle (Photoplate 20C). The latter, completed in 1991 is one of the largest developments in the City this century, and consists of a travertine-cladded balcony supported by plain columns and encircled by a wall of rebated cladding and semicircular capstones. In the centre, an ice-rink is surrounded by a pavement of travertine infilled with fine angular concrete, the whole being supported on a steel and concrete superstructure. In Budapest, local travertine has been used to replace decaying stonework in the Houses of Parliament since the 1920s. Measurements of stone deterioration have demonstrated its superiority over the limestone it replaced (Török 2004).

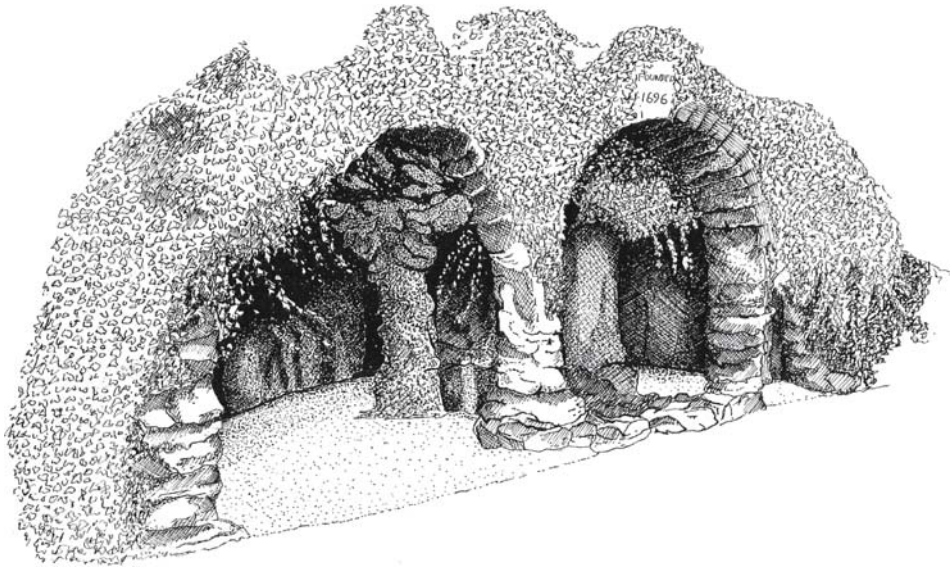

Fig. 95. A small vaulted grotto over the Old Bath Spring at Matlock Bath, UK. Drawing by Andrea Pentecost

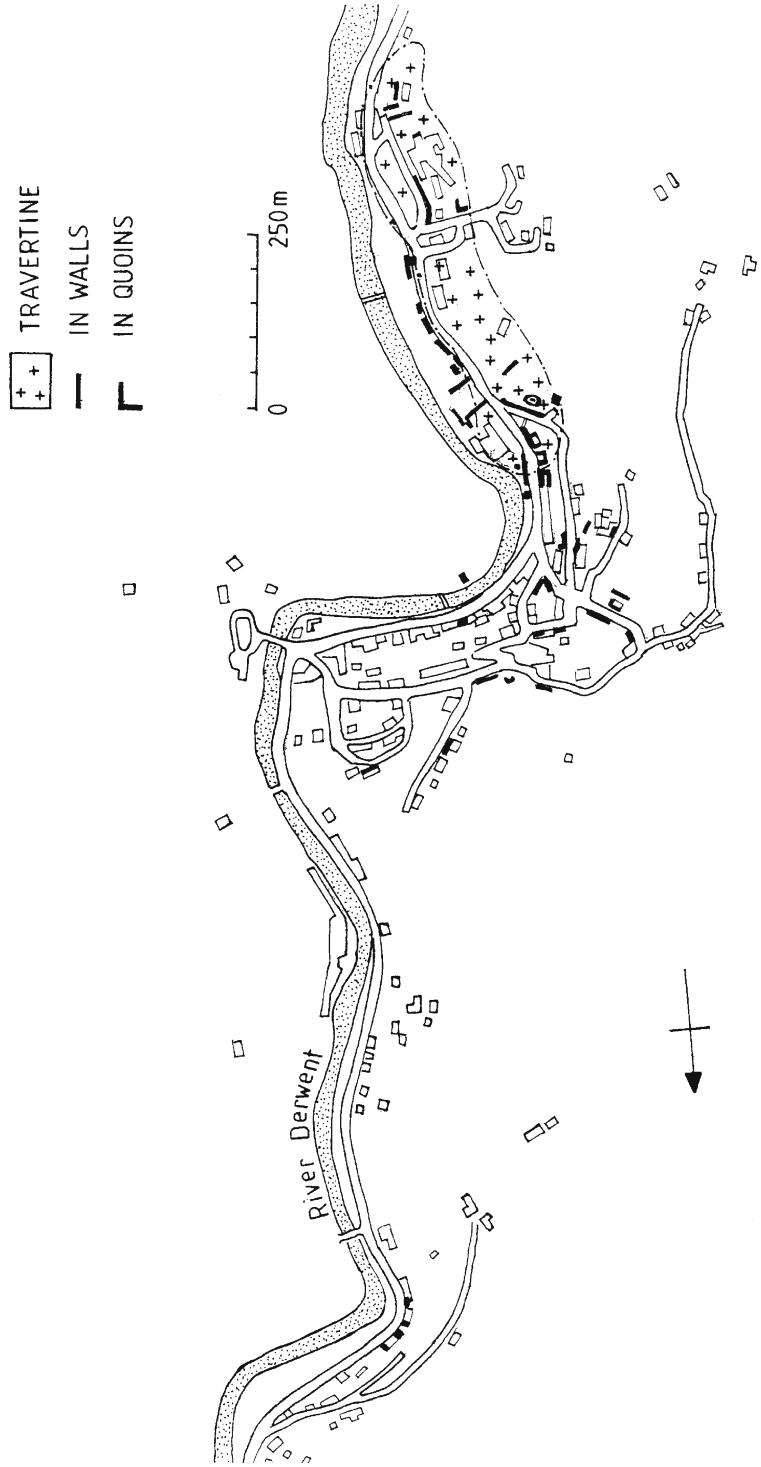

Fig. 96. Travertine use at Matlock Bath showing the extent of its use and the location of the deposit

17.3.5 A Case Study in English Travertine Use: The North Kent Churches

The county of Kent in England contains extensive tracts of low-lying limestone (Hythe Beds and Chalk) and one of the highest densities of Medieval churches in the country. Many of these churches originated in Saxon times but little of the original structure remains. After A.D. 1066, the Normans undertook an extensive re-building campaign, frequently incorporating travertine into the fabric. In this section, the use of travertine in these buildings is investigated in an attempt to provide a better understanding of how and when a scarce building material was used in these important buildings.

The Hythe Beds consist of a sequence of tough Cretaceous limestones and interbedded calcareous sandstones reaching a maximum thickness of 60 m and running approximately east-west through the counties of Kent and Surrey where they form a prominent escarpment up to 200 m high (Fig. 97 inset). The beds have a regional northern dip along the Wealden anticline and are succeeded by the Gault Clay and then thick pelagic limestones of the English Chalk. The area is dissected by the River Medway and its tributaries which cut completely through the limestone units and led to the establishment of early fortifications at Maidstone (Fig. 97, M) and Rochester (R). A series of smaller streams drain the dip slope of the Hythe Beds and scarp of the Chalk and small deposits of travertine are widespread in the upper reaches of many of these streams (Fig. 29). A number of streams also drain the scarp of the Hythe Beds but no travertine has been found in this area. The region of interest includes the Hythe Beds outcrop together with the southern Chalk margin and the upper Medway valley. It has been occupied since at least the Mesolithic period. The calcareous hills provided excellent soil for tillage and they were soon colonised by the Romans after their invasion of A.D. 43. Eighteen Roman villas/large buildings have been uncovered in the area and the port of Dvrobrivae was established at Rochester. Travertine has been found at four of these Roman sites; Boxley, Eccles, Maidstone and Rochester (Williams 1971). When the Romans left (c. A.D. 400) the buildings apparently fell into decay and were eventually abandoned.

Although Christianity came to Britain during the Roman occupation, it was not widespread, and the Anglo-Saxons, who later colonised Kent were not Christians. Pope Gregory sent Augustine to Kent in A.D. 597 and a church was subsequently built in Rochester in 604. Further churches were founded, though their superstructures were mainly of wood. When the Normans invaded in 1066 they found a church in every parish and replaced most of them with new stone, whilst retaining intact the scarce Saxon stone churches. The early Norman period was one of christian religious revival within the country.

Within the area, Saxon work has been identified in several churches, such as East Malling (Em, Fig. 97) and East Farleigh (Ef) and they contain some travertine. With few exceptions, all have been altered by later additions and rebuilding so it is not possible at present to demonstrate unequivocal Saxon use of the travertine. Major changes to church buildings occurred after 1066. Bishop Gundulf (?–c. 1108) was commissioned by King William to build Rochester castle and cathedral c. 1089 (Ro), the latter employing much travertine in the crypt. A year later, Gundulf founded West Malling Abbey, church and nearby keep (Wm), all of which employ travertine. He is also associated with the churches of Ryarsh, Trottiscliffe and West Farleigh that contain travertine (Fig. 98). In fact, the use of travertine in the Kent churches led Livett (1893) to state that 'tufa is the most characteristic stone found in early-Norman buildings'. Why the Normans in particular sought out this stone is uncertain. Normandy contains many travertine deposits and the material must have been known to them, but the author is unaware of any site where it may have been used in that region. Its use in quoins and window surrounds was popular probably because it was easy to dress – the Normans

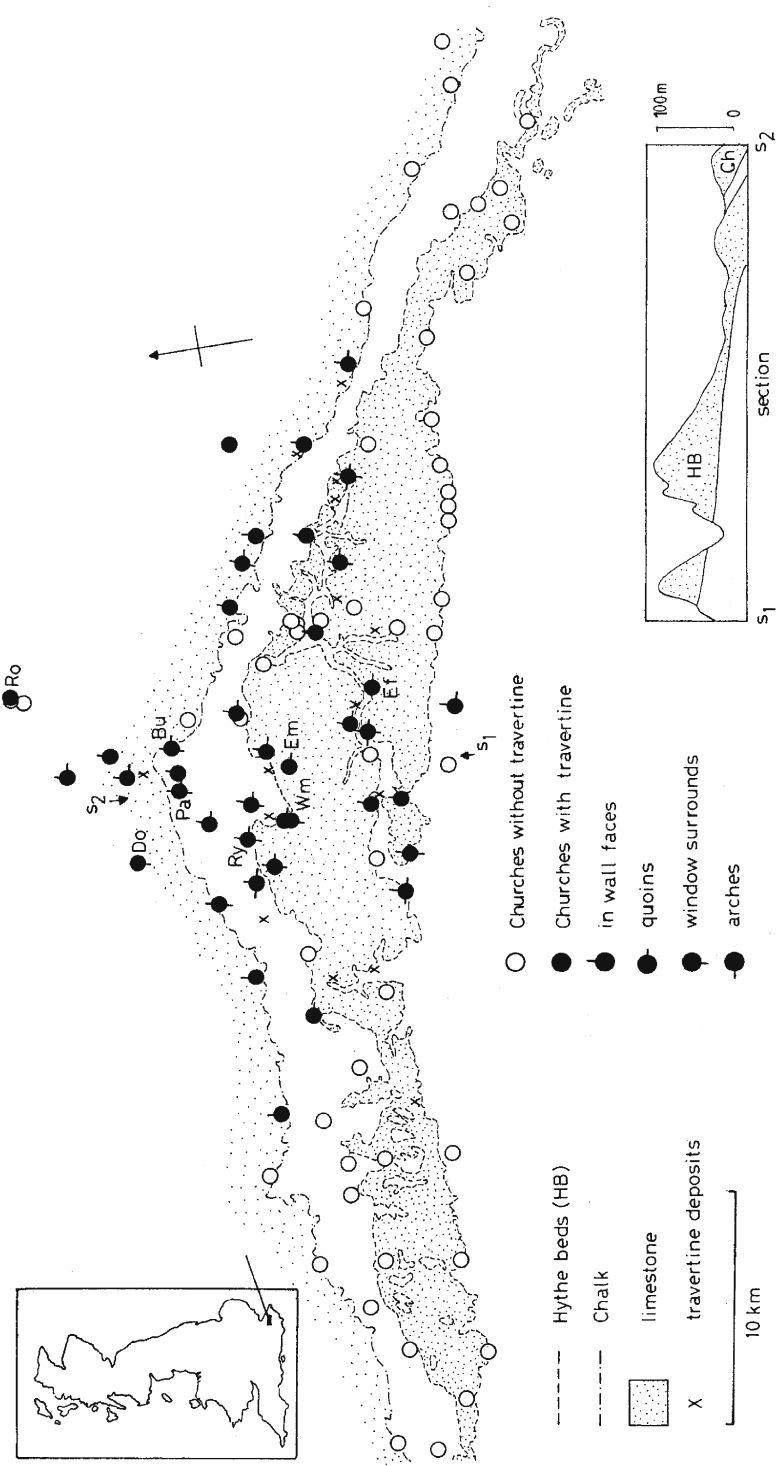

Fig. 97. Travertine use in Kent churches and the associated limestone outcrops and known travertine deposits

presumably used only the axe to shape it, since chisels were not introduced until 1174. There is no doubt that they quarried the material locally since several churches are adjacent to known Kent deposits, though the extent of the workable material was clearly limited and in no case are buildings constructed entirely of travertine. Even where it was used for quoins, other materials are often present. The quoin stones themselves are rarely dressed on all six faces and were not cut to a standard size. They range in thickness (ie. height) from about 13–39 cm, averaging about 20 cm. Typical dimensions are 16 x 16 x 43 cm and 12 x 22 x 33 cm. The variation might reflect a limited supply of large travertine blocks. There is in addition, an association between the building materials of some churches and adjacent Roman sites. The walls of Burham (Bu) and Snodland Church, for example contain travertine associated with Roman tile with Roman sites nearby. Early-Norman churches which have remained more or less unaltered in Kent are comparatively rare, examples being Dode (Do), Paddlesworth (Pa)and Hucking and all three contain travertine. Livett (1895) made a study of the two-celled churches at Dode and Paddlesworth. The church at Paddlesworth, which consists of a simple chancel and nave was built in several stages around 1100 and dressed travertine occurs patchily in the walls, in all six quoins and the upper window splays (Fig. 100). Livett suggested that its mode of occurrence might mean that a load of travertine may have been acquired from another, larger site. Alternatively it may indicate that a local source was discovered late in its construction. Most of these churches have however been enlarged or rebuilt and their Norman origins are often obscure. During enlargement, the Norman travertine was often retained within the

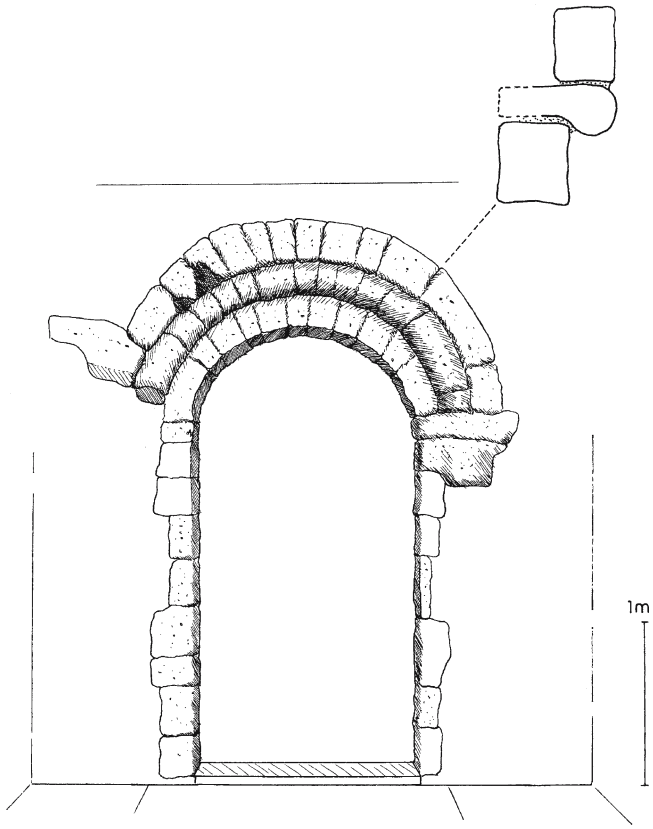

Fig. 98.
Norman door surround in West Farleigh Church, Kent. A section through the arch is shown above right

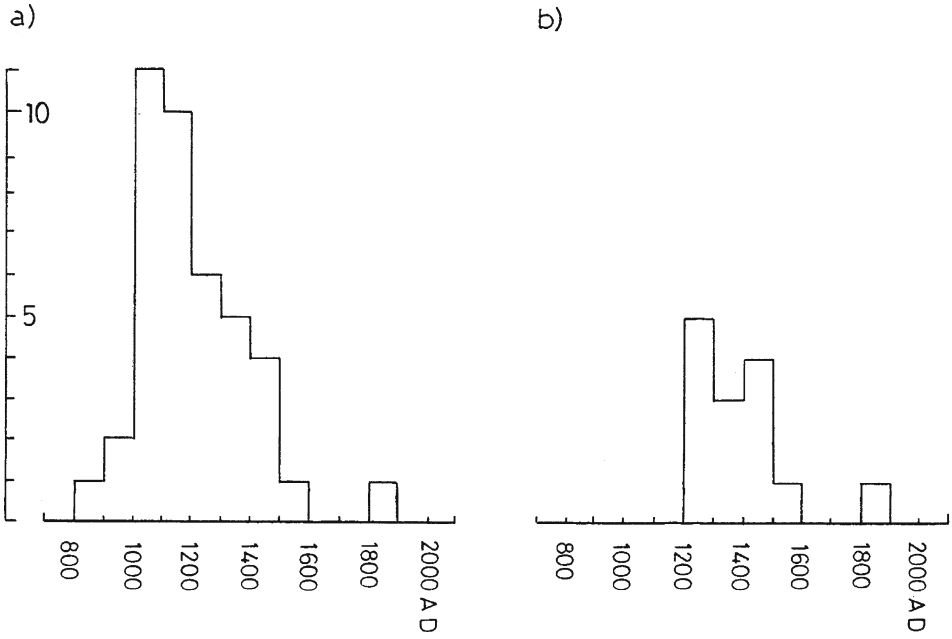

Fig. 99. Frequency of travertine use in Kent churches. a) All churches surveyed in the case study; b) churches where re-use is either known or strongly suspected

new structure. Indeed, attribution of Norman origins is often assumed on account of the travertine they contain. Examples include Aylesford, Leybourne, East Farleigh and Bearsted. A careful study of the early-Norman work in the Medway Valley led Livett to believe that a single gang of itinerant masons was responsible for most of the work.

Most of the Norman churches in this area contain travertine. The main building stone is the Hythe Beds limestone and of the 38 churches in the region with recognised Norman work only nine (24%) contain no trace of travertine. In a few cases such as Loose the absence of travertine is surprising since the adjacent valley contains large quantities.

The distribution of travertine-containing churches in the area (Fig. 98) demonstrates a concentration of use west of Maidstone. The calcareous Hythe Beds thin quickly to the east and west of here and little travertine has been uncovered which probably accounts for its absence in churches on the limbs of the outcrop. It is interesting to note that churches along the nearby Chalk scarp are also without travertine. Several are early-Norman which suggests that the travertine was dug primarily from the Hythe Beds and only used locally, even though several travertine deposits are known along the Chalk scarp.

Livett (1895) thought that travertine ceased to be dug in the area after 1120 because of deposit exhaustion or change in building practices. Nevertheless, there are several churches where travertine use and re-use occurs in later centuries. An analysis of the data shows that it was used in the area up to the 14th Century, but there is a rapid decline in its appearance after the early 12th Century (Fig. 99). A late example is Ryarsh (Ry), a Norman church with a travertine quoin in the vestry rebuilt in the late 19th Century. It should be noted that the evidence for fresh travertine use after the Norman period is based solely upon the observation that the earlier church structures have not been observed with it. This is hardly satisfactory, since earlier use may be covered by stucco, as at Bearsted, or the building period may have

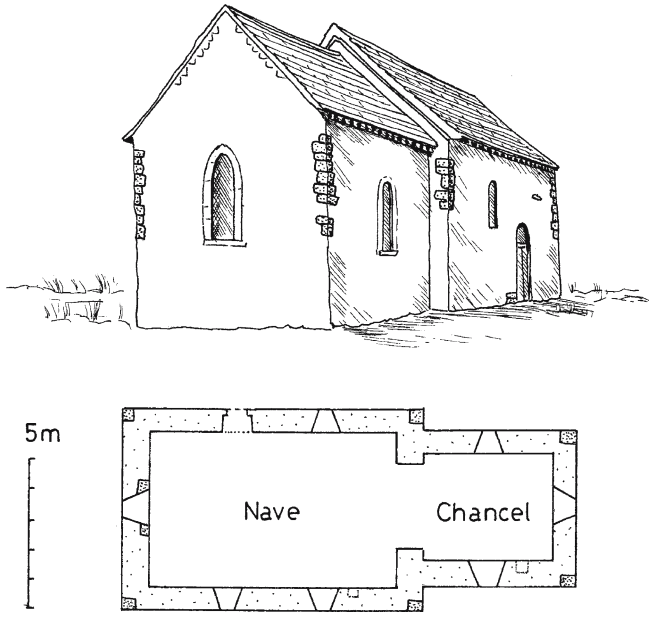

Fig. 100.
Paddlesworth Church, Kent. An early two-celled structure almost unaltered since its construction. The original roof was probably of thatch. Plan redrawn from Livett (1895). Travertine stippled

been misinterpreted. However, churches in other parts of the country attest to travertine use at later dates and this may well be the case in Kent, with 13th Century examples at Birling (walls, quoins) and 14th Century at Nettlestead (walls). Notable is the almost complete lack of travertine in churches founded after 1600.

During the survey, travertine was found in a total 40 of the 93 churches and abbeys investigated in North Kent. Most often it was found in the wall faces where it occurred as dressed and undressed blocks (34 churches). Its frequent random use suggests that broken pieces or those unsuitable for quoins were incorporated into the wall as fill. Use in quoins was noted in 23 churches, in window surrounds 10 and in arches only four. Within the region are the remains of five castles dating from the 11th to 13th Centuries, but travertine was used very sparingly, and only in the two fortifications attributable to Gundulf, namely those at Rochester and West Malling. The great majority of secular building in Kent was of wood, daub and plaster in medieval times owing to the readily availability and cheapness of wood compared with stone. Travertine was no doubt a highly prized material in this area and its use restricted to use in the most important ritualistic and defensible structures of the county.

17.4 Travertine in Art

Travertine use has never been confined to building. The dense, low-porosity forms resemble marble and can be sculpted in a similar manner. Intricate cutting and polishing is possible with these forms, and with the many kinds of speleothem where its translucency is especially valued. The mouldic porosity of many thermogene travertines, combined with all-round strength has found much use in large-scale sculpture combining inimitable surface patterns with simplicity of form. The rapid deposition of travertine has attracted attention throughout the ages, and several commercial enterprises exploit the phenomenon as 'petrifying springs'. They continue to fascinate and provide considerable future potential for development by sculptors.

17.4.1 Sculpture and Internal Decoration

Egyptian alabaster, some forms of which are closely akin to travertine, consisting of speleothem and spelean infills of calcite, has been used for making vessels since the First Dynasty (c. 3200 B.C.). A fine collection of objects having been discovered near the sepulchre of Udimu at Sakkara (Emery 1961). The vessels appear to have been shaped by cutting out the inside first, a method still practiced in that country. An alabaster statuette of Neteren dating to the 2nd Dynasty is in the Michailides Collection at Cairo. The use of alabaster continued and some exceptionally fine works were found in the tomb of Tutankhamun (1580 B.C.). Monumental sculptures also exist and include the great Marble Sphinx at Memphis attributed to Ramses II (c. 1250 B.C.) and believed to have come from the quarries at Hatnub. Another noteworthy piece is the huge sarcophagus of Seti (1292 B.C.) from the Valley of the Kings. An Etruscan sarcophagus made of alabaster is preserved in the Boston Museum and this material was also used by the Romans and quarried at Ain Tembalek and Tlemcen, (Merrill 1903) but in Italy, few early works in travertine *sensu stricto* have come to light. Some fine monuments depicting Roman families in bas-relief occur in the grounds of Villa Volkonsky, Rome (Photoplate 20D) dating from the Neronic period (A.D. 54–68). Sculpture in the round almost certainly existed but may not have survived intact. The author observed among a rubble pile by the Theatre of Marcellus (13 B.C.) a grotesque bas-relief (Photoplate 21D), presumably part of the decoration. Roman sculpture in travertine can also be observed at Tata, Hungary where there were substantial local supplies. Early medieval works are equally rare. Outside the Heimat Museum, Geislingen, stands a full size half-round statue of a man in local travertine dating from the 12th Century. It is in poor condition, has been crudely executed and nothing appears to be known of its origin (Photoplate 18E). Other examples occur in France. Blot (1986) mentions a sculpted pot of flowers at Blotzeim and other church sculpture is displayed in the Museum of Troyes and St. Martin-de Pris, Millau. In the Basilica san Pietro, Tuscania, Italy is a 12th Century travertine column with an ornately carved capital. During the Italian Renaissance, well-executed pieces were made by Bernini for the famous fountains of Rome. The Fountain of the Four Rivers (1647–51) in the Piazza Navona is a good example where travertine blocks support boldly carved horses rising majestically from the water.

An unusual decorative use of travertine is in the production of onyx marble windows in religious buildings. They may be seen in the cathedral at Orvieto, and the Mausoleum at Ravenna, Italy. Fine examples are also reported from some of the mosques of Istanbul, Turkey and in Mexico.

Prior to the 20th Century, little use was made of travertine in sculpture, but it has become more popular in recent times. The English sculptor Henry Moore (1898–1986) found it a good medium for his monolithic works and style. He began sculpting in the 1920s and produced more than 900 pieces during his life. Most of these were realised in bronze, but the majority of his later work in stone was executed in Italian travertine. One of his earliest travertine sculptures, a stout, ponderous piece, was produced in 1936 (untitled) soon after his first monolithic forms appeared. Few other works in travertine were made until after the Second World War, with a steady rise in production continuing into the 1970s. Moore had used other stones during this period, but travertine became a favourite in the 1970s and 80s when he was better known and could afford more expensive materials. However, all of his larger works were executed in Italy, since the cost of transport to England was prohibitive. One of his is most celebrated works in travertine is the Reclining Figure displayed outside the UNESCO building in Paris. This was executed from two blocks originally weighing around 60 tonnes, reduced to about 30 tonnes on completion 14 months later. The work began in 1957

and was his largest stone carving to date, though originally conceived to be much larger. Moore considered several materials for this work but decided upon travertine as its high reflection made good contrasts with the building's glass frontage. He was paid a total of £16000 ($29000) for the work, including expenses. Many of his travertine sculptures are of standing or reclining figures, notable among them being the Bone Skirt (1975), the Draped Reclining Figure (1978, Photoplate 20E) and the two sets of standing figures executed in 1981. These works were followed by the Mother and Child (1983). Most of the sculptures are oversize, and one of his grandest, the Large Animal Form (1969–70) measures 2.74 m in length. Abstract works include the 'Two Form' of 1975 which is one of his smaller marbles measuring 88 cm high and the Spindle Piece (4.47 m) of 1981. In these the grain lies horizontally and the surface is mostly smoothed with abrasive with the cavities left unfilled. Italian travertine is an excellent medium for monolithic sculpture and is well suited to flowing curved works rather than angular pieces which is why they suit Moore's style so well. Most of Moore's sculptures are open to broad interpretation and the travertines are best observed in sunlight where striking shadow effects can be observed. Some viewers believe that his later works, which Moore rarely sculpted himself, lack the vigour and imagination of his earlier pieces. Moore contracted the Henraux artisans, notably Giulio Cardini and Sem Ghelardini for much of his later work (Berthoud 1987).

The texture of most travertines used in sculpture is provided by their contrasting white and brown laminations, but most notably by the small cavities caused by gas inclusions (Photoplate 21D). These cavities, normally less than 1 cm across in the best quality marbles, give good finished surfaces especially suited to large works, and are very efffective in monoliths. The pieces darken upon weathering, a character appreciated by Moore. They remove the continuity of angular surfaces in small works, though this may be restored by filling. Monolithic forms however, remain best unfilled, as this can detract from the textural quality of the work.

Other 20th Century sculptors have also employed travertine such as Pietro Cascella (1921–) and Natalino Andolfatti (1933–). Large pieces may be seen in the Umberto Severi collection at Sant' Antonio, Italy. Another noteworthy monolith is the Pace Sulla Terra by Jacques Lipchitz (1971) which stands outside the Museum of Modern Art in Rome (Photoplate 21A).

Mass-produced souvenirs in travertine are to be found around the Tivoli quarries, Rome. Although of little artistic merit, these high quality marbles, subject to a series of well-placed saw cuts result in small, pleasing pieces such as the one illustrated (Photoplate 21B). In Mexico travertine onyx is fashioned into bookends and many other objects as souvenirs (Johnson 1965). This material is mainly a laminated flowstone excavated from collapsed cave systems (Ford and Pedley 1992). Travertine is also used widely in street furniture. It has occasionally been used in household furniture in the form of table-tops, slatted seats and vases. Onyx marble tables have been manufactured in Italy and elsewhere. Ornately carved fire surrounds have been exported worldwide from Italy.

17.4.2 Garden Decoration

Undressed travertine, especially that formed on cascades and dams has found wide use in garden decoration. An early use for such pieces, suggested by ancient writers is in grottoes (e.g. Ovid's *Metamorphoses*, 43 B.C.–C. A.D. 18). The use of travertine in gardens is extensive in South-East Asia, especially China. Barbour (1930) observed that the huge deposits at Niangtzekuan were used for gardens all over the northern provinces. Large pieces are used with effect in the gardens at Guangzou and at Guilin (Photoplate 21C), but they were not

used in the famous gardens at Suzhou, which date from Medieval times. Their use in continental Europe is noted by Davreux (1833), Fliche (1894) and Lohest (1901). In Britain, a number of small travertine quarries supply blocks for garden use, an activity which has continued for at least a century (Ford 1989). The travertine is used as both a decorative rockery stone and as a planting medium. The softer varieties provide a good base for calcicolous alpines. At the Cambridge Botanic Gardens, UK for example, *Arabis bryoides, Gypsophila aretoides* and *Minuartia stellata* along with *Saxifraga* and *Sempervirium* are planted within hollowed-out blocks of the material. The Chinese specialise in building miniature travertine mountains often with a form of bonsai art (Photoplate 22A). Recognising the rapidity of travertine accumulation around bryophytes in Spain, Weijermars et al. (1986) suggested using this property to produce natural overgrowths on artificial surfaces.

Occasionally, interest is added by playing a fountain of travertine-depositing water over a framework of travertine or other suitable material. With illumination, moss colonisation begins to build up around the fountainhead to form a picturesque column. In England, examples can be seen at Dulcote in Somerset, Matlock Bath in Derbyshire and at Settle, Yorks. Fabré (1986) recognised these forms as a 'travertin d'origine anthropique' and cited the 'champignons sur jet d'eau' at the Jardin de la Gare, Montpellier.

Blocks of travertine also find use in aquaria where they provide a good substratum for anemones and soft corals with suitable niches for eels. Barbour (1930) reports its use in Chinese fishponds.

17.4.3 Petrifying Springs

Perhaps the most remarkable of all uses to which travertine has been put are the encrustations built upon all manner of objects in the so-called 'petrifying springs' and wells. This phenomenon has been described on many occasions throughout history. Strabo (63 B.C.–A.D. 20) mentions a bird which flying over a spring, splashed the water on its wings and was turned to stone. The *Shu I Chi* (Records of Strange Things, c. A.D. 530) describes a chinese petrifying spring and the *han shui shih* (water-bearing stone). In Europe, such springs had been noted by Libavius (1597) and the earliest record in England appears to be of the Dripping Well, known in writing since at least the 16th Century, and probably appreciated even earlier. England has a number of these springs, so many in fact that Morton (1712) stated that for one county alone 'we have hundreds', and some of the names record this property, such as the Whitewell of Lancashire, and the Silver Well of Cheshire. Some of these springs are given the soubriquet 'Dropswell' though this does not appear to refer solely to their 'petrifying' properties.

The process of petrification refers to the replacement of one material by another, almost to the point of completion. This does not occur in 'petrifying springs' and they would be more appropriately, though less colourfully termed 'encrusting springs'. Interestingly, there is an early account of the true petrification of wood by calcium carbonate in a German aqueduct, but the discovery never appears to have been taken up (Stokes 1837). Both meteogene and thermogene travertines are deposited at petrifying springs and examples of both types are described below. In England, the most celebrated spring occurs at Knaresborough, Yorkshire, known locally as the Dropping (formerly Dripping) Well. Buckland (1883) described it as a 'huge frowning rock … overlooking the River Nidd'. The rock is a large overhanging block of travertine, almost entirely detached from the riverbank, over which spring water is guided in a series of channels (Fig. 101). The spring rises just above the bank and artificial channels guide the water so it forms a thin, continuous sheet of water on the travertine cliff. The lower edge of the face, which is undercut, is strung with horizontal lengths of wire, onto

which series of objects are suspended on further vertical wires (Photoplate 22D). Recently, soft teddy bears were popular, each separated from the other by a link to facilitate removal. Other items include ties, shoes, umbrellas, handbags and even braziers. Small absorbent articles such as toy bears are left under the water for about 6 months, but larger objects may remain over a year. The deposition rate is about 12 mm a^{-1} and the smooth cliff face is scraped to prevent the buildup of algae that spoil the 'petrifactions'. It is also done to help prevent the block toppling over. Sizeable lumps fell off in 1816 and 1821. Visitors are shown two protuberances on the cliff face, where a top hat and lady's bonnet were attached in 1853, indicating some accretion despite the scraping. The cleaning seems to have begun between 1800 and 1836 judging from dated prints. The Dropping Well is unusual for its employment of absorbent articles for encrustation, since these are not commonly utilised elsewhere.

At Matlock Bath in Derbyshire, 'petrifaction' has been practised for over a century using several of the superambient springs. The springwater rises at 20 °C and was piped to numerous outlets, some for petrifaction and others to bath-houses (Pentecost and Askew 1999). These wells, of which there have been many over the years, have traditionally been enclosed, a common practice on the continent. This serves to lower light intensity sufficiently to discourage the growth of plants. However, any enclosure is going to decrease the rate of degassing. At these wells, the usual method of supplying travertine to the objects was to spray it with fine droplets from a pipe or perforated spray head. When the author visited one of the wells in 2000, it was found to be occupied by a birdcage, a sewing machine, a telephone, and a pair of rugby boots. However, in Victorian times, bird's nests with eggs were among the most favourite objects. At Matlock the articles are left for about a year, after which they have acquired several millimetres of pale travertine.

The most renowned petrifying springs are those of the Auvergne region of France, a volcanic district where several springs deposit copious amounts of travertine. Among them are the waters of St Alyre, St. Nectaire and Mont Doré. The Grotte de Perou, St. Alyre at Clermont-Ferrand is one of the best known. The springs, rising from faulted granite, are guided by pipes into enclosures, one of which is a natural cave, where the waters, at 22 °C, cascade over a series of wooden shelves, called *echelles* upon which the objects are placed (Photoplate 22B). The articles, usually mass-produced casts of porcelain, are kept on the echelles for several months, when they become encrusted with a pure white crystalline travertine. Up to 30 shelves, about 30 cm apart may be placed in each echelle, and the objects are turned by hand every few days to ensure an even coating. Another, more sophisticated technique is also practiced, namely the production of high quality bas-relief casts. An original bas-relief, hammered or cut into copper plate is first produced and carefully cleaned and polished. The work, which rarely exceeds 20 x 20 cm, is placed face-up in an open metal box, and hot gutta-percha poured on top then left to set. Once cool, the reverse mould is pulled away and placed on the echelle, care being taken to ensure that the first layer of travertine is fine grained and even. For this, the mould is first placed only in spray at the base of the echelle, where the rate of deposition is least. Once a complete layer has formed, the mould is moved further up the echelle, where deposition is more rapid and the calcite crystals are more coarse, to provide strength to the backing. Deposition rates at the top of the echelle approach 10 cm a^{-1}. The moulds are left for a total of 12–18 months until 1–2 cm of travertine has accumulated, spending most of their time near the echelle base. By this time, the mould is completely encrusted and is then split to reveal the gutta-percha base. This is removed by warming the mould to 80 °C so that the base can be safely pulled away, leaving a detailed cast. The casts are usually framed and sold for considerable sums of money. The example illustrated in Photoplate 22E was sold for F350 ($60) in 1989. The casts are sometimes provided

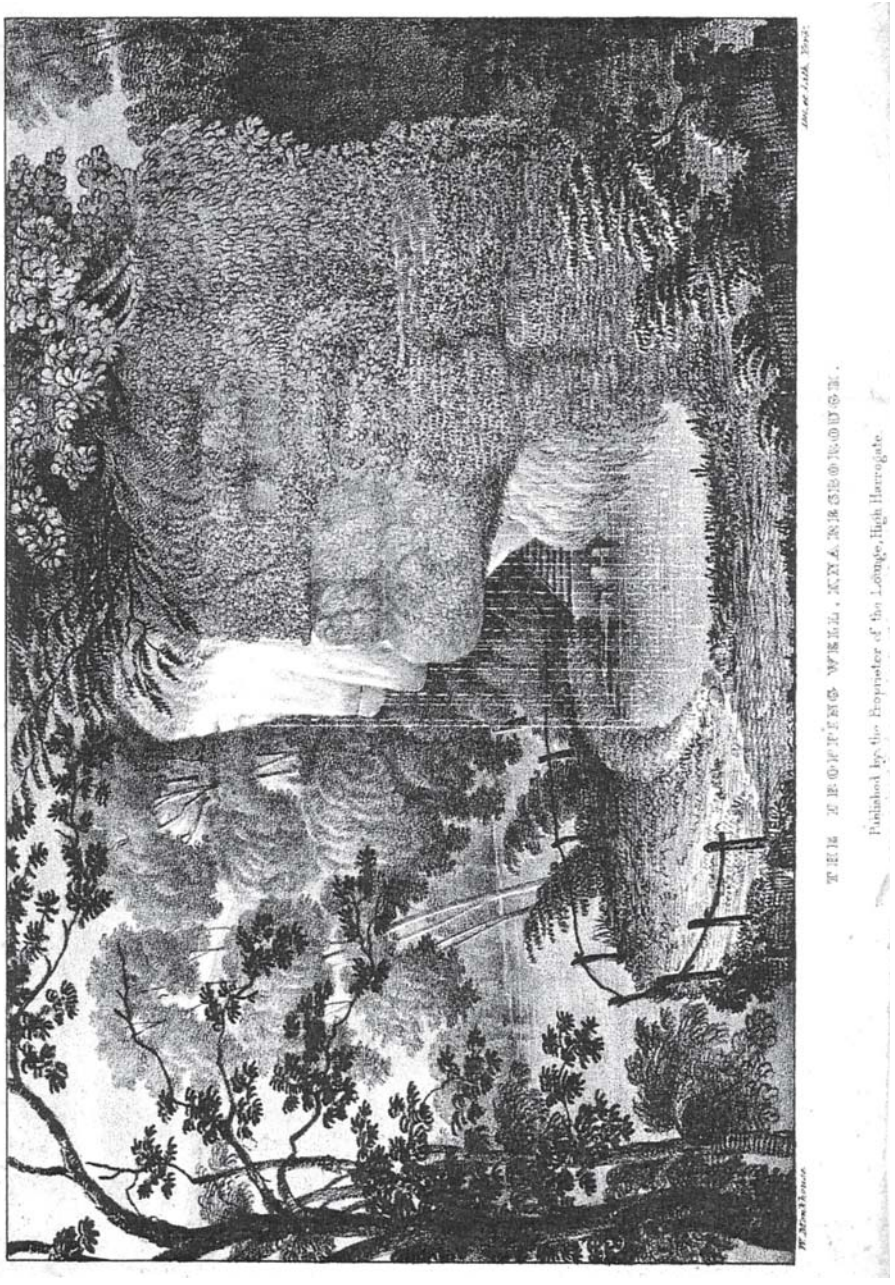

Fig. 101. A 19th Century print of the Dropping Well, a 'petrifying spring' by the River Nidd at Knaresborough, Yorkshire

with a back-light, since the crust is translucent. This technique has been used at St Alyre since the beginning of the 19th Century and still being refined. These petrifying springs are managed as small family businesses, in some cases, being handed down through several generations. Within recent years, the bas relief technique has been extended to produce cameos, utilising the finest water spray to initiate the encrustation. The spring water at St Alyre is low in oxygen and contains ~0.2 mmol L^{-1} ferrous iron. This is rapidly oxidised and deposited as ochre with the travertine, giving it a deep red colour. To form the sparkling white petrifactions such as the bird illustrated in Photoplate 22C, the iron is first removed by running the water along a channel of gentle gradient above the echelles. The iron precipitates before the travertine and is collected on deal shavings placed in the channel. To provide an ivory tint to the bas-reliefs, some of the spring water is diverted from the channel to allow some iron incorporation until the desired hue is reached. In the garden surrounding St Alyre may be found life-size 'petrifactions' of local village folk and animals. The latter had been stuffed prior to encrustation, but it is hoped that the same fate did not befall the villagers. A lion, on show at the Blaise Pascal spring, took 15 years to encrust, and weighs almost one tonne. Buckland (1883) also reports on the encrustation of stuffed animals at Knaresborough, UK. At all of the sites so far mentioned, the mineral deposited is calcite, and in the thermogene deposits of the Auvergne, the calcite rhombs exceed 150 μm across in the coarse encrustations. At the top of the echelles, the rhombic habit is well developed, but crystals, while remaining large, become increasingly anhedral lower down where the deposits have a reduced porosity.

The hot springs at Carslbad, Czech Republic, and Mammoth, Wyoming deposit aragonite and at both, petrifactions have been made and sold. This has long ceased at Mammoth (Weed 1889a) but continues as Carlsbad, where colourful effects are obtained by retaining the precipitated ocher (Photoplate 3D). Commercial petrifaction is also performed in other countries. At Bagni San Fillipo, Italy, travertine medallions were produced for many years. Raspé (1770) and Gosse (1820) observed that the water was led along channels to a series of pits containing wooden frames. The reverse moulds were made of plaster, sulphur or glass rubbed with soap, the latter being preferred. An unusual variant was the production of reverse prints. These were made by rubbing printing-ink into metal engravings and suspending them in the water. The flat travertine casts were pulled away revealing the ink impression on a white background. Reverse moulds of sulphur and glass proved less satisfactory than the guttapercha that was introduced in the Auvergne around 1830.

In China, Chang (1927) noted that grass and twigs were sometimes placed in travertine-depositing waters, and once consolidated, was used as a building material for a temple in Beijing. Some of the hot springs of Hokkaido, Japan are also used to petrify objects for souvenirs (Y. Kitano, *pers. comm.*). In Peru, Buckland (1883) noted the use of moulds for the production of travertine church ornaments in Lima.

Over the past century, the Navajo Indians have developed a metal-casting technique called 'channel work' using travertine molds. Small blocks of travertine are cut from stream beds and split into two flat slabs. The artwork is then drawn onto one of the smooth faces and chiselled out to make the mold and runner. The mold is closed with the second slab and molten silver introduced to form an attractive flat-backed casting (Untracht 1975).

Travertine-depositing springs have long been revered and used as ritualistic sites, though perhaps more for their gaseous exhalations than the rock itself. For example, the famous Oracle of Delphi has associated travertines (De Boer et al. 2001). At the Plutonium of Hierapolis CO_2 exhalations were guided into a structure under the temple (Bean 1971). In Australia, aboriginal artefacts have been found associated with mound springs and they are noted as important in aboriginal mythology (Ponder 1986).

17.4.4 Graphic Art and Tourism

The earliest known use of travertine in art occurs high on the Tibetan Plateau, near Lhasa, where a series of hand and foot impressions have been discovered associated with a fireplace at a thermogene site at 4200 m altitude (Zhang and Li 2002). The impressions have been dated using optically stimulated luminescence to about 20 Ka, near the height of the glacial maximum (Fig. 102). The impressions were made in a soft travertine mud which subsequently hardened, and appear to have been made deliberately. The prints are produced apparently at random, but the makers may have been aware that the impressions would harden in time.

Deposits of travertine have been drawn, painted and photographed on numerous occasions. Cascades in particular frequently appeal to the landscape artist, though speleothems have also been depicted. The falls at Tivoli and Marmore in Italy were often celebrated and many paintings and prints are in existence. Good examples may be found by Antoine Joinville (1801–1849) and Simon Denis (1755–1812). Often their inclusion is fortuitous as a backdrop to masses of white tumbling water. One of the many British examples is Gordale, Yorkshire. It was painted between 1811–1815 by the British artist James Ward (1769–1859) and can be seen at the Tate Gallery, London. As sites of curiosity, several petrifying springs have been illustrated such as Knaresborough in the UK (Fig. 101). Other famous attractions include the Plitvice Lakes, Croatia, Pamukkale, Turkey and Mammoth Hot Springs, Wyoming. In China, the travertine dams and turquoise lakes of Huanglong and Juizhaigou rate as some of most colourful natural landscapes on Earth. The tower karst islands of Phangnga, with their impressive overhanging remora in southern Thailand have long been photographed by tourists and made famous in the West after providing backdrops to the James Bond film *Man with the Golden Gun* (1974, Saltzman, Broccoli). Dunn's River Falls in Jamaica is likewise well known after its appearance in the Bond film *Dr. No* (1962, Saltzman, Broccoli). Pamukkale is one of the four top tourist attractions in Turkey and travertine deposition is carefully managed to maintain their dazzling appearance. The travertine bridges of the Taurus Mountains are considered by Bayari (2002) as a national heritage. Mention should also be made of travertine

Fig. 102.
Hand and foot impressions in a Tibetan travertine. From Zhang and Li (2002) reproduced with permission from the American Geophysical Union. Published 2002 by the American Geophysical Union

tourist caves such as the Olgahöhle, Germany, and that at Lillafured, Hungary. In fact the earliest known depiction of travertine is as speleothem in a bronze relief on the palace gates of Shalmaneser III, King of Assyria dated to c. 852 B.C. (Shaw 1997). Paillet (1986) describes medieval graffiti from the travertine walls of the chapel at St. Hilaire d'Ozilhan, St. Étienne. They include a number of animals and mounted horsemen dating around A.D. 1150.

Caves have long attracted visitors, much of the interest directed towards the formations contained within them. The number of 'show' and tourist caves is too large to detail here, but a good account can be found in Hill and Forti (1997). They list the 'top ten' caves for mineralogy. The most outstanding is Blue Cave of the Massif Central, France, but this is not a tourist cave.

17.5 Agriculture and Industry

Clastic travertines have occasionally been exploited as a source of agricultural lime for spreading on calcium-poor soils. An early English account is given by Vancouver (1810), where deposits were dug on a large scale in the south of England. Some travertines are still worked for this purpose as at Caerwys in Wales. In the United States, large-scale excavations were made from the late 19th to mid 20th Century in several parts of Virginia, where over a million tonnes was removed (Giannini 1990; Sweet and Hubbard 1990). These operations have now ceased, partly due to environmental concerns. Heavy industrial use has been very limited.

Deposits have often been calcined for slaked lime. In India, Chowdhury (1945) described kilns where hand-quarried travertine was layered with wood or coal and burnt for about a day. The lime was used to make bleaching powder or in paper mills. Travertines have been calcined in parts of Africa where sources of limestone are scarce. In Uganda, small deposits along Lake George are exploited in a region otherwise destitute of carbonate rocks (Barnes 1956). In England, lime burning has been practiced widely. Clastic travertines were favoured as they yield both a high $CaCO_3$ content and are easily exploited. At Cwm Nash, Wales, the valley deposits were quarried next to the sea and burnt *in situ* though nothing remains of the kilns today. Travertine as a source of lime has been documented at Falls Hollow, Virginia (Sweet and Hubbard 1990), in Brazil (Branner 1911) and South Africa (Vogel and Partridge 1983). Clastic deposits are normally preferred due to their ease of extraction, but their purity is usually inferior to autochthnonus accumulations such as those quarried in South Africa. In the UK, clastic deposits have occasionally been burnt for lime, as at Mealy Bank, Ingleton, where the kilns may still be seen, but this was a small local industry and there appears to be little use of them today. In Germany, Schmid (1972) notes the former use of travertine lime in plaster. In Denmark, it has been mined and used as an asphalt filler (Nielsen 1965).

Sweet and Hubbard (1990) consider travertine of little value as a desulphurisation base. It was once used locally as a flux for the smelting of both iron (Sweet and Hubbard 1990) and copper (Feth and Barnes 1979). Low-grade travertines are also quarried for road metal in Algeria and elsewhere. An unusual use is found in the extensive network of self-built channels at Pamukkale, Turkey, where the rapid deposition of travertine was exploited to provide a distribution system for irrigation water (Bean 1971; Altunel and Hancock 1993). The canals delivered water from the thermal springs on the hillside to the fields below the travertine mound, a distance of about 1 km (Photoplate 1B). The irrigation system shows numerous bifurcations and may also have served as a water distribution system for parts of the City of Hierapolis. They are probably contemporaneous with the city that flourished around A.D. 200. An earlier series of self-built canals is known from Hierve al Agua, Mexico where a travertine mound has been terraced and occupied since 700 B.C. (Caran et al. 1995).

17.6 Medicinal

Carbonate muds precipitating on the travertine mound at Bagnaccio, Italy are believed to possess healing properties by the local populace who use them as baths to heal skin ailments such as sores, minor cuts and rashes. These deposits are likely to be mildly antiseptic as they contain traces of sulphur. According to Rutty (1757), the 'petrifying' waters of Newnham Regis, Warwickshire, were taken as a diuretic and another at Newton Dale was used for curing distorted joints. Apparently, such waters were also sought by farmers to cure cattle of dysentery. At Carlsbad, de Boodt (1609) states that the

> dropstone … at the Caroline Baths is praised by surgeons for strengthening broken bones, where it has obtained the name of *Osteocolla* (bone-sticker) … the powder is drunk … and causes a powerful sweat.

Hot baths of travertine-depositing water are used worldwide, e.g. Carlsbad, Czech Republic; Saturnia, Bagni di Tivoli (Italy) and Masutomi (Japan) but the high levels of Ca and CO_2 do not appear to be specifically sought, and lead to serious lathering and scaling problems. There is also an extensive literature on the use of crushed speleothem in ritual, medicine and cosmetics (Shaw 1997). People have also made use of travertine in less obvious ways. In the Great Artesian Basin of Australia, local aboriginal tribes used travertine mounds as look-outs (Lampert 1989). The deposits often form natural barriers which may have proved useful in defence, and travertine sites often show signs of human occupation as discussed previously.

17.7 Economics and Tonnage

The price of travertine varies according to its use and availability. Loose, clastic forms have always been the cheapest. Vancouver (1810) recorded a price of two shillings (£0.1) per tonne for English agricultural grade. In the United States, Sweet and Hubbard (1990) quote $3 per tonne for similar crushed material in the mid 1940s, with quarrymen's wages of $0.9–2.5 per day. For flux grade travertine, the price was $0.25 per tonne in the early 1900s, rising to $0.93 in 1936, soon after which production ceased. Rockery grade travertine has always been more expensive owing to its relative scarcity and demand. In 1887 blocks quarried at Monsal Dale, UK were delivered to a nearby town for 16 s (£0.8) per tonne. In 1993, similar material sold for £3.00 or more per tonne in garden shops. Travertine blocks for building in Germany were sold at DM 85 ($38) per cubic metre in 1919 (Schmid 1972), and in 1972, the equivalent cost, for 1 x 1 x 0.04 m slabs was DM 1250 ($5600) per cubic metre. In 1992, Italian travertine 'marble', imported to the UK cost around £38 ($60) for polished slabs measuring 1 x 1 x 0.035 m, equivalent to £1080 ($1700) per cubic metre. In comparison, good quality marbles were priced at £45–100 per slab (Tiranti Ltd. UK). The price in 2004 is only slightly higher, but specially prepared surfaces are more expensive and may cost up to £50 per square metre.

Most of the travertine currently used in the UK is trucked direct from the Italian quarries, but increasingly it is sought from North Africa, Iran and Turkey. Numerous varieties are available and are traded under names such as 'Antico' or 'Classico'. In 1990, about 1000 tonnes was imported annually from Italy but this figure has been steadily increasing. Travertine is a valuable industry in Italy. For example, in 1934 64,950 tonnes was quarried, 69% of which came from Tivoli. In Turkey huge reserves are known and it is a major export material. Currently, (2004) huge quantities are quarried in over 25 countries, much of it going to the United States, Western Europe and the Middle East. In 2003, imports of cut travertine slab amounted to 6.5×10^6 m^2 and came mainly from Italy, Mexico and Turkey (Techstone.it website). Its use is likely to increase further as developing countries enlarge and improve their cities.

References

Abbott, A. (1999): 'Battle lines drawn between 'nanobacteria' researchers', *Nature*, 401, 105

Abell, P.I., Awramik, S.M., Osborne, R.H. and Tomellini, S. (1982): 'Plio-Pleistocene lacustrine stromatolites from Lake Turkana, Kenya: morphology, stratigraphy and stable isotopes', *Sed. Geol.,* 32, 1–26

Adams, C.S. and Swinnerton, A.C. (1937): 'The solubility of limestone', *Trans. Am. geophys. Un.,* 11, 504–508

Adolphe, J.P. and Rofes, G. (1973): 'Les concrétionnements calcaires de la Levriere', *Bull. Ass. Fr. Étude Quaternaire,* 35, 79–87

Adolphe, J.P. and Billy, C. (1974): 'Biosynthese de calcite par une association bactérienne aérobie', *C.R. Acad. Sci. Paris*, *Ser. D.,* 278, 2873–2875.

Adolphe, J.P., Hafchahinet, T., Lang, J. and Lucas, G. (1976): 'Sur le présence de concretions algaires dans les formations lacustres de la region de Zahle (Libon)', *Bull. Soc. Geol. Fr.,* 17, 701–710

Agardh, C.A. (1827): 'Aufzählung einer in den Österreichischen Ländern gefundenen neuen Gattung und Arten von Algen, nebst ihrer Diagnostik und beifügten Bemerkungen', *Flora*, 10, 625–640

Agricola, G. (1546): *De Natura Fossilium Libri VII*. Germany

Ahmamou, M., Conrad, G. and Plaziat, J. –Cl. (1989): 'Réinterpretation des conditions de dépôt des calcaires fluviatiles lacustres et palustres du bassin plio-quaternaire du Saiss de Fès (Maroc)', *Mediterranée,* 2, 41–49

Akdim, B., Desrochers, A. and Geurts, M. –A. (1994): 'Morphogenèse et pétrogenèse des travertins hydrothermaux de Skoura au Maroc méridional', *Z. Geomorph. N.F.,* 38, 355–372

Alexandrowicz, S.W. (1988a): 'The stratigraphy and malacofauna of the Holocene sediments of the Pradnik River valley', *Bull. Pol. Acad. Sci. Earth Sci.*, 36, 109–120

Alexandrowicz, S.W. (1988b): 'Cones of calcareous tufas in national parks of Tatra Mountains and Pieniny Mountains', *Ochr. Przyr.*, 46, 361–382

Ali A.A., Terral, J.-F., Guendon, J.-L., Roiron, P. (2003): 'Holocene palaeoenvironmental changes in southern France: a palaeobotanical study of travertine at St-Antonin, Bouches-du-Rhöne', *The Holocene*, 13, 293–298

Allard, P. (1988): 'Carbon and helium isotopic constraints on the origin of volcanic carbon from subduction zones', *Chem. Geol.,* 70, 36

Allen, C.C. and others (2000): 'Microscopic physical biomarkers in carbonate hot springs: implications in the search of life on Mars', *Icarus*, 147, 49–67

Allen, E.T. (1934): 'The agency of algae in the deposition of travertine and silica from thermal waters', *Am. J. Sci.*, 28, 373–389

Allen, E.T. and Day, A.L. (1935): 'Hot springs of Yellowstone National Park', *Carnegie Institute of Washington. Publication* 466, 1–525. Washington D.C

Allen, T.F.M. (1971): 'Multivariate approaches to the ecology of algae on terrestrial rock surfaces in North Wales', *J. Ecol.*, 59, 803–826

Alonso-Zarza, A.M. (2003): 'Palaeoenvironmental significance of palustrine carbonates and calcretes in the geological record', *Earth Sci. Revs.*, 60, 261–98

Altunel, E. and Hancock, P.L. (1993): 'Morphology and structural setting of Quaternary travertines at Pamukkale, Turkey', *Geol. J.,* 28, 335–346

Ambert, P. and Tavoso, A. (1981): 'Les formations quaternaires de la vallée du Tarn entre Millau et Saint-Rome de Tarn', *Paleobiologie-Continentale,* 12, 185–193

Ambert, P., Guendon, J.L. and Quinif, Y. (1989): 'Découverte d'un site du Paleolithique inferieur dans les Grands Causses (Creissels-Aveyron); contexte géologique et chronologique', *C.R. Acad. Sci. Ser. 2., Mec. Phys. Chim.*, 308, 63–69

Amundson, R. and Kelly, E. (1987): 'The chemistry and mineralogy of a CO_2-rich travertine depositing spring in the California Coast Range', *Geochim. Cosmochim. Acta,* 51, 2883–2890

Anadón, P. and Zamarreño, I. (1981): 'Paleogene nonmarine algal deposits of the Ebro basin, northeastern Spain', 140–154, in: Monty, C.L.V. (ed.), *Phanerozoic Stromatolites*, Berlin, (Springer-Verlag)

Andrews, J.E., Riding, R. and Dennis, P.F. (1997a): 'The stable isotope record of environmental and climatic signals in modern terrestrial microbial carbonates from Europe', *Palaeogeogr. Palaeoclim. Palaeoecol.,* 129, 171–189

Andrews, J.E., Gare, S.G. and Dennis, P.F. (1997b): 'Unusual isotopic phenomena in Welsh quarry water and carbonate crusts', *Terra Nova,* 9, 67–70

Andrews, J.E., Pedley, H.M. and Dennis, P.F. (1994): 'Stable isotope record of palaeoclimatic change in a British Holocene tufa', *The Holocene*, 4, 349–355

Andrews, J.E., Pedley, M. and Dennis, P.F. (2000): 'Palaeoenvironmental records in Holocene Spanish tufas: a stable isotope approach in search of reliable climatic archives', *Sedimentology,* 47, 961–978

Andrews, J.E., Greenaway, A.M., Dennis, P.F. and Barnes-Leslie, D.A. (2001): 'Isotopic effects on inorganic carbon in a tropical river caused by caustic discharges from bauxite processing', *Appl. Geochem.*, 16, 197–206

Anon (2003): 'Non-chemical water treatment technologies for cooling towers', Nelson Environmental Technologies Inc., http://neslonenvironmentaltechnologies.com/ACTWTechnicalpaper.html

Arana, R., López-Aguayo, F., Velilla, N. and Rodríguez Gallego, M. (1979): 'Mineralizaciones de hierro en el travertino de Lanjarón (Granada)', *Acta Geol. Hisp.,* 14, 106–112

Arenas, C., Gutiérrez, F., Osácar, C. and Sancho, C. (2000): 'Sedimentology and geochemistry of fluvio-lacustrine tufa deposits controlled by evaporite solution subsidence in the central Ebro Depression, NE Spain', *Sedimentology*, 47, 883–909

Arp, G., Hofmann, J. and Reitner, J. (1998): 'Microbial fabric formation in spring mounds ("microbialites") of alkaline salt lakes in the Badain Jaran Sand Sea, PR China', *Palaios*, 13, 581–592

Arp, G., Wedemeyer, N. and Reitner, J. (2001): 'Fluvial tufa formation in a hard-water creek (Deinschwanger Bach, Franconian Alb, Germany)', *Facies*, 44, 1–22

Atkinson, T.C. and Smith, D.I. (1976): 'The erosion of limestones', 151–177, in: T.F. Ford, C.H.D. Cullingford (eds), *The Science of Speleology*, London (Academic Press)

Auler, A.S. and Smart, P.L. (2001): 'Late Quaternary paleoclimate in semiarid northeastern Brazil from U-series dating of travertine and water-table speleothems', *Quat. Res.,* 55, 159–167

Aydar, C. and Dumont, J.F. (1979): 'Observations sur images Landsat d'alignements dans les travertins d'Antalya; discussion des relations probables entre neotectonique et hydrogeologique', *Bull. Min. Res. Explor. Inst. Ankara,* 92, 81–84

Baier, J.J. (1708): *Oryctographia Norica*, W. Michael (Nürnberg)

Bajaranus, M. (1924): 'Rezente Chironomidentuffe', *Arch. Hydrobiol.*, 14, 404

Baker, A. and Simms, M.J. (1998): 'Active deposition of calcareous tufa in Wessex, UK, and its implications for the 'late Holocene tufa decline', *The Holocene*, 8, 359–365

Baker, A., Smart, P.L. and Ford, D.C. (1993): 'Northwest European palaeoclimate as indicated by growth frequency variations of secondary calcite deposits', *Palaeogeogr. Palaeoclim. Palaeoecol.*, 100, 291–301

Baker, A., Ito, E., Smart, P.L. and Ewan, R.F. (1997): 'Elevated and variable values of ^{13}C in speleothems in a British cave system', *Chem Geol.*, 136, 263–270

Baker, A., Genty, D., Dreybrodt, W., Barnes, W.L., Mockler, N.J. and Grapes, J. (1998): 'Testing theoretically predicted stalagmite growth rate with Recent annually laminated samples: Implications for past stalagmite deposition', *Geochim. Cosmochim. Acta*, 62, 393–404

Balazs, D. (1977): 'The geographic distribution of karst areas', 13–15, in: T.D.Ford (ed.), *Proc. 7th Internat. Speleological Congress*, Sheffield, UK

Ballentine, C.J., O'nions, R.K., Oxburgh, E.R., Horvath, F. and Deak, J. (1991): 'Rare gas constraints on hydrocarbon accumulation, crustal degassing and groundwater flow in the Pannonian Basin', *Earth Planet Sci. Lett.,* 105, 229–246

Barbieri, M., Masi, U. and Tolomeo, L. (1979): 'Origin and distribution of strontium in the travertines of Latium (Central Italy)', *Chem. Geol.,* 24, 181–188

Barbour, G.B. (1930): 'The origin of the Niangtzekuan tufa', *Bull. Soc. Geol. China*, 9, 213

Bargar, K.E. (1978): 'Geology and thermal history of Mammoth Hot Springs, Yellowstone National Park, Wyoming', *U.S. Geol. Surv. Bull.,* 1444, 1–55

Barker, R. (1785): 'An account of a stag's head and horns, found at Alport, in the parish of Youlgreave, in the county of Derby', *Phil. Trans. R. Soc.,* 75, 353–355

Bar-Matthews, M., Ayalon, A., Matthews, A., Sass, E. and Halicz, L. (1996): 'Carbon and oxygen isotope study of the active water-carbonate system in a karstic Mediterranean cave: implications for paleoclimatic research in semiarid regions', *Geochim. Cosmochim. Acta,* 60, 337–347

Barnes, I. (1965): 'Geochemistry of Birch Creek, Inyo Co., California; a travertine-depositing creek in an arid climate', *Geochim. Cosmochim. Acta*, 29, 85–112

Barnes, I. and O'Neil, J.R. (1969): 'The relationship between fluids in some fresh alpine-type ultramafics and possible modern serpentinization; Western United States', *Geol. Soc. Am. Bull.,* 80, 1947–1960
Barnes, I. and O'Neil, J.R. (1971): 'Calcium-magnesium solid solutions from Holocene conglomerate cements and travertines in the Coast Range of California', *Geochim. Cosmochim. Acta,* 35, 699–717
Barnes, I., O'Neil, J.R., Rapp, J.B. and White, D.E. (1973): Silica-carbonate alteration of serpentine: Wall rock alternation of mercury deposits of the California Coast Ranges', *Econ. Geol.,* 68, 388–398
Barnes, I., Presser, T.S., Saines, M., Dickson, P. and Koster van Groos, A.F. (1982): 'Geochemistry of highly basic calcium hydroxide groundwater in Jordan', *Chem. Geol*., 35, 147–154
Barnes, I., Irwin, W.P. and White, D.E. (1984): 'Map showing world distribution of carbon dioxide springs and major zones of seismicity'. *U.S. Geological Survey Department of the Interior. Miscellaneous Investigations Series*. Map I-1528
Barnes, J.W. (1956): 'Pleistocene limestones of Lake George, Toro', *Uganda Geol. Surv. Rec.*, (for 1956), 55–59
Baron, M., Pentecost, A. and Parnell, J. (2003): 'Hot and cold spring deposits as a source of palaeo-fluid samples on Mars', *http://www.lpi.usra.edu/meetings/lpsc2003/a-f.html*
Bates, R.L. and Jackson, J.A. (1987): '*Glossary of Geology*', 3rd Ed., Alexandria, Va. (American Geological Institute)
Bathurst, R.G.C. (1954): 'First report of the committee on the Caerwys Tufa'. *Liverpool Manch. Geol. J.*, 1, 24–28
Bathurst, R.G.C. (1976): Carbonate Sediments and their Diagenesis,Developments in Sedimentology, 12, 658 pp., Amsterdam, (Elsevier)
Battistini, R. (1981): 'Le morphogénèse des plateforms de corrosion littorale dans les grês calcaires', *Rev. Geomorph. Dynamique,* 30, 81–94
Bayari, C.S. (2002): 'A rare landform: Yerköprü travertine bridges in the Taurids Karst Range, Turkey', *Earth Surface Processes Landf.,* 27, 577–590
Bayari, C.S. and Kurttas, T. (1997): 'Algae: an important agent in deposition of karstic travertines: observations on natural-bridge Yerköprü travertines, Aladaglar, Eastern Taurids, Turkey', 269–280, in: G. Gunay, A.I. Johnson, (eds), *Karst Waters and Environmental Impacts,* Rotterdam. (Balkema)
Beadle, L.C. (1974): '*The Inland Waters of Tropical Africa*', London (Longman)
Bean, G.E. (1971): *Turkey Beyond the Maeander, an Archaeological Guide.* 262 pp., London (Ernest Benn Ltd.)
Becker, G.F. (1888): 'The quicksilver deposits of the Pacific Coast', *Monogr. U.S. Geol. Surv.,* 13, 341–351
Beier, J.A. (1985): 'Diagenesis of Quaternary Bahamian beachrock: petrographic and isotopic evidence', *J. Sed. Petrol.*, 55, 755–761
Bell, P.R. and Lodge, E. (1963): 'The reliability of *Cratoneuron commutatum* (Hedw.) Roth. as an indicator moss', *J. Ecol.*, 51, 113–122
Bellinzoni, A.M., Caneva, G. and Ricci, S. (2003): 'Ecological trends in travertine colonisation by pioneer algae and plant communities', *Int. Biodet. Biodegr.,* 51, 203–210
Benson, L.V. (1978): 'Fluctuation in the level of the pluvial Lake Lahontan during the last 40,000 years', *Quat. Res.*, 9, 300–318
Benson, L.V. and Thompson, R.S. (1987): 'Lake-level variation in the Lahontan Basin for the past 50,000 years', *Quat. Res.*, 28, 69–85
Bernasconi, A., Glover, N. and Viljoen, R.P. (1980): 'The geology and geochemistry of the Senator antimony deposit, Turkey', *Miner. Deposita,* 15, 259–274
Berner, L. (1949): 'Biologies muscinées hygrophiles en Provence', *Rev. Bryol. Lichénol.*, 18, 59–65
Berthoud, R. (1987): '*The Life of Henry Moore*', 465 pp., London (Faber and Faber)
Bertrand, A. (1950): 'Les tufs à Chironomides des Pyrénées', *L'Entomoligiste*, 6, 13–18
Bertrand-Sarfati, J., Freytet, P. and Plaziat, J. –C. (1966): 'Les calcaires concrétionnés de la limite Oligocène-Miocene des environs de Saint-Pourcain-sur-Sioule: rôle des algues dans leur édification; analogue avec les stromatolithes et rapports avec la sedimentation', *Bull. Soc. Geol. Fr.*, 8, 652–662
Bertsch, K. (1927): 'Die diluviale Flora des Cannstatter Sauerwasserkalks', *Z. Botanik*, 19, 641–659
Beveridge, T.J. (1989): 'Role of cellular design in bacterial metal accumulation and mineralization', *Ann. Rev. Microbiol.,*43, 147–171
Bhaya, D., Schwarz, R. and Grossman, A.R. (2000): 'Molecular responses to environmental stress', 397–422, in: B.A. Whitton, M. Potts, (eds), *The Ecology of Cyanobacteria*, Dordrecht (Kluwer)
Bigazzi, G. and Rinaldi, G.F. (1973): 'Variazionii del contenuto di uranio nei sedimenti carbonatici di precipitazione chimica; possibili implicationi paleoclimatiche', *Atti. Mem. Soc. Tosc. Sci. Nat., Ser. A.,* 80, 233–243
Billings, W.D., Peterson, K.M., Shaver, G.R. and Trent, A.W. (1977): 'Root growth, respiration, and carbon dioxide evolution in a tundra soil', *Arct. Alp. Res.,* 9, 129–137
Billy, C. (1975): 'Isolement des constituants d'une bactérienne productrice de calcite', *C.R. Acad. Sci. Paris*, 281, 621–623

Binkley, K.L., Wilkinson, B.H. and Owen, R.M. (1980): 'Vadose beachrock cementation along a southeastern Michigan marl lake', *J. Sed. Petrol.,* 50, 953–962
Bischoff, J.L., Stine, S., Rosenbauer, R.J., Fitzpatrick, J.A. and Stafford Jr, T.W. (1993): 'Ikaite precipitation by mixing shoreline springs and lake water, Mono Lake, California, USA', *Geochim. Cosmochim. Acta,* 57, 3855–3865
Bishop, J.L., Murad, E., Lane, M.D. and Mancinelli, R.L. (2004): 'Multiple techniques for mineral identification on Mars: a study of hydrothermal rocks as potential analogues for astrobiology sites on Mars', *Icarus*, 169, 311–323
Black, J. (1757): Experiments upon magnesia alba, quicklime, and other alkaline substances. Edinburgh
Blackwell, B. and Schwarcz, H.P. (1986): 'U-series analyses of the lower travertine at Ehringsdorf, East Germany', *Quat. Res.*, 25, 215–222
Blake, D.M. (1947): 'Ancient Roman construction in Italy from the Prehistoric Period to Augustus', 421 pp., *Carnegie Institute of Washington,* Publication 570
Blake, D.M. (1959): 'Ancient Roman construction in Italy from Tiberias through the Flavians', 195 pp., *Carnegie Institute of Washington,* Publication 616
Blanchard, R. (1903): 'Observations sur la faune des eaux chaudes', *Soc. Biol. Paris C.r.*, 55, 947–950
Blaszac, M. (1972): 'Calcites in karst formations in the Czestochowa region', *Kwart. Geol.*, 16, 909–922
Blinn, D.W. and Sanderson, M.W. (1989): 'Aquatic insects in Montezuma Well, Arizona, USA: a travertine spring mound with high alkalinity and dissolved carbon dioxide', *Great Basin Nat.*, 49, 85–88
Blot, P. (1986): 'La tufologie, un nouveau domain d'études pour le domain continental'. *C.R. Congres-National Soc. savantes., Sci.,* 111, 199–210
Blum, J.L. (1957): 'An ecological study of the algae of the Saline River, Michigan', *Hydrobiologia*, 9, 361–408
Bogli, A. (1980): '*Karst Hydrology and Physical Speleology*', 284 pp., Berlin (Springer-Verlag)
Boni, C., Bono, P., Calderoni, G., Lombardi, S. and Turi, B. (1980): 'Indagine idrogeologica e geochimica sui rapporti tra ciclo carsico e circuito idrotermale nella Pianura Pontina (Lazio Meridionale)', *Geologia Applic. Idrogeol.*, 15, 203–247
Bono, P., Dreybrodt, W., Ercole, S., Percopo, C. and Vosbeck, K. (2001): 'Inorganic calcite precipitation in Tartare karstic spring (Lazio, central Italy): field measurements and theoretical prediction on depositional rates', *Environmental Geol.*, 41, 305–313
Boone, D.R. and Castenholz, R.W. (2001) (eds): '*Bergey's Manual of Systematic Bacteriology*', Volume 1, 721 pp., Baltimore (Williams & Wilkins)
Boros, A. (1925): 'Two fossil species of mosses from the Diluvial lime tufa of Hungary', *Bryologist*, 28, 29–32
Bottinga, Y. (1968): 'Calculation of fractionation factors for carbon and oxygen isotopic exchange in the system calcite-carbon dioxide-water', *J. Phys. Chem.,* 72, 800–808
Bottinga, Y. (1969): 'Calculated fractionation factors for carbon and hydrogen and exchange in the system calcite-carbon dioxide-graphite-methane-hydrogen-water vapor', *Geochim. Cosmochim. Acta,* 33, 49–64
Boule, M.M. (1902): 'Long excursion to the Auvergne', *Proc. Geol. Assoc.,* 17, 275–280
Bourguet, L. (1742): '*Traité des Petrifactions*', Paris (Briasson)
Bouyx, E. and Pias, J. (1971): 'Signification geologique, pedologique et palaeoclimatique des travertins d'Awpar (Vallée de Ghandak, Afghanistan Centrale)', *C.r. hebd. Séanc. Acad. Sci. Paris D.*, 273, 2468–2471
Bowen, D.G., Hughes, S., Sykes, G.A. and Miller, G.H. (1989): 'Land-sea correlations in the Pleistocene based on isoleucine epimerization in the non-marine molluscs', *Nature*, 340, 49–51
Boyer, M.L.H. and Wheeler, B.D. (1989): 'Vegetation patterns in spring-fed calcareous fens: calcite precipitation and constraints on fertility', *J. Ecol.*, 77, 597–609
Bradley, W.H. (1924): 'Fossil caddis fly cases from the Green River Formation, Wyoming', *Am. J. Sci.*, 7, 310–312
Bradley, W.H. (1929): 'Algae reefs and oolites of the Green River Formation', *U.S. Geol. Surv. Prof. Paper*, 154G, 203–223
Bradley, W.H. (1964): 'Geology of the Green River Formation and associated Eocene rocks in south-western Wyoming and adjacent parts of Colorado and Utah', *U.S. Geol. Surv. Prof. Paper*, 496-A
Bradley, W.H. (1974): '*Oocardium* tufa from the Eocene Green River Formation', *J. Paleont.*, 48, 1289–1290
Brady, P.V. and House, W.A. (1995): 'Surface-controlled dissolution and growth of minerals', 225–306, in: P.V. Brady, P.V. (ed.), *Physics and Chemistry of Mineral Surfaces*, Boca Raton, New York (CRC Press)
Braithwaite, C.J.R. (1979): 'Textures of recent fluvial pisolites and laminated crystalline crusts in Dyfed', *J. Sed. Petrol,* 49, 181–193
Bramwell, D. and Shotton, F.W. (1982): 'Rodent remains from the caddis-bearing tufa of Elder Bush Cave', *Quaternary Newsletter*, 38, 7–13
Brancaccio,L., d'Argenio, B., Ferreri, V., Stanzione, D., Turi, B. and Preite, M.M. (1986): 'Caratteri tessiturale e geochemici dei travertini di Rochetta a Volturno (Molise)', *Boll. Soc. Geol. Ital.*, 105, 267–277

Branner, J.C. (1911): 'Aggraded limestone plains of the interior of Bahia and the climate changes suggested by them', *Bull. Geol. Soc. Am.,* 22, 187–206

Brewer, R. (1964): '*Fabric and Mineral Analysis of Soils*', 470 pp., New York (J. Wiley & Sons)

Brnek-Kostic, A. (1989): 'Plitvice Lakes: A product of the eternal life cycles of organic and inorganic matter', 15–27., in: J. Movcan, A. Niksic, (eds), *Plitvice National Park: The World Heritage,* Zagreb (Turistkomerc)

Brock, T.D. (1978): '*Thermophilic Organisms andLife at High Temperatures*', 465 pp., New York (Springer-Verlag)

Brook, G.A., Folkoff, M.E. and Box, E.O. (1983): 'A world model of soil carbon dioxide', *Earth Surface Processes Landf.,* 8, 79–88

Brotto, M. (1986): 'Karst de gypse et accumulations de tufs en Queyras', *Mediterranée*, 1–2, 118–125

Brunnacker, K., Hennig, G.J., Juvigne, E., Loehre, H., Urban, B. and Zeese, R. (1982): 'Der Kartstein Travertin in der nördlichen Westeifel', *Decheniana*, 135, 179–204

Brunnacker, M. and Brunnacker, K. (1959): 'Der Kalktuff von Egloffstein (nördliche Frankenalb)', *Geol. Blätter Nordöst-Bayern*, 9, 135–140

Brunskill, G.J. (1969): 'Fayetteville Green Lake, New York. II. Precipitation and sedimentation of calcite in a meromictic lake with laminated sediments', *Limnol. Oceanogr.*, 14, 830–847

Brykczynski, M. and Skompsi, S. (1979): 'Holocene molluscan fauna and calcareous sinter from Glowina near Dobrzyn on the Vistula', *Kwartalnik Geoloczny*, 23, 429–434

Buccino, G., D'Argenio, B., Ferreri, V., Brancaccio, L., Ferreri, M., Panichi, C. and Stanzione, D. (1978): 'I travertini della bassa valle del Tanagro (Campania): Studio geomorfologico, sedimentologico e geochimico', *Boll. Soc. Geol. Ital.,* 97, 617–646

Buch, L. von (1802–09): Observations géognostiques recueillies pendant un voyage en Allemagne et en Italie, 2 vol., Berlin

Buchbinder, B. (1981): 'Morphology, microfabric and origin of stromatolites of the Pleistocene precursor of the Dead Sea, Israel', 181–196, in: Monty, C.L.V., (ed.), *Phanerozoic Stromatolites*, Berlin (Springer-Verlag)

Buchbinder, B., Begin, Z.B. and Friedmann, G.M. (1974): 'Pleistocene algal tufa of Lake Lisan, Dead Sea area, Israel', *Israel J. Earth Sci.,* 23, 131–138

Buck, S.G. (1980): 'Stromatolite and ooid deposits within the fluvial and lacustrine sediments of the Precambrian Ventersdorp Supergroup of South Africa', *Precamb. Res.*, 12, 311–330

Buckland, F.T. (1893): '*Curiosities of Natural History*', Second series, 353 pp., London (R. Bentley & Son)

Buckland, W. (1846): 'On the occurrence of nodules (called petrified potatoes) found on the shores of Lough Neagh in Ireland, *Q.J. Geol. Soc.,* 2, 103–104

Buhmann, D. and Dreybrodt, W. (1987): 'Calcite dissolution kinetics in the system H_2O-CO_2-$CaCO_3$ with participation of foreign ions', *Chem. Geol.*, 64, 89–102

Bunting, B.T. and Christensen, L. (1980): 'Micromorphology of calcareous crusts from the Canadian High Arctic', *Geologiska Foren. Stock. Forh.*, 100, 361–367

Burger, D. (1990): 'The travertine complex of Antalya / Southwest Turkey'. *Z. Geomorph. N.F. Suppl. Bd. 77*, 25–46

Burns, S.J., Fleitmann, D., Matter, A., Neff, U. and Mangini, A. (2001): 'Speleothem evidence from Oman for continental pluvial events during interglacial periods', *Geology*, 29, 623–626

Busenberg, E. and Plummer, L.N. (1985): 'Kinetic and thermodynamic factors controlling the distribution of SO_4^{2-} and Na in calcites and selected aragonites', *Geochim. Cosmochim. Acta,* 49, 713–725

Butcher, R.W. (1946): 'Studies in the ecology of rivers, VI. The algal growth in certain highly calcareous streams', *J. Ecol.*, 33, 268–283

Butzer, K.W. and Hanesn, G.L. (1968): *Desert and River in Nubia: Geomorphology and Prehistoric Environments at the Aswan Reservoir*, 562 pp., Madison, Milwaukee & London (University of Wisconsin Press)

Butzer, K.W., Stuckenrath, R., Bruzewicz, A.J. and Helgren, D.M. (1978): 'Late Cenozoic paleoclimates of the Gaap Escarpment, Kalahari margin, South Africa', *Quaternary Res.*, 10, 310–339

Caboi, R., Cidu, R., Fanfani, L., Zuddas, P. and Zuddas, P.P. (1991): 'Geochemistry of the Funtana Maore travertines (Central Sardinia, Italy)', *Miner. Petrog. Acta*, 34, 77–93

Cacciamale, G.B. (1892): 'Geologia arpinate', *Boll. Soc. Geol. Ital.*, 11, 293–333

Cady, S.L. and Farmer, J.D. (1996): 'Fossilization processes in siliceous thermal springs: trends in preservation along thermal gradients', 150–173, in: G.R. Bock, J.A. Goode,(eds), *Evolution of Hydrothermal Ecosystems on Earth (and Mars?)*, Ciba Foundation, Chichester, UK (J. Wiley & Sons)

Cai, Y.J., Zhang, M.L., Peng, Z.C., Lin, Y.S., An, Z.S., Zhang, G.Z.H. and Cao, Y.N. (2001): 'The $\delta^{18}O$ variation of a stalagmite from Qixang Cave, Guizhou Province and indicated climatic change during the Holocene', *Chinese Sci. Bull.*, 46, 1904–1908

Cailleux, A. (1965): 'Quaternary secondary chemical deposition in France', *Bull. Geol. Soc. Am. Spec. Paper*, 84, 125–139

Caldwell, D.E., Kieft, T.L. and Brannan, D.K. (1984): 'Colonization of sulfide-oxygen interfaces on hot spring tufa by *Thiothrix thiopara*', *Geomicrobiol. J.,* 3, 181–200

Campbell, K.A., Sannazzaro, K., Rodgers, K.A., Herdianita, N.R. and Browne, P.R.L. (2001): 'Sedimentary facies and mineralogy of the Late Pleistocene Umukiri silica sinter, Taupo Volcanic Zone, New Zealand', *J. Sed. Res.,* 71, 727–746

Campbell, K.A., Rodgers, K.A. and Brotheridge, J.M.A. (2002): 'An unusual modern silica-carbonate sinter from Pavlova Spring, Ngatamariki, New Zealand', *Sedimentology*, 49, 835–854

Canet, C., Prol-Ledesma, R.M., Melgarejo, J.C. and Reyes, A. (2003): 'Methane-related carbonates formed at submarine hydrothermal springs: a new setting for microbially-derived carbonates?', *Mar. Geol.*, 199, 245–261

Caran, S.C., Winsborough, B.M., Neely, J.A. and Valastro, D. Jr. (1995): 'Radiocarbon age of carbonate sediments (travertine, pedoconcretions, and biogenic carbonates): A new method based on organic residues, employing stable isotope control of carbon sources', *Curr. Res. Pleist.*, 12, 75–77

Carlisle, D. (1983): 'Concentrations of uranium and vanadium in calcretes and gypcretes', 185–195, in: R.C.L. Wilson (ed.), *Geol. Soc. Lond. Special Publ.* 11, London (Geological Society)

Carozzi, A.V. (1962): 'Observations on algal biostromes in the Great Salt Lake, Utah', *J. Geol.,* 70, 246–252

Carr, M.H. (1996): '*Water on Mars*', New York (Oxford University Press)

Carrier, A.M. and Standish, M.L. (1995): 'Polymer mediated crystal habit modification', 63–72, in: Z. Amjad, (ed.), *Mineral Scale Formation and Inhibition*, New York (Plenum)

Carthew, K.D., Taylor, M.P. and Drysdale, R.N. (2002): 'Aquatic insect larval constructions in tropical freshwater limestone deposits (tufa): preservation of depositional environments', *Gen. Appl. Entomol.*, 31, 35–41

Carthew, K.D. and Drysdale, R.N. (2003): 'Late Holocene fluvial change in a tufa-depositing stream: Davys Creek, New South Wales, Australia', *Australian Geogr.*, 34, 123–139

Casanova, J. (1986): 'East African Rift stromatolites', 201–210, in: R.W. Frostick (ed.), *Sedimentation in the African Rifts.* Geological Society of London Special Publication 25. London (Geological Society)

Casanova, J. (1994): 'Stromatolites from the East African Rift: a synopsis', 193–226; in: J. Bertrand-Sarfati, C.L.V. Monty (eds), *Phanerozoic Stromatolites II*, Dordrecht (Kluwer)

Casanova, J. and Lafont, R. (1985): 'Les cyanophycées encroûtants du Var (France)', *Verh. Int. ver. Limnol.,* 22, 2805–2810

Casanova, J. and Hillaire-Marcel, C. (1992): 'Chronology and paleohydrology of Late Quaternary high lake levels in the Manyara Basin (Tanzania) from isotopic composition (^{18}O, ^{13}C, ^{14}C, Th/U) of fossil stromatolites', *Quat. Res.*, 38, 205–226

Casanova, J. and Tiercelin, J-J. (1982): 'Constructions stromatolitiques en milieu carbonaté sodique: les oncolites des plains inondables du lac Magadi (Kenya)', *C.R. Acad. Sci. Paris, Série II,* 295, 1139–1144

Castanier, S., Le Métayer-Levrel, G. and Perthuisot, J.-P. (2000): 'Bacterial Roles in the Precipitation of Carbonate Minerals', 32–39 in: R. Riding, S.M. Awramik (eds), *Microbial Sediments*, Berlin (Springer-Verlag

Castenholz, R.W. (1973): 'Ecology of blue-green algae in hot springs', 379–414, in: N.G. Carr, B.A. Whitton, (eds), *The Biology of Blue-green Algae*. Oxford (Blackwell)

Castenholz, R.W. (1989): 'Genus *Chloroflexus*', 1698–1703, in: J.T. Staley, M.P. Bryant, N. Pfenig, J.G. Holt (eds), *Bergey's Manual of Systematic Bacteriology*, Vol. 3, Baltimore (Williams and Wilkins)

Castenholz, R.W. (2002): 'Cyanobacteria', 473–599, 2nd Edn., in: D. Boone, R.W. Castenholz (eds), *Bergey's Manual of Systematic Bacteriology,* Vol. 1. Baltimore (Williams and Wilkins)

Cathelineau, M., Dubessy, J., Marignac, C., Valori, A., Gianelli, G. and Puxeddu, M. (1989): 'Pressure-temperature-fluid composition changes from magmatic to present day stages in the Lardarello geothermal field', 137–140, in: D.L. Miles (ed.). *Proc. International Symposium on Water-rock Interaction*, Rotterdam (Balkema)

Caudwell, C. (1987): 'Étude expérimentale de la formation de micrite et de sparite dans les stromatolites deau douce à *Rivularia*', *Bull. Soc. Geol. Fr.*, 8, 299–306

Caudwell, C., Lang, J. and Pascal, A. (2001): 'Lamination in swampy-rivulets *Rivularia haematites* stromatolites in a temperate climate', *Sediment. Geol.,* 143, 125–147

Cavendish, H. (1767): 'Experiments on Rathbone-place water', *Phil. Trans. R. Soc.,* 57, 92–108

Cerling, T.E. and Quade, J. (1993): 'Stable carbon and oxygen isotopes in soil carbonates', 1–36, in: P.K. Swart, K.C. Lohmann, J. McKenzie, S.Savin, S, *Climate Change in Continental Isotopic Records*, Geophysical Monograph 78, , Washington, DC (American Geophysical Union)

Chafetz, H.S., Akdim, B., Julia, R., and Reid, A. (1998): 'Mn- and Fe-rich black travertine shrubs: bacterially (and nanobacterially) induced precipitates', *J. Sed. Petrol.*, 68, 404–412

Chafetz, H.S. and Folk, R.L. (1984): 'Travertines: depositional morphology and the bacterially constructed constituents', *J. Sed. Petrol*, 54, 289–316

Chafetz, H.S. and Guidry, S.A. (1999): 'Bacterial shrubs, crystal shrubs, and ray-crystal shrubs: bacterial vs. abiotic precipitation', *Sediment. Geol.*, 126, 57–74
Chafetz, H.S. and Meredith, J.C. (1983): ' Recent travertine pisolites (pisoids) from southeastern Idaho, U.S.A.' 450–455, in: T.M. Peryt (ed.), *Coated Grains*, New York, (Springer-Verlag)
Chafetz, H.S., Rush, P.F. and Utech, N.M. (1991a): 'Microenvironmental controls on mineralogy and habit of $CaCO_3$ precipitates: an example from an active travertine system', *Sedimentology*, 38, 107–126
Chafetz, H.S., Srdoc, D. and Horvantincic, N. (1994): 'Early diagenesis of Plitvice Lakes waterfall and barrier travertine deposits.' *Géogr. physique Quaternaire,* 48: 247–256
Chafetz, H.S., Utech, N.M. and Fitzmaurice, S.P. (1991b): 'Differences in the $\delta^{18}O$ and $\delta^{13}C$ signatures of seasonal laminae comprising travertine stromatolites', *J. Sed. Petrol.*, 61, 1015–1028
Chahida, M.R. (1988): 'Die Verbreitung des Tertiars und das Auftreten heisser Quellen in der Umgebung von Abergarm/Zefreh (Provinz Istafan, Iran)', *Steirische Beitr. Z. Hydrogeologie*, 39, 131–139
Chang, H.T. (1927): Lapidarium Sinicum. A Study of Rocks, Fossils and Metals as known in the ChineseLiterature, 2nd Edn. 432 pp., Peking (. Geological Survey of China)
Chanson, H. and Cummings, P.D. (1996): 'Air-water interface area in supercritical flows down small slope chutes', *Dept. of Civil Eng. Res. Series*, CE151, University of Queensland, Australia
Chapelle, F.H. and McMahon, P.B. (1991): 'Geochemistry of dissolved inorganic carbon in a coastal plain aquifer. 1. Sulfate from confining beds as an oxidant in microbial CO_2 production', *J. Hydrol. Amsterdam*, 127, 85–108
Chardon, M. (1992): 'Karstic denudation and tufa deposits in high alpine mountains (Alps, France)', *Z. Geomorph. N.F. Suppl. Bd.* 85, 19–38
Chave, K.E. and Schmalz, R.F. (1966): 'Carbonate-seawater reactions'. *Geochim. Cosmochim. Acta*, 30, 1037–1048
Chen, J., Zhang, D.D., Wang, S., Xiao, T. and Huang, R. (2004): 'Factors controlling tufa deposition in natural waters and waterfall sites', *Sediment. Geol.*, 166, 353–366
Chen, X., Zhu, X. and Zhou, X. (1988): 'A study of isotopes of karst water and travertine deposits at the Huanglong scenic spot', *Carsologica Sinica, 7*, 209–212
Chibowski, E., Holysz, L. and Szecres, A. (2003): 'Adhesion of *in situ* precipitated calcium carbonate in the presence and absence of magnetic field in quiescent conditions on different solid surfaces', *Wat. Res.*, 37, 4685–4692
Choquette, P.N. and Pray, C. (1970): 'Geologic nomenclature and classification of porosity in sedimentary carbonates', *Bull. Am. Ass. Petrol. Geol.*, 54, 207–250
Chowdhury, M.C.B.R. (1945): 'Tufa lime manufacture at Umaria, C.I.', *Quart. J. Geol. Mining Metall. Soc. India*, 17, 45–51
Cidu, R., Fanfani, L., Zuddas, P. and Zuddas, P. (1990): 'The travertine deposit at Funtana Maore (Central Sardinia, Italy)', *Chem. Geol.,* 84, 198–200
Cipriani, N., Ercoli, A., Malesani, P. and Vannucchi, S. (1972): 'I travertini di Rapolano Terme (Siena)', *Mem. Soc. Geol. Ital.,* 11, 31–46
Cipriani, N., Malesani, P., Vannucci, S. (1977): 'I travertini dell'Italia centrale', *Boll. Serv. Geol. Ital.,* 98, 85–115
Clapham, A.R. (1940): 'The role of bryophytes in the calcareous fens of the Oxford region', *J. Ecol.*, 28, 71–80
Clark, I.D. and Fontes, J. –C. (1990): 'Paleoclimatic reconstruction in Northern Oman based on carbonates from hyperalkaline groundwaters', *Quat. Res.,* 33, 320–336
Clark, I.D., Khoury, H.N., Salameh, E., Fritz, P., Goksu, Y., Wiesser, A., Fontes, J. –Ch., and Causse, C. (1991): 'Travertines in central Jordan: implications for palaeohydrology and dating', 551–565, *Proc. Int. Atomic Energy Symp. (IAEA)* SM-319, Vienna (IAEA)
Clark, I.D. and Lauriol, B. (1992): 'Kinetic enrichment of stable isotopes in cryogenic carbonates', *Chem. Geol.,* 102, 217–228
Clark, J.G.D. (1938): 'Microlithic industries from tufa deposits at Prestatyn, Flintshire and Blashenwell, Dorset', *Proc. Prehist. Soc.*, 4, 330–334
Clark, J.M. (1900): 'The water biscuits of Squaw Island, Canadaigua Lake, N.Y.', *Bull. N.Y. St. Mus.,* 8, 195–198
Clarke, F.W. (1916): 'Data of Geochemistry', *Bull. U.S. Geol. Surv.,* 616, 821 pp
Clerici, E. (1887): 'Il travertino di Fiano Romano', *Boll. Serv. Geol. D'Ital.*, 18, 99–121
Cloud, P. and Lajoie, K.R. (1980): 'Calcite-impregnated defluidisation structures in littoral sands of Mono Lake, California', *Science,* 210, 1009–1012
Cocozza, T. (1963): 'Nuovi dati stratigrafici e tettonici sul Monte Canino', *Geol. Romana*, 2, 15–40
Coey, J.M.D. and Cass, S. (2000): 'Magnetic water treatment', *J. Magnetism Magn. Mat.*, 209, 71–74
Cohn, F. (1862): 'Über die Algen des Karlsbader Sprudels, mit Rücksicht auf die Bildung des Sprudelsinters', *Abh. schles. Ges. vaterl. Cult.,* 2, 35–55

Cohn, F. (1864): 'Über die Entstehung des Travertin in den Wasserfällen von Tivoli', *Neues Jb. Min. Geol. Palaönt. Stuttgart,* 40: 580–610
Cohn, F. (1876): 'Kryptogamenflora von Schlesien', *Abh. Schles. Ges.*, No. 1, 47–53
Cole, J.M., Rasbury, E.T., Montanez, I.P., Pedone, V.I., Lanzirotti, A. and Hanson, G.N. (2004): 'Petrographic and trace element analysis of uranium-rich calcite, middle Miocene Barstow Formation,California, USA', *Sedimentology*, 51, 433–453
Cole, G.A. and Batchelder, G.L. (1969): 'Dynamics of an Arizona travertine-forming stream', *J. Ariz. Acad. Sci.,* 5, 271–283
Cole, G.A. and Watkins, R.L. (1977): '*Hyaella montezuma*, a new species (Crustacea: Amphipoda), from Montezuma Well, Arizona', *Hydrobiologia*, 52, 175–184
Collinsworth, B.C. and Rohr, D.M. (1986): 'An Eocene carbonate lacustrine deposit. Brewster County, West Texas', *Publ. West Texas Geol. Soc.*, No. 85–82, 117–124
Copeland, J.J. (1936): 'Yellowstone thermal Myxophyceae', *Ann. N.Y. Acad. Sci.*, 36, 5–225
Cortesi, C. and Leoni, M. (1955): 'Studio sedimentologico e geochimico del travertino di un sodaggio a Bagni di Tivoli', *Periodico di Mineralogia*, 27, 407–458
Couderc, J.P. (1977): 'Les groupements muscinaux des tufs de Tourraine', *Documents phytosociologiques*, 1, 37–50
Council, T.C. and Bennett, P.C. (1993): 'Geochemistry of ikaite formation at Mono Lake, California: implications for the origin of tufa mounds', *Geology,* 21, 971–974
Couteaux, M. (1969): 'Formation et chronologie palynologique des tufs calcaires du Luxembourg, Belgo-Grand-Ducal', *Bull. Ass. Fr. Étude Quaternaire*, 6, 179–206
Cox, G., James, J.M., Leggett, K.E.A. and Osborne, R.A.L. (1989): 'Cyanobacterially deposited speleothems: subaerial stromatolites', *Geomicrobiol. J.*, 7, 245–252
Craig, H. (1965): 'The measurements of oxygen isotope paleotemperatures', 1–24, in: E. Tongiorgi (Ed.), *Stable isotopes in Oceanographic Studies and Paleotemperatures*. Pisa (Consiglio Nazionale delle Richerche, Laboratorio di Geologia Nucleare)
Cramer, H.R. (1987): 'Hierapolis (Turkey) history and geology', *Bull. Georgia Acad, Sci.*, 45, 84
Crombie, M.K., Arvidson, R.E., Sturchio, N.C., El Alfy, Z. and Abu Zeid, K. (1997): 'Age and isotopic contstraints on Pleistocene pluvial episodes in the Western Desert, Egypt', *Palaeogeogr. Palaeoclim. Palaeoecol.*, 130, 337–355
Curl, R.L. (1972): 'Minimum diameter stalagmites', *Nat. Speleol. Soc. Bull.,* 34, 129–136
Curl, R.L. (1973): 'Minimum diameter stalagmites', *Nat. Speleol. Soc. Bull.,* 35, 1–9
Cuvier, G. (1812): 'Recherches sur les ossements fossiles de quadrupèdes…', Deterville, Paris
Dalby, D.H. (1966): 'The growth of *Eucladium verticillatum* in a poorly illuminated cave', *Rev. Bryol. Lichénol.*, 34, 288–301
Damm, B. (1968): 'Ein Riesenkegel aus Travertin (NW Iran)', *Der Aufschluss,* Sonderheft 19, 323–332
D'Amore, F., Fancelli, R., Nuti, S., Michard, G. and Paces, T. (1989): 'Origin of gases in Variscan massifs of Europe', 177–180, in: D.L. Miles (ed.), *Proceedings International Symposium on Water-rock interaction*, Rotterdam, (Balkema)
Dandurand, J.L., Gout, R., Hoefs, J., Menschel, G., Schott, J. and Usdowski, E. (1982): 'Kinetically controlled variations of major components and carbon and oxygen isotopes in a calcite-depositing spring', *Chem. Geol.,* 36, 299–315
Danielli, H.M. and Edington, M.A. (1983): 'Bacterial calcification in limestone caves', *Geomicrobiol. J.*, 3, 1–16
Danische, E. (1950): 'Gesteinbildende Mückenlarven im Wiehengebirge', *Jber. Naturw. Ver. Osnabr.*, 25, 87–92
D'Anna, A. and Courtin, J. (1986): 'Le point de vue du prehistorien', *Mediterranée*, 1–2, 31–38
D'Argenio, B., Ferreri, V., Stanzione, D., Brancaccio, L. and Ferreri, M. (1983): 'I travertini di Pontecagnano (Campania) geomorfologica, sedimentologica, geochemica', *Boll. Soc. Geol. Ital.,* 102, 123–136
Dart, R.A. (1926): 'Taungs and its significance', *Nat. Hist.*, 26, 315–327
Das, S. and Mohanti, M. (1997): 'Holocene microbial tufas: Orissa State, India', *Carbonates and Evaporites*, 12, 204–219
Daubrée, A. (1887): 'Les Régions Invisibles du Globe et des Espaces Célestes, Eaux SouterrainesTremblements de Terre- Météorites', 240 pp., Paris (Germer Bailleire)
Davies, K.H. and Keen, D.H. (1985): 'The age of the Pleistocene marine deposits at Portland, Dorset', *Proc. Geol. Ass.*, 96, 217–225
Davies, P.J. and Till, R. (1968): 'Stained dry cellulose acetate peels of ancient and Recent impregnated carbonate sediments', *J. Sed. Petrol.,* 38, 234–237
Davies, T.T. and Hooper, P.R. (1963): 'The determination of calcite:aragonite ratios in mollusc shells by X-ray diffraction', *Mineralog. Mag.,* 33
Davis, C.A. (1900): 'A contribution to the natural history of marl', *J. Geol.,* 8, 485–497

Davis, C.A. (1901): 'A second contribution to the natural history of marl', *J. Geol.,* 9, 491–506
Davis, J.S., Rands, D.G. and Hein, M.K. (1989): 'Biota of the tufa deposit of Falling Springs, Illinois', *Trans. Am. Microsc. Soc.*, 108, 403–409
Davis, R.V., Carter, P.W., Kamrath, M.A., Johnson, D.A. and Reed, P.E. (1995): 'The use of modern methods in the development of calcium carbonate inhibitors for cooling water systems', 33–46, in: Z. Amjad (ed.), *Mineral Scale Formation and Inhibition*, New York (Plenum)
Davreux, C.J. (1933): 'Essai sur la constitution géognostique de la province de Liège', *Mém. Cour. Acad. R. Belg.*, 9, 1–204
Debenham, N.C. and Aitken, M. (1984): 'Thermoluminesce dating of stalagmitic calcite', *Archaeometry*, 26, 155–170
De Boer, J.Z., Hale, J.R. and Chanton, J. (2001): 'New evidence for the geological origins of the ancient Delphic oracle (Greece)', *Geology,* 29, 707–710
De Boodt, A.B. (1609): '*Gemmarum et lapidum historia*', Hanover
De Bruyn, J.R. (1997): 'On the formation of periodic arrays of icicles', *Cold Reg. Sci. Tech.,* 25, 225–229
De Capitani, L., Fiorentine, P.M. and Terrani, M. (1974): 'Geochemistry of Ra in the supergene zone of a radioactive spring', *Atti Soc. Ital. Sci. Nat.,* 115, 157–169
Dehm, R. (1951): 'Mitteldiluviale Kalktuffe und ihre Molluskenfauna bei Schmiechen nahe Blaubeuren (Schwäbische Alb)', *Neues Jb. Geol. Paläont. Abh.*, 93, 247–276
Deines, P. (1989): 'Stable isotope variations in carbonatites', 301–359, in: K. Bell (ed), *Carbonatites Genesis and Function*. London, (Unwin Hyman)
Deines, P. (1992): 'Mantle carbon: concentration, mode of occurrence and isotopic composition', 133–146, in: M. Schidlowski, S. Golubic, M.M. Kimberley, D.M. McKirdy, P.A. Trudinger (eds), *Early Organic Evolution*. Berlin (Springer-Verlag)
Deines, P., Langmuir, D. and Harmon, R.S. (1974): 'Stable carbon isotope ratios and the existence of a gas phase in the evolution of carbonate ground waters', *Geochim. Cosmochim. Acta.,* 38, 1147
Del Giovine, A. (1986): 'Travertins Holocenes du Vauvenargues (Bouches du Rhone)', *Mediterranée*, 1–2, 81–91
Demovic, R., Hoefs, J. and Wedepohl, K.H. (1972): 'Geochemische untersuchungen an travertineen der Slowakei', *Contr. Min. Petrol.,* 37, 15–28
Devoto, G. (1965): 'Lacustrine Pleistocene in the lower Liri Valley', *Geol. Romana*, 4, 291–368
Dennen, K.O., Diecchio, R.J. and Stephenson, M.A. (1990): 'The geology of the Falling Spring travertine deposit, Alleghany Co., Virginia', 79–92, in: J.S. Herman, D.A. Hubbard (eds), *Travertine-marl: Stream Deposits in Virginia.* Virginia Division of Mineral Resources Publication 101, Charlottesville, Va (Virginia Division of Mineral Resources)
DeSaussure, R. (1961): 'Phototropic cave coral', *Cave Notes*, 3, 25–28
Dessau, G. (1968): 'Il berillio e l'arsenico nei travertini dell'Italia Centrale', *Atti Soc. Tosc. Sci. Nat.,* 75, 690–711
Dickson, J.A.D. (1966): 'Carbonate identification and genesis as revealed by staining', *J. Sed. Petrol.,* 36, 491–505
Dickson, J.A.D. (1990): 'Carbonate mineralogy and chemistry', 284–313 in: M.E. Tucker, V.P. Wright (eds). *Carbonate Sedimentology,* Oxford (Blackwell)
Diebel, K. and Pietrzeniuk, E. (1975): 'Ostrakoden aus dem holozänen Travertin von Bad Langensalza', *Quartärpaläontologie*, 1, 27–55
Diebel, K. and Pietrzeniuk, E. (1977): 'Ostrakoden aus dem Travertin von Taubach bei Weimar', *Quartärpaläontologie*, 2, 119–137
Diebel, K. and Pietrzeniuk, E. (1978): 'Die Ostrakodenfauna des eeminterglazialen Travertin von Burgtonna in Thüringen', *Quartärpaläontologie*, 3, 87–91
Dobat, K. (1966): 'Die Kryptogamenvegetation der Höhlen und Halbbhöhlen im Bereich der Schwäbischen Alb', *Abh. Karst u. Höhlenkunde,* E3, 1–153
Dobosi, V.T. (2003): 'Archeological finds in NE-Transdanubian travertine', *Acta Geol. Hung.*, 46, 205–214
Dobrovol'skiy Y.V., Dorofey, Y.N., Voronin, Y.V., Lyalko, V.I. and Krat, V.N. (1987): 'The mechanism and kinetics of travertine formation interpreted from carbon dioxide sources', *Geologicheskiy Zh.*, 47, 56–61
Donovan, R.N. (1973): 'Basin margin deposits of the Middle Old Red Sandstone at Dirlot, Caithness', *Scott. J. Geol.*, 9, 203–211
Dorale, J.A., Gonzalez, L.A., Reagan, M.K., Pickett, D.A., Murrell, M.T. and Baker, R.G. (1993): 'A high resolution record of Holocene climate change in speleothem calcite from Cold Water Cave, northeast Iowa', *Science*, 258, 1626–1630
Dove, P.M. and Hochella, M.F. Jr. (1993): 'Calcite precipitation mechanisms and inhibition by orthophosphate: in situ observations by Scanning Force Microscopy', *Geochim. Cosmochim. Acta*, 57, 705–714
Dowgiallo, J. (1976): 'Problems of the origin of Cl-HCO_3-Na mineral waters of the Polish Flysch Carpathians', 12–22, in: J. Cadek, T. Paces (eds), *Proceedings Int. Symposium on Water-rock Interaction*. Prague, (Geological Survey)

Drake, J.J. (1980): 'The effect of soil activity on the chemistry of carbonate groundwaters', *Water Resources Res.,* 16, 381–386

Drake, J. J (1983): 'The effects of geomorphology and seasonality on the chemistry of carbonate groundwater', *J. Hydrol.,* 61, 223–236

Dramis, F., Materazzi, M. and Cilla, G. (1999): 'Influence of climatic changes on freshwater travertine deposition: a new hypothesis', *Phys. Chem. Earth (A),* 24, 893–897

Dravis, J. (1979): 'Rapid and widespread generation of Recent oolitic hardgrounds on a high energy Bahamian Platform, Eleuthera Bank, Bahamas', *J. Sed. Petrol.*, 49, 195–207

Dreybrodt, W. (1980): 'Deposition of calcite from thin films of natural calcareous solutions and the growth of speleothems', *Chem. Geol.*, 29, 89–105

Dreybrodt, W. (1988): '*Processes in Karst Systems*', Berlin (Springer-Verlag), 288 pp

Dreybrodt, W. and Buhmann, D. (1991): 'A mass transfer model of dissolution and precipitation of calcite from solutions in turbulent motion', *Chem. Geol.*, 90, 107–122

Dreybrodt, W., Buhmann, D., Michaelis, J. and Usdowski, E. (1992): 'Geochemically controlled calcite precipitation by CO_2 outgassing: field measurements of precipitation rates in comparison to theoretical predictions', *Chem. Geol.*, 97, 285–294

Droste, R.L. (1997): '*Theory and Practice of Water and Wastewater Treatment*', 800 pp., New York (J. Wiley & Sons)

Drysdale, R.N. (1999): 'The sedimentological significance of hydropsychid caddis-fly larvae (Order: Trichptera) in a travertine-depositing stream: Louie Creek, Northwest Queensland, Australia', *J. Sed. Res.,* 69, 145–150

Drysdale, R.N. and Gale, S.J. (1997): 'The Indarri Falls travertine dam, Lawn Hill Creek, northwest Queensland, Australia', *Earth Surf. Proc. Landf.*, 22, 413–418

Drysdale, R.N. and Gillieson, D. (1997): 'Micro-erosion meter measurements of travertine deposition rates: a case study from Louie Creek, Northwest Queensland, Australia', *Earth Surface Proc. Landf.*, 22, 1037–1051

Drysdale, R.N., Taylor, M.P. and Ihlenfeld, C. (2003a): 'Factors controlling the chemical evolution of travertine-depositing rivers of the Barkly karst, northern Australia', *Hydrol. Process.*, 16, 2941–2962

Drysdale, R.N., Carthew, K.D. and Taylor, M.P. (2003b): 'Larval caddis-fly nets and retreats: a unique biosedimentary paleocurrent indicator for fossil tufa deposits', *Sediment. Geol.*, 161, 207–215

Drysdale, R.N., Lucas, S. and Carthew, K. (2003c): 'The influence of diurnal temperatures on the hydrochemistry of a tufa-depositing stream', *Hydrol. Process.*, 17, 3421–3441

Dublanski, V.N., Bajenova, L.D., Bashkin, A.I. and Teslenko, U.V. (1982): 'Quaternary calcareous tufa of the mountainous Crimea', *Akad. Nauk. Ukranski SSR* (for 1982), 1–33

Duchi, V. (1976): 'Determinazione del mercurio mediante spettrofotometria di assorbimento atomico senza fiamma; dossagio in travertini dell'Italia centrale', *Rend. Soc. Ital. Miner. Petrol.,* 32, 243–260

Duchi, V., Giordano, M.V. and Martini, M. (1978): 'Riesame del problema della precipitazione di calcite od aragonite da soluzione naturali', *Rend. Soc. Ital. Miner. Pet.,* 34, 605–618

Dunham, R.J. (1962): 'Classification of carbonate rocks according to depositional texture', 108–121, in: W.E. Ham (ed.), *Classification of Carbonate Rocks. Mem. Am. Ass. Petrol. Geol.,* 1. Tulsa, Oklahoma

Dunkerley, D.L. (1987): 'Deposition of tufa on Ryans and Stockyard Creeks, Chillagoe Karst, North Queensland: the role of evaporation', *Helictite*, 25, 30–35

Dunn, J.R. (1953): 'The origin of the deposits of tufa at Mono Lake', *J. Sed. Petrol.,* 23, 18–23

Duplessy, J.C., Lalou, C. and Gomes de Azevedo, M.A. (1969): 'Étude des conditions de concretionnement dans les grottes aou moyen des isotopes stables de l'oxygene et du carbone', *C.R. Acad. Sci. Ser. D.*, 268, 2327–2330

Duplessy, J.C., Labeyrie, J., Lalou, C. and Nguyen, H.V. (1970): 'Continental climate variations between 130,000 and 90,000 years B.P.', *Nature*, 226, 631–633

Durrenfeldt, A. (1978): 'Untersuchungen zur Besiedlungsbiologie von Kalktuff faunistosche, ökologische und elektronenmikroskopische Befunde', *Arch. Hydrobiol. Suppl.*, 54, 1–79

Dzhanelidze, C.P. (1969): 'Postglacial changes in the central Caucasus landscape during the Holocene', *Akad. Nauk. Gruz. SSR. Soobshch.*, 54, 369–372

Edington, J.M. and Hildrew, A.G. (1981): '*A key to the Caseless Caddis larvae of the British Isles, with notes on their ecology*', 45 pp., Freshwater Biological Association Publication 43, UK (Freshwater Biological Association)

Edmonds, W.J. and Martens, D.C. (1990): 'Influence of CaCO3 dissolution and deposition on flood plain soils in the Valley and Ridge province', 163–176, in: J.S. Herman, D.A. Hubbard (eds), *Travertine-marl: Stream Deposits in Virginia.* Virginia Division of Mineral Resources Publication 101, Charlottesville, Va. (Virginia Division of Mineral Resources)

Edmunds, W.M. 1971: Hydrogeochemistry of Groundwaters in the Derbyshire Dome with Special Reference to Trace Constituents. 52 pp., NERC Institute of Geological Sciences Report 71/7. HMSO, London

Edmunds, W.M. and Miles, D.L. (1991): 'The geochemistry of the Bath thermal waters', 143–156, in: G.A. Kellaway (ed.), *Hot Springs of Bath*, England (Bath City Council)

Edwards, R.W. and Heywood, J. (1960): 'Effect of a sewage effluent discharge on the deposition of calcium carbonate on shells of the snail *Potamopyrgus jenkinsii* (Smith)', *Nature*, 186, 492–493

Edwards, W.N. (1936): 'A Pleistocene Chironomid-tufa from Crémieu (Isère)', *Proc. Geol. Ass. Lond.*, 47, 197–198

Ehleringer, J.R. (1988): 'Carbon isotope ratios and physiological processes in aridland plants', 41–54, in: P.W. Rundel, J.R. Ehleringer, K.A. Nagy (eds), *Applications of Stable Isotope Ratios to Ecological Research*, New York (Springer-Verlag)

Eicher, U. and Siegenthaler, U. (1976): 'Palynological and oxygen isotope investigations on late-glacial sediment cores from Swiss lakes', *Boreas*, 5, 109–117

Eikenberg, J., Vezzu, G., Zumsteg, I., Bajo, S., Ruethi, M. and Wyssling, G. (2001): 'Precise two chronometer dating of Pleistocene travertine: the $^{230}Th/^{234}U$ and $^{226}Ra_{ex}/^{226}Ra(0)$ approach', *Quat. Sci. Revs.*, 20, 1935–1953

Ekmekci, M., Gunay, G. and Sinsek, S. (1995): 'Morphology of rimstone pools at Pamukkale, Western Turkey', *Cave and Karst Sci.*, 22, 103–106

Ellenberger, E. and Gottis, M. (1967): 'Sur les jeux de failles pliocenes et quaternaires dans l'arriere pays Narbonnaise', *Rev. Géogr. Phys. Geol. Dyn.,* 9, 153–159

Emeis, K. –C., Richnow, H.H., and Kempe, S. (1987): 'Travertine formation in Plitvice National Park, Yugoslavia: chemical versus biological control', *Sedimentology,* 34, 595–609

Emery, B. (1961): '*Archaic Egypt*', 269 pp., England (Penguin)

Emig, W.H. (1917): 'The travertine deposits of the Arbuckle Mountains Oklahoma, with reference to the plant agencies concerned in their formation', *Bull. Okla. geol. Surv.,* 29, 9–75

Emmons, W.H. and Larsen, E.S. (1913): 'The hot springs and the mineral deposits of Wagon Wheel Gap, Colorado', *Econ. Geol.,* 8, 235–246

Emrich, K., Ehhalt, D.H. and Vogel, J.C. (1970): 'Carbon isotope fractionation during the precipitation of calcium carbonate', *Earth Planet Sci. Lett.,* 8, 363–371

Eugster, H.P. and Hardie, L.A. (1978): 'Saline Lakes', 237–294, in: A. Lerman (ed.), *Lakes:Chemistry, Geology and Physics*', New York (Springer-Verlag)

Eulenstein, T. (1866): 'Die Tuffbildungen des Uracher Wasserfalls', *Jh. Ver. vaterl. Naturk. Württ.*, 22, 36–42

Evans, J.E. (1999): 'Recognition and implications of Eocene tufas and travertines in the Chadron Formation, White River Group, Badlands of South Dakota', *Sedimentology*, 46, 771–789

Evans, J.G. (1972): *Land Snails and Archaeology,* 436 pp., London (Seminar Press)

Evans, J.G. and Smith, I.F. (1983): 'Excavations at Cherhill, North Wiltshire, 1967', *Proc. Prehist. Soc.*, 49, 43–117

Fabré, G. (1986): 'Tufs et travertins du Languedoc mediterranéen et des Causses majeurs', *Mediterranée,* 1–2, 66–70

Fabré, G. and Fiche, J.L. (1986): 'Les concretionnements de l'Aqueduct Romain de Nîmes.' *Mediterranée,* 1–2, 129–130

Fairchild, I.J. and others (2000): 'Controls on trace-element (Sr-Mg) compositions of carbonate cave waters: implications for speleothem climatic waters', *Chem. Geol.,* 166, 255–269

Fairchild, I.J., Baker, A., Borsato, A., Frisia, S., Hinton, R.W., McDermott, F. and Tooth, A.F. (2001): 'Annual to subannual resolution of multiple trace-element trends in speleothems', *J. Geol. Soc. Lond.*, 158, 831–841

Fannin, N.G. (1969): 'Stromatolites from the Middle Old Red Sandstone of Western Orkney', *Geol. Mag.*, 106, 77–88

Fantidis, J. and Ehhalt, D.H. (1970): 'Variations in the C and O isotopic composition of stalagmites and stalactites. Evidence of non-equilibrium fractionation', *Earth Planet Sci. Lett.*, 10, 136–144

Farmer, J.D. and Des Marais, D.J. (1994a): 'Biological versus inorganic processes in stromatolite morphogenesis: observations from mineralizing sedimentary systems', 61–68, in: L.J. Stal, P. Caumette, P. (eds), *Microbial Mats,* Berlin (Springer-Verlag)

Farmer, J.D. and Des Marais, D.J. (1994b): 'Exopaleontology and the search for a fossil record on Mars', *Lunar Planetary Sci.,* 25, 367–368

Ferguson, J., Bubela, B. and Davies, P.J. (1978): 'Synthesis and possible mechanisms of formation of radial carbonate ooids', *Chem. Geol.*, 22, 285–308

Ferreri, M. (1985): ''Criteri di analisi di facies e classificazione dei travertini pleistocenici dell'Italia meriodionale', *Rend. Accad. Sci. Fis. Mat.*, 52, 121–147

Ferreri, M. and Stanzione, D. (1978): 'Contributo alla conoscenza geochimica dei travertini campani: travertini di Paestum e della bassa valle de Tanagro (Salerno)', *Rend. Acc. Sci. Fis. Mat. Napoli,* 45, 199–213

Feth, J.H. (1964): 'Review and annotated bibliography of ancient lake deposits (Precambrian to Pleistocene) in the western United States', *Bull. U.S. Geol. Surv.,* 1080, 1–119

Feth, J.H. and Barnes, I. (1979): 'Spring-deposited travertine in eleven western states', *U.S. Geol. Surv. Water Res. Investigation,* 79–35, Open file report
Fischbeck, R. and Müller, G. (1971): 'Monohydrocalcite, hydromagnesite, nesquehonite, dolomite, aragonite and calcite in speleothems of the Frankische Schweiz, Western Germany', *Contr. Min. Petrol.*, 33, 87–92
Fischer, H. (1956): 'Die Kalktuffvorkommen von St. Anton an der Jessnitz', *Verh. Geol. Bundesanst.*, 3, 267–274
Fjerdingstad, E. (1957): 'A lime incrusting algal community of a Danish well', *Revue. Algol.*, 4, 246–248
Fliche, M.M. (1894): 'Note sur les tufs calcaires de Kiffis (Sundgau, Alsace)', *Bull. Soc. Geol. Fr.*, *Serie 3*, (for 1894), 41–482
Flinn, D. and Pentecost, A. (1995): 'Travertine-cemented screes on the serpentinite seacliffs of Unst and Fetlar, Shetland', *Mineralogical Mag.,* 59, 259–265
Flowers, S. (1933): 'On Fossil Mosses', *Bryologist*, 36, 26–27
Flugel, E. (1982): *Microfacies analysis of Limestones*. Berlin, (Springer), pp. 633
Fodor, T., Scheuer, G. and Schweitzer, F. (1982): 'Comparison of fresh-water carbonate rocks of the Transylvanian-Eastern Carpathian Basin with those of Hungary', *Földt. Közlöny*, 112, 241–259
Folk, R.L. (1959): 'Practical petrographic classification of limestones', *Bull. Am. Ass. Petrol. Geol.,* 43, 1–38
Folk, R.L. (1962): 'Spectral subdivision of limestone types', 62–84, in: W.E. Ham (ed.), *Classification of Carbonate Rocks. Mem. Am. Ass. Petrol. Geol.,* 1.,Tulsa, Oklahoma
Folk, R.L. (1993): 'SEM imaging of bacteria and nannobacteria in carbonate sediments and rocks', *J. Sed. Petrol.*, 63, 990–999
Folk, R.L. (1994): 'Interaction between bacteria, nannobacteria, and mineral precipitation in hot springs of central Italy', *Géogr. Phys. Quat.*, 48, 233–246
Folk, R.L. and Assereto, R. (1976): 'Comparative fabrics of length-slow and length-fast calcite and calcitized aragonite in a Holocene speleothem, Carlsbad Caverns, New Mexico'. *J. Sediment. Petrol.,* 46: 486–496
Folk, R.L. and Chafetz, H.S. (1983): 'Pisoliths (pisoids) in Quaternary travertines of Tivoli, Italy', 474–487, in: T.M. Peryt (ed.), *Coated Grains*, Berlin (Springer-Verlag)
Folk, R.L., Chafetz, H.S. and Tiezzi, P.A. (1985): 'Bizarre forms of depositional and diagenetic calcite in hot-spring travertines, central Italy', 349–369, in: N. Scheidemann, P.Harris (eds), *Carbonate Cements*. Society of Economic Paleontologists and Mineralogists. Special Publication 36. Tulsa, Oklahoma
Fontes, J.C. and Pouchan, D. (1975): 'Les cheminées du lac Abbé (TFAI): stations hydroclimatiques de l'Holocene', *C.R. Acad. Sci. Paris,* 280, 383–386
Ford, D.C., Fuller, P.G. and Drake, J.J. (1970): 'Calcite precipitates at the soles of temperate glaciers', *Nature*, 226, 441–442
Ford, D.C. and Williams, P. (1989): *Karst Geomorphology and Hydrology,* London (Chapman and Hall)
Ford, T.D. (1989): 'Tufa- the whole dam story', *Cave Sci.*, 16, 39–49
Ford, T.D. and Pedley, H.M. (1992): 'Tufa deposits of the world', *J. Speleol. Soc. Japan,* 17, 46–63
Fornaca-Rinaldi, G., Panichi, C. and Tongiorgi, E. (1968): 'Some causes of the variation of the isotopic composition of carbon and oxygen in cave concretions', *Earth Planet Sci. Lett.*, 4, 321–324
Forsythe, R.D. and Zimbelman, J.R. (1995): 'A case for ancient evaporite basins on Mars', *J. Geophys. Res.,* 100E, 5553–5563
Forti, P. (1980): 'Grotta Pelagalli: nuovi rami ed inusuali cristallizzazioni', *Speleologia*, 3, 38
Fouke, B.W., Farmer, J.D., Des Marais, D.J., Pratt, L., Sturchio, N.C., Burns, P.C. and Discipulo, M.K. (2000): 'Depositional facies and aqueous-solid geochemistry of travertine-depositing hot springs (Angel Terrace, Mammoth Hot Springs, Yellowstone National Park, U.S.A.)', *J. Sed. Res.,* 70, 565–585
Fouke, B.W., Bonheyo, G.T., Sanzenbacher, B. and Frias-Lopez, J. (2003): 'Partitioning of bacterial communities between travertine depositional facies at Mammoth Hot Springs, Yellowstone National Park, Wyoming', *Can. J. Earth Sci.*, 40, 1531–1548
Fournier, G.F., Causse, C., Maraval, V. and Brousse, R. (1966): 'Sur quelques travertins perivolcaniques et sur leur florule de diatomées', *Bull. Ass. Fr. Étude Quaternaire*, 3, 202–207
Fournier, R.O. (1989): 'Geochemistry and dynamics of the Yellowstone Park hydrothermal system', *Ann. Rev. Earth. Planet. Sci.,* 17, 13–53
Francis, P. (1993): '*Volcanoes, a Planetary Perspective*', 443 pp., New York (Clarendon Press)
Franciskovic-Bilinski, S., Bilinski, H., Barisic, D., Horvantincic, N. and Daoxian, Y. (2003): 'Analysis of karst tufa from Guangxi, China', *Acta Geologica Sinica*, 77, 267–276
Frank, N., Braum, M., Hambach, U., Mangini, A. and Wagner, G. (2000): 'Warm period growth of travertine during the last interglaciation in Southern Germany', *Quat. Res.*, 54, 38–48
Franke, H.W. (1965): 'The theory behind stalagmite shape', *Studies in Speleology,* 1, 89–95
Franke, H.W. and Geyh, M.A. (1970): 'Zur wachstumsgeschwindigkeit von Stalagmiten', *Atompraxis*, 16, 46–48

Freeze, R.A. and Cherry, J.A. (1979): *Groundwater,*588 pp., New York (Prentice-Hall)
Frey, W. and Probst, W. (1974): 'Morphologische und vegetationsanalytische Untersuchungen an rezenten Kalktuffen im Keuper-gebiet des südlichen Schönbuchs', *Beitr. Naturk. Forsch. SüdwDtl.,* 33, 59–79
Freytet, P. (1990): 'Contribution à l'étude des tufs du Bassin de Paris: typologie des edifices tuffacés (stromatolitique) des chenaux fluviatiles', *Bull. Cent. Geomorphol. Caen*, 38, 9–27
Freytet, P. and Plaziat, J.C. (1982): 'Continental carbonate sedimentation and pedogenesis' Late Cretaceous and Early Tertiary of Southern France', *Contribution to Sedimentology*, 12, 1–213, Stuttgart (Schweizerbart'sche Verlag)
Freytet, P. and Plet, A. (1991): 'Les formations stromatolitiques (tufs calcaires) récentes de la region de Tournus (Saône et Loire).' *Geobios*, 24, 123–139
Freytet, P. and Plet, A. (1996): 'Modern freshwater microbial carbonates: The *Phormidium* stromatolites of southeastern Burgundy (Paris Basin, France).' *Facies*, 34: 219–238
Freytet, P. and Verrecchia, E.P. (1998): 'Freshwater organisms that build stromatolites: a synopsis of biocrystallization by prokaryotic and eukaryotic algae', *Sedimentology*, 45, 535–563
Freytet, P. and Verrecchia, E.P. (1999): 'Calcitic radial palisadic fabric in freshwater stromatolites: diagenetic and recrystallized feature or physicochemical sinter crust?', *Sediment. Geol.*, 126, 97–102
Friedmann, E.I. (1979): 'The genus *Geitleria:* distribution of *G. calcarea* and *G. floridana* n. sp.' *Plant Syst. Evol.*, 131: 169–178
Friedman, I (1970): 'Some investigations of the deposition of travertine from hot springs – 1. The isotopic chemistry of a travertine-depositing spring', *Geochim. Cosmochim. Acta,* 34, 1303–1315
Frisia, S., Borsato, A., Fairchild, I.J., McDermott, F. (2000): 'Calcite fabrics, growth mechanisms, and environments of formation in speleothems from the Italian Alps and Southwestern Ireland.' *J. Sed. Res.,* 70: 1183–1196
Frisia, S., Borsato, A., Fairchild, I.J., McDermott, F. and Selmo, E.M. (2002): 'Aragonite-calcite relationships in speleothems (Grotte de Clamouse, France): environment, fabrics, and carbonate geochemistry', *J. Sed. Res.,* 72, 687–699
Fritsch, F.E. and Pantin, C.F.A. (1946): 'Calcareous concretions in a Cambridgeshire stream', *Nature,* 157, 397–399
Fritz, A. (1976): 'Pollenanalytische Untersuchungen des Kalktuffes von St. Magdalena bei Feistritz im Gailtal (Kärnten)', *Carinthia II*, 166, 163–172
Fritz, P. (1965): 'Composizione isotopica dell'ossigeno e del carbonio nei travertini della Toscana', *Boll. Geofis. Teor. Applic.,* 7, 25–30
Fritz, P. (1968): 'Der Isotopengehalt der Mineralwasser von Stuttgart und Umgebung und ihrer mittel pleistozaenen Travertin-Ablagerungen', *Jber. Mitt. Oberrhein. Geol. Ver.,* 50, 53–69
Feuerborn, S.M. (1923): 'Die Larven der Psychodiden oder Schmetterlingsmücken. Ein Beitrag zur Ökologie des Feuchten', *Verh. Int. Ver. Limnol.*, 1, 181–213
Furness, S.M. and Grime, J.P. (1982): 'Growth rate and temperature responses in bryophytes II. A comparative study of species of contrasted ecology', *J. Ecol.*, 70, 525–536
Gaida, R. and Radtke, O. (1983): 'Datation des tufs calcaires quaternaires du Baixo Alentejo par les methodes Th/U et ESR', *Finisterra*, 18, 107–111
Galat, D.L. and Jacobsen, R.L. (1985): 'Recurrent aragonite precipitation in saline-alkaline Pyramid Lake', *Arch. Hydrobiol.*, 105, 137–160
Galli, G. and Sarti, C. (1989): 'Morphology and microstructure of Holocene freshwater-stream cyanobacterial stromatolites (Villa Ghigi, Bologna, Italy)', *Rev. Paleobiol. Revista,* 8, 39–50
Gams, H. (1932): 'Bryo-Cenology (Moss-Societies)', 323–366, in: F. Verdoorn (ed.), *Manual of Bryology*, The Hague (Martinus Nijhoff)
Garcia del Cura, M.A., Pedley, H.M., Ordoñez, S. and Gonzalez Martin, J.A. (2000): 'Petrology of a barrage tufa system (Pleistocene to Recent) in the Ruidera Lakes Natural Park (Central Spain)', *Geotemas*, 1, 359–363
Garcia-Ruiz, J.M., Hyde, S.T., Carnerup, A.M., Christy, A.G., Van Kranendonk, M.J. and Welham, N.J. (2003): 'Self-assembled silica-carbonate structures and detection of ancient microfossils', *Science*, 302, 1194–1197
Garnett, E.R., Andrews, J.E., Preece, R.C. and Dennis, P.F. (2004): 'Climatic change recorded by stable isotopes and trace elements in a British Holocene tufa', *J. Quat. Sci.*, 19, 251–262
Gascoyne, M. (1983): 'Trace element partition coefficients in the calcite-water system and their paleoclimatic significance in cave studies', *J. Hydrol.*, 61, 213–222
Gascoyne, M. (1992): 'Palaeoclimate determination from cave calcite deposits', *Quat. Sci. Revs.*, 11. 609–632
Genty, D. (1993): 'Mise en évidence d'alternances saisonnières dans la structure interne des stalagmites. Intérêt pur la reconstitution des paléoenvironments continentaux', *C.R. Acad. Sci. Paris*, *Série II*, 317, 1229–1236
Genty, D., Massault, M., Gilmour, M., Baker, A., Verheyden, S. and Kepens, E. (1999): 'Calculation of past dead carbon proportion and variability by the comparison of AMS 14C and TIMS ages on the Holocene stalagmites', *Radiocarbon*, 41: 251–270

Genty, D., Baker, A. and Vokal, B. (2001): 'Intra- and inter-annual growth rate of modern stalagmites', *Chem. Geol.*, 176, 191–212

Germann, F.E.E. and Ayres, H.W. (1941): 'The origin of underground carbon dioxide', *J. Phys. Chem.*, 46: 61–68

Geurts, M. -A., (1976): 'Formation des travertins de fond de vallée sous climat tempere oceanique, temperate climate', *C.R. Acad. Sci. Paris, Serie D.*, 282, 275–276

Geurts, M. -A. (1997): 'Ontogenèse des encorbellements inverses', *Études Géogr. Phys. Traveux, Supplement* 26, 51–59

Geurts, M. -A., Frappier, M. and Tsien, H.H. (1992): 'Morphogenèse des barrages de travertin de Coal River Springs, Sud-est du territoire du Yukon', *Géogr. phys. et Quaternaire,* 46, 221–232

Geurts, M.- A. and Watelet, A. (1994): 'Les travertins de Coal River Springs: physico-chimie des eaux', *Géogr. Phys. Quaternaire*, 48, 275–283

Gewelt, M. (1986): 'Datations ^{14}C de concrétions de grottes Belges: vitesse de croissance durant l'Holocene et implications paléoclimatiques', 293–321, in: K. Paterson, M.M. Sweeting (eds), *New Directions in Karst*, Norwich, UK (Geo Books)

Geyer, D. (1920): 'Die Mollusken des Cannstatter Sauerwasserkalks', *Jber. Mitt. Oberrein. Geol. Ver.*, 9, 61–66

Geyh, M.A. (1970): 'Zeitliche Abgrenzung con Idimaaenderungen mit ^{14}C-Daten von Kalksinter und organischen Substanzen', *Geol Jahrb. Beih.*, 98, 15–22

Gèze, B. (1968): '*La Espeleología Científica*', 192 pp., Barcelona (Martinez Roca)

Giannini, W.F. (1990): 'A commercial marl deposit near Winchester, Virginia', 93–100, in: J.S. Herman, D.A. Hubbard Jr. (eds), *Travertine-marl: Stream Deposits of Virginia*, Virginia Division of Mineral Resources Publication 101, Charlottesville, Va (Virginia Division of Mineral Resources)

Gibert, J.P., Laugier, R., Lefebvre, S. (1983): 'Sur la composition minerale et biologique d'un travertin hydrothermal: la source Alice-Aubignat a Chatel-Guyon (Puy de Dome)', *C.r. Sci. de l'Acad. Sci., Ser. 2. Mecan, Phys., Chemie.,* 296, 365–358

Gignoux, M. (1937): 'Architectures edifiées par les sources tuffeuses', *La Terre et la Vie,* 7, 33–42

Giller, P.S. and Malmqvist, B. (1998): *The Biology of Streams and Rivers*, 296 pp.,UK (Oxford University Press)

Ginsburg, R.N. (1953): 'Beachrock in south Florida', *J. Sed. Petrol.*, 23, 85–92

Giordani Soika, A.G. (1956): 'Studi di ecologia e biogeografia XVII- Su *Coenia beckeri*, musci endemico delle sorgenti solfuree di "Acque Albule" presso Tivoli (Diptera. Ephydridae)', *Boll. Mus. Civico Storia nat. Venezia*, 9, 17–20

Giovannoni, S.J., Revsbech, N.P., Ward, D.M. and Castenholz, R.W. (1987): 'Obligately phototrophic *Chloroflexus* primary production in anaerobic hot spring microbial mats' *Arch. Microbiol.*, 147, 80–87

Girard, C. and Bordas, F. (1901): 'Analyse de quelques travertins du bassin du Vichy', *Comptes Rendus Sci. de l'Acad. Sci.,* 132, 1423–1426

Gislason, S.R. (1989): 'Kinetics of water-air interactions in rivers: a field study in Iceland', 263–266, in: D.L. Miles (ed.), *Water-rock Interaction*, Rotterdam (Balkema)

Glazek, J. (1965): 'Recent oncolites in streams of North Vietnam and the Polish Tatra Mountains', *Roczn. Pol. Tow. Geol.*, 35, 221–242

Glazek, J., Harmon, R.S. and Nowak, K. (1980): 'Uranium series dating of the hominid-bearing travertine deposit at Bilzingsleben, GDR. and its stratigraphic significance', *Acta Geol. Pol.*, 30, 1–14

Glover, C. and Roberston, A.F.H. (2003): 'Origin of tufa (cool water carbonate) and related terraces in the Antalya area, SW Turkey', *Geol. J.*, 38, 329–358

Goetghebuer, M. (1933): 'Ceratopogonidae et Chironomidae nouveaux ou peu connus d'Europe', *Bull. Annls. Soc. r. Ent. Belg.*, 73, 209–221

Goldschmidt, V. (1913): *Atlas der Krystallformen,* 2 Vol., Heidelberg (Universität buchhandlung)

Goldsmith, J.R., Graf, D.L. and Joensuu, O.I. (1955): 'The occurrence of magnesian calcites in nature', *Geochim. Cosmochim. Acta,* 7, 212–230

Golubic, S. (1957): 'Vegetacija alga na Slapovima Rijeke Krke u Dalmaciji', *Rad. Jugosl. Akad. Znan. Umjetn.*, 312, 208–259

Golubic, S. (1969): 'Cyclic and non-cyclic mechanisms in the formation of travertine', *Verh. int. Verein. theor. angew. Limnol.,* 17, 956–961

Golubic, S. (1973): 'The relationship between blue-green algae and carbonate deposits, 434–472, in: N.G. Carr, B.A. Whitton (eds), *The Biology of Blue-green Algae,* Oxford (Blackwell)

Golubic, S. and Marcenko, E. (1958): 'Zur Morphologie und Taxonomie der Desmidiaceengattung *Oocardium*', *Schweiz. Z. Hydrol.*, 20, 177–185

Golubic, S. and Fischer, A.G. (1975): 'Ecology of calcareous nodules forming in Little Conestoga Creek near Lancaster, Pennsylvania.' *Verh. Int. Verein. Limnol.*, 19: 2315–2323

Gomes, N.A. de N.C. (1985): 'Modern stromatolites in a karst structure from the Malmani Subgroup. Transvaal Sequence, South Africa', *Trans. Geol. Soc. S. Afr.*, 88, 1–9
Gonfiantini, R., Panichi, C. and Tongiorgi, E. (1968): 'Isotopic disequilibrium in travertine deposition', *Earth Planet Sci. Lett.,* 5, 55–58
Gonzalez, L., Carpenter, S.J., Lohmann, K.C. (1992): 'Inorganic calcite morphology: Roles of fluid chemistry and fluid flow.' *J. Sed. Petrol.,* 62: 382–399
Gordon, D., Smart, P.L., Ford, D.C., Andrews, J.N., Atkinson, T.C., Rowe, P.J. and Christopher, N.S.J. (1989): 'Dating of Late Pleistocene interglacial and interstadial periods in the United Kingdonm from speleothem growth frequency', *Quat. Res.*, 31, 14–26
Gosse, L.A. (1820); 'Account of a visit made to the baths of St. Fillipo in Tuscany, with a description of the mode of forming stone medallions in basso relievo from the waters of the spring', *Edinb. Phil. J.,* 2, 290–300
Goudie, A.S. (1973): '*Duricrusts in Tropical and Subtropical Landscapes*', 174 pp., Oxford (Clarendon Press)
Goudie, A.S. (1996): 'Organic agency in calcrete development', *J. Arid Environments*, 32, 103–110
Goudie, A.S., Viles, H.A. and Pentecost, A. (1993): 'The late-Holocene tufa decline in Europe', *The Holocene,* 3, 181–186
Gradzinski, M., Jach, R. and Stworzewicz, E. (2001a): 'Origin of calcite-cemented Holocene slope breccias from the Dluga Valley (the Western Tatra Mountains)', *Ann. Soc. Geolog. Polon.,* 71, 105–113
Gradzinski, M., Szulc, J., Motyka, J., Stworzewicz, E. and Tyc, A. (2001b): 'Travertine mound and cave in a village of Laski. Silesian-Cracow Upland', *Ann. Soc. Geol. Polon.,* 71, 115–123
Gratz, A.J., Hillner, P.E. and Hansma, P.K. (1993): 'Step dynamics and spiral growth of calcite', *Geochim. Cosmochim. Acta*, 57, 491–495
Gray, J.R. and Edington, J.M. (1969): 'Effect of woodland clearance on stream temperature', *J. Fish Res. Bd. Can.*, 26, 399–403
Grechin, V.I. (1971): 'Siliceous Miocene rocks of Western Kamchatka', *Litologiya Miner. Resour.*, 6, 490–495
Green, C.P. and others (1984): 'Evidence of two temperate episodes in Late Pleistocene deposits at Marsworth, U.K.', *Nature*, 309, 778–781
Gregor, H.H. (1982): 'Die miozäne Flora aus dem Böttinger Thermalsinterkalk; eine Revision', *Stuttgart Beitr. Naturkd., ser. B.,* 88, 1–15
Gregory, J.W. (1911): 'Constructive waterfalls', *Scott. Geogr. Mag.,* 27, 537–546
Grigor'ev, D.P. (1961): '*Ontogeny of minerals*', Israel Program for Scientific Translations, Moscow, (Izdatel'stvo L'vovskogo University, 1965)
Groschopf, P. (1952): 'Pollenanalytische Datierung württembergischer Kalktuffe und der postglaziale klimablauf', *Jh. Geol. Abt. Württ. Statis. Landesamtes*, 2, 72–94
Grün, R. (2001): '*Trapped Charge Dating (ESR, TL, OSL)*', pp.47–62 in: D.R. Brothwell, A.M. Pollard (eds), *Handbook of Archaeological Sciences*, Chichester (J. Wiley & Sons)
Grün, R., Schwarcz, H.P., Ford, D.C. and Hentzsch, B. (1988): 'ESR dating of spring deposited travertine', *Quat. Sci. Rev.*, 7, 429–432
Gruninger, W. (1965): 'Rezente Kalktuffbildung im Bereich der Uracher Wasserfälle', *Abh. Karst u. Höhlenkunde,* E2, 1–113
Gruszczynski, M. and Mastella, L. (1986): 'Calcareous tufas in the area of the Mszana-Dolna tectonic window, Poland', *Rocznik Polskiego Towarz. Geol.,* 56, 117–131
Guido, M. (1972): '*Southern Italy: An Archeological Guide*', 222 pp., London (Faber)
Guo, L. and Riding, R. (1992): 'Aragonite laminae in hot water travertine crusts, Rapolano Terme, Italy'. *Sedimentology,* 39: 1067–1079
Guo, L. and Riding, R. (1994): 'Origin and diagenesis of Quaternary travertine shrub fabrics, Rapolano Terme, central Italy.' *Sedimentology,* 41: 499–520
Guo, L. and Riding, R. (1998): 'Hot-spring travertine facies and sequences, Late Pleistocene, Rapolano Terme, Italy', *Sedimentology,* 45, 163–180
Guo, L. and Riding, R. (1999): 'Rapid facies changes in Holocene fissure ridge hot spring travertines, Rapolano Terme, Italy', *Sedimentology,* 46, 1145–1158
Gwinner, M. (1959): 'Über "Talspinnen" am Nordrande der Schwäbische Alb und ihre holozänen Süsswasserkalk vorkommen', *Neues Jb. Geol. Pal. Min.,* 3, 121–131
Haites, T.B. (1959): 'Banff thermal springs, a fascinating problem', *J. Alberta Soc. Pet. Geol.,* 7, 23–32
Hajek, M., Hekera, P. and Hajkova, P. (2002): 'Spring fen vegetation and water chemistry in the Western Carpathian Flysch Zone', *Folia Geobot.,* 37: 205–224
Hallet, B. (1976): 'Deposits formed by subglacial precipitation of $CaCO_3$', *Bull. Geol. Soc. Am.*, 87, 1003–1015
Hancock, P.L., Chalmers, R.M.L., Altunel, E. and Cakir, Z. (1999): 'Travitonics: using travertine in active fault studies', *J. Struct. Geol.*, 21, 903–916

Hanold, W. and Weber, B. (1982): 'Schwarzer Calcit von der Schwäbischen Alb', *Der Aufluss*, 33, 45–48
Hanor, J.S. (1978): 'Precipitation of beachrock cements; mixing of marine and meteoric waters vs. degassing', *J. Sed. Petrol.*, 48, 489–501
Hardie, L. A. (1968): 'The origin of the recent non-marine evaporite deposit of Saline Valley, Inyo County, California'. *Geochim. Cosmochim. Acta*, 32, 1279–1301
Harmon, R.S., Thompson, P., Schwarcz, H.P. and Ford, D.C. (1975): 'Uranium-series dating of speleothems', *Bull. Nat. Speleol. Soc.*, 37, 21–33
Harmon, R.S., Glazek, J. and Nowak, K. (1980): '$^{230}Th/^{234}U$ dating of travertine from the Bilzingsleben archaeological site', *Nature*, 284, 132–135
Harrington, E.R. (1948): 'Craters and crater springs of the Rio Salado', *J. Geol.,* 56, 182–185
Hartkopf-Fröder, C., Hiss, M. and Leinfelder, R. R (1989): 'Holozäne Süsswasserkalke im Alme- und Aftetal südlich von Büren (Kreis Paderborn, Nordrhein-Westfalen)', *Münster. Forsch. Geol. Paläont.*, 69, 261–289
Hassack, C. (1888): 'Über das Verhaltnis von Pflanzen zu Bicarbonaten und über Kalkincrustation', 465–477, in: W. Pfeffer (ed.), *Untersuchungen aus dem Botanischen Institüt zu Tübingen,* Bande 2, Tübingen (Königliche Eberhard-Karls Universität)
Hatch, F.H., Rastall, R.H. and Black, M. (1938): '*The Petrology of the Sedimentary Rocks*', 408 pp.,London (Allen and Unwin)
Hay, R.L. and Reeder, R.J. (1978): 'Calcretes of Olduvai Gorge and the Ndolanya Beds of Northern Tanzania', *Sedimentology*, 25, 649–673
Hays, P.D. and Grossman, E.L. (1991): 'Oxygen isotopes in meteoric calcite cements as indicators of continental palaeoclimate', *Geology,* 19, 441–444
Headden, W.P. (1905): 'The Doughty Springs,a group of radium-bearing springs on the North Fork of the Gunnison River, Delta County, Colorado', *Proc. Col. Sci. Soc.,* 8, 1–30
Hearne, T. (1711): '*The Itinerary of John Leland*', vol. 6, Oxford
Heath, C.R., Leadbeater, B.S.C. and Callow, M.E. (1995): 'Effect of inhibitors on calcium carbonate deposition mediated by freshwater algae', *J. appl. Phycol.*, 7, 367–380
Heimann, A. and Sass, E. (1989): 'Travertines of the northern Hula Valley, Israel', *Sedimentology,* 36: 95–108
Heinrich, N. (1967): 'Les barrages de travertin du Williers (Lorraine Belge)', *Rev. Belge Géogr.,* 91, 79–87
Heizmann, E.P.J. and Fahlbusch,V. (1983): 'Die mittelmiozäne Wirbeltierfauna von Steinberg (Nördlinger Ries); Eine Übersicht', *Mitt. Bayer. St. Palaönt. u. Hist. Geol.*, 23, 83–93
Helmont, J.B. van (1648): *Ortus medicinae,* Amsterdam
Hendy, C.H. (1971): 'The isotopic geochemistry of speleothems – I. The calculation of the effects of different modes of formation on the isotopic composition of speleothems and their applicability as palaeoclimatic indicators', *Geochim. Cosmochim. Acta.,* 35, 801–824
Hendy, C.H. and Wilson, A.T. (1968): 'Paleoclimatic data from speleothems', *Nature*, 219, 48–51
Henley, R.W. (1996): 'Chemical and physical context for life in terrestrial hydrothermal systems', 61–82, in: G.R. Bock, J.A. Goode (eds), *Evolution of Hydrothermal Ecosystems on Earth (and Mars?)*, Ciba Foundation , Chichester, UK (J. Wiley & Sons)
Hennig, G.J., Grün, R., Brunnacker, K. and Pecsi, M. (1983a): 'Th-230/U-234 and ESR age determinations of spring deposited travertines in Hungary', *Eiszeitalter u. Gegenw.*, 33, 9–19
Hennig, G.J., Grün, R. and Brunnacker, K. (1983b): 'Speleothems, travertines and paleoclimates', *Quat. Res.*, 20, 1–29
Herbst, D.B. and Bradley, T.J. (1993): 'A population model for the alkali fly at Mono Lake: depth distribution and changing habitat availability', *Hydrobiologia*, 267, 191–201
Héribaud, J. (1920): 'Les Diatomées des Travertins d'Auvergne', *Impr. Médic. Scie. Bruxelles*, (for 1920), 1–206
Herman, J.S. and Lorah, M.M. (1987): 'CO_2 outgassing and calcite precipitation in Falling Spring Creek, Virginia, U.S.A., *Chem. Geol.*, 62, 251–262
Herman, J.S. and Lorah, M.M. (1988): 'Calcite precipitation rates in the field: measurement and prediction for a travertine-depositing stream', *Geochim. Cosmochim. Acta*, 52, 2347–2355
Herman, J.S. and Hubbard, D.A. Jr. (1990): 'A comparative study of travertine-marl-depositing streams in Virginia', 43–64, in: J.S. Herman, D.A. Hubbard Jr. (eds). *Travertine-Marl: Stream Deposits of Virginia*, Virginia Division of Mineral Resources Publication 101, Charlottesville, Va. (Virginia Division of Mineral Resources)
Herrmann, H. (1957): 'Die Entstehungsgeschichte der postglazialen Kalktuffe in der Umgebung von Weilheim (Oberbäyern)', *Neues Jb. Geol. Paläont. Abh.*, 105, 11–46
Hevisi, A. (1970): 'Az algák és Mohak szerepe a bükki forrasmeszko kepzodeseben', *Botanikai Közlem.*, 57, 233–244
Hewett, D.F., Shannon, E.V. and Gonyer, F.A. (1928): 'Zeolites from Richter Hot Springs, Grant County, Oregon', *Proc. U.S. Natn. Mus.,* 73, 18
Hill, C.A. (1978): 'Mineralogy of Ogle Cave', *Nat. Speleol. Soc. Bull.*, 40, 19–24

Hill, C.A. and Forti, P. (1997): *Cave Minerals of the World.* 2nd Edn., 463 pp., Alabama (National Speleological Society)

Hiltermann, H. (1977): 'Die Sinterkalke (Travertin) von Bad Laer am Teutoberger Wald', *Natur u. Heimat,* 37, 77–80

Høeg, O.A. (1929): 'Studies in stromatolites I. A postglacial marine stromatolite from southeastern Norway', *K. nor. Vid. Selsk. Skr.*, (for 1929), 1–60

Hoffer-French, K.J. and Herman, J.S. (1989): 'Evaluation of hydrological and biological influences on CO2 fluxes from a karst stream', *J. Hydrol.*, 108, 189–212

Hoffman, P.E. (1975): 'Shoaling-upward shale-to-dolomite cycles in the Rocknest Formation (Lower Proterozoic). Northwest Territories, Canada', 257–265, in: R.N. Ginsburg (ed.), *Tidal Deposits*, New York (Springer-Verlag)

Hoffman, P.E. (1976): 'Stromatolitic morphogenesis in Shark Bay, Western Australia', In Walter, M.R. (Ed.), pp. 261–271, *Stromatolites*, Elsevier, Amsterdam

Holdgate, M.W. (1955): 'The vegetation of some springs and wet flushes on Tarn Moor, near Orton, Westmorland', *J. Ecol.*, 43, 80–89

Holland, H.D., Kirsipu, T.W., Huebner, J.S. and Oxburgh, U.M. (1964): 'On some aspects of the chemical evolution of cave waters', *J. Geol.*, 72, 36–67

Holmes, P. (1965): *Principles of Physical Geology*, 1288 pp., 2nd edn. London, (T. Nelson)

Holyoak, D.T., Ivanovich, M. and Preece, R.C. (1983): 'Additional fossil evidence for the age of the interglacial tufas at Hitchin and Icklingham', *J. Conch.*, 31, 260–261

Horning, M. and Reynolds, B. (1995): 'The effects of natural and anthropogenic environmental changes on ecosystem processes at the catchment scale', *Trends Ecol. Evol.*, 10, 443–449

Horvatincic, N., Srdoc, D., Silar, J. and Tvrdikova, H. (1989): 'Comparison of the ^{14}C activity of groundwater and recent tufa from karst areas in Yugoslavia and Czechoslovakia', *Radiocarbon,* 31, 884–892

Horvatincic, N., Srdoc, D., Obelic, B. and Krajcar-Bronic, I. (1993): 'Environmental conditions for travertine formation in karst', 1–2, In: *Applications of isotope techniques in studying past and current environmental changes in the hydrosphere and atmosphere*, IAEA Symposium SM-329, Vienna (IAEA)

Horvatincic, N., Krajcar-Bronic, I. and Obelic, B. (2003): 'Differences in the ^{14}C age, d $\delta^{13}C$ and $\delta^{18}O$ of Holocene tufa and speleothem in the Dinaric Karst', *Palaeogeogr. Palaeoclim. Palaeoecol.,* 193, 139–157

House, W.A. (1981): 'Kinetics of crystallisation of calcite from calcium bicarbonate solutions', *J. chem. Soc.*, 77, 341–359

House, W.A. and Donaldson, L. (1985): 'Adsorption and coprecipitation of phosphate on calcite', *J. Colloid. Interf. Sci.,* 112, 309–324

House, W.A., Casey, H., and Smith, S. (1986a): 'Factors affecting the coprecipitation of inorganic phosphate with calcite in hardwaters –II', *Wat. Res.,* 20, 923–927

House, W.A., Casey, H., Donaldson, L. and Smith, S. (1986b): 'Factors affecting the coprecipitation of inorganic phosphate with calcite in hardwaters –1', *Wat. Res.,* 20, 917–922

Howard, A.P. (1948): 'An unusual type of natural bridge', *Am. J. Sci.,* 246, 593

Howsam, P. (1990): 'Well performance deterioration: an introduction to cause processes', 19–24, in: P. Howsam (ed.), *Water Wells: Monitoring, Maintenance and Rehabilitation*. London (Chapman and Hall)

Hrdlicka, A. (1925): 'The Taungs Ape', *Am. J. phys. Anthrop.*, 8, 379–392

Huang, Y. –M. and Fairchild, I.J. (2001): 'Partitioning of Sr^{2+} and Mg^{2+} into calcite under karst-analogue experimental conditions', *Geochim. Cosochim. Acta*, 65, 47–62

Huang, Y. -M. and others (2001): 'Seasonal variation in Sr, Mg and P in modern speleothems (Grotta di Ernesto, Italy)', *Chem. Geol.*, 175, 429–448

Hubbard, D.A. Jr. and Herman, J.S. (1990): 'Overview of travertine-marl volume', 1–4, in: J.S. Herman, D.A. Hubbard Jr.(eds), *Travertine-marl: Stream Deposits of Virginia,* Virginia Division of Mineral Resources, Publication 101, Charlottesville, Va. (Virginia Division of Mineral Resources)

Hubbard, D.A. Jr., Herman, J.S. and Bell, P.E. (1990): 'Speleogenesis in a travertine scarp: observations of sulfide oxidation in the subsurface', 177–184, in: J.S. Herman, D.A. Hubbard Jr. (eds), *Travertine-marl: Stream Deposits of Virginia,* Virginia Division of Mineral Resources, Publication 101, Charlottesville, Va. (Virginia Division of Mineral Resources)

Huckreide, R. (1975): 'Ein landschaftsgeschichtlich bedeutsamer Quellkalk im Tiroler Oberimm Tal', *Eiszeitalter Gegenw.*, 26, 181–189

Hull, E. (1872): 'A Treatise on the Building and Ornamental Stones of Great Britain and Foreign Countries', 333 pp., London

Humphreys, W.F., Awramik, S.M. and Jebb, M.H.P. (1995): 'Freshwater biogenic tufa in Madang Province, Papua New Guinea', *J.R. Soc. Western Australia*, 78, 43–54

Hunt, C.B. and Mabey, D.R. (1966): 'Stratigraphy and structure, Death Valley, California', *U.S. Geol. Surv. Prof. Paper*, 494-A, 1–162
Huntley, B. and Prentice, I.C. (1988): 'July temperatures in Europe from pollen data, 6000 years before present', *Science*, 241, 687–690
Hurley, P.M., Fairburn, H.W. and Pinson, W.H. Jr. (1966): 'Rb-Sr evidence in origin of potash-rich lavas in western Italy', *Earth Planet Sci. Lett.*, 5, 301–306
Hutcheon, I.E. and Abercrombie, H.J. (1989): 'The role of silicate hydrolysis in the origin of CO_2 in sedimentary basins', 321–324, in: D.L. Miles (ed). *Proc. International Symposium Water-rock Interaction*, Rotterdam (Balkema)
Hyde, H.A., Wade, A.E. and Harrison, S.G. (1978): '*Welsh Ferns*,' 6th Edn. 178 pp., Cardiff (National Museum of Wales)
Hynes, H.B.N. (1970): *The Ecology of Running Waters*, 555 pp., UK (Liverpool University Press)
Ichikuni, M. (1973): 'Partition of strontium between calcite and solution: effect of substitution by manganese', *Chem. Geol.,* 11, 315–319
Ichikuni, M. and Kikuchi, K. (1972): 'Retention of boron by travertines', *Chem. Geol.,* 9, 13–21
Ide, F.P. (1935): 'The effect of temperature on the distribution of the mayfly fauna of a stream', *Univ. Toronto Stud. Biol.*, 39, 9–76
Ihlenfield, C., Norman, M.D., Gagan, M.K., Drysdale, R.N., Maas, R. and Webb, J. (2003): 'Climatic significance of seasonal trace element and stable isotope variations in a modern freshwater tufa', *Geochim. Cosmochim. Acta*, 67, 2341–2357
Ingen-Housz, J. (1796): An Essay on the Food of Plants and the Restoration of Soils. London
Iler, R.K. (1979): 'The Chemistry of Silica, Solubility, Polymerization, Colloid and Surface Properties, and Biochemistry', 866 pp., New York (J. Wiley & Sons)
Irion, G. and Müller, G. (1968): 'Mineralogy, petrology and chemical composition of some calcareous tufa from the Schwäbische Alb, Germany', 157–171, in: G. Müller, G.M. Freidman (eds), *Carbonate Sedimentology in Central Europe*, New York, (Springer)
Iserentant, R. (1988): 'Les diatomées d'un travertin de Pente (<Cron>) en Lorraine', *Mem. Soc. Roy. Bot. Belg.*, 10, 17–25
Ishigami, T. and Suzuki, R. (1977): 'Factors affecting the crystalline form of calcareous sinters', *Geochem. Tokyo,* 11, 9–13
Ivandic, N. and Klavic, Z. (1996): 'Tourism revitalization in the Plitvice Lakes National Park in the Transition Period', *Turizam*, 44, 306–323
Ivanova, I.K. (1946): 'La stratigraphie des gisements de travertins du Mont Machouk aux environs de Piatigorsk', *Soc. Nat. Moscow B. Sect. Geol.*, 21, 21–44
Jaag, O. (1938): 'Die Kryptogamenflora des Rheinfalls und des Hochrheins von Stein bis Eglisau', *Mitt. Naturf. Ges. Schaffhausen,* 14, 1–158
Jackson, J.W. (1922): 'On the tufaceous deposits of Caerwys, Flintshire and the Mollusca contained therein', *Lancs. Cheshire. Nat.* 14, 147–158
Jacobson, R.L. and Langmuir, D. (1970): 'The chemical history of some spring waters in carbonate rocks', *Ground Water*, 8, 5–9
Jacobson, R.L. and Usdowski, E. (1975): 'Geochemical controls on a calcite precipitating spring', *Contr. Mineral. Petrol.,* 51, 65–74
Jakucs, K. (1977): *Morphogenetics of Karst Regions,* 284 pp., Bristol, (Adam Hilger)
James, N.P. and Choquette, P.W. (1984): 'Diagenesis 9. Limestones – the meteoric diagenetic environment', *Geoscience Canada,* 11, 161–194
Jánossy, D. (1977): 'Die fossilen Vogelreste aus den Travertinen von Taubach', *Quartärpaläontologie*, 2 (1976), 171–175
Janssen, A., Swennen, R., Podoor, N. and Keppens, E. (1999): 'Biological and diagenetic influence in recent and fossil tufa deposits from Belgium', *Sediment. Geol.*, 126, 75–95
Jehl. J.R. (1983): 'Tufa formation at Mono Lake, California', *California geol.,* 36, 3
Jennings, J.N. (1985): *Karst Geomorphology.* 293 pp., Oxford (Blackwell)
Jerz, H. (1983): 'Kalksinterbildung in Sudbayern und ihre zeitliche Einstufung', *Geol. Jb, Reihe A,* 71, 291–300
John, D.M., Champ, W.S.T. and Moore, J.A. (1982): 'The changing status of Characeae in four marl lakes in the Irish Midlands', *J. Life Sci. Roy. Dublin soc.,* 4, 47–71
Johnson, P.W. (1965): '*Field Guide to the Gems and Minerals of Mexico*', 105 pp.,Mentone, Ca. (Gem Books)
Johnston, J. (1915): 'The solubility-product of calcium and magnesium carbonates', *J. Am. Chem. Soc.,* 37, 2001–2020

Jones, F.G. and Wilkinson, B.H. (1978): 'Structure and growth of lacustrine pisoliths from recent Michigan marl lakes', *J. Sed. Petrol.,* 48, 1103–1111
Jones, B. and Kahle, C.F. (1986): Dendritic calcite crystals formed by calcification of algal filaments in a vadose environment. *J. Sed. Petrol.,* 56, 217–227
Jones, B. and Renaut, R.W. (1994): 'Crystal fabrics and microbiota in large pisoliths from Laguna Pastos Grandes, Bolivia.' *Sedimentology,* 41: 1171–1202
Jones, B. and Renaut, R.W. (1995): Noncrystallographic calcite dendrites from hot-spring deposits at Lake Bogoria, Kenya. *J. Sediment. Res.,* A65: 154–169
Jones, B. and Renaut, R.W. (1996): Skeletal crystals of calcite and trona from hot-spring deposits in Kenya and New Zealand. *J. Sed. Res.,* 66, 265–274
Jones, B. and Renaut, R.W. (2003): 'Hot spring and geysir sinters: the integrated product of precipitation, replacement, and deposition', *Can. J. Earth Sci.*, 40, 1549–1569
Jones, B.F. (1965): 'The hydrology and mineralogy of Deep Springs Lake, Inyo County, California', *U.S. Geol. Surv. Prof. Paper*, 502-A, 1–56
Jones, F.G. and Wilkinson, B.H. (1978): 'Structure and growth of lacustrine pisoliths from Recent Michigan marl lakes', *J. Sed. Petrol.,* 48, 1103–1111
Jones, R.L. and Keen, D.H. (1993): '*Pleistocene Environments in the British Isles*', Chapman and Hall, London, pp. 346
Julia, R. (1983): 'Travertines', 64–72, in: P.A. Scholle, D.G. Bebout, C.H. Moore (eds), *Carbonate Depositional Environments*, Tulsa, Ok. (American Association of Petroleum Geologists)
Julian, M. and Martin, J. (1981): 'Signification geomorphologique des tufs et des travertins', *Bull. Ass. Geogr. Fr.,* No. 479–480, 219–233
Jux, U. and Kempf, E.K. (1971): 'Stauseen durch Travertin absalz im Zentralafghanisanischen Hochgebirge', *Z.F. Geomorph. Suppl.,* 12, 107–137
Kahle, C.F. (1977): 'Origin of subaerial Holocene calcareous crusts: role of algae, fungi and sparmicritization', *Sedimentology,* 24, 413–435
Kahlke, H.D. (1978): 'Zusammenfassender Überblick zur stratigraphischen Stellung der travertine von Burgtonna in Thüringen', 171–174 in: H.D. Kahlke (ed.), *Das Pleistocene von Burgtonna, Quartaerpal. Abh. Ber. Inst. Quart. Weimar,* 3. Weimar
Kann, E. (1973): 'Bemerkungen zur Systematik und Ökologie einiger mit Kalk inkrustierter *Phormidium* arten', *Schweiz. Z. Hydrol.*, 35, 141–151
Kann, E. and Sauer, F. (1982): 'Die "Rotbunte Tiefenbiocoenose"', *Arch. Hydrobiol.*, 95, 181–195
Kano, A. and Fuji, H. (2000): 'Origin of the gross morphology and internal texture of tufas of Shirokawa Town, Ehime Prefecture, southwest Japan', *J. Geol. Soc. Jpn.*, 106, 397–412
Kano, A., Sakuma, K., Kaneko, N. and Naka, T. (1998): 'Chemical properties of surface waters in the limestone regions of western Japan: Evaluation of the chemical conditions for the deposition of tufas', *J. Sci. Hiroshima Univ. Ser. C.*, 11, 11–22
Kano, A., Kambayashi, T., Fujii, H., Matsuoka, J., Sakuma, K. and Ihara, T. (1999): 'Seasonal variation in water chemistry and hydrological conditions of tufa deposition of Shirokawa, Eihime Prefecture, southwestern Japan', *J. Geol. Soc. Jpn.*, 105, 289–304
Kargel, J.S. (1991): 'Brine volcanism and the interior structures of asteroids and icy satellites', *Icarus*, 94, 368–390
Katz, J.L. and Parsiegla, K.I. (1995): 'Calcite growth inhibition by ferrous and ferric iron', 11–20 in: Z. Amjad (ed), *Mineral Scale Formation and Inhibition*', New York (Plenum)
Kawaguchi, T. and Decho, A.W. (2001): 'Potential roles of extracellular polymeric secretions (EPS) in regulating calcification: a study of marine stromatolites, Bahamas', *Thalassus*, 17: 11–19
Kazmierczak, J., Ittekkot, V. and Degens, E.T. (1985): 'Biocalcification through time: environmental challenge and cellular response', *Paläont. Z.*, 59, 15–33
Kazmierczak, T.F., Tomson, M.B. and Nancollas, G.H. (1982): 'Crystal growth of calcium carbonate. A controlled composition kinetic study', *J. Phys. Chem.*, 86, 103–107
Keen, D.H. (1989): 'The molluscan fauna of a Flandrian tufa at Lower Beck, Malham, North Yorkshire', *J. Conch.*, 33, 173–178
Kele, S., Vaselli, O., Szabo, C. and Minissale, A. (2003): 'Stable isotope geochemistry of Pleistocene travertine from Budakalász (Buda Mts, Hungary)', *Acta Geol. Hung.*, 46, 161–175
Kelts, K. and Hsu, K.J. (1978): 'Freshwater carbonate sedimentation', 295–323, in: A. Lerman (ed.), *Lakes: Chemistry, Geology, Physics*, New York (Springer-Verlag)
Kempe, S. and Emeis, K. (1985): 'Carbonate chemistry and the formation of Plitvice Lakes', *Mitt. Geol.-Paläont. Inst. Iuiv. Hamburg (SCOPE/UNEP Sonderbd.),* 58, 351–383

Kempe, S., Kazmierczak, J., Landmann, G., Konuk, T. Reimer, A. and Lipp, A. (1991): 'Largest known microbialites discovered in Lake Van, Turkey', *Nature,* 349, 605–608
Kendall, A.C. (1993): 'Columnar calcite in speleothems: discussion', *J. Sed. Petrol.,* 63, 550–552
Kendall, A.C. and Broughton, P.L. (1978): 'Origin of fabrics in speleothems composed of columnar calcite crystals', *J. Sed. Petrol.,* 48, 519–538
Kerney, M.P. (1955): 'On the former occurrence of *Vertigo parcedentata* (A. L. Braun) in Hertfordshire', *J. Conch.*, 24, 55–58
Kerney, M.P. (1959): 'An interglacial tufa near Hitchin, Herts', *Proc. Geol. Ass.*, 70, 322–337
Kerney, M.P. (1976): 'Mollusca from an interglacial tufa in East Anglia, with the description of a new species of *Lyrodiscus* Pilsbury (Gastropoda: Zonitidae)', *J. Conch.*, 29, 47–50
Kerney, M.P. (1977): 'A proposed zonation scheme for Lake-Glacial and Postglacial deposits using land Mollusca', *J. Archaeol. Sci.*, 4, 387–390
Kerney, M.P., Preece, R.C. and Turner, C. (1980): 'Molluscan and plant biostratigraphy of some Late Devensian and Flandrian deposits in Kent', *Phil. Trans. R. Soc. Lond. B.*, 291, 1–43
Kerney, M.P. and Cameron, R.A.D. (1979): '*A Field Guide to the Land Snails of Britain and North-west Europe,*' 288 pp., London (Collins)
Kerr, R.C. and Turner, J.S. (1996): 'Crystallization and gravitationally controlled ponding during the formation of mound springs, terraces, and "black smoker" flanges', *J. Geophys. Res.,* 101, 25125–25137
Khoury, H., Salameh, E. and Udluft, P. (1984): 'On the Zerka Ma'in (Therma Kallirhoes) travertine/Dead Sea (hydrohemistry, geochemistry and isotopic composition)', *N. Jb. Geol. Paläont. Mh.,* 8, 472–484
Kieft, T.L. and Caldwell, D.E. (1984): 'Weathering of calcite, pyrite and sulfur by *Thiothrix thiopara* in a thermal spring', *Geomicrobiol. J.*, 3, 201–216
Kindle, E.M. (1923): 'The physical and biological characteristics of certain types of marlyte balls from Manitoba and Michigan', *Trans. R. Soc. Canada,* 17, 105–114
Kindle, E.M. (1927): 'The role of thermal stratification in lacustrine sedimentation', *Trans. R. Soc. Canada,* 21, 1–36
Kirby, C.S. and Rimstidt, J.D. (1990): 'The geology and geochemistry of the Falls Hollow travertine deposit', 33–42, in: J.S. Herman D.A. Hubbard Jr. (eds), *Travertine-marl: Stream Deposits in Virginia*, Virginia Division of Mineral Resources Publication 101, Charlottesville, Va. (Virginia Division of Mineral Resources)
Kirkland, B.L., Lynch, L., Rahnis, M.A., Folk, R.L., Molineux, J.J. and McLean, R.C.C. (1999): 'Alternative origins for nannobacteria-like objects in calcite', *Geology*, 27, 347–350
Kitano, Y. (1962): 'A study of polymorphic formation of calcium carbonate in thermal springs with emphasis on temperature', *Bull. Chem. Soc. Japan,* 35, 1980–1985
Kitano, Y. (1963): 'Geochemistry of calcareous deposits found in hot springs.' *J. Earth Sci. Nagoya Univ.*, 11: 68–100
Kitano, Y. and Hood, D.W. (1965): 'The influence of organic material on the polymorphic crystallization of calcium carbonate', *Geochim. Cosmochim. Acta,* 29, 29–41
Kite, J.S. and Allamong, D.M. (1990): 'The morphology and stratigraphy of calcareous sediments in a small alluvial-colluvial fan, New Creek Mountain, Mineral County, West Virginia', 139–150, in: J.S. Herman, D.A. Hubbard Jr. (eds), *Travertine-marl: Stream Deposits of Virginia,* Virginia Division of Mineral Resources Publication 101, Charlottesville, Va. (Virginia Division of Mineral Resources)
Kiuru, H. (1980): 'Preventing corrosion by mains water in cast iron and steel pipes by increasing the hardness of the water in Savonlinna waterworks', *Finn. J. Wat. Econ. Hydraulic Agric. Eng.*, 21, 10–13
Klähn, H. (1923): 'Die Petrogenese der Kalktuffe nebst einigen sich daraus ergebenden geologische Problemen', *Geol. Arch.,* 2, 298–316
Klähn, H. (1926): 'Über Kalkmagnesia wässer der Ungegend von Streitberg und Muggendorf (fränkischer Jura) und ihre Ausscheidungsprodukte', *Zbl. Miner. Geol. Paläont. Abt. B.* (for 1926), 390–400
Klähn, H. (1927): 'Vergleichende paläolimnologische, sedimentpetrographische und tektonische Untersuchungen an miocänen Seen der Schwäbische Alb', *Neues Jb. Min. Geol. Paläont.,* 55, 274–428
Klappa, C.F. (1979): 'Calcified filaments in Quaternary calcretes: organo-mineral interactions in the subaerial vadose environment', *J. Sed. Petrol.,* 49, 955–968
Knoll, A.H. and Walter, M.R. (1996): 'The limits of palaeontological knowledge: finding the gold among the dross', 198–213, in: G.R. Bock, J.A. Goode (eds), *Evolution of Hydrothermal Ecosystems on Earth (and Mars?)*, Ciba Foundation, Chichester, UK , (J. Wiley & Sons)
Koban, C.G. and Schweigert, G. (1993): 'Microbial origin of travertine fabrics- two examples from Southern Germany (Pleistocene Stuttgart travertines and Miocene Riedöschingen travertine)', *Facies*, 29, 251–264
Kolkwitz, R. and Kolbe, R. (1923): 'Zur Kenntnis der Kalktuffbildung durch Grünalgen', *Ber. Dt. Bot. Ges.*, 41, 312–316

Komarek, J. and Kann, E. (1973): 'Zur Taxonomie und Ökologie der Gattung *Homoeothrix*', *Arch. Protistenk.*, 115, 173–233
Konhauser, K.O., Phoenix, V.R., Bottrell, S.H., Adams, D.G. and Head, I.M. (2001): 'Microbial-sinter interactions in Icelandic hot spring sinter: possible analogues for some Precambrian siliceous stromatolites', *Sedimentology*, 48, 415–433
Konhauser, K.O., Jones, B., Reysenback, A.-L., and Renaut, R. (2003): 'Hot spring sinters: keys to understanding Earth's earliest life forms', *Can. J. Earth Sci.,* 40, 1713–1724
Korpás, L. (2003): 'Basic pattern of Quaternary travertine: a review with special regard to the Hungarian deposits', *Acta Geol. Hung.*, 46, 131–148
Koschel, R., Jurgen, B., Proft, G. and Recknagel, F. (1983): 'Calcite precipitation as a natural control mechanism for eutrophication', *Arch. Hydrobiol.*, 98, 380–408
Kovanda, J. (1974): 'Bemerkungen zur Geologie der Susswasserkalke Nordungarns (N. Hungary)', *Sborn. Geologick. Ved. Antropozoikum,* 10, 91–109
Kraglievich, J.L. and Reig, O.A. (1954): 'Un nuevo procionido del plioceno de Las Playas (provincia de Cordoba)', *Assoc. Geol. Argentina Rev.*, 9, 210–231
Krajcar-Bronic, I., Horvantincic, N., Srdoc, D. and Obelic, B. (1986): 'On the initial ^{14}C activity of karst aquifers with short mean residence time', *Radiocarbon*, 28, 436–440
Krajcar-Bronic, I., Horvatincic, N., Srdoc, D. and Obelic, B. (1992): 'Experimental determination of 14C initial activity of calcareous deposits', *Radiocarbon*, 34, 593–601
Kretzoi, M. and Dobosi, V.T. (1990): '*Vértesszölös, Man, Site and Culture*', 56 pp.,Budapest (Akadémiai Kiadó)
Krolopp, E. (1965): 'Mollusc fauna of the sedimentary formation of the Quaternary period, Hungary', *Acta Geol. Acad. Sci. Hung.*, 9, 153–160
Krolopp, E. (1969): 'Die jungpleistozäne Molluskenfauna von Tata (Ungarische VR)', *Ber. Dt. Ges. Geol. Wiss., Reihe A.*, 14, 491–505
Krolopp, E. (2003): 'The importance of mollusc fauna in the study of travertine deposits', *Földtany Közlöny*, 134, 219–225
Kronfeld, J., Vogel, J.C., Rosenthal, E. and Weinstein-Evron, M. (1988): 'Age and paleoclimatic implications of the Bet Shean travertines', *Quat. Res.,* 30, 298–303
Krumbein, W.E. and Giele, C. (1979): 'Calcification in a coccoid-cyanobacterium associated with the formation of desert stromatolites', *Sedimentology*, 26, 593–604
Krumbein, W.E. and Potts, M. (1979): '*Girvanella*-like structures formed by *Plectonema gloeophilum* Borzi (Cyanophyta) from the Borego Desert in S. California', *Geomicrobiol. J.*, 1, 211–218
Krüper, F. (1930): 'Über Verkalkungserscheinungen bei Dipteren-Larven und ihre Ursachen', *Arch. Hydrobiol.*, 22, 185–219
Kurck, C. (1901): 'Kalktuffen vid Benestad', *Bihang. Till. K. Svensk. Vet. Akad. Handl.*, 26, 1–79
Labeyrie, I., Duplessy, I.C., Delibrias, G., and Letolle, R. (1967): 'Étude des température des climats anciens par la mesure de l'oxygène 18, du carbon 13 et du carbon 14 dans les concretions des carvernes', 153–160, in: *Radioactive Dating and Methods of Low-level Counting,* Vienna (IAEA)
Lambert, A. (1955): 'Remarques sur les dépôts de travertins par les cours d'eau et sur leurs conséquences morphologiques', *Bull. Soc. Géogr. Fr.,* 5, 577–588
Lampert, R.J. (1989): 'Archaeology', 7–12, in: W. Zeidler, W.F. Ponder (eds), *Natural History of Dalhousie Springs*, Adelaide (South Australian Museum)
Lamplugh, G.W. (1902): 'Calcrete', *Geol. Mag.,* 9, 575
Lang, J. and Lucas, G. (1970): 'Contribution à l'étude de biohermes continentaux: barrages des lacs de Band-e-Amir (Afghanistan central)', *Bull. Soc. Géol. Fr.,* 12, 834–842
Lang, J. and Pierre, J.F. (1974): 'Contribution à l'étude des diatomées de quelques depôts carbonatées actuels hydrothermaux et lacustres de l'Afghanistan central', *Bull. Acad. Soc. Lorr. Sci.*, 13, 39–54
Lang, J., Pascal, A. and Salomon, J. (1992): 'Caractérisation pétrographique de divers carbonates continentaux holocenes du Jura français (Arbois, Chalain, Dortan). Implications paléogéographiques', *Z. Geomorph. N.F.,* 36, 273–291
Langmuir, D. (1971): 'The geochemistry of some carbonate groundwaters in central Pennsylvania', *Geochim. Cosmochim. Acta,* 35, 1023–1045
Lantos, M. (2004): 'Magnetostratigraphic correlation of Quaternary travertine sequences in NE Transdanubia', *Földtani Közlöny*, 134, 227–236
L'Apparent, A.F. de (1964): 'Region de Paris. Excursions Géologiques et Voyages Pédogogiques', Paris (Herman)
L'Apparent, A.F. de (1966): 'Les depôts de travertins des montagnes Afghanes à l'ouest de Kabul', *Rev. Géogr. phys. geol. Dyn.,* 8, 351–357

Larsen, D. (1994): 'Origin and paleoenvironmental significance of calcite pseudomorphs after ikaite in the Oligocene Creede Formation, Colorado', *J. Sed. Res.*, A64, 593–603

Latham, A.G. and Ford, D.C. (1993): 'The paleomagnetism and rock magnetism of cave and karst deposits', 1–216, in: D.F. Aissaoni, D.F. McNeill, N.F. Hurley (eds), *Applications of Paleomagnetism to Sedimentary Geology*, Society of Economic Paleontologists and Geologists, Tulsa, Oklahoma

La Touche, T.D. (1906): 'Note on the natural bridge in the Gokteik Gorge', *Record. Geol. Surv. India,* 33, 49–54

La Touche, T.D. (1913): 'Geology of the Northern Shan States', *Mem. Geol. Surv. India*, 39, 1–379

Lauritzen, S. –E., Haugen, J.E., Lovlie, R. and Gilje-Nielsen, H. (1994): 'Geochronological potential of isoleucine epimerization in calcite speleothems', *Quat. Res.,* 41, 52–58

Lebron, I. and Suarez, D.L. (1996): 'Calcite nucleation and precipitation kinetics as affected by dissolved organic matter at 25 °C and pH>7.5, *Geochim. Cosmochim. Acta*, 60, 65–76

Leeman, W.P., Doe, B.R. and Whelan, J. (1977): 'Radiogenic and stable isotope studies of hot spring deposits in Yellowstone National Park and their genetic implications', *Geochem. J.,* 11, 65–74

Leggitt, V.L. and Cushman, R.A. Jr. (2001): 'Complex caddis fly-dominated bioherms from the Eocene Green River Formation', *Sediment. Geol.*, 145, 377–396

Lehmann, H. (1954): 'Der tropische Kegelkarst auf den Grossen Antillen', *Erdkunde,* 8, 130–139

Leitmeier, H. (1909): 'Die Absatze des Mineralwassers von Rohitsch-Sauerbrunn in Steiermark', *Z. Kryst. Min.* 47, 104–123

Leland, J. (1538): '*The Itinerary of John Leland*', 9 vol., (published in 1711 by T. Hearne, from the original MS in the Bodleian Library, Oxford)

Leonard, J.W. (1939): 'Comments on the adequacy of accepted stream bottom sampling techniques', *Trans. 4th N. Amer. Wildlife Conf.*, (for 1939), 288–295

Leslie, A.B., Tucker, M.E. and Spiro, B. (1992): 'A sedimentological and stable isotopic study of travertines and associated sediments within Upper Triassic lacustrine limestones, South Wales, U.K.', *Sedimentology*, 39, 613–629

Li, B., Yuan, D., Lauritzen, S.-E., Qin, J. and Lin, Y. (1998): 'The Younger Dryas event and Holocene climate fluctuations recorded in a stalagmite from the Panlong Cave of Guilin', *Acta Geologica Sinica*, 72, 455–465

Li, W.X. and others (1989): 'High precision mass-spectrometric uranium-series dating of cave deposits and implications for paleoclimatic studies', *Nature*, 339, 534–536

Libavius, A. (1597): *De judico aquarum mineralium,* Francofurti

Liddle, R.A. (1928): *The Geology of Venezuela and Trinidad,* 552 pp., Texas (J. P. McGowan)

Likens, G.E., Bormann, F.H., Johnson, N.M., Fisher, D.W. and Pierce, R.S. (1970): 'Effects of forest cutting and herbicide treatment on nutrient budgets in the Hubbard Brook Watershed system', *Ecol. Monogr.*, 40, 23–47

Limondin-Lozouet, N. and Preece, R.C. (2004): 'Molluscan successions from the Holocene tufa of St Germain-le-Vasson, Normandy (France) and their biogeographical significance', *J. Quat. Sci.*, 19, 55–71

Lindgren, W. (1910): 'The hot springs at Ojo Caliente and their deposits', *Econ. Geol.,* 5, 22–27

Lindgren, W. (1933): '*Mineral Deposits*,' 4th Edn. 930 pp.,New York and London (McGraw Hill)

Lindner, L. and Petelski, K. (1984): 'Travertine dammed lakes and glaciers of the north western Hindu Kush', *Quaternary Studies Poland,* 5, 99–116

Ling, H.U., Thomas, D.P. and Tyler, P.A. (1989): 'Larger filamentous algae (Chlorophyta and Chrysophyta) from Dalhousie and other mound springs', 53–56, in W. Zeidler, W.F. Ponder(eds), *Natural History of Dalhousie Springs*, Adelaide (South Australian Museum)

Linge, H., Lauritzen, S.-E., and Lundberg, J. (2001): 'Stable isotope stratigraphy of a late Last Interglacial speleothem from Rana, northern Norway', *Quat. Res.,* 56, 155–164

Link, M.H., Osborne, R.H., and Awramik, S.M. (1978): 'Lacustrine stromatolites and associated sediments of the Pliocene Ridge Route Formation, Ridge Basin, California', *J. Sed. Petrol.*, 48, 143–158

Lipiarski, I. (1971): 'Lower Permian flora in the Karniowice Travertine, Kracow', *Pr. Inst. Geol.*, 58, 5–112

Lippmann, F. (1973): *Sedimentary Carbonate Minerals*, 228 pp, Heidelberg (Springer-Verlag)

Liu, Z., Svensson, U., Dreybrodt, W., Daoxian, Y. and Buhmann, D. (1995): 'Hydrodynamic control of inorganic precipitation in Huanglong Ravine, China: field measurements and theoretical prediction of deposition rates', *Geochim. Cosmochim. Acta*, 59, 3087–3097

Liu, Z. and Dreybdrodt, W. (1997): 'Dissolution kinetics of calcium carbonate minerals in H_2O-CO_2 solutions in turbulent flow. The role of the diffusion boundary layer and the slow reaction $H_2O + CO_2 = H^+ + HCO_3^-$', *Geochim. Cosmochim. Acta,* 61, 2879–2889

Livett, G.M. (1893): 'Early-Norman churches in and near the Medway Valley', *Archaeol. Cantiana*, 20, 137–154

Livett, G.M. (1895): 'Early Norman churches in and near the Medway Valley (II)', *Archaeol. Cantiana*, 21, 260–272

Livingstone, D., Pentecost, A. and Whitton, B.A. (1984): 'Diel variations in nitrogen and carbon dioxide fixation by the blue-green alga *Rivularia* in an upland stream', *Phycologia*, 23, 125–133
Livnat, A. and Kronfeld, J. (1985): 'Paleoclimatic implications of U-series dates for lake sediments and travertines in the Avava Rift Valley, Israel', *Quat. Res.*, 24, 164–172
Lohest, M. (1901): 'Le tuf de la vallée du Hoyoux', *Ann. Soc. Géol. Belge.*, 28, B295-B298
Lohest, M. and Forir, H. (1904): 'Les cascades de Barse et le tuf du Hoyoux', *Ann. Soc. Géol. Belg.*, 31, B155-B160
Lojen, S., Dolenec, T., Vokal, B., Cukrov, N., Mihelkcic, G. and Papesch, W. (2004): 'C and O stable isotope variability in recent freshwater carbonates (River Krka, Croatia)', *Sedimentology*, 51, 361–375
Lookene, E. (1968): 'Distribution and character of the spring deposits in the Otepaeae Hills', *Uchenye Zapiste Tertuskogo Gos. Univ.,* No. 213, 34–57
Lookene, E. and Utsal, K. (1971): 'The mineral composition and age of Holocene fresh-water carbonate sediments in Southern Estonia', *Uchenye Zapiske Tartuskogo Gos. Univ.*, 286, 164–194
Lorah, M.M. and Herman, J.S. (1988): 'The chemical evolution of a travertine-depositing stream: geochemical processes and mass transfer reactions', *Water Resources Res.*, 24, 1541–1552
Lorah, M.M. and Herman, J.S. (1991): 'Geochemical evolution and calcite precipitation rates in Falling Spring Creek, Virginia', 17–32, in: J.S. Herman, D.A. Hubbard Jr. (eds), *Travertine-marl: Stream Deposits of Virginia*, Virginia Division of Resources Publication 101, Charlottesville, Va. (Virginia Division of Mineral Resources)
Love, K.M. and Chafetz, H.S. (1988): 'Diagenesis of laminated travertine crusts, Arbuckle Mountains, Oklahoma.' *J. Sed. Petrol.,* 58: 441–445
Love, K.M. and Chafetz, H.S. (1990): 'Petrology of Quaternary travertine deposits, Arbuckle Mountains, Oklahoma', 65–78, in: J.S. Hermann, D.A. Hubbard Jr. (eds), *Travertine-marl: Stream Deposits of Virginia*, Virginia Division of Mineral Resources Publication 101, Charlottesville, Va. (Virginia Division of Mineral Resources)
Lowenstam, H.A. (1986): 'Mineralization processes in monerans and protoctists', 1–17, in: B.S.C. Leadbeater, R. Riding (eds), *Biomineralization in Lower Plants and Animals*, Oxford (Clarendon Press)
Lowenstam, H.A. (1990): 'S-layer similarity in matrix and mineral structure of a *Leptothrix* species (Bacteria)', 3–9, in: S. Suga, H.Nakahara (eds), *Mechanisms and Phylogeny of Mineralization in Biological Systems*, Tokyo (Springer-Verlag)
Lowenstam, H.A. and Wiener, S. (1982): 'Mineralization by organisms and the evolution of biomineralization', 191–204, in: P. Westbroek, E.W. De Jong (eds), *Biomineralization and Biological Metal Accumulation*, Holland (D. Riedel)
Lozek, V. (1969): 'Molluscan characteristics of the Pleistocene warm periods with particular reference to the last interglacial', *Ber. dt. Ges. geol. Wiss. Reihe A.,* 14, 439–469
Lu, Gouping, and Li, Xinjian (1992): 'A study of cold-water surface depositional landforms in Huanglong Scenic Spot, Sichuan Province', *J. Chengdu College Geol.,* 19, 55–64
Lu, G., Zheng, C., Donahoe, R.J. and Lyons, W.B. (2000): 'Controlling processes in a $CaCO_3$ precipitating stream in Huanglong Natural Scenic District, Sichuan, China', *J. Hydrol.*, 230, 34–54
Lund, J.W. (1996): 'Balneological use of thermal and mineral waters in the U.S.A.', *Geothermics,* 25, 103–147
Lund, J.W. (1978): 'Steamboat Springs, Nevada', *Geo-heat Center Quart. Bull.*, 3, 1–4
Lyell, C. (1829): 'On a recent formation of freshwater limestone in Forfarshire and on some recent deposits of freshwater marl', *Trans. Geol. Soc. Lond.,* 2, 73–96
Lynne, B.Y. and Campbell, K.A. (2003): 'Diagenetic transformations (opal-A to quartz) of low- and mid-temperature microbial textures in siliceous hot-spring deposits, Taupo Volcanic Zone, New Zealand', *Can. J. Earth Sci.*, 40, 1679–1696
Mabbutt, T.A. (1977): *Desert Landforms.* 340 pp., Mass. (MIT Press)
McConnaughey, T. (1989): '^{13}C and ^{18}O isotopic disequilibrium in biological carbonates II: *In vitro* simulation of kinetic isotope effects', *Geochim. Cosmochim. Acta,* 53, 163–171
McConnaughey, T.A., Labaugh, J.W., Rosenberry, D.O., Striegl, R.G., Reddy, M.A., Schuster, P.F. and Carter, V. (1994): 'Carbon budget for a groundwater-fed lake: calcification supports summer photosythesis', *Limnol. Oceanogr.*, 39, 1319–1332
McDermott, F. and others (1999): 'Holocene climate variability in Europe: evidence from $\delta^{18}O$, textural and extension-rate variations in three speleothems', *Quat. Sci. Revs.,* 18, 1021–1038
McDermott, F., Mattey, D.P. and Hawkesworth, C. (2001): 'Centennial-scale Holocene climate variability revealed by a high-resolution speleothem $\delta^{18}O$ record from SW Ireland', *Science*, 294, 1328–1331
McFall, C.C. (1968): 'Reconnaissance geology of the Concepcion Bay area, Baja, California', *Stanford Univ. Pubs. Geol. Sci.*, 10, 25

McFarland, E.R. and Sherwood, W.C. (1990): 'Description and origin of the calcite-rich Massanetta Variant Soil Series at Mount Crawford, Virginia, 151–16, in: J.S. Herman, D.A. Hubbard Jr. (eds), *Travertine-marl: Stream Deposits of Virginia.* Virginia Division of Mineral Resources, Publication 101, Charlottesville, Va. (Virginia Division of Mineral Resources)

McGannon, D.E. (1975): 'Primary fluvial oolites', *J. sed. Petrol.*, 45, 719–727

McKay, C.P. and Nedell, S.S. (1988): 'Are there carbonate deposits in Valles Marineris, Mars?', *Icarus*, 73, 142–148

McKay, D.S., Gibson, E.K., Thomas-Keprta, K.L., Vali, H., Romanek, C.S., Clemett, S.J., Chillier, X.D.F., Maechling, C.R. and Zare, R.N. (1996): 'Search for past life on Mars: possible relic biogenic activity in Martian meteorite ALH84001', *Science*, 273, 924–930

McKee, J.K. (1993a): 'Formation and geomorphology of caves in calcareous tufas and implications for the study of Taung fossil deposits', *Trans. R.Soc. S. Afr.,* 48, 307–322

McKee, J.K. (1993b): 'Faunal dating of the Taung hominid fossil deposit', *J. Human. Evol.*, 25, 363–376

McMillan, N.F. and Zeissler, H. (1986): 'The tufa deposit at Caerwys, North Wales, and its molluscan fauna', *Amateur Geologist*, 11, 3–11

Machado, B.I. (1967): 'Paleocene continental gastropods of Rio de Janeiro State, Brazil', *Bolm. Inst. Geocienc. Univ. fed. Rio de Janeiro*, 1, 7–22

Machel, H.G. (1985): 'Cathodoluminescence in calcite and dolomite and its chemical interpretation', *Geosci. Canada,* 12, 139–147

Machette, M.N. (1987): 'Calcic soils of the south-western United States', *Geol. Soc. Am. spec. Pap.*, 203, 1–21

Madigan, M.T. (1986): '*Chromatium tepidum* sp. nov. a new thermophilic photosynthetic bacterium of the family Chromatiaceae', *Int. J. Syst. Bact.*, 36, 222–227

Magdefrau, K. (1956): *Paläobiologie der Pflanzen,* 396 pp., Jena (Gustav Fischer)

Magnin, F., Guendon, J.L., Vaudour, J. and Martin, P. (1991): 'Les travertins; accumulations aux systemes karstiques, sequences sedimentaires et paleoenvironments quaternaires', *Bull. Soc. Geol. Fr.,* 162, 585–594

Maizels, J.K. (1987): 'Plio-Pleistocene raised channel systems of the western Sharqiya (Wahiba), Oman', 31–50, in: L.E. Frostik, I. Reid (eds), *Geol. Soc. Lond. Special Publ.*, 35, London

Malesani, P. and Vannucchi, S. (1975): 'Precipitazione di calcite o di aragonite dalle acque termominerale in relazione alla genesi e all'evoluzione dei travertini', *Atti della R. Accademia d'Italia,* 58, 761–776

Malusa, J., Overby, S.T. and Parnell, R. (2003): 'Potential for travertine formation: Fossil Creek, Arizona', *Appl. Geochem.*, 18, 1081–1093

Manfra, L., Masi, U. and Turi, B. (1974): 'Effeti isotopici nella diagenesi dei travertini', *Geol. Romana,* 13, 147–156

Manfra, L., Masi, U. and Turi, B. (1976): 'La composizione isotopica dei travertini del Lazio', *Geol. Romana,* 15, 127–174

Mania, D. (1978): 'Zur Molluskenfauna aus der jungpleistozänen Deckschichtenfolge über dem Travertin von Burgtonna in Thüringen', *Quartärpal. Abh. Ber. Inst. Quart. Weimar,* 3, 203–205

Marker, A.F.M. (1976): 'The benthic algae of some streams in Southern England. I. Biomass of the epolithon in some small streams', *J. Ecol.*, 64, 343–358

Marker, A.F.M. and Casey, H. (1982): 'The population and production dynamics of benthic algae in an artificial re-circulating hard water stream', *Phil. Trans. R. Soc. Lond. B. Biol Sci.,* 298, 265–308

Marker, M.E. (1971): 'Waterfall tufas: a facet of karst geomorphology in South Africa', *Z.F. Geomorph. Suppl.*, 12, 138–152

Marker, M.E. (1973): 'Tufa formation in the Transvaal, South Africa', *Z. Geomorph.*, 17, 460–473

Markovic, M.J.D. (1950): 'Flore fossile du travertin de la vallée de Gradasnica, près de Soko Banja', *Mus. Hist. Nat. Pays Serbe B., Ser. A.*, 3, 119–130

Marston, R.A. (1982): 'The geomorphic significance of log steps in forest streams', *Ann. Am. Ass. Geogr.*, 72, 99–108

Martel, E.A. (1894): *Les Abimes, Les Eaux Souterraines, Les Cavernes, Les Sources, La Spelaeologie*. 578 pp., Paris (Delagrave)

Martín-Algarra, A., Martín-Martín, M., Andreo, B., Julia, R. and González-Gómez, C. (2003): 'Sedimentary patterns in perched spring travertines near Granada (Spain) as indicators of the paleohydrological and paleoclimatological evolution of a karst massif', *Sediment. Geol.*, 161, 217–228

Mathe, G. (1982): 'Der Kalktuff von Niedervogelsgang in Elbsandsteingebirge', *Abh. St. Mus. Miner. Geol. Dresden*, 31, 177–180

Mathews, H.L., Prescott, G.W. and Obenshain, S.S. (1965): 'The genesis of certain calcareous floodplain soils of Virginia', *Proc. Soil Sci. Soc. Am.*, 29, 729–732

Matonickin, I. and Pavletic, Z. (1962): 'Entwicklung der Lebensgemeinschaften und ihre Bedeutung für die Bildung und Erhaltung von Kalktuff-Wasserfällen', *Arch. Hydrobiol.,* 58, 467–473

Mawson, D. (1929): 'Some South Australian algal limestones in the process of formation', *Q.J. Geol. Soc. Lond.,* 85, 613–620
Meiggs, R. (1973): '*Roman Ostia*', 598 pp., Oxford (Clarendon Press)
Meixiang, Z. and Wei, T. (1987): 'Surface hydrothermal minerals and their distribution in the Tengchong geothermal area, China', *Geothermics,* 16, 181–195
Melezhik, V.A. and Fallick, A.E. (2001): 'Palaeoproterozoic travertines of volcanic affiliation from a ^{13}C-rich rift lake environment', *Chem. Geol.,* 173, 293–312
Merrill, G.P. (1903): '*Stones for Building and Decoration*', 506 pp., New York (J. Wiley and Sons)
Merz, M. and Zankl, H. (1993): 'The influence of culture conditions on growth and sheath development of calcifying cyanobacteria', *Facies*, 29, 75–80
Merz-Preiss, M. and Riding, R. (1999): 'Cyanobacterial tufa calcification in two freshwater streams: ambient environment, chemical thresholds and biological processes', *Sediment. Geol.*, 126, 103–124
Meunier, S. (1899): 'Observations relatives au dépôt de certains travertins calcaires', *C.R. Acad. Sci. Paris*, 129, 659–660
Meyer, H.J. (1984): 'Influence of impurity on the growth rate of calcite', *J. Cryst. Growth,* 66, 639–646
Meyrick, R.A. (2000): 'Holocene molluscan faunal history and environmental change from a tufa at Direndall, Luxembourg', *Bull. Soc. Préhist. Luxembourgeoise*, 22, 55–75
Meyrick, R.A. (2003): 'Holocene molluscan faunal history and environmental change at Kloster Mühle, Rheinland-Pfalz, western Germany', *J. Quat. Sci.*, 18, 121–132
Meyrick, R.A. and Preece, R.C. (2001): 'Molluscan successions from two Holocene tufas near Northampton, English Midlands', *J. Biogeogr.*, 28, 77–93
Michaelis, J., Usdowski, E. and Menschel, G. (1985): 'Partitioning of ^{13}C and ^{12}C on the degassing of CO_2 and the precipitation of calcite: Rayleigh type fractionation and a kinetic model', *Am. J. Sci.,* 285, 318–325
Minckley, W.L. (1963): 'The ecology of a spring stream Doe Run, Meade County, Kentucky', *Wildlife Monographs,* 11, 1–124
Mitchell, R.S. (1985): '*Dictionary of Rocks*', 228 pp., New York (Van Nostrand)
Mongini, M. (1973): 'Transformazione naturali ed umane delle cascate di Tivoli', *Riv. Geol. Ital.,* 80, 62–77
Monty, C.L.V. (1976): 'The origin and development of cryptalgal fabrics', 193–250, in: M.R. Walter (ed.). *Stromatolites.* Studies in Sedimentology 20, Amsterdam (Elsevier)
Monty, C.L.V. and Mas, J.R. (1981): 'Lower Cretaceous (Wealdian) blue-green algal deposits of the Province of Valencia, eastern Spain,' 85–120, in: C.L.V. Monty (ed.), *Phanerozoic Stromatolites.* Berlin (Springer-Verlag)
Moore, G.W. and Halliday, W.R. (1953): 'Nomenclature of erratic cave deposits', *Calif. Caver*, 5, 2–5
Morse, J.W. (1983): 'The kinetics of calcium carbonate dissolution and precipitation', 227–264 in: R.J. Reeder, (ed.), *Carbonates: Mineralogy and Chemistry, Reviews in Mineralogy,* Vol. 11, Washington D.C. (Mineralogical Society of America)
Morton, J. (1706): ' A letter from the Reverend Mr. Morton, A.M. and S.R.S. to Dr. Hans Sloane, S.R. Secr.', *Phil. Trans. R. Soc. Lond.*, 25, 2210–2214
Morton, J. (1712): '*The Natural History of Northamptonshire*', Northampton, UK
Mosseray, R. (1938): 'Principaux groupements végetaux observés dans le district jurassique belge', *Bull. Soc. Roy. Bot. Belg.,* 70, 148–161
Moulin, M.P. (1966): 'Importance et répartition paléogeographique des Cyanophycées dans le complexe fluvio-lacustre dit des "Calcaires de Castres" (Tarn)', *Actes Soc. Linn. Bordeaux B.*, 103, 1–12
Mountain, B.W., Benning, L.G. and Boerema, J.A. (2003): 'Experimental studies on New Zealand hot spring sinters: rates of growth and textural development', *Can. J. Earth Sci.,* 40, 1643–1667
Muffler, L.J.P. and White, D.E. (1968): 'Origin of CO_2 in the Salton Sea geothermal system, southeastern California, U.S.A.', *Proc. 23rd International Geological Congress*, *Prague.*, 17, 185–194
Müller, G. (1968): 'Exceptionally high strontium concentrations in fresh water onkolites and mollusk shells of Lake Constance', 116–127 in: G. Müller, G.M. Friedman (eds), *Recent Developments in Carbonate Sedimentology in Central Europe*, Berlin (Springer-Verlag)
Müller, G. (1971): 'Aragonite precipitation in freshwater lakes', *Nature*, 229, 18
Müller, G. and Oti, M. (1981): 'The occurrence of calcified planktonic green algae in freshwater carbonates', *Sedimentology*, 28, 897–907
Müller, G., Botz, R. and Linz, E. (1986): 'Oxygen and carbon isotope composition of calcareous tufa and speleothems from the Schwäbische Alb, W. Germany', *Neues Jb. Min. Mh.,* (1986): 289–296
Murray, G. (1895): 'Calcareous pebbles formed by algae', *Phycol. Bull.*, 3, 74–77
Murray, J.W. (1954): 'The deposition of calcite and aragonite in caves', *J. Geol.,* 62, 481–492
Nancollas, G.H. (1979): 'The growth of crystals in solution', *Adv. Colloid Interf. Sci.*, 10, 215–252

Nancollas, G.H. and Reddy, M.M. (1971): 'The crystallization of calcium carbonate. II. Calcite growth mechanism', *J. Coll. Interf. Sci.*, 37, 824–830

Naumann, C.F. (1850): *Lehrbuch der Geognosie,* Vol. 1. Leipzig (W. Engelman)

Needham, J. (Ed.) (1954): *Science and Civilization in China,* vol. 3, Cambridge (Cambridge University Press)

Neev, D. and Emery, K.O. (1967): 'The Dead Sea. Depositional processes and environments of evaporites', *Israel Geol. Surv. Bull.*, 41, 1–147

Newton, M.S. and Grossman, E.L. (1988): 'Late Quaternary chronology of tufa deposits, Walker Lake, Nevada', *J. Geol.,* 96, 417–433

Nickel. E. (1983): 'Environmental significance of freshwater oncoids, Eocene Guarga Formation, southern Pyrenees, Spain', 308–329, in: T.M. Peryt (ed.), *Coated Grains*, Berlin (Springer-Verlag)

Nicod, J. (1981): 'Répartition classification, relation avec les milieux karstiques et karstification', *Bull-Ass. Géogr. Fr. Paris,* No. 479–80, 181–187

Nielsen, A.V. (1965): 'Ekskursion til egren vest og nordvest for Kobenhavn', *Medd. Dansk. Geol. Foren.*, 16, 265–267

Nordhagen, R. (1921): 'Kalktuffstudier i Gudbrandsdalen', *Skr. Norske Vidensk-Akad. Mat. Nat. Kl.*, 9, 1–155

Nowak, J. (1938): 'Die Frage der Grenzen des polnischen Ölbeckens der Flyschzone', *Bull. Int. Acad. Sci. Pol. Cl. Math.-Nat. Ser. A.*, No. 7–7, 354–356

O'Connor, D.J. and Dobbins, W.E. (1958): 'Mechanism of reaeration in natural streams', *Trans. Am. Soc. Civil Eng.*, 123, 641–684

Ogawa, N. and Furukawa, Y. (2002): 'Surface instability of icicles', *Phys. Rev. E.,* 66, 041202

Ohle, W. (1937): 'Kalksystematik unserer Binnengewässer und der Kalkgehalt Rügener Bäche', *Geol. der Meere und Binnengewässer*, 1, 291–316

Okumura, M. and Kitano, Y. (1986): 'Coprecipitation of alkali metal ions with calcium carbonate', *Geochim. Cosmochim. Acta*, 50, 49–58

Omelon, C.R., Pollard, W.H. and Marion, G.M. (2001): 'Seasonal formation of ikaite ($CaCO_3.6H_2O$) in saline spring discharge at Expedition Fiord, Canadian High Arctic: assessing conditional constraints for natural crystal growth', *Geochim Cosmochim. Acta*, 65, 1429–1437

O'Neil, J.R., Clayton, R.N. and Mayeda, T.K. (1968): 'Oxygen isotope fractionation in divalent metal carbonates', *J. Chem. Phys.*, 51, 5547–5558

O'Neil, J.R. and Barnes, I. (1971): 'C^{13} and O^{18} compositions in some freshwater carbonates associated with ultramafic rocks and serpentinites: western United States', *Geochim. Cosmochim. Acta,* 35, 687–697

Opdyke, B.N., Gust, D. and Ledwell, J.R. (1987): 'Mass transfer from smooth alabaster surfaces in turbulent flows', *Geophys. Res. Lett.*, 14, 1131–1134

Ordoñez, S. and Garcia del Cura, M.A. (1983): 'Tertiary fluvial carbonates in Central Spain', 485–497, in: J.D. Collinson, J. Lewin (eds), *Modern and Ancient Fluvial Systems,* International Association of Sedimentologists Special Publication 6. Oxford (Blackwell)

Ordoñez, S., Gonzalez, J.A. and Garcia del Cura, M.A. (1986): 'Pétrographie et morphologie des édifices tuffeux quaternaires du centre de l'Espagne', *Mediterranée*, 1–2, 52–60

Osinski, G. (2003): 'Shocked into life', *New Scientist*, 13th September, 2003, 40–43

Özkul, M., Varol, B. and Alcicek, M.C. (2002): 'Depositional environments and petrography of the Denizli travertines', *Miner. Res. Expl. Bull.,* 125, 13–29

Ozol, A.A. (1974): 'Geochemistry of boron in travertine of the Pamir Mountains', *Akad. Nauk. SSSR. Dokl.*, 217, 926–928

Pache, M., Reitner, J. and Arp, G. (2001): 'Geochemical evidence for the formation of a large Miocene "travertine" mound at a sublacustrince spring in a soda lake (Wallerstein Castle Rock, Nördinger Ries, Germany)', *Facies*, 45, 311–230

Palissy, B. (1564): *'Recepte Véritable, par laquelle tous les hommes de la France pourront aprendre a Multiplier at Augmenter leurs Thresors'*, La Rochelle (Berton)

Paquette, J. and Reeder, R.J. (1995): 'Relationship between surface structure, growth mechanism, and trace element incorporation in calcite', *Geochim. Cosmochim. Acta*, 59, 735–749

Pareyn, C. and Salimeh, H. (1990): 'Dislocation catastrophique d'un tuf lapidifie dans l'arriere-pays d'Honfleur (Calvados, France)', *Bull. Centre Géomorph. Caen*, 38, 151–159

Paillet, J. –J., (1986): 'L'utilisation des concrétions de aqueduct de Nimes en tant que materiau du construction', *Mediterranée*, 1–2, 152–159

Panichi, C. and Tongiorgi, E. (1976): 'Carbon isotopic composition of CO_2 from springs, fumaroles, mofettes, and travertines of central and southern Italy', 815–825, in: *Proc. 2nd U.N. Symposium on Development and Use of Geothermal Resources*, San Francisco 1975

Pankow, J.F., Asher, W.E. and List, E.J. (1984): 'Carbon dioxide transfer at the gas/water interface as a function of system turbulence', 101–111, in: W. Brutsaert, G.H. Jirka (eds), *Gas Transfer at Water Surfaces*, Holland (Reidel.)
Panow, E. (1936): 'Permo-Carboniferous animal fossils from the travertine of Karniowice', *Roczn. Pol. Tow. Geol.*, 12, 36–41
Pant, G.B. and Tewari, S.D. (1984): 'On some aquatic bryophyte communities of Nainital and its environs (Western Himalayas)', *Geophytology,* 14, 137–142
Pant, G.B. and Tewari, S.D. (1988): 'An assessment of bryophytic vegetation of Naini Tal and Environs II. *J. Indian Bot. Soc.,* 67, 285–296
Paprocki, H., Holzenthal, R.W. and Cressa, C. (2003): 'A new species of *Smicridea* McLachan (Trichoptera: Hydropsychidae) from Venezuela and its role in travertine biogenesis', *J. North Am. Benthol. Soc.*, 22, 401–409
Parihar, N.S. and Pant, G. (1982): 'Bryophytes as rock builders – bryophytic communities associated with travertine formation at Sahasradhara, Dehra Dun', 277–295, in: D.D. Nautiyal (ed.), *Phyta, Studies of Living and Fossil Plants.* India (Allahabad)
Pavletic, Z. (1955): 'Die kalktuffbildenden Bryophyten in den Gewässern Südkroatiens und Bosniens', *Rev. Bryol. Lichenol.*, 24, 93–95
Pavletic, Z. and Golubic, S. (1956): '*Oocardium stratum* Naeg. in den Karstgewässern Südkroatiens', *Bull. Sci. Cons. Acads. RPF. Yougosl.*, 2, 110–111
Pazdur, A. (1988): 'The relations between carbon isotope composition and apparent age of freshwater tufaceous sediment', *Radiocarbon*, 30, 7–18
Pazdur, A., and Pazdur, M.F. (1986): '^{14}C dating of calcareous tufa from different environments', *Radiocarbon*, 28, 534–538
Pazdur, A. and Pazdur, M.F. (1988): 'Stable isotopes of Holocene calcareous tufa in southern Poland as paleoclimatic indicators', *Quat. Res.*, 30, 177–189
Pazdur, A., Pazdur, M.F. and Szulc, J. (1988): 'Radiocarbon dating of Holocene calcareous tufa in southern Poland', *Radiocarbon*, 30, 133–152
Peabody, F.E. (1954): 'Travertine and cave deposits of the Kaap Escarpment of South Africa, and the type locality of *Australopithecus africanus* Dart,' *Bull. Geol. Soc. Am.,* 65, 671–706
Pécsi, M. (1973): 'Geomorphological position and absolute age of the Lower Paleolithic site at Vértesszôllôs, Hungary', *Földr. Közlem.*, 21, 109–119
Pécsi, M, Scheuer, G. and Schweitzer, F. (1982): 'Geomorphological position and chronological classification of Hungarian travertines', 117–133, in: M. Pécsi (ed.), *Quaternary Studies in Hungary,* Geographical Research Institute, Budapest (Hungarian Academy of Sciences)
Pedley, H.M. (1980): 'The occurrence and sedimentology of a Pleistocene travertine in the Fiddien Valley, Malta', *Proc. Geol. Assoc.,* 91, 195–202
Pedley, H.M. (1987): 'The Flandrian (Quaternary) Caerwys tufa, North Wales: an ancient barrage tufa deposit', *Proc. Yorks. Geol. Soc.,* 46, 141–152
Pedley, H.M. (1990): 'Classification and environmental models of cool freshwater tufas', *Sedim. Geol.,* 68, 143–154
Pedley, H.M. (1992): 'Freshwater (phytoherm) reefs: the role of biofilms and their bearing on marine reef cementation', *Sedim. Geol.,* 79, 255–274
Pedley, H.M. (1993): 'Sedimentology of the late Quaternary barrage tufas in the Wye and Lathkill valleys, north Derbyshire.' *Proc. Yorks. Geol. Soc.,* 49, 197–206
Pedley, H.M. (1994): 'Prokaryote-microphyte biofilms and tufas: a sedimentological perspective', *Kaupia,* 4, 45–60
Pedley, H.M., Andrews, J., Ordonez, S., Garcia del Cura, M., Martin, J.-A. G. and Taylor, D. (1996): 'Does climate control the morphological fabric of freshwater carbonates? A comparative study of Holocene barrage tufas from Spain and Britain', *Palaeogeogr. Palaeoclim, Palaeoecol.*, 121, 239–257
Pedley, H.M., Hill, I., Denton, P. and Brasington, J. (2000): 'Three-dimensional modelling of a Holocene tufa system in the Lathkill Valley, north Derbyshire, using ground-penetrating radar', *Sedimentology*, 47, 721–737
Pentecost, A. (1978): 'Blue-green algae and freshwater carbonate deposits', *Proc. R. Soc. Lond.,* B200, 43–61
Pentecost, A. (1981): 'The tufa deposits of the Malham district, North Yorkshire', *Fld. Stud.,* 5, 365–387
Pentecost, A. (1982): 'A quantitative study of calcareous and Tintenstriche algae from the Malham district, Northern England', *Br. Phycol. J.*, 17, 443–456
Pentecost, A. (1985a): 'Association of cyanobacteria with tufa deposits: identity, enumeration and nature of the sheath material revealed by histochemistry', *Geomicrobiol. J.,* 4, 285–298
Pentecost, A. (1985b): '*Alnus* leaf impressions from a postglacial tufa in Yorkshire', *Ann. Bot.*, 56, 779–782

Pentecost, A. (1987a): 'Some observations on the growth rates of mosses associated with tufa deposits and the interpretation of some Postglacial bryoliths', *J. Bryol.*, 14, 543–550
Pentecost, A. (1987b): 'Growth and calcification of the freshwater cyanobacterium *Rivularia haematites*', *Proc. R. Soc. Lond. B.*, 232, 125–136
Pentecost, A. (1988a): 'Growth and calcification of the cyanobacterium *Homoeothrix crustacea*', *J. Gen. Microbiol.*, 134, 2665–2671
Pentecost, A. (1988b): 'Observations on growth rates and calcium carbonate deposition in the green alga *Gongrosira*', *New. Phytol.*, 110, 249–253
Pentecost, A. (1989): 'Growth and calcification of *Calothrix*-dominated oncolites from Northern England', 443–454, in: R.E. Crick (ed.), *Origin, Evolution and Modern Aspects of Biomineralization in Lower Plants and Animals.* New York (Plenum)
Pentecost, A. (1990a): 'The algal flora of travertine', 117–128, in: J.S. Herman, D.A.Hubbard Jr. (eds), *Travertine-marl: Stream Deposits of Virginia*, Virginia Division of Mineral Resources Publication 101, Charlottesville, Va. (Virginia Division of Mineral Resources)
Pentecost, A. (1990b): 'The formation of travertine shrubs: Mammoth Hot Springs, Wyoming.' *Geol. Mag.,* 127: 159–168
Pentecost, A. (1990c): 'Calcification processes in algae and cyanobacteria', 3–20, in: R. Riding (ed.), *Calcareous Algae and Stromatolites,* Berlin (Springer-Verlag)
Pentecost, A. (1990d): 'The identity of suspended particles in a calcite-depositing stream and their significance in trapping and binding phenomena', *Limnologica,* 21, 251–255
Pentecost, A. (1991a): 'A note on the vegetation of some English crons', *Naturalist*, 116, 125–131
Pentecost, A. (1991b): 'Algal and bryophyte flora of a Yorkshire (U.K.) hill stream: a comparative approach using biovolume estimations', *Arch. Hydrobiol.*, 121, 181–201
Pentecost, A. (1991c): 'A new and interesting site for the calcite-encrusted desmid *Oocardium stratum* Naeg. in the British Isles', *Br. Phycol. J.,* 26, 297–301
Pentecost, A. (1991d): 'Springs that turn life to stone', *New Scientist*, December 1991, 42–44
Pentecost, A. (1992a): 'Growth and distribution of endolithic algae in some North Yorkshire streams (UK),' *Br. Phycol. J.,* 27, 145–151
Pentecost, A. (1992b): 'Carbonate chemistry of surface waters in a temperate karst region: the southern Yorkshire Dales, U.K.', *J. Hydrol.,* 139, 211–232
Pentecost, A. (1992c): 'A note on the colonisation or limestone rocks by cyanobacteria', *Arch. Hydrobiol.*, 124, 167–172
Pentecost, A. (1993): 'British travertines: a review', *Proc. Geol. Ass.,* 104, 23–39
Pentecost, A. (1994): 'Formation of laminate travertines at Bagno Vignone, Italy.' *Geomicrobiol. J.*, 12, 239–252
Pentecost, A. (1995a): 'The Quaternary travertine deposits of Europe and Asia Minor', *Quaternary Science Reviews,* 14, 1005–1028
Pentecost, A. (1995b): 'The microbial ecology of some Italian hot-spring travertines', *Microbios,* 81, 45–58
Pentecost, A. (1995c): 'Geochemistry of carbon dioxide in six travertine-depositing waters of Italy', *J. Hydrol.,* 167, 263–278
Pentecost, A. (1995d): 'Significance of the biomineralizing microniche in a *Lyngbya* (cyanobacterium) travertine', *Geomicrobiol. J.*, 13, 213–222
Pentecost, A. (1996a): *The sulphur spas of Harrogate*. London, (King's College)
Pentecost, A. (1996b): 'Moss growth and travertine deposition: the significance of photosynthesis, evaporation and degassing of carbon dioxide', *J. Bryol.*, 19, 229–234
Pentecost, A. (1998): 'The significance of calcite (travertine) formation by algae in a moss-dominated travertine from Matlock Bath, England', *Arch. Hydrobiol.,* 143, 487–509
Pentecost, A. (1999a): 'The origin and development of the travertines and associated thermal waters at Matlock Bath, Derbyshire', *Proc. Geol. Ass.,* 110, 217–232
Pentecost, A. (1999b): 'A note on sand ripples developing in sandstone rock seepages of the Weald, UK.', *Earth Surf. Proc. Landforms,* 24, 1257–1259
Pentecost, A. (2000): 'A note on the stable carbon isotope composition of bryophytes in calcareous aquatic habitats and its relationship to carbon dioxide assimilation', *J. Bryol.,* 22, 13–15
Pentecost, A. (2001): 'Microdistribution of algae in an Italian thermogene travertine', *Arch. Hydrobiol.*, 152, 439–449
Pentecost, A. (2003a): 'Cyanobacteria associated with hot spring travertines', *Can. J. Earth Sci.*, 40, 1447–1457
Pentecost, A. (2003b): 'Taxonomic identity, ecology and distribution of the calcite-depositing cyanobacterium *Phormidium incrustatum* (Oscillatoriaceae)', *Crypt. Algol.*, 24, 307–321

Pentecost, A. and Fletcher, A.F. (1974): 'Tufa, an unusual lichen substrate', *Lichenologist*, 6, 100–102
Pentecost, A. and Riding, R. (1986): 'Calcification in cyanobacteria', pp. 73–90, In Leadbeater, B.S.C. and Riding, R. (eds), Biomineralization of Lower Plants and Animals, Clarendon Press, Oxford
Pentecost, A. and Lord, T.C. (1988): 'Postglacial tufas and travertines from the Craven district of Yorkshire', *Cave Sci.,* 15, 15–19
Pentecost, A. and Terry, C. (1988): 'Inability to demonstrate calcite precipitation by bacterial isolates from travertine', *Geomicrobiol. J.*, 6, 185–194
Pentecost, A. and Tortora, P. (1989): 'Bagni di Tivoli, Lazio: a modern travertine depositing site and its associated microorganisms', *Boll. Soc. Geol. Ital.,* 108, 315–324
Pentecost, A. and Spiro, B. (1990): 'Stable carbon and oxygen isotope composition of calcites associated with modern freshwater cyanobacteria and algae', *Geomicrobiol. J.,* 8, 17–26
Pentecost, A., Thorpe, P.M., Harkness, D.D. and Lord, T.C. (1990): 'Some radiocarbon dates for tufas of the Craven district of Yorkshire'. *Radiocarbon,* 32, 93–97
Pentecost, A. and Viles, H.A. (1994): 'A review and reassessment of travertine classification', *Géogr. phys. Quaternaire,* 48, 305–314
Pentecost, A., Bayari, S. and Yesertener, C. (1997): Phototrophic microorganisms of the Pamukkale travertine Turkey: their distribution and influence on travertine deposition. *Geomicrobiol. J.,* 14, 269–283
Pentecost, A. and Askew, K. (1999): *The Thermal Springs of Matlock Bath, their History and Properties: with an Account of the Matlock Petrifying Wells*, 26 pp., London (King's College)
Pentecost, A., Viles, H.A., Goudie, A.S. and Keen, D.H. (2000a): 'The travertine deposit at Shelsley Walsh, Hereford & Worcestershire', *Trans. Woolhope Nat. Fld. Club*, 50, 25–36
Pentecost, A., Peterken, G.F. and Viles, H.A. (2000b): 'The travertine dams of Slade Brook, Gloucestershire: their formation and conservation', *Geology Today*, Jan. 2000
Pentecost, A. and Whitton, B.A. (2000): 'Limestone', 257–279, in: B.A. Whitton, M. Potts, M. (eds), *The Ecology of Cyanobacteria*, Dordrecht (Kluwer)
Pentecost, A. and Zhang, Z. (2000): 'The travertine flora of Juizhaigou and Munigou, China and its relationship with calcium carbonate deposition', *Cave Karst Sci.,* 27, 71–78
Pentecost, A. and Zhang, Z. (2001): 'A review of Chinese travertines', *Cave Karst Sci.*, 28, 15–28
Pentecost, A. and Zhang, Z. (2002): 'Bryophytes from some travertine-depositing sites in France and the U.K.: relationships with climate and water chemistry', *J. Bryol.,* 24, 233–241
Pentecost, A. and Edwards, H.G.M. (2003): 'Raman spectroscopy and light microscopy of a modern and subfossil microstromatolite: *Rivularia haematites* (cyanobacteria, Nostocales)', *Int. J. Astrobiol.*, 1, 357–363
Penzig, O. (1915): 'Noduli calcarei d'origine vegetale', *Malpighia,* 27, 401–405
Perez, L.A. and Zidovic, D.F. (1995): 'Scale control by using a new non-phosphorus, environmentally friendly scale inhibitor', 47–62, in: Z. Amjad (ed.), New York (Plenum)
Perry, C.T. (1994): 'Freshwater tufa stromatolites in the basal Purbeck Formation (Upper Jurassic), Isle of Portland, Dorset', *Geol. J.*, 29, 119–135
Peryt, T.M. (1983): 'Classification of coated grains', 3–6, in: T.M. Peryt (ed.), *Coated Grains*, Berlin (Springer-Verlag)
Petrbok, J. (1935): 'Mollusken der Holozänen Travertine bei Swischtov a.d. Donau', *Archiv. Molluskenk.* 67, 75–77
Petrelli, M., Perugini, D., Moroni, B. and Poli, G. (2003): 'Determination of travertine provenance from ancient buildings using self-organising maps and fuzzy logic', *Appl. Artif. Intell.*, 17, 885–900
Pevalek, I. (1935): 'Der Travertin und die Plitvice Seen', *Verh. Int. Ver. Limnol.*, 7, 165–181
Pfannenstiel, M. and Forcart, L. (1957): 'Der Kalktuff von Bursa', *Abh. Math. Nat. Kl.*, 3, 65–95
Phillips, S.E., Milnes, A.R. and Foster, R.C. (1987): 'Calcified filaments: an example of biological influences in the formation of calcrete in South Australia', *Austr. J. Earth Sci.*, 25, 405–428
Pia, J. (1933): 'Die Rezenten Kalksteine', *Min. petrog. Mitt. Ergänzungsband,* 1, 1–419
Pia, J. (1934): 'Die Kalkbildung durch Pflanzen. Eine Übersicht', *Beih. Bot. Zbl. A.,* 52, 1–72
Picknett, R.G. (1964): 'A study of calcite solutions at 10 °C', *Trans. Cave Res. Group*, 7, 39–62
Pietsch, W. (1984): 'Die Standortverhältnisse im Naturschutzgebiet 'Kalktuff-Niedermoor' (Vorderrhön)', *Archiv. Naturschutz u. Landschfsforsch.*, 24, 259–273
Piperov, N., Kamenskiy, I.L. and Tolstikhin, I.N. (1988): 'Noble gas isotopes in Bulgarian hot springs', *Geochem. Internat.*, 25, 43–51
Pitois, F., Jigorel, A. and Bertru, G. (2001): 'Colonization dynamics of an encrusting cyanobacterial mat in a hardwater river (Eaulne, France)', *Geomicrobiol. J.,* 18, 139–155
Pitty, A.F. (1968): 'Calcium carbonate content of karst water in relation to flow-through time', *Nature,* 217, 939–940

Plant, L.J. and House, W.A. (2002): 'Precipitation of calcite in the presence of inorganic phosphate', *Colloids Surfaces A: Physicochem. Eng. Aspects,* 203, 143–153
Platner, E. (1830): *Beschriebung der Stadt Rom,* Stuttgart and Tübingen
Plummer, L.N., Wigley, T.L.M. and Parkhurst, D.L. (1978): 'The kinetics of calcite dissolution in CO_2-water systems at 5 °C to 50 °C and 0.0 to 1.0 atm CO_2', *Am. J. Sci.*, 278, 179–216
Pobeguin, T. (1954): 'Contribution a l'étude des carbonates de calcium. Précipitation du calcaire par les végétaux. Comparison avec le monde animal', *Ann. Sci. Nat. Bot.,ser. 11.,* 15, 29–109
Poelt, J. (1954): 'Moosgesellschaften im Alpenvorland I', *Sber. Akad. Wiss. Wien*, 163, 141–174
Pomerol, C. (1973): *The Cainozoic Era*, (English translation by D.W. Humphries, E.E. Humphries), New York (J. Wiley and Sons)
Ponder, W.F. (1986): 'Mound springs of the Great Artesian Basin', 403–420, in: P. De Deckker, W.D. Williams, (eds), *Limnology in Australia*, Melbourne, (CSIRO)
Popp, N. and Wilkinson, B.H. (1983): 'Holocene lacustrine ooids from Pyramid Lake, Nevada', 142–153, in: T. Peryt (ed.), *Coated Grains.* Berlin (Springer-Verlag)
Porter, H. (1861): '*The Geology of Peterborough and its Vicinity*', 126 pp., Peterborough, UK (T. Chadwell)
Powell, C. (1903): 'Observations on some calcareous pebbles', *Minnesota bot. Stud.*, 3, 75–77
Prát, S. (1929): 'Étude sur la biolithogénèse. Résumé de l'ouvarge "Biolithogenese" paru en tchèque en 1929 (Prague Académie Tchèque)', *Bull. Int. Acad. Tchèque Sci.*, 30, 75–78
Preece, R.C. (1979): 'The molluscan fauna of an early Postglacial tufa at Totland, Isle of Wight', *J. Conch.*, 30, 35–42
Preece, R.C. (1980): 'The biostratigraphy and dating of the tufa deposit at the Mesolithic site at Blashenwell, Dorset, England', *J. Archaeol. Sci.*, 7, 345–362
Preece, R.C. (1991): 'Radiocarbon-dated molluscan successions from the Holocene of central Spain', *J. Biogeogr.*, 18, 409–426
Preece, R.C. and Robinson, J.E. (1982): 'Molluscan and ostracod faunas from Post-glacial tufaceous deposits in County Offaly', *Proc. Roy. Irish Acad.* 82B, 115–131
Preece, R.C., Turner, C. and Green, H.S. (1982): 'Field excursion to the tufas of the Wheeler Valley and to Pontnewydd and Cefn Caves', 9 pp., *Quaternary Research Association Field Guide*, UK (Quaternary Research Association)
Preece, R.C. and Robinson, J.E. (1984): 'Late Devensian and Flandrian environmental history of the Ancholme Valley: molluscan and ostracod evidence', *J. Biogeogr.*, 11, 319–352
Preece, R.C., Bennett, K.D. and Robinson, J.E. (1984): 'The biostratigraphy of an early Flandrian tufa at Inchrory, Glen Avon, Banffshire', *Scott. J. Geol.*, 20, 143–159
Preece, R.C., Thorpe, P.M. and Robinson, J.E. (1986a): 'Confirmation of an interglacial age for the Condat tufa (Dordogne, France) from biostratigraphic and isotopic data', *J. Quat. Sci.*, 1, 57–65
Preece, R.C., Coxon, P. and Robinson, J.E. (1986b): 'New biostratigraphic evidence of the Postglacial colonization of Ireland and for Mesolithic forest disturbance', *J. Biogeogr.*, 13, 487–509
Preece, R.C. and Day, S.P. (1994): 'Comparison of Post-glacial molluscan and vegetational successions from a radiocarbon-dated tufa sequence in Oxfordshire', *J. Biogeogr.*, 21, 463–478
Printz, H. (1964): 'Die Chaetophoralen der Binnengewasser – Eine Systematische Übersicht', *Hydrobiologia*, 24, 1–376
Prinz, W. (1908): 'Les crystallizations des grottes de Belgique', *Nouv. Mém. Brlg. Géol.* Ser. 4, No. 2
Privittera, M. and Guidice, R.L. (1986): 'Sulla briovegetation dei Tufi Calcarei dell'Ennese (Sicilia)', *Cryptogam. Bryol. Lichénol.*, 7, 129–140
Rabenhorst, M.C. and Wilding, L.P. (1986): 'Pedogenesis on the Edwards Plateau, Texas. III. New model for the formation of petrocalcic horizons', *Soil. Sci. Soc. Am. J.*, 50, 693–699
Radbruch, D.H. (1957): 'Hypothesis regarding the origin of thinolite tufa at Pyramid Lake, Nevada', *Bull. Geol. Soc. Am.,* 68, 1683–1688
Raspail, F.V. (1833): '*Nouveau Système de Chimie Organique*', 16 pp., Paris
Raspé, R.É. (1770): 'De modo marmoris albi producendi, dissertatio epistolaris Domino Maty, Societus Regiae', *Phil. Trans. R. Soc.*, 60, 47–53
Rastall, R.H. (1926): 'Note on the geology of the Bath springs', *Geol. Mag.,* 63, 98–104
Raymahashay, B.C. and Chaturvedi, L.N. (1976): 'Regional geology and geochemistry of the Manikaran-Kaso geothermal area, India', 223–229, in: J. Cadek, T. Paces (eds), *Proc. Int. Symp. Water-rock Interaction,* Prague (Geological Survey)
Raymond, M.R. (1937): 'A limnological study of the plankton of a concretion-forming marl lake', *Trans. Am. Microsc. Soc.,* 56, 405–430

Reddy, M.M. (1986): 'Effect of magnesium ions on calcium carbonate nucleation and crystal growth in dilute aqueous solutions at 25 °C', 169–182, in: F.A. Mumpton (ed.), *Studies in Diagenesis*, U.S. Geological Survey Bulletin 1578

Reddy, M.M. (1988): 'Physical-chemical mechanisms that affect regulation of crystallization', 3–8, in: C.S. Sikes, A.P. Wheeler (eds), *Chemical Aspects of Regulation of Mineralization*, Mobile, Al. (University of South Alabama)

Reddy, M.M. (1995): 'Carbonate precipitation in Pyramid Lake, Nevada', 21–32, in: Z. Amjad (ed.), *Mineral Scale Formation and Inhibition*, New York (Plenum)

Reddy, M.M. and Gaillard, W.D. (1981): 'Kinetics of calcium carbonate (calcite)-seeded crystallization: influence of solid/solution ratio on the reaction rate constant', *J. Colloid Interf. Sci.*, 80, 171–178

Reddy, M.M., Plummer, L.N. and Busenberg, E. (1981): 'Crystal growth of calcite from calcium bicarbonate solutions at constant P_{CO2} and 25 °C: a test of a calcite dissolution model', *Geochim. Cosmochim. Acta*, 45, 1281–1289

Reeves, C.C. (1983): 'Pliocene channel calcrete and suspended-channel drainage in West Texas and New Mexico', 179–183, in: R. C .L. Wilson (ed.), *Residual Deposits. Geol. Soc. Lond. Spec. Publ.* 11. London (Geological Society)

Reid, C. (1897): 'An early Neolithic kitchen midden and tufaceous deposit, at Blashenwell near Corfe Castle', *Proc. Dorset nat. Hist. Antiq. Fld. Club,* 17, 67–75

Reiff, W. (1955): 'Über den pleistozanen Sauerwasserkalk von Stuttgart-Münster-Bad Canstatt', *Jber. Mitt. oberrhein. Geol. Ver.*, 37, 56–91

Renberg, I. and Wick, M. (1985): 'Soot particle counting in recent lake sediments: An indirect dating method', *Ecol. Bull.*, 37, 53–57

Reysenbach, A.-L., Ehringer, M. and Hershberger, K. (2000): 'Microbial diversity at 83 °C in Calcite Springs, Yellowstone National Park: another environment where the *Aquificiales* and "Korarchaeota" coexist', *Extremophiles*, 4, 61–67

Rhodes, F.H.T. (1954): 'Insects from a travertine deposit in Upper Teesdale, Co. Durham', *Durham Univ. Phil. Soc. Proc.*, 11, 131–135

Riccetti, R. (1988): '*Il Duomo di Orvieto*', 282pp., Edizioni Laterza, Bari

Richter, D.K. and Besenecker, H. (1983): 'Subrecent high-Sr aragonitic ooids from hot springs near Tekke Ilica, Turkey', 154–162, in: T.M. Peryt (ed.), *Coated Grains*, Berlin, (Springer-Verlag)

Ricker, W.E. (1934): 'An ecological classification of certain Ontario streams', *Univ. Toronto Stud. Biol.*, 37, 1–114

Riding, R. (1979): 'Origin and diagenesis of lacustrine algal bioherms at the margin of the Ries Crater, Upper Miocene, S. Germany', *Sedimentology*, 26, 645–680

Riding, R. (1991): 'Classification of microbial carbonates', 21–51, in: R. Riding, (ed.), *Calcareous Algae and Stromatolites*, Berlin (Springer-Verlag)

Riding, R. (1999): 'The term stromatolite: towards an essential definition', *Lethaia*, 32, 321–330

Riding, R. (2000): 'Microbial carbonates: the geological record of calcified bacterial-algal mats and biofilms', *Sedimentology*, 47, (Suppl. 1), 179–214

Rieger, T. (1992): 'Calcareous tufa formations. Searles Lake and Mono Lake', *Calif. Geol.* (for 1992), 99–109

Rightmire, C.T. (1978): 'Seasonal variation in P_{CO2} and ^{13}C content of soil atmosphere', *Water Resources Res.*, 14, 691–692

Riley, J.P. and Chester, R. (1971): *Introduction to Marine Chemistry.* 465 pp., London and New York (Academic Press)

Rippka, R., Deruelles, J., Waterbury, J.B., Herdman, M. and Stanier, R.Y. (1979): 'Generic assignments, strain histories and properties of pure cultures of cyanobacteria', *J. Gen. Microbiol.*, 111, 1–61

Risacher, F. and Eugster, H.P. (1979): 'Holocene pisoliths and encrustations associated with spring-fed surface pools, Pastos Grandes, Bolivia', *Sedimentology,* 26, 253–270

Robèrge, J. and Caron, D. (1983): 'The occurrence of an unusual type of pisolite: the cubic cave pearls of Castelguard Cave, Columbia Icefields, Alberta, Canada', *Arctic Alpine Res.*, 15, 517–522

Roberts, M.S., Smart, P.L. and Baker, A. (1998): 'Annual trace element variations in a Holocene speleothem', *Earth Planet Sci. Lett.*, 154, 237–246

Roberts, M.S., Smart, P.L., Hawkesworth, C.J., Perkins, W.T. and Pearce, N.J.G. (1999): 'Trace element variations in coeval Holocene speleothems from GB Cave, southwest England', *The Holocene*, 9, 707–713

Roberts, P.V. (1984): 'Dependence of oxygen transfer rate on energy dissipation during surface aeration and in stream flow', 347–355, in: W. Brutsaert, G.H.Jirka (eds), *Gas Transfer at Water Surfaces*, Holland (D. Riedel)

Roddy, H.J. (1915): 'Concretions in streams formed by the agency of blue-green algae and related plants', *Proc. Am. phil. Soc.,* 54, 246–258

Rong, K., Li, J., An, Y., and He, F. (1996): 'A study of biogenesis of karst speleothem: an example from Zhijin Cave of Guizhou', *Guizhou Geology*, 13, 177–180

Ronov, A.B. (1964): 'Common tendencies in the chemical evolution of the Earth's crust', *Geochem. Int.*, 4, 713–737
Roques, H. (1964): 'Contribution à l'étude statique et cinétique des systèmes gas carbonique-eau-carbonate', *Ann. Speléologie*, 19, 258–484
Rothpletz, A. (1892): 'On the formation of oolite', *Am. Geol.*, 10, 279–282
Rowe, J.J., Fournier, R.O. and Morey, G.W. (1973): 'Chemical analysis of thermal waters in Yellowstone National Park, Wyoming, 1960–65', *Bull. U.S. Geol. Surv.,* 1303, 1–33
Rowlands, D.L.G. and Webster, R.K. (1971): 'Precipitation of vaterite in lake water', *Nature Phys. Sci.*, 229, 158
Roy, S. (1992): 'Environments and processes of Mn deposition', *Econ. Geol.*, 87, 1218–1236
Rubinson, M. and Clayton, R.N. (1969): 'Carbon-13 fractionation between calcite and aragonite" *Geochim. Cosmochim. Acta,* 33, 997–1002
Rudder, S. (1779): *A New History of Gloucestershire,* Cirencester, UK (S. Rudder)
Russell, M.J., Ingham, J.K., Zedef, V., Maktav, D., Sunar, F., Hall, A.J. and Fallick, A.E. (1999): 'Search for signs of ancient life on Mars: expectations from hydromagnesite microbialites, Salda Lake, Turkey', *J. Geol. Soc. Lond.*, 156, 869–888
Rutte, E. (1954): 'Gesteinbildende Algen aus dem Eozän von Kleinkems am Idsteiner Klotz in Baden', *Jb. Geol. Paläont. Monatsch.*, (1953), 495–506
Rutty, J. (1757): '*A Methodological Synopsis of Mineral Waters*', 660 pp., London (W. Johnston)
Rytz, W. (1934): 'Die interglazialen Tuffe von Castelneu bei Montpellier', *Mitt. Naturf. Ges. Bern.*, (for 1934), 36–38
Saines, M., Dickson, P.A. and Lambert, P.T. (1980): 'An occurrence of calcium hydroxide groundwater in Jordan', *Ground Water*, 18, 503
Sakai, H. and Matsubaya, O. (1977): 'Stable isotope of Japanese geothermal systems', *Geothermics,* 5, 97–124
Sallis,J. D., Juckes, W. and Koutsoukos, P.G. (1995): 'Phosphocitrate: potential to influence deposition of scaling salts and corrosion', 87–98, in: Z. Amjad (ed.), *Mineral Scale Formation and Inhibition*, New York (Plenum)
Salomon, J.N. (1986): 'Aspects morphologiques des karsts Eocenes du Sud-Ouest Malgache', 409–426, in: K. Paterson, K., M.M. Sweeting (eds), *New Directions in Karst,* Norwich (Geobooks)
Salomons, W. and Mook, W.G. (1976): 'Isotope geochemistry of carbonate dissolution and reprecipitation in soils', *Soil. Sci.*, 122, 15–24
Salomons, W., Goudie, A.S. and Mook, W.G. (1978): 'Isotopic composition of calcrete deposits from Europe, Africa and India', *Earth Surf. Proc.*, 3, 43–57
Sano, Y. (1996): 'Helium and carbon isotope study on magmatic hydrothermal processes at subsurface region', *Mem. Geol. Soc. Jpn.*, 46, 83–90
Saporta, G. de (1868): 'Prodrome d'une flore fossile des travertins anciens de Sézanne', *Mem. Soc. Géol. Fr.*, 8, 1–287
Savelli, C. and Wedepohl, K.H. (1969): 'Geochemische Untersuchungen an Sinterkalken (Travertinen)', *Contr. Min. Petrol.,* 21, 238–256
Schauroth, V. and Zerrenner, H. (1851): 'Breifliche Mittheilungen', *Z. dt. Geol. Ges.*, 3, 135–137
Schäfer, A. and Staf, K.R.G. (1978): 'Permian Saar-Nahe Basin and recent Lake Constance (Germany): two environments of lacustrine algal carbonates', *Spec. Publs. Int. ass. Sedimentology*, 2, 83–107
Scheuer, G. and Schweitzer, F. (1973): 'Development of Hungarian travertine sequences in the Quaternary', *Föld. Közl.,* 22, 133–144
Scheuer, G. and Schweitzer, F. (1981): 'Origin of the freshwater limestones of Hungary and comparative studies', *Föld. Közl.,* 111, 67–97
Scheuer, G. and Schweitzer, F. (1985): 'Types and forms of travertine cones', *Föld. Közl.,* 115, 385–398
Scheuer, G. and Schweitzer, F. (1989): 'Genetics and occurrence of Holocene travertines in Hungary', *Studies in Geography in Hungary, Akademici Kiado, Budapest*, 25, 39–48
Schloesing, M.T. (1872): 'Sur la dissolution du carbonate de chaux par l'acide carbonique', *C.R.Hebd. de l'Academie des Sciences A.,* 75, 70–73
Schöttle, M. and Müller, G. (1967): 'Recent carbonate sedimentation in the Gnadensee (L. Constance), Germany', 148–156, in: G. Müller, G.M. Friedmann (eds), *Carbonate Sedimentology in Central Europe,* New York, (Springer-Verlag)
Schmid, K. –H. (1972): 'Abbau und Verwendung von Kalktuff im Echaztal', *Abh. Kartst. u. Höhlenkd*, A7, 40–49
Schmulz, R.F. (1971): 'Formation of beachrock at Eniwetok Atoll', 17–24, in: O.P.Bricker (ed.), *Carbonate Cements*, Baltimore, Md. (Johns Hopkins University Press)
Schneider, J. (1977): 'Carbonate construction and decomposition by epilithic and endolithic microorganisms in salt and freshwater', 248–260, in: E. Flügel (ed.), *Fossil Algae, Recent Results and Developments*. Berlin (Springer-Verlag)
Schnitzer, U.A. (1974): 'Kalkinkrustation und Kalksinterknollen in Lias-Quellwässern bei Elsenberg (Bl. Erlangen-Nord)', *Geol. Bl. Nordöst-Bayern*, 24, 188–191

Schock, M.R. (1989): 'Understanding corrosion control strategies for lead', *J. Am. Water Wks. Ass.*, 81, 89–100
Scholl, D.W. (1960): 'Pleistocene algal pinnacles at Searles Lake, California', *J. Sed. Petrol.,* 30, 414–431
Scholl, D.W. and Taft, W.H. (1964): 'Algae, contributors to the formation of calcareous tufa, Mono Lake, California', *J. Sed. Petrol.,* 34, 309–319
Schreiber, B.C., Smith, D. and Schreiber, E. (1981): 'Spring peas from New York State: nucleation and growth of freshwater hollow ooliths and pisoliths', *J. Sed. Petrol.*, 51, 1341–1346
Schreve, D.C. and Bridgland, D.R. (2002): 'Correlation of English and German Middle Pleistocene fluvial sequences based on mammalian biostratigraphy', *Netherlands J. Geosci.*, 81, 357–373
Schultze-Lam, S., Ferris, F.G., Konhauser, K.O. and Wiese, R.G. (1995): 'In situ silicification of an Icelandic hot spring microbial mat: implications for microfossil formation', *Can. J. Earth Sci.,* 32, 2021–2026
Schwarcz, H.P. (1980): 'Absolute age determination of archeological sites by uranium series dating of travertines', *Archaeometry*, 22, 3–24
Schwarcz, H.P. (1990): 'Dating travertine', 113–116, in: J.S. Herman, D.A. Hubbard Jr., *Travertine-Marl: Stream Deposits of Virginia*, Virginia Division of Mineral Resources, Publication 101, Charlottesville, Va. (Virginia Division of Mineral Resources)
Schwarcz, H.P., Blackwell, B., Goldberg, P. and Marks, A.E. (1979): 'Uranium series dating of travertine from archaeological sites, Nahan Zin, Israel', *Nature*, 277, 558–560
Schwarcz, H.P. and Latham, A.G. (1984): 'Uranium series age determination of travertines from the site of Vertesszollos, Hungary', *J. Archaeol. Sci.*, 11, 327–336
Schwedt, G. (1987): 'Römische Wasserleitung in der Eifel', *Naturwissensch.-Rundsch.*, 40, 58–62
Schweigert, G. (1991): 'Die Flora der Eem-interglazialen Travertine von Stuttgart-Untertürkeim (Baden-Württemburg)', *Stuttgarter Beitr. Z. Naturkunde B.,* 178, 1–43
Scoffin, T.P. and Stoddart, D.R. (1983): 'Beachrock and intertidal cements', 401–425, in: A.S. Goudie, K. Pye (eds), *Chemical Sediments and Geomorphology*, London (Academic Press)
Scrope, G.J.P. (1858): *The Geology and Extinct Volcanoes of Central France*, 258 pp., London
Segré, A.G. (1957): 'Contributo allo studio del quaternario dell'Agro Pontino; il travertino di Cisterna di Latina; giacimento del paleolitico superiore e del bronzo', *Quaternaria,* 4, 191–194
Segré, A.G. and Ascenzi, A. (1956): 'Giacimenti del paleolitico superiore e del bronzo nei travertini di Cisterna' (Latina). Parte 1: Geologia, Paleontologia, Palenologia. *Riv. Antropologia,* 43, 367–382
Semikhatov, M.A., Gebelein, C.D., Cloud, P., Awramik, S.M. and Benmore, W.C. (1979): 'Stromatolite morphogenesis – progress and problems', *Can. J. Earth Sci.*, 16, 992–1015
Settepassi, F. and Verdel, U. (1965): 'Continental Quaternary Mollusca of the Lower Liri Valley (southern Latium)', *Geol. Romana*, 4, 369–451
Shaw, T.R. (1997): 'Cave minerals of the world: a historical introduction', 1–24, in C.A. Hill, P. Forti (eds), *Cave Minerals of the World.* 2nd Edn, Huntsville, Alabama (National Speleological Society)
Shepard, W.D. (1990): '*Microcylloepus formicoideus* (Coleoptera: Elmidae), a new riffle beetle from Death Valley National Monument, California', *Entomol. News*, 101, 147–153
Shieh, Y.N. and Taylor, H.P. Jr. (1969): 'Oxygen and carbon isotope studies of contact metamorphism of carbonate rocks', *J. Petrol.,* 10, 307–331
Shopov, Y.Y. (1997): 'Luminescence of cave minerals', 244–248, in: C.A. Hill, P. Forti (eds), *Cave Minerals of the World*, Huntsville, Alabama (National Speleological Society)
Shuster, E.T. and White. W.B. (1971): 'Seasonal fluctuations in the chemistry of limestone springs: a possible means of characterising carbonate aquifers', *J. Hydrol.,* 14, 93–128
Sikes, C.S. and Wierzbicki, A. (1995): 'Mechanisms of regulation of crystal growth in selected biological systems', 185–206, in: Z. Amjad (ed.), *Mineral Scale Formation and Inhibition*, New York (Plenum)
Skoflek, I. (1990): 'Plant remains from the Vertesszölös travertine', 77–124, in: M. Kretzoi, V.Y. Dobosi (eds), *Vertesszöllös Site, Man and Culture*, Budapest (Akadémiai Kiado)
Skuja, A. (1937): 'Algae', 1–105, in: H. Handel-Mazzetti (ed.), *Symbolae Sinicae.*, Teil 1, Vienna
Smith, A.M. and Mason, T.R. (1991): 'Pleistocene multiple-growth, lacustrine oncoids from the Poacher's Point Formation, northern Namibia', *Sedimentology,* 38, 591–599
Smith, I.R. (1975): '*Turbulence in Lakes and Rivers*', 79 pp.,Freshwater Biological Association Scienctific Publication 29, Cumbria, UK (Freshwater Biological Association)
Smith, P.C. (1989): 'Hydrogeology', 19–26, in: W. Zeidler, W.F. Ponder (eds), *The Natural History of Dalhousie Springs*, Adelaide (South Australian Museum)
Soens, M. and Gullentops, F. (1969): 'Molluskenfauna van een actuele en een fossiele tuf in midden-Belgie', *Bull. Soc. Belg. Geol. Palaeontol. Hydrol.*, 78, 39–47

Soligo, M., Tuccimei, P., Barberi, R., Delitala, M.C., Miccadei, E. and Taddeuci, A. (2002): 'U/Th dating of freshwater travertine from Middle Velino Valley (Central Italy): paleoclimatic and geological implications', *Palaeogeogr. Palaeoclim. Palaeoecol.,* 184, 147–161

Speer, J.A. (1983): 'Crystal chemistry and phase relations of orthorhombic carbonates', *Revs. Mineral.,* 11, 145–190

Spiro, B. and Pentecost, A. (1991): 'One day in the life of a stream – a diurnal inorganic carbon mass balance for a travertine-depositing stream (Waterfall Beck, Yorkshire)', *Geomicrobiol. J.,* 9, 1–11

Spötl, C., Unterwurzacher, M., Mangini, A. and Longstaffe, F.J. (2002): 'Carbonate speleothems in the dry, inneralpine Vinschgau Valley, northernmost Italy: witness of changes in climate and hydrology since the last glacial maximum', *J. Sed. Res.,* 72, 793–808

Sprenger, E. (1930): 'Bacillariales aus den Thermen und der Umgebung von Karlsbad', *Arch. Protisenk.*, 71, 502–542

Srdoc, D., Obelic, B. and Horvatincic, N. (1980): 'Radiocarbon dating of calcareous tufa: how reliable data can we expect?', *Radiocarbon*, 22, 858–862

Srdoc, D., Horvatincic, N., Obelic, B. and Sliepevic, A. (1983): 'Radiocarbon dating of tufa in paleoclimatic studies', *Radiocarbon*, 25, 421–427

Srdoc, D., Krajkar-Bronic, I., Horvatincic, N. and Obelic, B. (1986a): 'Increase in 14C activity on dissolved inorganic carbon along a river course', *Radiocarbon*, 28, 515–521

Srdoc, D., Horvatincic, N., Obelic, B., Krakcar-Bronic, I. and O'Malley, P. (1986b): 'The effects of contamination of calcareous sediments on their radiocarbon ages', *Radiocarbon*, 28, 510–514

Srdoc, D., Horvantincic, N., Obelic, B. and Krajcar-Bronic, I. (1987): 'Rudjer Boskovic Institute Radiocarbon measurements IX', *Radiocarbon*, 29, 115–134

Statham, I. (1977): 'A note on tufa-depositing springs in Glenasmole, Co. Dublin', *Irish Geogr.*, 10, 14–18

Steidtmann, E. (1936): 'Travertine-depositing waters near Lexington, Virginia', *J. Geol.*, 44, 193–200

Steinen, R.P., Gray, N.A. and Mooney, J. (1987): 'A Mesozoic hot spring deposit in the Hertford Basin of Connecticut', *J. Sed. Petrol.,* 57, 319–326

Steiner, W. (1977): 'Das geologische Profil des Travertin-Komplexes von Taubach bei Weimar', *Abh. Ber. Inst. Quartaerpal. Weimar*, 2, 83–118

Steiner, W. and Wagenbreth, O. (1971): 'Zur geologischen Situation der altsteinzeitlichen Rasplätze in Unteren Travertin von Ehringsdorf bei Weimar', *Alt-Thüringen,* 11, 47–75

Stetter, K.O. (1996): 'Hyperthermophiles in the history of life', 1–18, in: J. Bock, J.A. Goode (eds), *Evolution of Hydrothermal Ecosystems on Earth (and Mars?)*, Ciba Foundation, Chichester (J. Wiley and Sons)

Steven, T.A. and Ratté, J.C. (1965): 'Geology and structural control of ore deposition in the Creede district, San Juan Mountains, Colorado', *U.S. Geol. Surv. Prof. Paper*, 487, 1–90

Stiller, M., Rounick, J.S. and Shasha, S. (1985): 'Extreme carbon-isotope enrichments in evaporitic brines', *Nature*, 316, 434–435

Stirn, A. (1964): 'Kalktuffvorkommen und Kalktufftypen der Schwäbische Alb', *Abh. Karst u. Höhlenkunde,* E1, 1–92

Stirn, A. (1972): 'Die Olgahöhle – Entstehung und Formen', *Abh. Karst u. Höhlenkunde,* A7, 27–39

Stockner, J.G. (1968): 'Algal growth and primary productivity in a thermal stream', *J. Fish. Res. Bd. Can.*, 25, 2037–2058

Stoffers, P. (1975): 'Recent carbonate sedimentation in the lakes of Plitvice (Yug.)', *N. Jb. Miner. Mh.,* 9, 412–418

Stoffers, P. and Botz, R. (1994): 'Formation of hydrothermal carbonate in Lake Tanganyika, East-Central Africa', *Chem. Geol.,* 115, 117–122

Stokes, C. (1837): 'Note respecting a piece of recent wood partly petrified by carbonate of lime, with some remarks on fossil wood', *Trans. Geol. Soc.,* 5, 207–214

Straccia, F.G., Wilkinson, B.H. and Smith, G.R. (1990): 'Miocene lacustrine algal reefs: southwestern Snake River Plain, Idaho', *Sed. Geol.,* 67, 7–23

Strong, A.E. and Eadie, B.J. (1978): 'Satellite observations of calcium carbonate precipitations in the Great Lakes', *Limnol. Oceanogr.*, 23, 872–887

Strong, G.E., Giles, J.R.A. and Wright, V.P. (1993): 'A Holocene calcrete from North Yorkshire: implications for interpreting palaeoclimates using calcretes', *Sedimentology*, 39, 333–347

Stuart, A.J. (1991): 'Mammalian extinctions in the Late Pleistocene of northern Eurasia and North America', *Biol. Rev.*, 66, 453–562

Stumm, W. and Morgan, J.J. (1996): *Aquatic Chemistry*. 3rd Edn., New York (J. Wiley and Sons)

Sturchio, N.C. (1990): 'Radium isotopes, alkaline earth diagenesis, and age determination of travertine from Mammoth Hot Springs, Wyoming, U.S.A.', *Appl. Geochem.*, 5, 631–640

Sturchio, N.C., Pierce, K.L., Murrell, M.T. and Sorey, M.L. (1994): 'Uranium-series ages of travertines and timing of the last glaciation in the northern Yellowstone area, Wyoming-Montana', *Quat. Res.*, 41, 265–277

Sturm, M. and Matter, A. (1972): 'Sedimente und Sedimentionsvorgänge im Thunersee', *Eclogae Geol. Helv.*, 65, 563–590
Sturrock, P.L.K., Benjamin, L., Loewenthal, R.E. and Marais, G.R. (1976): 'Calcium carbonate precipitation kinetics part 1: pure system kinetics', *Water S.A.*, (for 1976), 101–109
Sugiyama, S., Awaya, T., Hirano, T. and Oki, Y. (1985): 'Scanning electron microscope observation of $CaCO_3$ deposits, Yugowara thermal area', *Bull. Hot Springs Res. Inst.,* 16, 63–75
Summers, W.K. (1972): 'Practical corrosion and incrustation guide lines for water wells', *Groundwater*, 10, 12–17
Sunagawa, I. (1987): 'Morphology of minerals', 509–587, in: I. Sungawa (ed.), *Morphology of Crystals*, Tokyo (Terra Scientific Publishing)
Surdam, R.C. and Wolfbauer, C.A. (1975): 'Green River Formation, Wyoming – a playa-lake complex', *Geol. Soc. Am. Bull.*, 86, 335–345
Surdam, R.C. and Wray, J.L. (1976): 'Lacustrine stromatolites, Eocene Green River Formation, Wyoming', 535–542, in: M.R. Walter (ed.), *Stromatolites*, *Developments in Sedimentology* 20*,* Amsterdam (Elsevier)
Suzuki, R. (1978): 'Fluoride in calcareous sinters', *Geochem. Tokyo,* 12, 5–8
Svetov, A.P. (1974): 'Types and products of Jatulian and Suysarian basaltic vulcanism in central and southern Karelia and their role in volcanogenic-sedimentary lithogenesis', 94–102, in: G.S. Dzotsenidze, *Problemy Vulkanogenio-osadochnogo Litogeneza*, Moscow (Izd. Nauka)
Swartz, J.F. (1990): 'Depositional environments and pedogenic alteration of palustrine and lacustrine deposits; an example from the Lower Cretaceous Baum Limestone, south-central Oklahoma', Unpublished Masters Thesis, Department of Geology, University of Oklahoma
Sweet, P.C. and Hubbard, D.A. Jr. (1990): 'Economic legacy and distribution of Virginia's Valley and Ridge province travertine-marl deposits', 129–138, in: J.S. Herman, D.A. Hubbard Jr. (eds), *Travertine-marl: Stream Deposits in Virginia*, Virginia Division of Mineral Resources Publication 101, Charlottesville, Va. (Virginia Division of Mineral Resources)
Sweeting, M.M., Bao, F.S. and Zhang, D. (1991): 'The problem of palaeokarst in Tibet', *Geographical J.*, 157, 316–325
Symoens, J.J. (1949): 'Note sur des formations de tuf calcaire observés dans le bois d'Hautmont (Wauthier-Braine)', *Bull. Soc. r. Bot. Belg.*, 82, 81–90
Symoens, J.J. (1950): ' Note sur les tufs calcaires de la vallée du Hoyoux', *Lejeunia Rev. Bot.*, 14, 13–17
Symoens, J.J. (1955): 'Découverte de tufs a Chironomides dans la région mosane', *Travaux de l'Ass. Int. Limnol. Théor. appliq.*, 12, 604–607
Symoens, J.J., Duvigneaud, P. and Vanden Bergen, C. (1951): 'Aperçu sur la végétation des tufs calcaires de la Belgique', *Bull. Soc. Roy. Bot. Belg.*, 83, 329–352
Symeons, J.J. and Malaisse, F. (1967): 'Sur une formation de tuf calcaire observé sur le versant est du plateau desKundelungu', *Bull. Acad. Roy. Sci. D'outre-Mer*, 13, 1148–1151
Symoens, J.J. and Van der Werff, A. (1951): 'Note sur les formations de tuf calcaire des environs de Consdorf (Grande Duché de Luxembourg)', *Bull. Soc. Roy. Bot. Belg.*, 83, 213–218
Szabo, B.J. (1990): 'Ages of travertine deposits in Eastern Grand Canyon National Park, Arizona', *Quat. Res.*, 34, 24–32
Szkatula, A., Balanda, M. and Kopk, M. (2002): 'Magnetic treatment of industrial water. Silica activation', *Eur. Phys. J. Appl. Phys.*, 18, 41–49
Szulc, J. (1983): 'Genesis and classification of travertine deposits', *Przeglad Geologiczny,* 4, 231–236
Szulc, J. and Cwizewicz, M. (1989): 'The Lower Permian freshwater carbonates of the Slawkow Graben, southern Poland: sedimentary facies and stable isotope study', *Palaeogeogr. Palaeoclim. Palaeoecol.*, 70, 107–120
Taborosi, D., Hirakawa, K. and Stafford, K.W. (2003): 'Speleothem-like calcite and aragonite deposits on a tropical carbonate coast', *Cave and Karst Sci.*, 30, 23–32
Talling, J.F. (1976): 'The depletion of carbon dioxide from lake water by phytoplankton', *J. Ecol.*, 64, 79–121
Talma, A.S. and Netterberg, F. (1983): 'Stable isotope abundancies in calcretes', 221–233, in: R.C.L. Wilson (ed.), *Residual Deposits*, *Geol. Soc. London Spec. Pub.,* 13, London (Geological Society)
Tan, M., Liu, D., Zhong, H., Qin, X., Li, H., Zhao, S., Li, T., Lu, J. and Lu, X. (1998): 'Preliminary study on climatic signals of stable isotopes from Holocene speleothems under monsoon condition', *Chinese Sci. Bull.*, 43, 506–509
Tan, M., Qin, X., Shen, L., Wang, Y., Li, T., Song, L., Wang, L. and Liu, D. (1999): 'Bioptical microcycles of laminated speleothems from China and their chronological significance.' *Chinese Sci. Bull.*, 44, 1604–1607
Tarutani, T., Clayton, R.N. and Mayeda, T.K. (1969): 'The effects of polymorphism and magnesium substitution on oxygen isotope fractionation between calcium carbonate and water', *Geochim. Cosmochim. Acta*, 33, 986–996
Taylor, A. (1919): 'Mosses as formers of tufa and of floating islands', *Bryologist*, 22, 38–39

Tedford, R.H., Banks, M.R., Kemp, N.R., McDougall, I. and Sutherland, F.L. (1975): 'Recognition of the oldest known fossil marsupials from Australia', *Nature*, 255, 141–142
Thienemann, A. (1933): 'Mückenlarven bilden Gesteine', *Natur und Museum*, 63, 370–378
Thienemann, A. (1934): 'Eine gesteinbildende Chironomide *Lithotanytarsus emarginatus* (Goetghebuer)', *Z. Morphol. Ökol. Tiere.*, 28, 480–496
Thienemann, A. (1935): 'Gesteinbildung durch Mückenlarven', *Forsch. Fortschr.*, 11, 24–25
Thienemann, A. (1936): 'Alpine Chironomiden (Ergebnisse von Untersuchungen in der Gegend von Garmisch-Partenkirchen, Oberbayern)', *Arch. Hydrobiol.*, 30, 167–262
Thienemann, A. (1950): 'Verbreitungsgeschichte der Süßwassertierwelt Europas. Versuch einer historischen Tiergeographie der europäishen Binnengewässer', *Die Binnengewässer*, 18, 1–809
Thiselton-Dyer, W.T. (1891): 'Note on Mr. Barber's paper on *Pachytheca*', *Ann. Bot.*, 5, 225
Thomas, R.L., Kemp, A.L. and Lewis, C.F.M. (1973): 'The surficial sediments of Lake Huron', *Can. J. Earth Sci.*, 10, 226–271
Thompson, J.B. (2000): 'Microbial whitings', 250–260, in: R. Riding, S.M. Awramik (eds), *Microbial Sediments*, Berlin (Springer-Verlag)
Thompson, J.B. and Ferris, F.G. (1990): 'Cyanobacterial precipitation of gypsum, calcite and magnesite from natural alkaline lake water', *Geology,* 18, 995–998
Thompson, P., Schwarcz, H.P. and Ford, D.C. (1976): 'Stable isotope geochemistry, geothermometry, and geochronology of speleothems from West Virginia', *Geol. Soc. Am. Bull.,* 87, 1730–1738
Thorpe, P.M. (1981): *Isotope Studies of UK Tufa Deposits and Associated Source Waters,* Unpublished D. Phil. Thesis, School of Geography, Oxford, UK
Thorpe, P.M., Otlet, R.L. and Sweeting, M.M. (1981a): 'Hydrological implications from ^{14}C profiling of UK tufa', *Radiocarbon,* 22, 897–908
Thorpe, P.M., Holyoak, D.T., Preece, R.C. and Willing, M.J. (1981b): 'Validity of corrected ^{14}C dates from calcareous tufa', pp. 151–156, *Actes du Colloque de l'AGF. Formations carbonatées externes, tufa et travertins*, Paris
Thrailkill, J. (1965): 'Studies in the excavation of limestone caves and the deposition of speleothems', unpublished PhD thesis, Princeton University, Princeton, N.J
Thrailkill, J. (1971): 'Carbonate deposition in Carlsbad Caverns', *J. Geol.,* 79, 683–695
Thunmark, S. (1926): 'Bidrag till Kännendomen om recenta kalktuffer', *Geol. Föreningens*, 48, 541–583
Tilden, J.E. (1897): 'On some algal stalactites of the Yellowstone National Park', *Bot. Gaz.*, 24, 194–199
Tiercelin, J.-J., and others (1987): 'Le demi-graben de Baringo-Bogoria, Rift Gregory, Kenya, 30,000 ans d'histoire hydrologique et sedimentaire', *Bull. Centres Rech. Explor-Prod. Elf-Aquitaine*, 11, 249–540
Tiratsoo, E.N. (1972): *Natural Gas*. 2nd Edn. Beaconsfield, England, (Scientific Press)
Tobias, P.V., Vogel, J.C., Oschadleus, H.D., Partridge, T.C. and McKee, J.K. (1993): 'New isotopic and sedimentological measurements of the Thabaseek deposits (South Africa) and the dating of the Taung hominid', *Quat. Res.*, 40, 360–367
Tomascak, P.B., Hemming, N.G. and Hemming, S.R. (2003): 'The lithium isotopic composition of waters of the Mono Basin, California', *Geochim. Cosmochim. Acta,* 67, 601–611
Török, A. (2004): 'Comparison of the process of decay of two limestones in a polluted urban environment', *Land Reconst. Management*, 3, 73–92
Townson, R. (1797): *Travels in Hungary, with a Short Account of Vienna in the Year 1797*, 506 pp., London
Trewin, N.H., Fayers, S.R. and Kelman, R. (2003): 'Subaqueous silicification of the contents of small ponds in an early Devonian hot-spring complex, Rhynie, Scotland', *Can. J. Earth Sci.,* 40, 1697–1712
Troester, J.W. and White, W.B. (1986): 'Geochemical investigations of three tropical karst drainage basins in Puerto Rico', *Ground Water,* 24, 475–482
Tsivoglou, E.C. and Neal, L.A. (1976): 'Tracer measurement of reaeration: III, predicting the reaeration capacity of inland streams', *J. Water Poll. Contr. Fed.*, 48, 2669–2689
Tucan, F. (1939): 'Onyx Marmor und Aragonit aus der Umgebung von Tetoro', *Bull. Int. Acad. Yougosl. Sci.,* 32, 11–17
Tucker, M.E. and Wright, V.P. (1990): *Carbonate Sedimentology*. London, Blackwell, pp. 482
Turekian, K.K. and Wedepohl, K.H. (1961): 'Distribution of elements in some major units of the earth's crust', *Bull. Geol. Soc. Am.,* 72, 175–182
Turi, B. (1986): 'Stable isotope geochemistry of travertines', 207–235, in: B.P. Fritz, J.C.Fontes (eds), *Handbook of Environmental Isotope Geochemistry*, Amsterdam (Elsevier)
Turner, J.V. and Fritz, P. (1983): 'Enriched ^{13}C composition of interstitial waters in sediments of a freshwater lake', *Can. J. Earth Sci.,* 20, 616–621
Twenhofel, W.H. (1939): '*Principles of Sedimentation*', McGraw-Hill, New York

UNEP (2004): www.unep-wcmc.org/sites/
Unger, F. (1861): 'Beitrage zur Physiologie der Pflanzen', *Sber. Akad. Wiss. Wien. Math. Nat. Kl., Abt. II*, 43, 497–516
Unterwurzacher, M. (2002): 'Der Laaser Onyx – Karbonatsinter aus dem Vinschgau', *Der Schlern,* 76, 5–10
Untracht, O. (1975): '*Metal Techniques for Craftsmen*', London (Robert Hale), pp. 509
Urbain, P. (1953): 'Contribution de l'hydrogeologie thermale à la tectonique; l'aire d'emergence d'Hammam Meskoutine (Départment de Constantine)', *Bull. Soc. Géol. Fr. Série VI*, 3, 247–251
Usdowski, E., Hoefs, J. and Menschel, G. (1979): 'Relationship between ^{13}C and ^{18}O fractionation and changes in major element composition in a recent calcite-depositing spring – a model of chemical variations with inorganic $CaCO_3$ precipitation', *Earth Sci. Planet. Lett.,* 42, 267–276
Vaillant, F. (1991): 'Contribution à l'étude du genre *Phyllotelmatoscopus* Vaillant 1982 (Diptera: Psychodidae)', *Bull. Inst. Roy. Soc. Nat. Belg. Ent.*, 61, 211–218
Vaillant, F. and Withers, P. (1993): 'Quelques *Pericoma* du groups *trifasciata* (Diptera: Psychodidae, Psychodinae)', *Bull. Soc. Ent. Suisse*, 66, 99–112
Valero-Garcés, B.L., Arenas, C. and Delgado-Huertas, A. (2001): 'Depositional environments of Quaternary lacustrine travertines and stromatolites from high–altitude Andean lakes, northwestern Argentina', *Can. J. Earth Sci.,* 38, 1263–1283
Vallardi, F. (1982): '*Marmi Italiani*', 2 vol., Rome (Istituto Commercio Estero)
Van, N.H., Lang, J., Elbez, G., Lalou, C. and Lucas, G. (1973): 'Existence d'un desequilibre elevé entre les isotopes de l'uranium. Influence sur la datation des travertinsde Bamyan (Afghanistan central) par la methode $^{230}Th/^{234}U$. *C.R. hebd. Séanc. Acad. Sci., Paris,* 276, 2233–2236
Vancouver, C. (1810): *'General View of the Agriculture of Hampshire, Including the Isle of Wight, drawn up for the Board of Agriculture and Internal Improvement'*, 520 pp., London
Van Everdingen, R.O. (1969): 'Degree of saturation with respect to $CaCO_3$, $CaMg(CO_3)_2$, and $CaSO_4$ for some thermal and mineral springs in the S. Rocky Mountains, Alberta and B.C.', *Can. J. Earth Sci.*, 6, 1421–1431
Van Everdingen, R.O., Shakur, M.A. and Krouse, H.R. (1985): 'Role of corrosion by the H_2SO_4 fallout in caves developed in a travertine deposit – evidence from sulphur and oxygen isotopes', *Chem. Geol.,* 49, 205–211
Van Oye, P. (1937): 'Biologie et écologie des formations calcaires du Jurassique Belge', *Biol. Jaarb.*, 4, 236–265
Vannote, R.L., Minshall, G.W., Cummins, K.W., Sedell, J.R. and Cushing, C.E. (1980): 'The river continuum concept', *Can. J. Fish. Aquatic Sci.*, 37, 130–137
Varnedoe, W.W. (1965): 'A hypothesis for the formation of rimstone dams and gours', *Bull. natn. speleol. Soc.*, 27, 151–152
Varol. B., Kazanci, N. and Okan, Y. (1984): 'Fresh-water algal bioherms and stromatolites fo Eocene age around Kinck, northwest of Ankara', *Bull. Geol. Soc. Turkey*, 27, 119–129
Vaudour, J. (1986): 'Introduction à l'étude des édifices travertineux holocenes', *Mediterranée*, 1–2, 3–10
Veni, G. (1994): *'Geomorphology, Hydrogeology, Geochemistry, and Evolution of the Karstic Lower Glen Rose Aquifer, South-central Texas'*, Unpublished Ph.D. Dissertation, University of Texas, Austin, Tx
Vent, W. (1978): 'Die Flora des Travertins von Burgtonna un Thüringen', *Quartarpaläontol.*, 3, 59–66
Verheyden, S., Keppens, E., Fairchild, I.J., McDermott, F. and Weis, D. (2000): 'Mg, Sr and Sr isotope geochemistry of a Belgian Holocene speleothem: implications for paleoclimate reconstruction', *Chem. Geol.*, 169, 131–144
Verhulst, A. (1914): 'Essai sur le tuf calcaire, les eaux incrustantes et leur vegetation dans le Jurassique Belge', *Bull. Soc. Roy. Boty. Belg.,* 53, 69–85
Vernet, J.L. (1986): 'Travertins et végétations holocenes méditerranéennes', *Mediterranée*, 1–2, 25–29
Vernet, J.L., Ambert, P., Andre, J. and others (1984): 'Palaeoenvironements quaternaires dans la region de Millau (Masif Central) a partir des travertins, des macroflores et des faunes', 125–131, in: L. David, J.C. Gall (eds), *Congress of Paleoecology*. Geobios-Memoire-Special no. 8, Lyons, France
Verrecchia, E.P. and Verrecchia, K.E. (1994): Needle-fiber calcite: a critical review and a proposed classification. *J. Sed. Res.*, A64, 650–664
Verrecchia, E.P., Dumon, J. –L. and Verrecchia, K.E. (1993): 'Role of calcium oxalate biomineralization by fungi in the formation of calcretes: a case study from Nazareth, Israel', *J. Sed. Petrol.*, 63, 1000–1006
Verzilin, N.N. and Kalmykova, N A. (1989): 'Lithological features of the Tsagan-Tsab section of the zeolite-bearing deposits of southeastern Mongolia', *Vestnik-Leningradskogo Univ. Geologiya-Geografiya*, (for 1989), 3–12
Viehmann, I. (1963): 'Un nou proces de geneza a perlelor de caverna', *Trav. Inst. Spéol. "E. Racovita"*, 1–2, 295–303
Viles, H.A. and Goudie, A.S. (1990a): 'Reconnaisance studies of the tufa deposits of the Napier Range, N.W. Australia', *Earth Surf. Proc. Landf.,* 15, 425–443
Viles. H.A. and Goudie, A.S. (1990b): 'Tufas, travertines and allied carbonate deposits', *Progr. Phys. Geogr.,* 14, 19–41
Viles, H.A. and Pentecost, A. (1999): 'Geomorphological controls on tufa deposition at Nash Brook, South Wales, United Kingdom', *Cave and Karst Sci.*, 26, 61–68

Villumsen, A. and Grelk, B. (1978): 'Sedimentological and microprobe studies of the lime tufas of Aastrup', *Den. Geol. Unders. Aarbog.,* (for 1976), 89–114
Vitek, J. (1973): 'Mikroformy zvetravani travertinu no Dreveniku u Spisskeho Podhradi', *Zprav. Geografik. Ustavu,* 10, 23–30
Vogel, J.C. (1970): 'Carbon-14 dating of groundwater', 225–239, in: *Isotope Hydrology*, Vienna (IAEA)
Vogel, J.C. (1985): 'Further attempts at dating the Taung tufas. In Tobias, P.V. (Ed.), pp. 189–194, *Hominid Evolution: past, present and future*. A.R. Liss, New York
Vogel, J.C. and Partridge, T.C. (1983): 'Preliminary radiometric ages for the Taung tufas', 507–514, in: J.C. Vogel (ed.), *Late Cainozoic Palaeoclimates of the Southern Hemisphere*. Rotterdam (Balkema)
Von der Dunk, K. and Von der Dunk, K. (1980): 'Algen und Moose bauen einen Aquäduct aus Tuff', *Mikrokosmos,* 69, 50–55
Wagenbreth, O. (1968): 'Geologische-gesteinskundliche und ökonomische Gesichtspunkle für den Abbau und die Verwendung der Travertine Thüringens', *Z. Angew. Geol.,* 14, 128–134
Walch, J.E.I. (1773): '*Von den incrustierten Körpen – Die Naturgeschichte der Versteinerungen*', Vol. 1, Nürnberg
Walcott, C.D. (1914): 'Cambrian geology and paleontology III: Precambrian Algonkian algal flora', *Smithsonian Misc. Coll.*, 64, 77–156
Wallner, J. (1933): '*Oocardium stratum* Naeg. Eine wichtige tuffbildende Alge Südbayerns', *Planta*, 20, 287–293
Wallner, J. (1934a): 'Beitrag zur Kenntnis der *Vaucheria*-Tuffe', *Zbl. Bakt. Parasiteku. Infekt.* Abt. II, 90, 150–154
Wallner, J. (1934b): 'Über die Beteiligung Kalkablagernder Pflanzen bei der Bildung südbayerischen Tuffe', *Bibl. Bot.*, 111, 1–30
Wallner, J. (1935a): 'Über die Kalkbildung in der Gattung *Cosmarium*', *Beih. Bot. Zbl. Abt. A.*, 53, 586–590
Wallner, J. (1935b): 'Über die Verbreitungsökologie der Desmidiacee *Oocardium*', *Planta*, 23, 249–263
Wallner, J. (1935c): 'Eine gesteinebildende Süsswasser-Alge Deutschlands', *Natur. und Volk*, 66, 85–91
Wallner, J. (1936): 'Zur Kenntnis der Gattung *Oocardium*', *Hedwigia*, 75, 130–136
Wang, X. (1985): 'Some characteristics of stable isotopes of oxygen and carbon in speleothems of Guilin', *Carsalogica Sinica,* 3, 149–154
Wang, X. (1986): 'U-dating and $\delta^{18}O$, $\delta^{13}C$ features of speleothems in Maomaotou Big Cave, Guiling', *Chinese Sci. Bull.*, 31, 835–838
Walter, L.M. and Morse, J.W. (1985): 'The dissolution kinetics of shallow marine carbonates in seawater. A laboratory study', *Geochim. Cosmochim. Acta,* 49, 1503–1513
Walter, M.R. (1976): 'Introduction', 1–3, in: M.R. Walter (ed.), *Stromatolites, Studies in Sedimentology, 20*, Amsterdam (Elsevier)
Walter, M.R. (1983): 'Archaean stromatolites: evidence of the Earth's earliest benthos', 187–213, in: J.W. Schopf (ed.), *Earth's Earliest Biosphere*, Princeton, NJ.(Princeton University Press)
Walter, M.R., Bauld, J., and Brock, T.D. (1976): 'Microbiology and morphogenesis of columnar stromatolites (*Conophyton*, *Vacerrilla*) from hot springs in Yellowstone National Park', pp. 273–310 in Walter, M.R. (ed.), *Stromatolites*, Elsevier, Amsterdam
Walter, M.R., DesMarais, D., Farmer, J.D. and Hinman, N.W. (1996): 'Lithofacies and biofacies of Mid-Paleozoic thermal spring deposits in the Drummond Basin, Queensland, Australia', *Palaios*, 11, 497–518
Waltham, A.D., Brook, D. and Bottrell, S. (1993): 'The caves and karst of Xingwen, China', *Cave Sci.,* 20, 75–86
Walther, K. (1942): 'Die Moosflora der *Cratoneuron commutatum*- Gesellschaft in den Karawanken', *Hedwigia*, 81, 127–130
Ward, D.M., Tayne, T.A., Anderson, K.L. and Bateson, M.M. (1987): 'Community structure and interactions among members in hot spring cyanobacterial mats', *Symp. Soc. Gen. Microbiol.*, 41, 179–210
Waring, G.A. (1965): 'Thermal springs of the United States and other countries of the world, a summary. Revised by R.R. Blankenship and R. Bentall. *U.S. Geol. Surv. Prof. Paper,* 492, 1–383
Warren, J.K. (1982): 'The hydrological significance of Holocene tepees, stromatolites, and boxwork limestones in coastal salinas in South Australia', *J. Sed. Petrol.,* 52, 1171–1201
Warwick, G.T. (1952): 'Rimstone pools and associated phenomena', *Trans. Cave. Res. Group GB.,* 2, 153–165
Warwick, T. (1953): 'The nature of shell encrustations in some aquatic molluscs', *Proc. Malac. Soc. Lond.*, 30, 71–73
Watts, N.L. (1980): 'Quaternary pedogenic calcretes from the Kalahari (southern Africa): mineralogy, genesis and diagenesis', *Sedimentology*, 27, 661–686
Weed, W.H. (1889a): 'The formation of travertine and siliceous sinter by the vegetation of hot springs', *Ann. Report. U.S. Geol. Surv. 1887–1888,* 9, 619–676
Weed, W.H. (1889b): 'The diatom marshes and diatom beds of the Yellowstone National Park', *Bot. Gaz.*, 14, 117–120

Weed, W.H. (1889c): 'On the formation of siliceous sinter by the vegetation of thermal springs', *Am. J. Sci.*, 37, 351–359
Weijermars, R., Mulder-Blanken, C.W. and Wiegers, J. (1986): 'Growth rate observation from the moss-built Checa travertine terrace, central Spain', *Geol. Mag.*, 123, 279–286
Weiss, M.P. (1969): 'Oncolites, paleoecology, and Laramide tectonics, central Utah.' *Bull. Am. Assoc. Petrol. Geol.* 53, 1105–1120
Weiss, M.P. (1970): 'Oncolites forming on snails (*Goniobasis*)', *J. Palaeontol.*, 44, 765–769
Went, F.W. (1969): 'Fungi associated with stalactite growth', *Science*, 166, 385–386
West, R.G. (1964): 'Inter-relations of ecology and Quaternary palaeobotany', *J. Ecol. Suppl.*, 52, 47–57
Westphal, F. (1959): Neue Wirbeltierreste (Fledermause, Froesche, Reptilien) aus dem obermiozänen Travertin von Böttingen (Schwäbische Alb)', *Neues Jb. Geol. Paläont. Abh.*, 107, 341–365
Wetzel, R.G. (2001): *Limnology*. 3rd Edn, 767 pp., San Diego, Ca. (Academic Press)
Wharton, R.A., Parker, B.C., Simmons, G.M. Jr., Seaburg, K.G. and Love, F.G. (1982): 'Biogenic calcite structures forming in Lake Fryxell, Antarctica', *Nature*, 295, 403–405
Wheeler, A.P., Rusenko, K.W., Swift, D.M. and Sikes, C.S. (1988): 'Regulation of *in vitro* and *in vivo* $CaCO_3$ crystallization by fractions of oyster shell organic matrix', *Mar. Biol.*, 98, 71–80
White, D.E. (1957): 'Magmatic, connate and metamorphic waters', *Geol. Soc. Am. Bull.* 68, 1659–1682
White, D.E., Hem, J.D. and Waring, G.A. (1963): 'Chemical composition of sub-surface waters', *U.S. Geological Survey Professional Paper* 440F, 67pp
White, D.E., Fournier, R.O., Muffler, C.J.P. and Truesdell, A.H. (1975): 'Physical results of research drilling in thermal areas of Yellowstone National Park, Wyoming', *U.S. Geol. Surv. Pof. Paper* 892, 63–64
White, W.B. (1976): 'Cave minerals and speleothems' 267–327, in: T.D. Ford, C.H.D. Cullingford (eds), *The Science of Speleology*, London (Academic Press)
White, W.B. (1981): 'Reflectance spectra and color in speleothems', *Nat. Spel. Soc. Bull.,* 43, 20–26
White, W.B. (1982): 'Mineralogy of the Butler Cave – Sinking Creek system', *Nat. Spel. Soc. Bull.,* 44, 90–97
White, W.B. (1988): *Geomorphology and Hydrology of Karst Terrains.* 464 pp., Oxford, UK (Oxford University Press)
White, W.B. (1994): 'The anthodites from Skyline Caverns, Virginia: the type locality', *NSS Bull.*, 56, 23–26
White, W.B. and Deike, G.H. (1962); 'Secondary mineralization in Wind Cave, South Dakota', *Nat. Spel. Soc. Bull.,* 24, 74–87
Whitten, D.A. and Brooks, J.V.R. (1972): '*The Penguin Dictionary of Geology*', 496 pp.,London (Penguin)
Whitton, B.A. (1987): 'The biology of the Rivulariaceae', 513–524, in: P. Fay, C. van Baalen (eds), *The Cyanobacteria – A Comprehensive Review*, Amsterdam (Elsevier)
Wiegel, J. and Ljungdahl, L.G. (1981): '*Thermoanaerobacter ethanolicus*, gen. nov., a new, extreme thermophilic, anaerobic bacterium', *Arch. Microbiol.*, 128, 343–348
Wigley, T.M.L. (1971): 'Ion pairing and water quality measurements', *Can. J. Earth Sci.,* 8, 468–476
Wigley, T.M.L. (1975): 'Carbon 14 dating of groundwaters from closed and open systems', *Water Resources Res.*, 11, 324–328
Wilken, G. (1980): 'Morphology of inhibitor treated $CaCO_3$ precipitate', *Desalination*, 33, 201–210
Williams, J.H. (1971): 'Roman building-materials in south-east England', *Britannia*, 2, 166–195
Williams, W.D. (1981): 'Salt lakes', 1–14, in: W.D. Williams (ed.), *Developments in Hydrobiology,* 5, The Hague (W. Junk)
Williams, R. (1989): '*Limekilns and Limeburning*', 45 pp.,Buckingham, UK (Shire Publications)
Wilmotte, A. and Herdman, M. (2001): 'Phylogenetic relationships among the cyanobacteria based on 16S rRNA sequences', 487–493, in: D.R. Boone, R.W. Castenholz (eds), *Bergey's Manual of Systematic Bacteriology*, 2nd Edn., Vol. 1., New York (Springer-Verlag)
Wilson, L.R. and Guest, M.E. (1961): 'Travertine formation associated with mosses at Turner Falls and Prices Falls, Oklahoma', *Oklahoma Geol. Notes*, 21, 310–316
Winsborough, B.M. (2000): 'Diatoms and benthic microbial mats', 76–83, in: R. Riding, S.M. Awramik (eds), *Microbial Sediments*, Berlin (Springer-Verlag)
Winsborough, B.M. and Seeler, J. –S. (1984): 'The relationship of diatom epiflora to the growth of limnic stromatolites and microbial mats', 395–407, in: M. Ricard (ed.), *Proc. 8th Diatom Symposium,* Paris
Winsborough, B.M. and Golubic, S. (1987): 'The role of diatoms in stromatolite growth: two examples from modern freshwater settings', *J. Phycol.,* 23, 195–201
Winsborough, B.M., Seeler, J. -S., Golubic, S., Folk, R.L. and Maguire, B. (1994): 'Recent freshwater lacustrine stromatolites, stromatolitic mats and oncoids from Northeastern Mexico', 71–100, in: J. Bertrand-Sarfati, C.L.V. Monty (eds), *Phanerozoic Stromatolites II*, Netherlands (Kluwer)
Winsborough, B.M., Caran, S.C., Neely, J.A. and Valastro, S. Jr. (1996): 'Calcified microbial mats date prehistoric canals – radiocarbon assay of organic extracts from travertine', *Geoarchaeology,* 11, 37–50
Woese, C.R., Kandler, O. and Wheelis, M.L. (1990): 'Towards a natural system of organisms: proposal for the domains Archaea, Bacteria and Eucarya', *Proc. Nat. Acad. Sci. USA,* 87, 4576–4579

Wood, B. (2002): 'Who are we?', *New Scientist*, October, 2002, 44–47
Woodburn, J.G. (1936): 'Tests of broad-crested weirs', *Trans. Am. Soc. Civ. Eng.*, 96, 387–453
Woodward, F.I. (1987): '*Climate and Plant Distribution*', 174 pp., Cambridge UK (Cambridge University Press)
Woodward, F.I. (1988): 'Temperature and distribution of plant species', 59–75, in: S.P. Long, F.I. Woodward (eds), *Plants and Temperature*, Cambridge UK (Society of Experimental Biology)
Wopfner, H. and Twidale, C.R. (1967): 'Geomorphological history of the Lake Eyre Basin', 119–143, in: J.N. Jennings, J.A. Mabbutt (eds). *Landform Studies from Australia and New Guinea.* Cambridge, UK (Cambridge University Press)
Wright, J.S. (2000): 'Tufa accumulations in ephemeral streams: observations from the Kimberley, north-west Australia', *Australian Geogr.*, 31, 333–347
Wright, V.P. (1990): 'A micromorphological classification of fossil and recent calcic and Petrocalcic microstructures', 401–407, in: L.A. Douglas (ed.), *Soil Micromorphology: a Basic and Applied Science. Developments in Soil Science*, 19, Amsterdam (Elsevier)
Wright, V.P. and Tucker, M.E. (1991): 'Calcretes: introduction', *Int. Ass. Sedimentol.,* 2, 1–22
Yang H., Zhu, W.X. and Huang, R. (1985): 'Research on travertine formation in the rivers of Guizhou', 39–47, in: *Karst Landforms and Caves*, Beijing (Science Press)
Yong Lao and Benson, L. (1988): 'Uranium series age estimates and paleoclimatic significance of Pleistocene tufas from the Lahontan Basin, California and Nevada', *Quat. Res.,* 30, 165–176
Yoshimura, K., Iwaya-Inoue, M., Someya, T. and others. (1996): 'Contribution of cyanobacteria to the formation of tufa in the entrance to Akiyoshi-dô Cave, Yamaguchi', *J. Spel. Soc. Japan*, 20, 27–37
Yoshimura, K., Liu, Z., Cao, J., Yuan, D., Inokura, Y. and Noto, M. (2004): 'Deep source CO_2 in natural waters and its role in extensive tufa deposition in the Huanglong Ravines, Sichuan, China', *Chem. Geol.*, 205, 141–153
Yurtsever, Y. (1976): 'Worldwide survey of stable isotopes in precipitation', *Report Section Isotope Hydrology, IAEA*, 1–40
Zaguzin, V.P., Zaguzina, T.A. and Pogrebnyak, Y.F. (1980): 'Concentrations of tungsten and molybdenum in mineral waters and travertines of Transbaikalia', *Geochimiya*, 17, 297–301
Zakrzewski, M.A. (1984): 'Minerals of the bravoite-vilamaninite series and cuprian siegenite from Karniowice, Poland', *Canadian Mineralogist*, 22, 499–502
Zammit-Maempel, G. (1977): '*An outline of Maltese Geology*', Malta
Zeidler, W. and Ponder, W.F. (1989): '*History of Dalhousie Springs*', 116 pp., Adelaide (South Australia Museum)
Zeissler, H. (1969): 'Möglichkeiten und Probleme quantitativer Arbeit mit fossilen Mollusken, dargestellt an einem Beispiel aus dem Ehringsdorfer Travertin (DDR.)', *Ber. Dt. Ges. geol. Wiss. Ser. A.*, 14, 507–531
Zeissler, H. (1975): 'Konchylien im Ehringsdorfer Pleistozäne', *Ger. Zent. Geol. Inst. Abh.*, *Teil* 2, 15–90
Zeissler, H. (1977a): 'Eine bisher übersehene Fossilgruppe ungeklärter Zugenhörigkeit aus Taubach und anderen Thüringer Quartärablagerungen', *Quartärpaläont.*, 2 (1976), 161–165
Zeissler, H. (1977b): 'Konchylien aus den Pleistozän von Taubach, Grube Vollmar', *Quartärpaläont.*, 2 (1976), 139–160
Zhang, Dian., Zhang, Y., Zhu, A. and Cheng, X. (2001): 'Physical mechanisms of river waterfall tufa (travertine) formation', *J. Sed. Res.,* 71, 205–216
Zhang, Dian and Li, S.H. (2002): 'Optical dating of Tibetan human hand- and footprints: An implication for the palaeoenvironment of the last glaciation of the Tibetan Plateau', *Geophys. Res. Lett.*, 29, pt. 16, 1–3
Zhang, Jie (1993): 'On bio-effects on the development of karst-dammed lakes in limestone areas, Minshan Mountain Range, NW Sichuan', *Carsalogica Sinica*, 5, 30–30
Zhang, Q.-S., Tao. J., Huang, C. and Gu, C. (1990): 'A discovery of late Cenozoic fossil plants in Kunlun Mountains', *Chinese Sci. Bull.*, 35, 197–205
Zhang, Yingjun and Mo, Z. (1982): 'The origin and evolution of Orange Fall', *Acta Geographica*, 37, 303–316
Zhang, Z. (1993): 'A catalogue of Musci in Maolan karst forest area, Lipo County, Guizhou', *J. Guizhou Normal University*, 11, 33–42
Zhang, Z. (1996): 'Contributions to the bryoflora of Guizhou, S.W. China: new records and habitat notes on mosses from Huangguoshu karst area', *J. Bryol.,* 19, 149–152
Zhang, Z. (1998): 'A preliminary taxonomical study on tufa-bryophytes in Guizhou, SW China', *Chenia*, 5, 173–176
Zhang, Z. and Pentecost, A. (2000): 'New and noteworthy bryophytes from the travertines of Guizhou and Sichuan', *J. Bryol.,* 22, 66–68
Zhdanov, G.S. (1965): '*Crystal Physics*', translated by A.F. Brown. 500 pp., Edinburgh (Oliver and Boyd)
Zheng, M., Tang, J. and Zhang, F. (1993): 'Chinese saline lakes', *Hydrobiologia*, 267, 23–36
Ziegler, M. (1972): 'Honau und die Olgahöhle', *Abh. Karst u. Höhlenkunde,* A7, 3–18
Zyka, V. (1958): 'Die Rolle der Ölfeldwässer bei der Akkumulation und Verteilung der chemischen Elemente', *Acta geol. Hung.,* 5, 435–478
Zyka, V. and Vtelensky, J. (1960): 'Geochemie slovenkých travertinu', *Geol. Pr. Zpravy,* 17, 147–196

Photoplates

Photoplate 1
Travertine Mounds and Cascades

A A pair of small (5 m high) recently active thermogene mounds near Auburn, Wyoming, USA

B One of the self-built canals at Pamukkale, Turkey. Note break in the canal wall caused by earth movements and the main travertine mound in the background

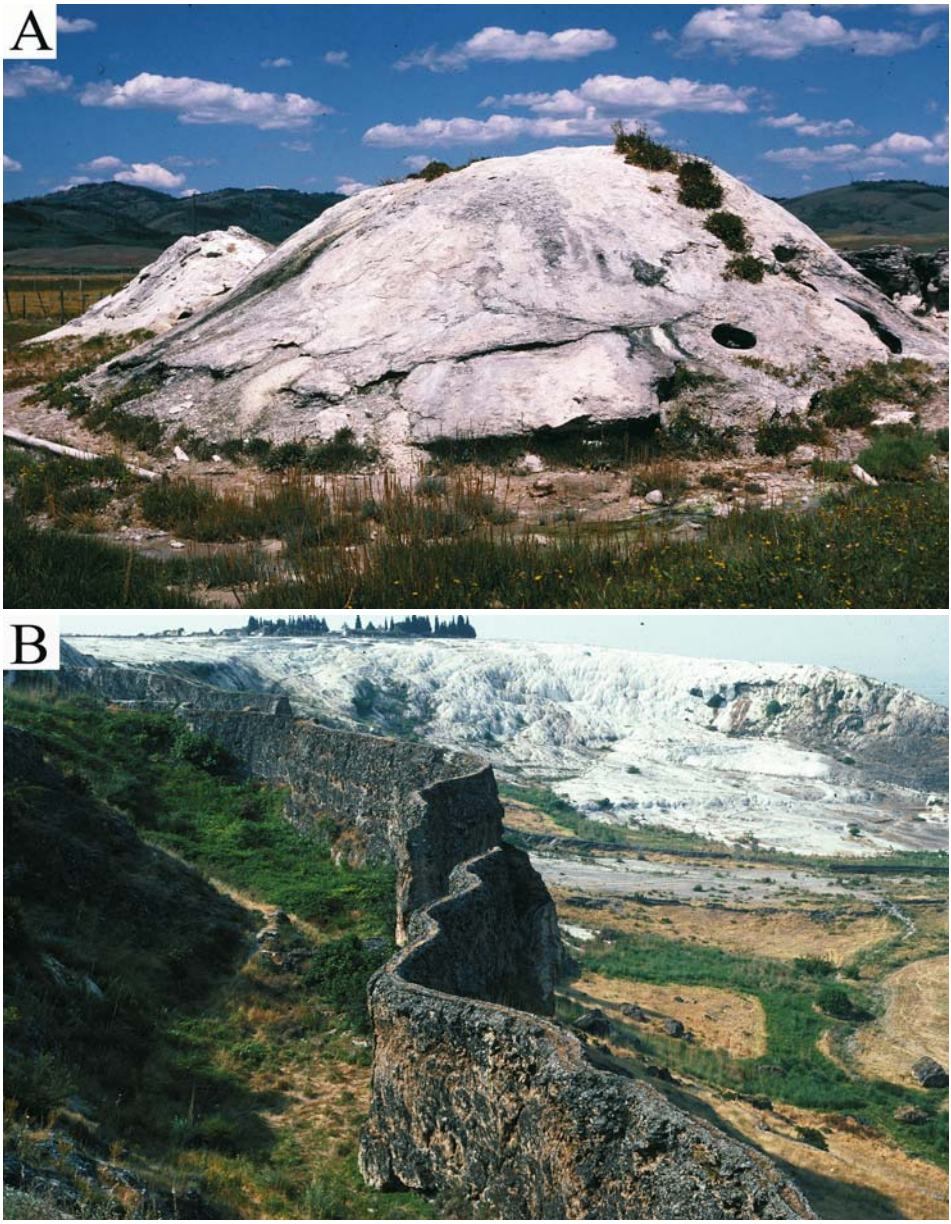

C Prices Falls, Arbuckle Mountains, Oklahoma, USA. One of a series of small erosively-shaped cascades colonised by the cyanobacterium *Phormidium incrustatum*

D Part of the steep prograding section of the Gütersteiner Falls, Germany colonised by the moss *Palustriella commutata*

E Canary Terrace, Mammoth Hot Springs, Wyoming, USA. A complex series of minidams in the foreground with streaks of colourful photosynthetic bacteria on the large mound in the background

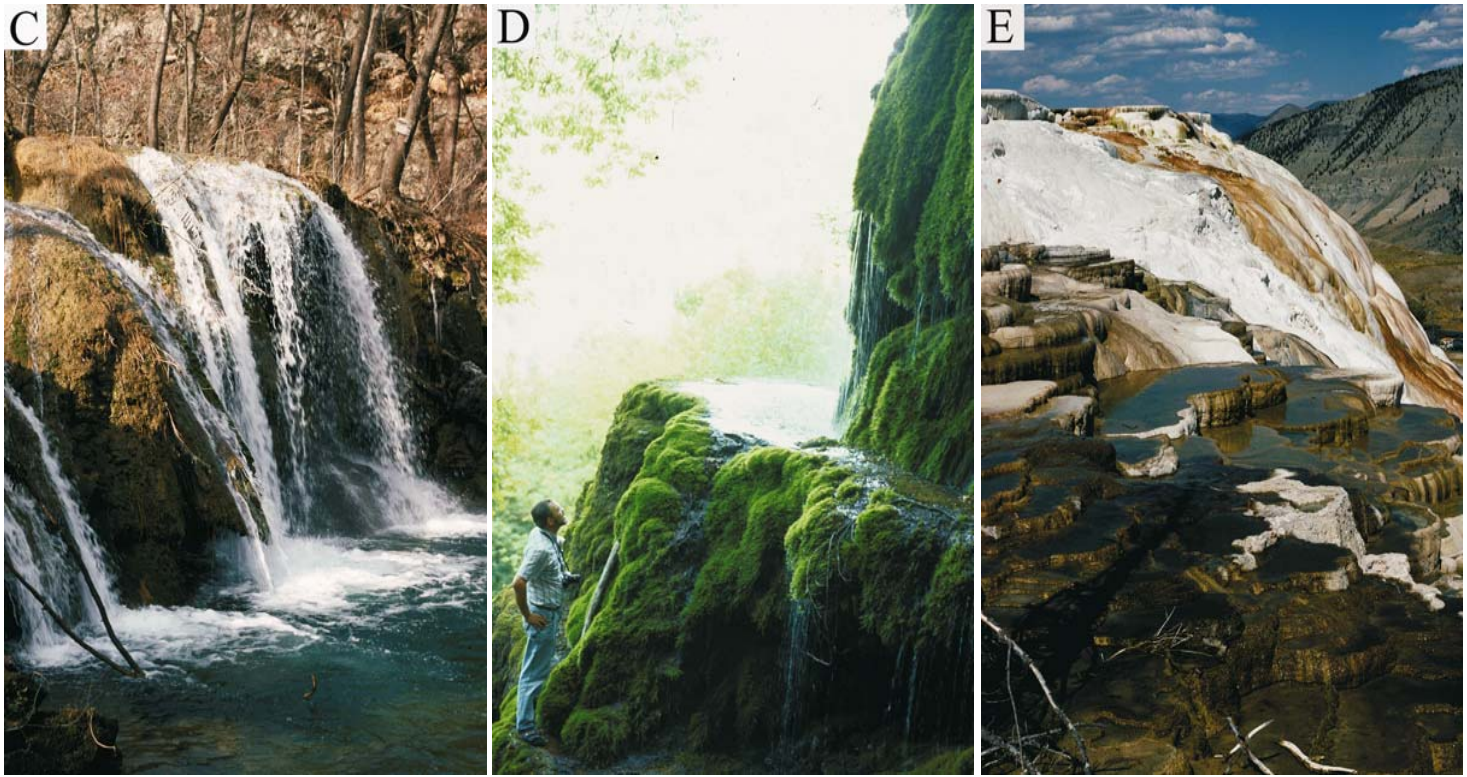

Photoplate 2
Organisms Colonising Travertine

A A fire salamander stands atop a fertile cushion of *Palustriella commutata* var. *commutata* searching for invertebrates on a German travertine-depositing stream. To left is a dense green cushion of the moss *Hymenostylium recurvirostrum*

B A stem of the moss *Bryum pseudotriquetrum* characterised by its rusty-red tomentum supports two *Pericoma trifasciata* moth flies with pubescent and iridescent wings. Below, two *Pericoma* larvae forage among the liverwort *Pellia endiviifolia*


A


B

Photoplate 3
Travertine Morphologies and Encrustations

A Prograding draperies of the Reotier travertine deposit by the Durance River, French Alps
B Small travertine dams in Huanglong Ravine, Sichuan, China containing fine carbonate sediments under turquoise-blue water. The drop walls in the foreground are colonised by

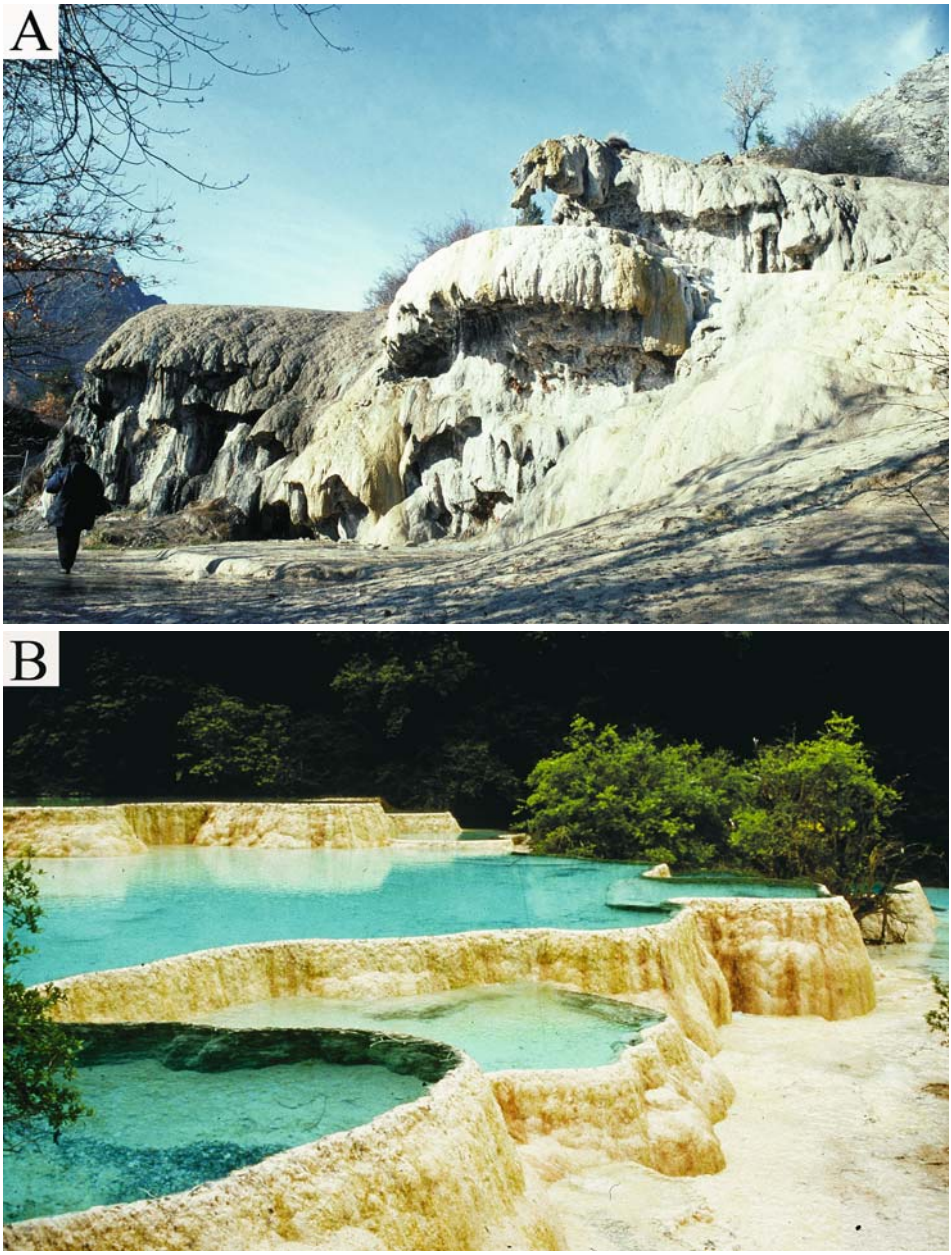

diatoms, principally *Gomphonema* giving a yellow-brown coloration from which the deposits are named (photo A. Waltham)

C Heavily encrusted waterwheel near Augusta, Western Australia. The travertine is colonised by the cyanobacterium *Schizothrix* and filamentous green algae

D Iron-rich encrustation resembling a rose flower obtained from a metal armature immersed in the 'petrifying' springs at Carlsbad, Czech Republic

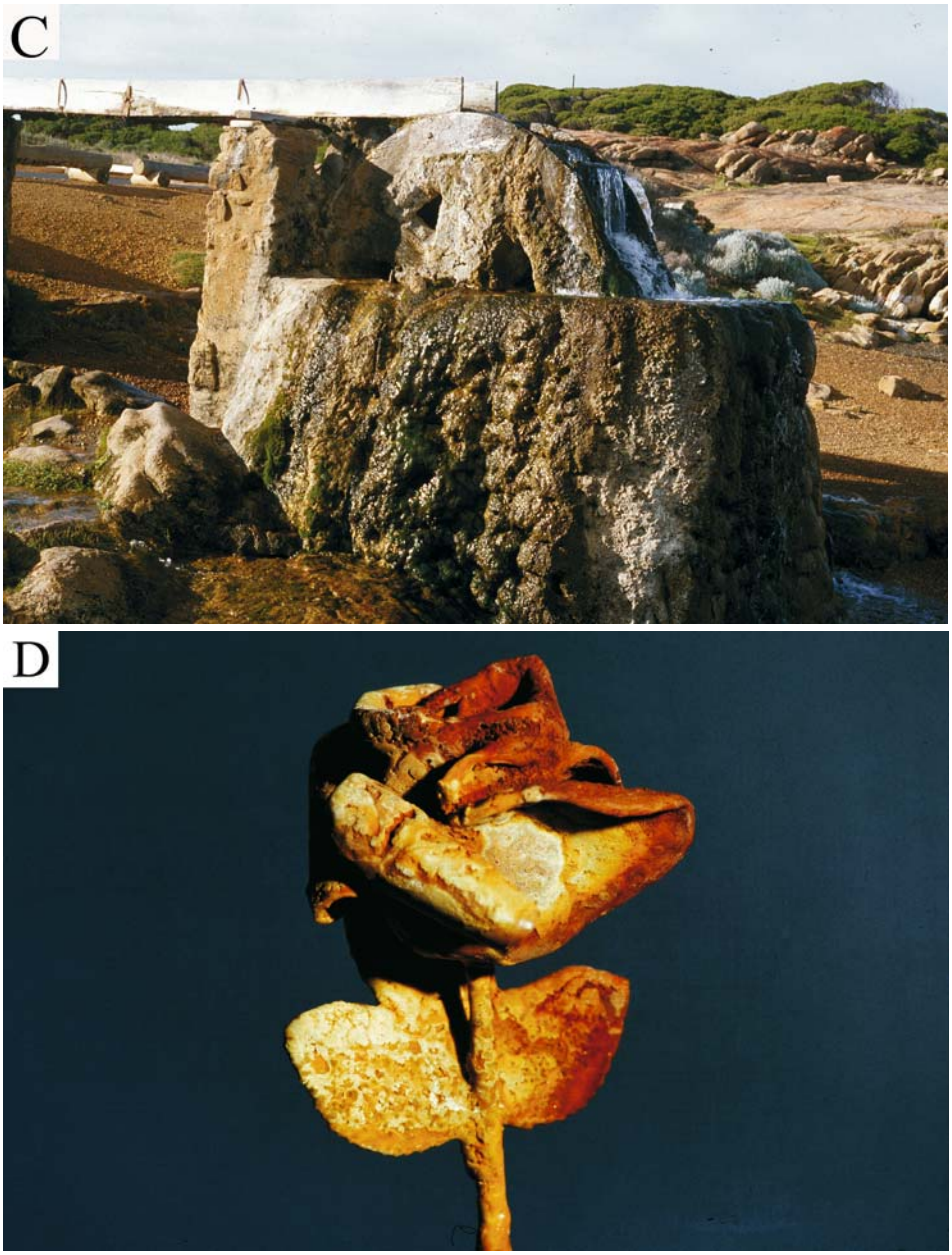

Photoplate 4
Micrite and Sparite in Thin Section

A Laminated micrite (dark areas) alternating with pale microspar mosaic. The micrite layers are 300–500 μm in thickness and the band on the left contains fine wavy layers about 40 μm wide, possibly representing daily accumulation. Interpretation is difficult at this site because the deposit is artificially irrigated to maintain a highly reflective surface. Pamukkale main mound, Turkey. Vertical section, deposit surface to left. Transmitted light. Bar 200 μm

B Clotted micrite in a matrix of microspar. Clots are 20–40 μm wide. The deposit contains burrowing porosity, the large hole probably being formed by an insect larva. No microbial structures are evident. Vertical section, surface to top. Transmitted light. El Riego, Mexico. Bar 100 μm

C Clotted and peloidal micrite in a matrix of sparite. Vertical section, surface to left. Transmitted light. Matlock Bath, UK. Bar 50 μm

D Palisade of microspar surrounded by micrite from a minidam at Huanglong Ravine, Sichuan, China. Vertical section, surface to left. Crossed nicols. Bar 50 μm

E Radial spar developed around bryophyte stems in a cascade travertine about 4000 years old. Section parallel to surface, crossed nicols. Gordale Lower Mound, Yorkshire, UK. Bar 25 μm

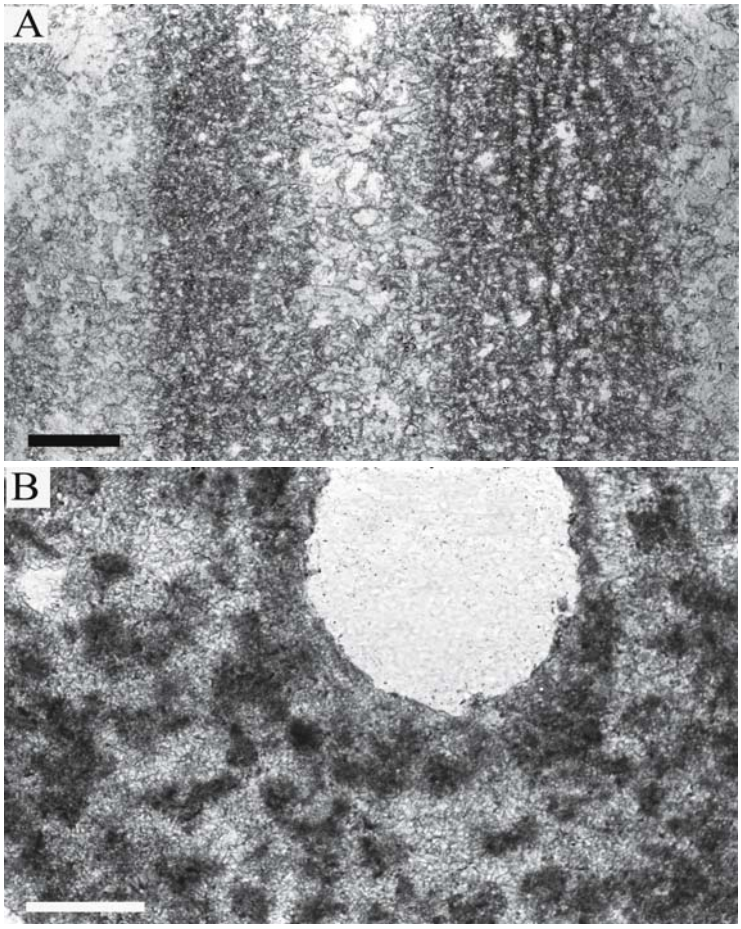

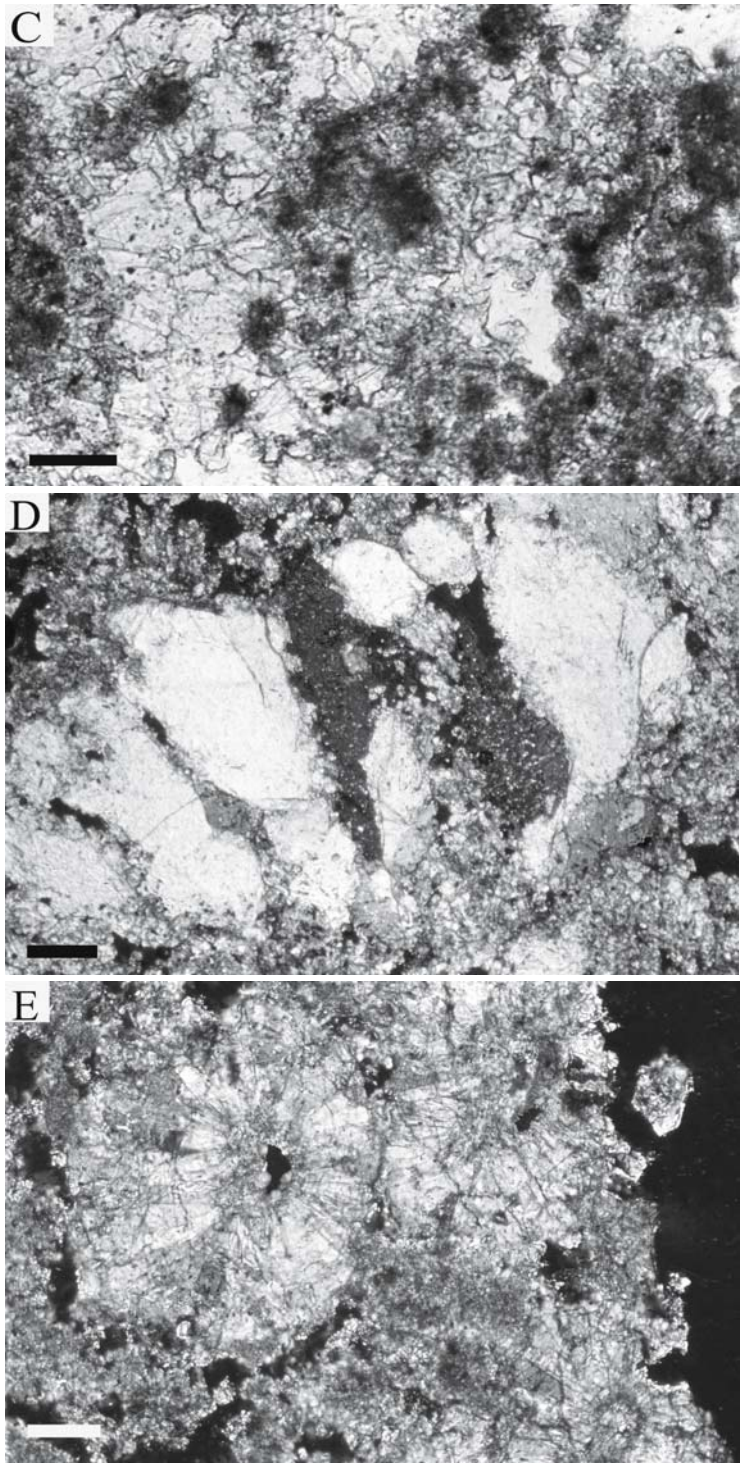
C
D
E

Photoplate 5
Sparite and Dendritic Calcite

A Drusy calcite lining cavities formed by shelter- and framework porosity in a Holocene *Palustriella* travertine from Matlock Bath, UK. Some of the crystals appear to be scalenohedra. Crossed nicols, vertical section. Bar 100 μm

B Radial-fibrous calcite developing on a fragment of shale. Colloform banding and ballooning crystal aggregates with sweeping extinction can be seen. Vertical section, crossed nicols. Invasive meteogene deposit at Ingleton, UK. Bar 100 μm

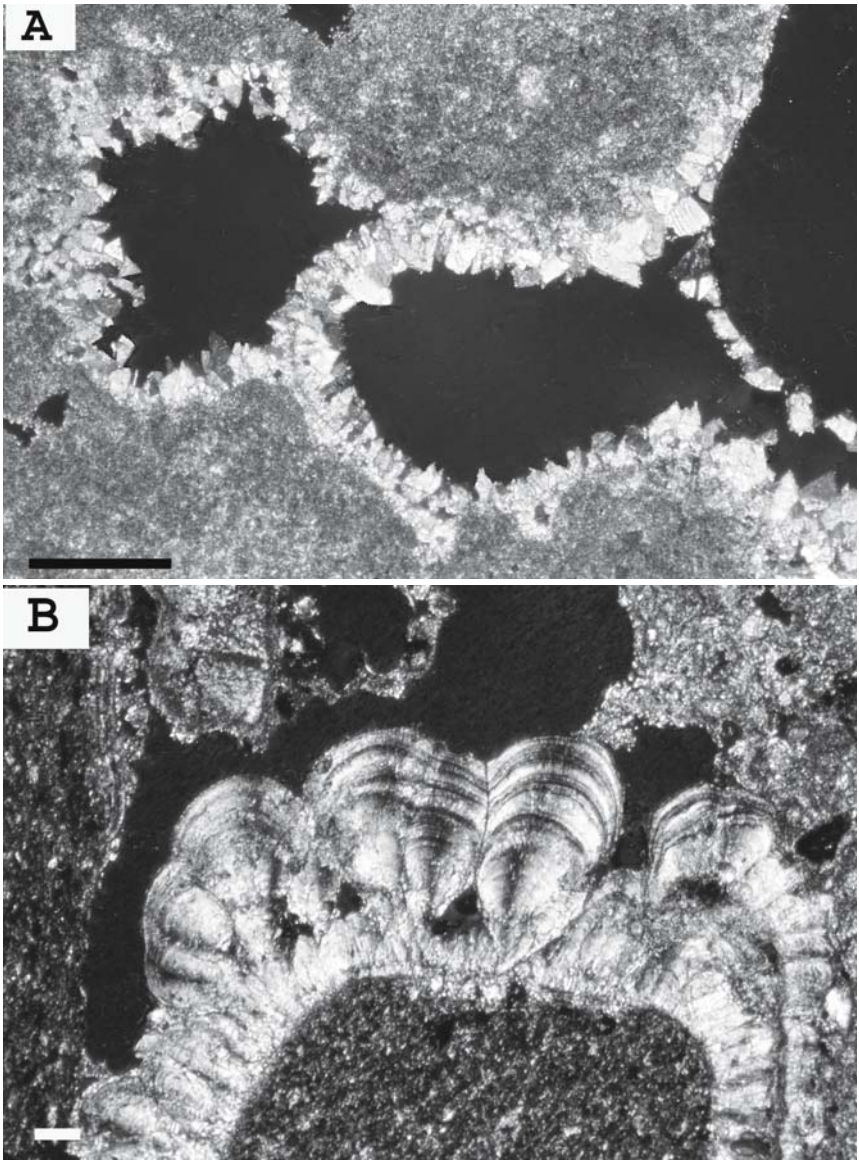

C Feather crystals from a travertine minidam. Individual 'elements' of the feathers consist of fibrous calcite with sweeping extinction forming complex interlocking units 180–300 μm long by 50–100 μm wide with jagged margins. Note the faint superimposed lamination. Plane transmitted light, vertical section. Suio modern thermogene deposit, Italy. Bar 5 mm

D Dendritic feather crystals forming complex aggregates perpendicular to the deposit surface. The branches are non-crystallographic and the feathers exhibit sweeping extinction. Crossed nicols, vertical section. Bagni Vignoni modern thermogene travertine, Italy. Bar 100 μm

E Feather crystals of calcite showing crystallographic branching. Crossed nicols, vertical section. Pamukkale lower mound, Turkey. Bar 50 μm

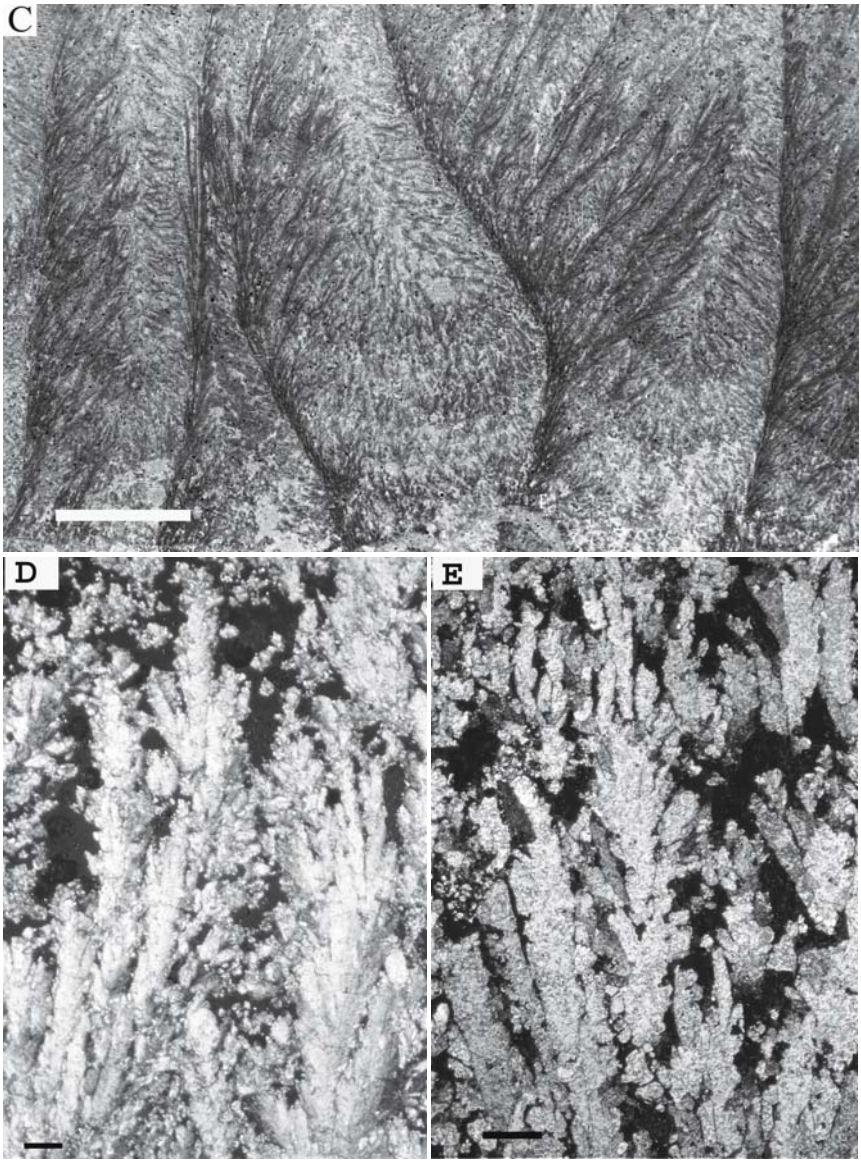

Photoplate 6
Shrubs

A Bacterial shrubs in a smooth block of Bagni di Tivoli travertine, Italy. Small oncoids ('pisoids') can be seen in places above the shrub layer. Top of deposit to left. Bar 1 cm

B Thin section through a shrub showing branched structures composed of dark clotted micrite closely associated with the remnants of bacteria. Shrubs are normally ensheathed with a layer of microspar as shown here. Cave Bruno Poggi, Bagni di Tivoli, Italy. Vertical section, plane transmitted light. Bar 100 μm

C Dense feather-like shrubs in a thermal (?thermogene) travertine of probable Pleistocene age. The smallest structural units consist of fibrous calcite containing numerous bacterium-sized inclusions rendering them dark under plane transmitted light. Vertical section. San Marcos Mesa. Cuatro Cienegas, Mexico. Bar 1 mm

D Modern aragonite shrub from Canary Terrace, Mammoth Hot Springs, Wyoming. Most of the aragonite needles building these shrubs are below the resolution of this image. Plane transmitted light, vertical section. Bar 100 μm

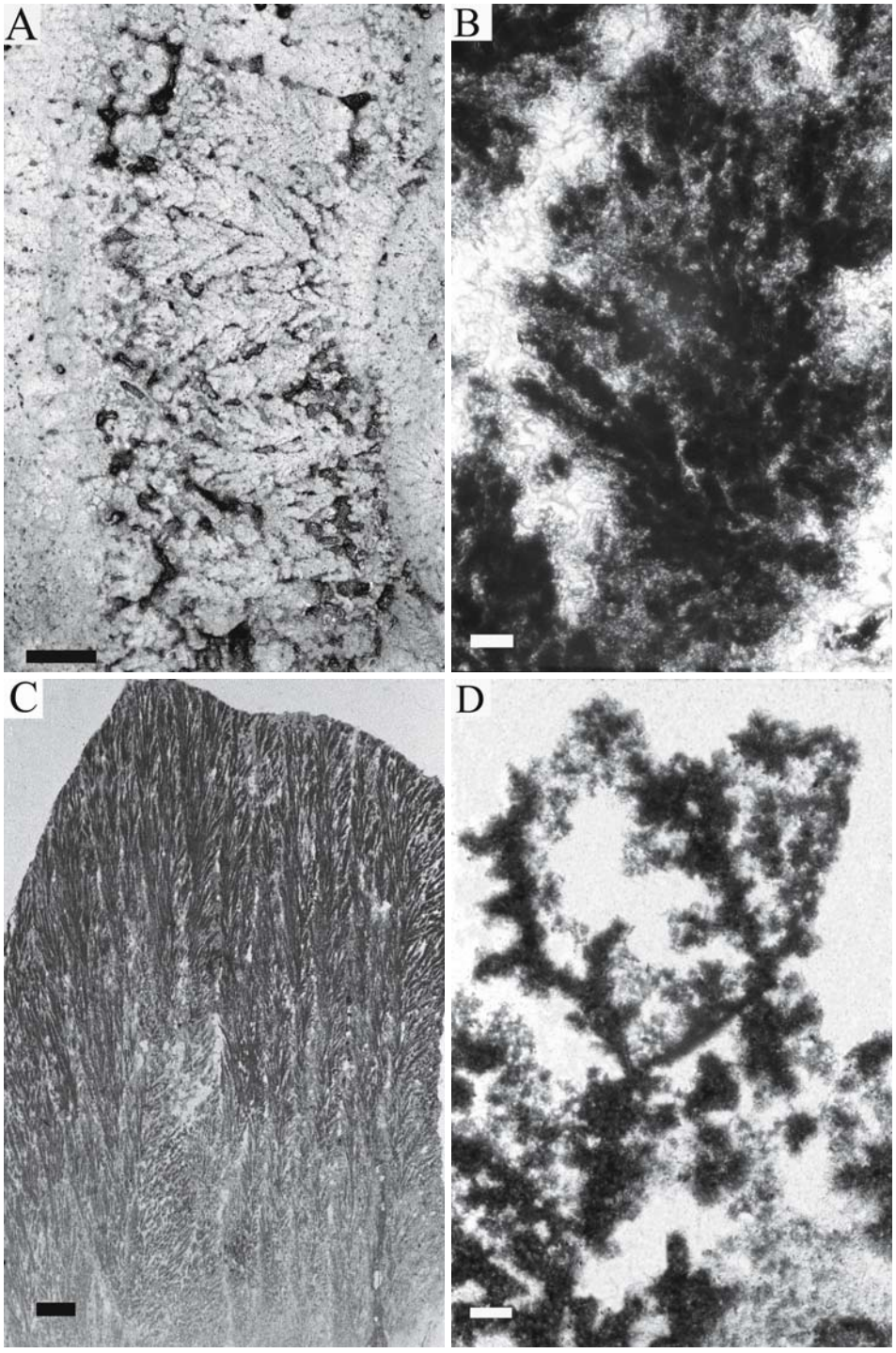
A
B
C
D

Photoplate 7
Mesofabrics

A High framework porosity produced by encrustation of the moss *Palustriella commutata* var. *commutata*. Matlock Bath, UK. Bar 1 cm

B 'Foam rock' formed from encrusted gas bubbles forming at the travertine surface. Early Pleistocene, Sütto, Hungary. Bar 2 cm

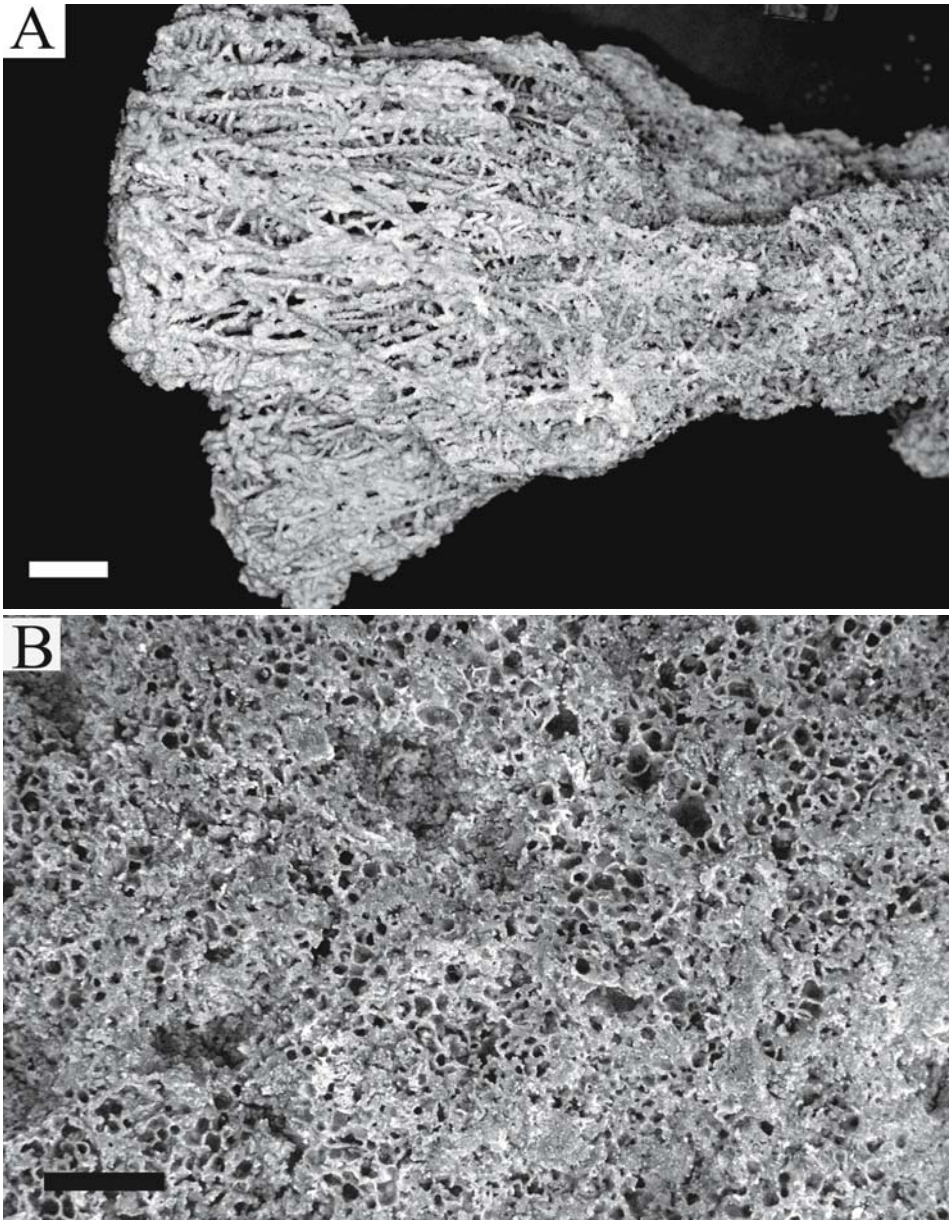

C Layers of floe developed in an originally water-filled depression in the Bagno Vignoni travertine, Italy. Bar 2.5 cm
D Small ooids ('pisoids') in a polished vertical section of the Pleistocene Bagni di Tivoli travertine, Italy. (Photograph by P. Tortora). Bar 5 cm
E Encrusted modern *Vaucheria* from Wateringbury, UK. Modern. Bar 1 cm

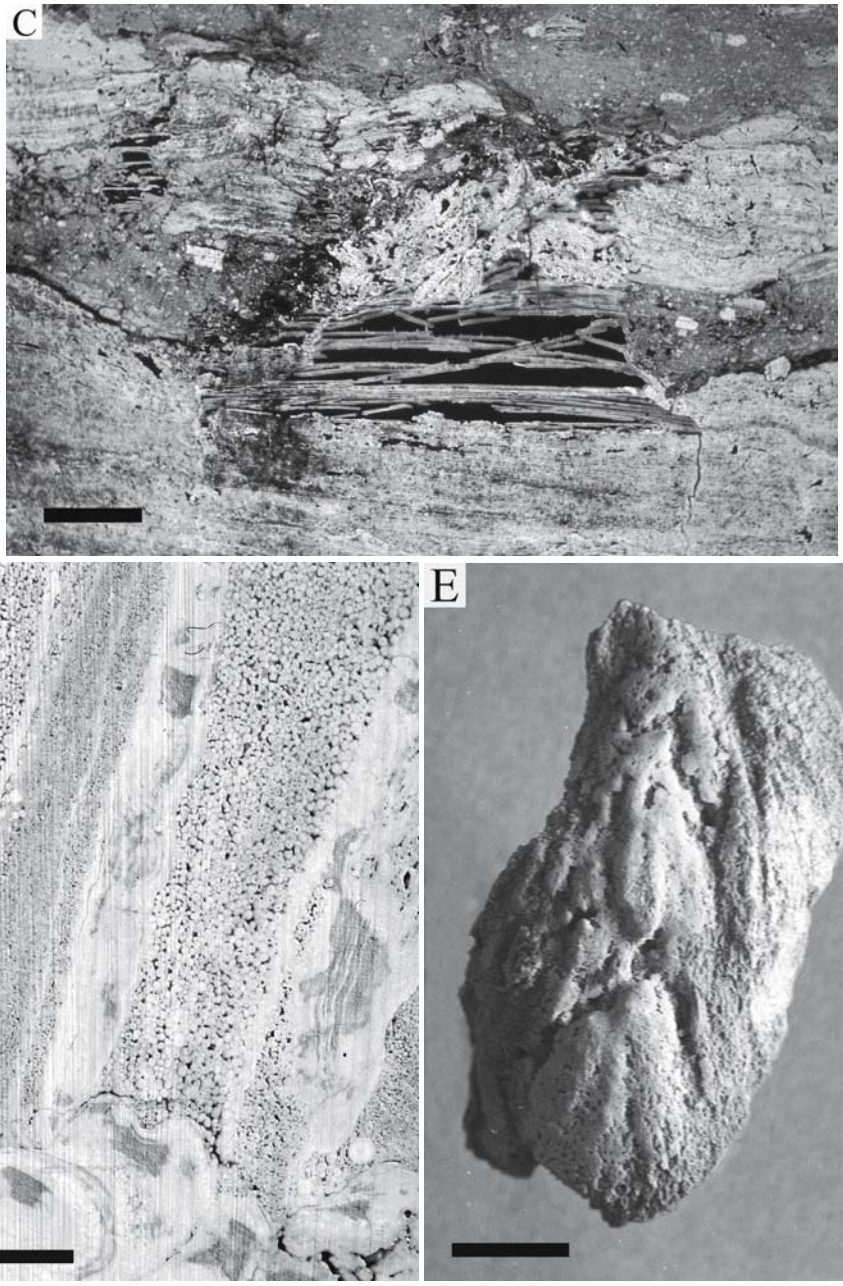

Photoplate 8
Oncoids and Lamination

A A collection of modern oncoids from a wooded cool-temperate meteogene stream illustrating the range of shapes and sizes. Oncoids are colonised by the cyanobacterium *Phormidium incrustatum*. The more elongate specimens probably formed around fragments of twig. Priory Mill, Oxfordshire, UK. Bar 2.5 cm

B Sections through the above oncoids showing annual lamination. Bar 2.5 cm

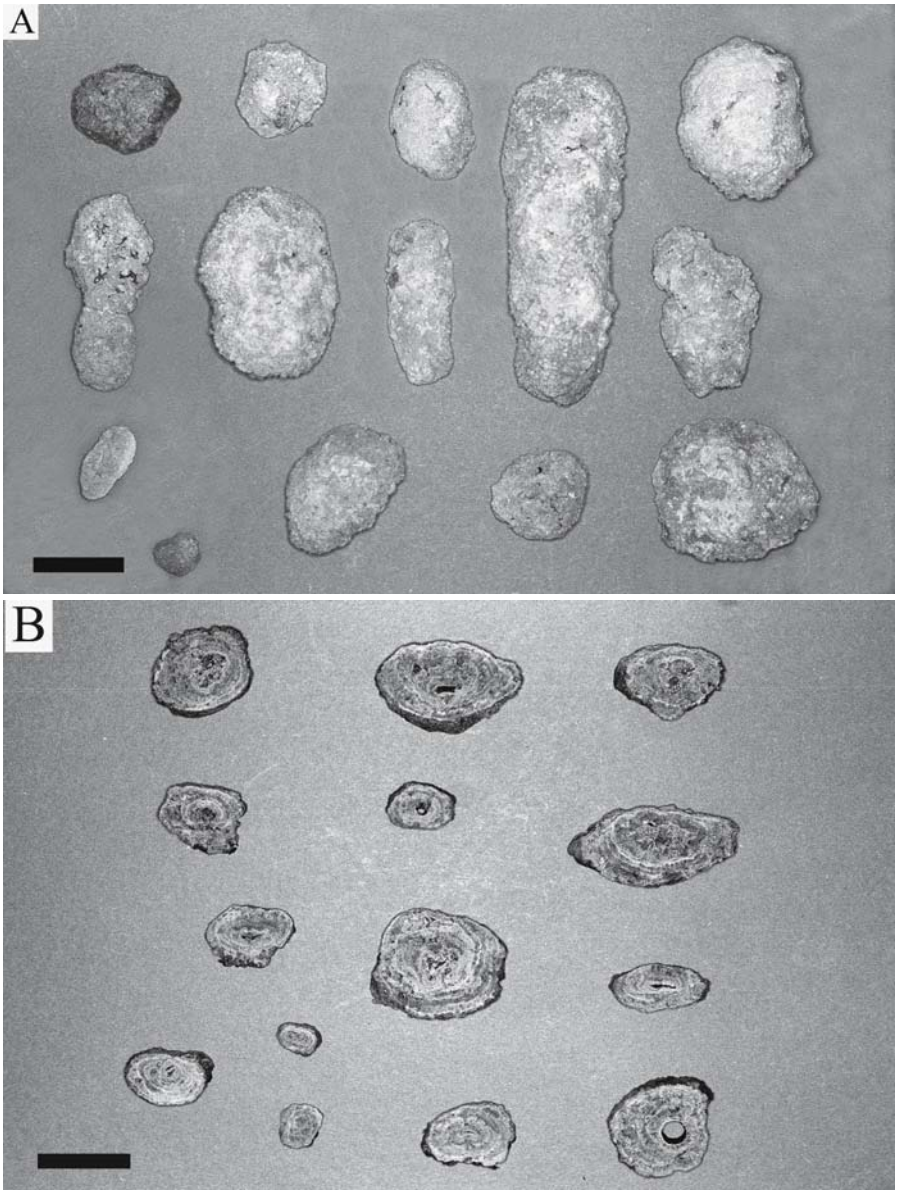

C Fine daily lamination in a modern thermogene deposit at Bagni Vignoni, Italy. The dark layers consist mainly of micrite and are formed at night. Radiating feather crystals of calcite which run across these layers can be seen at the right. Vertical section, transmitted light. Bar 2 mm

D Annual alternate lamination in a modern *Phormidium incrustatum* travertine. The dark layers were formed in the spring and summer and are thicker than the pale winter layers. Pommelsbrunn, Franconian Alb, Germany. Bar 1 cm

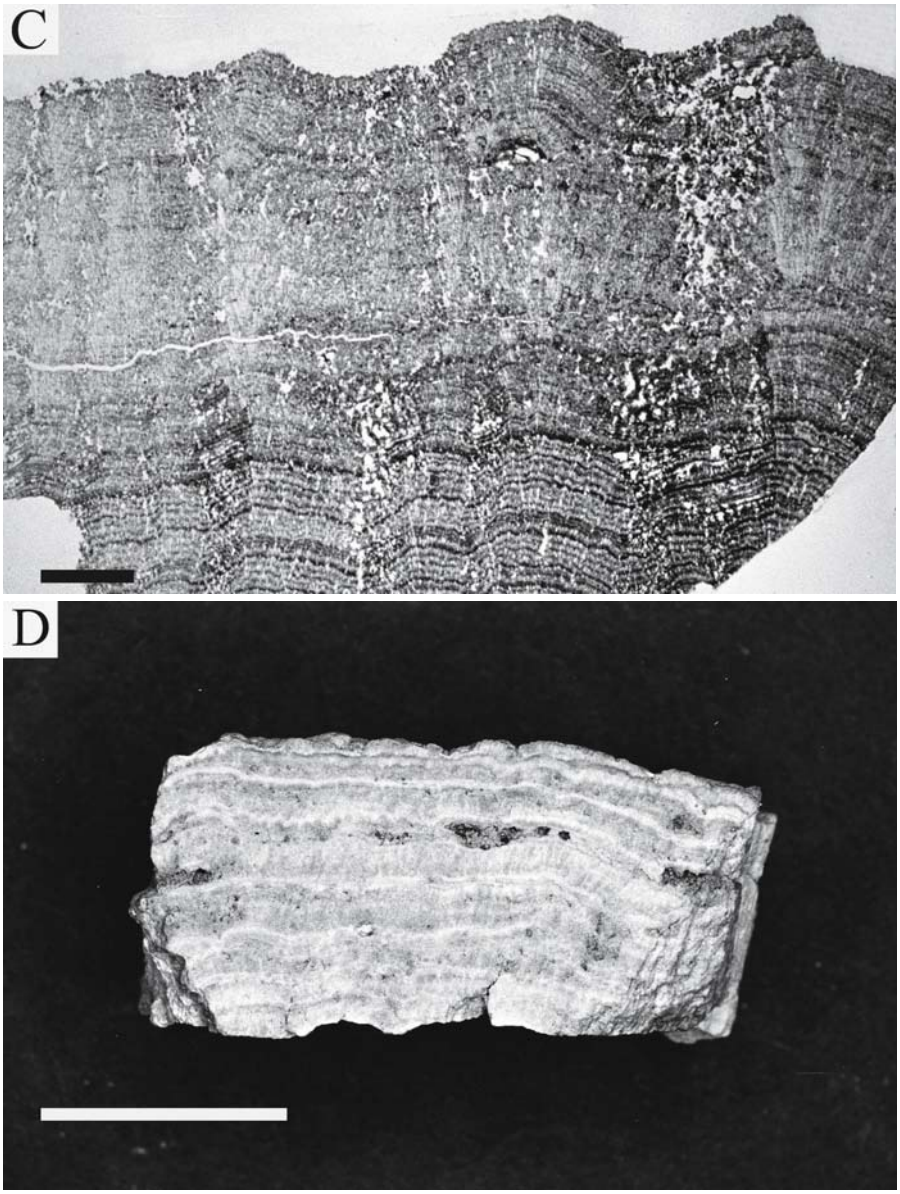

Photoplate 9
Mounds, Fissure Ridges and Cascades

A A small thermogene mound surrounding a large smooth-walled cavity partly filled with water. Heber, Utah
B Section through a fissure-ridge showing deposition of travertine parallel to the opening fracture. The fracture is now filled with clastics. Pamukkale, Turkey
C Partially active fissure ridge over 50 m in length. Rapolano Terme, Siena, Italy
D The Urach Waterfall, Schwäbische Alb, Germany. Water cascades over a prominent travertine nose on the limestone cliff and forms an extensive braided cascade below

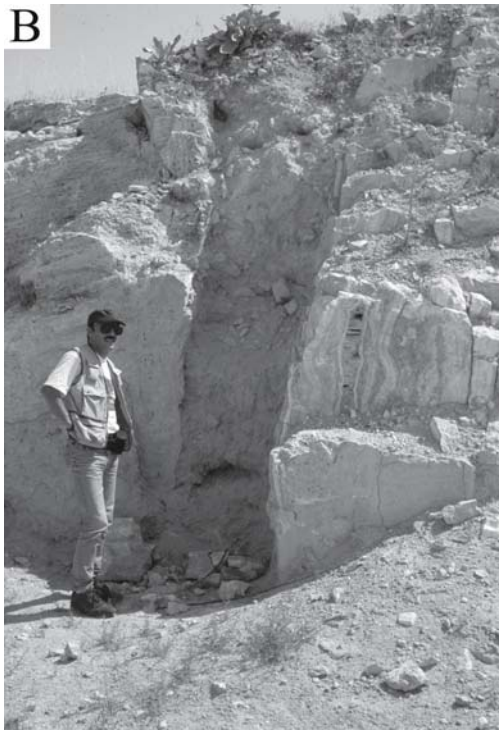
B

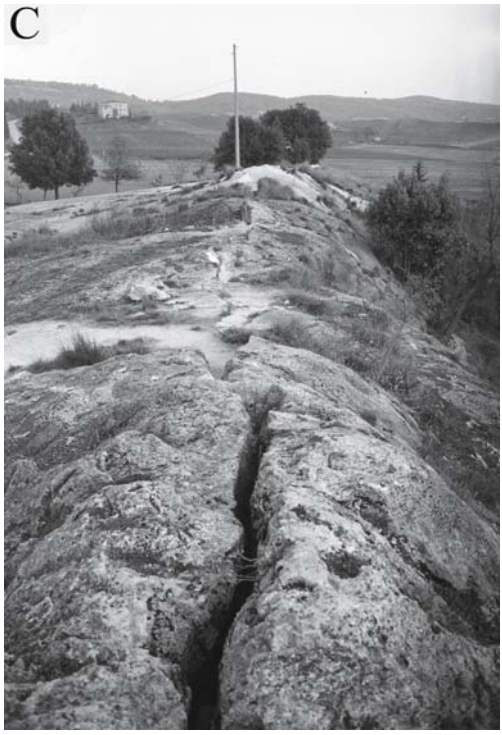
C


D

Photoplate 10
Travertine Dams

A Intricate minidam patterns at Egerszalók, Bükk Mountains, Hungary. This small mound formed under a dripping pipe conducting hot water from a trial borehole. 10 cm scale at left

B Minidam crests captured in morning sunlight showing their contour-like form. The most narrowly spaced dams are on the steepest slopes. Upper mound of Pamukkale, Turkey. 10 cm scale at left

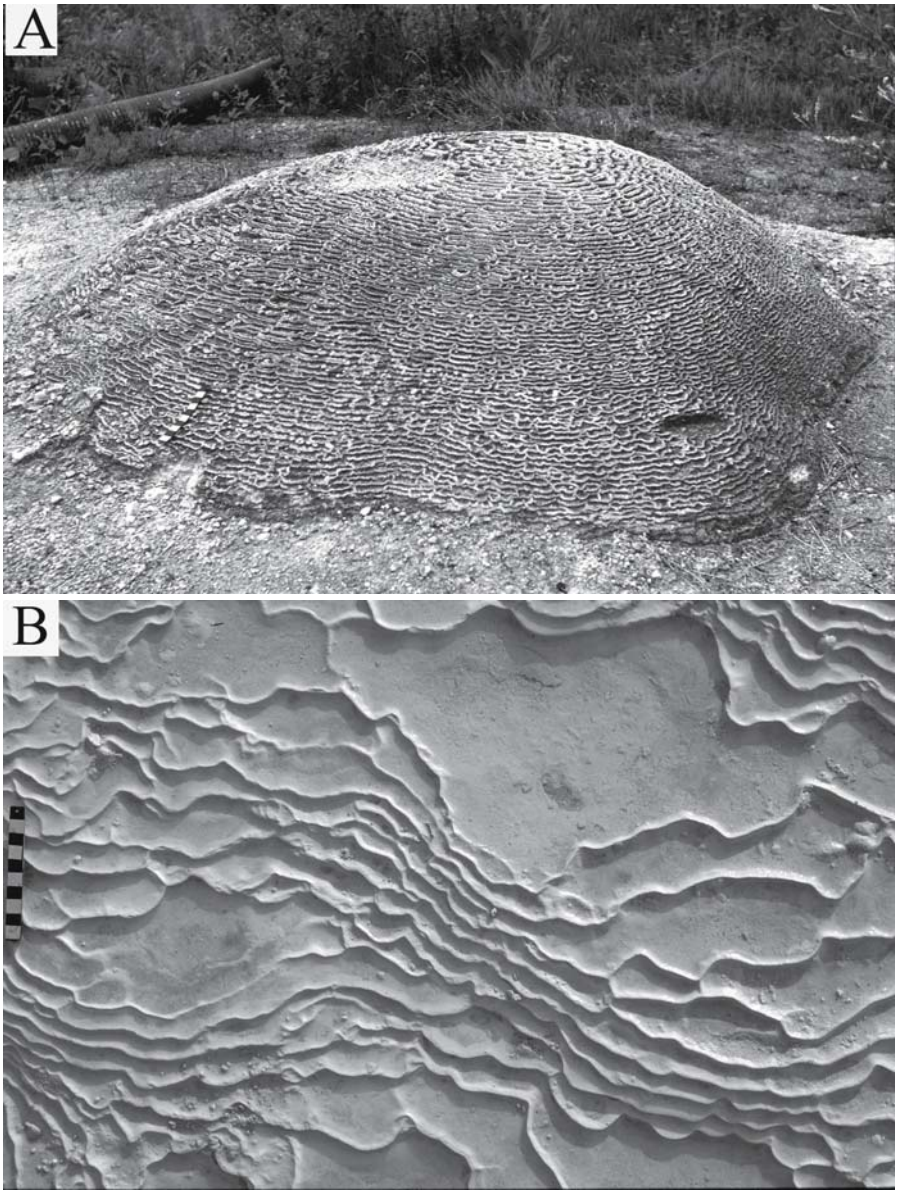

C Pearl Shoal, Jiuzhaigou, China. An extensive riffle on the surface of an almost flat, gently sloping surface of actively depositing travertine forming part of the crest of a large and complex lake-dam system

D The 'Bathers Basins' at Pamukkale, Turkey. A popular tourist attraction showing the shallow ponds supported by massive drop-walls

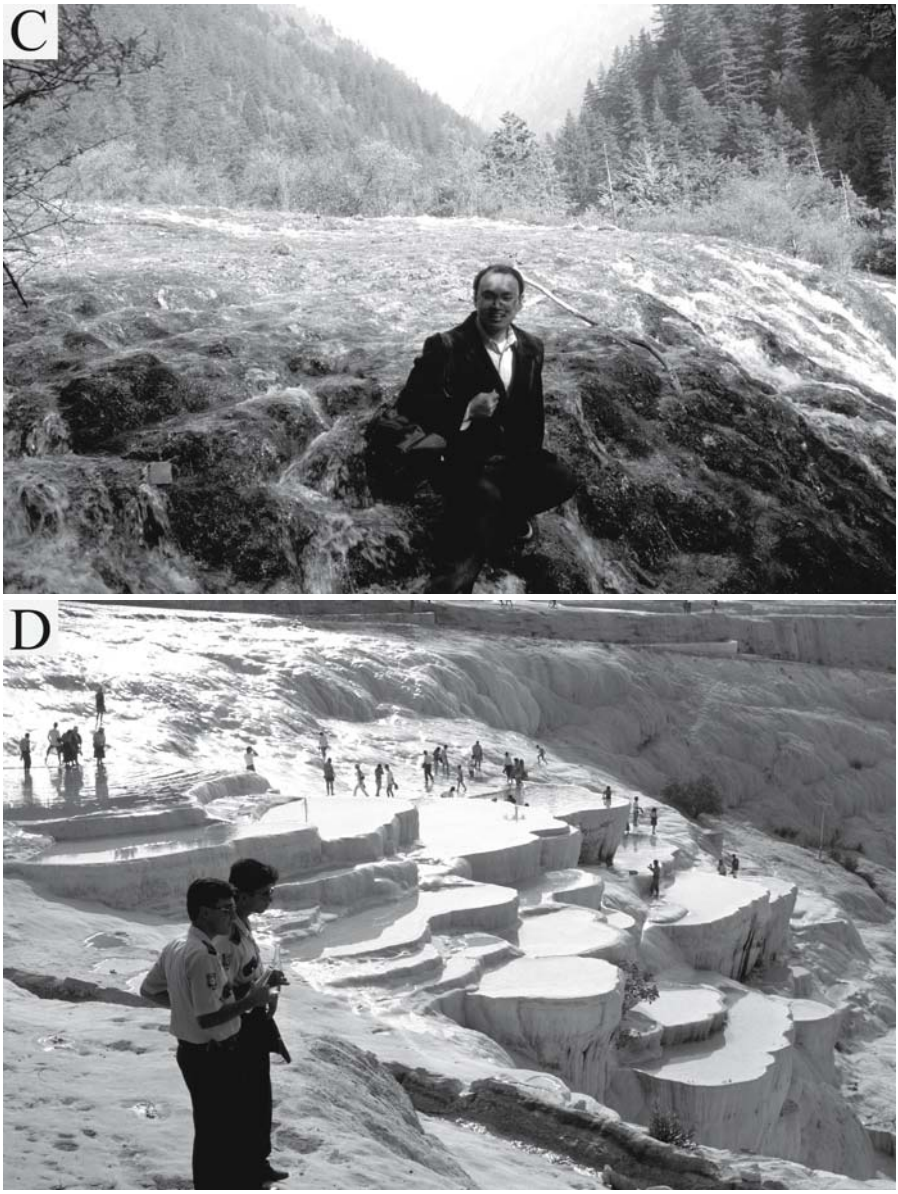

Photoplate 11
Travertines in Streams, Lakes and Seepages

A Stream crust consisting of oncoids and thin stream bed encrustations covered by shallow water and colonised by the cyanobacterium *Phormidium incrustatum*. Harrietsham, UK
B Thin lake crusts on littoral limestone cobbles containing abundant diatoms, *Rivularia* and *Schizothrix* and burrowed by the caddis fly larva *Tinodes*. Malham Tarn, UK. Bar 2 cm
C Stromatolitic reefs up to 1 m across, covered in a thick biofilm of diatoms at the edge of Pozzo Azulas, Cuatro Cienegas, Mexico
D Paludal deposit of travertine consisting of loose clastic material accumulating in hollows and small capillary-fed mossy mounds up to 30 cm high. Great Close Mire, Malham, UK
E Holocene cemented rudite exposed in an eroding river bank near Malham Tarn, UK. 5 cm lens cap near centre of image

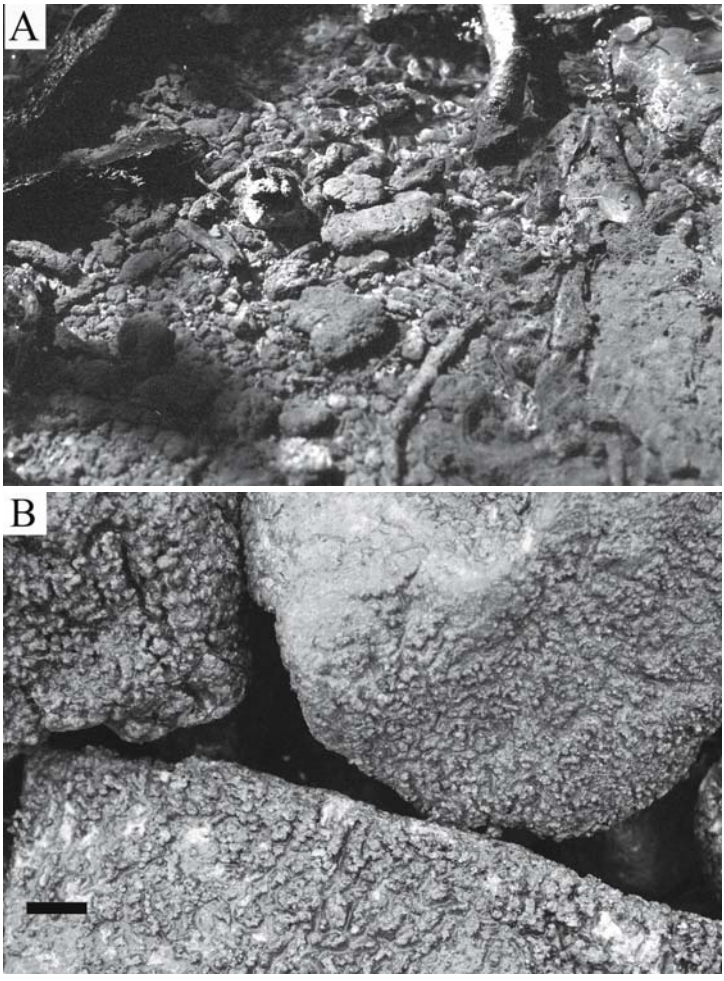


C


D

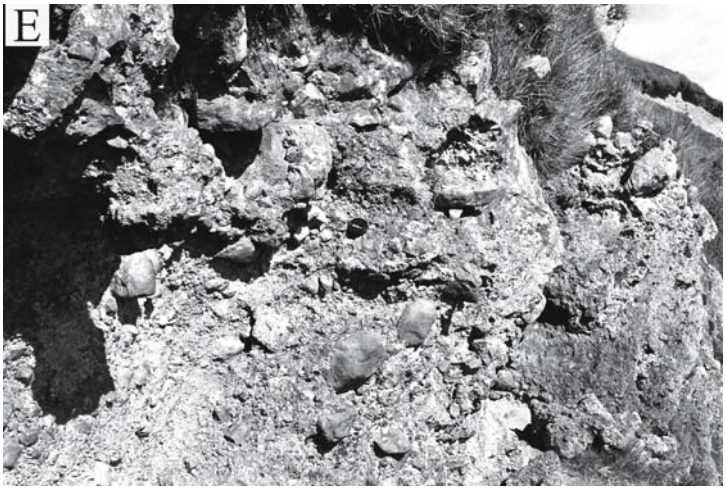
E

Photoplate 12
Speleothem, Caves and Diverse Deposits

A A cave cone consisting of an accumulation of floe on the floor of Szemlöhegy Cave, Budapest, Hungary. 10 cm scale at left

B Exposed bar of clastic travertine deposited on the inner curve of a small meander during periods of spate. Lathkilldale, UK

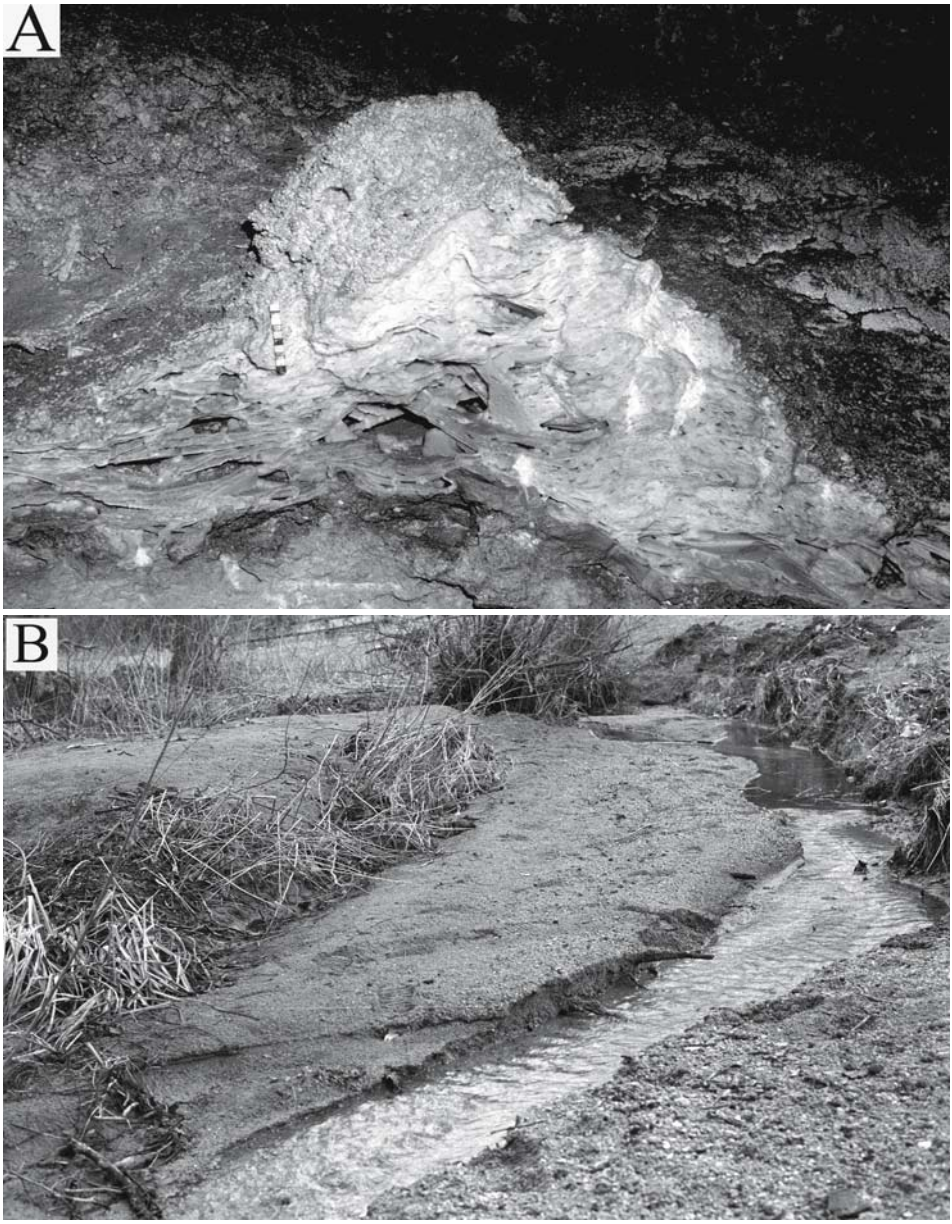

C Large karstic depression in the Antalya travertine deposit, Turkey
D Arbol del Navidad (The 'Christmas Tree'), Chiapas, Mexico
E A small travertine cave formed under a relict cascade deposit, Terni Falls, Italy. Scale 10 cm

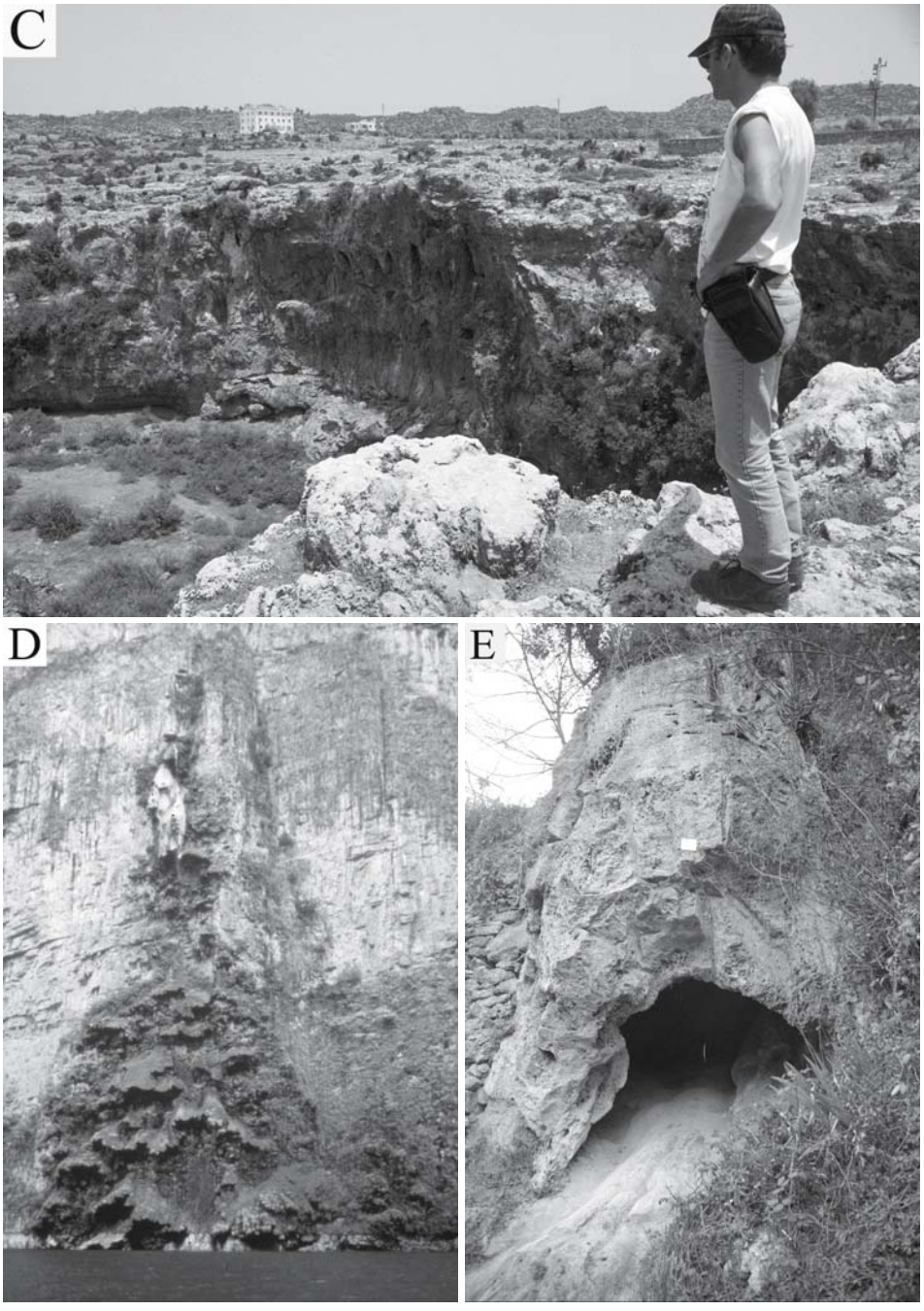

Photoplate 13
Scanning Electron Micrographs of the Travertine Surface (All Au-Pd Coated)

A Calcite rhombohedra with well-defined faces on the surface of the meteogene Santuario di Quintilio deposit near Tivoli, Italy. Bar 100 μm

B Aragonite sheaves and spherulites from a minidam surface at Minerva Terrace, Mammoth Hot Springs, Wyoming. Bar 10 μm

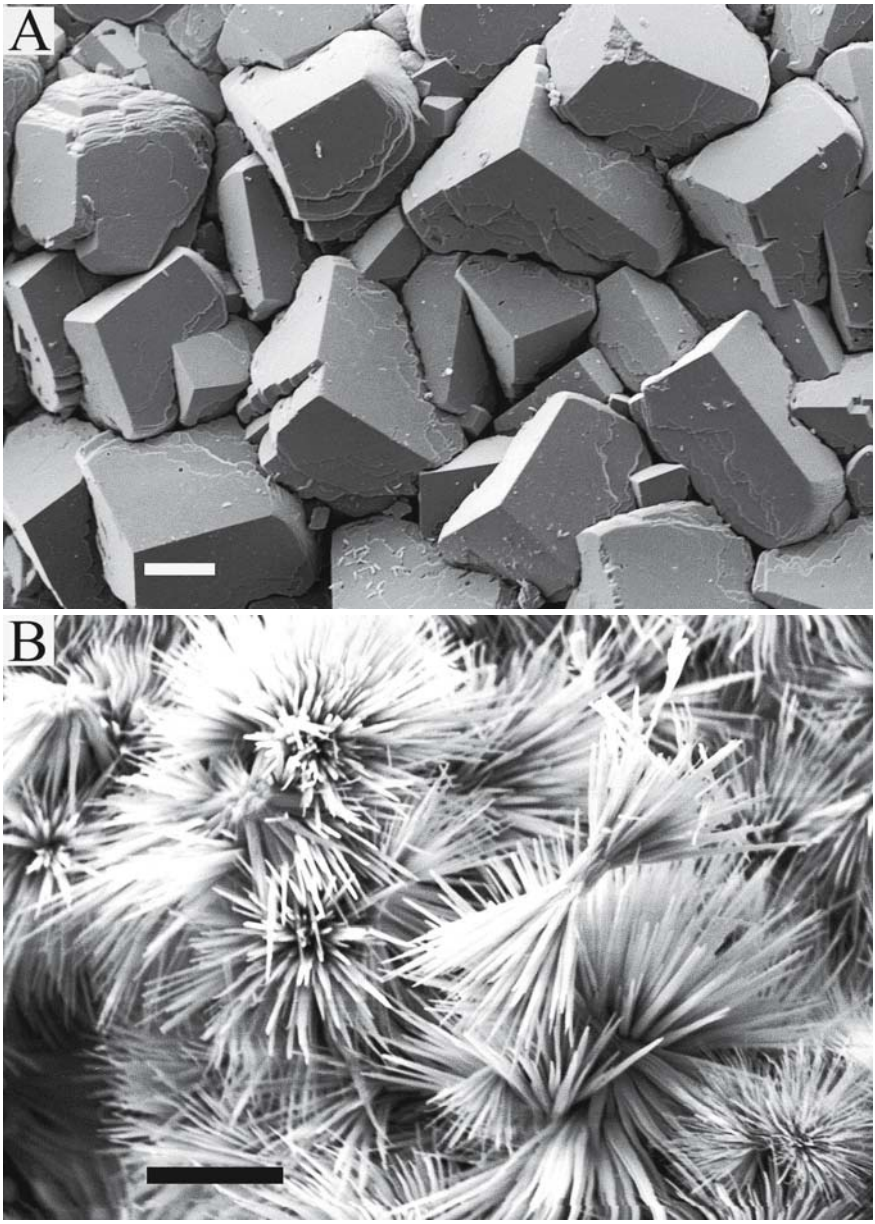

C Calcite crystals developing around the desmid *Oocardium stratum*. This alga grows at the end of mucilaginous tubes which occupied the holes in the crystal. Several cells of *Oocardium* can be seen at the surface. Cam Gill, Yorkshire, UK. Bar 20 μm

D *Achnanthes minutissima* a common diatom on the surface of a travertine composed of micrite. Waterfall Beck, UK. Bar 5 μm

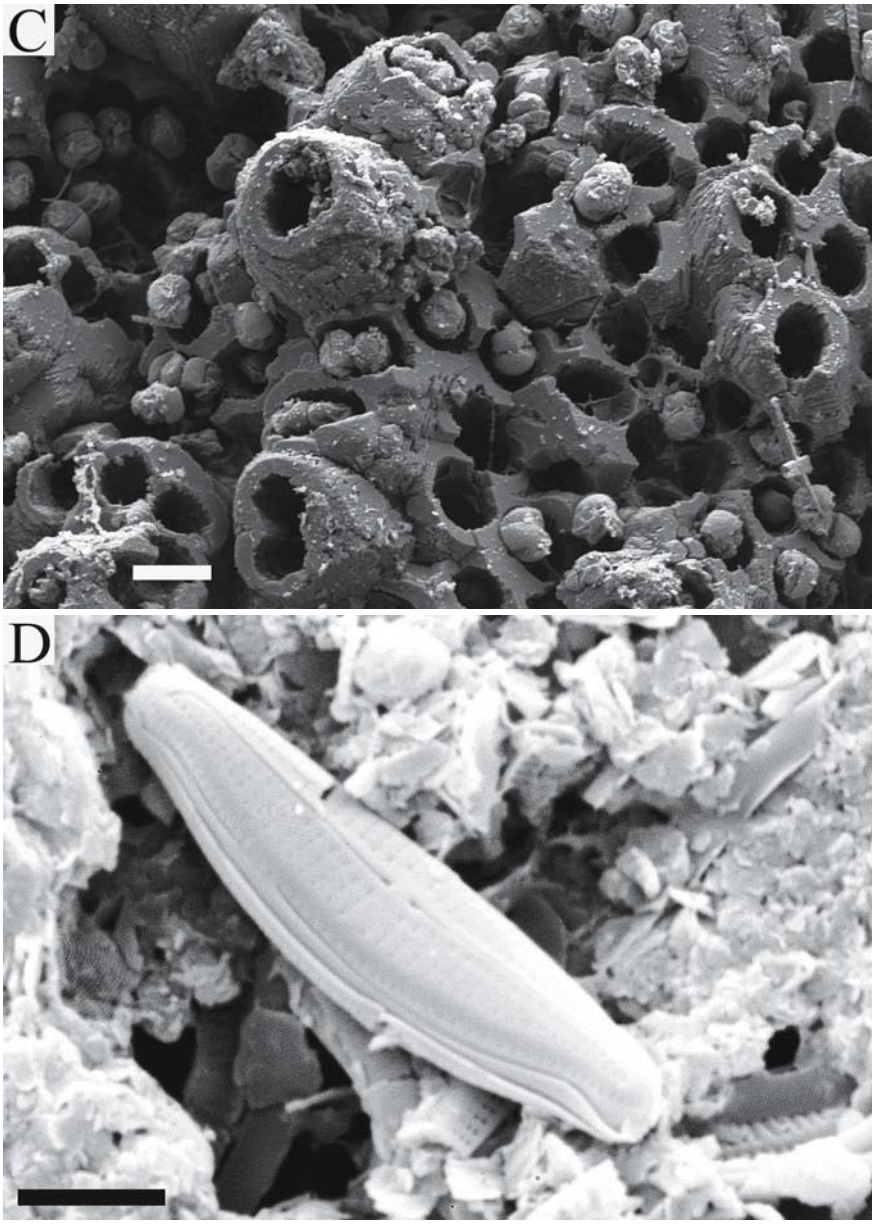

Photoplate 14
Bacteria and Algae Inhabiting Travertine

A Photosynthetic bacteria colonising microspar at Lago delle Collonelle, Bagni di Tivoli, Italy. The bacteria, probably *Chromatium*, are easily detached and have left small cavities in the crystals. Scanning electron micrograph. Bar 10 μm

B Nodular encrusted colonies of *Phormidium incrustatum* on a meteogene stream crust, Fleinsbrunnenbach. Schwäbische Alb, Germany. Bar 5 mm

C Thin vertical section through a meteogene cascade travertine colonised by the cyanobacterium *Phormidium incrustatum*. The trichomes appear as thin pale streaks surrounded by a mucilaginous sheath encrusted with micrite. Croscombe, UK. Plane transmitted light. Travertine surface to page top. Bar 100 μm

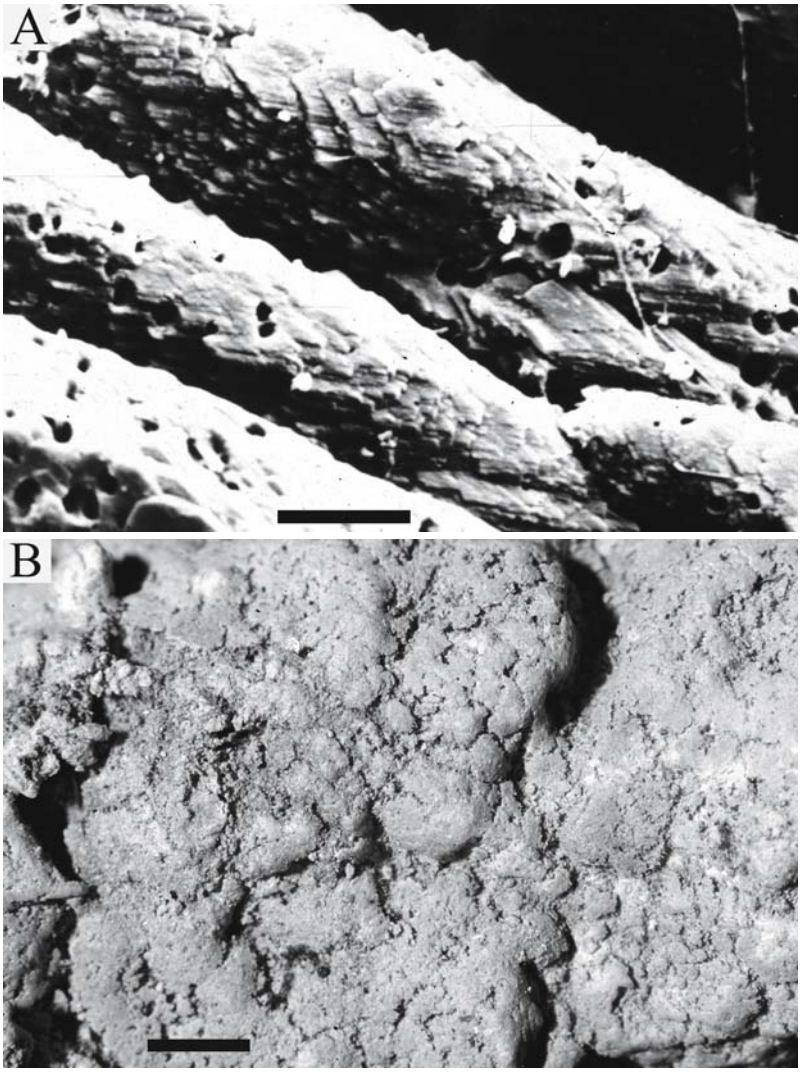

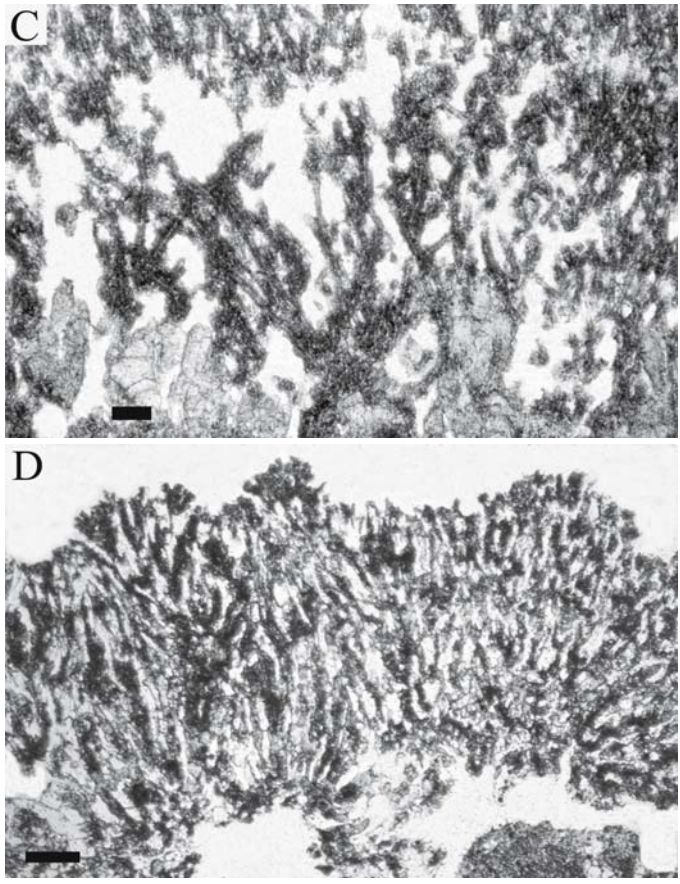

D Thin vertical section through a stream crust colonised by the cyanobacterium *Schizothrix fasciculata*. Bundles of narrow trichomes occupy the clear areas and are surrounded by micrite, much of which is closely associated with the outer mucilaginous sheath. Waterfall Beck, UK. Plane transmitted light. Travertine surface to top of page. Bar 100 μm

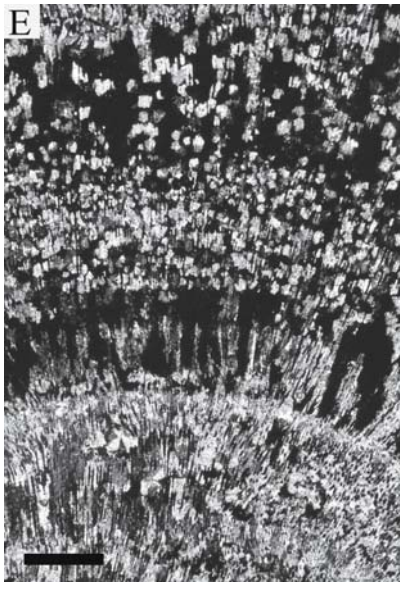

E Sagittal section through a calcified colony of *Rivularia haematites*. Several layers with different degrees of calcification with microspar can be observed representing physical and chemical changes within the stream water, and photosynthesis within the colony. The trichomes run vertically across the image and are surrounded by thick sheaths in which the mineral is embedded, but are difficult to see under crossed polars. Gordale Beck, UK. Bar 250 μm

Photoplate 15
Algae and Bryophytes of Travertine

A Vertical section through colonies of the green alga *Oocardium stratum* on a modern meteogene travertine. Crystals of microspar develop around the colonies and their structure appears to be controlled by them. Within the crystals the unmineralised mucilagous stalks can be clearly seen but few cells are visible. Lahage Cron, Belgium. Crossed nicols. Bar 200 µm

B Vertical section through a meteogene travertine colonised by the diatom *Didymosphenia geminata*. Both valve and girdle views are seen, together with the mucilaginous stalks, some of which are surrounded by micrite. Gordale Beck, UK. Plane transmitted light, surface of deposit to left. Bar 100 µm

C Thin section through a modern meteogene deposit colonised by the Xanthophyte alga *Vaucheria geminata*. This section has been cut perpendicular to the filament bundles to show small euhedral calcite crystals surrounding the cell wall. Many of these crystals appear to

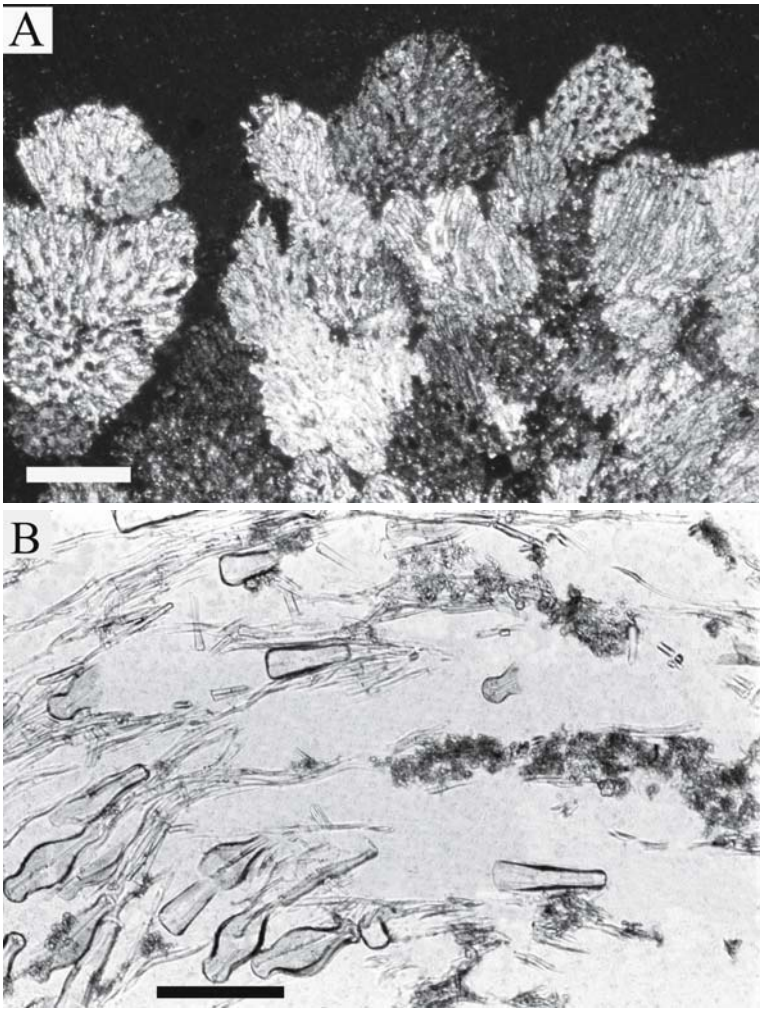

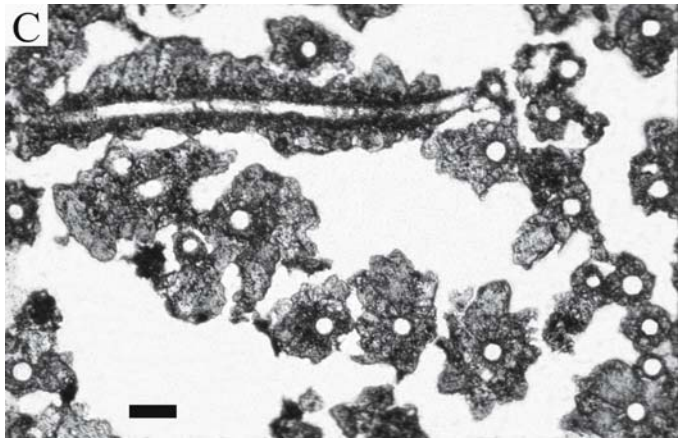

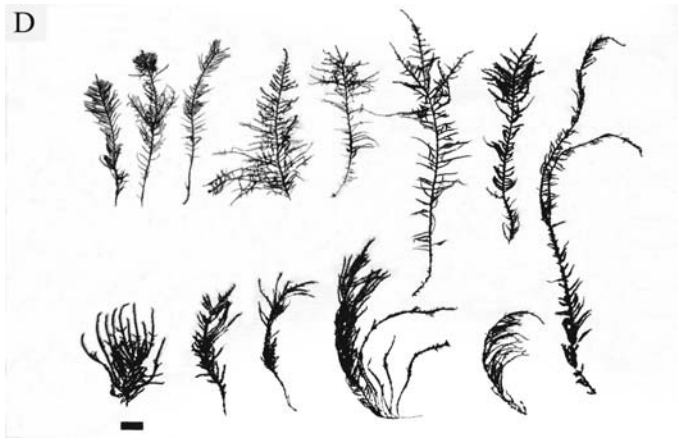

develop from a thin layer of micrite in contact with the cell wall. Wateringbury, UK. Plane transmitted light. Bar 100 μm

D Silhouttes of the moss *Palustriella commutata* showing the variation in growth resulting from differences in water flow. Above: *P. commutata* var. *commutata* ; The five plants on the left were collected from capillary flow regimes, while the two larger plants on the right represent intermediate forms collected from an area of rapidly dripping water on a cascade. Below: *P. commutata* var. *falcata*; The five plants on the left were obtained from a cascade with rapidly flowing water. The long plant on the right was collected from water flowing at 2 m s^{-1}. Note the short side-branches in this specimen. Samples from a range of deposits in the UK. Bar 1 cm

E The moss *Rhynchostegium riparioides* from Waterfall Beck, UK. Bar 1 cm

Photoplate 16
Bryophytes and Higher Plants

A *Eucladium verticillatum*, a common moss of shaded travertine deposits in Western Europe. Gordale Beck, UK. Bar 5 mm
B *Vesicularia montangei* from the travertines of Sahasra-dhara, India. Bar 5 mm

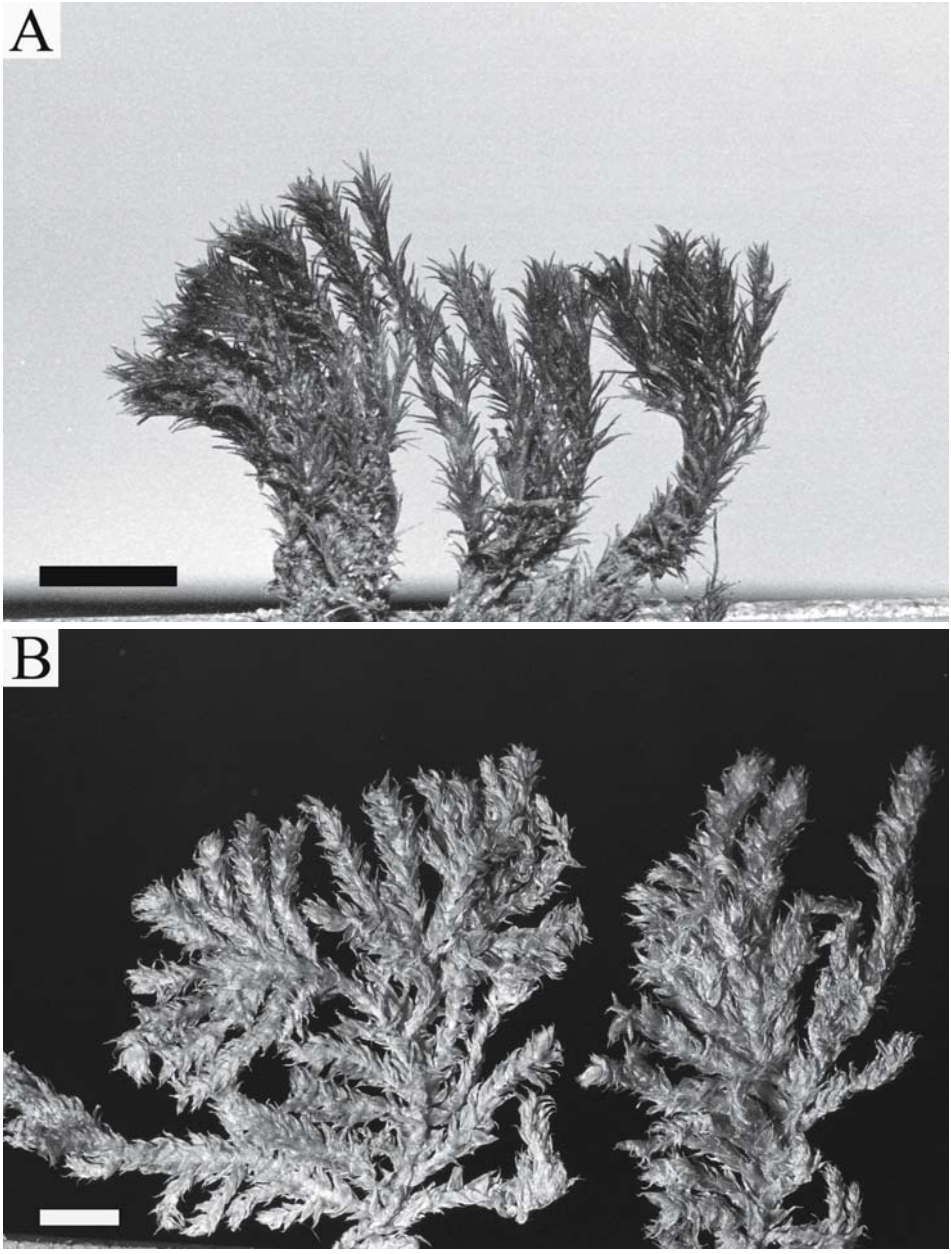

C The liverwort *Pellia endiviifolia* from the travertines of Waterfall Beck, UK. Bar 1 cm

D Zhaga Water Forest, Sichuan, China. An area of deciduous woodland developed on an extensive braided travertine deposit

E *Eupatorium cannabinum* growing on a prograding cascade travertine in semi-shade, Gütersteiner Falls, Germany

Photoplate 17
Related Deposits

A Two oogonia and an antheridium of *Chara hispida* from a marlpond in Kent, UK. The oogonia are surrounded by spiral cells capped by five coronal cells. On fertilisation, the spiral cells become calcified, detach from the alga and may be preserved in lake sediments as 'gyrogonites'. SEM micrograph. Bar 0.5 mm

B *Chara* preserved in life position by intense calcification of the stems to form a highly porous 'petrified forest' sold as a curio. Munigo, Sichuan, China. Bar 2 cm

C Beachrock at Seilebost, Harris, UK. Note lamination of the sediment by the dog's tail. Dark patches are of cyanobacteria, mainly *Calothrix contarenii*

D Waterpipe encrusted with calcite. The pipe originally had an internal diameter of 12 cm and the deposit has reduced the cross-sectional area by about 75%. Matlock Bath, UK

E Siliceous sinter terrace and cone. Upper Geysir Basin, Yellowstone National Park, Wyoming

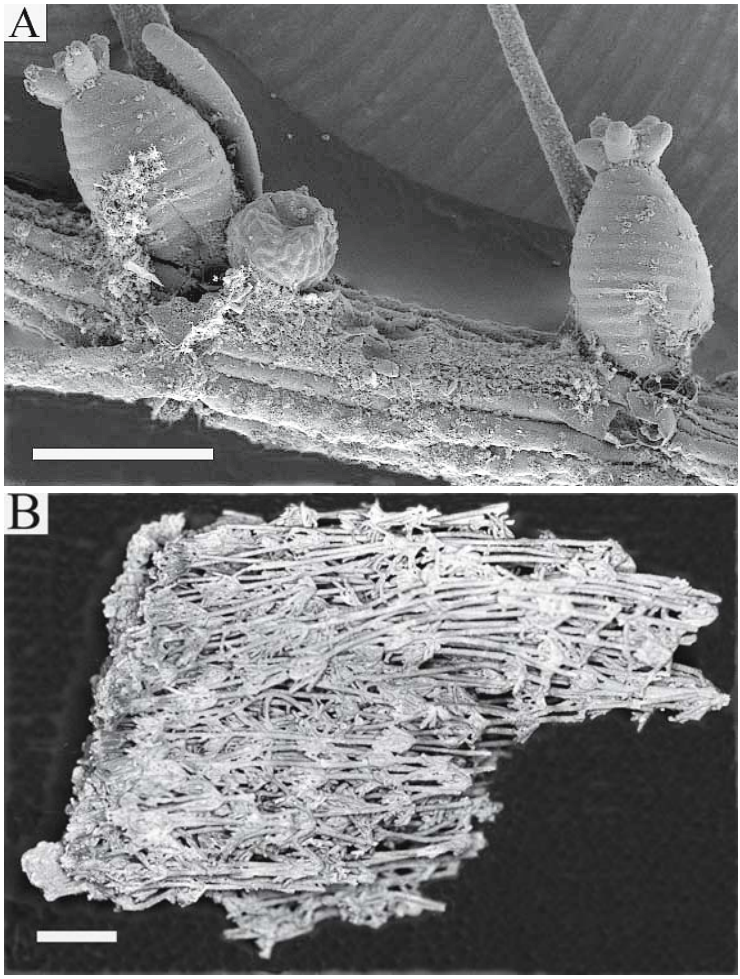

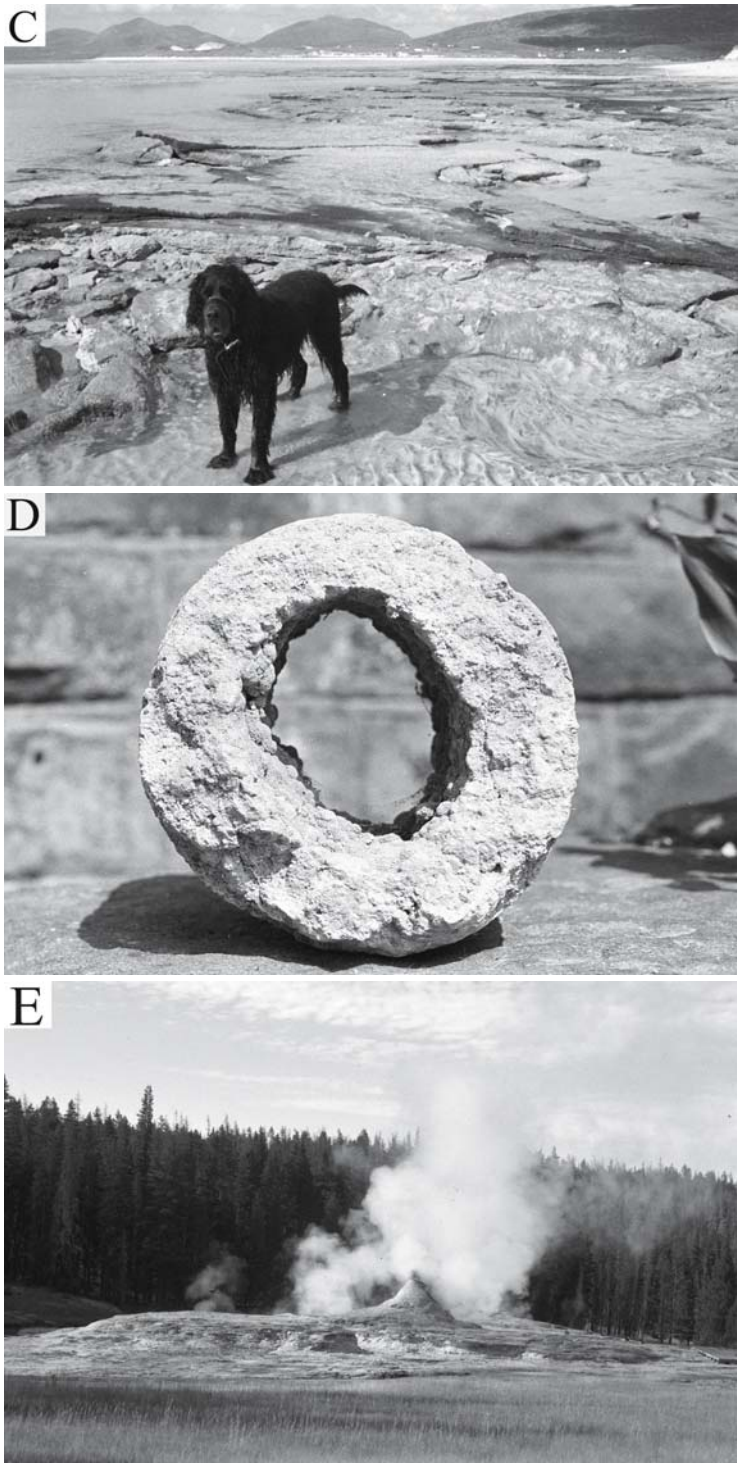
C
D
E

Photoplate 18
Fossils and Travertine Use

A The wing-nut, *Pterocarya fraxinifolia*
B Cave Bruno Poggi, Bagni di Tivoli, Italy. One of the largest travertine quarries in this district where the rock is won along three major benches about 6 m in thickness
C Temple of Aedes Spei, Forum Holitorium, Rome. The travertine columns have been built into the wall of a church
D Fossil Forest, Lulworth, UK showing encrustations of travertine surrounding moulds of tree trunks *in situ*. Upper Jurassic
E Travertine sculpture, Geislingen Church, Germany. Probably part of a medieval tomb, but age unknown

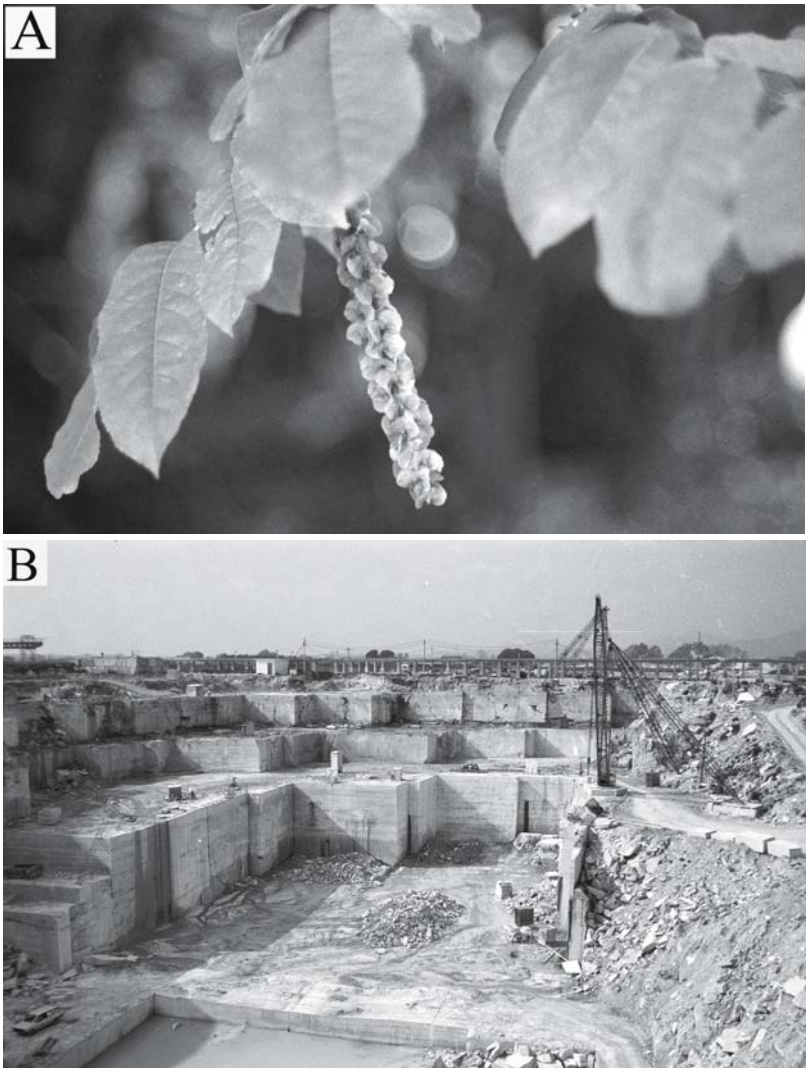


C

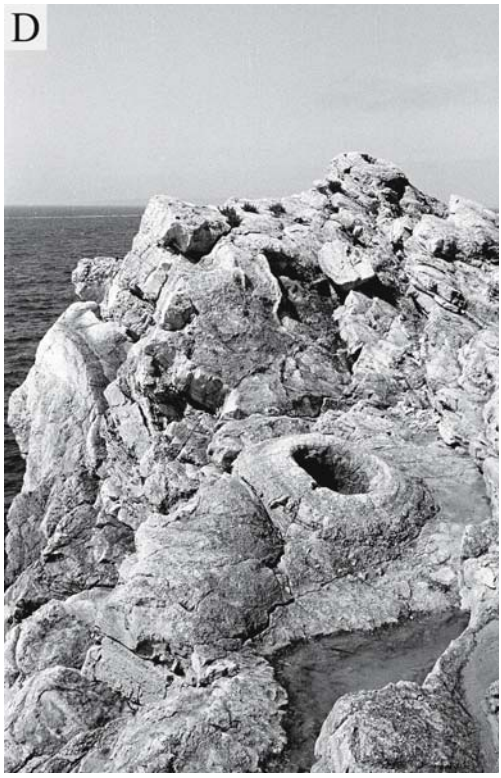
D

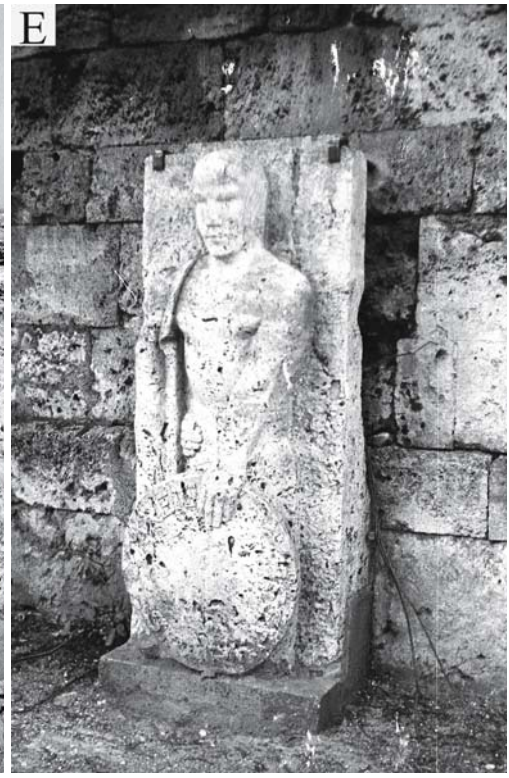
E

Photoplate 19
Travertine Use in Buildings

A Ponte della Badia, Vulci showing the large travertine voussoirs
B Porta Maggiore (formerly P. Prenestina), Rome, with inscriptions of Roman emporers faintly visible on the attic. The tomb of M. Eurysaces is partly visible behind the arch on the left
C Travertine substructures in the Roman Theatre at Hierapolis, Turkey
D The Roman Pharos, with the church of St Mary in the Castle behind. Dover, UK
E Travertine tomb dating from c. A.D. 100, partly embedded in recent travertine. The Necropolis at Hierapolis, Turkey


C


D


E

Photoplate 20
Travertine in Buildings and Sculpture

A Modern vaulted gateway partly built of dressed local travertine. Berkeley Castle, UK
B Marl Cottage, Derbyshire, built almost entirely of a local travertine
C Broadgate Circle, London
D Bas-reliefs on the side of a Roman tomb, Villa Volkonsky, Rome
E Draped Reclining Figure by Henry Moore (1978; LH 706). With permission from the Henry Moore Foundation, Much Hadham, UK


C


D


E

Photoplate 21
Travertine in Art

A *Pace sulla Terra* by J. Lipchitz, Museum of Modern Art, Rome
B Hedgehog souvenir from Tivoli, Italy. Piece measures 9 cm in width
C Meteogene travertine employed in a circular rockery surrounded by water. Guilin, China. Largest piece is about 4 m high
D Grotesque mask found among rubble by the Theatre of Marcellus, Rome. Mask is about 30 cm wide
E 'Jellybabe'. Carved from a small (25 cm) block of Bagni Vignoni travertine

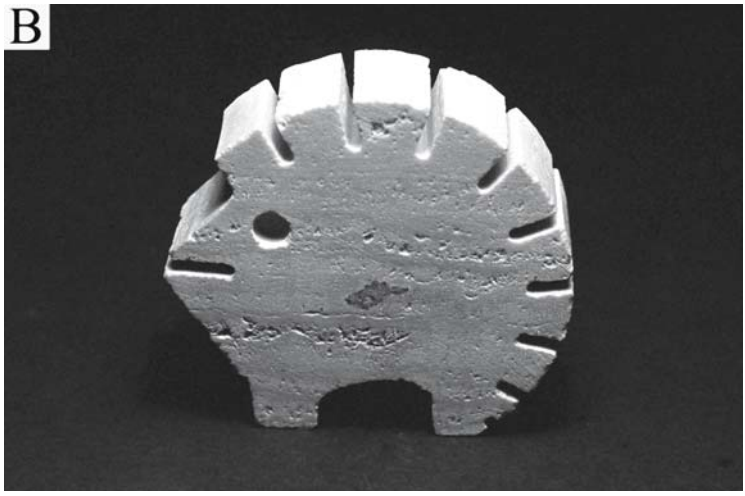

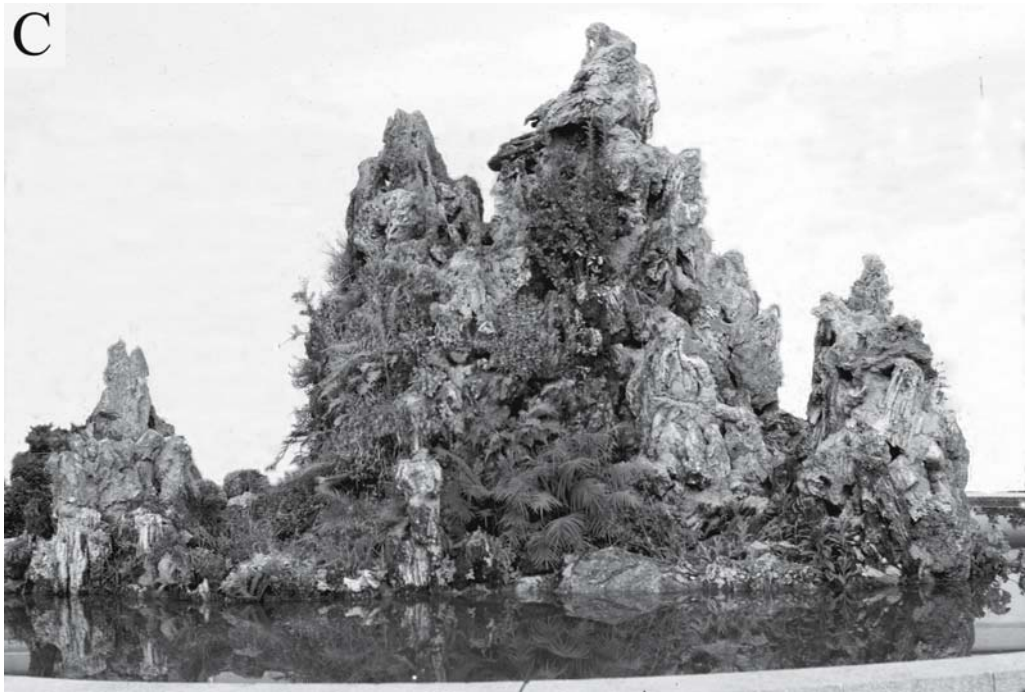
C


D

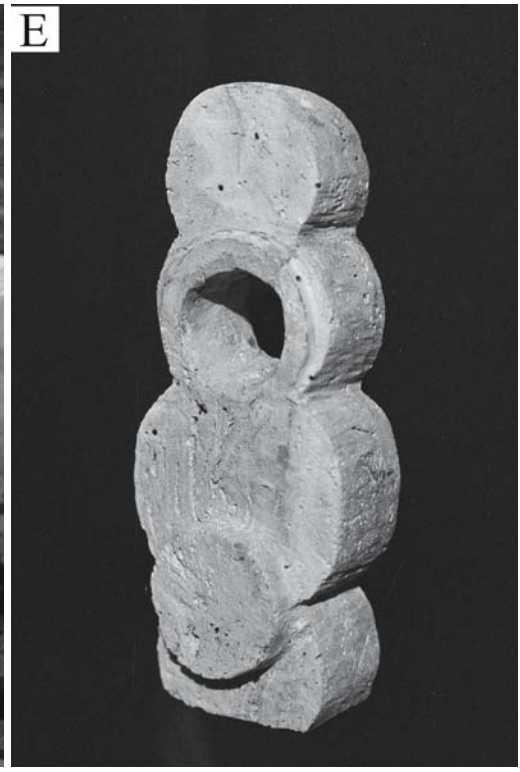
E

Photoplate 22
Travertine in Art Continued

A Decorative pieces of travertine used as a background and planting medium for small calcicolous herbs. Huangguoshu, Guangxi, China
B Two echelles stacked with moulds ready for encrustation. Grotte de Pérou, St. Alyre, Clermont-Ferrand, France
C A 'petrified' passerine bird on display at the Clermont-Ferrand petrifying springs, France
D Teddy bears, ties and brassieres are among the articles 'petrified' at the Knaresborough Dropping Well, UK
E Travertine bas-relief produced at the Grotte de Pérou, France. This work measures 9.5 x 12.5 cm

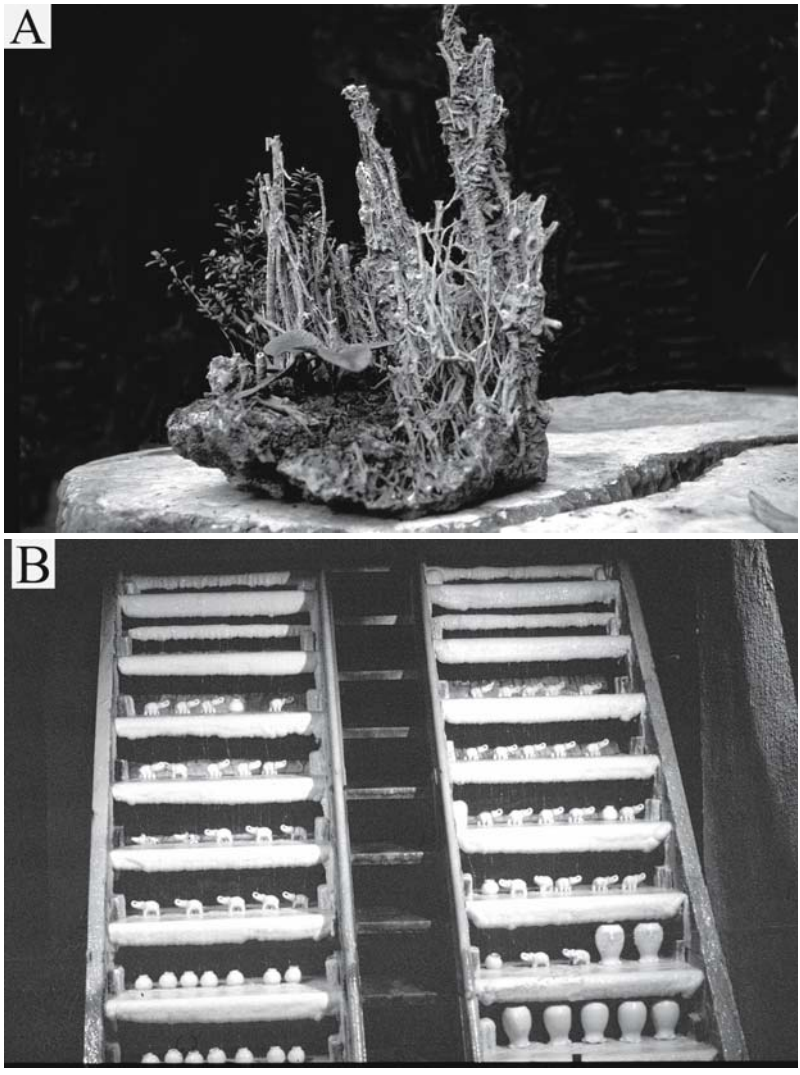


C


D


E

Index

C

G

H

M

N

S

U

V

W

Y

Z